Wydział Chemii
Uniwersytet im. Adama Mickiewicza w Poznaniu

mgr inż. Anna Kawka

Synteza, analiza spektroskopowa oraz badania biologiczne *in silico* nowych koniugatów steroidowych zawierających układy triazolowe

Synthesis, spectroscopic analysis and *in silico* biological studies of new steroid conjugates containing triazole systems

Rozprawa doktorska w formie cyklu artykułów naukowych

Poznań, 2025 r.

Praca doktorska została wykonana w Zakładzie Produktów Bioaktywnych
Wydziału Chemii
Uniwersytetu im. Adama Mickiewicza w Poznaniu

Promotor: prof. UAM dr hab. Tomasz Pospieszny
Promotor pomocnicza: dr inż. Hanna Koenig

Pragnę wyrazić głęboką wdzięczność Profesorowi UAM dr. hab. Tomaszowi Pospiesznemu, mojemu Promotorowi, za nieocenione wsparcie, mądrość i inspirację, które były filarami mojego rozwoju naukowego. Pańska opieka i życzliwość uczyniły tę współpracę czymś znacznie więcej niż tylko naukowym doświadczeniem.

Moją serdeczne podziękowania kieruję do Pani dr inż. Hanny Koenig, której cierpliwość, wyrozumiałość i nieoceniona pomoc towarzyszyły mi w trakcie całego procesu tworzenia tej pracy.

Michalinie,
dziękuję za Twoje wsparcie, cierpliwość i motywację, które sprawiły, że nigdy nie przestałem wierzyć w siebie i swoje możliwości.

Mojej Rodzinie,
za umożliwienie realizacji własnych celów, które pozwoliły mi dotrzeć do tego miejsca.

Pamięci mojego ukochanego Dziadka, którego obecność na zawsze pozostanie w moim sercu i którego miłość inspirowała mnie na każdym kroku tej drogi.

Spis treści

Życiorys naukowy

Urodziłam się 1 sierpnia 1997 roku w Inowrocławiu. W 2016 roku ukończyłam III Liceum Ogólnokształcące im. Królowej Jadwigi w Inowrocławiu.

W październiku tego samego roku rozpoczęłam studia licencjackie na Wydziale Chemii im. Adama Mickiewicza w Poznaniu na kierunku chemia, specjalność chemia sądowa. W 2018 roku trafiłam do Zakładu Produktów Bioaktywnych, gdzie realizując temat pracy licencjackiej zajmowałam się syntezą czwartorzędowych soli alkiloamoniowych pochodnych kwasów żółciowych. Kontynuując badania pod opieką Pana prof. UAM dr. hab. Tomasza Pospiesznego, w ramach pracy magisterskiej podjęłam się syntezy nowych biokoniugatów steroidowych zawierających pierścienie 1,2,3-triazolowe. W 2021 roku uzyskałam dyplom magisterski za pracę *Synteza, charakterystyka spektroskopowa oraz badania teoretyczne nowego koniugatu steroidowego modyfikowanego pierścieniem 1,2,3-triazolowym*.

Moje zainteresowania tematyką biokoniugatów steroidowych sprawiły, że badania te postanowiłam rozszerzyć podejmując naukę w Szkole Doktorskiej Nauk Ścisłych na Wydziale Chemii Uniwersytetu im. Adama Mickiewicza w Poznaniu w grupie badawczej prof. UAM dr. hab. Tomasza Pospiesznego.

Rezultaty swoich prac zaprezentowałam na dwudziestu jeden konferencjach o zasięgu ogólnopolskim i międzynarodowym (w formie jedenastu komunikatów ustnych i dziesięciu posterów). Zostałam laureatką dwóch prestiżowych nagród za najlepsze wystąpienia ustne.

Jestem współautorką siedmiu artykułów naukowych (w tym sześciu z pierwszym autorstwem, a w trzech jako autor korespondencyjny), gdzie zostały opisane szczegółowo wyniki przeprowadzonych badań nad koniugatami steroidowymi, jak również publikacji powstałej przy współpracy z Katedrą i Zakładem Bromatologii Uniwersytetu im. Karola Marcinkowskiego w Poznaniu. Prace te ukazały się w renomowanych czasopismach z listy filadelfijskiej. Moje osiągnięcia naukowe są poparte imponującymi wynikami, ponieważ sumaryczny Impact Factor wynosi 20,1, natomiast całkowita punktacja ministerialna to 530 pkt.

Poza działalnością naukową aktywnie angażuję się w popularyzację chemii, m.in. poprzez prowadzenie warsztatów edukacyjnych dla uczniów oraz udział w corocznym Poznańskim Festiwalu Nauki i Sztuki. Ponadto, jestem również członkinią Polskiego Towarzystwa Chemicznego.

Wykaz artykułów naukowych i monografii w czasopismach naukowych lub w materiałach pokonferencyjnych wraz z danymi bibliograficznymi

LP	OPIS BIBLIOGRAFICZNY	PKT	IF
P1	**Anna Kawka***, Hanna Koenig, Tomasz Pospieszny, *Triazole-Based Modification of Bile Acids: Promising Strategies for Combating Infections and Cancer – A Review*, Rozdział [w] *Na pograniczu chemii, biologii i fizyki - rozwój nauk. Tom 6.* Wydawnictwo Naukowe UMK, Toruń, Polska, **2025**.	20	–
Koncepcja pracy, przygotowanie oryginalnego manuskryptu, metodologia, analiza danych, analiza formalna, udział w dyskusji z recenzentami, edycja tekstu, wizualizacja, nadzór administracyjny.			
P2	**Anna Kawka***, Hanna Koenig, Tomasz Pospieszny*, *Steroid and Bioactive Molecule Conjugates: Improving Therapeutic Approaches in Disease Management*, Bioorganic Chemistry, **2024**, 153, 107933, DOI: 10.1016/j.bioorg.2024.107933	100	4.5
Koncepcja pracy, przygotowanie oryginalnego manuskryptu, metodologia, gromadzenie danych, analiza formalna, analiza danych, wizualizacja, udział w dyskusji z recenzentami, edycja tekstu, nadzór administracyjny.			
P3	**Anna Kawka***, Damian Nowak, Hanna Koenig, Tomasz Pospieszny, *Exploring Triazole-Connected Steroid-Pyrimidine Hybrids: Synthesis, Spectroscopic Characterization, and Biological Assessment*, ACS Omega, **2024**, 9, 37995–38014, DOI: 10.1021/acsomega.4c04800	70	3.7
Koncepcja pracy, synteza związków, metodologia, analiza formalna, przygotowanie oryginalnego manuskryptu, udział w dyskusji z recenzentami, edycja tekstu, wizualizacja.			
P4	**Anna Kawka**, Hanna Koenig, Tomasz Pospieszny*, *From Squalamine to Triazole Ring Derivatives Exploring the Versatility of Steroidal Bioconjugates*, Rozdział [w] *Studies in Natural Products Chemistry* Edited by Atta-ur Rahman, Elsevier, Amsterdam, Netherlands **2024**, 82, 247–283, ISBN: 978-0-443-15756-1	20	–
Koncepcja pracy, przygotowanie oryginalnego manuskryptu, metodologia, gromadzenie danych, analiza danych, wizualizacja, udział w dyskusji z recenzentami, edycja tekstu.			
P5	Michalina Banaszak*, Małgorzata Dobrzyńska, **Anna Kawka**, Ilona Górna, Dagmara Woźniak, Juliusz Przysławski, Sławomira Drzymała-Czyż, *Role of Omega-3 Fatty Acids EPA and DHA as Modulatory and Anti-Inflammatory Agents in Noncommunicable Diet-Related Disorders – Reports From the Last 10 Years*, Clinical Nutrition ESPEN, **2024**, 63, 240–258, DOI: 10.1016/j.clnesp.2024.06.053	40	2.9

Koncepcja pracy, napisanie manuskryptu, edycja tekstu.

P6	**Anna Kawka**, Hanna Koenig, Damian Nowak, Tomasz Pospieszny*, *Quasi-Podands with 1,2,3-Triazole Rings from Bile Acid Derivatives: Synthesis, and Spectroscopic and Theoretical Studies*, Journal of Organic Chemistry, **2024**, 89 (11), 7561–7572, DOI: 10.1021/acs.joc.4c00195	140	3.3 3.6**

Koncepcja pracy, synteza związków, metodologia, analiza formalna, przygotowanie oryginalnego manuskryptu, wizualizacja.

P7	Grzegorz Hajdaś, **Anna Kawka**, Hanna Koenig, Damian Kułaga, Katarzyna Sosnowska, Lucyna Mrówczyńska, Tomasz Pospieszny*, *Click chemistry as a method for the synthesis of steroid bioconjugates of bile acids derivatives and sterols*, Steroids, **2023**, 199, 109282, DOI: 10.1016/j.steroids.2023.109282	70	2.1 2.9**

Synteza związków, koncepcja pracy, metodologia, analiza formalna, analiza danych, edycja tekstu, wizualizacja.

P8	**Anna Kawka**, Grzegorz Hajdaś, Damian Kułaga, Hanna Koenig, Iwona Kowalczyk, Tomasz Pospieszny*, *Molecular Structure, Spectral and Theoretical Study of New Type Bile Acid–Sterol Conjugates Linked via 1,2,3-Triazole Ring*, Journal of Molecular Structure, **2023**, 273, 134313, DOI: 10.1016/j.molstruc.2022.134313	70	4.0 3.8**

Koncepcja pracy, synteza związków, metodologia, analiza formalna, analiza danych, przygotowanie oryginalnego manuskryptu, udział w dyskusji z recenzentami, edycja tekstu, wizualizacja.

*autor korespondencyjny; **Impact Factor w dniu opublikowania artykułu

Publikacje wchodzące w skład rozprawy doktorskiej: P1, P2, P3, P4, P6, P8

Autor korespondencyjny w trzech publikacjach: P1, P2 i P3.

Wykaz uczestnictwa w ogólnopolskich i międzynarodowych konferencjach naukowych

Komunikaty ustne

1. **Anna Kawka**, Hanna Koenig, Tomasz Pospieszny, *Synthesis of new steroid-pyrimidine conjugates connected with 1,2,3-triazole ring*, XVII Kopernikańskie Seminarium Doktoranckie, Toruń, 6–7 czerwca **2024**.
2. **Anna Kawka**, Hanna Koenig, Tomasz Pospieszny, *Synthesis of new steroid-uracil conjugates using the „click" chemistry method*, Natural Science Baltic Conference, online, 20–21 kwietnia **2024**.
3. **Anna Kawka**, Hanna Koenig, Tomasz Pospieszny, *Synteza nowych koniugatów steroidowo-pirymidynowych z zastosowaniem metody chemii „click"*, IV Ogólnopolska Konferencja Doktorantów Nauk Ścisłych i Przyrodniczych „Bio Idea 4.0", Lublin, 3 lutego **2024**.
4. **Anna Kawka**, Hanna Koenig, Tomasz Pospieszny, *Zastosowanie chemii „click" do syntezy koniugatów kwasów żółciowych zawierających pierścienie 1,2,3-triazolowe*, Sympozjum Młodych Naukowców Wydziału Fizyki, Warszawa, 18–20 września **2023**.
5. **Anna Kawka**, Hanna Koenig, Tomasz Pospieszny, *Zastosowanie chemii „click" do syntezy nowych koniugatów steroidowych pochodnych kwasów żółciowych o potencjalnej aktywności biologicznej*, III Międzynarodowa Multidyscyplinarna Konferencja Doktorantów US 2.0 „MKDUS 2.0", Szczecin, 21–23 czerwca **2023**.
6. **Anna Kawka**, Hanna Koenig, Tomasz Pospieszny, *Synteza nowych quasi-podandów pochodnych kwasów żółciowych metodą chemii „click"*, I Ogólnopolska Konferencja PUTChemikon, Poznań, 6 maja **2023**.*
7. **Anna Kawka**, Hanna Koenig, Tomasz Pospieszny, *Synteza nowych quasi-podandów pochodnych kwasów żółciowych z wykorzystaniem chemii „click"*, V Pomorskie Sympozjum Studentów Chemii, online, 25–26 marca **2023**.
8. **Anna Kawka**, Hanna Koenig, Tomasz Pospieszny, *Synteza oraz badania biologiczne nowych koniugatów kwasów żółciowych zawierających pierścienie 1,2,3- triazolowe*, IV Ogólnopolskie Sympozjum Chemii Bioorganicznej, Organicznej i Biomateriałów „BioOrg", Poznań, 3 grudnia **2022**.*
9. **Anna Kawka**, Hanna Koenig, Tomasz Pospieszny, *Synteza nowych koniugatów kwasów żółciowych zawierających pierścienie 1,2,3-triazolowe*, Sympozjum Młodych Naukowców Wydziału Fizyki, Warszawa, 20–22 września **2022**.
10. **Anna Kawka**, Hanna Koenig, Tomasz Pospieszny, *Synteza i analiza spektroskopowa nowych koniugatów kwasów żółciowych i cholesterolu zawierających pierścień 1,2,3-triazolowy*, IX Sympozjum Doktorantów Chemii, Łódź, 19–20 maja **2022**.
11. **Anna Kawka**, Hanna Koenig, Tomasz Pospieszny, *Zastosowanie chemii „click" w syntezie dimerów steroidowych zawierających pierścień 1,2,3-triazolowy*, IV Pomorskie Sympozjum Studentów Chemii, online, 23–24 kwietnia **2022**.

Sesja posterowa

1. Marta Marzec, Izabela Nowak, **Anna Kawka**, Tomasz Pospieszny, *Optymalizacja syntezy nanocząstek lipidowych z wykorzystaniem soli żółciowych*, XLVIII Międzynarodowe Seminarium Naukowo-Techniczne „Chemistry for Agriculture and Human Health", Karpacz, 24–27 listopada **2024**.
2. **Anna Kawka**, Hanna Koenig, Tomasz Pospieszny, *Steroid-pyrimidine hybrids as potential agents with high biological activity*, XXV International Symposium „Advances in the Chemistry of Heteroorganic Compounds", Łódź, 21–22 listopada **2024**.
3. **Anna Kawka**, Grzegorz Hajdaś, Hanna Koenig, Tomasz Pospieszny*, Biokoniugaty steroidowo-triazolowe jako potencjalne środki farmakoterapeutyczne o dużej aktywności biologicznej*, 66. Zjazd Naukowy Polskiego Towarzystwa Chemicznego, Poznań, 15–20 września **2024**.
4. **Anna Kawka**, Hanna Koenig, Tomasz Pospieszny, *New steroid-thiouracil conjugates containing 1,2,3-triazole rings with potential biological activity*, 11th Workshop of the Selenium and Sulfur Redox and Catalysis Network (WSeS-11), Toruń, 25–26 lipca **2024**.
5. **Anna Kawka**, Hanna Koenig, Tomasz Pospieszny, *Biokoniugaty steroidowo-uracylowe zawierające pierścienie 1,2,3-triazolowe*, XI Ogólnopolska Konferencja Naukowa „INNOWACJE W PRAKTYCE", Lublin, 6–7 czerwca **2024**.
6. **Anna Kawka**, Hanna Koenig, Tomasz Pospieszny, *Synteza koniugatów steroidowo-uracylowych połączonych pierścieniami 1,2,3-triazolowymi o potencjalnej aktywności biologicznej*, Ogólnopolska Konferencja Naukowa „Zrównoważony rozwój w obszarze kosmetyków i detergentów", Kędzierzyn-Koźle, 12 kwietnia **2024**.
7. **Anna Kawka**, Grzegorz Hajdaś, Hanna Koenig, Tomasz Pospieszny, *Zastosowanie chemii „click" w syntezie biokoniugatów steroidowych pochodnych kwasów żółciowych i steroli*, 47. Międzynarodowe Seminarium Naukowo-Techniczne „Chemistry for Agriculture", Karpacz, 26–29 listopada **2023**.
8. **Anna Kawka**, Hanna Koenig, Tomasz Pospieszny, *Synthesis and theoretical studies of new steroid bioconjugates containing 1,2,3-triazole rings*, XXIV International Symposium „Advances in the Chemistry of Heteroorganic Compounds", Łódź, 24 listopada **2023**.
9. **Anna Kawka**, Grzegorz Hajdaś, Hanna Koenig, Tomasz Pospieszny, *Synteza oraz badania biologiczne nowych dimerów steroidowych połączonych pierścieniem 1,2,3-triazolowym*, 65. Zjazd Naukowy Polskiego Towarzystwa Chemicznego, Toruń, 18–22 września **2023**.
10. **Anna Kawka**, Hanna Koenig, Tomasz Pospieszny, *Zastosowanie chemii „click" do syntezy koniugatów kwasów żółciowych zawierających pierścienie 1,2,3-triazolowe*, 65. Zjazd Naukowy Polskiego Towarzystwa Chemicznego, Toruń, 18–22 września **2023**.

*Otrzymanie I nagrody za zaprezentowanie najlepszego komunikatu ustnego.

Spis rysunków

Spis schematów

Spis tabel

Wykaz skrótów

^{1}H NMR	protonowy magnetyczny rezonans jądrowy (*ang. Proton Nuclear Magnetic Resonance*)
^{13}C NMR	węglowy magnetyczny rezonans jądrowy (*ang. Carbon-13 Nuclear Magnetic Resonance*)
AIDS	zespół nabytego niedoboru odporności (*ang. Acquired Immunodeficiency Syndrome*)
AKR1C4	dehydrogenaza 3α-hydroksysteroidowa (*ang. 3α-hydroxysteroid dehydrogenase type 1*)
AKR1D1	5β-reduktaza Δ4-3-oksosteroidowa (*ang. Δ4-3-oxosteroid 5β-reductase*)
AMACR	racemaza α-metyloacylo-CoA (*ang. α-methylacyl-CoA racemase*)
BA	kwasy żółciowe (*ang. Bile Acids*)
BAAT	kwas żółciowy-CoA:aminokwas *N*-acylotransferaza
BACS	syntetaza kwasu żółciowego CoA (*ang. Bile Acyl-CoA Synthetase*)
BCOX	oksydaza rozgałęzionych acylo-CoA (*ang. Branched-Chain acyl-CoA Oxidase*)
BDP	białko D-bifunkcyjne (*ang. D-bifunctional Protein*)
BSH	hydrolaza soli żółciowych (*ang. Bile Salt Hydrolase*)
CA	kwas cholowy (*ang. Cholic Acid*)
CDCA	kwas chenodeoksycholowy (*ang. Chenodeoxycholic Acid*)
CH25H	25-hydroksylaza cholesterolowa (*ang. Cholesterol 25-hydroxylase*)
CH27H	27-hydroksylaza cholesterolowa (*ang. Cholesterol 27-hydroxylase*)
CoA	koenzym A (*ang. Coenzyme A*)
CTX	ksantomatoza mózgowo-ścięgnista (*ang. Cerebrotendinous Xanthomatosis*)
CuAAC	cykloaddycja azydkowo-alkinowa katalizowana miedzią (*ang. Cu(I)-Catalyzed Azide-Alkine Cycloaddition*)
CYP7A1	7α-hydroksylaza cholesterolowa (*ang. Cholesterol 7 alpha-hydroxylase*)
CYP7B1	7α-hydroksylaza oksysterolowa (*ang. 25-hydroxycholesterol 7-alpha-hydroxylase*)
CYP8B1	12α-hydroksylaza sterolowa (*ang. Sterol 12-alpha-hydroxylase*)
CYP27A1	27-hydroksylaza sterolowa (*ang. Sterol 27-hydroxylase*)
CYP46A1	24-hydroksylaza cholesterolowa (*ang. Cholesterol 24-hydroxylase*)
DBU	1,8-diazabicyklo[5.4.0] undek-7-en (*ang. 1,8-Diazabicyclo[5.4.0]undec-7-ene*)
DCA	kwas deoksycholowy (*ang. Deoxycholic Acid*)
DMF	dimetyloformamid (*ang. Dimethylformamide*)
DPPA	azydek difenylofosforanu (*ang. Diphenylphosphoryl Azide*)
EDC*HCL	chlorowodorek 1-etylo-3-(3-dimetyloaminopropylo)karbodiimid (*ang. 1-Ethyl-3-(3-dimethylaminopropyl)carbodiimide Hydrochloride*)
ESI-MS	spektrometria masowa z jonizacją elektrosprayową (*ang. Electrospray Ionisation Mass Spectrometry*)
EI-MS	spektrometria masowa z jonizacją elektronową (*ang. Electron Ionisation Mass Spectrometry*)
FT-IR	spektroskopia w podczerwieni z transformacją Fouriera (*ang. Fourier Transform Infrared Spectroscopy*)

GIAO	metody orbitali atomowych niezależnych od miernika (*ang. Gauge-Independent Atomic Orbital*)
GIAO/B3LYP/6-311G	*ang. Gauge-Independent Atomic Orbital/ Becke, 3-parameter, Lee-Yang-Parr/ Triple-split valence basis set with six core orbitals and three valence orbitals split into one, one, and one Gaussian functions*
HCT116	linia komórek raka jelita grubego (*ang. Human Colon Carcinoma 116*)
HIV	ludzki wirus niedoboru odporności (*ang. Human Immunodeficiency Viruses*)
HOF	ciepło tworzenia (*ang. Heat of Formation*)
HMG-CoA	reduktaza 3-hydroksy-3-metyloglutarylokoenzymu A (*ang. 3-hydroxy-3-methyl-glutaryl-coenzyme A reductase*)
HSD3B7	oksyreduktaza 3β-hydroksy-Δ5-C27 steroidowa (*ang. Hydroxy-delta-5-steroid dehydrogenase, 3 beta- and steroid delta-isomerase 7*)
IC_{50}	połowa maksymalnego stężenia hamującego (*ang. Half maximal Inhibitory Concentration*)
IMR-32	linia komórek neuroblastoma ludzkiego (nazwa własna)
K562	linia komórek białaczki szpikowej (nazwa własna)
LAH	wodorek litowo-glinowy (*ang. Lithium Aluminium Hydride*)
LCA	kwas litocholowy (*ang. Lithocholic Acid*)
LSD1	demetylaza-1 specyficzna dla lizyny (*ang. Lysine-Specific histone Demehylase 1A*)
MCF-7	linia komórek raka piersi (*ang. Michigan Cancer Foundation-7*)
MIC	minimalne stężenie hamujące (*ang. Minimal Inhibitory Concentration*)
***p*-TsOH**	kwas *p*-toluenosulfonowy
PASS	przewidywane spektrum aktywności substancji (*ang. Prediction of Activity Spectra for Substances*)
PA	prawdopodobieństwo wystąpienia danej aktywności biologicznej (*ang. Probability „to be Active”*)
PI	prawdopodobieństwo braku wystąpienia danej aktywności biologicznej (*ang. Probability „to be Inactive”*)
PC-3	linia komórek ludzkiego raka prostaty
PDB ID	identyfikator z banku danych o białkach (*ang. Protein Data Bank Identifier*)
PM5	metoda parametryczna 5 (*ang. Parametric Method 5*)
SCPx	białko transportujące sterolu x (*ang. Sterol Carrier Protein x*)
***tert*-BuOH**	alkohol *tert*-butylowy
THF	tetrahydrofuran
VLCS	syntetaza długołańcuchowych acylo-CoA (*ang. Very-long-chain acyl-CoA synthetases*)

Wstęp

Natura stanowi nieustające źródło aktywnych biologicznie związków heterocyklicznych o zróżnicowanych właściwościach fizycznych, chemicznych i biologicznych. Dostępne środki terapeutyczne często wykazują niestabilność, słabą rozpuszczalność lub oporność gospodarza, co powoduje ich nieskuteczność. Sprzęganie dwóch biologicznie aktywnych cząsteczek niesie wiele korzyści wynikających z braku toksyczności systemowej, zredukowaniu skutków ubocznych oraz, co najważniejsze, zwalczeniu lekooporności komórek docelowych. Biokoniugat to połączenie dwóch lub więcej jednostek strukturalnych o odmiennych właściwościach biologicznych, co sprawia, że utworzona cząsteczka zyskuje spotęgowaną aktywność.

Steroidy obejmują obszerną grupę związków pochodzenia naturalnego występujących we wszystkich komórkach eukariotycznych, wykazujących znaczącą aktywność biologiczną. Istotnie interesujące są kwasy żółciowe oraz β-sterole. Związki te posiadają charakterystyczny dla steroidów sztywny czteropierścieniowy rdzeń cyklopentanoperhydrofenantrenowy o różnym stopniu nienasycenia, właściwości amfipatyczne oraz podatną na modyfikację grupę hydroksylową w pozycji C-3. Ważne są również glikozydy nasercowe (np. scylaren A, digitoksyna) oraz hormony roślinne (np. brassinolid) i zwierzęce (np. estron, testosteron).

Kwasy żółciowe (np. litocholowy, deoksycholowy, cholowy) stanowią główny składnik żółci, wspomagając emulgowanie tłuszczy, natomiast jako surfaktanty obniżają napięcie powierzchniowe. Charakteryzują się ponadto łańcuchem bocznym zakończonym grupą karboksylową obecnym w pozycji C-17 szkieletu steroidowego oraz grupami hydroksylowymi (3α-OH; 3α-OH, 12α-OH; 3α-OH, 7α-OH, 12α-OH) o różnej reaktywności.

Wśród β-steroli zainteresowanie wzbudza cholesterol będący składnikiem zwierzęcych błon komórkowych, zapewniając im sztywność. Jest prekursorem w biosyntezie witaminy D_3, hormonów płciowych oraz kwasów żółciowych.

Fundamentalne znaczenie ma naturalny biokoniugat steroidowy – skwalamina, wyizolowana z komórek kolenia pospolitego (*Squalus acanthias*), wykazująca się właściwościami przeciwko flawiwirusom, HAV, HBV i HCV. Związek ten zastosowano jako antybiotyk działający na szereg szczepów bakterii, jak również w terapii onkologicznej, w leczeniu zwyrodnienia plamki żółtej oka i retinopatii cukrzycowej. Z kolei syntetyczny glikosteroid – deksametazon, cechuje aktywność przeciwzapalna, przeciwalergiczna i immunosupresyjna. Jest niezwykle cenny w leczeniu obrzęku i nowotworu mózgu, a także rekonwalescencji po urazach głowy i zabiegach neurochirurgicznych. Co ciekawe, został zastosowany w łagodzeniu powikłań dróg oddechowych spowodowanych COVID-19.

Ze względu na ogromną różnorodność właściwości biologicznych i fizykochemicznych, steroidy stały się doskonałymi związkami w syntezie organicznej. Transformacje grup funkcyjnych poprzez reakcję estryfikacji prowadzą do wytwarzania nowych pochodnych. Dodatkowe grupy mogą wpływać na zmianę lipofilowości, rozpuszczalności oraz selektywności receptora. Z perspektywy poszukiwania nowych leków steroidowych najistotniejsze jest to, że jako związki lipofilowe mogą skutecznie pokonywać błony komórkowe.

Niezwykle kluczowym aspektem w opracowywaniu ścieżek syntezy dimerycznych i wielkocząsteczkowych biokoniugatów steroidowych jest zastosowanie chemii „click". Wykorzystanie tej efektywnej, prostej i wysokowydajnej reakcji prowadzi do utworzenia linkerów 1,2,3-triazolowych. Unikalna struktura układów triazolowych pozwala im łatwo

łączyć się z enzymami oraz receptorami w układach biologicznych poprzez wiązania wodorowe, oddziaływania dipol-dipol lub siły van der Waalsa. Wykazują odporność na hydrolizę oraz degradację metaboliczną. Sprzężenie steroidów z pierścieniami 1,2,3-triazolowymi ma szczególne znaczenie z perspektywy aktywności farmakoterapeutycznej nowo powstałej cząsteczki biokoniugatu.

Z danych literaturowych wynika, że drobne przekształcenie struktury steroidowej silnie oddziałuje na układ biologiczny. Ich specyficzny układ przestrzenny pełni kluczową funkcję dla interakcji z receptorami białkowymi. Unikatowe cechy strukturalne i biologiczne steroidów przyczyniły się do wykorzystania ich jako potencjalnego materiału w projektowaniu leków o działaniu przeciwnowotworowym, przeciwdrobnoustrojowym, przeciwzapalnym, jak również o aktywności neuroprotekcyjnej.

Na podstawie pozytywnych wyników dotychczasowych badań wykazano, że związki steroidowe spełniają kluczowe kryteria w kontekście projektowania nowych środków terapeutycznych, a także mogą pełnić funkcję efektywnych nośników leków. Uwzględniając analizę literatury przedmiotu oraz wcześniejsze osiągnięcia badawcze zespołu prof. Pospiesznego, celem mojej pracy było opracowanie szlaku syntezy nowych biokoniugatów steroidowych o potencjalnej aktywności biologicznej.

Bazując na obiecujących danych literaturowych zsyntetyzowano 30 nowych pochodnych kwasów żółciowych i steroli. Wykorzystując reakcję chemii „click" wbudowano w strukturę każdej cząsteczki łącznik w postaci pierścienia 1,2,3-triazolowego. Zsyntetyzowane związki można podzielić na trzy grupy: dimery kwasów żółciowych i steroli, quasi-podandy oraz biokoniugaty steroidowo-pirymidynowe. Pełna analiza spektroskopowa i spektrometryczna pozwoliła na potwierdzenie wszystkich otrzymanych struktur. Przeprowadzone obliczenia semiempiryczne wyznaczyły ich energię tworzenia i modele molekularne. Na podstawie badań *in silico* z wykorzystaniem programu PASS oraz wykonanie dokowania molekularnego określono wstępną teoretyczną aktywność biologiczną koniugatów steroidowych. Sprecyzowanie powinowactwa utworzonych cząsteczek do miejsc aktywnych zdefiniowanych domen białkowych uwarunkowało ich obiecujący potencjał przeciwhipercholesterolemiczny, przeciwbakteryjny, przeciwgrzybiczny oraz przeciwnowotworowy.

Rezultaty przeprowadzonych w ramach pracy doktorskiej badań zostały szczegółowo opisane i opublikowane, podobnie jak wyczerpujące artykuły przeglądowe, w renomowanych czasopismach z listy filadelfijskiej.

Część literaturowa

1. Steroidy

Związki pochodzenia naturalnego o zróżnicowanych właściwościach biologicznych zajmują wyjątkowe miejsce w chemii organicznej [1,2]. Szczególnie ważne są steroidy, które zapewniają prawidłowe funkcjonowanie wszystkich komórek organizmów żywych. Biorą udział w przemianach metabolicznych oraz w transporcie wewnątrzkomórkowym [3]. Kwasy żółciowe (np. litocholowy, deoksycholowy, cholowy) działają jako emulgatory, pomagając w trawieniu i wchłanianiu lipidów oraz kontrolują metabolizm glukozy [4]. Sterole (np. cholesterol, ergosterol, stigmasterol) są komponentami struktury błon komórkowych prokariotów i eukariotów (Rys. 1). Cholesterol (**1**) uczestniczy także w biosyntezie hormonów steroidowych [5]. Te z kolei (np. estrogeny, androgeny) odpowiadają za ekspresję genów, normalną syntezę białek oraz podstawowe działanie regulacyjne i modyfikacyjne tkanek docelowych [6]. Hormony roślinne, takie jak brassinosteroidy (np. brassinolid) kontrolują przebieg procesu fotosyntezy, prawidłowy wzrost roślin oraz działanie innych fitohormonów [7]. Kortykosteroidy odgrywają kluczową rolę w metabolizmie węglowodanów i regulacji stanu zapalnego [6].

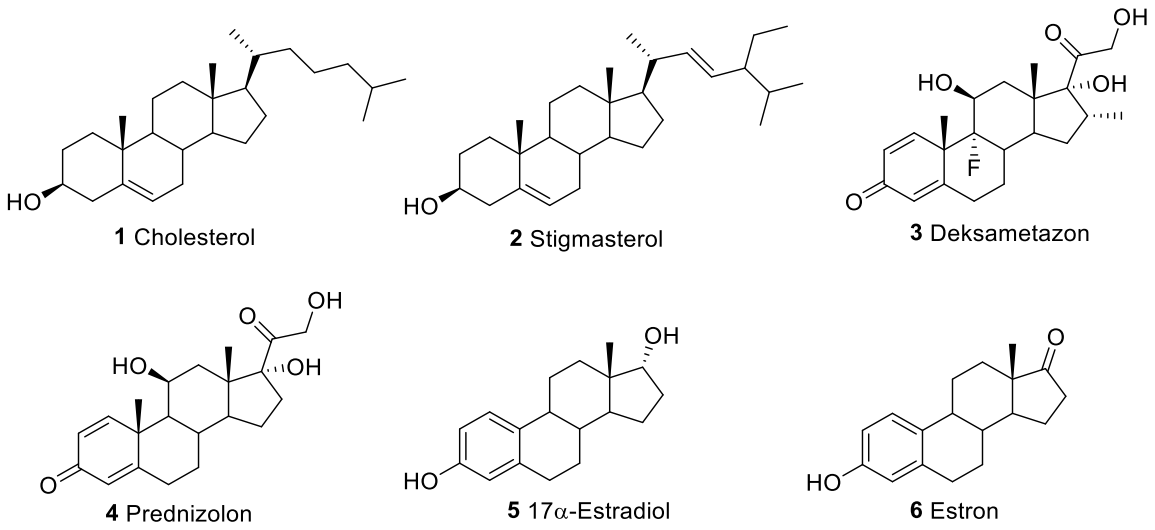

Rysunek 1. Wybrane pochodne steroidów.

1.1. Sterole

Alkohole steroidowe jako kluczowe związki lipidowe odgrywają istotną rolę w funkcjonowaniu organizmów żywych. Sterole są integralnymi składnikami błon komórkowych, wpływając na ich strukturę, płynność i funkcje biologiczne. Biorą udział jako główny substrat w biosyntezie ważnych związków bioaktywnych, takich jak hormony steroidowe, witaminy z grupy D lub kwasy żółciowe. Komórki roślinne zwykle zawierają fitosterole, takie jak stigmasterol, β-sitosterol, kampesterol albo fukosterol. W komórkach grzybów można wyróżnić mykosterole – głównie ergosterol będący promotorem ergokalcyferolu (**8**), znanego powszechnie jako witamina D_2 (Rys. 2) [8,9]. Jednak największe zainteresowanie wzbudza sterol budujący błony komórkowe u ssaków – cholesterol, dlatego jego właściwości zostaną szerzej omówione.

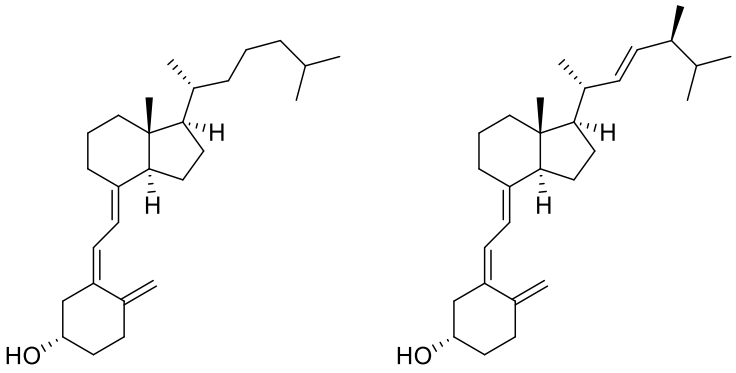

7
Cholekalcyferol
Witamina D_3

8
Ergokalcyferol
Witamina D_2

Rysunek 2. Struktury witamin D – pochodnych ergosterolu i cholesterolu.

1.1.1 Cholesterol

β-sterole podobnie jak pozostałe steroidy kontrolują homeostazę procesów biologicznych zachodzących w celu prawidłowego funkcjonowania organizmu. Ze względu na udział w szeregu przemian metabolicznych cholesterol jest jednym z niewielu związków steroidowych, którego właściwości fizykochemiczne zostały niezwykle dokładnie przeanalizowane. Cholesterol (**1**) należy do zoosteroli, w których jako element budulcowy stabilizuje błonę komórkową, jednocześnie zapewniając jej odpowiednią elastyczność i płynność (Rys. 3).

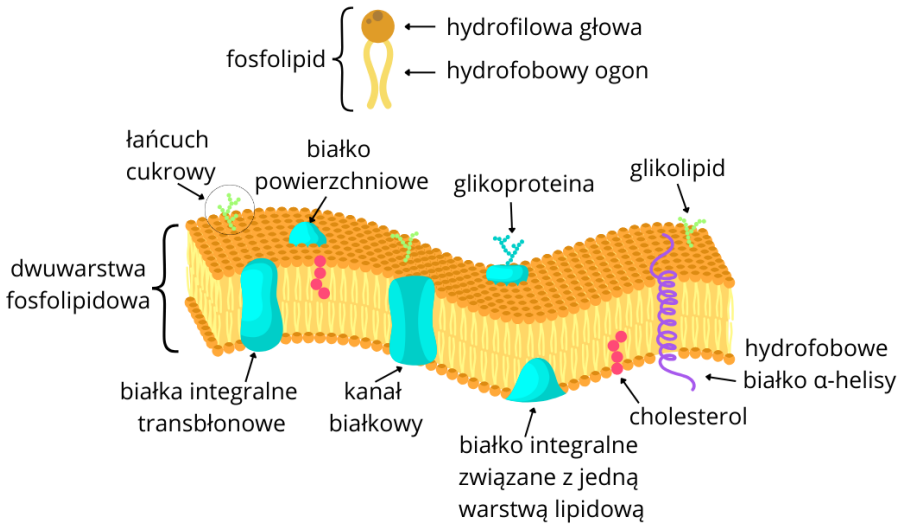

Rysunek 3. Budowa błony białkowo-lipidowej.

Umożliwia to transport substancji do i z komórki. Ponadto, jego obecność w komórkach mózgu wpływa na utrzymanie struktury neuronów. Cholesterol jest prekursorem w syntezie hormonów steroidowych (np. kortyzolu, aldosteronu), hormonów płciowych (np. testosteronu, progesteronu) i kwasów żółciowych, jak również witaminy D_3 (cholekalcyferolu)

odpowiedzialnej za regulację gospodarki wapniowo-fosforanowej. Natomiast jako kluczowy składnik mieliny (osłonki otaczającej włókna nerwowe) ma znaczący udział w szybkim i skutecznym przesyłaniu sygnałów nerwowych [10].

Cholestanol (5α-dihydrocholesterol) (**9**) jest nasyconą formą cholesterolu, a jego struktura rożni się wyłącznie zredukowanym wiązaniem podwójnym w pozycji C-5 i C-6 w cząsteczce (Rys. 4). Głównie powstaje w wyniku jego przemian metabolicznych. W organizmie występuje w śladowych ilościach, ale jego obecność ma diagnostyczne znaczenie w przypadku rzadkich schorzeń. Podwyższony poziom cholestanolu może być związany z chorobą ksantomatozą mózgowo-ścięgnistą (CTX). To zaburzenie metaboliczne spowodowane nieprawidłową przemianą kwasów żółciowych prowadzącą do gromadzenia cholestanolu w organizmie, a w konsekwencji do postawania złogów w ścięgnach, uszkodzeniem układu nerwowego bądź zaćmą [11,12].

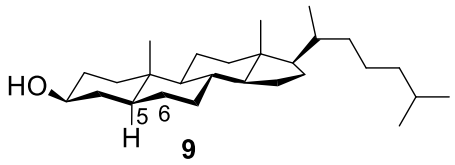

9

Rysunek 4. Budowa cholestanolu.

1.1.2. Stereochemia cholesterolu

Unikalna struktura przestrzenna cholesterolu, wynikająca ze stereochemii jest kluczowa dla jego funkcjonalności. Będąc steroidem niezmiennie posiada podstawowy element ich budowy – szkielet cyklopentano[α]perhydrofenantrenu. Sprzężone pierścienie tworzą płaską cząsteczkę z konfiguracją *cis* pierścieni B/C oraz *trans* C/D. Zoosterol cechuje 8 centrów stereogenicznych determinujących charakterystyczne ułożenie grup funkcyjnych i łańcucha bocznego. Z perspektywy syntezy organicznej ważna jest ekwatorialna grupa hydroksylowa znajdująca się w konfiguracji β (nad płaszczyzną pierścienia A) przy atomie węgla C-3 (Rys. 5). Nadaje cząsteczce amfipatycznego charakteru oraz umożliwia jej modyfikacje. Natomiast obecność rozgałęzionego łańcucha bocznego przy atomie węgla C-17 wpływa na zdolność sterolu do wbudowywania się w błony komórkowe. Co więcej, cholesterol występuje w organizmach jako jeden enancjomer, dzięki czemu łatwo wchodzi w interakcje z innymi biomolekułami. Przestrzenna budowa cholesterolu ułatwia jego dopasowywanie się do fosfolipidów w dwuwarstwie i warunkuje transformację struktury [13,14].

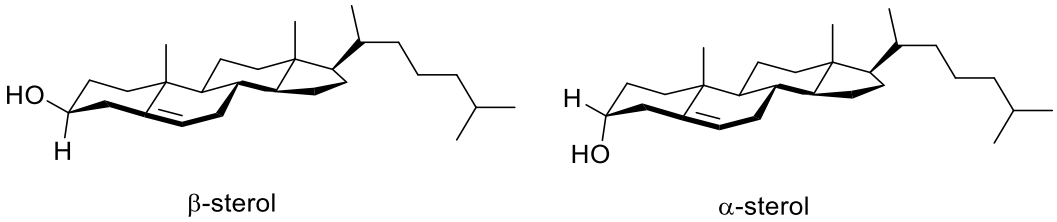

Rysunek 5. Epimery cholesterolu.

1.2. Kwasy żółciowe

1.2.1. Charakterystyka i znaczenie biologiczne kwasów żółciowych

Kwasy żółciowe jako cząsteczki aktywne biologicznie są wytwarzane w organizmach wszystkich kręgowców w wyniku przemian metabolicznych cholesterolu [15]. Obecność 24-węglowej struktury spowodowała, że powszechnie u ssaków noszą miano kwasów żółciowych C24 (Rys. 6). Wynika to z obecności trzech sześcioczłonowych pierścieni A, B i C, pięcioczłonowego pierścienia D oraz pięciowęglowego łańcucha bocznego z grupą karboksylową w pozycji C-24 [16,17]. Kwas litocholowy (3α-hydroksycholanowy) (**10**), kwas deoksycholowy (kwas 3α,12α-dihydroksycholanowy) (**11**) i kwas cholowy (3α,7α,12α-trihydroksycholanowy) (**12**) wzbudzają największe zainteresowanie jako reagenty w syntezie organicznej [18–20].

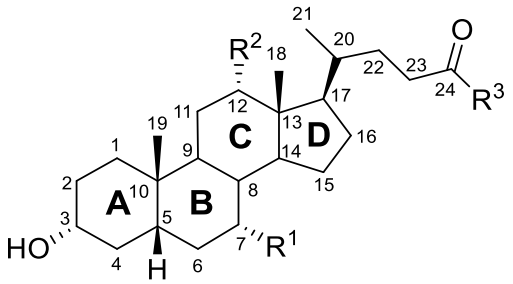

Nr	R^1	R^2	R^3	Nazwa
10	H	H	OH	Kwas litocholowy
11	H	OH	OH	Kwas deoksycholowy
12	OH	OH	OH	Kwas cholowy
13	OH	H	OH	Kwas chenodeoksycholowy
14	OH	H	$NHCH_2CO_2H$	Kwas glikochenodeoksycholowy
15	OH	H	$NHCH_2CH_2SO_3H$	Kwas taurochenodeoksycholowy
16	OH	OH	$NHCH_2CO_2H$	Kwas glikocholowy
17	OH	OH	$NHCH_2CH_2SO_3H$	Kwas taurocholowy

Rysunek 6. Szkielet steroidowy kwasów żółciowych.

Kwasy żółciowe stanowią główny składnik żółci, gdzie występują w formie sprzężonych soli z glicyną (75 %) lub tauryną (25 %) [21]. Jednocześnie zwiększa to ich rozpuszczalność w wodzie w warunkach fizjologicznych [22]. Około 95% kwasów żółciowych

jest wchłaniane w jelicie, następnie trafia z krwią do wątroby i ponownie do żółci, by wrócić do jelita (tzw. krążenie jelitowo-wątrobowe). Pozostałe 5% jest wydalane, a straty uzupełnia synteza *de novo* w wątrobie [23–25].

Główne właściwości fizjologiczne kwasów żółciowych obejmują transport lipidów poprzez ich solubilizację oraz usuwanie cholesterolu do przewodu pokarmowego, skąd jego wchłanianie jest ograniczone. Funkcje te wynikają z ich amfipatycznego charakteru, który wiąże się z obecnością hydrofilowej i hydrofobowej powierzchni [26–28]. Z kolei koniugacja z kwasami tłuszczowymi, cholesterolem i monoglicerydami BA prowadzi do ich micelizacji i umożliwia emulgowanie tłuszczy [29,30]. Tworzenie miceli powoduje zwiększenie powierzchni tłuszczu narażonej na działanie lipaz trzustkowych, co umożliwia bardziej efektywne trawienie i wchłanianie lipidów przez komórki jelita cienkiego [31]. Micele powstałe z udziałem kwasów żółciowych wspomagają również rozpuszczanie i absorpcję witamin rozpuszczalnych w tłuszczach [32]. Biorąc pod uwagę ogólny udział BA w krążeniu jelitowo-wątrobowym ich zadania ograniczają się przede wszystkim do: regulacji homeostazy cholesterolu, zapobiegania tworzeniu się kamieni żółciowych i nerkowych, działania przeciwdrobnoustrojowego oraz funkcji regulacyjnych. Udowodniono, że ich receptory są obecne w większości narządów i tkanek, stąd mogą pełnić rolę cząsteczek sygnałowych. Kwasy żółciowe uczestniczą w proliferacji komórek, reakcjach detoksykacji i regulacji układu odpornościowego [33–37].

1.2.2. Stereochemia kwasów żółciowych

Szkielet steroidowy BA posiada 7 chiralnych atomów węgla (tj. C-5, C-8, C-9, C-10, C-13, C-14, C-17), co wskazuje na 128 stereoizomerów. Jednak surowe ograniczenia związane z kondensacją pierścieni cyklicznych wpłynęły na istnienie tylko kilku z nich. Pierścienie A/B naturalnych steroidów przyjmują konformację przestrzenną *cis* lub *trans*. Jest to charakterystyczna cecha układów sześcio– i pięcioczłonowych, co potwierdza rotacja pomiędzy strukturami *cis* i *trans*-dekaliny (Rys. 7) [38,39].

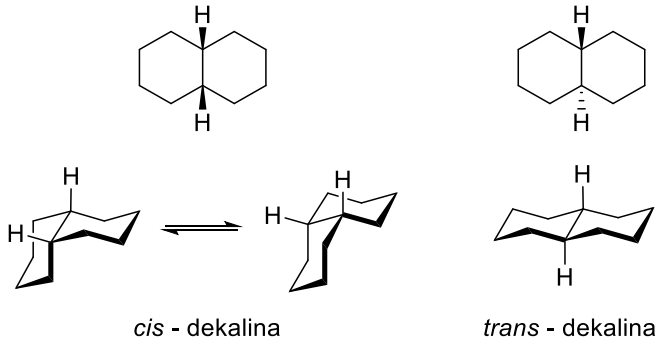

Rysunek 7. Konformacje przestrzenne dekaliny.

Sposób ułożenia się skondensowanych pierścieni A/B podczas transformacji determinuje występowanie dwóch rodzajów szeregów w konfiguracji przestrzennej steroidów:

- *allo* – typowy w przypadku większości steroli. Charakterystyczny jak w *trans*-dekalinie układ pierścieni A/B; płaska cząsteczka, w której grupa metylowa CH_3-19 i atom wodoru występują naprzeciw siebie, a dodatkowo można utworzyć dwie konformacje

krzesłowe. Sztywna struktura tego typu układu ogranicza wydajność syntez prowadzących do otrzymania niekorzystnej energetycznie konformacji łódkowej (Rys. 8a).

- normalny – preferowany w przypadku kwasów żółciowych. Podobny jak w *cis*-dekalinie układ pierścieni A/B, grupa metylowa CH_3-19 i atom wodoru występują po jednej stronie pierścienia. Specyficzna i stabilna wykrzywiona struktura decyduje o pozostaniu wysoko korzystnej energetycznie konformacji krzesełkowej bez względu na typ syntezy (Rys. 8b) [40].

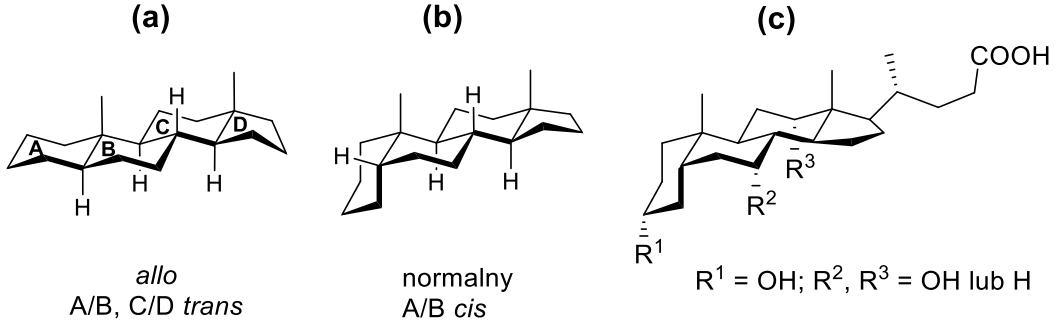

Rysunek 8. Rodzaje ułożeń pierścieni A, B, C i D w cząsteczkach steroidów.

Zgodnie z tym założeniem u wyższych kręgowców szkielet steroidowy kwasów żółciowych przyjmuje konformację *cis* pierścieni A/B (Rys. 8c). Charakterystyczne dla ich struktury są również: czystość enancjomeryczna, sztywny układ pierścieni alicyklicznych, 11 chiralnych atomów węgla, zróżnicowane chemicznie grupy hydroksylowe w pozycjach C-3α, C-7α, C-12α oraz alifatyczny łańcuch przy atomie węgla C-17 zakończony grupą karboksylową [41,42]. Wymienione dwie ostatnie cechy nadają im szczególnych właściwości fizykochemicznych, dzięki którym stały się materiałem budulcowym w projektowaniu nowych cząsteczek będących antybiotykami, sztucznymi kanałami jonowymi, receptorami jonowymi, nośnikami leków oraz surfaktantami [43–47].

Amfipatyczny charakter kwasów żółciowych wynika z hydrofilowej i hydrofobowej części ich struktury. Grupy hydroksylowe i karboksylowy łańcuch boczny tworzą tzw. α-ścianę (hydrofilową) (Rys. 9). Z kolei grupy metylowe C-18 i C-19 nadają im hydrofobowego charakteru, dając tzw. β-ścianę [48]. Wpływa to na wysoką aktywność powierzchniową kwasów żółciowych, dzięki której mogą tworzyć w roztworach wodnych małe agregaty lub micele mniejsze niż 10 monomerów [49,50].

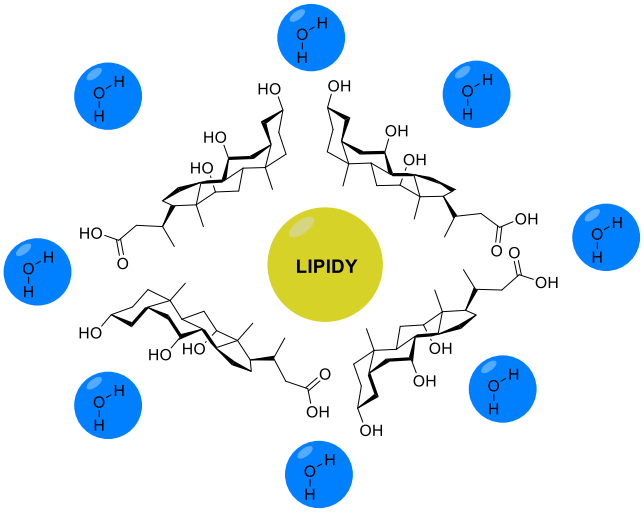

Rysunek 9. Micelizacja na przykładzie kwasu cholowego [**P3**].

Liczba i rozkład różnych reaktywnie grup hydroksylowych decyduje o podatności kwasów na szereg reakcji, takich jak acetylowanie, estryfikacja, hydroliza bądź redukcja. Ze względu na położenie ekwatorialną grupę 3α-OH łatwo zmodyfikować, co jest najbardziej utrudnione w przypadku grupy 12α-OH z powodu dużego zatłoczenia sterycznego w jej otoczeniu [51].

1.2.3. Biosynteza kwasów żółciowych

Kwasy żółciowe są produkowane w wątrobie z cholesterolu jako pierwszorzędowe kwasy żółciowe, przy udziale 17 enzymów katalizujących 17 różnych reakcji. U ssaków proces ten odbywa się w cytozolu, siateczce śródplazmatycznej (mikrosomach), mitochondriach i peroksysomach (Schemat 1). Jednocześnie ma on ogromne znaczenie dla kontrolowania homeostazy cholesterolu, ponieważ odpowiada za katabolizm połowy jego dobowej produkcji [52,53].

Istnieją dwa szlaki syntezy kwasów żółciowych: klasyczny (główny, neutralny) i alternatywny (kwasowy). Pierwszy z nich determinuje produkcję 90 % kwasów żółciowych u osób dorosłych, natomiast drugi pozostałych 10 % i przeważa u noworodków oraz pacjentów z chorobami wątroby [54].

Główna ścieżka syntezy rozpoczyna się od hydroksylacji pierścienia sterolowego w pozycji C-7 obecności 7α-hydroksylazy cholesterolowej (CYP7A1) (Schemat 2). Utworzony produkt pośredni jest następnie atakowany przez 27-hydroksylazę sterolową (CYP27), która modyfikuje łańcuch boczny, dając kwas chenodeoksycholowy. W celu syntezy kwasu cholowego tę transformację poprzedza jeszcze hydroksylacja w pozycji C-12 katalizowana przez 12α-hydroksylazę (CY8B1). W tym przypadku szybkość procesu metabolicznego zależy od aktywności enzymu CYP7A1, a aktywność enzymu CY8B1 wpływa na hydrofilowość steroidu i reguluje stosunek produkcji dwóch kwasów pierwotnych (CA i CDCA) [55].

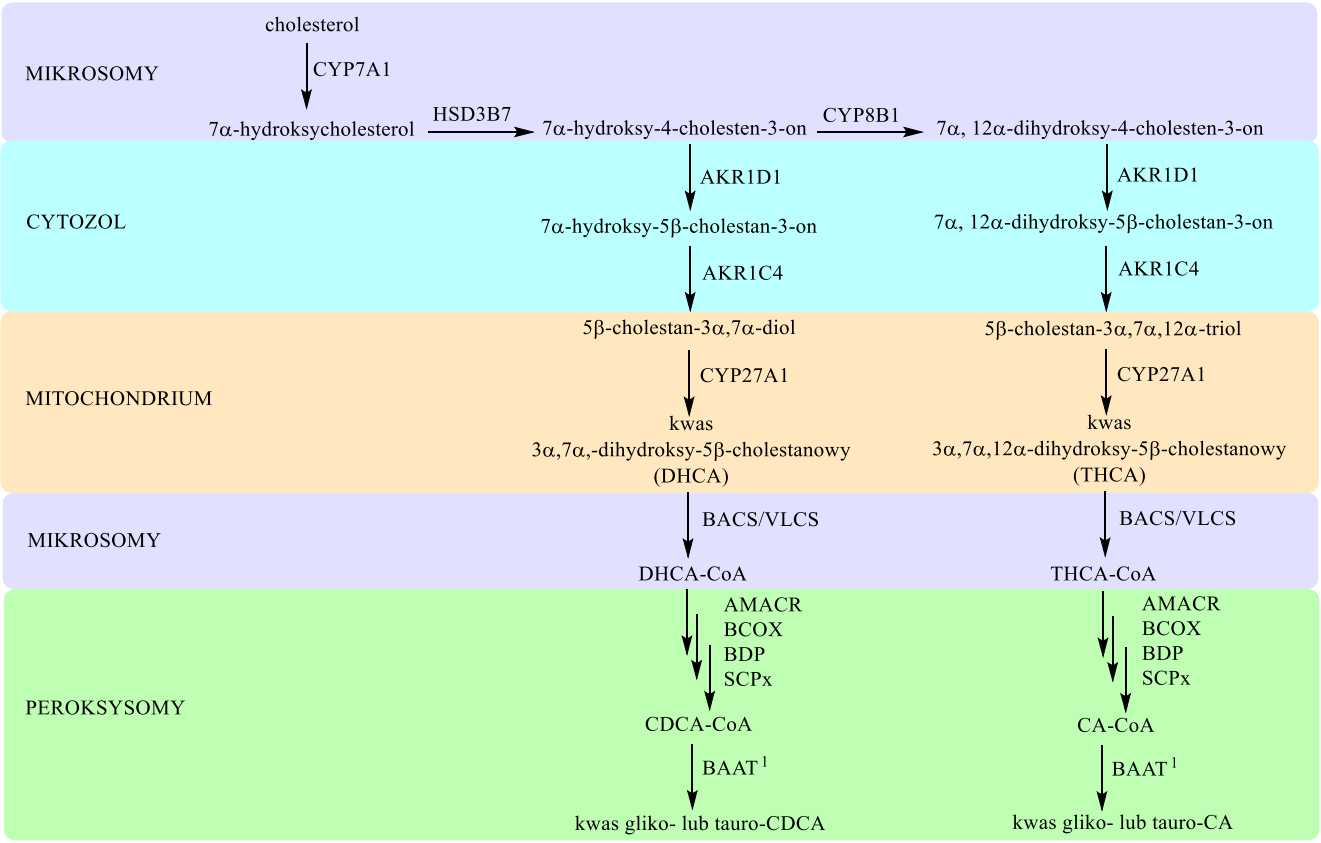

AKR1C4 – dehydrogenaza 3α-hydroksysteroidowa; AKR1D1 – 5β-reduktaza Δ4-3-oksosteroidowa; AMACR – racemaza α-metyloacylo-CoA; BAAT – Kwas żółciowy-CoA:aminokwas *N*-acylotransferaza; BACS – syntetaza kwasu żółciowego CoA; BCOX – oksydaza rozgałęzionych acylo-CoA; BDP – białko D-bifunkcyjne; CA – kwas cholowy; CDCA – kwas chenodeoksycholowy; CYP27A1 – 27-hydroksylaza sterolowa; CYP7A1 – 7α-hydroksylaza cholesterolowa; CYP7B1 – 7α-hydroksylaza oksysterolowa; DHCA – kwas 3α,7α-dihydroksycholestanowy; HSD3B7 – oksyreduktaza 3β-hydroksy-Δ5-C27 steroidowa; SCPx – białko transportujące sterolu x; THCA – kwas 3α,7α,12α-trihydroksycholestanowy; VLCS – syntetaza długołańcuchowych acylo-CoA

Schemat 1. Szlak syntezy pierwszorzędowych kwasów żółciowych (CDCA i CA).

Alternatywny szlak w przeciwieństwie do klasycznego zakłada syntezę głównie CDCA. Na początku odbywa się hydroksylacja łańcucha bocznego cholesterolu na końcu C-27 przez enzym CYP27 Następnie aktywność 7α-hydroksylazy oksysterolowej (CYP7B1) prowadzi do dalszych przekształceń 27α-hydroksysterolu do kwasu 3β,7α-dihydroksy-5-cholestenowego. Kolejne modyfikacje tego związku dają w konsekwencji kwas CDCA. Warto zauważyć, że hydroksysterole mogą być również wytwarzane w organach innych niż wątroba, takich jak płuca lub mózg, jednak przetransportowanie do niej nie wyklucza ich udziału w kwasowej ścieżce biosyntezy BA. Alternatywna ścieżka chroni osoby ze schorzeniami wątroby przed hipercholesterolemią [56,57].

W wyniku działania dwóch enzymów, takich jak syntaza kwasu żółciowego-CoA i *N*-acylotransferaza kwasu żółciowego-CoA, kwas cholowy i chenodeoksycholowy ulegają sprzężeniu z tauryną i glicyną, po którym wędrują do żółci, gdzie są przechowywane w pęcherzykach żółciowych. Utworzone sole cechuje wyższa hydrofilowość, kwasowość oraz mniejsza cytotoksyczność [58,59].

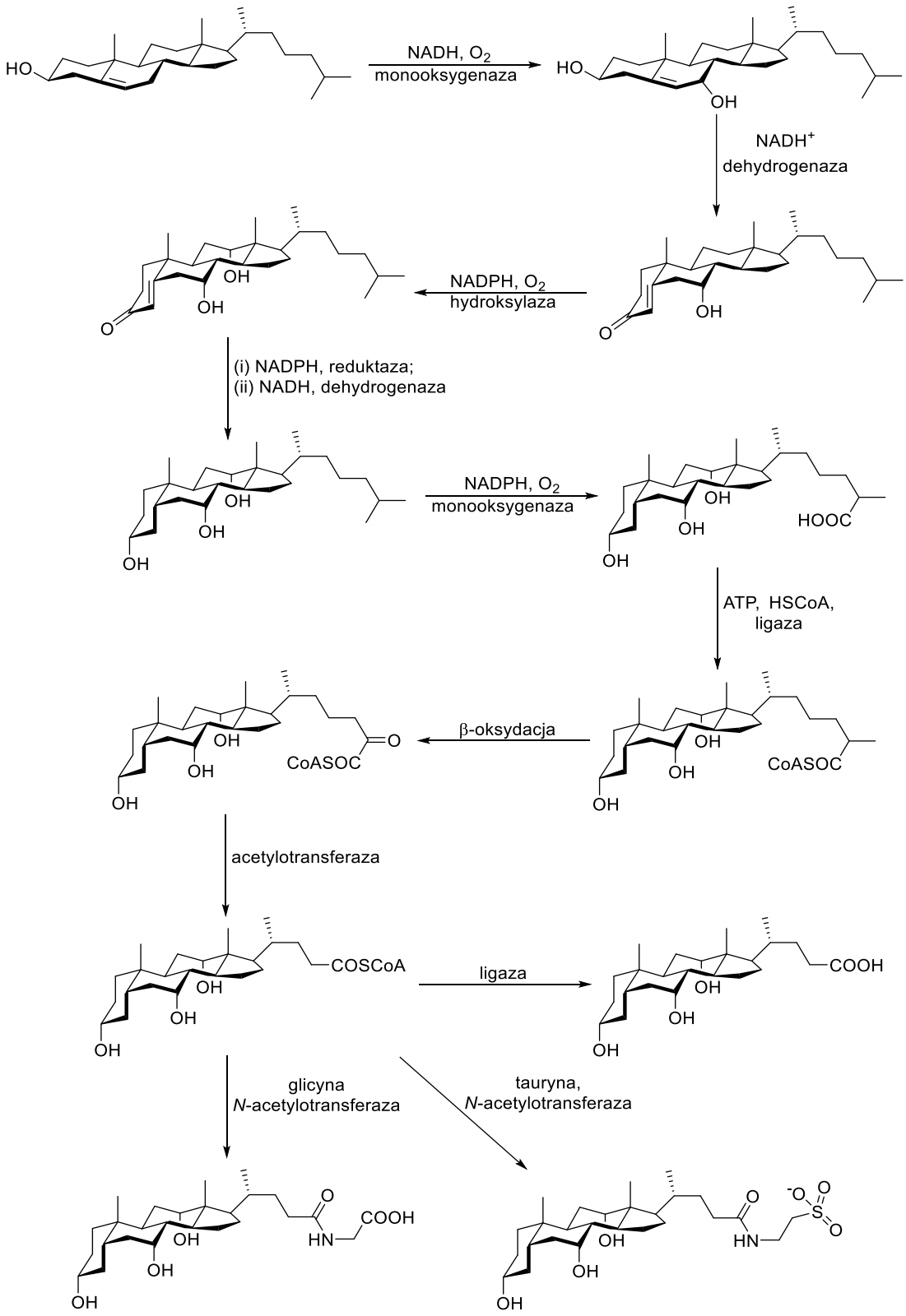

Schemat 2. Transformacje struktury cholesterolu podczas biosyntezy na przykładzie kwasu cholowego.

Większość (około 95%) kwasów żółciowych po emulgowaniu tłuszczy w jelicie cienkim zostaje wtórnie wchłonięta przez odcinek jelita krętego i przeniesiona do wątroby. Pozostałe 5 % ulega biotransformacji przez bakterie jelitowe, w wyniku której dehydoksylacja odpowiednio CA i CDCA prowadzi do powstania drugorzędowych kwasów żółciowych: kwasu deoksycholowego i kwasu litocholowego. Aktywność bakteryjnej hydrolazy soli żółciowych (BSH) przy udziale bakterii z rodzaju *Bacteroides*, *Clostridium*, *Bifidobacterium* oraz *Lactobacillus* powoduje dekoniugację. W kolejny etap zaangażowana jest bakteryjna 7α-dehydroksylaza, która eliminuje grupę 7-OH z kwasów CA i CDCA, co z kolei prowadzi do utworzenia odpowiednio kwasów DCA i LCA [60].

Kwas litocholowy wykazuje słabą rozpuszczalność w wodzie i toksyczność. Niemalże w całości jest wydalany z kałem, ale około 2 % po powrocie do wątroby ulega przemianom w celu usunięcia z moczem. Natomiast kwas deoksycholowy cechuje bakteriobójczość, dzięki której może zapobiegać przerostowi mikrobioty w jelicie. Z drugiej jednak strony kwasy wtórne są promotorami zmian patologicznych jelita grubego, często prowadzących do nowotworu [61].

1.3. Znaczenie aktywności biologicznej steroidów

Skwalamina (**18**) to jeden z kluczowych naturalnych koniugatów steroidowo-poliaminowych o monumentalnych znaczeniu dla chemii związków bioaktywnych (Rys. 10). Została wyizolowana z wątroby kolenia pospolitego (*Squalus acanthias*), u którego silnie wspiera układ odpornościowy przed chorobami nowotworowymi i wirusowymi [62]. Ten aminosterolowy antybiotyk, będący koniugatem spermidyny i 24-siarczanu 7α,24ζ-dihydroksy-5α-cholestanu, rozpuszcza się w wodzie dzięki hydrofobowemu szkieletowi steroidowemu, grupie hydroksylowej i aminowej [63]. Stereochemia i ładunek związku umożliwiają przenikanie przez błonę komórkową, transportując białka związane elektrostatycznie z błoną cytoplazmatyczną [64]. Skwalamina hamuje agregację α-synukleiny, zapobiegając chorobie Parkinsona, ograniczając toksyczne agregaty i neutralizując już istniejące [65]. Wykazuje aktywność biobójczą wobec szerokiego spektrum mikroorganizmów (w tym wirusa HIV). Spowalnia również rozwój nowotworów mózgu, wspierając działanie cytotoksycznych leków przeciwnowotworowych w raku płuc, sutka, jajnika i prostaty [66].

(a)

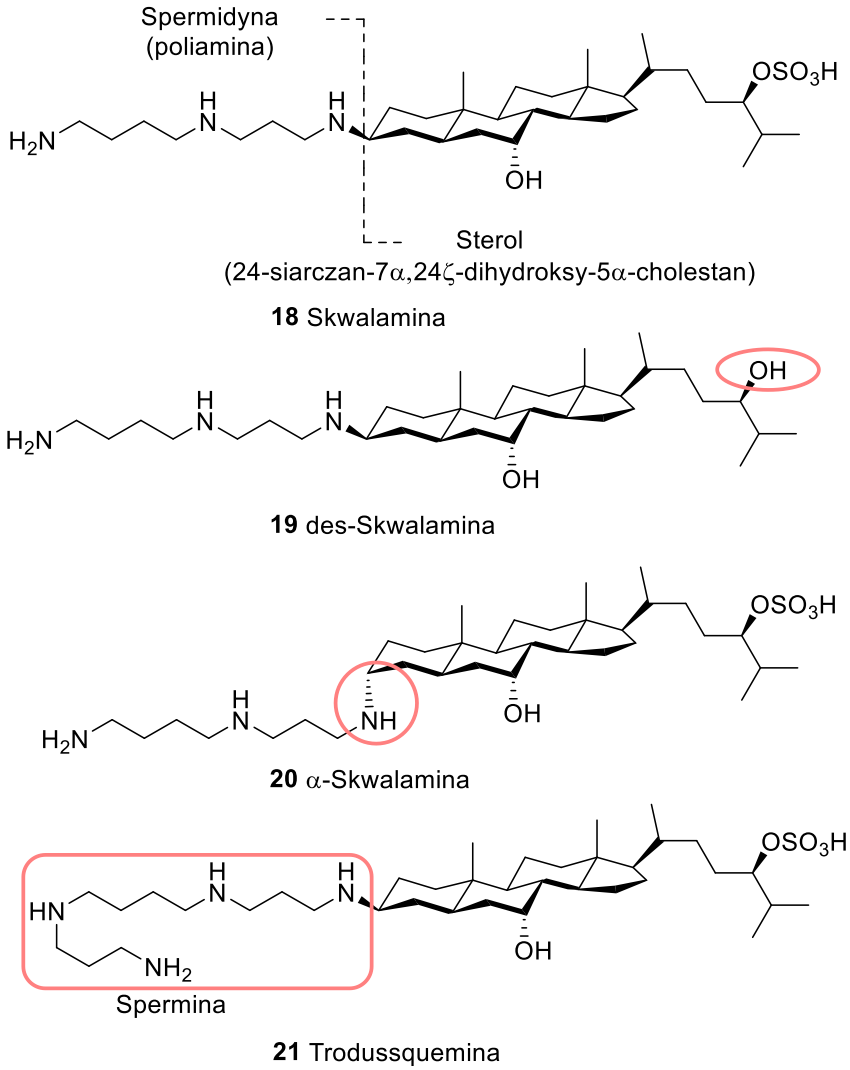

(b)

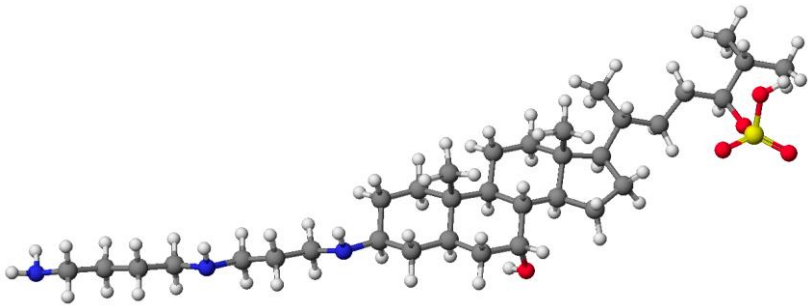

Rysunek 10. Skwalamina i jej pochodne (**a**) oraz model molekularny (**b**).

Zróżnicowanie właściwości biologicznych i fizykochemicznych związków naturalnych zadecydowało o wykorzystaniu ich w syntezie bioorganicznej. Przekształcenie grup funkcyjnych w wyniku estryfikacji, eteryfikacji, utlenieniu, redukcji bądź amidowania

prowadzi do utworzenia nowych pochodnych o ulepszonych właściwościach farmakokinetycznych (lipofilowości, rozpuszczalności) i farmakodynamicznych (inna selektywność receptora) (Rys. 11). Charakter lipofilowy steroidów pozwala im na pokonywanie barier biologicznych, jednak łatwo może ulec zmianie w wyniku wprowadzenia bardziej polarnych grup funkcyjnych, co znacznie zwiększy ich rozprowadzenie i czas działania w organizmie. Sztywny szkielet steroidowy umożliwia im penetrację komórki oraz wiązanie z receptorem hormonalnym lub białkowym. Struktura cząsteczki i cechy biologiczne steroidów wpłynęły na wykorzystanie ich w projektowaniu leków o aktywności przeciwnowotworowej, przeciwbakteryjnej, przeciwgrzybiczej, przeciwwirusowej lub przeciwzakrzepowej oraz stosowanych w leczeniu choroby Alzheimera. Ponadto, znalazły zastosowanie również w innych dziedzinach jako receptory molekularne, quasi-podandy, szczypce molekularne czy receptory wychwytujące kationy i aniony [67–70].

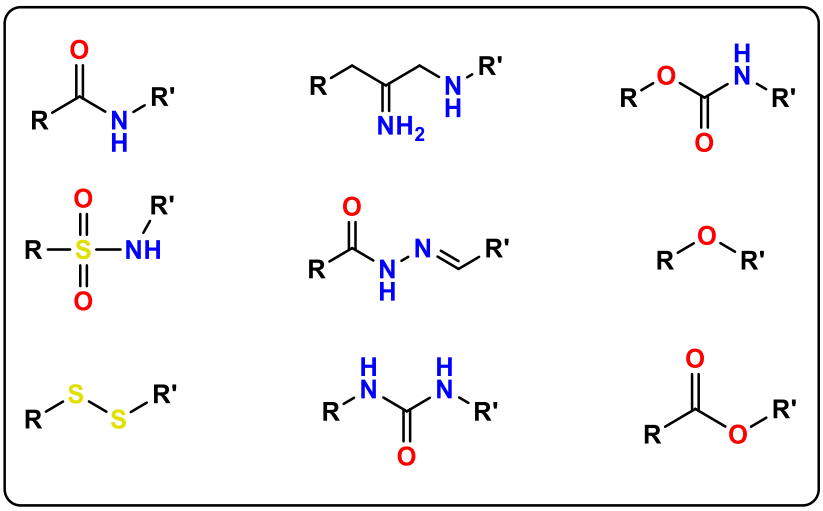

Rysunek 11. Możliwe drogi sprzęgania związków steroidowych z innymi molekułami [**P1**].

2. Chemia „click”

W 2001 roku profesor Sharpless i współpracownicy zaproponowali rewolucyjną metodę projektowania i syntezy nowych złożonych cząsteczek. Chemia „click” (chemia „kliknięć”) odnosi się do wysoko wydajnych reakcji chemicznych, które są proste w wykonaniu, szybkie, selektywne i nie dają produktów ubocznych. Odpowiednio zaprojektowane fragmenty molekularne łatwo ulegają połączeniu w precyzyjny sposób [71,72].

Podstawowe zasady chemii „click” obejmują koncepcje takie jak modularność, wysoka wydajność oraz efektywność atomowa, która z kolei jest kluczowa dla reguł tzw. „zielonej chemii”. Ze względu na te cechy metoda ta znalazła szerokie zastosowanie głównie w dziedzinach związanych z farmaceutykami, chemią medyczną i materiałową oraz biologią chemiczną [72]. Wśród najbardziej znanych reakcji opierających się na schemacie „click” należą cykloaddycja azydkowo-alkinowa katalizowana miedzią (CuAAC – *Copper–Catalyzed Azide–Alkyne Cycloaddition*), reakcje tiol-enowe oraz reakcje Dielsa-Aldera (Schemat 3) [74].

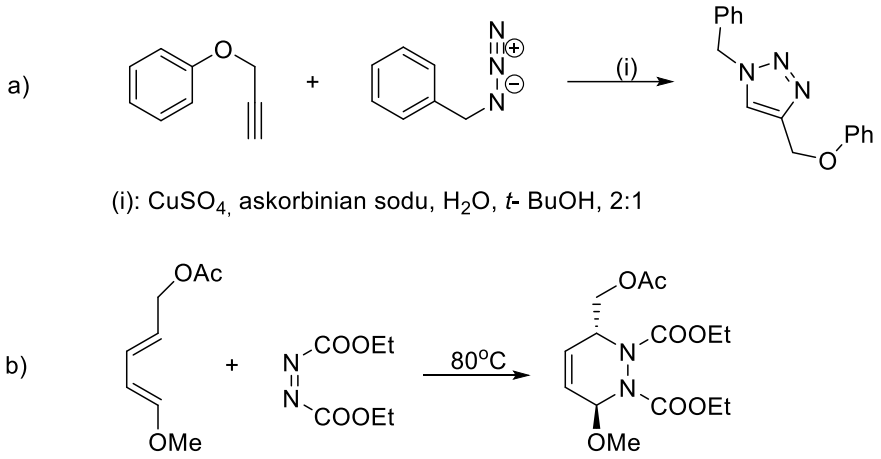

Schemat 3. Wybrane reakcji chemii „click": cykloaddycja azydkowo-alkinowa (a) i reakcja Dielsa-Aldera (b).

2.1. Typy reakcji chemii „click"

Istnieją przemiany chemiczne, które wymagają określonych warunków termodynamicznych, wskutek których zostanie utworzony tylko jeden produkt końcowy.

Jedną z podstawowych reakcji cyklicznych chemii „click", w której tworzy się wiązanie atom węgla–heteroatom jest cyklooaddycja [4+2], zwana również reakcją Dielsa-Aldera (Schemat 3b). Z kolei cykloaddycja 1,3-dipolarna dąży do utworzenia nowych koniugatów heterocyklicznych złożonych z wielu zróżnicowanych pięcio– i/lub sześcioczłonowych pierścieni, gdzie synteza rozpoczyna się od sprzężenia dwóch nienasyconych związków (Schemat 3a) [75].

Wyróżnia się cztery najważniejsze rodzaje przekształceń przebiegające zgodnie z zasadami chemii „click":

(1) addycja do wielokrotnego wiązania węgiel–węgiel:
- addycja Michaela (Schemat 4a);
- synteza azyrydyn (Schemat 4b);
- epoksydacja (Schemat 4c);
- dihydroksylacja (Schemat 4d);

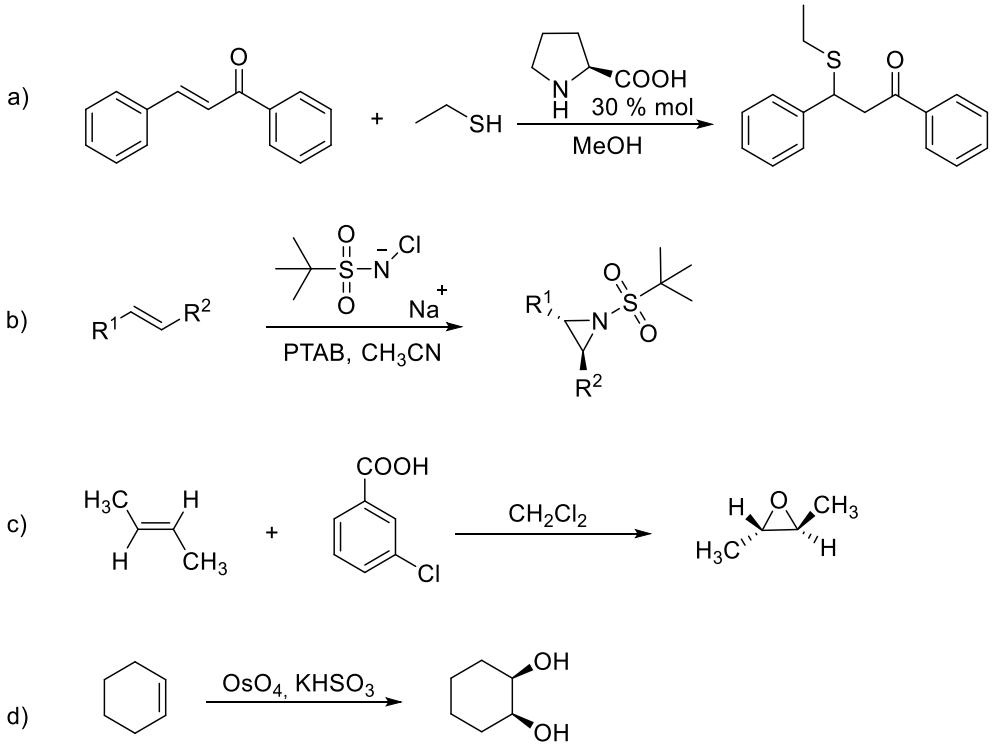

Schemat 4. Addycja nukleofilowa Michaela (a), synteza azyrydyn (b), epoksydacja (c) oraz dihydroksylacja (d).

(2) reakcje substytucji nukleofilowej:

- szczególnie transformacja, w wyniku której pęka wiązanie, co skutkuje otwarciem pierścienia w układach heterocyklicznych związków elektrofilowych, takich jak azyrydyny, epoksydy, cykliczne siarczany;

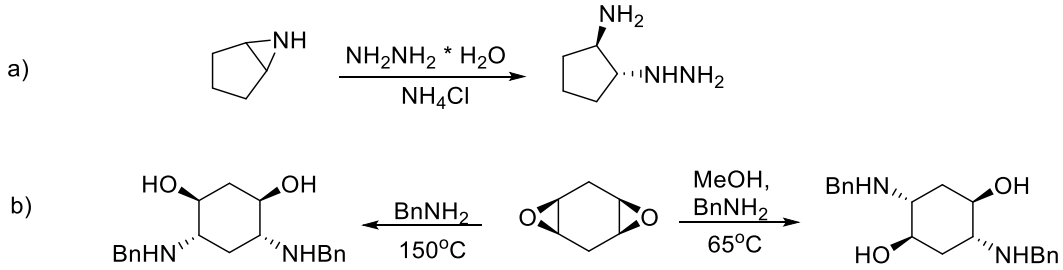

Schemat 5. Reakcje związane z otwarciem pierścienia azyrydyny (a) lub epoksydu (b).

(3) cykloaddycja związków nienasyconych:

- cykloaddycja 1,3-dipolarna, w tym cykloaddycja Dielsa-Aldera;

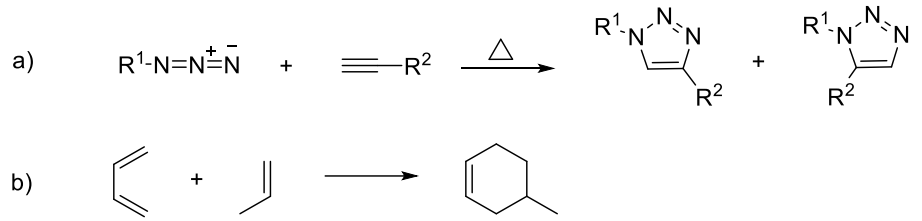

Schemat 6. Cykloaddycja 1,3-dipolarna (a) oraz cykloaddycja Dielsa-Aldera (b).

(4) modyfikacje związków karbonylowych typu „non-aldol":

- otrzymywanie eterów oksymowych, hydrazonów oraz aromatycznych układów heterocyklicznych.

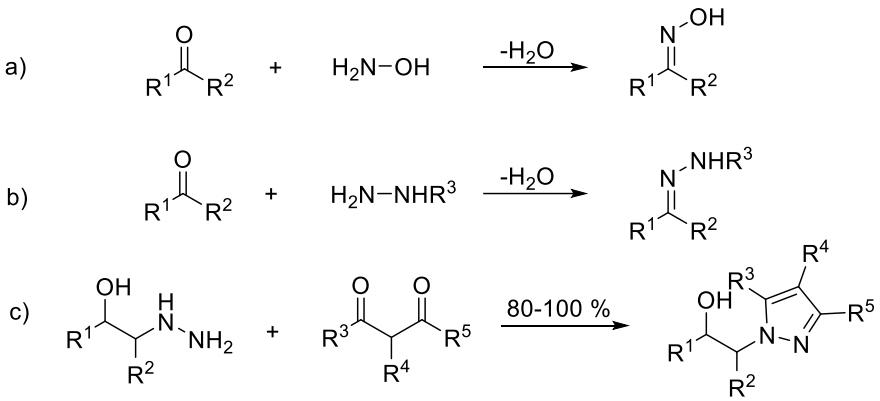

Schemat 7. Reakcje typu „non-aldol": synteza oksymów (a), hydrazonów (b) oraz układów aromatycznych (c).

Warto zauważyć, że wszystkie syntezy „click" charakteryzuje wysoka aktywność termodynamiczna, gdzie konieczny nakład energii jest wyższy niż 20 kcal/mol.

2.2. Cykloaddycja azydkowo-alkinowa katalizowana jonami miedzi (CuAAC)

Fundamentalną reakcją chemii „click" jest 1,3-dipolarna cykloaddycja azydkowo-alkinowa katalizowana jonami miedzi, znana jako reakcja Huisgena. Ten rodzaj reakcji pericyklicznej stosuje 1,3-dipol oraz dipolarofil jako substraty wyjściowe. Pierwszy z nich wskazuje na związek zbudowany dwubiegunowo, tj. składający się z elektrofilowego i nukleofilowego końca (taki jak azydek, ozon, diazometan). Natomiast dipolarofil charakteryzuje się pewnym stopniem nienasycenia spowodowanym deficytem elektronów. Wskutek sprzężenia terminalnych alkinów z azydkami w obecności miedzi, dzięki któremu dochodzi do cyklicznego przejścia elektronów π powstaje zwykle jeden produkt posiadający co najmniej dwa stabilizujące układ pierścieni wiązania [76,77].

Klasyczna reakcja Huisgena przebiegała w podwyższonej temperaturze, na skutek czego utworzony produkt był mieszaniną 1,4- i 1,5-dipodstawionych 1,2,3-triazoli. Kluczowe jest zastosowanie jonów miedzi(I) jako katalizatora, wskutek czego reakcja jest regioselektywna, wydajniejsza oraz blisko 10^6 szybsza niż przemiana przeprowadzona

wyłącznie w wyższej temperaturze (Schemat 8). Utworzony 1,4-dipodstawiony 1,2,3-triazol cechuje stabilność i brak toksyczności, natomiast użyte substraty najczęściej brak reaktywności w stosunku do grup funkcyjnych molekuły, jak również brak wpływu grup azydkowych i alkinowych na jej bioaktywność [78].

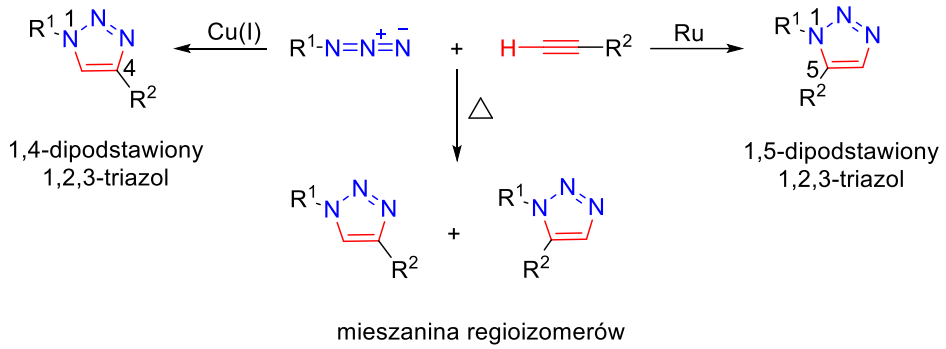

Schemat 8. Regioselektywność reakcji Huisgena zależna od jej warunków.

2.2.1. Sposoby wprowadzenia jonów Cu(I)

Dostarczenie do mieszaniny reakcyjnej jonów miedzi(I) decyduje o prawidłowym kierunku reakcji. Zastosowanie warunków wodnych (np. układu *tert*-butanol/woda) wskazuje na technikę *in situ*, w której jony Cu(I) uzyskuje się z pięciowodnego siarczanu(VI) miedzi(II) albo octanu miedzi(II), redukując te sole odpowiednimi odczynnikami, takimi jak askorbinian sodu, miedź metaliczna, hydrazyna lub tris(2-karboksyetylo)fosfina (jak na Schemacie 3a).

W układzie niepolarnym oraz wykorzystując kompleksy soli miedzi z nadmiarem zasady (np. trietyloaminy) zostanie utworzony acetylenek miedzi. Jony miedzi(I) można pozyskać również stosując niektóre halogenki miedzi (CuI, CuBr), tlenki miedzi(I) i (II) oraz nanoklastery Au_4Cu_4 [75,79–81].

Z kolei kataliza heterogeniczna należy do wydajnych i tanich metod syntezy 1,4-dipodstawionych pochodnych 1,2,3-triazoli (Schemat 9b). Katalizator miedziowy znajduje się na nośniku węglowym (Cu/C). Zakonserwowany wodnym roztworem azotanu(V) miedzi(II) węgiel drzewny poddaje się destylacji wody i suszeniu, w wyniku czego tlenki miedzi(I) i (II) pokrywają powierzchnię katalizatora (Schemat 9a). W tego typu układzie można łatwo usunąć reduktor i katalizator bądź wygodnie wybrać rozpuszczalnik, jak również zmienić warunki reakcji dodając trietyloaminę lub podwyższając temperaturę [82].

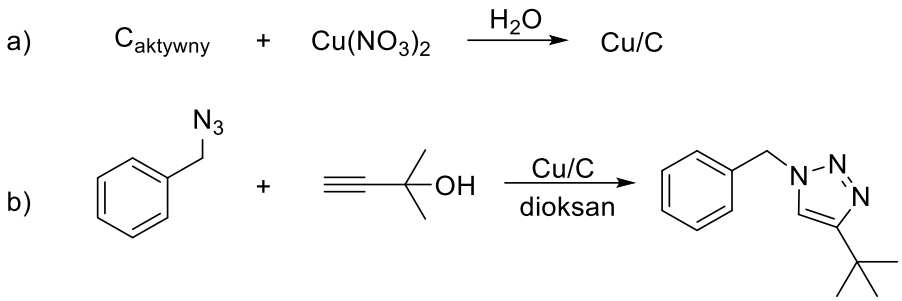

Schemat 9. Wybrana reakcja typu katalizy heterogenicznej.

2.2.2. Mechanizm reakcji CuAAC

Cykloaddycja azydkowo-alkinowa katalizowana jonami miedzi(I) jest efektywnym procesem charakteryzującym się kilkuetapowym mechanizmem (Schemat 10). Jony miedzi(I) pełnią kluczową rolę w aktywacji alkinu, umożliwiając utworzenie trójczłonowego kompleksu z azydkiem. W pierwszym etapie następuje koordynacja jonów Cu(I) do wiązania potrójnego alkinu, zwiększając jego elektrofilowość (**A**). Aktywowany acetylenek miedzi zostaje zaatakowany przez azydek, tworząc przejściowy kompleks metaloorganiczny (**B**). Następnie reorganizacja wiązań prowadzi do zamknięcia pięcioczłonowego pierścienia, dając strukturę 1,2,3-triazolu (**C**, **D** i **E**). Uzyskany 1,4-podstawiony 1,2,3-triazol charakteryzuje wysoka odporność chemiczna i termiczna, a jedynym produktem ubocznym jest cząsteczka wody, co czyni reakcję zgodną z zasadami zielonej chemii [83,84].

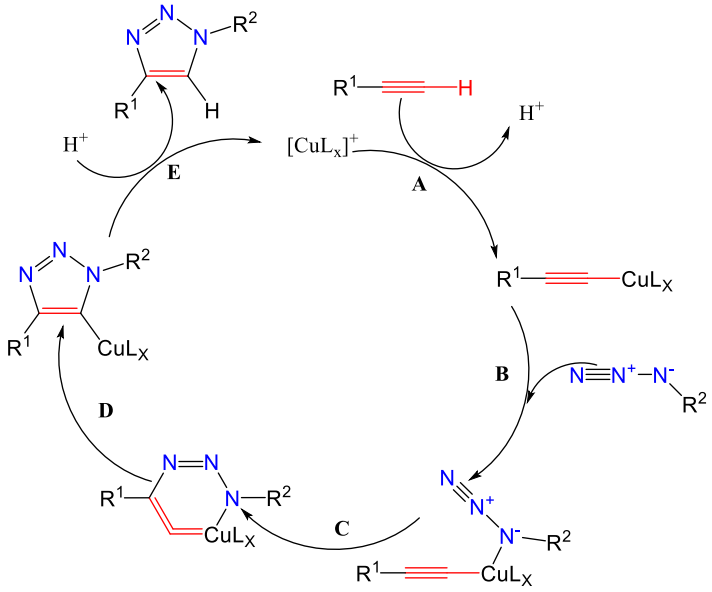

Schemat 10. Mechanizm reakcji CuAAC.

Ze względu na wydajność sięgającą często 100% oraz chemoselektywność wynikającą z eliminacji izomerycznych związków ubocznych, reakcja ta ma przełomowe znaczenie w syntezie organicznej. Dodatkowo, zwykle przeprowadzana jest w temperaturze nieprzekraczającej 65°C, co minimalizuje ryzyko związane z degradacją substratów. Zastosowanie warunków wodnych zwiększa jej ekologiczność. Prostota, niezawodność i minimalne wymogi oczyszczania sprawiły, że stała się filarem chemii „click", znajdując zastosowanie w syntezie leków, modyfikacji polimerów oraz w chemii biomolekularnej (znakowanie białek i kwasów nukleinowych) [85].

2.3. 1,2,3-triazolowe koniugaty steroidowe

Układy 1,2,3-triazolowe to pięcioczłonowe krystaliczne związki heterocykliczne. Cechuje je rozpuszczalność w wodzie oraz wysoka odporność na stres oksydacyjny/redukujący, hydrolizę i degradację metaboliczną. Ich wyjątkową właściwością jest możliwość wiązania się z receptorami lub enzymami wskutek oddziaływań takich jak wiązania wodorowe, siły van der Waalsa lub interakcje hydrofobowe [86]. Ze względu na niepodatność tych wiązań na rozszczepienie przez proteazy są one porównywane do wiązań peptydowych. Pochodne 1,2,3-triazolowe wyróżnia doskonała aktywność biologiczna, szczególnie ważna w leczeniu chorób związanych: z nowotworami, zakażeniami (przez pasożyty, bakterie, grzyby, wirusy), nadciśnieniem tętniczym, depresją, cukrzycą, ośrodkowym układem nerwowym oraz chorobą Alzheimera [87–90].

2.3.1. Wprowadzenie grupy azydkowej do szkieletu steroidowego

Zaprojektowano i opisano wiele ścieżek syntetycznych przekształcających odpowiednie grupy funkcyjne szkieletu steroidowego w grupę azydkową. Najczęściej stosowaną metodą jest modyfikacja grupy hydroksylowej w pochodną tosylową lub mesylową. Następnie w wyniku reakcji substytucji nukleofilowej anion azydkowy oddziałuje na elektrofil [91]. W zależności od konfiguracji przestrzennej wyróżnia się dwa różne mechanizmy tej reakcji: bez inwersji lub z inwersją konfiguracji produktu końcowego.

2.3.1.1. Reakcja Mitsunobu – bez inwersji konfiguracji

Pierwszy z dostępnych rozwiązań zakłada, że azydkowa pochodna przyjmuje stereochemię alkoholu. W celu dokonania początkowej inwersji konfiguracji związku przeprowadza się reakcję Mitsunobu (Schemat 11). Otrzymana struktura mesylowa jest podatna na atak nukleofilowego azydku sodu, co w konsekwencji daje związek azydku z zachowaną konfiguracją przyjętą wcześniej przez alkohol [92].

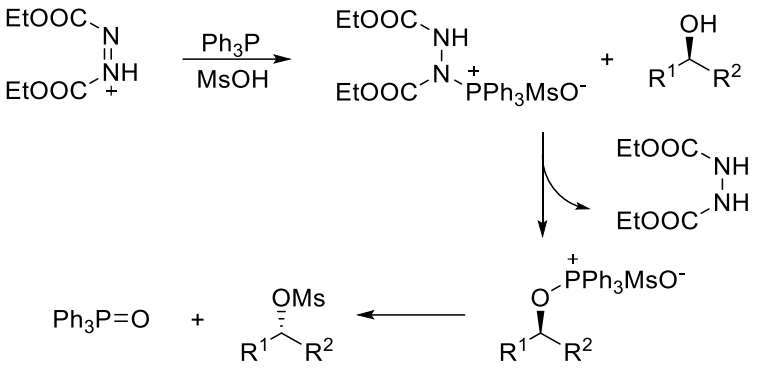

Schemat 11. Mechanizm reakcji Mitsunobu.

2.3.1.2. Reakcja z inwersją konfiguracji

Druga metoda zakłada otrzymanie pochodnej steroidowej o konfiguracji przeciwnej względem wyjściowego alkoholu (Schemat 12). W tym celu należy zastosować inne odczynniki wprowadzające grupę mesylową niż te obecne w reakcji Mitsunobu. Opracowano również syntezy, gdzie produktem pośrednim jest pochodna tosylowa, która ulegając podobnym reakcjom substytucji nukleofilowej zostaje przekształcona w azydek [93].

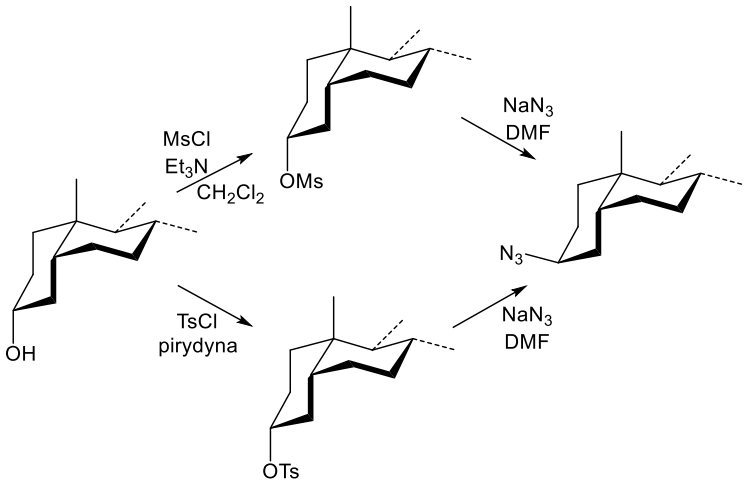

Schemat 12. Synteza przebiegająca z inwersją konfiguracji.

Istnieje również ścieżka wykorzystująca halogenoacetoksy podstawione pochodne steroidów. Wzbogacenie szkieletu steroidowego w ugrupowanie azydkowe opiera się na substytucji atomu halogenu (najczęściej bromu). Reakcja ta jest zwykle stosowana w przypadku kwasów żółciowych (Schemat 13) [94,95].

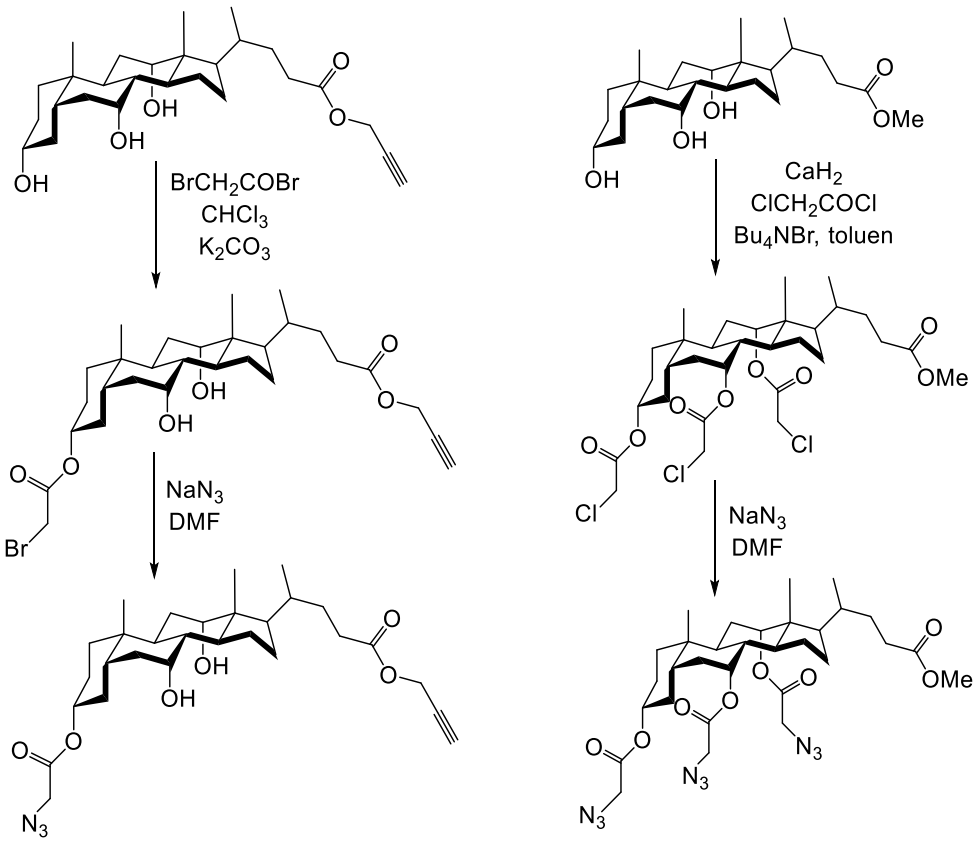

Schemat 13. Halogenoacetoksy podstawienie kwasu cholowego.

Z kolei modyfikacje łańcucha bocznego kwasów żółciowych polegają głównie na reakcjach zmierzających do zredukowania grupy karboksylowej do grupy hydroksylowej. Utworzony alkohol można przekształcić ponownie w pochodną mesylową, która następnie ulega sprzężeniu z azydkiem sodu (Schemat 14) [96].

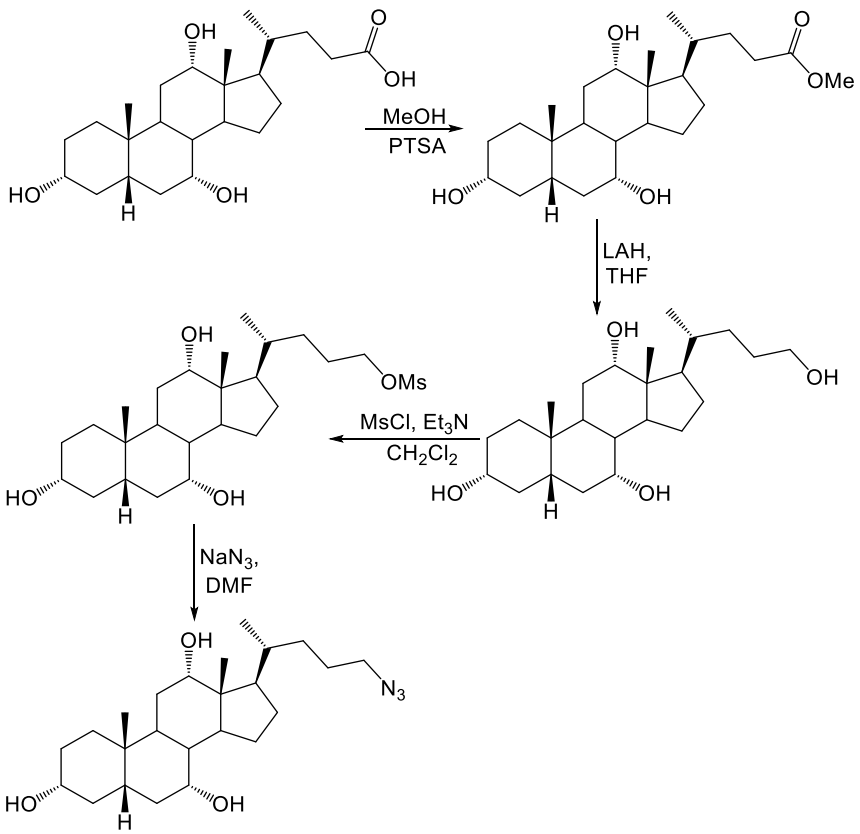

Schemat 14. Wprowadzenie grupy azydkowej w łańcuch boczny steroidu.

Zaprojektowano również metodę rozpoczynającą się od transformacji grupy karboksylowej łańcucha bocznego w monoester glikolu etylenowego. W wyniku mesylowania grupy hydroksylowej glikolu, a w kolejnym etapie reakcji powstałego związku przejściowego z azydkiem sodu otrzymano strukturę pochodnej steroidowej z wbudowaną grupą azydkową (Schemat 15) [97].

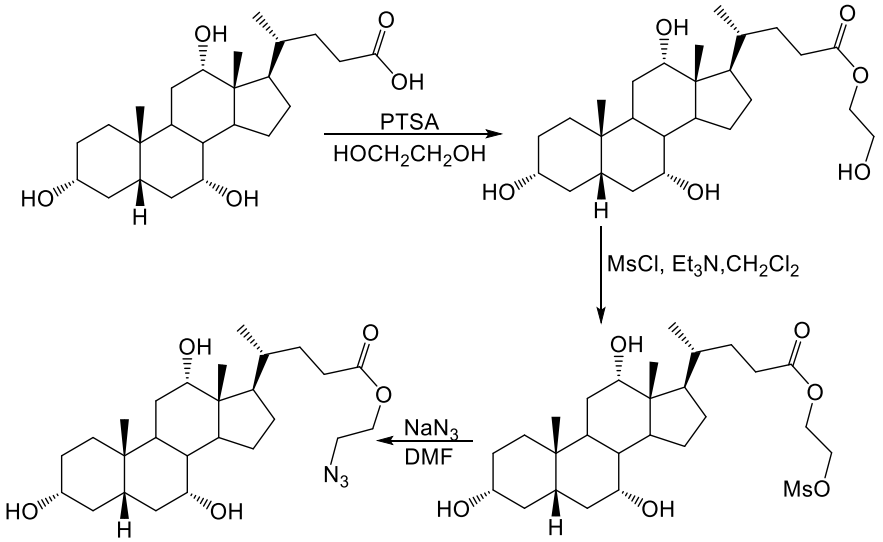

Schemat 15. Modyfikacja grupy karboksylowej z wykorzystaniem glikolu.

Grupa badawcza kierowana przez Zhu dążyła do syntezy inhibitorów α-2,3-sialulotransferazy. Seria przeprowadzonych reakcji chemicznych wzbogaciła łańcuch boczny kwasu litocholowego o grupę azydkową (Schemat 16). Proces rozpoczęto od estryfikacji steroidu, a następnie uzyskany litocholan metylu zredukowano do alkoholu (przy użyciu LAH). W kolejnym etapie działanie azydku difenylofosforanu (DPPA) i DBU na alkohol przekształciło grupę hydroksylową w łańcuchu bocznym w grupę difenylofosforanu. Uzyskany związek został przekonwertowany w azydek steroidowy, wykorzystując nadmiar azydku sodu, eter koronowy i katalityczne ilości jodku tetrabutyloamoniowego [98].

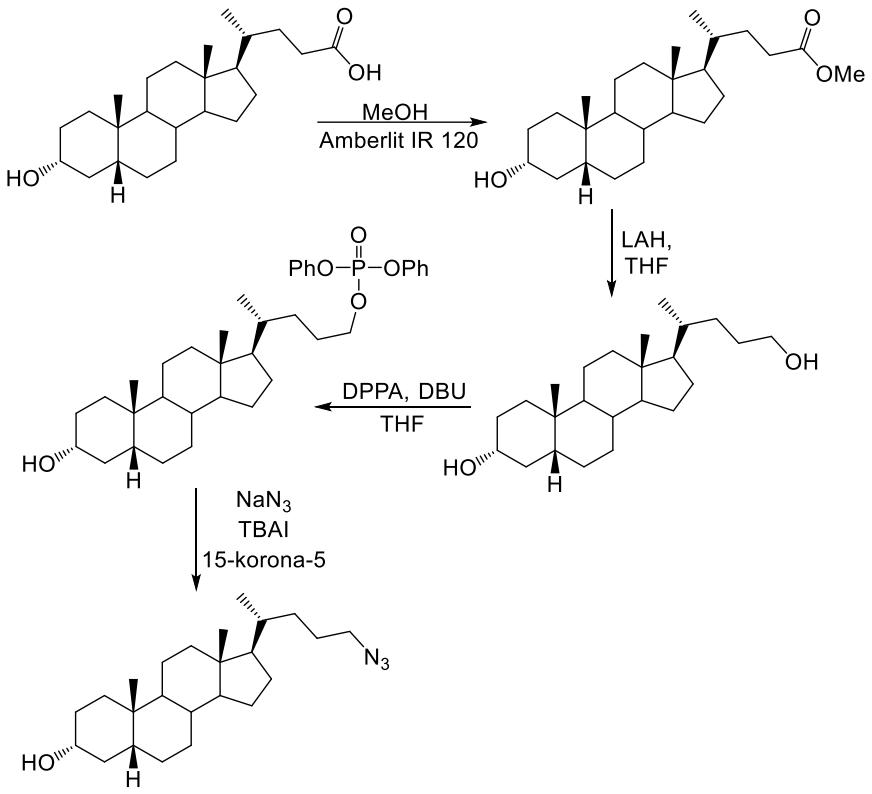

Schemat 16. Przekształcenie kwasu litocholowego w azydek w syntezie inhibitorów α-2,3-sialulotransferazy

2.3.2. Wprowadzenie grupy alkinowej do szkieletu steroidu

Opisano kilka sposobów wprowadzających terminalną grupę alkinową w cząsteczkę steroidu, jednak najbardziej znane jest zastosowanie glikolu etylenowego (Schemat 17) [99].

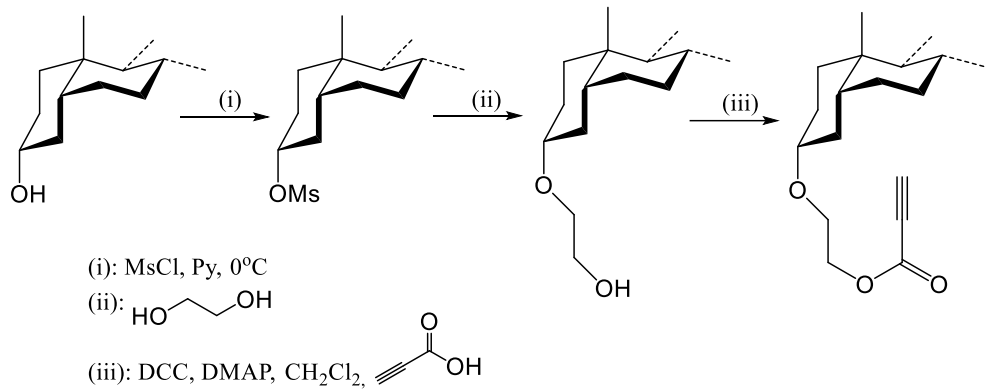

Schemat 17. Wprowadzenie grupy alkinowej w pozycję C-3 steroidu.

Natomiast grupa karboksylowa łańcucha bocznego kwasów żółciowych ulega łatwo reakcji estryfikacji z użyciem alkoholu propargilowego (Schemat 18) [100,101].

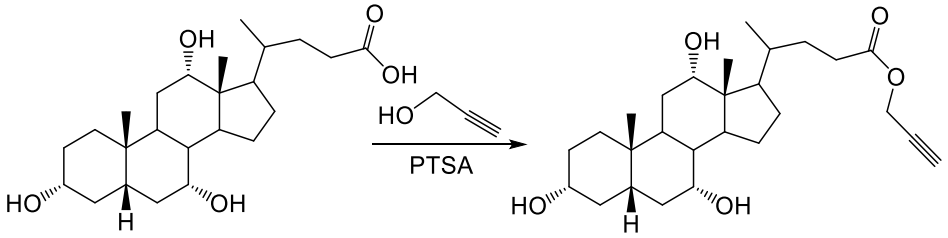

Schemat 18. Przekształcenie grupy karboksylowej łańcucha bocznego w terminalny alkin.

Dobór odpowiedniego katalizatora syntezy znacząco wpływa na jej kierunek. W obecności EDC*HCl istnieją dwie drogi reakcji. Ester z wiązaniem potrójnym będzie produktem końcowym reakcji, jeśli wezmą w niej udział tylko i wyłącznie kwas żółciowy i alkohol propargilowy. Wprowadzenie do układu reakcyjnej propargiloaminy skutkuje powstaniem amidu (Schemat 19) [102].

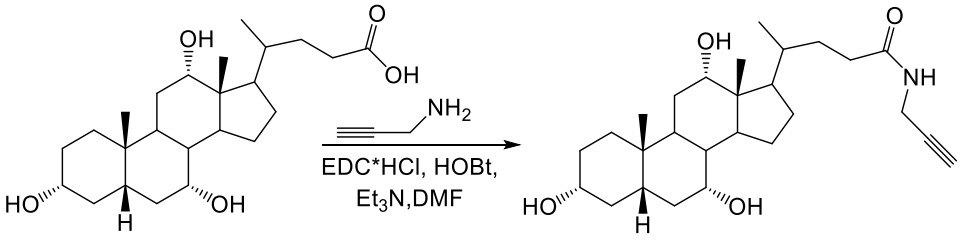

Schemat 19. Synteza amidu steroidowego w obecności tritetyloaminy.

Suh zaproponował metodę syntezy 1,2,3-triazolowych koniugatów witaminy D, w której wykorzystał terminalny alkin podstawiony grupą trimetylosililową (Schemat 20). Powstały w wyniku reakcji związek (A) został poddany serii przemian chemicznych, prowadzących do uzyskania 1,2,3-triazolowej pochodnej witaminy D [103].

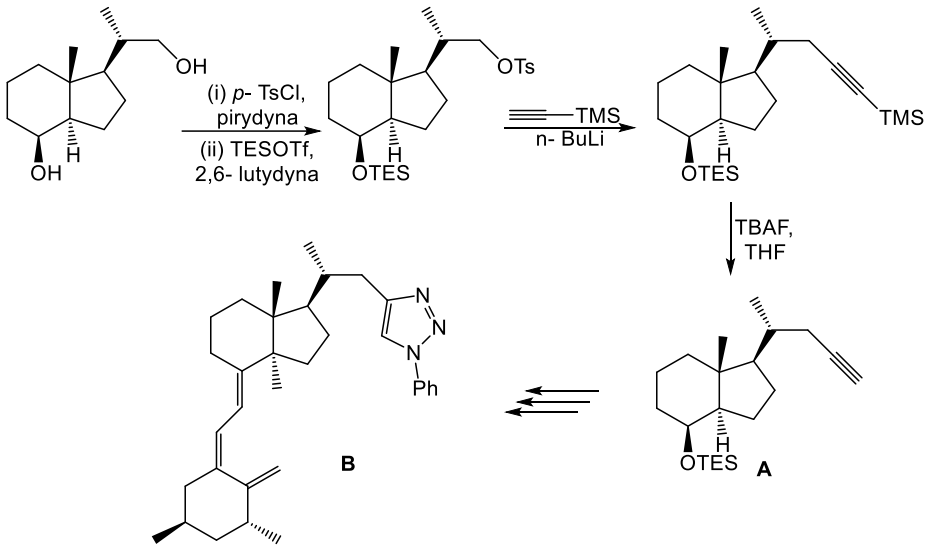

Schemat 20. Synteza 1,2,3-triazolowej pochodnej witaminy D.

2.4. Koniugaty steroidowo-triazolowe o aktywności biologicznej

Kwasy żółciowe, jak już wymieniono, wyróżniają się sztywnym rdzeniem steroidowym, wysoką aktywnością grup funkcyjnych oraz wyjątkowymi właściwościami amfifilowymi. Te unikalne cechy decydują o ich ogromnej roli jako materiału biologicznego do syntez związków o potencjalnym zastosowaniu w przemyśle farmakoterapeutycznym. Są prekursorami do otrzymywania związków makrocyklicznych, takich jak szczypce molekularne, elementy struktur biologicznych oraz koniugatów flukonazolu [96,104]. Wydajne metody gwarantują efektywną syntezę związków steroidowych o aktywności biologicznej.

2.4.1. Koniugaty steroidowe o aktywności przeciwgrzybicznej i przeciwbakteryjnej

Flukonazol (**22**) jest związkiem z grupy triazoli, będący antybiotykiem oraz pełniący funkcję inhibitora syntezy ergosterolu (Rys. 12). Jego struktura opiera się na pierścieniu triazolowym związanym z fluorowanym benzenem oraz grupy hydroksylowej. Lekooporność grzybów obniżyła jego skuteczność, co spowodowało, że stał inspiracją w projektowaniu koniugatów steroidowo-triazolowych. Sprzężenie właściwości biologicznych związków steroidowych z aktywnością układów triazolowych daje pochodne o potencjalnym zastosowaniu jako leki przeciwgrzybicze o zwiększonej biobójczości i szerszym spektrum działania.

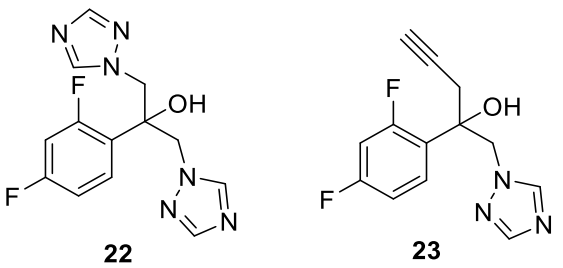

Rysunek 12. Flukonazol (**22**) i jego alkinowa (**23**) pochodna.

Pochodne odpowiednich kwasów żółciowych (deoksycholowego i cholowego) połączono pierścieniem 1,2,3-triazolowym ze zmodyfikowaną cząsteczką flukonazolu (**23**) (Rys. 13). Część steroidowa odgrywała rolę nośnika leku, a wbudowany triazol zwiększył funkcjonalność biologiczną uzyskanej molekuły. Grzyby z rodzaju *Candida*, takie jak *C. parapsilosis*, *C. albicans* i *C. Sporothrix* wykazywały prawie 100 % śmiertelność po zastosowaniu wobec nich nowych koniugatów (**24**–**27**), których aktywność przeciwgrzybicza oscylowała w zakresie MIC 3,12–6,25 mg/ml [96,105,106].

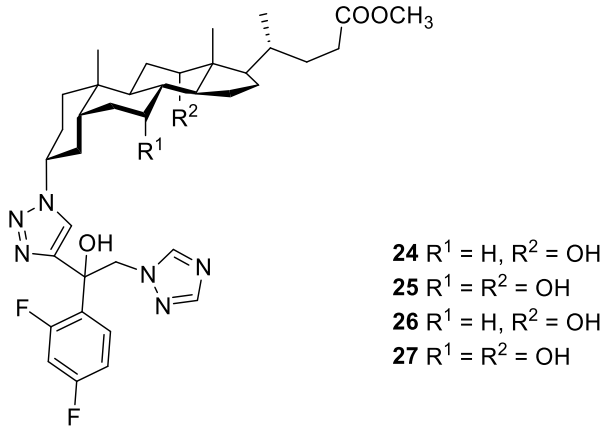

Rysunek 13. Koniugaty kwasów żółciowych i flukonazolu.

Wykorzystując metodę „click" sprzężono cząsteczkę mentolu z kwasami żółciowymi. Wybrane kwasy steroidowe poddano estryfikacji w obecności bromku propargilu i K_2CO_3, a metylowany mentol przekształcono w azydek stosując NaN_3 w DMF. Następnie związki użyto jako reagenty w reakcji „click" (Schemat 21). Otrzymane pochodne 1,2,3-triazolu (**28-30**) charakteryzowały się lepszą aktywnością przeciwko szczepom *Enterococcus faecium* (MIC < 10 μM) niż mentol (MIC = 410 μM), kwasy żółciowe (MIC = 10, 20, 157, 410 μM) oraz antybiotyk cefiksym (MIC = 35410 μM) [107].

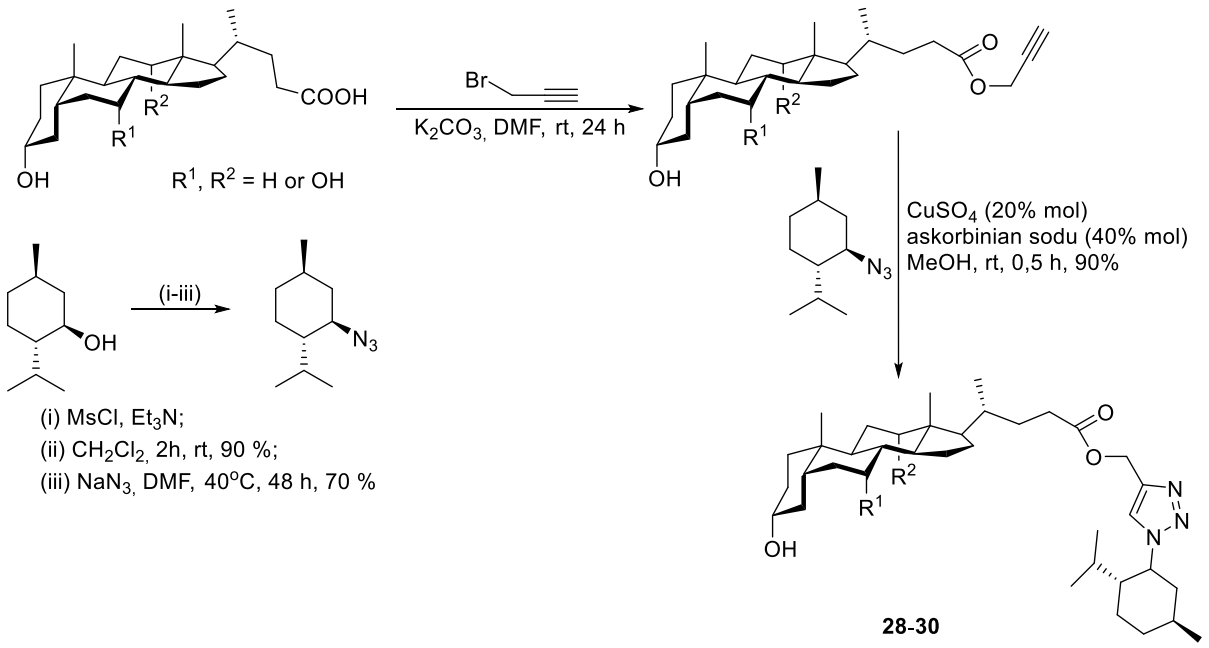

Schemat 21. Otrzymywanie koniugatów kwasów żółciowych i mentolu (**28**–**30**).

Związki o właściwościach farmakologicznych często zawierają grupy β-laktamowe. W strukturze penicyliny rozpoznano czteroczłonowe laktamy [108]. Rosnąca lekooporność bakterii i grzybów wymusiła zaprojektowanie hybryd opartych na związkach heterocyklicznych. Otrzymano koniugaty kwasów żółciowych połączone pierścieniem 1,2,3-triazolowym z cząsteczką pochodnej β-laktamu, które były skuteczne wobec szczepów grzybów: *C. albicans* (128 μg/ml), *Cryptococcus neoformans*, *Yarrowia lipolytica* (8 μg/ml), *Fusarium oxysporum*, *Benjaminiella poitrasii* (32 μg/ml) oraz bakteriom z rodzaju: *Escherichia coli* i *Staphylococcus aureus* (Rys. 14) [102].

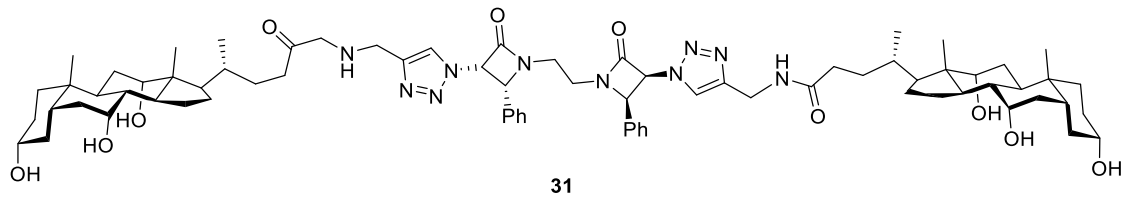

Rysunek 14. Koniugat kwas żółciowy-β-laktam.

Koniugaty aminocholestanów połączone z pierścieniem imidazolowym lub pirydynowym (**32**–**33**) działały przeciwko kilku szczepom bakterii *S. aureus* (MIC < 4 μg/ml) (Rys. 15) [109].

Niezwykle skuteczne okazały się pochodne kwasu cholowego i lizyny. Związek (**34**) wykazywał aktywność wobec *S. aureus*, *E. Coli* i *C. albicans* (MIC < 8 μg/ml) oraz nie powodował degradacji erytrocytów ludzkich (Rys. 15). Natomiast inna pochodna tego

kwasu żółciowego była wysoce skuteczna przeciwko szczepom opornym *S. aureus* 1704, *E. Coli* 4052 i *C. auris* [110].

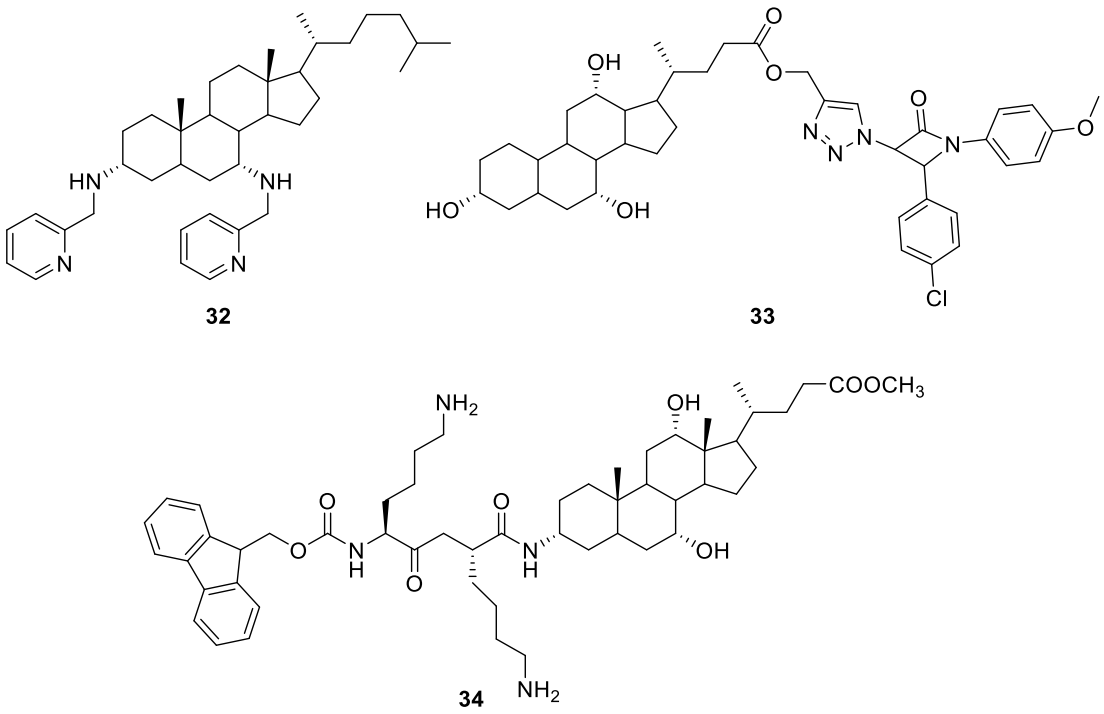

Rysunek 15. Koniugaty steroidowe o właściwościach antybakteryjnych i antygrzybicznych.

2.4.2. Koniugaty steroidowe o aktywności przeciwpasożytniczej

Pasożyty Leishmania to pierwotniaki z rodzaju *Leishmania*, przenoszone przez ukąszenia muchówek z rodziny *Phlebotominae*, Wywołują leiszmaniozę, objawiającą się zmianami skórnymi, śluzówkowymi lub trzewnymi [111]. Z kolei malaria to choroba zakaźna wywoływana przez pasożyty z rodzaju *Plasmodium*, przenoszona na ludzi przez ukłucia samic komarów z rodzaju *Anopheles*. Objawia się gorączką, dreszczami, bólami mięśni i powikłaniami zagrażającymi życiu [112].

Biokoniugaty kwasu cholowego i 6-tiopuryny (**35**–**36**) otrzymane metodą „click" wykazywały w badaniach *in vivo* znacznie wyższą aktywność biologiczną niż chlorochina (lek stosowany w leczeniu malarii) oraz powodowały śmiertelność pasożyta Leishmanna (Rys. 16). Testy pod kątem cytotoksyczności nie stwierdziły ich ingerencji w tkanki ssaka [113].

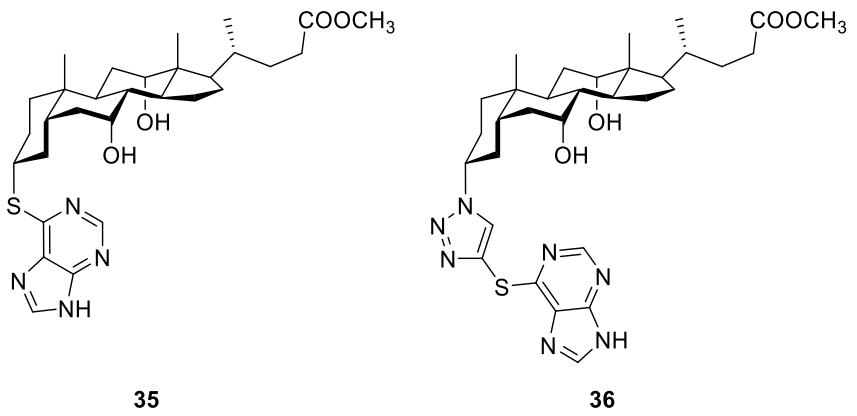

Rysunek 16. Koniugaty steroidowo-tiopurynowe o aktywności przeciwpasożytniczej.

Podobną skuteczność wobec leiszmaniozy oraz prątka *Mycobacterium tuberculosis* określono dla związków triazolowych, zbudowanych z aminocholiny i kwasu żółciowego (Schemat 22). Koniugat (**38**) wykazywał właściwości przeciwgruźlicze przeciwko *M. tuberculosis* (MIC = 8,8 μM) porównywalne ze stosowanymi lekami [114].

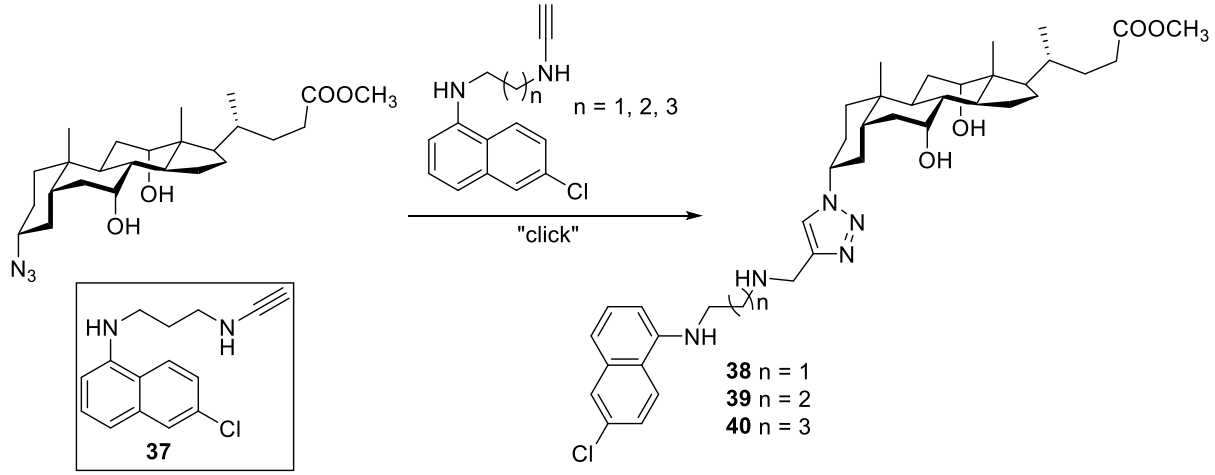

Schemat 22. Synteza koniugatów aminocholiny i kwasu cholowego.

2.4.3. Koniugaty steroidowe o aktywności przeciwnowotworowej

Projektowanie syntez związków o potencjalnym wykorzystaniu w terapiach przeciwnowotworowych ma fundamentalne znaczenie dla chemii organicznej. Z doniesień literaturowych wynika, że wzrastające zainteresowanie chemią steroidów zaowocowało opracowaniem efektywnych koniugatów o dużej aktywności wobec różnorodnych komórek raka [115]. Szczególną wartość mają te sprzężone z nukleozydami (Schemat 23) [116].

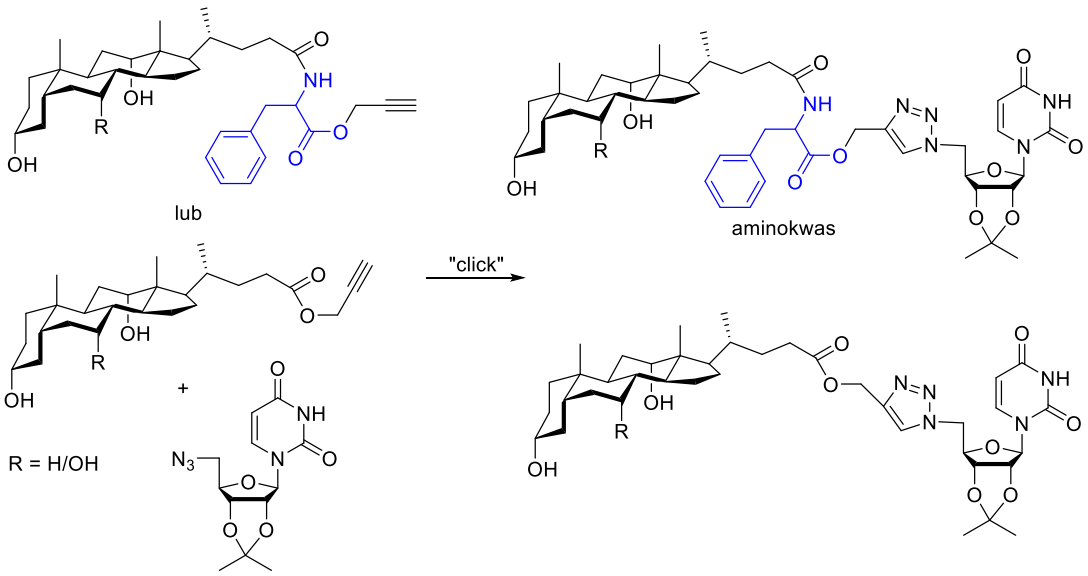

Schemat 23. Synteza steroidowo-urydynowych pochodnych triazolowych.

Agarwal i współpracownicy opisali pochodne kwasu żółciowego i aminokwasów zawierające układ 1,2,3-triazolowy (**41**–**48**) (Schemat 23, Rys. 17). Na podstawie testów *in vitro* potwierdzono ich aktywność przeciwko trzem liniom komórek nowotworowych (PC-3, MCF-7, IMR-32). Te same koniugaty wykazywały również działanie przeciwgruźlicze i były bezpieczne dla przeciętnej linii komórek ludzkiej nerki [117].

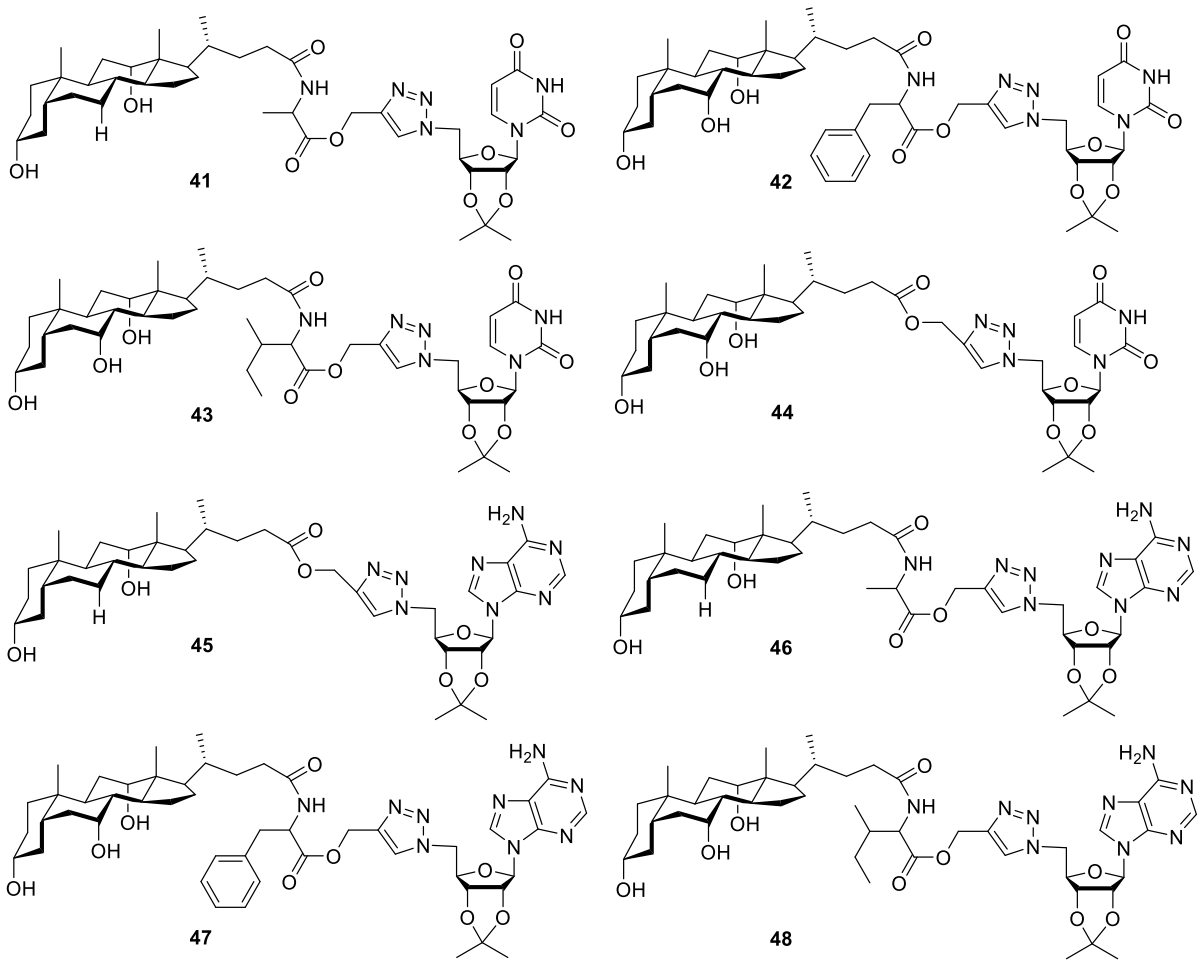

Rysunek 17. Biokoniugaty kwas żółciowy-nukleozyd zawierające pierścienie 1,2,3-triazolowe.

Natomiast koniugaty kwasu litocholowego i aminokwasów opracowano, aby sprawdzić ich potencjał inhibitujący sialilotransferazę. Enzym ten uczestniczy w kluczowym procesie biologicznym przerzutów komórek nowotworowych, zwanym hipersialilacją. Oceniono, że uzyskane w reakcji „click" pochodne steroidowe (**49**–**51**) hamują aktywność enzymu przy wartościach IC_{50} równym 6, 7 i 5 μM (Rys. 18) [98].

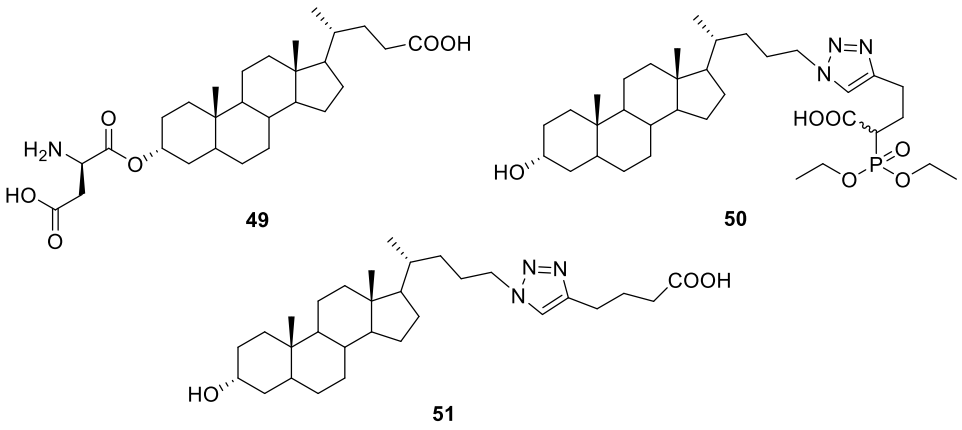

Rysunek 18. Pochodne kwasu litocholowego (**49**–**51**) jako inhibitory sialilotransferazy.

Podobne hybrydy triazolowe oparte na szkielecie steroidowym również wykazywały aktywność antyproliferacyjną przeciwko liniom komórek K562 oraz HCT116 (Rys. 19). Biokoniugat, tzw. dU-nor-CDC (**52**) powodował apoptozę przy IC_{50} = 42,9 μM (wobec K562), natomiast dU-UDC (**53**) był skuteczny przeciwko obu liniom komórek raka (IC_{50} = 16,5 i 22,0 μM, odpowiednio dla K562 i HCT116) [118].

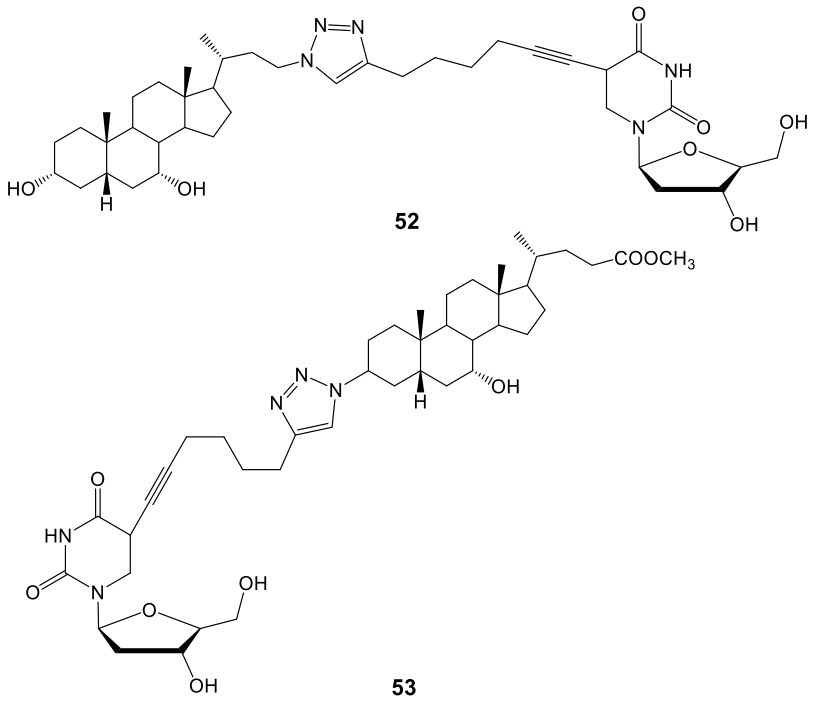

Rysunek 19. Biokoniugaty steroidowe powodujące apoptozę komórek raka.

Dane literaturowe donoszą również o biokoniugatach kwasu żółciowego i deoksyadenozyny łączony linkerem 1,2,3-triazolowym (Rys. 20). W wyniku kilkuetapowej syntezy utworzone struktury (**54**–**56**) o właściwościach przeciwnowotworowych wobec

komórek raka białaczki K562 i Jurkat, o aktywności IC50 odpowiednio 8,51 ± 4,05 μM i 10,47 ± 2,64 μM [119].

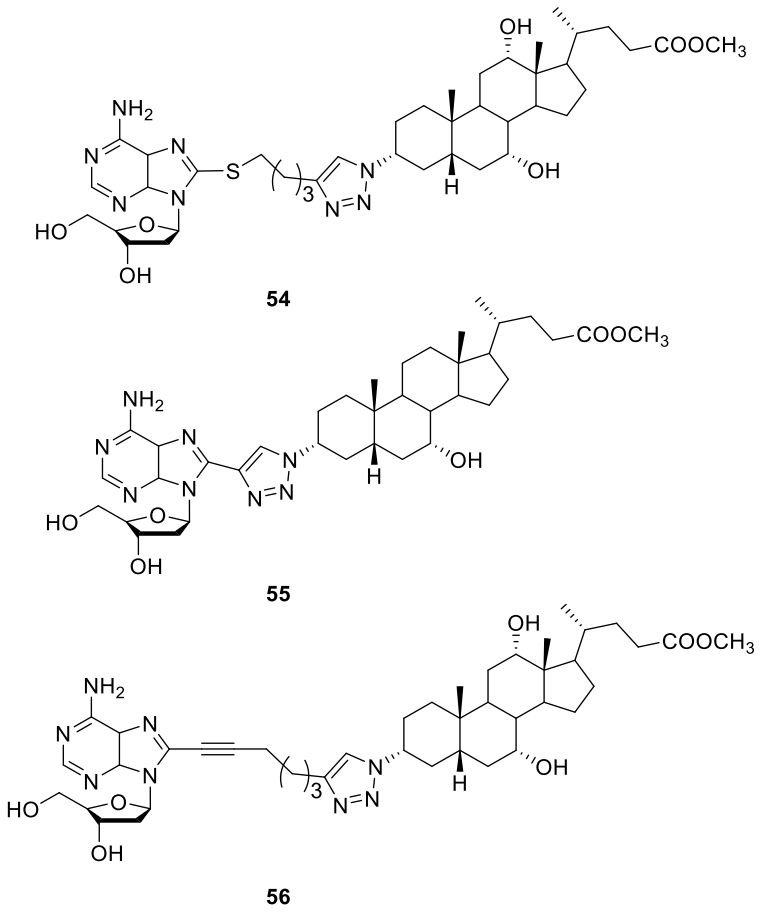

Rysunek 20. Hybrydy kwasów żółciowych i deoksyadenozyny.

Dendrymery, znane również jako „kieszenie molekularne", wykazują niezwykłą aktywność antyproliferacyjną. Udało się zaprojektować wydajną ścieżkę syntezy dendrymerów pierwszej generacji (chlodendrymerów), które następnie przekształcono w azydodendrymery drugiej generacji (Schemat 24). Jednocześnie cząsteczka kwasu żółciowego została efektywnie zmodyfikowana poprzez wprowadzenie grupy alkinowej. Testy MTT określiły, że pochodne steroidów zawierające pierścień triazolowy (**61**–**62**) skutkowały apoptozą komórek glejaka C6 przy IC_{50} = 10,48 μM [120].

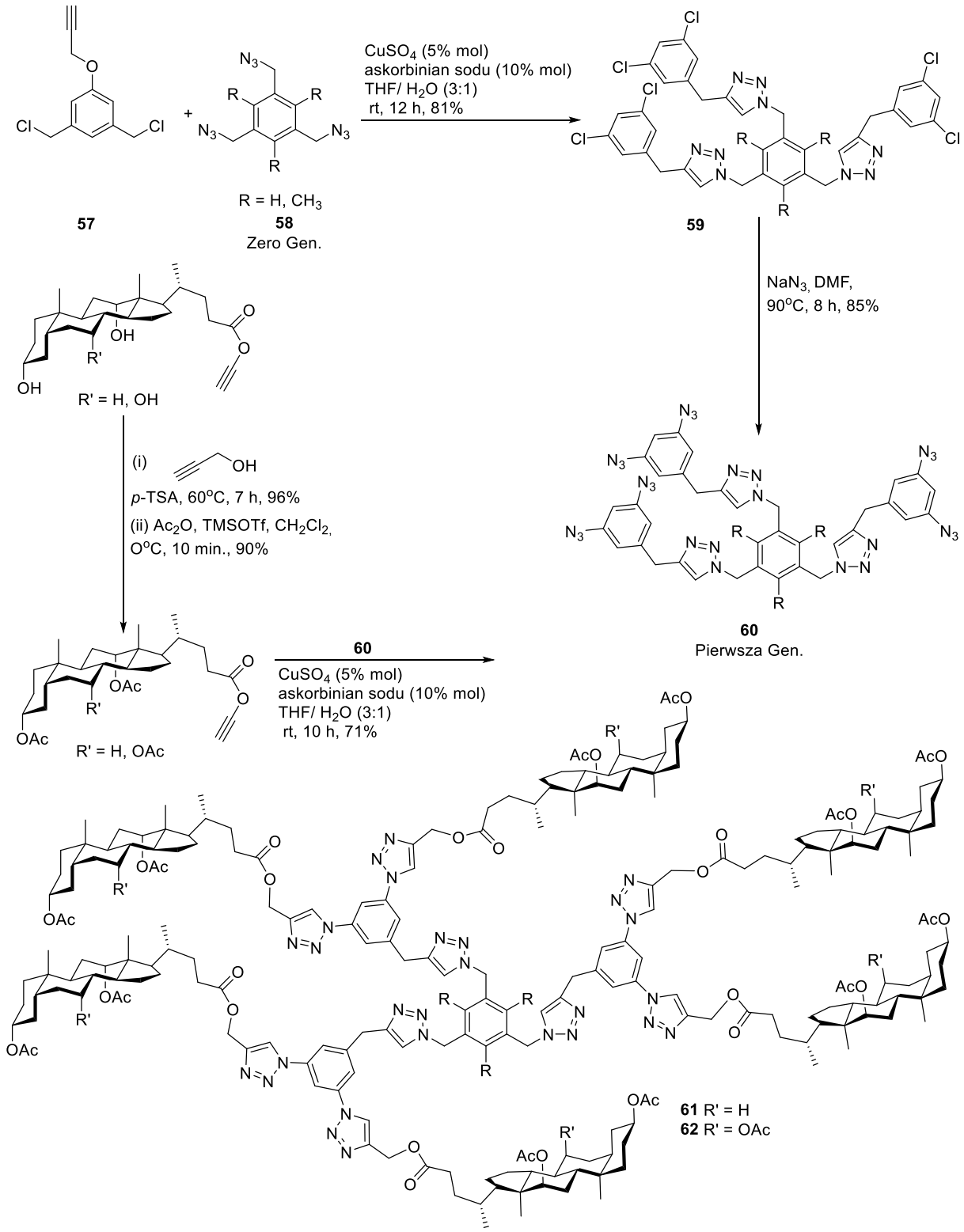

Schemat 24. Synteza dendrymerów (tzw. „kieszeni molekularnych") o właściwościach antynowotworowych.

2.5. Znaczenie biologiczne syntezy koniugatów steroidowych i chemii „click”

Synteza nowych biokoniugatów steroidowych wskutek amplifikacji układów 1,2,3-triazolowych w cząsteczkę steroidu odgrywają kluczową rolę w rozwoju chemii związków naturalnych [121–125]. Chemia „click” umożliwia dostosowywanie właściwości związków steroidowych, co najczęściej prowadzi do powstania skuteczniejszych leków o minimalnych skutkach ubocznych. Dzięki koniugatom steroidowym można badać interakcje w układach biologicznych, wyjaśniając procesy fizjologiczne oraz mechanizmy chorób. Precyzyjny i selektywny charakter reakcji „click” promuje projektowanie cząsteczek o niezwykłym znaczeniu dla medycyny i biotechnologii. Sprzyja to tworzeniu efektywnych terapii, zaawansowanych biomateriałów i innowacyjnych technologii, korzystnych dla nauki i społeczeństwa.

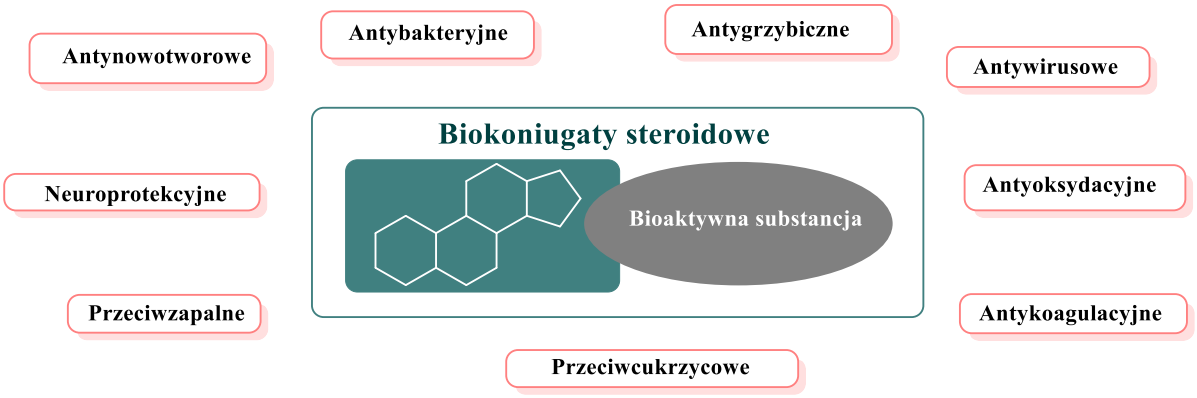

Rysunek 21. Potencjał farmakoterapeutyczny opisanych w literaturze koniugatów steroidowych [**P1**].

Część eksperymentalna

Rozwój nowoczesnych terapii w farmakologii i chemii bioorganicznej bazuje na projektowaniu nowych związków o wielokierunkowym działaniu biologicznym. Biokoniugaty steroidowe o unikalnej aktywności biobójczej zyskały szczególne miejsce w opracowywaniu potencjalnych leków. Część eksperymentalna tej pracy opiera się na fundamentalnym zrozumieniu właściwości pochodnych steroidowych. Moje dotychczasowe badania w tym obszarze zaowocowały sześcioma publikacjami naukowymi, w których jestem pierwszą autorką, w tym w trzech z nich pełniłam również rolę autora korespondencyjnego.

Aby lepiej usytuować zakres badań własnych, w poniższym wprowadzeniu streszczono trzy kluczowe artykuły przeglądowe podsumowujące aktualne osiągnięcia naukowe dotyczące modyfikacji steroidów, ich potencjału terapeutycznego oraz możliwych zastosowań klinicznych. Podkreślają one znaczenie triazolowych modyfikacji kwasów żółciowych, koniugatów skwalaminy oraz zastosowania chemii „click" w tworzeniu nowych związków o działaniu przeciwnowotworowym, przeciwdrobnoustrojowym i neuroprotekcyjnym.

Biokoniugaty steroidowe stanowią obiecujące narzędzie w nowoczesnej chemii bioorganicznej i farmakologii. Oferują szerokie zastosowania terapeutyczne dzięki swojej unikalnej strukturze, wielokierunkowej aktywności biologicznej oraz niskiej toksyczności. Zawarte w pracach przeglądowych [**P1**], [**P2**] i [**P4**] badania podkreślają szczególne znaczenie modyfikacji chemicznych steroidów, takich jak skwalamina, kwasy żółciowe oraz koniugaty zawierające pierścienie 1,2,3-triazolowe, szczególnie w kontekście terapii przeciwnowotworowej, przeciwdrobnoustrojowej i przeciwpasożytniczej.

Biokoniugaty steroidowe wykazują wysoką skuteczność w zwalczaniu opornych szczepów bakterii i grzybów. Opisywane pochodne flukonazolu z kwasami żółciowymi, dzięki pierścieniowi 1,2,3-triazolowemu, zyskały większą stabilność i aktywność biologiczną wobec patogenów, takich jak *Candida albicans*. Podobne wyniki osiągnięto dla koniugatów steroidowych-triazolowych z mentolem, które przewyższyły skuteczność tradycyjnych antybiotyków.

Koniugaty steroidowe, takie jak związki kwasów żółciowych i nukleozydów, wykazały selektywną aktywność wobec komórek nowotworowych, m.in. raka piersi, prostaty czy neuroblastomy. Zastosowanie chemii „click" umożliwiło projektowanie makrocząsteczek o zwiększonej biodostępności i zdolności do celowanego działania przeciwnowotworowego.

Steroidowo-triazolowe pochodne kwasów żółciowych wykazały wyjątkową aktywność wobec *Mycobacterium tuberculosis* oraz pasożytów, takich jak *Leishmania*. Badania *in vivo* dowiodły, że niektóre koniugaty przewyższają działanie istniejących leków przeciwmalarycznych, takich jak chlorchicyna, zachowując przy tym niską toksyczność lub będąc całkowicie bezpieczne dla komórek ludzkich.

Koniugaty steroidowe odgrywają istotną rolę w syntezie nośników leków oraz materiałów supramolekularnych, takich jak hydrożele czy dendrymery. Dzięki ich właściwościom amfipatycznym możliwe jest precyzyjne dostarczanie leków przeciwnowotworowych, diagnostycznych czy przeciwbakteryjnych.

W artykułach [**P1**] i [**P4**] omówiono różnorodne możliwości zastosowań biokoniugatów steroidowych w chemii supramolekularnej, farmakologii i medycynie. Szczególną uwagę poświęcono skwalaminie, naturalnemu steroidowi izolowanemu z wątroby rekina (*Squalus acanthias*). Skwalamina, będąca biokoniugatem spermidyny

i 7α,24-dihydroksy-5α-cholestanu, wykazuje silne właściwości przeciwdrobnoustrojowe, przeciwwirusowe (w tym przeciw HIV) oraz przeciwnowotworowe. Badania wskazały na zdolność skwalaminy do hamowania angiogenezy, co spowalnia rozwój nowotworów płuc, piersi i jajników. W artykule podkreślono znaczenie modyfikacji chemicznych skwalaminy oraz jej pochodnych. Zastosowanie chemii „click" umożliwiło syntezę nowych koniugatów z pierścieniami triazolowymi, co zwiększyło ich stabilność oraz aktywność biologiczną. Opisano również koniugaty skwalaminy i kwasów żółciowych, które wykazały wysoką skuteczność wobec szczepów bakterii Gram-dodatnich i grzybów, takich jak *Candida albicans*. Ponadto, artykuł podkreśla rolę biokoniugatów steroidowych w syntezie nowych związków makrocyklicznych, takich jak organożele i receptory molekularne wykrywające biomarkery i kompleksujące cząsteczki gościa w układach biologicznych. Koniugaty kwasów żółciowych z flukonazolem wykazały prawie 100% skuteczność w zwalczaniu szczepów grzybów, takich jak *C. albicans* i *Sporothrix schenckii*. Doniesienia literaturowe wskazują na ogromny potencjał biokoniugatów steroidowych w opracowywaniu nowych leków celowanych, cząsteczek transportujących, jak również w terapii chorób przewlekłych i zakaźnych. Szczególny nacisk położono na możliwości precyzyjnego projektowania ich właściwości dzięki modyfikacjom chemicznym.

Artykuł przeglądowy [**P2**] podsumowuje szerokie zastosowanie biokoniugatów steroidowych w terapii chorób. Opisane związki naturalne, dzięki swojej unikalnej strukturze i właściwościom farmakologicznym, stanowią idealne nośniki bioaktywnych molekuł, takich jak aminokwasy, węglowodany czy peptydy. Połączenia te umożliwiają poprawę biodostępności, selektywności oraz ograniczenie toksyczności leków. Podkreślono szczególne znaczenie koniugatów steroidowych w terapii nowotworowej, zwłaszcza jako inhibitorów enzymów zaangażowanych w metabolizm steroidów (np. sulfotazy steroidowej) oraz jako środków wiążących receptory hormonalne. Koniugaty estradiolu z doksorubicyną wykazały zwiększoną skuteczność wobec komórek raka piersi zależnych od estrogenu. Ponadto glikozydy steroidowe, takie jak diosgenina, wykazały silne właściwości przeciwnowotworowe wobec komórek raka szyjki macicy. Kolejną istotną grupą są koniugaty steroidów z aminokwasami, które znajdują zastosowanie w terapii chorób neurodegeneracyjnych, takich jak choroba Alzheimera. Koniugaty sarsasapogeniny z aminokwasami wykazały potencjał neuroprotekcyjny poprzez hamowanie stresu oksydacyjnego i zwiększenie ekspresji neurotroficznych czynników wzrostu. Artykuł wskazuje także na potencjał steroidów w syntezie nowych hydrożeli i systemów dostarczania leków, co czyni je obiecującymi narzędziami w medycynie regeneracyjnej i nanotechnologii. Opisano m.in. steroidowe hydrożele do immobilizacji nanocząsteczek złota i srebra, co może mieć zastosowanie w terapii przeciwnowotworowej i diagnostyce.

Prace przeglądowe [**P1**], [**P2**] i [**P4**] podkreślają ogromny potencjał biokoniugatów steroidowych w rozwoju nowoczesnych leków. Ich wszechstronność, wynikająca z możliwości chemicznej modyfikacji, czyni je obiecującym narzędziem w walce z nowotworami, infekcjami i chorobami pasożytniczymi. Wyniki badań wskazują na konieczność dalszych prac nad ich właściwościami farmakologicznymi, aby w pełni wykorzystać ich potencjał terapeutyczny.

Opierając się na ogromnym spektrum doniesień literaturowych można postawić hipotezę, że sprzężenie szkieletu steroidowego kwasów żółciowych lub steroli z jednostką pierścienia 1,2,3-triazolową może prowadzić do otrzymania koniugatów o znacznym potencjale terapeutycznym.

Ze względu na dotychczasowy istotny wkład związków steroidowych w rozwój syntezy bioorganicznej cel pracy doktorskiej obejmował otrzymanie i charakterystykę:

(1) 12α-OAc i 7α-OAc,12α-OAc 3α-bromoacetoksy podstawionych pochodnych kwasu deoksycholowego i kwasu cholowego (**64**–**65**);
(2) 12α-OAc i 7α-OAc,12α-OAc 3α-azydoacetoksy podstawionych pochodnych kwasu deoksycholowego i kwasu cholowego (**67**–**68**);
(3) 12α-OAc i 7α-OAc,12α-OAc 3α-propargilowych podstawionych pochodnych kwasu deoksycholowego i kwasu cholowego (**78**–**79**);
(4) 3β-propargilowej pochodnej cholestanolu (**70**);
(5) dimerów steroidowych kwasów żółciowych i steroli zawierających układ 1,2,3-triazolowy (**71**–**76**);
(6) quasi-podandów kwasów żółciowych ze sztywną platformą pierścienia aromatycznego połączoną pierścieniami 1,2,3-triazolowymi (**82**–**85**);
(7) koniugatów steroidowo-pirymidynowych połączonych linkerami 1,2,3-triazolowymi (**93**–**103**);

W ramach rozszerzonej charakterystyki otrzymanych związków:

(8) przeprowadzono pełną analizę spektroskopową otrzymanych koniugatów steroidowych;
(9) wykonano obliczenia semiempiryczne z wykorzystaniem metody PM5;
(10) określono przewidywaną aktywność biologiczną *in silico* przy wykorzystaniu metody PASS;
(11) określono potencjalne powinowactwa otrzymanych koniugatów do miejsc aktywnych wybranych domen białkowych w celu oceny ich aktywności przeciwbakteryjnej, przeciwgrzybicznej oraz przeciwnowotworowej.

Uzyskane wyniki dostarczyły istotnych informacji na temat innowacyjnych biokoniugatów steroidowo-triazolowych i ich możliwego zastosowania terapeutycznego.

1. Dimery kwasów żółciowych i steroli

Głównym założeniem współczesnej chemii bioorganicznej jest projektowanie i synteza nowych związków o potencjalnych zastosowaniach farmakoterapeutycznych. Szczególną uwagę przykuwa wykorzystanie chemii „click", w tym reakcji cykloaddycji Huisgena, do tworzenia biokoniugatów steroidowych. W ramach przeprowadzonych badań zsyntetyzowano innowacyjne koniugaty kwasów żółciowych (stanowiących „ogon") i steroli (tzw. „głowa"), połączone za pomocą pierścienia 1,2,3-triazolu. Uzyskane związki zostały dokładnie scharakteryzowane metodami spektroskopowymi (NMR, FT-IR), spektrometrii mas (ESI-MS) oraz półempirycznymi i teoretycznymi obliczeniami chemicznymi, co pozwoliło ocenić ich potencjał terapeutyczny oraz stabilność fizykochemiczną [**P8**].

1.1. Synteza nowych biokoniugatów steroidowych

Dokonałam selektywnej syntezy bromoacetoksy podstawionych pochodnych kwasu litocholowego (**63**) lub acylowanych pochodnych kwasów deoksycholowego (**64**) i cholowego

(**65**) (Schemat 25). Prezentowane badania stanowią pierwsze raporty dotyczące syntezy i charakterystyki spektroskopowej związków kwasów deoksycholowego i cholowego, które znajdują szerokie zastosowanie w syntezie organicznej. Pochodne te zostały utworzone w wyniku reakcji odpowiedniego estru metylowego (lub 12α-OAc oraz 7α-OAc, 12α-OAc estru metylowego) z bromkiem kwasu bromooctowego w bezwodnym dichlorometanie.

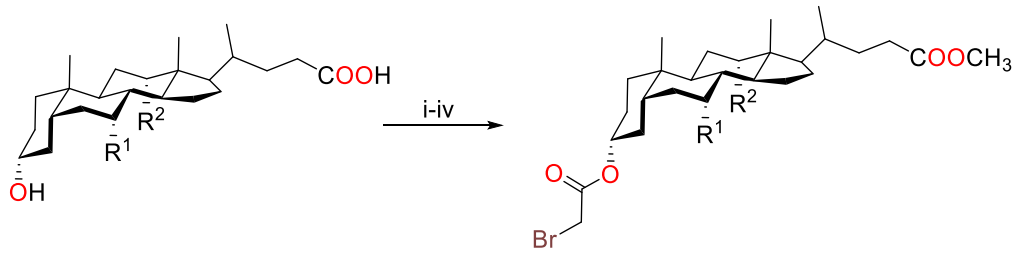

10-12 **63-65**

(i) MeOH, *p*- TsOH; (ii) Ac_2O, Py, DMAP (dla **11**&**12**); (iii) K_2CO_3, MeOH (dla **11**&**12**; (iv) $BrCH_2COBr$, $CH_2Cl_{2(bezw)}$

Nr	R^1	R^2	Wydajność [%]
63	H	H	98
64	H	OAc	92,7
65	OAc	OAc	70

Schemat 25. Synteza bromoacetoksy pochodnych kwasów żółciowych (**63**–**65**) [**P8**].

Warto podkreślić, że reaktywność grup hydroksylowych względem reakcji acetylowania, hydrolizy bądź redukcji wygląda następująco: 3α-OH > 7α-OH > 12α-OH. Wynika to z ekwatorialnego położenia grupy 3α-OH. W reakcjach tych wykazano jednocześnie, że stosowanie metanolu wobec czynnika zasadowego (K_2CO_3) prowadzi do selektywnej hydrolizy grup 3α-OAc, 7α-OAc, 12α-OAc (o ile są obecne).

W celu otrzymania azydoacetoksy podstawionych pochodnych kwasów żółciowych (**66**–**68**) przeprowadziłam reakcję substytucji nukleofilowej (S_N2). Odpowiednie halogenoacetoksy podstawione pochodne steroidów (**63**–**65**) sprzężono z azydkiem sodu w obecności aprotycznego rozpuszczalnika (THF) i w podwyższonej temperaturze (50°C), uzyskując wysokie wydajności reakcji (do 95 %) (Schemat 26).

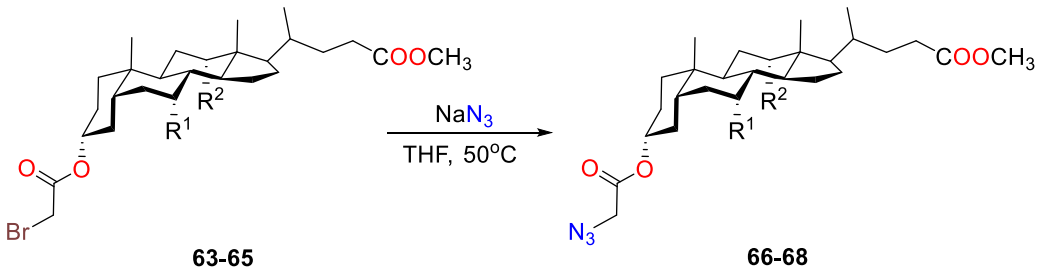

63-65 66-68

Nr	R^1	R^2	Wydajność [%]
66	H	H	95
67	H	OAc	88,6
68	OAc	OAc	78

Schemat 26. Synteza azydoacetoksy pochodnych kwasów żółciowych (**66**–**68**) [**P8**].

W wyniku estryfikacji steroli z udziałem kwasu propargilowego i katalitycznej ilości *p*-TsOH otrzymano terminalne alkiny cholesterolu i cholestanolu (**69**–**70**) (Schemat 27). Aktywacja tych steroidów zwiększyła ich elektrofilowość, co było niezbędne przed kluczową reakcją „click".

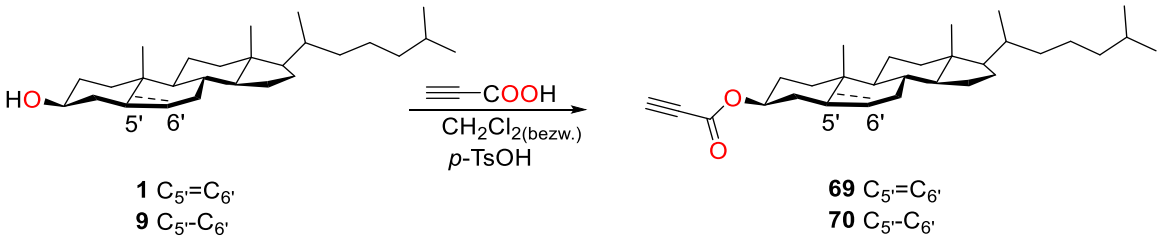

1 $C_{5'}$=$C_{6'}$
9 $C_{5'}$-$C_{6'}$

69 $C_{5'}$=$C_{6'}$
70 $C_{5'}$-$C_{6'}$

Schemat 27. Synteza alkinowych pochodnych steroli (**69**–**70**) [**P8**].

Zaprojektowane warunki syntez otrzymywania bromoacetoksypochodnych estrów metylowych pochodnych kwasów litocholowego, deoksycholowego oraz cholowego, jak również propargilowych pochodnych steroli opisano po raz pierwszy w pracy [**P8**]. Z analizy danych literaturowych wynika, że nie podjęto również wcześniej prób ich syntez, podobnie jak azydków steroidowych, dlatego dla związków (**64**), (**65**), (**67**), (**68**) i (**70**) przeprowadzono pełną charakterystykę spektroskopową.

3α-azydoacetoksy pochodne kwasów żółciowych (**66**–**68**) oraz 3β-propargilowe pochodne steroli (**69**–**70**) zastosowałam jako substraty w syntezie nowych biokoniugatów steroidowych połączonych pierścieniem 1,2,3-triazolowym. W warunkach reakcji specyficznych dla metody „click", tj. przy użyciu pięciowodnego siarczanu miedzi(II), askorbinianu sodu, w mieszaninie rozpuszczalników *tert*-butanol/woda (5:1) oraz w temperaturze nieprzekraczającej 65°C otrzymano z zadowalającą wydajnością

(51–80%) nieznane dotąd w literaturze chemicznej biokoniugaty kwasów żółciowych (**71**–**76**) ze sterolami o właściwościach proleków (Schemat 28).

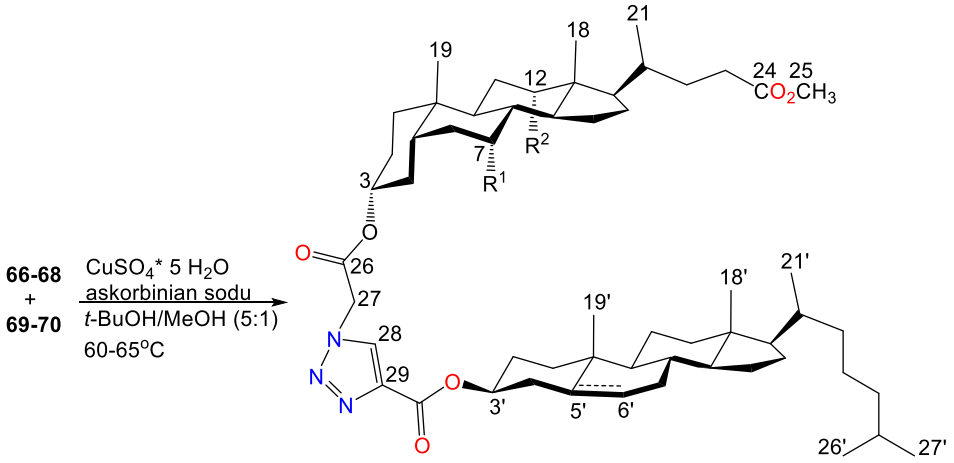

Nr	R^1	R^2	$C_{5'}$---$C_{6'}$	Wydajność [%]
71	H	H	$C_{5'}$=$C_{6'}$	79,7
72	H	OAc	$C_{5'}$=$C_{6'}$	55,7
73	OAc	OAc	$C_{5'}$=$C_{6'}$	60
74	H	H	$C_{5'}$–$C_{6'}$	51
75	H	OAc	$C_{5'}$–$C_{6'}$	53
76	OAc	OAc	$C_{5'}$–$C_{6'}$	52

Schemat 28. Synteza koniugatów kwasów żółciowych i steroli połączonych pierścieniem 1,2,3-triazolowym (**71**–**76**) [**P8**].

Wszystkie powyższe biokoniugaty zostały scharakteryzowane spektroskopowo (^{1}H NMR, ^{13}C NMR, FT-IR) i spektrometrycznie (ESI-MS). Stałe przesiewowe dla atomów ^{13}C i ^{1}H obliczono i przeanalizowano metodą GIAO/B3LYP/6–311G (d,p). Teoretyczne parametry porównano z uzyskanymi parametrami eksperymentalnymi otrzymując bardzo dobre rezultaty. W badaniach *in silico* wyznaczono aktywność farmakologiczną badanych związków oraz przeprowadzono dokowanie molekularne (domeny białkowe: 2Q85, 1KZN, 1EZF) [**P8**].

1.2. Analiza spektroskopowa

Na widmach ^{1}H NMR związków (**71**–**76**) zaobserwowano diagnostyczne przesunięcia chemiczne w postaci singletów w zakresie 8,24–8,20 ppm pochodzące od protonu obecnego w pierścieniach 1,2,3-triazolowych (Rys. 22). Z kolei sygnały wskazujące na położenie protonów grupy metylenowej 3α-OCO–CH_2–triazol są obecne w zakresie 5,22–5,17 ppm. Widoczne przesunięcia chemiczne położone przy 5,04–4,86 ppm odpowiadają protonom przyłączonym w pozycjach 3'α-H w szkielecie sterolu oraz 3β-H w szkielecie kwasów żółciowych. Sygnały pochodzące od protonów związanych z grupami acetylowymi 7α-$OCOCH_3$ oraz 12α-$OCOCH_3$ zaobserwowano jako singlety w zakresie 2,14–2,09 ppm dla wszystkich koniugatów. Natomiast przy 1,05–0,65 ppm zdiagnozowano charakterystyczne przesunięcia chemiczne odpowiadające protonom z grup metylowych CH_3-18/18' (singlet), CH_3-19/19' (singlet) i CH_3-21/21' (dublet) połączonych z rdzeniem steroidowym, jak również CH_3-26' i CH_3-27' obecne w rozgałęzionym łańcuchu bocznym wyłącznie sterolu.

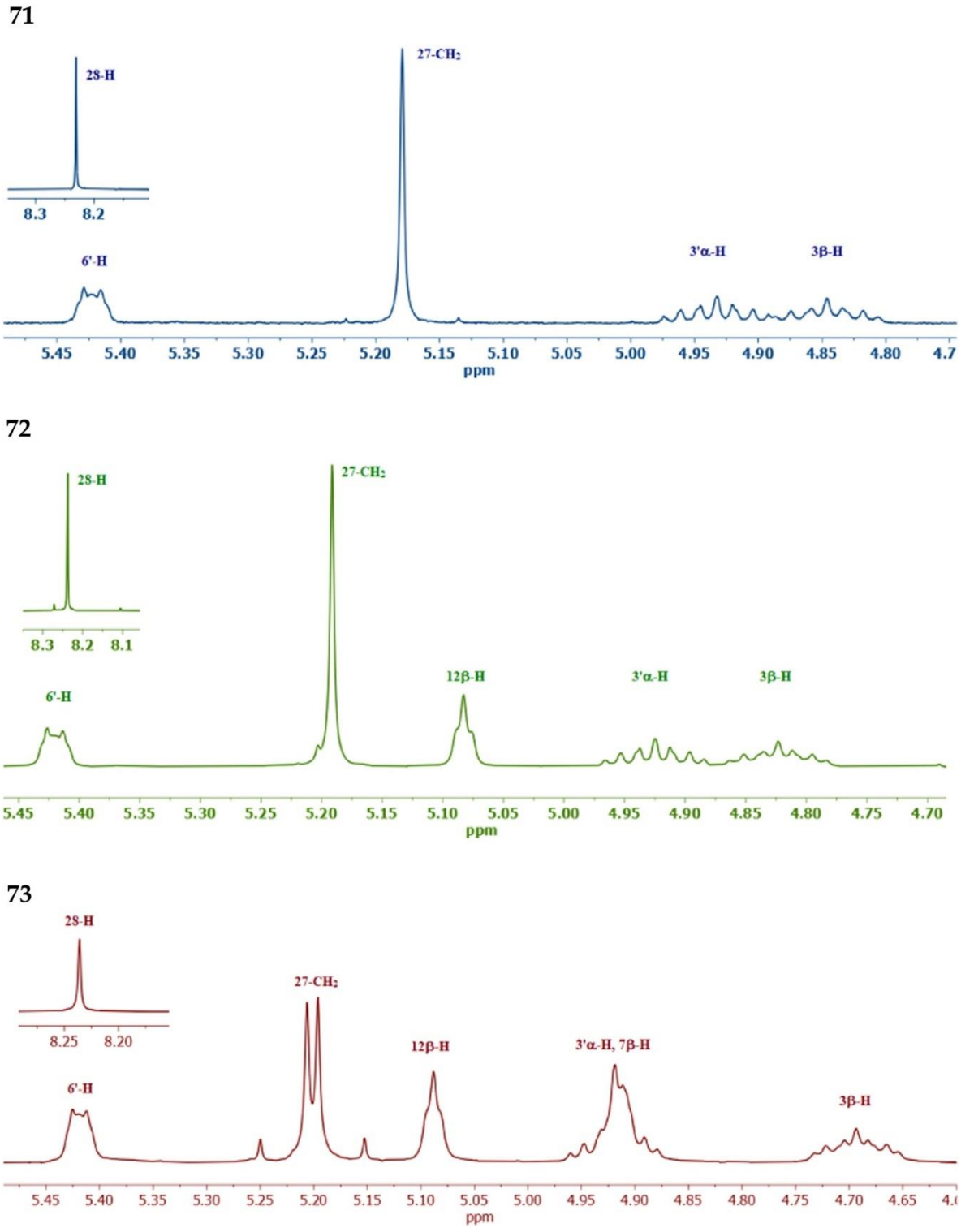

Rysunek 22. Fragmenty widm ^{1}H NMR związków (**71**–**73**) w zakresie diagnostycznych przesunięć chemicznych [**P8**].

Na podstawie interpretacji wykonanych widm ^{13}C NMR stwierdzono, że sygnały przesunięte w kierunku wyższych wartości ppm pochodzą od atomów węgla grup karbonylowych, obecnych zarówno w grupie estrowej przy atomach C-24 (174,73–174,47 ppm), jak i przy atomach 12α-OCO (170,45–170,40 ppm) oraz przy atomach 7α-OCO

(170,28–170,22 ppm). Dla wszystkich biokoniugatów steroidowych w zakresie 128,83–128,74 ppm zaobserwowano sygnał związany z triazolowym atomem węgla. Sygnały w zakresie 77,48–75,15 ppm skorelowano z atomami węgla połączonymi z atomem tlenu przy C-3/3', C-7 i C-12 w szkielecie steroidowym. Z kolei przesunięcia atomów węgla z grup metylowych, tj. C-18/18', C-19/19', C-21/21', C-26' i C-27' szkieletu steroidowego zaobserwowano przy najniższych wartościach (22,94–12,02 ppm) (Rys. 23).

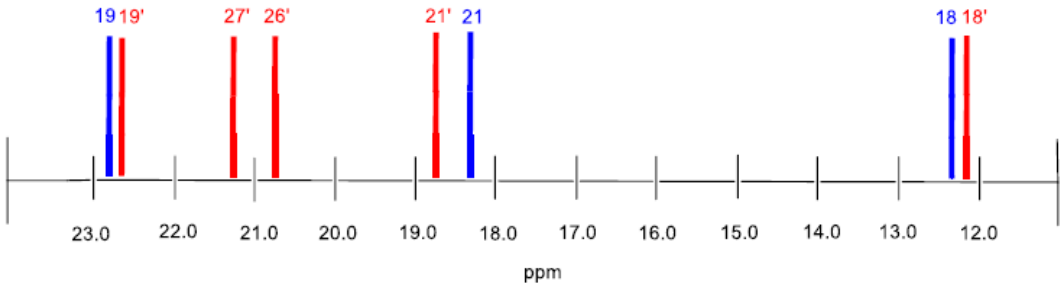

Rysunek 23. Fragment widma ^{13}C NMR pochodnej kwasu litocholowego i cholesterolu (**71**) [**P8**].

Charakterystyczne pasma w widmach FT-IR wskazywały na obecność kluczowych grup funkcyjnych. W wyniku dokładnej analizy widm substratów i otrzymanych w reakcji „click" produktów, dla obu grup związków (tj. substratów i produktów) pasma w zakresie 1753–1738 cm^{-1} odpowiadały drganiom atomów węgla grup karbonylowych. Jednocześnie na podstawie porównania tych widm oraz z uwagi na nieobecność charakterystycznych dla grup propargilowych i azydkowych pasm w zakresie 2111–2106 cm^{-1} na analizowanych widmach koniugatów (**71**–**76**) zweryfikowano ich otrzymanie.

Przeprowadzona analiza spektrometryczna ESI-MS potwierdziła masy cząsteczkowe zsyntetyzowanych koniugatów kwasów żółciowych i steroli. Na postawie widm masowych wszystkich nowych związków udowodniono obecność ich głównych jonów o większym powinowactwie do jonów sodu $[M+Na]^+$, a o mniejszej intensywności związanej jonami potasu $[M+K]^+$.

Oddziaływania między- i wewnątrzcząsteczkowe oraz konformacje cząsteczek zostały szczegółowo zbadane poprzez porównanie danych eksperymentalnych, uzyskanych w fazie skondensowanej, z wynikami obliczeń wykonanych dla fazy gazowej. W analizie porównano eksperymentalne przesunięcia chemiczne (^{1}H i ^{13}C NMR) z wartościami obliczonymi dla wybranego biokoniugatu, wykorzystując metodę GIAO. Otrzymane korelacje były liniowe i opisane równaniem $\delta_{exp}=a+b\sigma_{calc}$, gdzie wartości parametrów wynosiły odpowiednio: dla ^{13}C a=216,9071 i b=–1,848, a dla ^{1}H a=30,6665 i b=–0,9303. Wysokie współczynniki determinacji (r^2=0,9942 dla ^{13}C NMR oraz r^2=0,9905 dla ^{1}H NMR) potwierdzają poprawność zoptymalizowanej geometrii cząsteczek (Rys. 24).

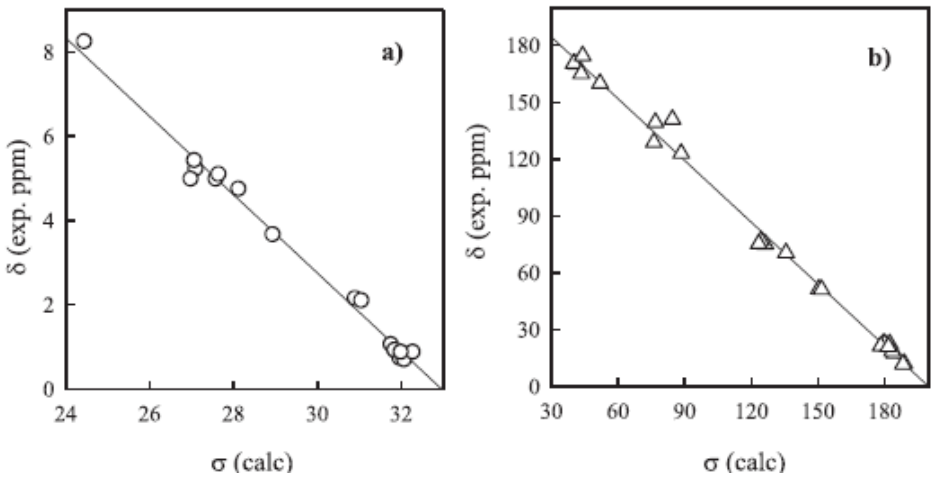

Rysunek 24. Eksperymentalne przesunięcia chemiczne (δ_{exp}, $CDCl_3$) w związku (**73**) w funkcji izotropowych stałych ekranowania magnetycznego (σ_{calc}) z obliczeń GIAO/B3LYP/6–311G(d,p); (a) protony i (b) atomy węgla-13 [**P8**].

1.3. Obliczenia semiempiryczne (PM5)

PM5 jest metodą półempiryczną stosowaną w chemii kwantowej, umożliwiającą szybkie i efektywne modelowanie struktur molekularnych oraz ich właściwości. Wykorzystuje uproszczone równania Schrödingera, uzupełnione o parametry empiryczne, dodane na podstawie wyników eksperymentalnych i dokładnych obliczeń *ab initio*.

Obliczenia metodą PM5 odegrały kluczową rolę w analizie właściwości fizykochemicznych i strukturalnych otrzymanych biokoniugatów kwasów żółciowych i steroli (Tabela 1). Zoptymalizowana geometria cząsteczek posłużyła do analiz dokowania molekularnego. Wartości ciepła tworzenia (HOF) niektórych struktur biokoniugatów, uzyskane w obliczeniach metodą PM5, są wynikiem kilku kluczowych czynników związanych z ich strukturą molekularną i właściwościami chemicznymi. W biokoniugatach zawierających pierścień 1,2,3-triazolowy oraz liczne podstawniki (np. grupy acetylowe) obserwuje się duże oddziaływania steryczne między fragmentami cząsteczki. Pierścień triazolowy odgrywa kluczową rolę w rozkładzie elektronów w cząsteczce. Jego zdolność do sprzężenia π–π z innymi elementami struktury może zarówno stabilizować, jak i destabilizować cząsteczkę, w zależności od rozmieszczenia grup funkcyjnych. Warto zauważyć, że wartość ciepła tworzenia HOF maleje wraz ze wzrostem grup estrowych, dlatego też za najbardziej stabilny energetycznie związek można uznać biokoniugaty kwasu cholowego (**73**) i (**76**). Porównując pochodne steroli należy uwzględnić wpływ obecnego wiązania podwójnego przy atomach węgla $C_{5'}$=$C_{6'}$ w cząsteczce cholesterolu, wskutek którego jego związki wykazywały minimalnie niższą trwałość (Rys. 25). Zastosowanie fragmentów sterolowych i kwasów żółciowych prowadzi do uzyskania struktur o mieszanym charakterze hydrofobowym i hydrofilowym. Tego typu właściwości mogą powodować lokalne napięcia w strukturze cząsteczki, wpływając na jej stabilność energetyczną. Wskazują również, które elementy strukturalne mogą być modyfikowane w przyszłych badaniach, aby uzyskać bardziej stabilne i potencjalnie bioaktywne związki.

a)

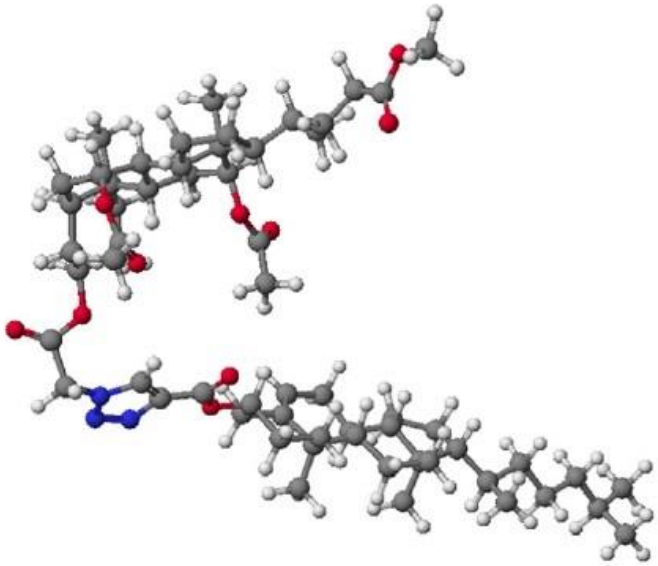

b)

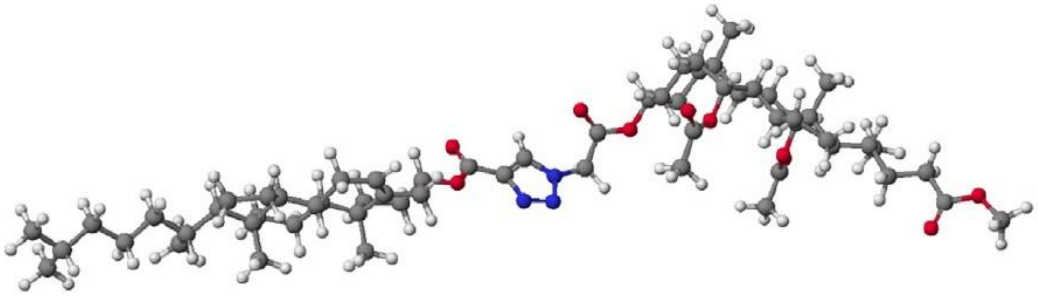

Rysunek 25. Model molekularny w konformacji *syn* (**a**) oraz *anti* (**b**) pochodnej kwasu cholowego i cholesterolu (**73**) [**P8**].

Tabela 1. Ciepło tworzenia (HOF) [kcal/mol] kwasów żółciowych, steroli i koniugatów steroidowych [**P8**].

Nr	HOF	HOF_{syn}	HOF_{anti}	ΔHOF_1	ΔHOF_2	ΔHOF_3	ΔHOF_4
10	–229,2756	–	–	–	–	–	–
11	–266,8560	–	–	–	–	–	–
12	–309,8662	–	–	–	–	–	–
1	–145,2016	–	–	–	–	–	–
9	–167,9130	–	–	–	–	–	–
71	–	–370,9984	–370,8825	–141,7228	–141,6069	–225,7968	–225,6809
72	–	–448,9483	–456,2749	–182,0923	–189,4189	–303,7467	–311,0733
73	–	–533,3628	–542,0610	–223,4966	–232,1948	–388,1612	–396,8450
74	–	–394,2004	–393,6084	–164,9248	–164,3328	–226,2874	–225,6954
75	–	–471,8692	–479,4003	–205,0132	–212,5443	–3,039,562	–311,4873
76	–	–557,2032	–557,2743	–247,3370	–247,4081	–389,2902	–389,3613

$\Delta HOF_1 = HOF_{\text{koniugaty } syn}$ (**71**–**76**) $–HOF_{\text{kwasy żółciowe}}$ (**7**–**9**). $\Delta HOF_2 = HOF_{\text{koniugaty } anti}$ (**71**–**76**) $–HOF_{\text{kwasy żółciowe}}$ (**10**–**12**). $\Delta HOF_3 = HOF_{\text{koniugaty } syn}$(**71**–**76**) $–HOF_{\text{sterole}}$(**1**, **9**). $\Delta HOF_4 = HOF_{\text{koniugaty } anti}$ (**71**–**76**) $–HOF_{\text{sterole}}$(**1**, **9**).

1.4. Aktywność biologiczna

Badania *in silico* metodą PASS

Synteza i izolacja nowych związków chemicznych, jak również modyfikacja struktury już znanych połączeń, wymagają oceny ich właściwości farmakologicznych oraz potencjalnego działania toksycznego. Tradycyjne badania *in vitro*, a następnie *in vivo*, są jednak czasochłonne i kosztowne. W związku z tym coraz większą rolę odgrywają analizy *in silico*, przeprowadzane z wykorzystaniem narzędzi takich jak program PASS.

Metoda ta pozwala nie tylko na skrócenie czasu poszukiwań biologicznie aktywnych związków, lecz także na wskazanie ich potencjalnych właściwości biologicznych. Dzięki temu możliwe jest szybsze wytypowanie prawdopodobnych związków do dalszych badań farmakologicznych. Program PASS, opierając się na strukturze cząsteczki, przewiduje zarówno jej potencjalne działanie farmakologiczne, jak i toksyczne. Mechanizm działania programu polega na porównaniu struktury badanego związku z danymi zawartymi w obszernej bazie, obejmującej około 1 000 000 biologicznie aktywnych związków i 5500 różnych aktywności biologicznych.

Program PASS znajduje szczególne zastosowanie przy analizie związków zawierających elementy substancji pochodzenia naturalnego lub metabolitów wtórnych. Narzędzie to oblicza prawdopodobieństwo wystąpienia danej aktywności biologicznej (PA) oraz jej braku (PI). Wysokie wartości PA (> 0,7) wskazują na duże prawdopodobieństwo potwierdzenia aktywności w badaniach eksperymentalnych. Dla wartości PA w przedziale 0,5–0,7 szansa ta jest mniejsza, a przy PA < 0,5 jest ona bardzo niska.

Warto również zauważyć, że obecność elementów znanych i aktywnych biologicznie w strukturze badanego związku zwiększa prawdopodobieństwo potwierdzenia aktywności biologicznej. Założenia te czynią program PASS niezwykle przydatnym narzędziem w procesie diagnozowania potencjalnych właściwości farmakologicznych.

Bazując na wynikach testów *in silico* uzyskanych dla otrzymanych koniugatów steroidowych można wnioskować o ich zróżnicowanych właściwościach biologicznych. Istnieje wysokie prawdopodobieństwo wykazywania przez cząsteczki działania przeciwbakteryjnego oraz przeciwgrzybicznego. Wiąże się to z interakcjami z lipidowymi strukturami błon komórkowych drobnoustrojów prowadzących do ich destabilizacji. Biokoniugaty wykazują przewidywane właściwości antagonistyczne wobec cholesterolu. W Tabeli 2 pokazano wybrane przewidywane aktywności biologiczne koniugatów (**71**–**76**).

Tabela 2. Przewidywana aktywność biologiczna wybranych koniugatów [**P8**].

PA > 0,70	**71**	**72**	**73**	**74**	**75**	**76**
Inhibitor gliceryloeteromonooksygenazy	–	0,71	0,75	0,72	0,75	0,79
Antagonista cholesterolu	0,84	0,76	0,76	0,71	–	–
Hipolipidemia	0,76	0,78	0,85	–	–	0,78
Antyhipercholesterolemia	0,73	–	0,75	–	–	–
Zapalenie trzustki	0,83	0,80	0,79	0,90	0,86	0,84

Aktywność przeciwbakteryjna

Badania dokowania molekularnego wykazały, że biokoniugaty mają zdolność do oddziaływania z białkami kluczowymi dla metabolizmu bakterii (Rys. 26). Szczególną uwagę zwrócono na zdolność do hamowania wzrostu bakterii Gram-dodatnich i Gram-ujemnych. Wśród analizowanych drobnoustrojów znalazły się:

- *Escherichia coli* – bakteria Gram-ujemna związana z zakażeniami dróg moczowych, przewodu pokarmowego i ran [126].
- *Staphylococcus aureus* – bakteria Gram-dodatnia odpowiedzialna za poważne zakażenia skórne, a także infekcje szpitalne [127].

Wyniki wskazują, że aktywność przeciwbakteryjna koniugatów jest ograniczona, jednak stwarzają perspektywę do dalszych modyfikacji chemicznych w celu zwiększenia ich skuteczności.

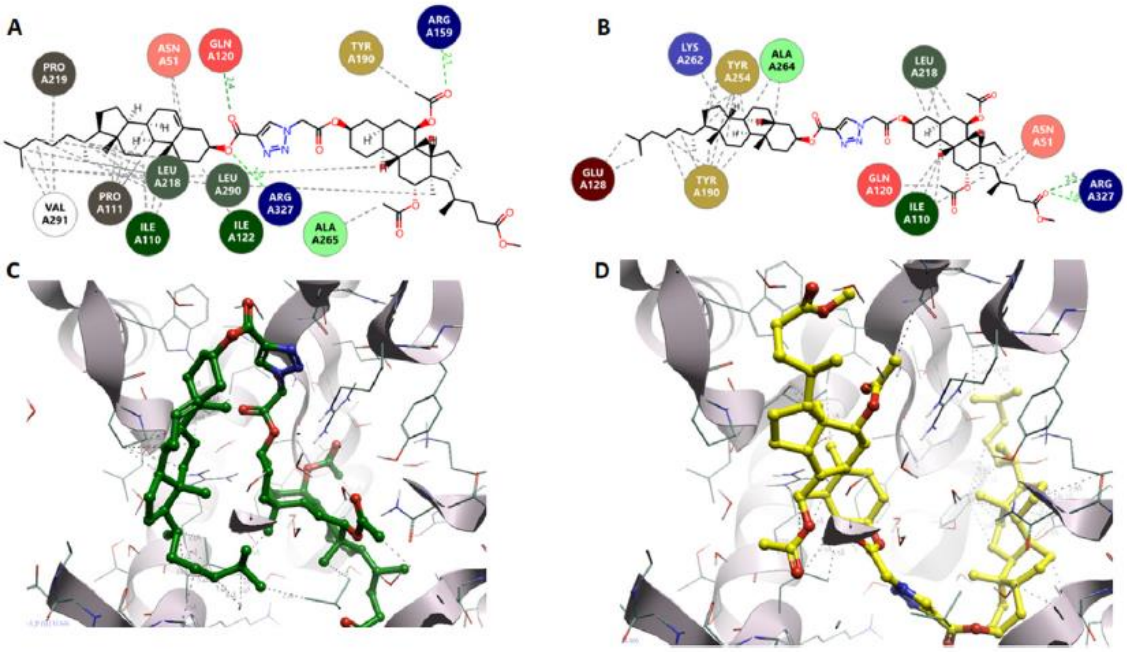

Rysunek 26. Interakcje ligandów i sposób wiązania dla związków (**73**) i (**76**) w 2Q85. A, C – oznacza ligand (**73**) (zielony); B, D – oznacza ligand (**76**) (żółty) [**P8**].

Aktywność przeciwgrzybiczna

Wykazano wyraźnie większe działanie przeciwgrzybiczne w porównaniu z działaniem przeciwbakteryjnym otrzymanych biokoniugatów steroidowych (**71**–**76**). Najsilniejszą aktywność przeciwgrzybiczną zaobserwowano wobec następujących szczepów grzybów:

- *Candida albicans* – grzyb odpowiedzialny za infekcje kandydozowe, szczególnie u osób z obniżoną odpornością [128].
- *Aspergillus niger* – pleśń mogąca wywoływać choroby płuc, w tym aspergilozę [129].
- *Cryptococcus neoformans* – drożdżak związany z ciężkimi zakażeniami ośrodkowego układu nerwowego u pacjentów z HIV/AIDS [130].

Koniugaty działają na kluczowe enzymy grzybów, co wskazuje na ich potencjał jako inhibitorów specyficznych szlaków metabolicznych.

Obecność pierścienia 1,2,3-triazolowego oraz właściwości amfifilowe związków mogą zakłócać funkcjonowanie błon komórkowych drobnoustrojów, prowadząc do ich uszkodzenia. Dokowanie molekularne sugeruje, że zsyntetyzowane koniugaty mogą wiązać się z enzymami odpowiedzialnymi za syntezę ściany komórkowej drobnoustrojów oraz za procesy metaboliczne, co prowadzi do ich dezaktywacji (Rys. 27).

Dzięki swojej chemicznej strukturze koniugaty są odporne na degradację enzymatyczną, co zwiększa ich trwałość w środowisku biologicznym i potencjalnie wydłuża czas działania. Ich potencjalne zastosowania obejmują terapie antygrzybiczne szczególnie w zakażeniach wywołanych przez *Candida albicans* oraz możliwość wykorzystania ich jako składników preparatów przeciwdrobnoustrojowych o szerokim spektrum działania.

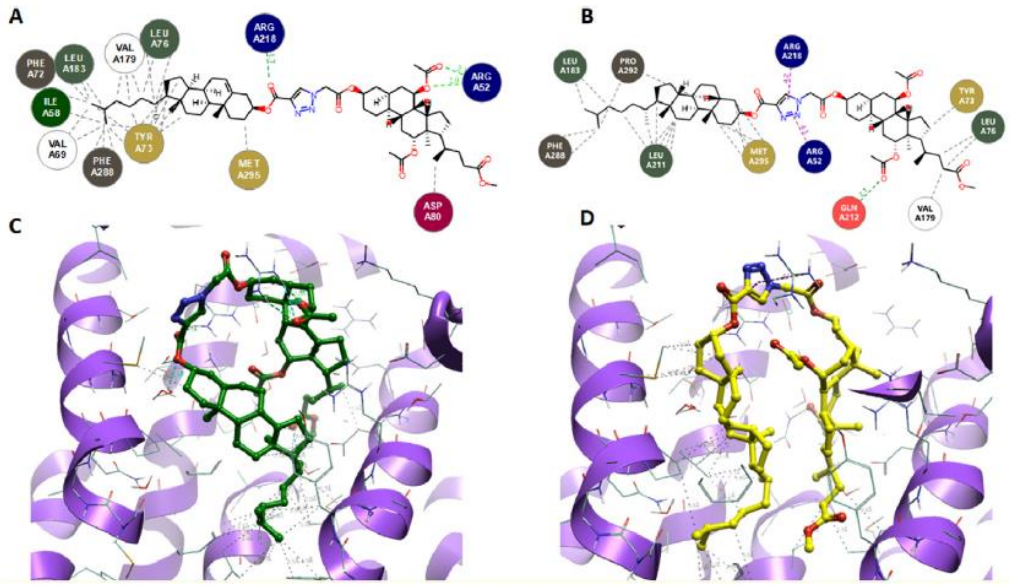

Rysunek 27. Interakcje ligandów i sposób wiązania dla związków (**73**) i (**76**) w 1EZF. A, C – oznacza ligand (**73**) (zielony); B, D – oznacza ligand (**76**) (żółty) [**P8**].

Zdolność koniugatów do wykazywania selektywnego działania przeciwko wybranym szczepom drobnoustrojów, szczególnie grzybów, czyni je obiecującymi kandydatami do dalszych badań. Ich stabilność chemiczna i specyficzne mechanizmy działania otwierają nowe możliwości terapeutyczne, zwłaszcza w kontekście rosnącej oporności drobnoustrojów na istniejące leki.

2. Quasi-podandy kwasów żółciowych

2.1. Synteza tripodstawionych pochodnych kwasów żółciowych

Zachęcona powyższym sukcesem przeprowadziłam reakcje syntezy quasi-podandów pochodnych kwasów żółciowych zawierających w strukturze pierścienie 1,2,3-triazolowe [**P6**]. Otrzymałam i przeanalizowałam właściwości fizykochemiczne propargilowej (**77**) oraz nowoopracowanych syntez 12α-acetoksy– oraz 7α,12α-diacetoksy propargilowych pochodnych kwasów żółciowych (**78**–**79**) (Schemat 29). Opierając się na założeniach chemii „click", stanowiącej podstawową metodę nowoczesnej syntezy organicznej, zaprojektowałam reakcję otrzymywania wielkocząsteczkowych związków zawierających pierścienie 1,2,3-triazolowe (**82**–**85**). Tego typu układy cechuje stabilność w polarnych rozpuszczalnikach, wysoka odporność na procesy redukcji i utleniania oraz aktywność w tworzeniu wiązań wodorowych zwiększających ich trwałość.

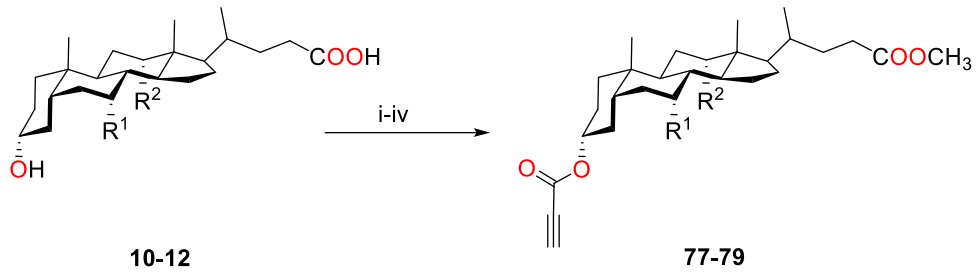

10-12 **77-79**

(i) MeOH, *p*-TsOH; (ii) Ac_2O, Py, DMAP (dla **11**&**12**); (iii) K_2CO_3, MeOH (dla **11**&**12**); (iv) CHCCOOH, $CH_2Cl_{2(bezw.)}$, *p*-TsOH

Nr	R^1	R^2	Wydajność [%]
77	H	H	49
78	H	OAc	57
79	OAc	OAc	30

Schemat 29. Wprowadzenie grupy alkinowej w pozycję C-3 szkieletu steroidowego kwasów żółciowych [**P6**].

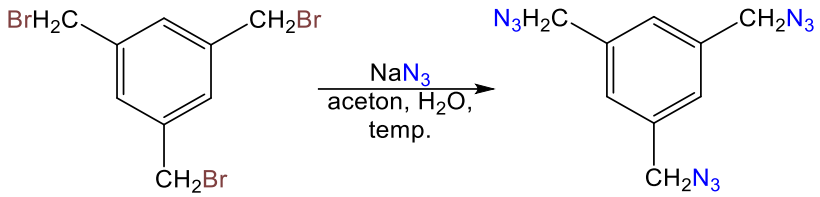

80 **81**

Schemat 30. Synteza 1,3,5-tris(azydometyleno)benzenu (**81**) [**P6**].

Serię quasi-podandów zsyntetyzowałam w reakcji estrów (lub acetylowanych estrów, nieznanych jak dotąd w literaturze) propargilowych kwasów żółciowych z 1,3,5-tris(azydometyleno)benzenem w mieszaninie *tert*-BuOH/H_2O, z dodatkiem $CuSO_4$*$5H_2O$, askorbinianu sodu i w podwyższonej temperaturze (65°C). Na Rysunku 28 przedstawiono wszystkie tripodstawione koniugaty otrzymane z wysoką wydajnością. Ponadto, wyizolowano również dipodstawioną pochodną kwasu litocholowego (**82**) (Rys. 28). Monopodstawione pochodne kwasów żółciowych sprzężone z pierścieniem 1,2,3-triazolowym (z dwiema grupami azydkowymi N_3) nie powstają ze względu na ich niską trwałość. Otrzymanie dipodstawionych pochodnych występuje sporadycznie. Warto podkreślić, że opisaną dipodstawioną pochodną kwasu litocholowego (**82**) charakteryzuje wyższa wartość HOF w porównaniu z tripodstawioną pochodną tego kwasu (**83**), co świadczy o jej niestabilności (Tabela 3).

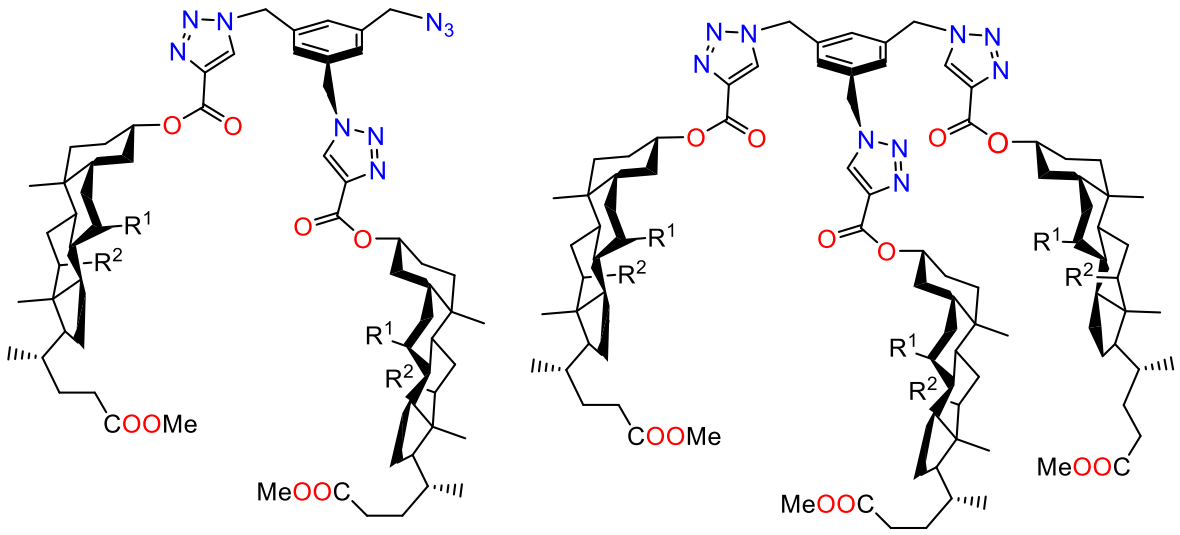

82 83-85

Nr	R^1	R^2	Wydajność [%]
82	H	H	11
83	H	H	88
84	H	OAc	77
85	OAc	OAc	57

Rysunek 28. Quasi-podandy kwasów żółciowych zawierające układy 1,2,3-triazolowe [**P6**].

Zastosowanie reakcji 1,3-dipolarnej cykloaddycji (reakcji Huisgena) wykorzystującej katalityczne ilości miedzi(I) okazało się niezmiennie atrakcyjną i selektywną metodą syntezy pierścieni 1,2,3-triazolowych.

Zaprojektowane powyżej biokoniugaty (**82**–**85**) posiadają wbudowaną sztywną platformę pierścienia aromatycznego. Sprawia to, że ich cząsteczki będą sprawniej przyjmowały odpowiednią konformację. Płaski pierścień benzenowy może determinować wchodzenie w interakcje z powierzchnią biopolimerów, jak również stanowić swego rodzaju kotwicę w układach biologicznych.

Identyfikacja i scharakteryzowanie sześciu nowych związków (**78**, **79**) oraz (**82**–**85**) obejmowały wszechstronną analizę za pomocą technik spektralnych (^{1}H NMR, ^{13}C NMR, FT-IR), spektrometrii mas (ESI-MS) i metody semiempirycznej PM5 [**P6**].

2.2. Analiza spektroskopowa

Charakterystyka spektroskopowa dostarczyła kluczowych informacji o strukturze związków, potwierdzając obecność pierścienia 1,2,3-triazolowego. Na widmach wszystkich koniugatów kwasów żółciowych zaobserwowano diagnostyczne przesunięcia chemiczne w zakresie 8,10–8,06 ppm odpowiadające protonom obecnym w pierścieniach 1,2,3-triazolowych. Ponadto w widmie ^{1}H NMR związku (**82**) widoczne jest istotne dla

identyfikacji przesunięcie chemiczne w postaci singletu przy 8,06 ppm, które można przypisać dwóm protonom pierścieni triazolowych, co świadczy o otrzymaniu dipodstawionej triazolowej pochodnej kwasu litocholowego. Co więcej, w widmach tego związku zaobserwowano również charakterystyczny sygnał przy 4,37 ppm, który można przypisać protonom z grupy $-CH_2-N_3$ (Rys. 29). Przesunięcia chemiczne w zakresie 5,09–4,81 ppm przypisano protonom 3β-H, 7β-H i 12β-H w szkielecie steroidowym. Natomiast sygnały przy niższych wartościach (0,95–0,73 ppm) pochodziły od protonów z grup metylowych CH_3-21, CH_3-19 i CH_3-18.

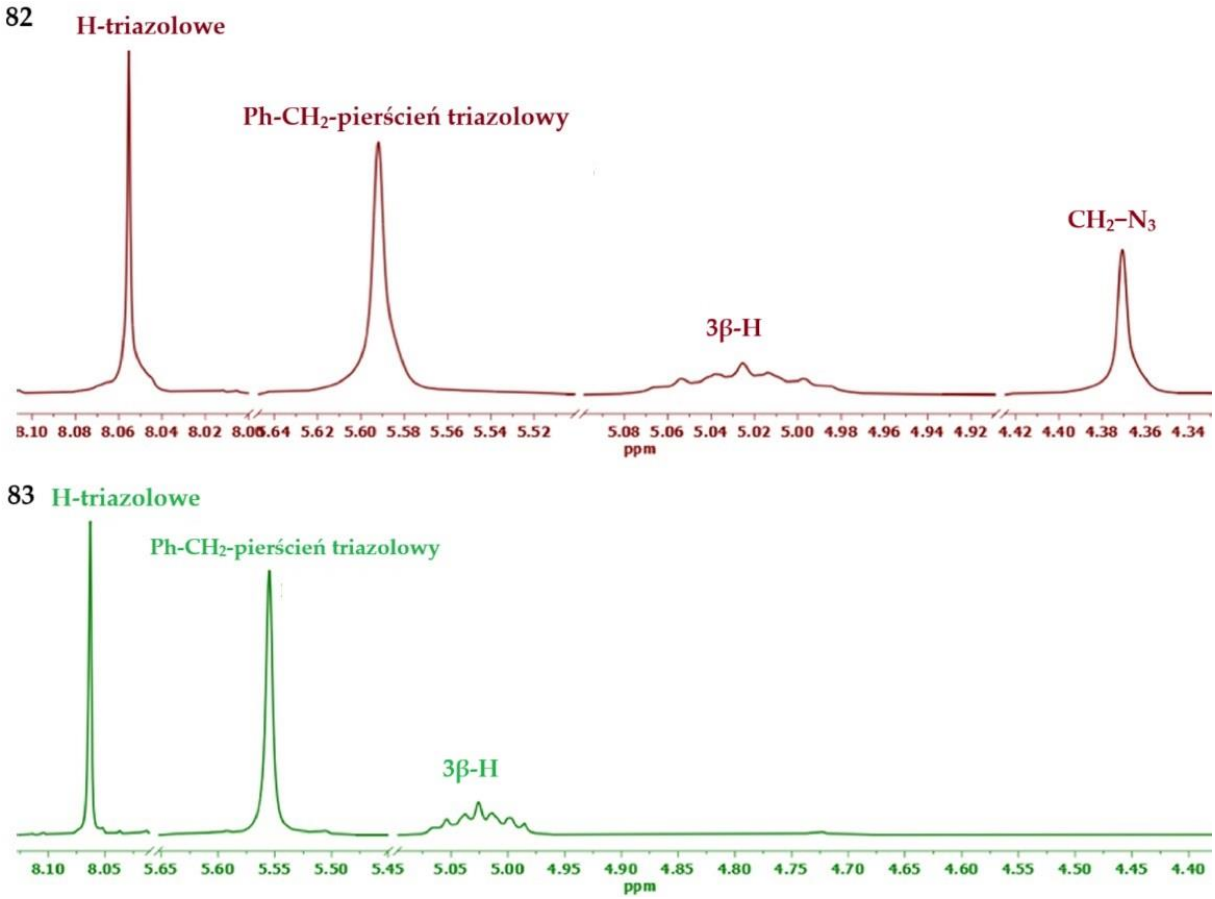

Rysunek 29. Porównanie sygnałów zaobserwowanych na widmach ^{1}H NMR di- (**82**) i tripodstawionej (**83**) pochodnej kwasu litocholowego [**P6**].

Z kolei na wszystkich widmach ^{13}C NMR zidentyfikowano charakterystyczny sygnał z zakresie 129,5–123,8 ppm wskazujący na atom węgla z pierścienia 1,2,3-triazolowego. Przesunięcia odpowiadające atomom węgla z grup karbonylowch obecnych w cząsteczkach koniugatów zaobserwowano przy najwyższych wartościach (172,50–170,17 ppm). Niezmiennie, sygnały pochodzące od atomów węgla z grup metylowych, takich jak C-21, C-19 i C-21 połączonych bezpośrednio ze rdzeniem steroidowym kwasów żółciowych były widoczne przy w zakresie 23–10 ppm.

W widmach FT-IR zaobserwowano charakterystyczne pasma dla kluczowych grup funkcyjnych. Grupy karbonylowe (C=O) dawały intensywne pasma w zakresie

1745–1730 cm^{-1}, co potwierdza obecność estrów acetylowych. W przypadku propargilowych pochodnych kwasów żółciowych zaobserwowano pasma w zakresie 2120–2100 cm^{-1}, których nie odnotowano dla wykonanych widm FT-IR otrzymanych tripodstawionych triazolowych koniugatów steroidowych. W przypadku dipodstawionego koniugatu kwasu litocholowego (**82**) dostrzeżono pasmo pochodzące od grupy azydkowej N_3 przy liczbie falowej 2099 cm^{-1} (Rys. 30).

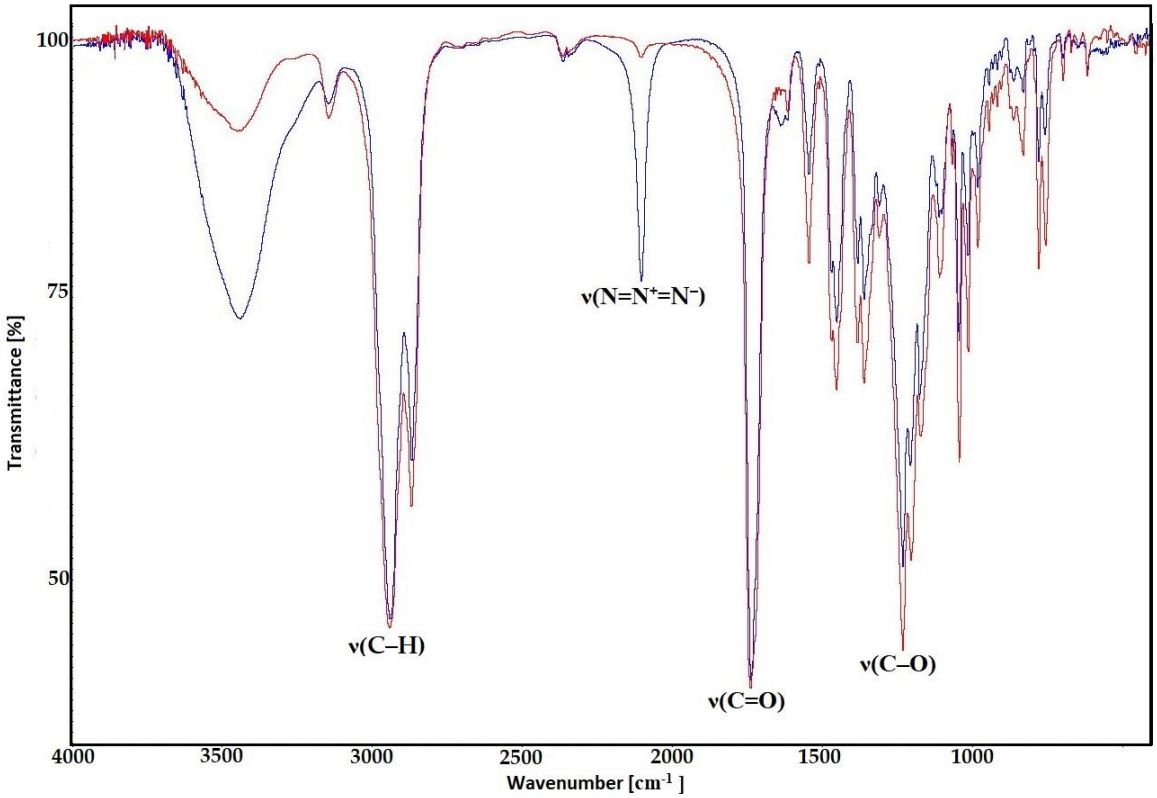

Rysunek 30. Porównanie otrzymanych widm FT-IR związku (**82**) (z grupą N_3, niebieski) oraz pozostałych związków (**83**–**85**) (czerwony) [**P6**].

Analiza wyników pozyskanych z otrzymanych widm spektrometrii masowej oraz wysoka zgodność danych eksperymentalnych z teoretycznymi dodatkowo potwierdzają poprawność struktur. Korelacja przesunięć chemicznych (^1H i ^{13}C) między wartościami eksperymentalnymi i obliczonymi (metodą GIAO) wykazała bardzo wysoką zgodność (^{13}C NMR: $r^2 = 0,9942$, ^1H NMR: $r^2 = 0,9905$). Jony molekularne o odpowiednich wartościach mas cząsteczkowych wskazują na utworzone zgodnie z oczekiwaniami struktury biokoniugatów. Fragmentacja masowa jonów molekularnych uzyskanych cząsteczek zweryfikowała obecność pierścieni 1,2,3-triazolowych bądź grup acetylowych.

Analiza spektroskopowa stanowi podstawę do dalszych badań nad właściwościami biologicznymi związków.

2.3. Obliczenia semiempiryczne (PM5)

Analiza wyników badań teoretycznych, opartych na obliczeniach metodą PM5, wskazuje, że monopodstawione pochodne kwasów żółciowych połączone pierścieniem 1,2,3-triazolowym (z dwiema wolnymi grupami N_3) nie powstają ze względu na bardzo wysokie wartości ciepła tworzenia. W przypadku kwasu litocholowego zaobserwowano powstawanie dipodstawionych pochodnych, jednak ich stabilność była niska (Tabela 3). Wszystkie quasi-podandy wykazywały obecność interakcji π–π (typu „sandwich") pomiędzy dwoma pierścieniami triazolowymi, przy czym obliczona separacja międzypłaszczyznowa wynosiła około 5,8 Å. Odległość ta jest większa o około 1,7 Å w porównaniu z klasycznymi interakcjami π–π, co wynika z faktu, że pierścień triazolowy jest bezpośrednio połączony ze sztywnym szkieletem aromatycznym, co wymusza zwiększoną odległość. Ponadto przestrzenne rozmieszczenie cząsteczek kwasów żółciowych i pierścieni 1,2,3-triazolowych może sprzyjać tworzeniu stabilnych kompleksów typu gospodarz-gość (Rys. 31).

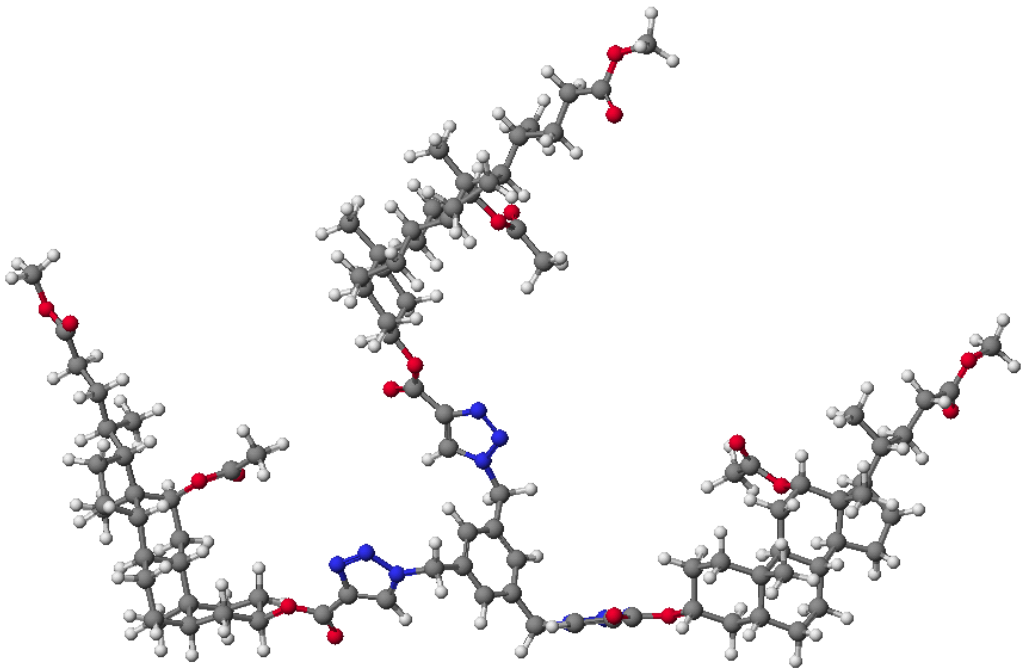

Rysunek 31. Model molekularny koniugatu kwasu deoksycholowego z pierścieniami 1,2,3-triazolowymi (**84**) [**P6**].

Tabela 3. Ciepło tworzenia (HOF) [kcal/mol] otrzymanych pochodnych kwasów żółciowych [**P6**].

Nr	HOF [kcal/mol]
77	−212,7209
78	–298,6465
79	−383,8356
82	−286,8410
83	−550,9153
84	−809,8199
85	−1063,6189

2.4. Aktywność biologiczna

Przewidywana aktywność biologiczna (PASS)

Na podstawie badań *in silico* przewidziano potencjalną aktywność biologiczną zsyntetyzowanych związków. Ich potencjał farmakologiczny jest związany głównie z regulacją metabolizmu cholesterolu, dlatego mogą znaleźć zastosowanie jako antagoniści cholesterolu lub inhibitory enzymów metabolizmu lipidów [**P6**].

Dokowanie molekularne

Reduktaza HMG-CoA jest kluczowym enzymem odpowiedzialnym za syntezę cholesterolu w wątrobie. Badania nad nowymi inhibitorami reduktazy HMG-CoA mają istotne znaczenie dla zdrowia publicznego, ponieważ podwyższony poziom cholesterolu jest jednym z głównych czynników ryzyka chorób układu sercowo-naczyniowego, takich jak miażdżyca czy zawał serca. Jej hamowanie może skutecznie ograniczać produkcję cholesterolu, prowadząc do obniżenia jego stężenia we krwi [131, 132].

Zsyntetyzowane związki wykazują większe powinowactwo do domeny białka 1HW8 (PDB ID, reduktaza HMG-CoA) w porównaniu z mewastatyną, osiągając energię wiązania na poziomie –6,9 kcal/mol przy średniej energii –6,8 kcal/mol. Wyniki te wskazują, że nowe cząsteczki mogą potencjalnie pełnić rolę skutecznych inhibitorów reduktazy HMG-CoA (Rys. 32 i 33). Otrzymane związki, wykazujące większe powinowactwo do enzymu niż obecnie stosowana mewastatyna, mogą przyczynić się do opracowania bardziej efektywnych i bezpiecznych terapii obniżających poziom cholesterolu. Wprowadzenie takich innowacyjnych leków mogłoby nie tylko poprawić jakość życia pacjentów, ale także zredukować obciążenie systemu ochrony zdrowia związanego z leczeniem powikłań chorób sercowo-naczyniowych.

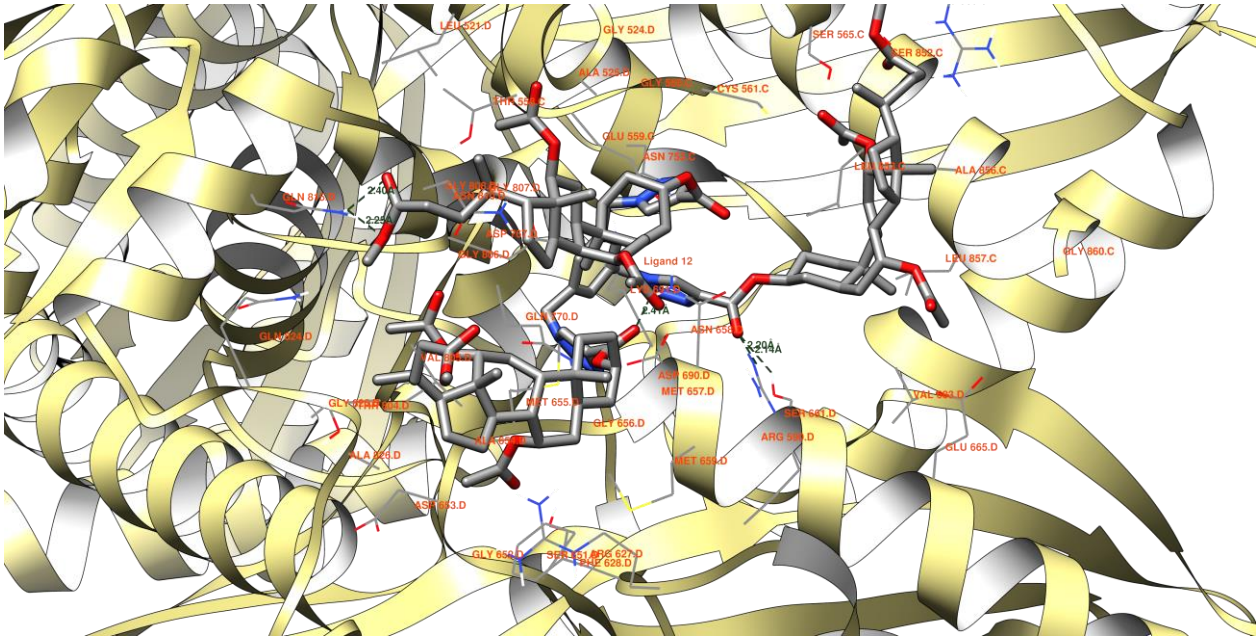

Rysunek 32. Tworzenie wiązań wodorowych przez ligand (**85**) z miejscem aktywnymi domeny białka 1HW8 [**P6**].

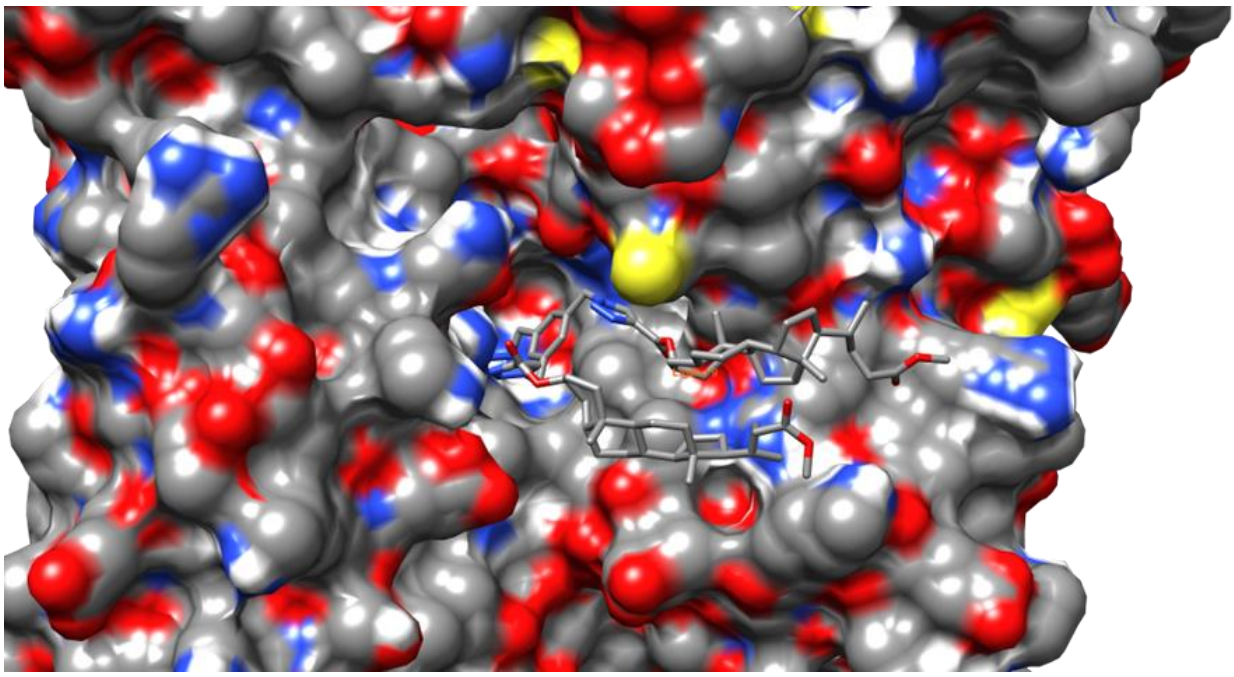

Rysunek 33. Możliwe wiązania wodorowe ligandu (**82**) pomiędzy miejscami wiązania domeny białka 1HW8. Energia wiązania wynosi –8,7 kcal/mol (średnia energia wiązania wynosi –8,4 kcal/mol) [**P6**].

3. Koniugaty steroidowo-pirymidynowe

3.1. Synteza koniugatów zawierających pierścienie 1,2,3-triazolowe

Unikatowa struktura i właściwości biologiczne steroidów determinują ich zastosowanie jako doskonałą platformę do modyfikacji chemicznych. Połączenie kwasów żółciowych lub steroli z zasadami pirymidynowymi, takimi jak uracyl i 2-tiouracyl umożliwia projektowanie biokoniugatów o potencjalnym działaniu wobec wirusów, bakterii, grzybów oraz komórek nowotworowych [133–136]. Zasady pirymidynowe jako kluczowy element strukturalny kwasów nukleinowych charakteryzuje zdolność do specyficznego oddziaływania z białkami enzymatycznymi i receptorami biologicznymi [137]. Włączenie cząsteczki uracylu bądź 2-tiouracylu do szkieletu steroidowego może istotnie poprawić ich farmakokinetykę oraz selektywność.

Przeprowadziłam syntezy modelowe z użyciem nowoopracowanych struktur *N*(1),*N*(3)-dipropargilowej pochodnej uracylu (**88**), *N*(1),*S*-dipropargilowej pochodnej 2-tiouracylu (**89**) i *N*(3),*S*-dipropargilowej pochodnej 2-tiouracylu (**90**) z 3α-azydooctanami odpowiednich kwasów żółciowych (**66**–**68**) oraz 3β-azydooctanami steroli (**91**–**92**) (Schemat 31 i 32). W wyniku reakcji „click" otrzymano 11 nowych 1,4-dipodstawionych 1,2,3-triazolowych koniugatów steroidowo-pirymidynowych (**93**–**103**) z wysokimi wydajnościami (Rys. 34). Zsyntetyzowane związki poddano szczegółowej analizie spektroskopowej (^{1}H NMR, ^{13}C NMR, FT-IR), spektrometrycznej (ESI-MS, EI-MS), wykonano obliczenia teoretyczne (PM5) oraz określono *in silico* ich potencjalną aktywność farmakologiczną (PASS, dokowanie molekularne) [**P3**].

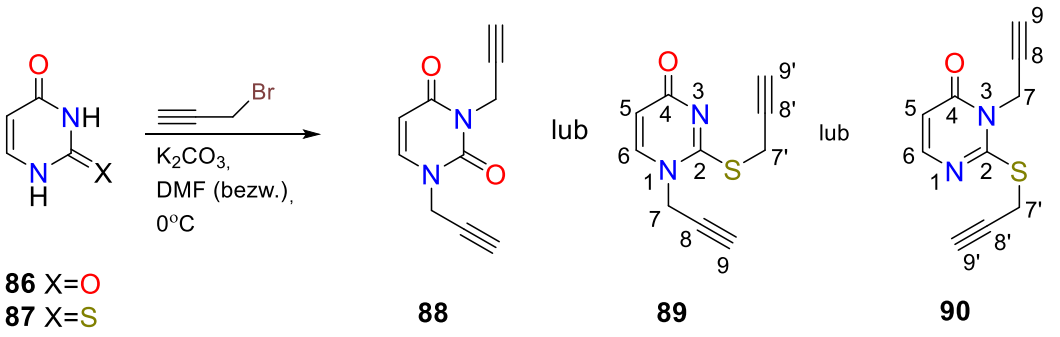

Schemat 31. Synteza dipropargilowych pochodnych uracylu (**88**) i nowoopracowanych dipropargilowych pochodnych 2-tiouracylu (**89**–**90**) [**P3**].

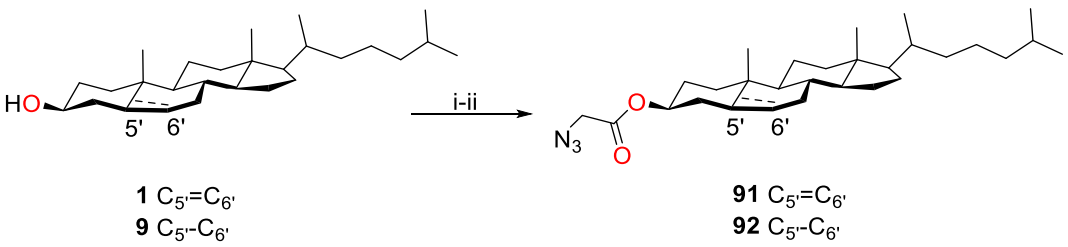

Schemat 32. Synteza 3β-azydooctanowych pochodnych steroli (**91**–**92**) [**P3**].

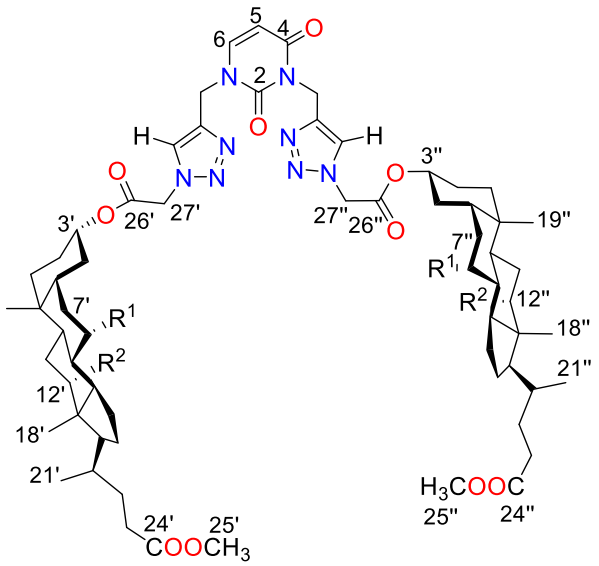

93-95

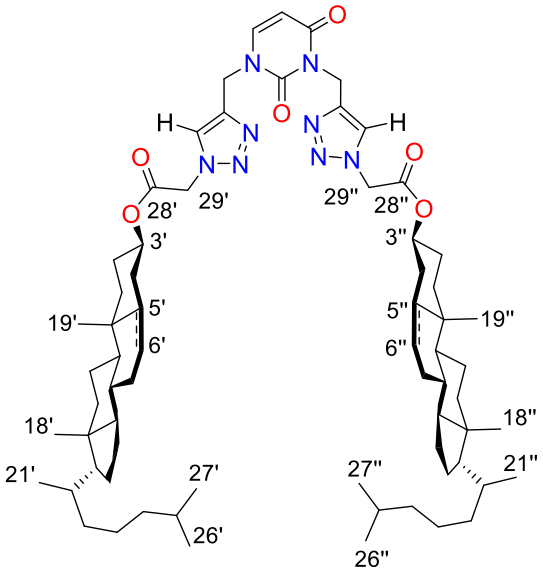

96-97

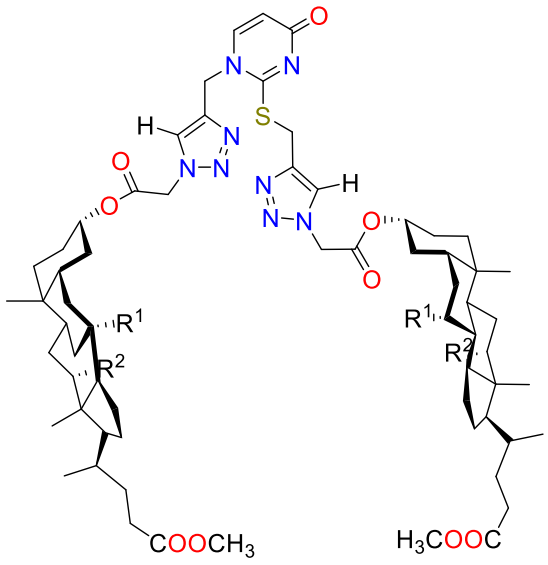

98-100

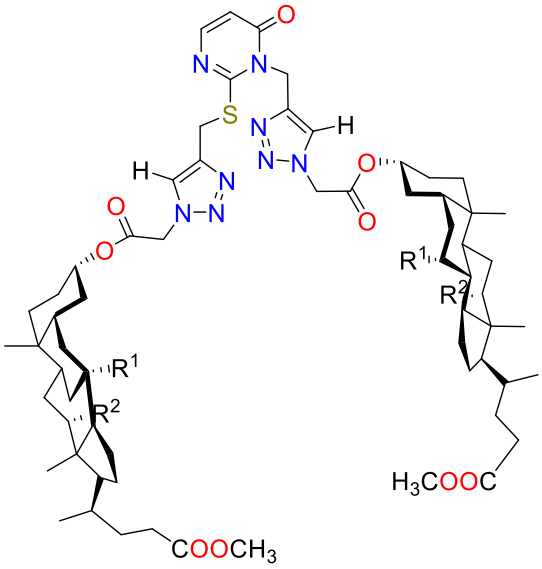

101-103

Nr	R^1	R^2	$C_{5'}$---$C_{6'}$	Wydajność [%]
93	H	H	–	72
94	H	OAc	–	63
95	OAc	OAc	–	78
96	–	–	$C_{5'}$=$C_{6'}$	65
97	–	–	$C_{5'}$–$C_{6'}$	75
98	H	H	–	34
99	H	OAc	–	47
100	OAc	OAc	–	43
101	H	H	–	60
102	H	OAc	–	78
103	OAc	OAc	–	67

Rysunek 34. Koniugaty steroidowo-pirymidynowe połączone pierścieniami 1,2,3-triazolowymi (**93**–**103**) [**P3**].

3.2. Analiza spektroskopowa

Analiza spektralna (^{1}H NMR, ^{13}C NMR, FT-IR, EI-MS, ESI-MS) dostarczyła kompleksowych informacji o strukturze i stabilności nowych koniugatów steroidowo-pirymidynowych.

W widmie ^{1}H NMR dipropargilowych pochodnych 2-tiouracylu (**89**–**90**) charakterystyczne przesunięcia chemicznie dawały sygnał w postaci dubletów, które zaobserwowano przy 8,30 i 7,77 ppm i przypisano protonom CH-6 oraz przy 6,50 i 6,26 z CH-5 (Rys. 35). Sygnały odpowiadające protonom przy atomie węgla w wiązaniu CH_2−N(1) pojawiają się jako podwójne singlety przy 5,03 i 4,85 ppm, podobnie jak przesunięcia chemiczne pochodzące od protonów obecnych w grupie metylenowej CH_2−S przy 4,02 i 3,91 ppm. W zakresie 2,53−2,19 ppm zidentyfikowano charakterystyczne sygnały w postaci tripletów pochodzące od protonów przy wiązaniu C≡CH.

89

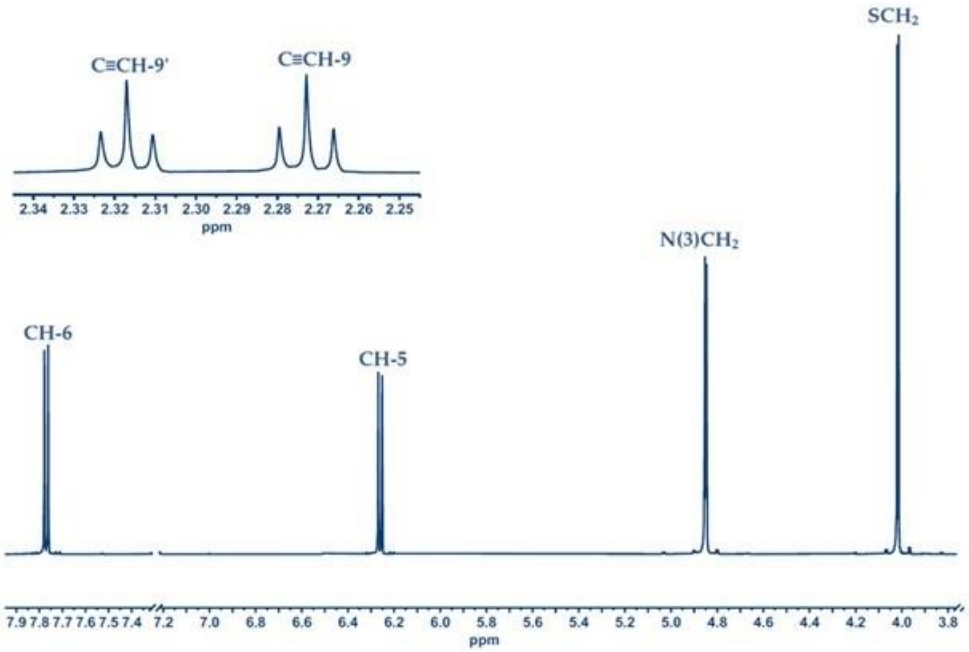

90

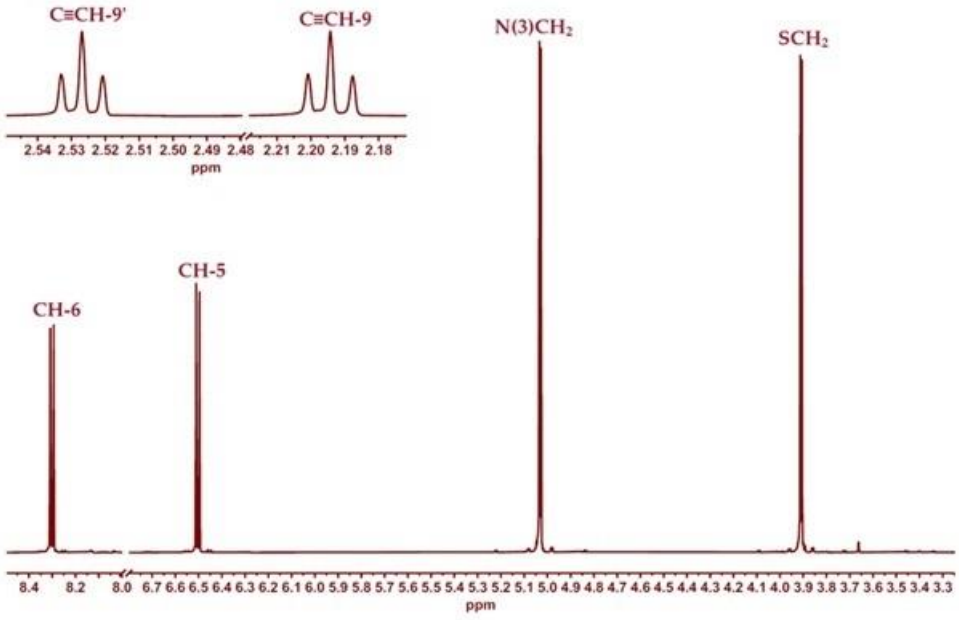

Rysunek 35. Fragmenty widm ^{1}H NMR alkinowych pochodnych 2-tiouracylu (**89**, **90**) [**P3**].

Diagnostyczne przesunięcia chemiczne pochodzące od protonów z pierścieni 1,2,3-triazolowych zaobserwowano dla wszystkich koniugatów (**93–103**) jako singlety w zakresie 7,90–7,70 ppm (Rysunek 36). Charakterystyczne sygnały w postaci dubletów odpowiadające protonom przy atomach węgla CH-6 i CH-5 zaobserwowano przy 8,26–8,25 i 6,45 ppm (dla związków **101**–**103**), 7,77–7,75 i 6,22–6,20 ppm (dla związków **98**–**100**),

7,46–7,45 i 5,75–5,74 ppm (dla związków **93**–**97**). Protony obecne w grupach metylenowych N−CH_2−triazol i S-CH_2−triazol można zinterpretować jako singlety położone odpowiednio przy 5,54−5,52 (N(3)), 5,34−5,33 (N(1)) i 4,56−4,50 ppm. Przesunięcia chemiczne pochodzące od protonów z grup metylenowych CH_2 łączących szkielet steroidu z pierścieniem triazolowym są położone w widmach ^{1}H NMR koniugatów steroid−uracyl (**93**–**97**) w zakresach 5,25−5,23 i 5,13−5,11 ppm. W przypadku związków (**98**−**103**) podobne sygnały w postaci singletów zaobserwowano przy 5,15−5,08 ppm. Na widmach ^{1}H NMR wszystkich związków (**93–103**) występują charakterystyczne przesunięcia chemiczne w zakresie 4,86–4,61 ppm należące do protonów przy 3'α-H i 3'β-H. Dla pochodnej cholesterolu (**96**) diagnostyczny jest szeroki singlet odpowiadający protonowi 6'-H przy 5,38 ppm.

95

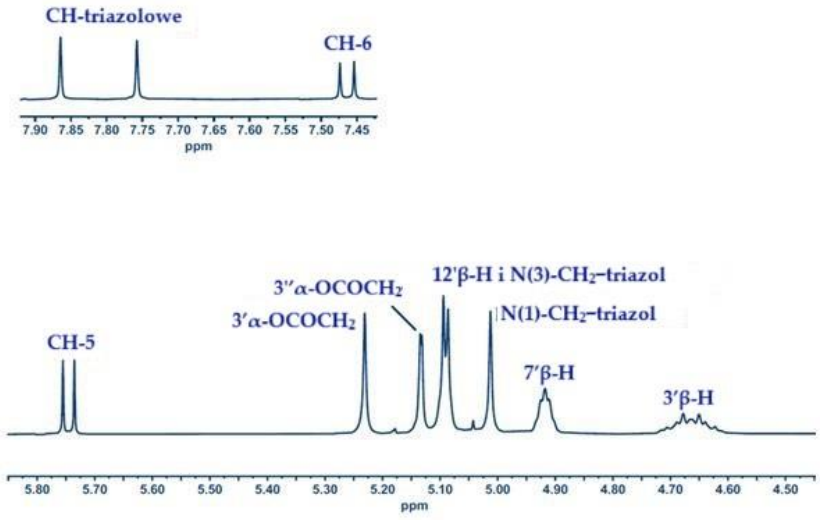

99

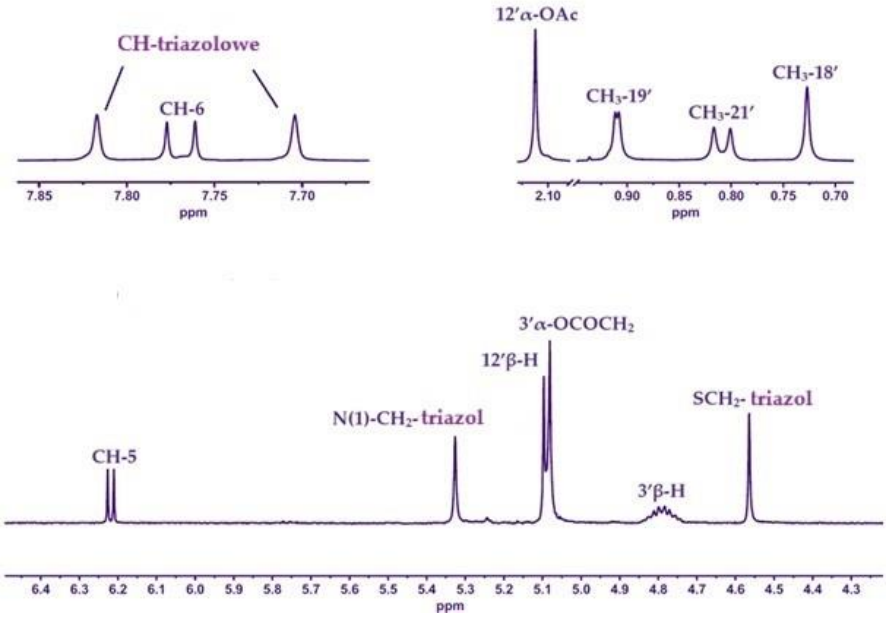

Rysunek 36. Diagnostyczne sygnały widma ^{1}H NMR zidentyfikowane dla triazolowych związków kwasu cholowy-uracyl (**95**) i kwas deoksycholowy-tiouracyl (**99**) [**P3**].

Interpretacja widm ^{13}C NMR związków (**89**) i (**90**) wskazuje na sygnały pochodzące od atomów węgla C(4)=O, C(2)–S, C-6, C-5 odpowiednio przy 169,8–160,7, 167,5–160,7, 157,8–151,9 i 110,8–104,1 ppm. Sygnały od atomów C≡C obserwowano w zakresie 79,7–70,5 ppm, natomiast sygnały odpowiadające atomom węgla z grup metylenowych CH_2 obserwowano w zakresie 54,1–19,4 ppm.

Na widmach ^{13}C NMR wszystkich koniugatów (**93–103**) sygnały diagnostyczne odpowiadające atomom węgla z pierścienia triazolowego, takie jak C=CH, dają sygnały odpowiednio przy 145,7–138,8 i 125,4–123,3 ppm. Z drugiej strony, atom węgla z połączenia metylenowego steroid-CH_2−pierścienia triazolowy zaobserwowano przy 51,2–51,0 ppm.

Na widmach FT-IR występują charakterystyczne dla grup karbonylowych pasma drgań rozciągających przy maksimum absorpcji w zakresie 1745–1730 cm^{-1}. Pasma absorpcji związane z wiązaniami N–H w cząsteczce uracylu i 2-tiouracylu są obecne w zakresie 3220–3120 cm^{-1}, co potwierdza udział pierścienia pirymidynowego w strukturze biokoniugatów.

Analiza widm EI-MS dostarczyła informacji o przyłączeniu grup propargilowych do odpowiednich atomów azotu (N(1) lub N(3)) i siarki w otrzymanych pochodnych 2-tiouracylu (**89**–**90**) (Schemat 33). Z kolei po interpretacji widm ESI-MS utworzonych biokoniugatów (**93–103**) zweryfikowano ich masy cząsteczkowe. Zaproponowana fragmentacja masowa struktur potwierdziła stabilność układów 1,2,3-triazolowych.

Pierścień pirymidynowy w związku (**89**) ulega otwarciu w wyniku pierwotnej fragmentacji typu α, prowadząc do powstania dwóch alternatywnych ścieżek fragmentacyjnych skutkujących powstaniem różnych jonów analitycznych. W jednej z dróg fragmentacji, dalszy rozpad typu α, a następnie reakcja typu retro-Dielsa–Aldera, prowadzi do powstania jonu nieparzysto elektronowego obserwowanego przy m/z = 107. W drugiej ścieżce, w wyniku indukowanego rozpadu α, generowany jest jon parzysto elektronowy o m/z = 97.

W przypadku związku (**90**), będącego pochodną typu N(3)S, obserwuje się dwa możliwe przebiegi fragmentacji typu α, obejmujące eliminację rodnika $C_3H_3^*$ z atomu azotu z ugrupowania N(3), bądź atomu siarki. W obu przypadkach prowadzi to do powstania jonów parzysto elektronowych o m/z = 165.

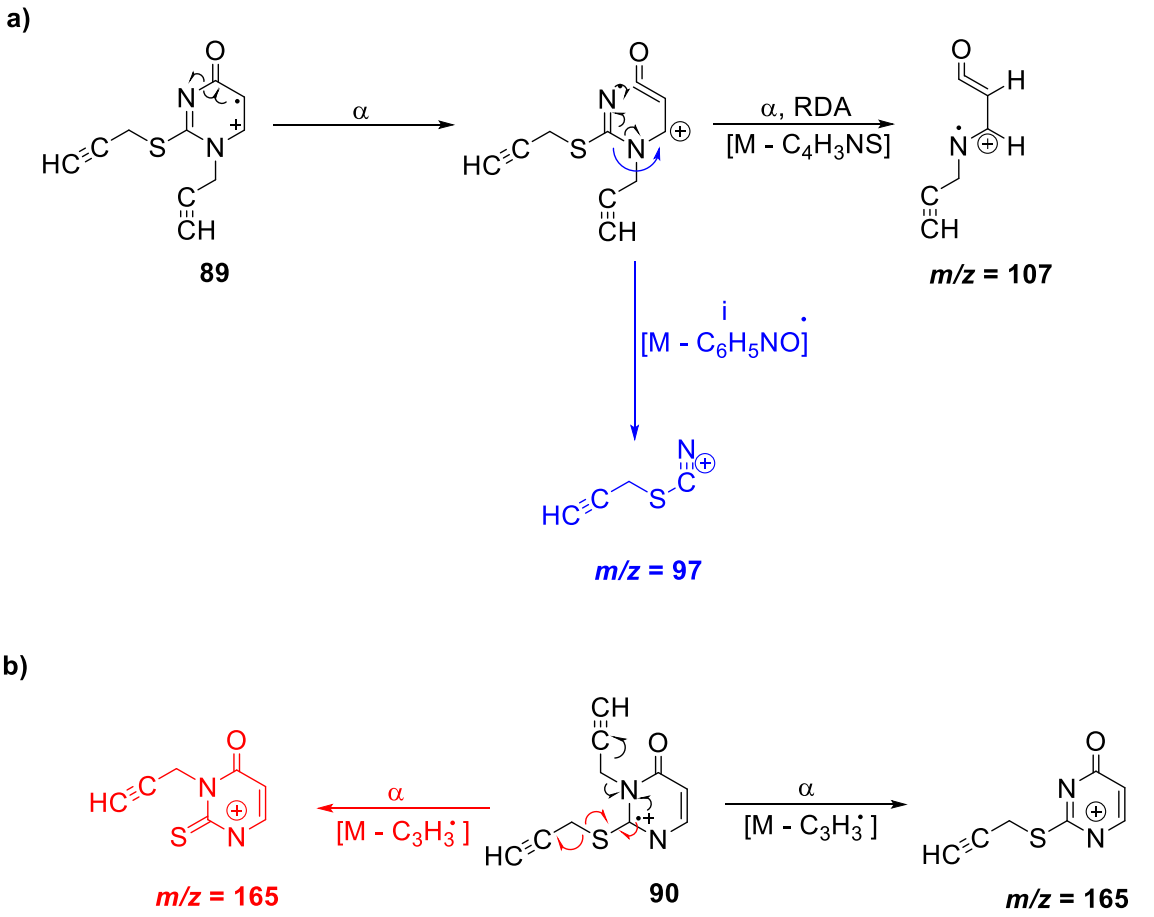

Schemat 33. Możliwe fragmentacje związków (**89**) i (**90**) podczas analizy EI-MS [**P3**].

3.3. Obliczenia semiempiryczne (PM5)

Obliczone wartości ciepła tworzenia dla koniugatów wskazują na stabilność energetyczną hybryd steroidowo-uracylowych (**93**–**97**) (Tabela 4). Najwyższą trwałością charakteryzują się związki kwasu cholowego (**95**, **100**, **103**), co może być związane z obecnością grup 7α-OAc, 12α-OAc oraz wiązaniem estrowym w łańcuchu bocznym (Rys. 37). Obecność atomu siarki w pochodnych 2-tiouracylu spowodowały wyższe wartości HOF ze względu na steryczne oddziaływania w cząsteczce oraz większą polaryzowalność. Obliczenia wskazały na obecność silnych wewnątrzcząsteczkowych wiązań wodorowych między grupami karbonylowymi a pirymidynowymi, które stabilizują utworzone struktury. Obecność pierścienia 1,2,3-triazolowego sprzyja trwałości układu dzięki interakcjom π–π i zwiększeniu sztywności strukturalnej.

Tabela 4. Ciepła tworzenia uzyskane dla pochodnych pirymidyn (**88**–**90**) i dla koniugatów steroidowych (**93**–**103**) [**P3**].

Nr	Ciepło tworzenia HOF [kcal/mol]
88	28,9829
89	97,0622
90	90,6298
93	–439,5148
94	–606,8373
95	–784,1348
96	–272,6631
97	–321,9369
98	–370,6792
99	–546,0568
100	–712,6079
101	–379,0817
102	–548,2400
103	–712,2926

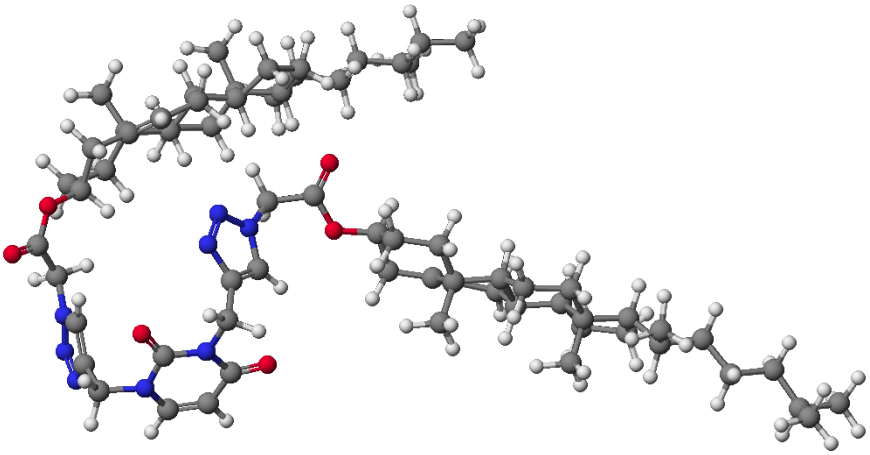

96

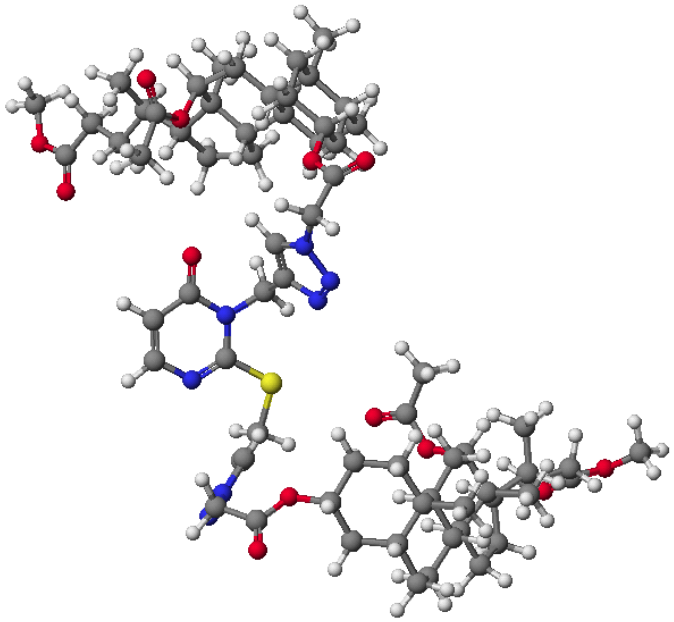

102

Rysunek 37. Modele molekularne koniugatu cholesterolu z uracylem (**96**) i kwasu deoksycholowego z 2-tiouracylem (**102**) [**P3**].

3.4. Aktywność biologiczna

Otrzymane hybrydy steroidowo-pirymidynowe połączone pierścieniem 1,2,3-triazolowym wykazują szerokie spektrum potencjalnych właściwości biologicznych, co zostało potwierdzone za pomocą metod predykcyjnych (PASS) oraz dokowania molekularnego.

Na podstawie badań *in silico* przewidziano, że wybrane biokoniugaty steroidowe wykazały potencjalną aktywność przeciw bakteriom Gram dodatnim (*Staphylococcus aureus*) i Gram ujemnym (*Escherichia coli*), jak również grzybom z rodzaju *Candida albicans*. Ich działanie przeciwdrobnoustrojowe jest związane z oddziaływaniem z enzymami kluczowymi w metabolizmie wymienionych patogenów, takimi jak syntaza skwalenu (1EZF) i giraza-DNA (1KZN) (Rys. 38 i 39). Białko 1EZF bierze udział w biosyntezie ergosterolu, niezbędnego składnika błony komórkowej u grzybów, a 1KZN jest istotna dla prawidłowej replikacji DNA w komórkach bakterii. Wyższa energia powinowactwa koniugatów niż ligandy natywne wskazują na ich potencjał proleków (Tabela 5).

Tabela 5. Otrzymane wartości energii powinowactwa [kcal/mol] koniugatów do określonych domen białkowych [**P3**].

Domena białka ID	Nazwa ligandu				
	1EZF	**1KZN**	**2H94**	**2Q85**	**5V5Z**
Natywny	–11.9	–9.1	–14.6	–10.9	–10.5
89	–5.7	–5.7	–6.2	–5.9	–5.9
90	–6.2	–5.2	–5.6	–5.7	–5.6
93	–11.4	–7.1	–9.5	–11.3	–11.3
94	–11.4	–8.3	–9.9	–12.7	–10.8
95	–11.1	–6.4	–9.6	–9.7	–10.6
96	–11.4	–8.7	–10.3	–11.6	–12.1
97	–11.6	–7.4	–10.0	–10.8	–11.3
98	–10.8	–8.0	–10.7	–11.3	–11.2
99	–10.9	–7.1	–9.9	–10.7	–10.6
100	–10.2	–8.0	–9.3	–11.6	–9.7
101	–11.3	–8.8	–10.2	–11.2	–11.9
102	–10.9	–7.6	–10.2	–9.5	–10.8
103	–10.4	–8.2	–9.3	–10.1	–10.1

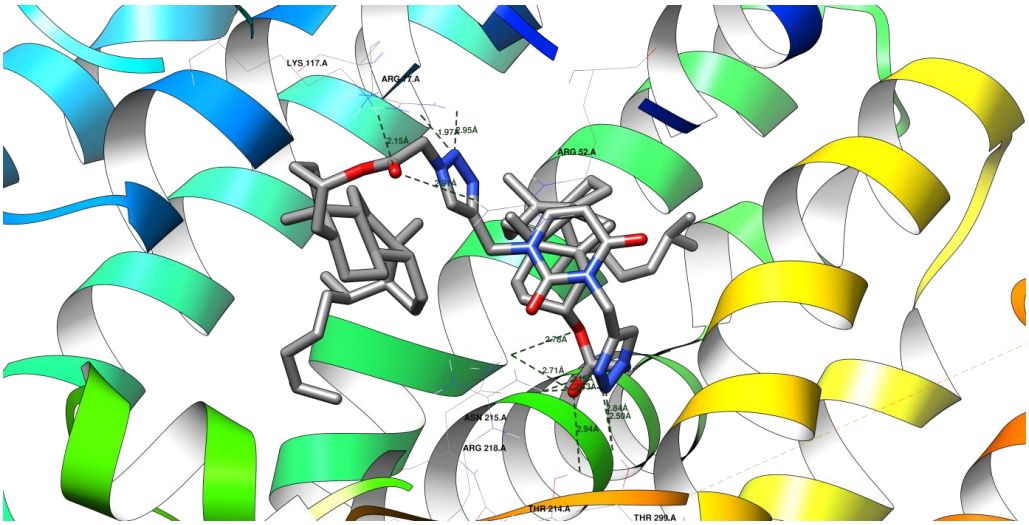

Rysunek 38. Wiązania wodorowe utworzone pomiędzy koniugatem (**97**) a miejscem aktywnym syntazy skwalenu (1EZF) określające potencjalną aktywność przeciwgrzybiczną [**P3**].

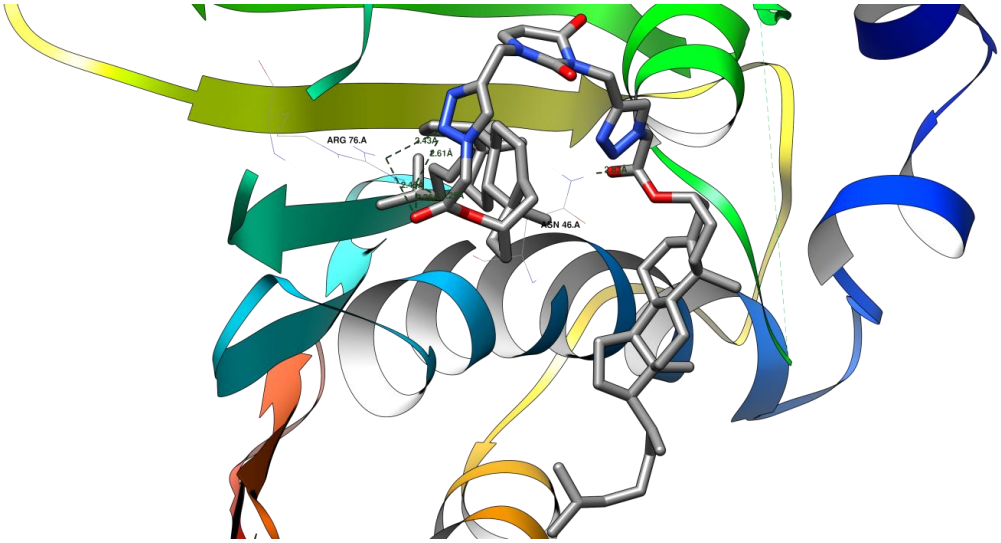

Rysunek 39. Wiązania wodorowe utworzone między ligandem pochodnej cholesterolu (**96**) a domeną białkową bakterii (1KZN) określający potencjalną aktywność przeciwbakteryjną [**P3**].

Testy *in silico* metodą PASS prognozują zdolność pochodnych 1,2,3-triazolowych do ochrony komórek przed stresem oksydacyjnym (Tabela 6). Przewidywana aktywność cytoprotekcyjna wiąże się z amfipatycznością kwasów żółciowych i steroli. Wyniki pokazują, że otrzymane struktury zostały zidentyfikowane jako potencjalne inhibitory enzymów (monooksygenazy gliceryloeterowej i alkiloacetyloglicerofosfatazy) związanych z reakcjami zapalnymi skóry. Ponadto, związki te posiadają charakter antycholestatyczny, co może mieć znaczenie w leczeniu zaburzeń przewodu żółciowego.

Tabela 6. Przewidywana aktywność biologiczna wybranych koniugatów steroidowo-pirymidynowych [**P3**].

Aktywność biologiczna 50 <	**Koniugat**				
	93	**96**	**97**	**98**	**102**
Inhibitor monooksygenazy gliceryloeterowej	71	61	73	69	69
Inhibitor alkiloacetyloglicerofosfatazy	68	–	71	–	52
Choroby skóry	69	64	67	59	–
Cytoprotekcyjna	61	–	–	57	60
Zaburzenia metabolizmu żółci	56	–	61	–	–
Dermatologiczna	57	59	57	52	54
Niepłodność u kobiet	53	58	57	–	–
Choroby związane z prostatą	53	58	53	–	–
Antygrzybiczna	52	58	54	50	50
Antyalergiczna	52	54	54	–	–
Inhibitor CYP17	–	65	–	–	–
Inhibitor reduktazy DELTA14-sterolowej	–	60	–	–	–

Przeprowadzone dokowanie molekularne określiło działanie przeciwnowotworowe biokoniugatów steroidowo-pirymidynowych (Tabela 7, Rys. 40). Wykazując wyższą energię powinowactwa do białka związanego z regulacją ekspresji genów i cyklu komórkowego (LSD1, demetylaza-1 specyficzna dla lizyny) niż powinowactwo ligandu natywnego predysponują do hamowania wzrostu komórek nowotworowych poprzez mechanizmy epigenetyczne.

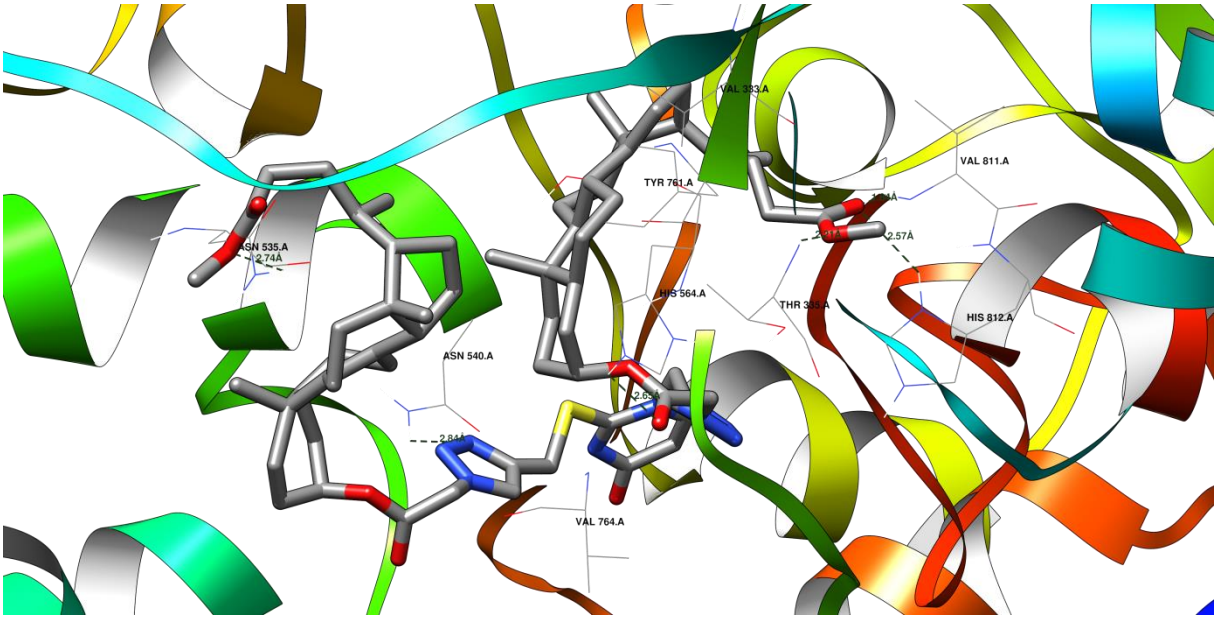

Rysunek 40. Potencjalne wiązania wodorowe między ligandem (**98**) a miejscem aktywnym białka związanego z proliferacją komórek nowotworowych (2H94) [**P3**]**.**

Dzięki wysokiej specyficzności względem enzymów docelowych mogą one znaleźć zastosowanie w terapiach nowotworowych, leczeniu infekcji oraz jako związki wspomagające ochronę komórek przed uszkodzeniami.

Podsumowanie

Artykuły przeglądowe dostarczyły szczegółowego wglądu na aktualny stan wiedzy dotyczący syntezy biokoniugatów steroidowych i ich właściwości biologicznych. Poruszana tematyka skupiała się na skwalaminie jako fundamentalnym związku promującym projektowanie nowych pochodnych steroidowych o zastosowaniu w terapiach przeciwnowotworowych, przeciwwirusowych i przeciwdrobnoustrojowych. Zwrócono również uwagę na ich zdolność do hamowania angiogenezy i agregacji białek w chorobach neurodegeneracyjnych.

Silną aktywnością biobójczą wyróżniają się koniugaty oparte na szkielecie steroidowym kwasów żółciowych z wbudowanymi pierścieniami 1,2,3-triazolowymi, potęgującymi ich zastosowanie w układach biologicznych. Modyfikacje rdzenia steroidowego z wykorzystaniem reakcji chemii „click" prowadzą do otrzymywania potencjalnych leków [**P1**, **P2, P4**].

Wyniki uzyskane w badaniach własnych wniosły istotny wkład w rozwój wiedzy o nowych biokoniugatów steroidowych, szczególnie w zakresie ich syntezy, charakterystyki spektroskopowej i przewidywanych właściwości farmakologicznych.

Opracowano efektywne warunki syntezy jedenastu nowych pochodnych kwasów żółciowych i steroli, w tym sześciu biokoniugatów połączonych pierścieniami 1,2,3-triazolowymi, które scharakteryzowano spektroskopowo. Związki te wyróżnia stabilność chemiczna, co dowiodły obliczenia teoretyczne. Wykazano, że nowe koniugaty wykazują potencjalną aktywność biologiczną w kierunku działania przeciwgrzybicznego i przeciwbakteryjnego [**P8**].

Zsyntetyzowano dwie propargilowe acetylowe pochodne kwasów żółciowych oraz cztery struktury quasi-podandów kwasów żółciowych zawierających pierścienie 1,2,3-triazolowe. Takie układy mogą tworzyć kompleksy supramolekularne. Analiza spektroskopowa i wyniki obliczeń semiempirycznych metodą PM5 potwierdziły poprawność otrzymanych struktur i trwałość wszystkich cząsteczek. Koniugaty wyróżnia potencjał antyhipercholesterolemiczny [**P6**]

Z kolei trzynaście nowych hybryd steroidowo-pirymidynowych charakteryzuje zdolność do oddziaływań z enzymami uczestniczącymi w metabolizmie lipidów i w procesach przeciwnowotworowych. Analizy dokowania molekularnego wskazały na ich potencjalną aktywność antyproliferacyjną oraz na zastosowanie tych związków w terapii przeciwko grzybom i bakteriom [**P3**].

Zaprojektowane struktury trzydziestu nowych pochodnych kwasów żółciowych i steroli wniosły nowe perspektywy wiedzy w dziedzinie chemii bioorganicznej. Opracowane koniugaty zawierające pierścienie 1,2,3-triazolowe wykazują wysoką przewidywaną aktywność farmakologiczną, szczególnie przeciwnowotworową, przeciwdrobnoustrojową i cytoprotekcyjną. Prezentowane wyniki stanowią punkt wyjścia dla dalszych badań nad zastosowaniem uzyskanych koniugatów steroidowo-triazolowych w medycynie, farmakologii lub jako nośniki substancji bioaktywnych.

Tabela 7. Wykaz numeracji związków w artykułach naukowych (**Nr_A**) w porównaniu z obowiązującymi w pracy (**Nr_P**).

Artykuły

P8		**P6**		**P3**	
Nr_A	**Nr_P**	**Nr_A**	**Nr_P**	**Nr_A**	**Nr_P**
8	64	**5**	78	**4**	89
9	65	**6**	79	**5**	90
11	67	**9**	82	**16**	93
12	68	**10**	83	**17**	94
16	70	**11**	84	**18**	95
17	71	**12**	85	**19**	96
18	72	–	–	**20**	97
19	73	–	–	**21**	98
20	74	–	–	**22**	99
21	75	–	–	**23**	100
22	76	–	–	**24**	101
–	–	–	–	**25**	102
–	–	–	–	**26**	103

Bibliografia

1. Floss, H.G. Natural Products Derived from Unusual Variants of the Shikimate Pathway. *Nat. Prod. Rep.* **1997**, *14*, 433, doi:10.1039/np9971400433.
2. Nicolaou, K. C.; Montagnon, T. Molecules That Changed the World *J. Chem. Educ.* **2009**, *86*, 1372, doi:10.1021/ed086p1372.
3. Kandi, S.; Godishala, V.; Rao, P.; Ramana, K.V. Biomedical Significance of Terpenes: An Insight. *Biomed.&Biotech.* **2015**, *3*, 8–10, doi:10.12691/bb-3-1-2.
4. Mukhopadhyay, S.; Maitra, U. Chemistry and Biology of Bile Acids. *Cur. Sci.* **2004**, *87*, 18.
5. Bloch, K. Sterol Molecule: Structure, Biosynthesis, and Function. *Steroids* **1992**, *57*, 378–383, doi:10.1016/0039-128X(92)90081-J.
6. Dewick, P. M. *Medicinal Natural Products A Biosynthetic Approach 3rd Ed.,* John Wiley & Sons, Ltd.: Chichester, UK, **2009**, 247–298.
7. Tang, J.; Han, Z.; Chai, J. Q&A: What Are Brassinosteroids and How Do They Act in Plants? *BMC Biology* **2016**, *14*, 113, doi:10.1186/s12915-016-0340-8.
8. Okamura, W.H.; Midland, M.M.; Hammond, M.W.; Abd.Rahman, N.; Dormanen, M.C.; Nemere, I.; Norman, A.W. Chemistry and Conformation of Vitamin D Molecules. *J. Steroid Biochem. Mol. Biol.* **1995**, *53*, 603–613, doi:10.1016/0960-0760(95)00107-B.
9. Rodriguez-Estrada, M.T.; Tatay, A.C.; Cardenia, V.; Garcia-Llatas, G. Fats and Sterols. In *Reference Module in Biomedical Sciences*; Elsevier, **2014**, doi: 10.1016/B978-0-12-801238-3.00228-2
10. Benveniste, P. Biosynthesis and Accumulation of Sterols. *Annu. Rev. Plant Biol.* **2004**, *55*, 429–457, doi:10.1146/annurev.arplant.55.031903.141616.
11. Björkhem, I.; Leitersdorf, E. Sterol 27-Hydroxylase Deficiency: A Rare Cause of Xanthomas in Normocholesterolemic Humans. *Trends Endocrinol. Metab.* **2000**, *11*, 180–183, doi:10.1016/S1043-2760(00)00255-1.
12. Hoenig, M.R.; Rolfe, B.E.; Campbell, J.H. Cholestanol: A Serum Marker to Guide LDL Cholesterol-Lowering Therapy. *Atherosclerosis* **2006**, *184*, 247–254, doi:10.1016/j.atherosclerosis.2005.09.007.
13. Morzycki, J.W. Recent Advances in Cholesterol Chemistry. *Steroids* **2014**, *83*, 62–79, doi:10.1016/j.steroids.2014.02.001.
14. Oakes, V.; Domene, C. Influence of Cholesterol and Its Stereoisomers on Members of the Serotonin Receptor Family. *J. Mol. Biol.* **2019**, *431*, 1633–1649, doi:10.1016/j.jmb.2019.02.030.
15. Ferdinandusse, S.; Houten, S.M. Peroxisomes and Bile Acid Biosynthesis. *Biochim. Biophys. Acta* **2006**, *1763*, 1427–1440, doi:10.1016/j.bbamcr.2006.09.001.

16. Thomas, C.; Pellicciari, R.; Pruzanski, M.; Auwerx, J.; Schoonjans, K. Targeting Bile-Acid Signalling for Metabolic Diseases. *Nat. Rev. Drug Discov.* **2008**, *7*, 678–693, doi:10.1038/nrd2619.

17. di Gregorio, M.C.; Cautela, J.; Galantini, L. Physiology and Physical Chemistry of Bile Acids. *Int. J. Mol. Sci.* **2021**, *22*, 1780, doi:10.3390/ijms22041780.

18. Babu, P.; Sangeetha, N.M.; Maitra, U. Supramolecular Chemistry of Bile Acid Derivatives: Formation of Gels. *Macromol. Sym.* **2006**, *241*, 60–67, doi:10.1002/masy.200650909.

19. Pavlović, N.; Goločorbin-Kon, S.; Đanić, M.; Stanimirov, B.; Al-Salami, H.; Stankov, K.; Mikov, M. Bile Acids and Their Derivatives as Potential Modifiers of Drug Release and Pharmacokinetic Profiles. *Front. Pharmacol.* **2018**, *9*, 1283, doi:10.3389/fphar.2018.01283.

20. Wang, Z.; Qiang, X.; Peng, Y.; Wang, Y.; Zhao, Q.; He, D. Design and Synthesis of Bile Acid Derivatives and Their Activity against Colon Cancer. *RSC Med. Chem.* **2022**, *13*, 1391–1409, doi:10.1039/D2MD00220E.

21. Chiang, J.Y.L. Bile Acids: Regulation of Synthesis. *J. Lipid Res.* **2009**, *50*, 1955–1966, doi:10.1194/jlr.R900010-JLR200.

22. Galantini, L.; di Gregorio, M.C.; Gubitosi, M.; Travaglini, L.; Tato, J.V.; Jover, A.; Meijide, F.; Soto Tellini, V.H.; Pavel, N.V. Bile Salts and Derivatives: Rigid Unconventional Amphiphiles as Dispersants, Carriers and Superstructure Building Blocks. *Curr. Opin. Colloid Interface Sci.* **2015**, *20*, 170–182, doi:10.1016/j.cocis.2015.08.004.

23. Roberts, M.S.; Magnusson, B.M.; Burczynski, F.J.; Weiss, M. Enterohepatic Circulation. *Clin. Pharmacokinet.* **2002**, *41*, 751–790, doi:10.2165/00003088-200241100-00005.

24. Warren, D.B.; Chalmers, D.K.; Hutchison, K.; Dang, W.; Pouton, C.W. Molecular Dynamics Simulations of Spontaneous Bile Salt Aggregation. *Colloids Surf. A: Physicochem. Eng. Asp.* **2006**, *280*, 182–193, doi:10.1016/j.colsurfa.2006.02.009.

25. Li, T.; Chiang, J.Y.L. Bile Acid Signaling in Metabolic Disease and Drug Therapy. *Pharmacol. Rev.* **2014**, *66*, 948–983, doi:10.1124/pr.113.008201.

26. Hofmann, A.F. Bile Acids: The Good, the Bad, and the Ugly. *Physiology* **1999**, *14*, 24–29, doi:10.1152/physiologyonline.1999.14.1.24.

27. Higuchi, W.I.; Tzeng, C.-S.; Chang, S.-J.; Chiang, H.-J.; Liu, C.-L. Estimation of Cholesterol Solubilization by a Mixed Micelle Binding Model in Aqueous Tauroursodeoxycholate: Lecithin:Cholesterol Solutions. *J. Pharm. Sci* **2008**, *97*, 340–349, doi:10.1002/jps.21096.

28. Rudling, M.; Laskar, A.; Straniero, S. Gallbladder Bile Supersaturated with Cholesterol in Gallstone Patients Preferentially Develops from Shortage of Bile Acids. *J. Lipid Res.* **2019**, *60*, 498–505, doi:10.1194/jlr.S091199.

29. Hofmann, A.F. The Continuing Importance of Bile Acids in Liver and Intestinal Disease. *Arch. Intern. Med.* **1999**, *159*, 2647–2658, doi:10.1001/archinte.159.22.2647.

30. Coreta-Gomes, F.M.; Vaz, W.L.C.; Wasielewski, E.; Geraldes, C.F.G.; Moreno, M.J. Quantification of Cholesterol Solubilized in Dietary Micelles: Dependence on Human Bile Salt Variability and the Presence of Dietary Food Ingredients. *Langmuir* **2016**, *32*, 4564–4574, doi:10.1021/acs.langmuir.6b00723.

31. Jang, S.I.; Fang, S.; Kim, K.P.; Ko, Y.; Kim, H.; Oh, J.; Hong, G.Y.; Lee, S.Y.; Kim, J.M.; Noh, I.; et al. Combination Treatment with N-3 Polyunsaturated Fatty Acids and Ursodeoxycholic Acid Dissolves Cholesterol Gallstones in Mice. *Sci. Rep.* **2019**, *9*, 12740, doi:10.1038/s41598-019-49095-z.

32. Fiorucci, S.; Mencarelli, A.; Palladino, G.; Cipriani, S. Bile-Acid-Activated Receptors: Targeting TGR5 and Farnesoid-X-Receptor in Lipid and Glucose Disorders. *Trends Pharmacol. Sci.* **2009**, *30*, 570–580, doi:10.1016/j.tips.2009.08.001.

33. Kim, I.; Ahn, S.-H.; Inagaki, T.; Choi, M.; Ito, S.; Guo, G.L.; Kliewer, S.A.; Gonzalez, F.J. Differential Regulation of Bile Acid Homeostasis by the Farnesoid X Receptor in Liver and Intestine. *J. Lipid Res.* **2007**, *48*, 2664–2672, doi:10.1194/jlr.M700330-JLR200.

34. Mimaki, Y.; Kuroda, M.; Kameyama, A.; Sashida, Y.; Hirano, T.; Oka, K.; Maekawa, R.; Wada, T.; Sugita, K.; Beutler, J.A. Cholestane Glycosides with Potent Cytostatic Activities on Various Tumor Cells from *Ornithogalum Saundersiae* Bulbs. *Bioorg. Med. Chem. Lett.* **1997**, *7*, 633–636, doi:10.1016/S0960-894X(97)00071-1.

35. Jiao, Y.; Lu, Y.; Li, X. Farnesoid X Receptor: A Master Regulator of Hepatic Triglyceride and Glucose Homeostasis. *Acta Pharmacol. Sin.* **2015**, *36*, 44–50, doi:10.1038/aps.2014.116.

36. Baxter, J.D.; Webb, P. Metabolism: Bile Acids Heat Things Up. *Nature* **2006**, *439*, 402–403, doi:10.1038/439402a.

37. Magotti, P.; Bauer, I.; Igarashi, M.; Babagoli, M.; Marotta, R.; Piomelli, D.; Garau, G. Structure of Human *N*-Acylphosphatidylethanolamine-Hydrolyzing Phospholipase D: Regulation of Fatty Acid Ethanolamide Biosynthesis by Bile Acids. *Structure* **2015**, *23*, 598–604, doi:10.1016/j.str.2014.12.018.

38. Summons, R.E.; Bradley, A.S.; Jahnke, L.L.; Waldbauer, J.R. Steroids, Triterpenoids and Molecular Oxygen. *Philos. Trans. R. Soc. Lond. B. Biol. Sci.* **2006**, *361*, 951–968, doi:10.1098/rstb.2006.1837.

39. Kołodziejczyk, A. *Naturalne związki organiczne*; Wydawnictwo Naukowe PWN: Warszawa, **2012**, 427–436.

40. Lednicer, D. *Steroid Chemistry at a Glance*; John Wiley & Sons, Ltd: Chichester, UK, **2010**.

41. Kuhajda, K.; Kandrac, J.; Kevresan, S.; Mikov, M.; Fawcett, J.P. Structure and Origin of Bile Acids: An Overview. *Eur. J. Drug Metab. Pharmacokinet.* **2006**, *31*, 135–143, doi:10.1007/BF03190710.

42. Pospieszny, T. Steroidal conjugates: Synthesis, spectroscopic, and biological studies, *Studies in Natural Products Chemistry* **2015**, *46*, 169–172.

43. Savage, P.B. Cationic Steroid Antibiotics. *Curr. Med.l Chem. - Anti-Infective Agents* **2002**, *1*, 293–304, doi:10.2174/1568012023354776.

44. Pospieszny, T. Molecular Pockets, Umbrellas and Quasi Podands from Steroids: Synthesis, Structure and Applications. *Mini Rev. Org. Chem.* **2015**, *12*, 258–270, doi:10.2174/1570193X1203150429105154.

45. Mishra, R.; Mishra, S. Updates in Bile Acid-Bioactive Molecule Conjugates and Their Applications. *Steroids* **2020**, *159*, 108639, doi:10.1016/j.steroids.2020.108639.

46. Altinkok, C.; Acik, G.; Karabulut, H.R.F.; Ciftci, M.; Tasdelen, M.A.; Dag, A. Synthesis and Characterization of Bile Acid-Based Polymeric Micelle as a Drug Carrier for Doxorubicin. *Polym. Advan. Technol.* **2021**, *32*, 4860–4868, doi:10.1002/pat.5478.

47. Sue, K.; Cadelis, M.M.; Troia, T.; Rouvier, F.; Bourguet-Kondracki, M.-L.; Brunel, J.M.; Copp, B.R. Investigation of α,ω-Disubstituted Polyamine-Cholic Acid Conjugates Identifies Hyodeoxycholic and Chenodeoxycholic Scaffolds as Non-Toxic, Potent Antimicrobials. *Antibiotics* **2023**, *12*, 404, doi:10.3390/antibiotics12020404.

48. Monte, M.J.; Marin, J.J.; Antelo, A.; Vazquez-Tato, J. Bile Acids: Chemistry, Physiology, and Pathophysiology. *World J. Gastroenterol.* **2009**, *15*, 804, doi:10.3748/wjg.15.804.

49. Coello, A.; Meijide, F.; Núñez, E.R.; Tato, J.V. Aggregation Behavior of Bile Salts in Aqueous Solution. *J. Pharm. Sci.* **1996**, *85*, 9–15, doi:10.1021/js950326j.

50. Poša, M.; Bjedov, S.; Sebenji, A.; Sakač, M. Wittig Reaction (with Ethylidene Triphenylphosphorane) of Oxo-Hydroxy Derivatives of 5β-Cholanic Acid: Hydrophobicity, Haemolytic Potential and Capacity of Derived Ethylidene Derivatives for Solubilisation of Cholesterol. *Steroids* **2014**, *86*, 16–25, doi:10.1016/j.steroids.2014.04.018.

51. Natalini, B.; Sardella, R.; Gioiello, A.; Ianni, F.; Di Michele, A.; Marinozzi, M. Determination of Bile Salt Critical Micellization Concentration on the Road to Drug Discovery. *J. Pharm. Biom. Anal.* **2014**, *87*, 62–81, doi:10.1016/j.jpba.2013.06.029.

52. Russell, D.W. The Enzymes, Regulation, and Genetics of Bile Acid Synthesis. *Annu. Rev. Biochem.* **2003**, *72*, 137–174, doi:10.1146/annurev.biochem.72.121801.161712.

53. Björkhem, I.; Leoni, V.; Meaney, S. Genetic Connections between Neurological Disorders and Cholesterol Metabolism. *J. Lipid Res.* **2010**, *51*, 2489–2503, doi:10.1194/jlr.R006338.

54. Quinn, R.A.; Melnik, A.V.; Vrbanac, A.; Fu, T.; Patras, K.A.; Christy, M.P.; Bodai, Z.; Belda-Ferre, P.; Tripathi, A.; Chung, L.K.; et al. Global Chemical Effects of the Microbiome Include New Bile-Acid Conjugations. *Nature* **2020**, *579*, 123–129, doi:10.1038/s41586-020-2047-9.

55. Li, T.; Francl, J.M.; Boehme, S.; Chiang, J.Y.L. Regulation of Cholesterol And Bile Acid Homeostasis by the Cholesterol 7α-Hydroxylase/Steroid Response Element-Binding Protein 2/Microrna-33A Axis in Mice. *Hepatology* **2013**, *58*, 1111, doi:10.1002/hep.26427.

56. Kevresan, S.; Kuhajda, K.; Kandrac, J.; Fawcett, J.P.; Mikov, M. Biosynthesis of Bile Acids in Mammalian Liver. *Eur. J. Drug Metab. Pharmacokinet.* **2006**, *31*, 145–156, doi:10.1007/BF03190711.

57. Sarenac, T.; Mikov, M. Biosynthesis and Biotransformation of Bile Acids. *Hosp. Pharm. Int. Multi. J.* **2017**, *4*, 469–485, doi:10.5937/hpimj1701469S.

58. Solaas, K.; Ulvestad, A.; Söreide, O.; Kase, B.F. Subcellular Organization of Bile Acid Amidation in Human Liver: A Key Issue in Regulating the Biosynthesis of Bile Salts. *J. Lipid Res.* **2000**, *41*, 1154–1162, doi: 10.1016/S0022-2275(20)32022-8.

59. Pellicoro, A.; van den Heuvel, F.A.J.; Geuken, M.; Moshage, H.; Jansen, P.L.M.; Faber, K.N. Human and Rat Bile Acid–CoA:Amino acid N-Acyltransferase Are Liver-Specific Peroxisomal Enzymes: Implications for Intracellular Bile Salt Transport. *Hepatology* **2007**, *45*, 340, doi:10.1002/hep.21528.

60. Ridlon, J.M.; Kang, D.-J.; Hylemon, P.B. Bile Salt Biotransformations by Human Intestinal Bacteria. *J. Lipid Res.* **2006**, *47*, 241–259, doi:10.1194/jlr.R500013-JLR200.

61. Ridlon, J.M.; Gaskins, H.R. Another Renaissance for Bile Acid Gastrointestinal Microbiology. *Nat. Rev. Gastroenterol. Hepatol.* **2024**, *21*, 348–364, doi:10.1038/s41575-024-00896-2.

62. Zasloff, M.; Adams, A.P.; Beckerman, B.; Campbell, A.; Han, Z.; Luijten, E.; Meza, I.; Julander, J.; Mishra, A.; Qu, W.; Taylor, J. M.; Weaver, S.C.; Wong, G.C.L. Squalamine as a broad-spectrum systemic antiviral agent with therapeutic potential. *Biol. Sci.* **2011**, *108* (38), 15978–15983, doi: 10.1073/pnas.1108558108.

63. Moore, K.S.; Wehrli, S.; Roder, H.; Rogers, M.; Forrest, J.N.; McCrimmon, D.; Zasloff, M. Squalamine: An Aminosterol Antibiotic from the Shark. *Proc. Natl. Acad. Sci. USA* **1993**, *90*, 1354–1358, doi:10.1073/pnas.90.4.1354.

64. Brunel, J.; Salmi, C.; Loncle, C.; Vidal, N.; Letourneux, Y. Squalamine: A Polyvalent Drug of the Future? *Curr. Cancer Drug Targets* **2005**, *5*, 267–272, doi:10.2174/1568009054064642.

65. Limbocker, R.; Staats, R.; Chia, S.; Ruggeri, F.S.; Mannini, B.; Xu, C.K.; Perni, M.; Cascella, R.; Bigi, A.; Sasser, L.R.; et al. Squalamine and Its Derivatives Modulate the Aggregation of Amyloid-β and α-Synuclein and Suppress the Toxicity of Their Oligomers. *Front. Neurosci.* **2021**, *15*, 680026, doi:10.3389/fnins.2021.680026.

66. Mammari, N.; Salles, E.; Beaussart, A.; El-Kirat-Chatel, S.; Varbanov, M. Squalamine and Its Aminosterol Derivatives: Overview of Biological Effects and Mechanisms of Action of Compounds with Multiple Therapeutic Applications. *Microorganisms* **2022**, *10*, 1205, doi:10.3390/microorganisms10061205.

67. Agarwal, D.S.; Anantaraju, H.S.; Sriram, D.; Yogeeswari, P.; Nanjegowda, S.H.; Mallu, P.; Sakhuja, R. Synthesis, Characterization and Biological Evaluation of Bile Acid-Aromatic/Heteroaromatic Amides Linked via Amino Acids as Anti-Cancer Agents. *Steroids* **2016**, *107*, 87–97, doi:10.1016/j.steroids.2015.12.022.

68. Ruwizhi, N.; Adeyemi, S.A.; Ubanako, P.; Morifi, E.; Fonkui, Y.T.; Ndinteh, D.T.; Choonara, Y.E.; Aderibigbe, B.A. Cholesterol-Based Conjugates: Synthesis, Characterization and *In Vitro* Biological Studies. *Chem. Select.* **2021**, *6*, 11985–11993, doi:10.1002/slct.202102784.

69. Bansal, R.; Suryan, A. A Comprehensive Review on Steroidal Bioconjugates as Promising Leads in Drug Discovery. *ACS Bio. Med. Chem. Au* **2022**, *2*, 340–369, doi:10.1021/acsbiomedchemau.1c00071.

70. Shansky, Y.; Bespyatykh, J. Bile Acids: Physiological Activity and Perspectives of Using in Clinical and Laboratory Diagnostics. *Molecules* **2022**, *27*, 7830, doi:10.3390/molecules27227830.

71. Narayan, S.; Muldoon, J.; Finn, M.G.; Fokin, V.V.; Kolb, H.C.; Sharpless, K.B. „On Water": Unique Reactivity of Organic Compounds in Aqueous Suspension. *Angew. Chem. Int. Ed.* **2005**, *44*, 3275–3279, doi:10.1002/anie.200462883.

72. da S M Forezi, L.; Cardoso, M.F.C.; Gonzaga, D.T.G.; de C da Silva, F.; Ferreira, V.F. Alternative Routes to the Click Method for the Synthesis of 1,2,3-Triazoles, an Important Heterocycle in Medicinal Chemistry. *Curr. Top. Med. Chem.* **2018**, *18*, 1428–1453, doi:10.2174/1568026618666180821143902.

73. Kumar, V.; Lal, K.; Naveen; Tittal, R.K. The Fate of Heterogeneous Catalysis & Click Chemistry for 1,2,3-Triazoles: Nobel Prize in Chemistry 2022. *Catal. Commun.* **2023**, *176*, 106629, doi:10.1016/j.catcom.2023.106629.

74. Malkoch, M.; Thibault, R.J.; Drockenmuller, E.; Messerschmidt, M.; Voit, B.; Russell, T.P.; Hawker, C.J. Orthogonal Approaches to the Simultaneous and Cascade Functionalization of Macromolecules Using Click Chemistry. *J. Am. Chem. Soc.* **2005**, *127*, 14942–14949, doi:10.1021/ja0549751.

75. Woo, H.; Kang, H.; Kim, A.; Jang, S.; Park, J.C.; Park, S.; Kim, B.-S.; Song, H.; Park, K.H. Azide-Alkyne Huisgen [3+2] Cycloaddition Using CuO Nanoparticles. *Molecules* **2012**, *17*, 13235–13252, doi:10.3390/molecules171113235.

76. Huisgen, R. Kinetics and Mechanism of 1,3-Dipolar Cycloadditions. *Angew. Chem., Int. Ed. Engl.* **1963**, *2*, 633–645, doi:https://doi.org/10.1002/anie.196306331.

77. Amblard, F.; Cho, J.H.; Schinazi, R.F. Cu(I)-Catalyzed Huisgen Azide−Alkyne 1,3-Dipolar Cycloaddition Reaction in Nucleoside, Nucleotide, and Oligonucleotide Chemistry. *Chem. Rev.* **2009**, *109*, 4207–4220, doi:10.1021/cr9001462.

78. Hein, J.E.; Fokin, V.V. Copper-Catalyzed Azide–Alkyne Cycloaddition (CuAAC) and beyond: New Reactivity of Copper(I) Acetylides. *Chem. Soc. Rev.* **2010**, *39*, 1302–1315, doi:10.1039/B904091A.

79. Tron, G.C.; Pirali, T.; Billington, R.A.; Canonico, P.L.; Sorba, G.; Genazzani, A.A. Click Chemistry Reactions in Medicinal Chemistry: Applications of the 1,3-Dipolar Cycloaddition between Azides and Alkynes. *Med. Res. Rev.* **2008**, *28*, 278–308, doi:10.1002/med.20107.

80. Fang, Y.; Bao, K.; Zhang, P.; Sheng, H.; Yun, Y.; Hu, S.-X.; Astruc, D.; Zhu, M. Insight into the Mechanism of the CuAAC Reaction by Capturing the Crucial Au_4Cu_4–π-Alkyne Intermediate. *J. Am. Chem. Soc.* **2021**, *143*, 1768–1772, doi:10.1021/jacs.0c12498.

81. Ramapanicker, R.; Chauhan, P. Click Chemistry: Mechanistic and Synthetic Perspectives. In *Click Reactions in Organic Synthesis*; Wydawnictwo Wiley–VCH Verlag GmbH & Co. KGaA, Weinheim, Germany, **2016**, 1–24.

82. Lipshutz, B.H.; Taft, B.R. Heterogeneous Copper-in-Charcoal-Catalyzed „Click" Chemistry. *Angew. Chem.* **2006**, *118*, 8415–8418, doi:10.1002/ange.200603726.

83. Grudzka-Flak, I. Reakcje Addycji, Cykloaddycji i Sprzęgania w Syntezie Nowych Pochodnych Arenów i Heteroarenów z Podstawnikami Bitienylowymi. Praca doktorska, Katowice, **2016**.

84. Liang, L.; Astruc, D. The Copper(I)-Catalyzed Alkyne-Azide Cycloaddition (CuAAC) „Click" Reaction and Its Applications. An Overview. *Coord. Chem. Rev.* **2011**, *255*, 2933–2945, doi:10.1016/j.ccr.2011.06.028.

85. Kumar, A.; Kumar, V.; Singh, P.; Tittal, R.K.; Lal, K. Ionic Liquids for the Green Synthesis of 1,2,3-Triazoles: A Systematic Review. *Green Chem.* **2024**, *26*, 3565–3594, doi:10.1039/D3GC04898E.

86. Bonandi, E.; Christodoulou, M.S.; Fumagalli, G.; Perdicchia, D.; Rastelli, G.; Passarella, D. The 1,2,3-Triazole Ring as a Bioisostere in Medicinal Chemistry. *Drug Discov. Today* **2017**, *22*, 1572–1581, doi:10.1016/j.drudis.2017.05.014.

87. Agalave, S.G.; Maujan, S.R.; Pore, V.S. Click Chemistry: 1,2,3-Triazoles as Pharmacophores. *Chem. Asian J.* **2011**, *6*, 2696–2718, doi:10.1002/asia.201100432.

88. Guo, H.-Y.; Chen, Z.-A.; Shen, Q.-K.; Quan, Z.-S. Application of Triazoles in the Structural Modification of Natural Products. *J. Enzyme Inhib. Med. Chem.* **2021**, *36*, 1115–1144, doi:10.1080/14756366.2021.1890066.

89. Alam, M.M. 1,2,3-Triazole Hybrids as Anticancer Agents: A Review. *Arch. Pharm.* **2022**, *355*, 2100158, doi:10.1002/ardp.202100158.

90. Li, Q.; Qi, S.; Liang, J.; Tian, Y.; He, S.; Liao, Q.; Xing, S.; Han, L.; Chen, X. Review of Triazole Scaffolds for Treatment and Diagnosis of Alzheimer's Disease. *Chem.-Biol. Interact*. **2023**, *382*, 110623, doi:10.1016/j.cbi.2023.110623.

91. Aflak, N.; Ben El Ayouchia, H.; Bahsis, L.; El Mouchtari, E.M.; Julve, M.; Rafqah, S.; Anane, H.; Stiriba, S.-E. Sustainable Construction of Heterocyclic 1,2,3-Triazoles by Strict Click [3+2] Cycloaddition Reactions Between Azides and Alkynes on Copper/Carbon in Water. *Front. Chem*. **2019**, *7*, 81,doi:10.3389/fchem.2019.00081.

92. Aher, N.G.; Pore, V.S.; Patil, S.P. Design, Synthesis, and Micellar Properties of Bile Acid Dimers and Oligomers Linked with a 1,2,3-Triazole Ring. *Tetrahedron* **2007**, *63*, 12927–12934, doi:10.1016/j.tet.2007.10.042.

93. Suarez, P.L.; Gándara, Z.; Gómez, G.; Fall, Y. Vitamin D and Click Chemistry. Part 1: A Stereoselective Route to Vitamin D Analogues with Triazole Rings in Their Side Chains. *Tetrahedron Lett.* **2004**, *45*, 4619–4621, doi:10.1016/j.tetlet.2004.04.117.

94. Evanoff, D.D.; Chumanov, G. Synthesis and Optical Properties of Silver Nanoparticles and Arrays. *Chemphyschem* **2005**, *6*, 1221–1231, doi:10.1002/cphc.200500113.

95. Pospieszny, T.; Koenig, H.; Kowalczyk, I.; Brycki, B. Spectroscopic Methods and Theoretical Studies of Bromoacetic Substituted Derivatives of Bile Acids. *Acta Chim. Slov.* **2015**, *62*, 15–27, doi:10.17344/acsi.2014.608.

96. Pore, V.S.; Aher, N.G.; Kumar, M.; Shukla, P.K. Design and Synthesis of Fluconazole/Bile Acid Conjugate Using Click Reaction. *Tetrahedron* **2006**, *62*, 11178–11186, doi:10.1016/j.tet.2006.09.021.

97. Luo, J.; Chen, Y.; Zhu, X. Highly Efficient Synthesis and Inclusion Properties of Star-Shaped Amphiphilic Derivatives of Cholic Acid. *Synlett* **2007**, *2007*, 2201–2204, doi:10.1055/s-2007-984909.

98. Chang, K.-H.; Lee, L.; Chen, J.; Li, W.-S. Lithocholic Acid Analogues, New and Potent α-2,3-Sialyltransferase Inhibitors. *Chem. Commun.* **2006**, 629, doi:10.1039/b514915k.

99. Zhang, Z.; Ju, Y.; Zhao, Y. Synthesis of 1,2,3-Triazole-Containing Bile Acid Dimers and Properties of Inverse Micellar Mimic. *Chem. Lett.* **2007**, *36*, 1450–1451, doi:10.1246/cl.2007.1450.

100. Pospieszny, T.; Koenig, H.; Kowalczyk, I.; Brycki, B. Synthesis, Spectroscopic and Theoretical Studies of New Quasi-Podands from Bile Acid Derivatives Linked by 1,2,3-Triazole Rings. *Molecules* **2014**, *19*, 2557–2570, doi:10.3390/molecules19022557.

101. Kumar, A.; Chhatra, R.K.; Pandey, P.S. Synthesis of Click Bile Acid Polymers and Their Application in Stabilization of Silver Nanoparticles Showing Iodide Sensing Property. *Org. Lett.* **2010**, *12*, 24–27, doi:10.1021/ol902351g.

102. Vatmurge, N.S.; Hazra, B.G.; Pore, V.S.; Shirazi, F.; Chavan, P.S.; Deshpande, M.V. Synthesis and Antimicrobial Activity of β-Lactam–Bile Acid Conjugates Linked *via* Triazole. *Bioorg. Med. Chem. Lett.* **2008**, *18*, 2043–2047, doi:10.1016/j.bmcl.2008.01.102.

103. Suh, B.-C.; Jeon, H.; Posner, G.H.; Silverman, S.M. Vitamin D Side Chain Triazole Analogs *via* Cycloaddition „Click" Chemistry. *Tetrahedron Lett.* **2004**, *45*, 4623–4625, doi:10.1016/j.tetlet.2004.04.118.

104. Ropponen, J.; Tamminen, J.; Kolehmainen, E.; Rissanen, K. Synthesis and Characterization of Novel Steroidal Dendrons. *Synthesis* **2003**, 2226–2230, doi:10.1055/s-2003-41041.

105. Pore, V.S.; Jagtap, M.A.; Agalave, S.G.; Pandey, A.K.; Siddiqi, M.I.; Kumar, V.; Shukla, P.K. Synthesis and Antifungal Activity of 1,5-Disubstituted-1,2,3-Triazole Containing Fluconazole Analogues. *Med. Chem. Commun.* **2012**, *3*, 484, doi:10.1039/c2md00205a.

106. Aher, N.G.; Pore, V.S.; Mishra, N.N.; Kumar, A.; Shukla, P.K.; Sharma, A.; Bhat, M.K. Synthesis and Antifungal Activity of 1,2,3-Triazole Containing Fluconazole Analogues. *Bioorg. Med. Chem. Lett.* **2009**, *19*, 759–763, doi:10.1016/j.bmcl.2008.12.026.

107. Khaligh, P.; Salehi, P.; Bararjanian, M.; Aliahmadi, A.; Khavasi, H.R.; Nejad-Ebrahimi, S. Synthesis and *in Vitro* Antibacterial Evaluation of Novel 4-Substituted 1-Menthyl-1,2,3-Triazoles. *Chem. Pharm. Bull.* **2016**, *64*, 1589–1596, doi:10.1248/cpb.c16-00463.

108. Shiri, P. Novel Hybrid Molecules Based on Triazole-β-Lactam as Potential Biological Agents. *Mini Rev. Med. Chem.* **2021**, *21*, 536–553, doi:10.2174/1389557520666201027160436.

109. Kim, H.-S.; Jadhav, J.R.; Jung, S.-J.; Kwak, J.-H. Synthesis and Antimicrobial Activity of Imidazole and Pyridine Appended Cholestane-Based Conjugates. *Bioorg. Med. Chem. Lett.* **2013**, *23*, 4315–4318, doi:10.1016/j.bmcl.2013.05.098.

110. Singla, P.; Kaur, M.; Kumari, A.; Kumari, L.; Pawar, S.V.; Singh, R.; Salunke, D.B. Facially Amphiphilic Cholic Acid-Lysine Conjugates as Promising Antimicrobials. *ACS Omega* **2020**, *5*, 3952–3963, doi:10.1021/acsomega.9b03425.

111. Mann, S.; Frasca, K.; Scherrer, S.; Henao-Martínez, A.F.; Newman, S.; Ramanan, P.; Suarez, J.A. A Review of Leishmaniasis: Current Knowledge and Future Directions. *Curr. Trop. Med. Rep.* **2021**, *8*, 121–132, doi:10.1007/s40475-021-00232-7.

112. Fikadu, M.; Ashenafi, E. Malaria: An Overview. *Ind. Eng. Chem. Res.* **2023**, *16*, 3339–3347, doi:10.2147/IDR.S405668.

113. Corrales, R.C.N.R.; de Souza, N.B.; Pinheiro, L.S.; Abramo, C.; Coimbra, E.S.; Da Silva, A.D. Thiopurine Derivatives Containing Triazole and Steroid: Synthesis, Antimalarial and Antileishmanial Activities. *Biom. Pharm.* **2011**, *65*, 198–203, doi:10.1016/j.biopha.2010.10.013.

114. Shiradkar, M.; Suresh Kumar, G.V.; Dasari, V.; Tatikonda, S.; Akula, K.C.; Shah, R. Clubbed Triazoles: A Novel Approach to Antitubercular Drugs. *Eur. J. Med. Chem.* **2007**, *42*, 807–816, doi:10.1016/j.ejmech.2006.12.001.

115. Navacchia, M.L.; Marchesi, E.; Perrone, D. Bile Acid Conjugates with Anticancer Activity: Most Recent Research. *Molecules* **2020**, *26*, 25, doi:10.3390/molecules26010025.

116. Agarwal, D.S.; Sakhuja, R.; Beteck, R.M.; Legoabe, L.J. Steroid-Triazole Conjugates: A Brief Overview of Synthesis and Their Application as Anticancer Agents. *Steroids* **2023**, *197*, 109258, doi:10.1016/j.steroids.2023.109258.

117. Agarwal, D.S.; Siva Krishna, V.; Sriram, D.; Yogeeswari, P.; Sakhuja, R. Clickable Conjugates of Bile Acids and Nucleosides: Synthesis, Characterization, *in Vitro* Anticancer and Antituberculosis Studies. *Steroids* **2018**, *139*, 35–44, doi:10.1016/j.steroids.2018.09.006.

118. Navacchia, M.; Marchesi, E.; Mari, L.; Chinaglia, N.; Gallerani, E.; Gavioli, R.; Capobianco, M.; Perrone, D. Rational Design of Nucleoside–Bile Acid Conjugates Incorporating a Triazole Moiety for Anticancer Evaluation and SAR Exploration. *Molecules* **2017**, *22*, 1710, doi:10.3390/molecules22101710.

119. Perrone, D.; Bortolini, O.; Fogagnolo, M.; Marchesi, E.; Mari, L.; Massarenti, C.; Navacchia, M.L.; Sforza, F.; Varani, K.; Capobianco, M.L. Synthesis and *in Vitro* Cytotoxicity of Deoxyadenosine–Bile Acid Conjugates Linked with 1,2,3-Triazole. *New J. Chem.* **2013**, *37*, 3559, doi:10.1039/c3nj00513e.

120. Anandkumar, D.; Rajakumar, P. Synthesis and Anticancer Activity of Bile Acid Dendrimers with Triazole as Bridging Unit through Click Chemistry. *Steroids* **2017**, *125*, 37–46, doi:10.1016/j.steroids.2017.06.007.

121. Ibrahim-Ouali, M.; Dumur, F. Recent Syntheses of Steroid Derivatives Using the CuAAC „Click" Reaction. *Arkivoc* **2021**, *2021*, 130–149, doi:10.24820/ARK.5550190.P011.543.

122. Bendi, A.; Vashisth, C.; Yadav, S.; Pundeer, R.; Raghav, N. Recent Advances in the Synthesis of Cholesterol-Based Triazoles and Their Biological Applications. *Steroids* **2024**, *211*, 109499, doi:10.1016/j.steroids.2024.109499.

123. Ameziane El Hassani, I.; Rouzi, K.; Ameziane El Hassani, A.; Karrouchi, K.; Ansar, M. Recent Developments Towards the Synthesis of Triazole Derivatives: A Review. *Organics* **2024**, *5*, 450–471, doi:10.3390/org5040024.

124. Bariya, D.; Anand, V.; Mishra, S. Recent Advances in the Bile Acid Based Conjugates/Derivatives towards Their Gelation Applications. *Steroids* **2021**, *165*, 108769, doi:10.1016/j.steroids.2020.108769.

125. Patel, S.; Challagundla, N.; Rajput, R.A.; Mishra, S. Design, Synthesis, Characterization and Anticancer Activity Evaluation of Deoxycholic Acid-Chalcone Conjugates. *Bioorg. Chem.* **2022**, *127*, 106036, doi:10.1016/j.bioorg.2022.106036.

126. Kaper, J.B.; Nataro, J.P.; Mobley, H.L.T. Pathogenic *Escherichia Coli*. *Nat. Rev. Microbiol.* **2004**, *2*, 123–140, doi:10.1038/nrmicro818.

127. Backx, M.; Healy, B. Serious Staphylococcal Infections. *Clin. Med. (Lond.)* **2008**, *8*, 535–538, doi:10.7861/clinmedicine.8-5-535.

128. Talapko, J.; Juzbašić, M.; Matijević, T.; Pustijanac, E.; Bekić, S.; Kotris, I.; Škrlec, I. *Candida Albicans*-The Virulence Factors and Clinical Manifestations of Infection. *J. Fungi (Basel)* **2021**, *7*, 79, doi:10.3390/jof7020079.

129. Hocking, A.D. *Aspergillus* and Related Teleomorphs. In *Food Spoilage Microorganisms*; Blackburn, C. de W., Ed.; Woodhead Publishing Series in Food Science, Technology and Nutrition; Woodhead Publishing, **2006**, 451–487.

130. Zhao, Y.; Ye, L.; Zhao, F.; Zhang, L.; Lu, Z.; Chu, T.; Wang, S.; Liu, Z.; Sun, Y.; Chen, M.; Liao, G.; Ding, C.; Xu, Y.; Liao, W.; Wang, L. *Cryptococcus Neoformans*, a Global Threat to Human Health. *Infect. Dis. Poverty* **2023**, *12*, 20, doi:10.1186/s40249-023-01073-4.

131. Ishikawa, T.; Hosaka, Y.Z.; Beckwitt, C.; Wells, A.; Oltvai, Z.N.; Warita, K. Concomitant Attenuation of HMG-CoA Reductase Expression Potentiates the Cancer Cell Growth-Inhibitory Effect of Statins and Expands Their Efficacy in Tumor Cells with Epithelial Characteristics. *Oncotarget* **2018**, *9*, 29304–29315, doi:10.18632/oncotarget.25448.

132. Friesen, J.A.; Rodwell, V.W. The 3-Hydroxy-3-Methylglutaryl Coenzyme-A (HMG-CoA) Reductases. *Genome Biol.* **2004**, *5*, 248, doi:10.1186/gb-2004-5-11-248.

133. Yu, B.; Shi, X.-J.; Zheng, Y.-F.; Fang, Y.; Zhang, E.; Yu, D.-Q.; Liu, H.-M. A Novel [1,2,4] Triazolo [1,5-*a*] Pyrimidine-Based Phenyl-Linked Steroid Dimer: Synthesis and Its Cytotoxic Activity. *Eur. J. Med. Chem.* **2013**, *69*, 323–330, doi:10.1016/j.ejmech.2013.08.029.

134. Kumar, K.; Liu, N.; Yang, D.; Na, D.; Thompson, J.; Wrischnik, L.A.; Land, K.M.; Kumar, V. Synthesis and Antiprotozoal Activity of Mono- and Bis-Uracil Isatin Conjugates against the Human Pathogen *Trichomonas Vaginalis*. *Bioorg. Med. Chem.* **2015**, *23*, 5190–5197, doi:10.1016/j.bmc.2015.04.075.

135. Arenas-González, A.; Mendez-Delgado, L.A.; Merino-Montiel, P.; Padrón, J.M.; Montiel-Smith, S.; Vega-Báez, J.L.; Meza- Reyes, S. Synthesis of Monomeric and Dimeric Steroids Containing [1,2,4]Triazolo[1,5-*a*]Pyrimidines. *Steroids* **2016**, *116*, 13–19, doi:10.1016/j.steroids.2016.09.014.

136. Cortés-Percino, A.; Vega-Báez, J.L.; Romero-López, A.; Puerta, A.; Merino-Montiel, P.; Meza-Reyes, S.; Padrón, J.M.; Montiel-Smith, S. Synthesis and Evaluation of Pyrimidine Steroids as Antiproliferative Agents. *Molecules* **2019**, *24*, 3676, doi:10.3390/molecules24203676.

137. Andreeva, O.V.; Garifullin, B.F.; Zarubaev, V.V.; Slita, A.V.; Yesaulkova, I.L.; Volobueva, A.S.; Belenok, M.G.; Man'kova, M.A.; Saifina, L.F.; Shulaeva, M.M.; et al. Synthesis and Antiviral Evaluation of Nucleoside Analogues Bearing One Pyrimidine Moiety and Two D-Ribofuranosyl Residues. *Molecules* **2021**, *26*, 3678, doi:10.3390/molecules26123678.

Streszczenie

Synteza, analiza spektroskopowa oraz badania biologiczne *in silico* nowych koniugatów steroidowych zawierających układy triazolowe

mgr inż. Anna Kawka

Promotor: prof. UAM dr hab. Tomasz Pospieszny

Promotor pomocnicza: dr inż. Hanna Koenig

Praca doktorska koncentruje się na projektowaniu, syntezie, izolacji i oczyszczeniu oraz charakterystyce spektroskopowej i przewidywaniu aktywności biologicznej nowych biokoniugatów steroidowych. Opracowane związki stanowią połączenie fragmentów kwasów żółciowych oraz zasad pirymidynowych za pomocą pierścieni 1,2,3-triazolowych, uzyskanych w wyniku reakcji typu „click", w kontekście poszukiwania nowych związków o potencjale farmakologicznym. Rozprawa obejmuje zarówno przegląd literaturowy, jak i oryginalne badania eksperymentalne i teoretyczne.

W części literaturowej omówiono znaczenie biokoniugatów steroidowych, takich jak skwalamina i jej pochodne, w terapiach farmakologicznych. Zwrócono szczególną uwagę na zastosowanie chemii „click" w modyfikacji kwasów żółciowych i steroli. Takie podejście umożliwia tworzenie stabilnych i bioaktywnych struktur supramolekularnych. Skrupulatnie przeanalizowano współczesne osiągnięcia w zakresie koniugatów steroidowo-triazolowych jako inhibitorów enzymów i potencjalnych leków przeciwinfekcyjnych.

W części badawczej opracowano trzy grupy nowych związków: (1) koniugaty kwasów żółciowych i steroli z pierścieniami 1,2,3-triazolowymi wykazują przewidywaną aktywność przeciwgrzybiczną i przeciwbakteryjną; (2) quasi-podandy z układami triazolowymi strukturalnie przypominają układy supramolekularne podatne na tworzenie kompleksów typu gospodarz-gość, co otwiera możliwości w nanotechnologii i systemach dostarczania leków, zwłaszcza w leczeniu hipercholesterolemii; (3) hybrydy steroidowo-pirymidynowe (z uracylem i 2-tiouracylem) charakteryzuje zdolność do interakcji z enzymami metabolizmu lipidów i potencjalne zastosowanie w terapiach przeciwnowotworowych, przeciwdrobnoustrojowych i dermatologicznych.

Wyniki analiz spektroskopowych (^{1}H i ^{13}C NMR, FT-IR) i spektrometrycznych (ESI-MS, EI-MS) oraz obliczeń teoretycznych (PM5, GIAO) potwierdziły poprawność struktur molekularnych i stabilność chemiczną związków. Badania *in silico* metodą PASS oraz dokowania molekularnego wykazały ich szerokie spektrum potencjalnej aktywności biologicznej, obejmujące działanie przeciwnowotworowe, przeciwdrobnoustrojowe, cytoprotekcyjne i przeciwzapalne.

Praca przyczynia się do rozwoju chemii bioorganicznej, oferując nowe perspektywy w projektowaniu związków terapeutycznych o wielokierunkowym działaniu biologicznym.

Abstract

Synthesis, spectroscopic analysis and *in silico* biological studies of new steroid conjugates containing triazole systems

mgr inż. Anna Kawka

Supervisor: prof. UAM dr hab. Tomasz Pospieszny

Assistant supervisor: dr inż. Hanna Koenig

The doctoral thesis focuses on the design, synthesis, isolation, purification, spectroscopic characterisation and prediction of biological activity of new steroid bioconjugates. The developed compounds constitute a combination of fragments of bile acids and pyrimidine bases using 1,2,3-triazole rings obtained by a „click" reaction in the context of searching for new compounds with pharmacological potential. The dissertation includes both a literature review and original experimental and theoretical studies.

The literature section discusses the importance of steroid bioconjugates in pharmacological therapies, such as squalamine and its derivatives. Special attention was paid to the use of „click" chemistry in the modification of bile acids and sterols. This approach allows the creation of stable and bioactive supramolecular structures. The contemporary achievements in steroid-triazole conjugates as enzyme inhibitors and potential anti-infective drugs were meticulously analysed.

In the research part, three groups of new compounds were developed: (1) bile acid and sterol conjugates with 1,2,3-triazole rings exhibit predicted antifungal and antibacterial activity; (2) quasi-podands with triazole systems structurally resemble supramolecular systems susceptible to forming host-guest complexes, which opens up opportunities in nanotechnology and drug delivery systems, especially in treating hypercholesterolemia; (3) steroid-pyrimidine hybrids (with uracil and 2-thiouracil) are characterized by the ability to interact with lipid metabolism enzymes and potential use in anticancer, antimicrobial and dermatological therapies.

The results of spectroscopy analyses (^{1}H and ^{13}C NMR, FT-IR), spectrometry analyses (ESI-MS, EI-MS) and theoretical calculations (PM5, GIAO) confirmed the correctness of the molecular structures and chemical stability. *In silico* studies using PASS and molecular docking methods have shown their broad spectrum of potential biological activity, including anticancer, antimicrobial, cytoprotective and anti-inflammatory effects.

The work contributes to the development of bioorganic chemistry, offering new perspectives in designing therapeutic compounds with multidirectional biological activity.

Artykuły naukowe wchodzące w skład dysertacji doktorskiej oraz materiały uzupełniające

TRIAZOLE-BASED MODIFICATIONS OF BILE ACIDS: PROMISING STRATEGIES FOR COMBATING INFECTIONS AND CANCER – A REVIEW

Anna Kawka, Hanna Koenig, Tomasz Pospieszny
Department of Bioactive Products, Faculty of Chemistry,
Adam Mickiewicz University, Poznań
email: anna.kawka@amu.edu.pl

Abstract: The specific structure and high biological activity of bile acids resulted in their use in the design of new compounds with negligible toxicity and significant pharmacological activity. Natural steroid conjugates occupy a special place among natural products due to their participation in most metabolic pathways. Literature data indicate that in recent years, there has been a significant increase in interest in isolating, synthesizing, and modifying new steroid conjugates with broad physical, biological, and pharmacotherapeutic properties. Bile acid derivatives containing the 1,2,3-triazole ring are fundamental in drug discovery. Previous studies of steroid-triazole conjugates confirm their essential importance as compounds with high biocidal, antibacterial, and anticancer properties.

Keywords: bile acids, 1,2,3-triazole ring, anticancer and antimicrobial activity

1. Introduction

Compounds of natural origin play an essential role in the search for new molecules with biocidal properties. Their high availability and unique structure have made them used in the design of new drug syntheses [1, 2]. Bile acids are formed as products of cholesterol (**1**) metabolism (fig. 1). Their glycine/taurine-conjugated salts are stored in the gallbladder. Bile acids (e.g., lithocholic acid, deoxycholic acid, cholic acid) are responsible for the digestion of lipids in the small intestine. As surfactants, they help to lower surface tension and emulsify fats. Moreover, they regulate glucose homeostasis, cholesterol, fat transport, and enterohepatic circulation [3–6].

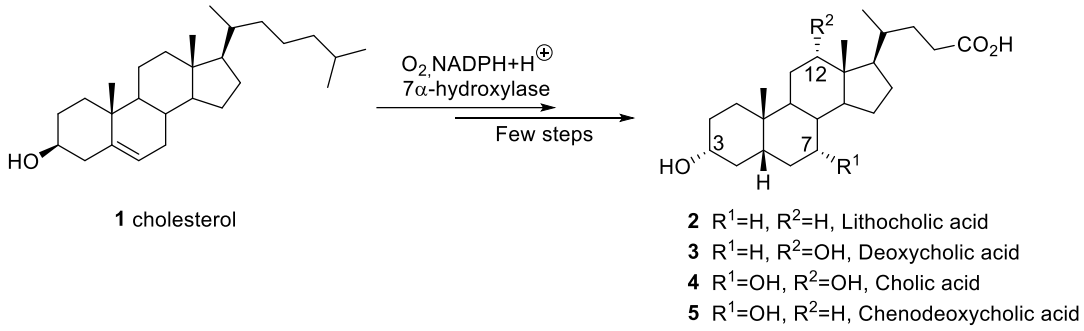

1 cholesterol

2 R^1=H, R^2=H, Lithocholic acid
3 R^1=H, R^2=OH, Deoxycholic acid
4 R^1=OH, R^2=OH, Cholic acid
5 R^1=OH, R^2=H, Chenodeoxycholic acid

Fig. 1. Shortened scheme of the biosynthesis of bile acids from cholesterol (**2**–**5**)

Bile acids (**2**–**5**) have a chiral rigid skeleton, a long side chain with a carboxyl group, and hydroxyl groups (3α–OH, 7α–OH, 12α–OH) with different reactivity and amphiphilic properties. Their low cost and several physicochemical properties make them ideal building materials in drug design. Most importantly, this use of bile acids entirely minimizes the risk of unwanted side effects [7–9]. Successful attempts to modify steroid molecules have often been carried out through coupling chemistry. The obtained steroid-triazole conjugates were distinguished by low toxicity, susceptibility to multidrug resistance, and bioavailability. They have become leading compounds in designing new biomolecules with biocidal and especially anticancer activity [10–14].

1,2,3-triazole systems are five-membered heterocyclic compounds of crystalline nature. They are soluble in water and alcohol. They resist oxidative/reductive stress, hydrolysis, and metabolic degradation. Triazole derivatives can also bind to receptors (or enzymes) through interactions, such as hydrogen bonding, van der Waal's forces, or hydrophobic interactions [15, 16]. It is worth noting that bonds formed in this way are resistant to cleavage by, for example, proteases. As a result, triazole systems can be analogues of the peptide bond [17]. Literature data show that 1,2,3-triazole compounds are characterized by exceptional pharmacotherapeutic activity, especially antihypertensive, antimalarial, antidiabetic, anticonvulsant, antioxidant, antidepressant, antiplasmoid, antimicrobial, antibacterial, anti-inflammatory, and antituberculosis [18–34].

Usually, 1,2,3-triazole derivatives are obtained by thermal 1,3-dipolar cycloaddition of azides and alkynes using a catalytic amount of copper(I) ions (fig. 2). The "Huisgen reaction" synthesizes macromolecular steroid-triazole conjugates [35–37]. The specific structure, amphipathic nature, and high activity of functional groups of bile acids determine their crucial importance in bioorganic synthesis. Steroid acids have become a precursor to preparing macrocyclic compounds or fluconazole derivatives, which have potent pharmacotherapeutic activity [38, 39].

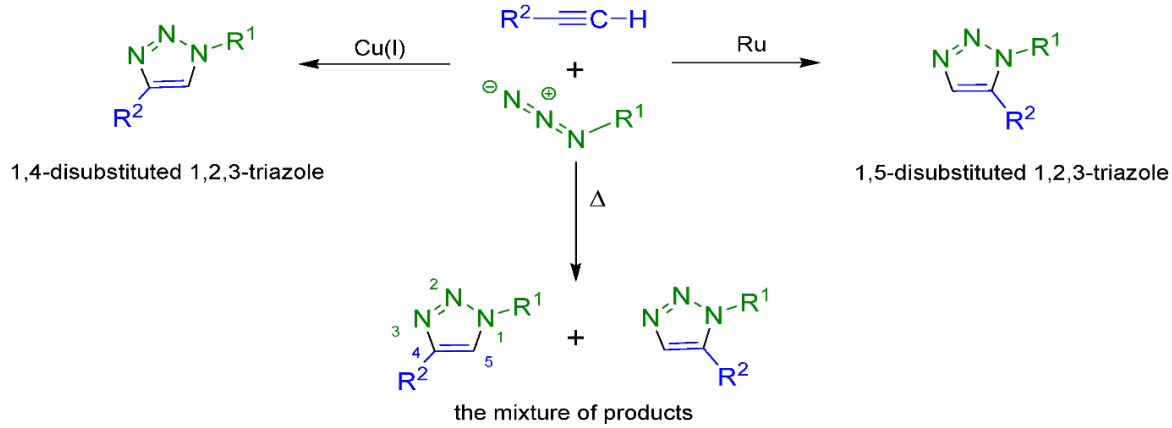

Fig. 2. Scheme of the preparation of 1,4- or 1,5-disubstituted 1,2,3-triazole rings

2. Steroid-triazole conjugates with biological activity

2.1. Bioconjugates with antibacterial and antifungal properties

Fluconazole is a potent compound used as an antibiotic in antifungal and antibacterial therapy (fig. 3). The growing resistance of bacteria to this drug made it necessary to change its structure.

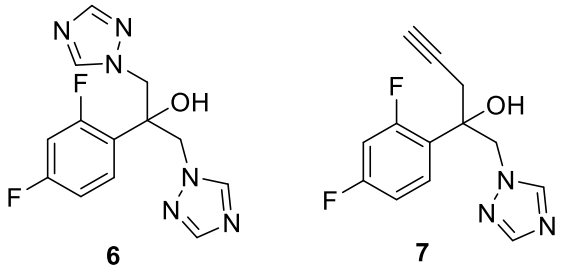

Fig. 3. Fluconazole (**6**) and its alkyne derivative (**7**)

A molecule of a suitable bile acid linked to fluconazole *via* a 1,2,3-triazole ring was designed (fig. 4). In this way, the amphipathic nature of bile acids was used as a drug transporter inhibiting bacterial strains' growth. On the other hand, thanks to the presence of the triazole ring, the new biomolecule gained resistance to enzymatic degradation. Compounds obtained (**8**–**11**) were almost entirely effective against strains of *Candida parapsilosis*, *Candida albicans*, and *Sporothrix scheckii* (MIC = 3.12–6.25 mg/ml) [39–41].

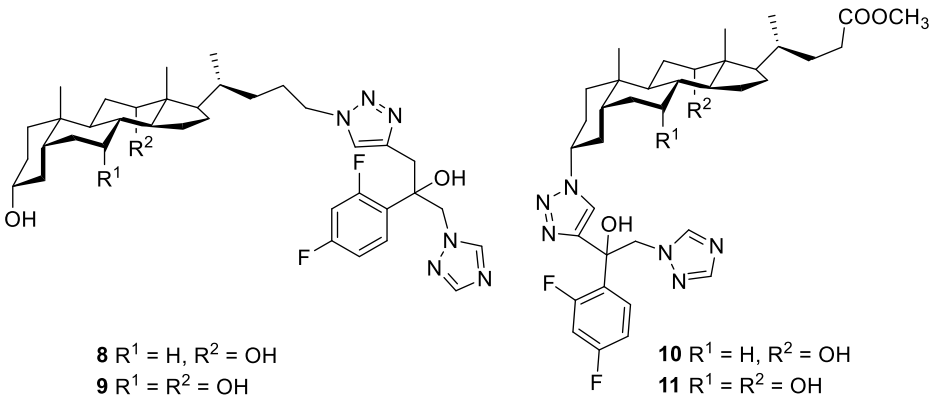

Fig. 4. Conjugates of fluconazole and bile acids (**8**–**11**) with antifungal activity

A similar "click" reaction was performed for the menthol molecule (fig. 5). The corresponding bile acids were esterified with propargyl bromide in the presence of K_2CO_3. On the other hand, in the reaction of methylated menthol with NaN_3 in DMF, a compound was obtained, which, by coupling with a bile acid derivative, gave triazole. The obtained 1,2,3-triazole derivatives (**12**–**14**) showed higher antimicrobial activity (MIC < 10 μM) against strains *Enterococcus faecium* menthol (MIC = 410 μM) and bile acids (MIC = 10, 20, 157, 410 μM). Interestingly, their antimicrobial activity was much stronger than the antibiotic cefixime (MIC = 35410 μM) [42].

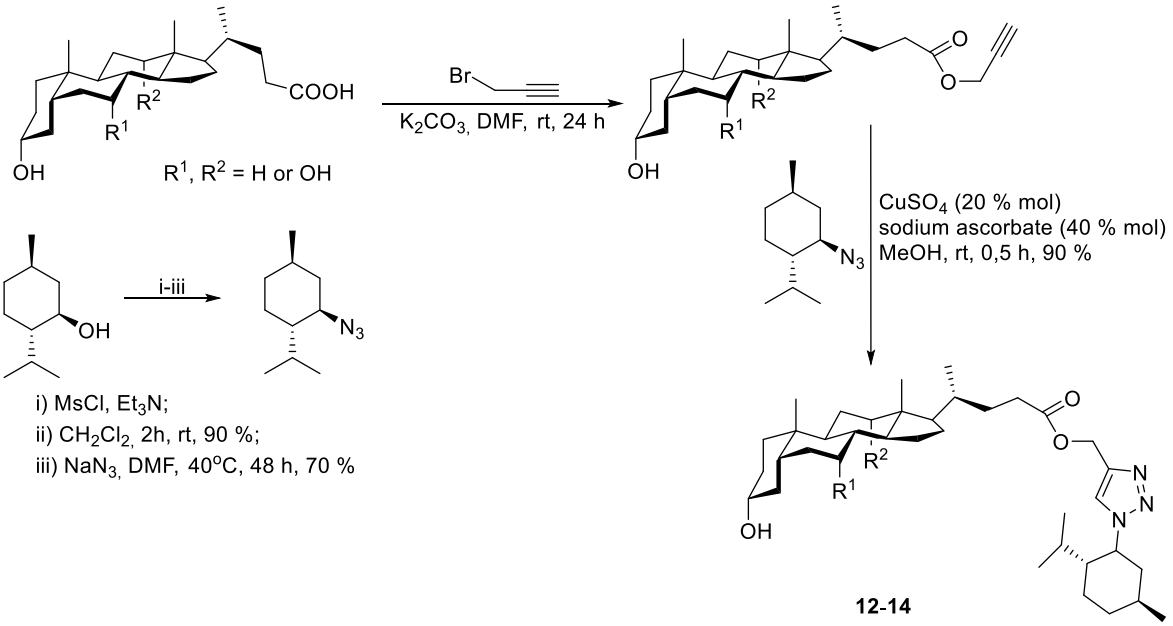

Fig. 5. Scheme of the preparation of triazole derivatives of menthol (**12**–**14**) [42]

2.2. Bioconjugates with antiparasitic effect

Corrales et al. efficiently synthesized novel triazole derivatives of cholic acid and 6-thiopurine (fig. 6). The conjugates obtained (**15**–**19**) were tested for their biological activity and cytotoxicity. Research *in vivo* confirmed their antimalarial efficacy far superior

to chloroquine (a substance used in patients diagnosed with malaria). Conjugate (**19**) was more effective than chloroquine on the 7th day of the study and all other compounds after 12 days. On the other hand, the tests performed *in vivo* indicate their action against Leishman's parasite. Most importantly, the resulting compounds are not toxic to mammalian cells [43, 44].

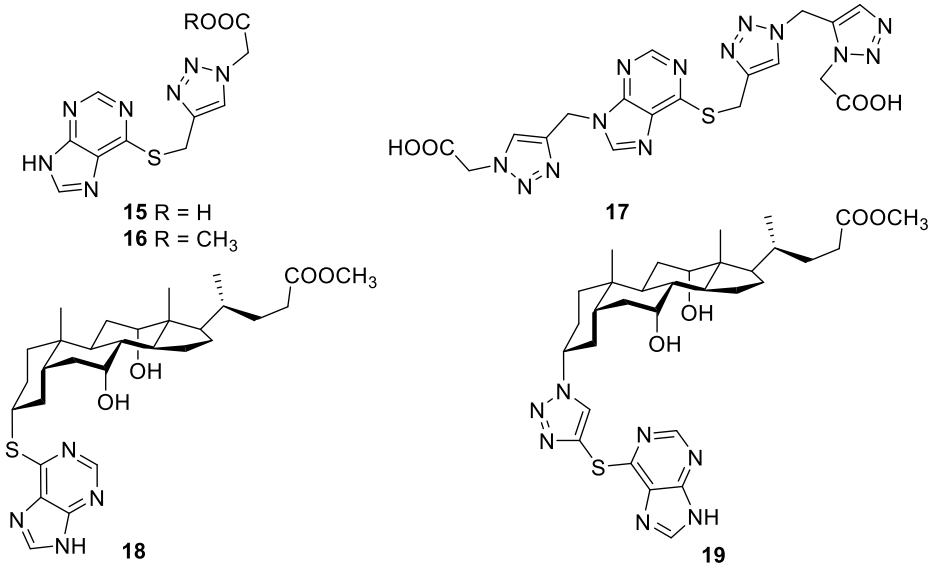

Fig. 6. Steroid-purine conjugates (**15**–**19**) with anti-leishmanial activity [43, 44]

The amino choline-bile acid compounds (**20**–**23**) exhibit exceptional activity against Leishman's parasite and *Mycobacterium tuberculosis*.(fig. 7). Conjugate (**20**) exhibits a similar inhibitory effect against *M. tuberculosis* (MIC = 8.8 μM) as available antituberculosis drugs. Biological testing of all structures (**21**–**23**) confirms their activity towards *promastigote* and *amastigota L. major*as well as leishmanicidal and antituberculosis properties [45].

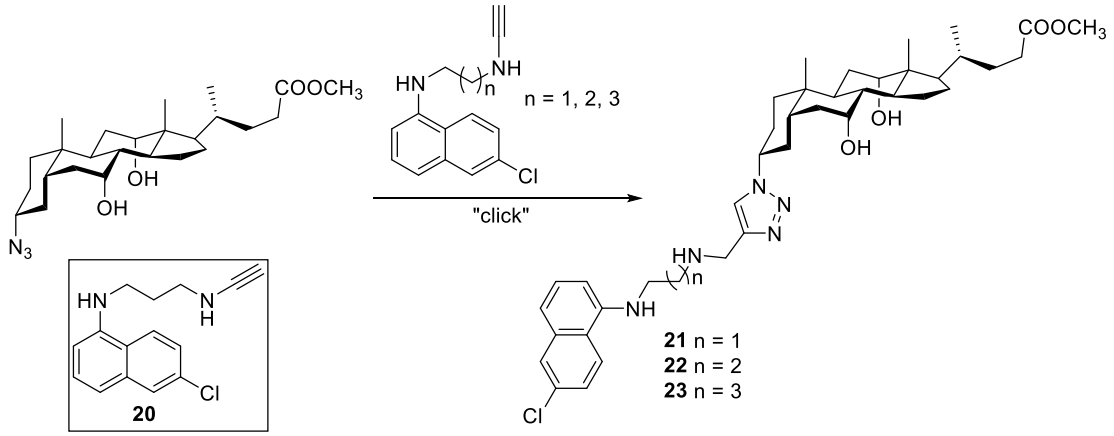

Fig. 7. 1,2,3-triazole derivatives of cholic acid with aminocholine (**21**–**23**) [45]

2.3. Anticancer bioconjugates

Agarwal et al. designed novel bile acid and nucleoside molecules linked by a 1,2,3-triazole linker with antitumor activity (fig. 8). Studies have been carried out *in vitro* against three cancer cell lines (PC-3, MCF-7, IMR-32). Tests have shown that compounds (**25**) and (**27**) are characterized by the highest efficacy of MCF-7 (IC50 = 8.084 μM) and IMR-32 (IC50 = 8.71 μM) cells. It is worth noting that all compounds were tested for cytotoxicity and antituberculosis activity. Compound (**28**) has significant antituberculosis activity (MIC = 4.09 μM), while all compounds are not toxic to the human kidney [46].

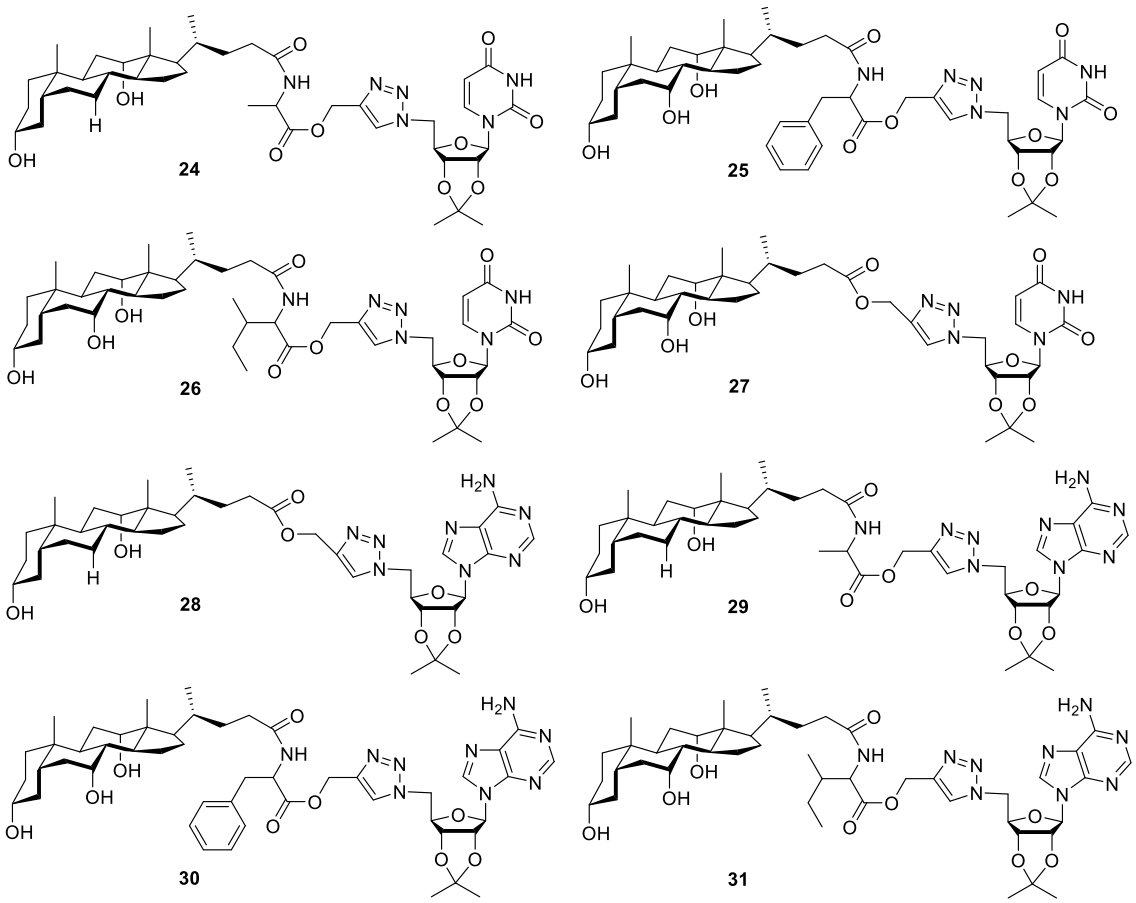

Fig. 8. Steroid-nucleoside conjugates (**24**–**31**) [46]

Incredible anticancer activity is distinguished by dendrimers called "molecular pockets". Efficient synthesis of first-generation dendrimers (chlorodendrimers) was developed, which were subsequently appropriately converted into second-generation azidodendrimers (fig. 9). On the other hand, the bile acid molecule was effectively enriched with an alkyne group. Finally, triazole derivatives (**34**–**35**) exhibited MTT activity against C6 glioma cells (IC50 = 10.48 μM) [47].

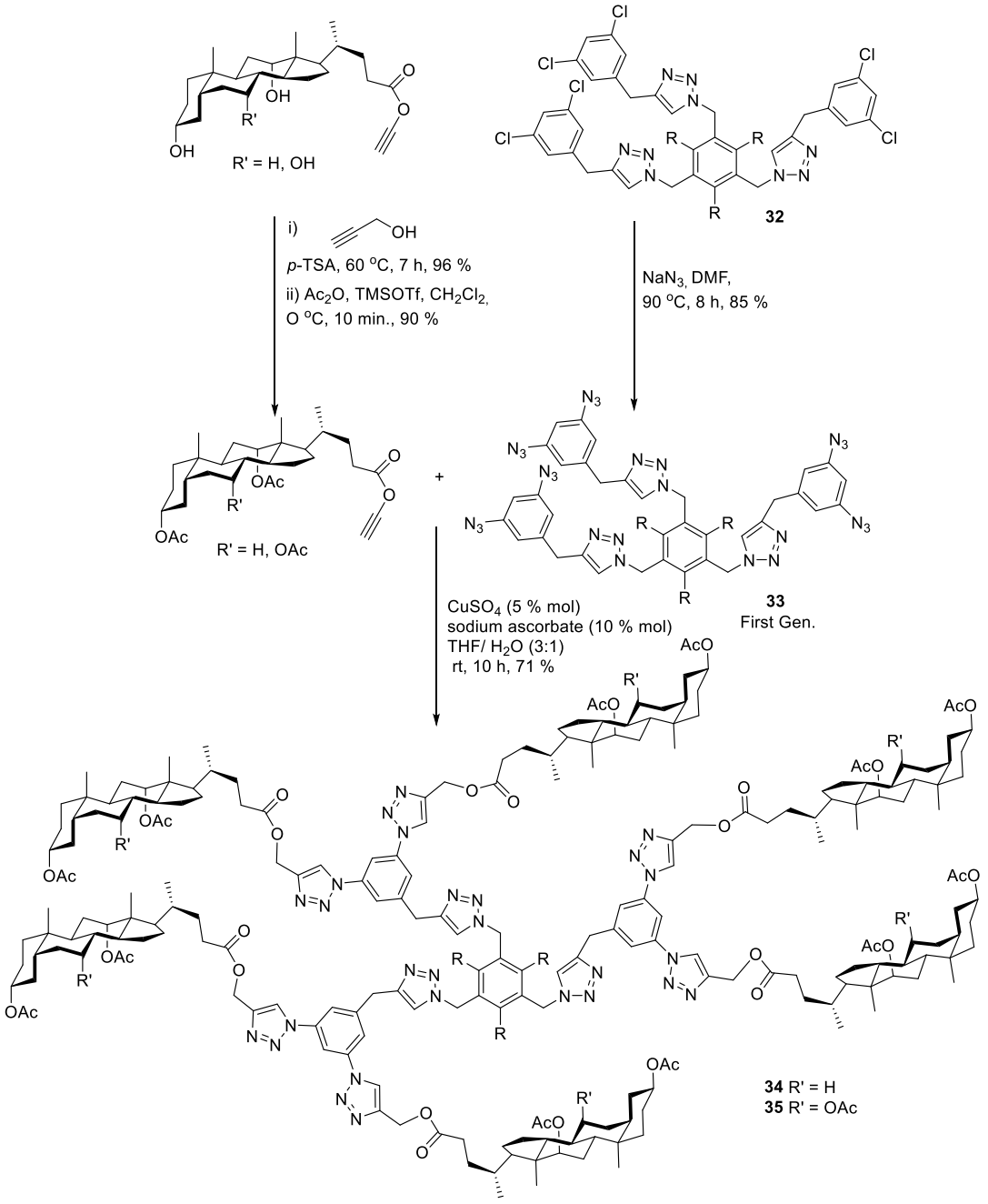

Fig. 9. Scheme of the synthesis of "molecular pockets" (**34**–**35**) [47]

Jurášek et al. described ribbon-type steroid dimers linked by a heterocyclic cholic acid moiety (**37**), ethienoic acid (**38**), or estrone (fig. 10). Appropriately modified reactants were subjected to a "click" reaction. The obtained 1,2,3-triazole derivatives showed antitumor activity against several cell lines. Compound (**37**) was effective against CCRF-CEM and K562 lines (IC50 = 5.4 and 5.35 μM), and compound (**38**) against K562 and CEM-DNR-BULK (IC50 = 5.37 and 5.48 μM) [48].

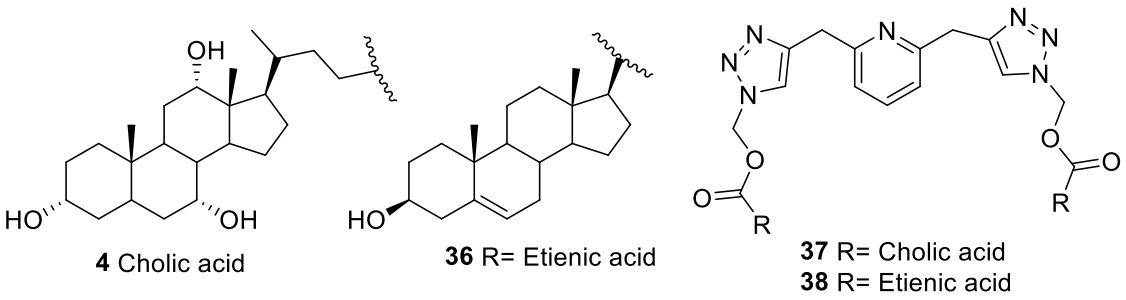

Fig. 10. Ribbon-type steroid dimers (**37**–**38**) [48]

Designed deoxyadenosine 1,2,3-triazole bile acid derivatives have been studied for activity against leukaemia (Jurkat and K562), colorectal (HCT116), ovarian (A2780), and human skin fibroblasts. Multistage bile acid and deoxyadenosine structure transformations were carried out [49, 50]. As a result, 1,2,3-triazole conjugates (**39**–**41**) (fig. 11). Compound (**40**) distinguishes the highest anticancer activity against cells of the K562 (IC50 = 8.51 ± 4.05 μM) and Jurkat (IC50 = 10.47 ± 2.64 μM) lines. In addition, compounds (**39**) and (**41**) are also active against K562 and Jurkat (IC50 = 172.36 ± 9.60 μM, 35.86 ± 11.60 μM, 35.65 ± 2.23 μM and 36.17 ± 1.51 μM, respectively) [51].

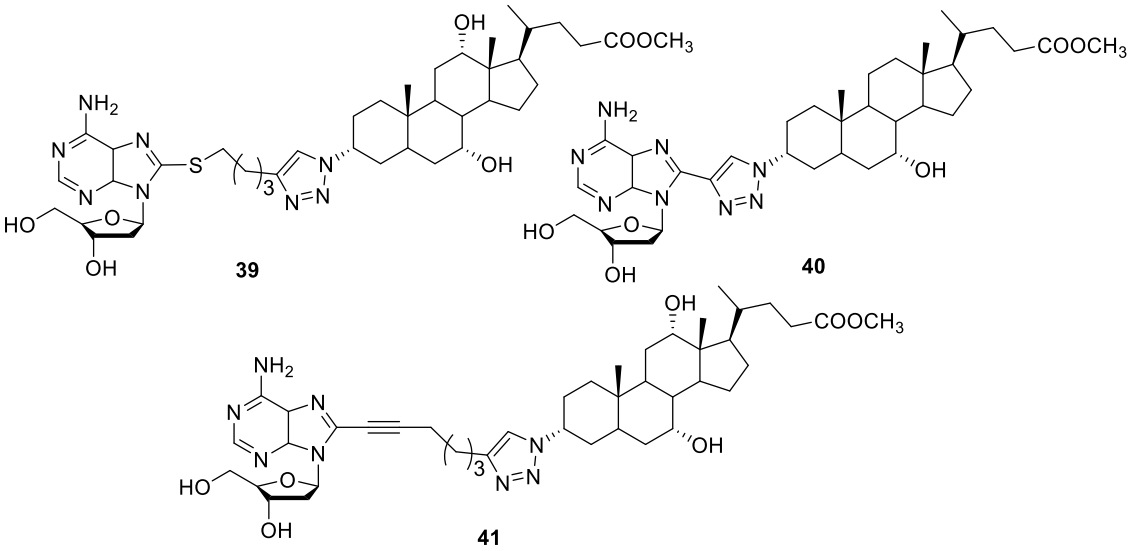

Fig. 11. Bile acid derivatives with deoxyadenosine (**39**–**41**) [49–51]

Subsequently, Perrone's research group synthesized bile acid conjugates-nucleoside with a C-3 and C-24 triazolyl bond (fig. 12). Their activity against human leukaemia cells (K562), colon cancer (HCT116), and skin fibroblasts (FIBRO) was determined. Unfortunately, their activity was low, so the structures were enriched with adenosine, deoxyadenosine, and deoxyuridine (fig. 13). The acid-deoxyadenosine compound (**53**) was efficacious against K562 (IC50 = 8.5 ± 4.0 μM). Against C-3 of the triazolyl-linked bile acid-adenosine conjugate (**54**) was found to be effective against K562 and HCT116 (IC50

of 43.5 ± 1.3 μM and 23.1 ± 1.7 μM). For triazolyl junctions, C-24 was active (**49**), where the IC50 was 16.2 ± 2.2 μM and 17.0 ± 2.5 μM against K562 and HCT116, respectively. For (**50**), an activity of 23.6 ± 1.2 μM for K562 only was determined. For bile acid–deoxyuridine compounds (**55**–**56**), the IC50 for K562 and HCT116 at 21.5 ± 2.0 μM and 23.5 ± 1.6 μM, respectively. Moreover, for C-24 triazolyl compounds (**51**–**52**), the activity against 2.9 ± 1.9 μM and 24.8 ± 1.5 μM, respectively [52].

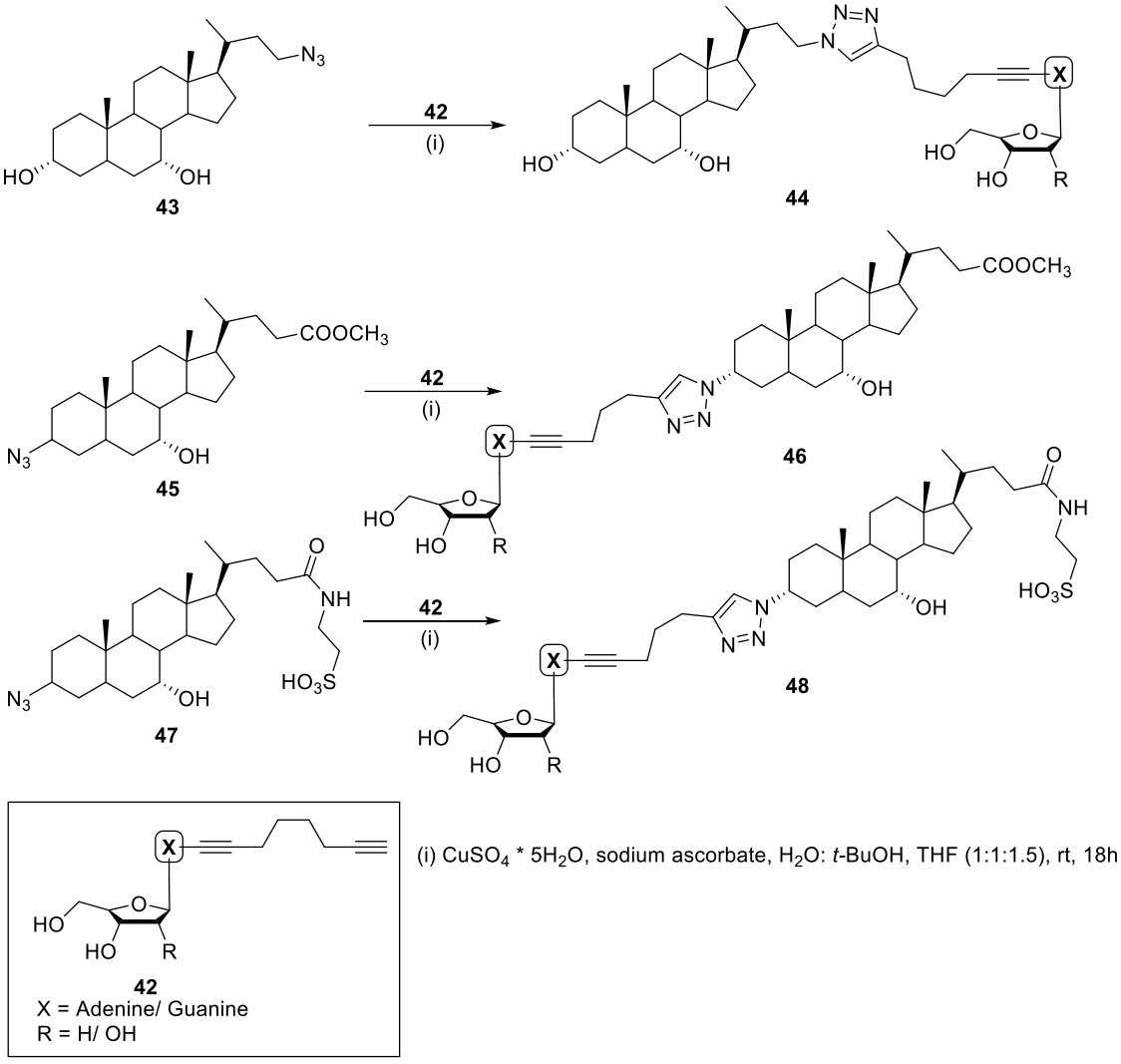

Fig. 12. Scheme of the synthesis of C-3 (**46**, **48**) and C-24 (**44**) triazolyl linked bile acid-nucleoside conjugates [52]

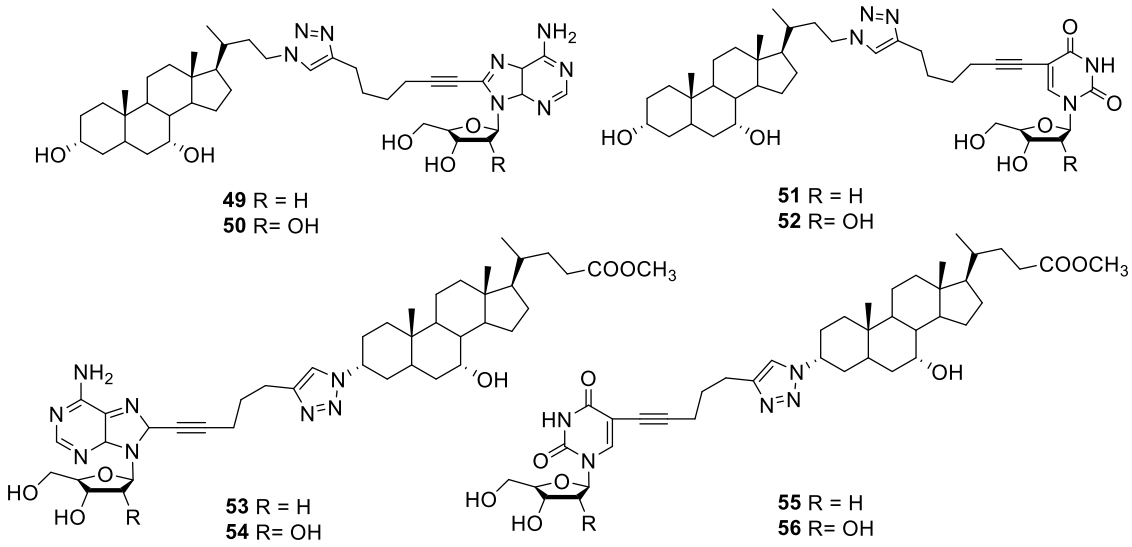

Fig. 13. Steroid-nucleoside conjugates (**49**–**56**) with anticancer activity [52]

New triazolyl steroid-nucleoside conjugates were tested to evaluate their activity against human cell lines for prostate cancer (PC-3), breast cancer (MCF-7), neuroblastoma (IMR-32), and toxicity against human renal embryo (HEK 293 T) (fig. 14). In addition, their antituberculosis activity against *M. tuberculosis* H37Rv (strain ATCC 27.294) confirmed. Multistep synthesized conjugates (**57**–**65**) were compared with the activity of doxorubicin against MCF-7 (IC50 = 0.44 ± 0.05 μM) and IMR-32 (IC50 = 0.043 ± 0.05 μM) cells. Compounds (**65**) and (**60**) showed apoptosis for these cells, where their IC50 values were 8.71 μM and 8.08 μM, respectively. Moreover, they did not destroy human HEK293 T kidney cells [46].

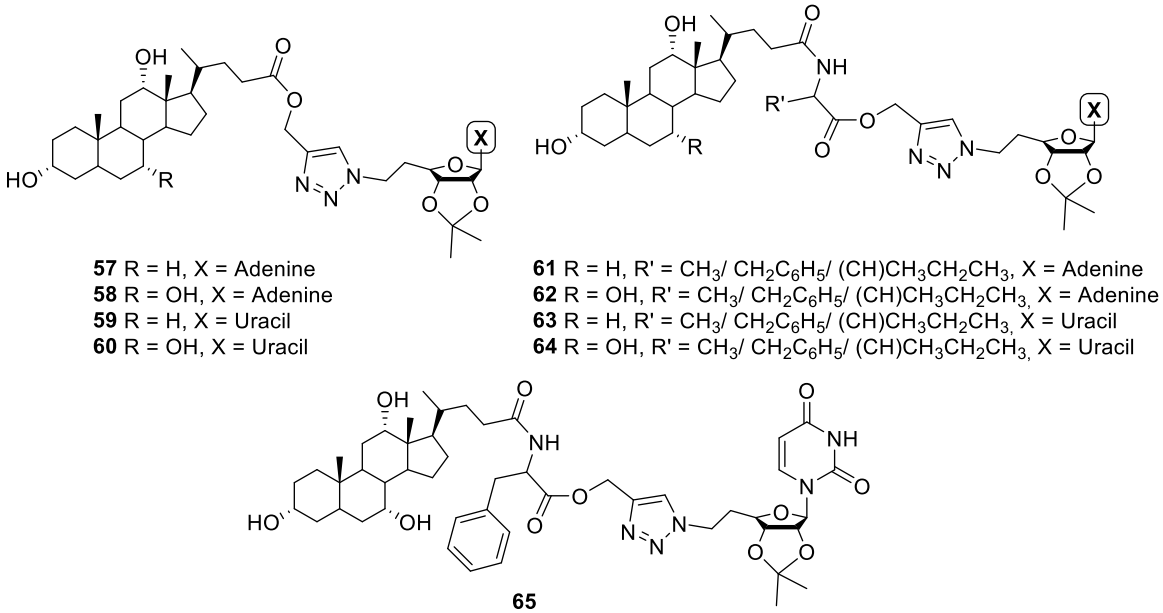

Fig. 14. Triazolyl conjugates deoxycholic/cholic-nucleoside acid (**57**–**65**) [46]

The synthesis of bile acids combined with triazolyl aryl ketones with antitumor properties against human breast cancer cells (MCF7) and mouse breast cancer cells (4 T1) was also developed (fig. 15). In the studies, it was assessed that the conjugate (**66**) is effective against MCF7 at IC50 = 2.61 ± 0,70 μM, a (**67**) at IC50 = 5.71 ± 1.00 μM. In addition, compound (**68**) also exhibits activity against T1 cells (IC50 = 8.76 ± 1.29 μM). All conjugates (**66**–**68**) were not toxic to HEK293. Moreover, the study determined higher apoptosis in MCF-7 for compound (**68**) than (**66**). In the case of four T1 cells, apoptosis was similar for both compounds. In addition, it was found that the addition of cholic acid and the absence of aryl ketone substitution significantly increased the biological activity of the obtained molecules [53].

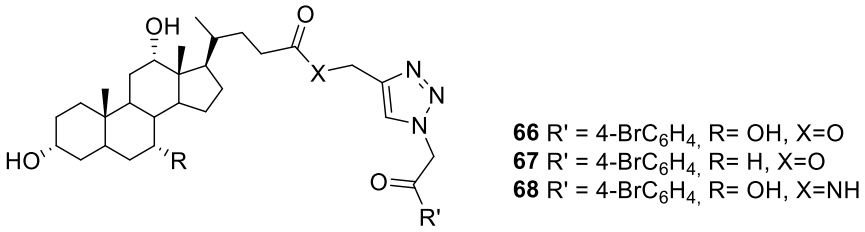

Fig. 15. Triazolyl aryl ketones derivatives of bile acids (**66**–**68**) [53]

2.4. Other types of bile acid bioconjugates with biological potential

The synthesis of novel bile acid dimers and sterols with a unit of 1,2,3-triazole (**69**–**74**) (fig. 16) was carried out. A complete spectroscopic analysis(^{1}H NMR, ^{13}C NMR, FT-IR), spectrometric (ESI-MS), molecular docking and calculations semi-empirically were performed. Research *in silico* indicates their biological activity [54].

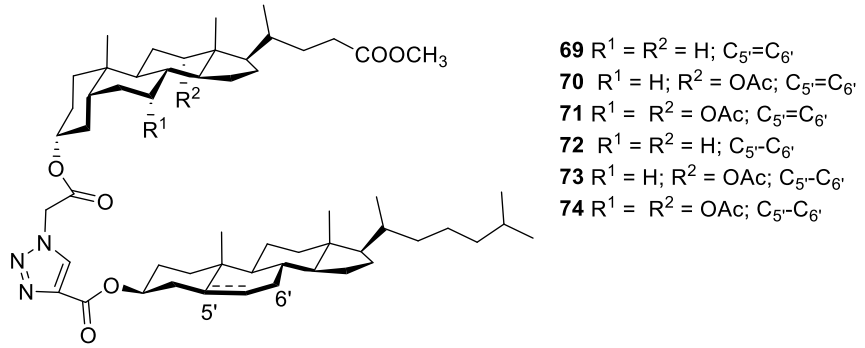

Fig. 16. Dimers of bile acids and sterols (**69**–**74**) [54]

3. Conclusions

This review briefly presents the advances in synthesizing novel bile acid conjugates containing 1,2,3-triazole systems with antibacterial, antiparasitic, and anticancer properties. The research focuses on various microbial strains and cancer cell lines. The presented

research results shed new light on the design of syntheses in the search for new drugs.

Literature

[1] Bai C., Schmidt A., Freedman L. P. Steroid Hormone Receptors and Drug Discovery: Therapeutic Opportunities and Assay Designs. ASSAY Drug Dev. Tech. 2003, 1, 843–852.

[2] Tamminen J., Kolehmainen E. Bile Acids as Building Blocks of Supramolecular Hosts. Molecules 2001, 6, 21–46.

[3] Mikov M., Fawcett J. P., Kuhajda K., Kevresan S. Pharmacology of Bile Acids and Their Derivatives: Absorption Promoters and Therapeutic Agents. Eur. J. Drug Metab. Pharmacokinet. 2006, 31, 237–251.

[4] Saltz L. B. Adjuvant Therapy for Colon Cancer. Surg. Oncol. Clin. N. Am. 2010, 19, 819–827.

[5] Kandi S., Godishala V., Rao P., Ramana K. V. Biomedical Significance of Terpenes: An Insight. Biomedicine 2015, 3, 8–10.

[6] Horáčková Š., Plocková M., Demnerová K. Importance of Microbial Defence Systems to Bile Salts and Mechanisms of Serum Cholesterol Reduction. Biotechnol. Adv. 2018, 36, 682–690.

[7] Sievänen E. Exploitation of Bile Acid Transport Systems in Prodrug Design. Molecules 2007, 12, 1859–1889.

[8] Fernández L. R., Svetaz L., Butassi E., Zacchino S. A., Palermo J. A., Sánchez M. Synthesis and Antifungal Activity of Bile Acid-Derived Oxazoles. Steroids 2016, 108, 68–76.

[9] Pospieszny T. Molecular Pockets, Umbrellas and Quasi Podands from Steroids: Synthesis, Structure and Applications. Mini-Rev. Org. Chem. 2015, 12, 258–270.

[10] Pospieszny T. Design and Synthesis of New Bile Acid-Sterol Conjugates Linked *via* 1,2,3-Triazole Ring. Helv. Chim. Acta 2015, 98, 1337–1350.

[11] Mishra R., Mishra S. Updates in Bile Acid-Bioactive Molecule Conjugates and Their Applications. Steroids 2020, 159, 108639.

[12] Agarwal D. S., Sakhuja R., Beteck R. M., Legoabe L. J. Steroid-Triazole Conjugates: A Brief Overview of Synthesis and Their Application as Anticancer Agents. Steroids 2023, 197, 109258.

[13] Patel S., Challagundla N., Rajput R. A., Mishra S. Design, Synthesis, Characterization and Anticancer Activity Evaluation of Deoxycholic Acid-Chalcone Conjugates. Bioorg. Chem. 2022, 127, 106036.

[14] Zolottsev V., Latysheva A. S., Pokrovsky V. S., Khan I. I., Misharin A. Y. Promising Applications of Steroid Conjugates for Cancer Research and Treatment. Eur. J. Med. Chem. 2021, 210, 113089.
[15] Becer C. R., Hoogenboom R., Schubert U. S. Click Chemistry Beyond Metal-Catalyzed Cycloaddition. Angew. Chem. Int. Ed. Engl. 2009, 48, 4900–4908.
[16] Devaraj N. K., Finn M. G. Introduction: Click Chemistry. Chem. Rev. 2021, 121, 6697–6698.
[17] Bonandi E., Christodoulou M. S., Fumagalli G., Perdicchia D., Rastelli G., Passarella D. The 1,2,3-Triazole Ring as a Bioisostere in Medicinal Chemistry. Drug Discov. Today 2017, 22, 1572–1581.
[18] Liu J., Liu Q., Yang X., Xu S., Zhang H., Bai R., Yao H., Jiang J., Shen M., Wu X. Xu J. Design, Synthesis, and Biological Evaluation of 1,2,4-Triazole Bearing 5-Substituted Biphenyl-2-Sulfonamide Derivatives as Potential Antihypertensive Candidates. Bioorg. Med. Chem. 2013, 21, 7742–7751.
[19] Manohar S., Khan S. I., Rawat D. S. Synthesis of 4-aminoquinoline-1,2,3-triazole and 4-aminoquinoline-1,2,3-triazole-1,3,5-triazine Hybrids as Potential Antimalarial Agents. Chem. Biol. Drug. Des. 2011, 78, 124–136.
[20] Chu, X. M., Wang C., Wang W. L., Liang, L. L., Liu W., Gong K. K., Sun K. L. Triazole Derivatives and Their Antiplasmodial and Antimalarial Activities. Eur. J. Med. Chem. 2019, 166, 206–223.
[21] Wang G., Peng Z., Wang J., Li X., Li J. Synthesis, *in Vitro* Evaluation and Molecular Docking Studies of Novel Triazine-Triazole Derivatives as Potential α-Glucosidase Inhibitors. Eur. J. Med. Chem. 2017, 125, 423–429.
[22] Guan L. P., Jin Q. H., Tian G. R., Chai K. Y., Quan Z. S. Synthesis of Some Quinoline-2(1H)-One and 1, 2, 4 - Triazolo [4 ,3-a] Quinoline Derivatives as Potent Anticonvulsants. J. Pharm. Pharm. Sci. 2007, 10, 254–262.
[23] Song M. X., Deng X.Q. Recent Developments on Triazole Nucleus in Anticonvulsant Compounds: A Review. J. Enzyme Inhib. Med. Chem. 2018, 33, 453–478.
[24] Shaikh M. H., Subhedar D. D., Arkile M., Khedkar V. M., Jadhav N., Sarkar D., Shingate B. B. Synthesis and Bioactivity of Novel Triazole Incorporated Benzothiazinone Derivatives as Antitubercular and Antioxidant Agent. Bioorg. Med. Chem. Lett. 2016, 26, 561–569.
[25] Khan I., Ali S., Hameed S., Rama N. H., Hussain M. T., Wadood A., Uddin R., Ul-Haq Z., Khan A., Ali S., Iqbal Choudhary M. Synthesis, Antioxidant Activities and Urease

Inhibition of Some New 1,2,4-Triazole and 1,3,4-Thiadiazole Derivatives. Eur. J. Med. Chem. 2010, 45, 5200–5207.

[26] Kaplancıklı Z. A., Özdemir A., Turan-Zitouni G., Altıntop M. D., Can Ö. D. New Pyrazoline Derivatives and Their Antidepressant Activity. Eur. J. Med. Chem. 2010, 45, 4383–4387.

[27] Seck I., Ciss I., Diédhiou A., Baldé M., Ka S., Ba L. A., Ndoye S. F., Figadère B., Seon-Meniel B., Gomez G. 1,2,3-Triazenes and 1,2,3-Triazoles as Antileishmanial, Antitrypanosomal, and Antiplasmodial Agents. Med. Chem. Res. 2023, 32, 158–164.

[28] Zoumpoulakis P., Camoutsis C., Pairas G., Soković M., Glamočlija J., Potamitis C., Pitsas A. Synthesis of Novel Sulfonamide-1,2,4-Triazoles, 1,3,4-Thiadiazoles and 1,3,4-Oxadiazoles, as Potential Antibacterial and Antifungal Agents. Biological Evaluation and Conformational Analysis Studies. Bioorg. Med. Chem. 2012, 20, 1569–1583.

[29] Mathew V., Keshavayya J., Vaidya V. P., Giles D. Studies on Synthesis and Pharmacological Activities of 3,6-Disubstituted-1,2,4-Triazolo[3,4-b]-1,3,4-Thiadiazoles and Their Dihydro Analogues. Eur. J. Med. Chem. 2007, 42, 823–840.

[30] Labanauskas L., Udrenaite E., Gaidelis P., Brukštus A. Synthesis of 5-(2-,3- and 4-Methoxyphenyl)-4H-1,2,4-Triazole-3-Thiol Derivatives Exhibiting Anti-Inflammatory Activity. Il Farmaco 2004, 59, 255–259.

[31] Sztanke K., Pasternak K., Rzymowska J., Sztanke M., Kandefer-Szerszeń M. Synthesis, Structure Elucidation and Identification of Antitumoural Properties of Novel Fused 1,2,4-Triazine Aryl Derivatives. Eur. J. Med. Chem. 2008, 43, 1085–1094.

[32] Dheer D., Singh V., Shankar R. Medicinal Attributes of 1,2,3-Triazoles: Current Developments. Bioorg. Chem. 2017, 71, 30–54.

[33] Alam M. M. 1,2,3-Triazole Hybrids as Anticancer Agents: A Review. Arch. Pharm. 2022, 355, 2100158.

[34] Zhou C. H., Wang Y. Recent Researches in Triazole Compounds as Medicinal Drugs. Curr. Med. Chem. 2012, 19, 239–280.

[35] Meldal M., Tornøe C.W. Cu-Catalyzed Azide−Alkyne Cycloaddition. Chem. Rev. 2008, 108, 2952–3015.

[36] Bock V. D., Hiemstra H., van Maarseveen J. H. CuI-Catalyzed Alkyne–Azide “Click” Cycloadditions from a Mechanistic and Synthetic Perspective. Eur. J. Org. Chem. 2006, 2006, 51–68.

[37] Hein C. D., Liu X. M., Wang D. Click Chemistry, A Powerful Tool for Pharmaceutical Sciences. Pharm. Res. 2008, 25, 2216–2230.

[38] Pospieszny T. Chapter 6 – Steroidal Conjugates: Synthesis, Spectroscopic, and Biological Studies. In Studies in Natural Products Chemistry; Atta-ur-Rahman Ed., Elsevier, 2015, 46, 169–200.

[39] Pore V. S., Aher N. G., Kumar M., Shukla P. K. Design and Synthesis of Fluconazole/Bile Acid Conjugate Using Click Reaction. Tetrahedron 2006, 62, 11178–11186.

[40] Pore V. S., Jagtap M. A., Agalave S. G., Pandey A. K., Siddiqi M. I., Kumar V., Shukla P. K. Synthesis and Antifungal Activity of 1,5-Disubstituted-1,2,3-Triazole Containing Fluconazole Analogues. Med. Chem. Commun. 2012, 3, 484.

[41] Aher N. G., Pore V. S., Mishra N. N., Kumar A., Shukla P. K., Sharma A., Bhat M. K. Synthesis and Antifungal Activity of 1,2,3-Triazole Containing Fluconazole Analogues. Bioorg. Med. Chem. Lett. 2009, 19, 759–763.

[42] Khaligh P., Salehi P., Bararjanian M., Aliahmadi A., Khavasi H. R., Nejad-Ebrahimi S. Synthesis and *in Vitro* Antibacterial Evaluation of Novel 4-Substituted 1-Menthyl-1,2,3-Triazoles. Chem. Pharm. Bull. 2016, 64, 1589–1596.

[43] Corrales R. C. N. R., de Souza N. B., Pinheiro L. S., Abramo C., Coimbra E. S., Da Silva, A. D. Thiopurine Derivatives Containing Triazole and Steroid: Synthesis, Antimalarial and Antileishmanial Activities. Biomed. Pharmacother. 2011, 65, 198–203.

[44] Shiradkar M., Suresh Kumar G. V., Dasari V., Tatikonda S., Akula K. C., Shah R. Clubbed Triazoles: A Novel Approach to Antitubercular Drugs. Eur. J. Med. Chem. 2007, 42, 807–816.

[45] Antinarelli L. M., Carmo A. M., Pavan F. R., Leite C. Q. F., Da Silva A. D., Coimbra E.S., Salunke D.B. Increase of Leishmanicidal and Tubercular Activities Using Steroids Linked to Aminoquinoline. Org. Med. Chem. Lett. 2012, 2, 16.

[46] Agarwal D. S., Siva Krishna V., Sriram D., Yogeeswari P., Sakhuja R. Clickable Conjugates of Bile Acids and Nucleosides: Synthesis, Characterization, *in Vitro* Anticancer and Antituberculosis Studies. Steroids 2018, 139, 35–44.

[47] Anandkumar D., Rajakumar P. Synthesis and Anticancer Activity of Bile Acid Dendrimers with Triazole as Bridging Unit through Click Chemistry. Steroids 2017, 125, 37–46.

[48] Jurášek M., Džubák P., Sedlák D., Dvořáková H., Hajdúch M., Bartůněk P., Drašar P. Preparation, Preliminary Screening of New Types of Steroid Conjugates and Their Activities on Steroid Receptors. Steroids 2013, 78, 356–361.

[49] Łotowski Z., Guzmański D. New Acyclic Dimers of Cholic Acid with Oxamide and Hydrazide Spacers. Monatsh. Chem. 2006, 137, 117–124.
[50] Capobianco M. L., Marchesi E., Perrone D., Navacchia M. L. Labeling Deoxyadenosine for the Preparation of Functional Conjugated Oligonucleotides. Bioconjugate Chem. 2013, 24, 1398–1407.
[51] Perrone D., Bortolini O., Fogagnolo M., Marchesi E., Mari L., Massarenti C., Navacchia M. L., Sforza F., Varani K., Capobianco M. L. Synthesis and *in Vitro* Cytotoxicity of Deoxyadenosine–Bile Acid Conjugates Linked with 1,2,3-Triazole. New J. Chem. 2013, 37, 3559.
[52] Navacchia M., Marchesi E., Mari L., Chinaglia N., Gallerani E., Gavioli R., Capobianco M., Perrone D. Rational Design of Nucleoside–Bile Acid Conjugates Incorporating a Triazole Moiety for Anticancer Evaluation and SAR Exploration. Molecules 2017, 22, 1710.
[53] Agarwal D. S., Mazumdar S., Italiya K. S., Chitkara D., Sakhuja R. Bile-Acid-Appended Triazolyl Aryl Ketones: Design, Synthesis, *in Vitro* Anticancer Activity and Pharmacokinetics in Rats. Molecules 2021, 26, 5741.
[54] Kawka A., Hajdaś G., Kułaga D., Koenig H., Kowalczyk I., Pospieszny T. Molecular Structure, Spectral and Theoretical Study of New Type Bile Acid–Sterol Conjugates Linked *via* 1,2,3-Triazole Ring. J. Mol. Struct. 2023, 1273, 134313.

WYDAWNICTWO NAUKOWE
UNIWERSYTETU
MIKOŁAJA KOPERNIKA

Toruń, dnia 29 stycznia 2025 r.

WN-7531/2025

Zaświadczenie

Wydawnictwo Naukowe UMK informuje, że Pani mgr. inż. Anna Kawka jest autorką artykułu pt. *Triaole–Based Modifications of Bile Acids: Promising Strategies for Combating Infections and Cancer – A Review,* o objętości 1/2 arkusza wydawniczego. Artykuł ukaże się do końca kwietnia 2025 r. w publikacji zbiorowej *Na pograniczu chemii, biologii i fizyki - rozwój nauk Tom 6 Kopernikańskie Seminarium Doktoranckie* pod redakcją prof. dra hab. Edwarda Szłyka.

Starszy Specjalista
mgr Blanka Heberlejn

Bioorganic Chemistry 153 (2024) 107933

Contents lists available at ScienceDirect

Bioorganic Chemistry

journal homepage: www.elsevier.com/locate/bioorg

Review Article

Steroid and bioactive molecule conjugates: Improving therapeutic approaches in disease management

Anna Kawka *, Hanna Koenig, Tomasz Pospieszny *

Department of Bioactive Products, Faculty of Chemistry, Adam Mickiewicz University, Uniwersytetu Poznańskiego 8 Street, 61-614 Poznań, Poland

ARTICLE INFO

Keywords:
Natural compounds
Conjugates
Steroids hybrids
Biological activity
Medical chemistry

ABSTRACT

Conjugates of steroids and other natural bioactive molecules (such as amino acids or carbohydrates) have proven promising compounds with diverse biological effects. This literature review summarises the importance of steroid conjugates in a broad spectrum of therapeutic applications. Steroid conjugates exhibit improved pharmacokinetic properties, improved target specificity, and reduced side effects compared to the parent compounds. This increases their clinical usefulness. Their versatility extends to drug delivery systems, enabling precise modulation of drug release kinetics and bioavailability. Moreover, steroid conjugates are vital in treating inflammatory and neurodegenerative diseases, hormonal disorders, cancer therapy, and combating microbial infections. The review presents the current state of research on steroid conjugates, highlighting the crucial role of steroid conjugates in modern medicine and their potential to revolutionise therapeutic paradigms and improve patient outcomes. Steroid compounds are excellent for developing agents with better bioavailability and are used as drug carriers or hydrogelators.

1. Introduction

Nature is a vast source of biologically active heterocycles with varying degrees of optimisation. Molecules derived naturally from biosynthetic pathways exhibit diverse physical, chemical, and biological properties [1,2]. The decreasing effectiveness of therapeutic agents due to their poor solubility, instability, or host resistance forces the search for new drugs. Coupling a carrier molecule with a biologically active substance has many benefits, such as systemic non-toxicity, minimisation of side effects, and overcoming drug resistance of target cells [3,4].

The conjugation of two biologically active molecules has influenced the enormous development of biomedicine, materials science, and pharmaceutical sciences [5–8]. A bioconjugate should be understood as a structure of two or more molecular units with different biological properties. With this technique, the molecule formed gains a double benefit by combining the properties of individual units, thus acquiring new activity [9,10]. Literature data indicate that steroid bioconjugates have the most excellent application in improved biomolecules with pharmacological potential [11–14].

Fig. 1 shows the different conjugation approaches to form new compounds known in the literature (Fig. 1). Bioconjugates are formed by reactions between functional groups on other molecules or by a cross-linking agent. Cross-linking agents such as EDC (*1-Ethyl-3-(3-(Dimethylamino)propyl)Carbodiimide hydrochloride*) and DCC (*Dicyclohexyl Carbodiimide*) are used to form covalent bonds without an extra atom. Small molecule coupling controls the selectivity and toxicity of bioconjugates. The basic idea of bioconjugation is to connect molecules through covalent bonds. At least one of the molecules must be of biological origin or be part of a biomolecule [9]. Antibody-drug conjugates are therapeutic agents in which antibodies are conjugated with biologically active drugs. The FDA (*U.S. Food and Drug Administration*) has approved three such conjugates; more than 40 are in clinical trials [8]. Among these compounds, it is worth distinguishing between PEGylated (*Polyethylene Glycol*) adenosine deaminase (Adagen) used in the treatment of severe immunodeficiency and PEGylated L-asparaginase (Oncaspar, acute lymphoblastic leukaemia) [15]. In addition, other approved conjugates are m.in, Pegintron, Pegasus, Neulasta, and Mylotarg [16–19]. It is worth noting that among the antibody-drug couplings, anticancer drugs such as Adcetris (treatment of Hodgkin lymphoma) and Kadcyla (therapy of breast cancer) deserve special attention [20,21].

Steroids include a group of natural compounds found in all eukaryotic cells. These compounds are characterised by a rigid four-ring cyclopentanoperhydrophenanthrene framework (Fig. 2),

* Corresponding authors.
E-mail addresses: anna.kawka@amu.edu.pl (A. Kawka), tposp@amu.edu.pl (T. Pospieszny).

https://doi.org/10.1016/j.bioorg.2024.107933
Received 20 August 2024; Received in revised form 25 October 2024; Accepted 27 October 2024
Available online 5 November 2024

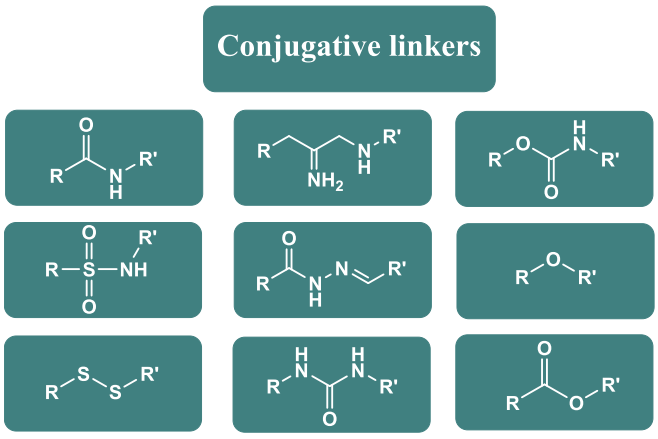

Fig. 1. Selected pathways of molecule bioconjugation.

hydrophobicity, varying degrees of functionalisation, and amphipathic properties [22]. Among steroids, bile acids (e.g. lithocholic acid, deoxycholic acid, cholic acid), plant (e.g. stigmasterol) and animal (e.g. cholesterol) sterols, corticosteroids (e.g. cortisol), sex hormones (e.g. progesterone, androgens) and sapogenin (e.g. sarsasapogenin) deserve special attention. The most important functions of bile acids include the absorption and control of lipid and glucose metabolism [23]. Corticosteroids play a crucial role in carbohydrate metabolism and regulating inflammation. On the other hand, sex hormones such as estrone, pregnenolone, or testosterone are responsible for the proper functioning of the entire body [24,25].

Due to the enormous diversity of biological and physicochemical properties, steroids have become an excellent choice for bioorganic synthesis [26,27]. Transformations of functional groups through the formation of ester, ether, or amide bonds consistently produce new derivatives (Fig. 1). However, additional groups may change pharmacokinetic properties (e.g. lipophilicity, solubility) and pharmacodynamic properties (e.g. receptor selectivity). As lipophilic compounds, they can easily cross cell membranes (e.g. blood–brain barrier), which is crucial in the design of steroid drugs. Introducing polar groups can change their lipophilicity, affecting the distribution in the body and the duration of action. It is worth noting that a slight transformation of the steroid molecule causes a massive change in biological systems. The rigid structure of the steroid nucleus makes it easier for them to penetrate the cell and, consequently, to interact with a specific hormone receptor. Steroids are characterised by particular stereochemistry (spatial arrangement), crucial for interacting with protein receptors. Minor differences in stereochemistry can determine the activity of the drug, namely whether it will be an agonist, antagonist, or inactive. The *cis/trans* configuration between the rings, especially A/B, also plays a significant role in receptor binding specificity. Several structural and biological characteristics of steroids have influenced their use in drug design [28–30]. Some known steroid conjugates increase the expression of genes of essential transport proteins. Also fundamental are derivatives with anticancer, antibacterial, antifungal, antimicrobial, antiviral (including HIV), anticoagulant, anti-inflammatory, antioxidant or insecticidal (pesticides) activity [31–46]. Moreover, they have neuroprotective potential in Alzheimer's disease and affect transcription factors [47].

Recently, several reviews have been published highlighting the diverse therapeutic benefits of steroid and amino acid conjugates and bile acids with bioactive molecules [48,49]. Research on the therapeutic use of steroid bioconjugates in cancer therapy is intensively conducted, confirmed by numerous scientific reports [50,51]. Therefore, we decided to comprehensively review structurally diverse steroid bioconjugates that may have potential therapeutic relevance. PubChem, Web of Science, Scopus and Reaxys databases were searched for studies on the multidirectional biocidal activity of steroid conjugates with natural compounds from the last two decades (2004–2024). The focus was on specific terms such as „steroid conjugates", „amino acid

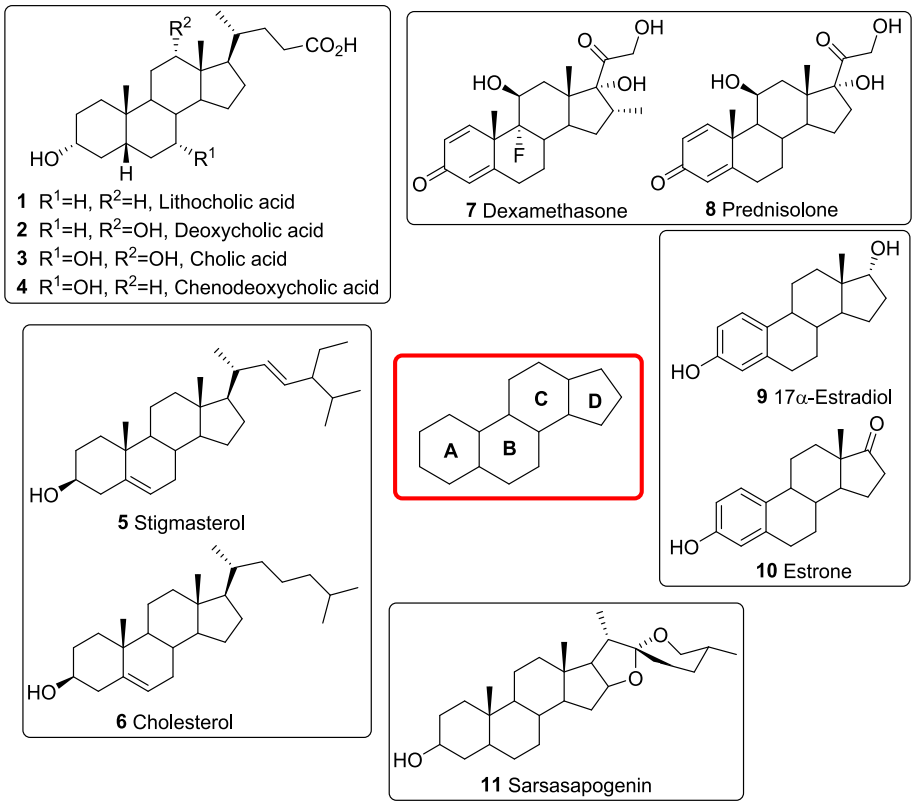

Fig. 2. Selected steroid compounds (**1**–**11**).

conjugates", „bile acid bioconjugates", „anticancer agents", or „biocidal activity". The most critical aspect was experimental articles, while theoretical and review articles were considered to have supplementary scientific value. This review covers the diverse biological applications of steroid bioconjugates and may benefit the broader scientific community searching for new drugs. It is worth mentioning that the dominant position was taken by steroid-amino acid conjugates that can be used as antimicrobials or in chemotherapy [52,53].

2. Steroid conjugates of anticancer significance

Recently, scientists have emphasised the design of steroid conjugates with anticancer properties (see Table 2). An exciting approach is developing compounds acting as enzyme inhibitors crucial for steroid metabolism, such as steroid sulfatase (STS) and hydroxysteroid dehydrogenase (HSD). STS inhibitors, such as Irosustat, have been studied in the context of breast and endometrial cancer due to their ability to inhibit estrogen metabolism, leading to the inhibition of tumour cell proliferation [54]. In turn, HSD inhibitors, including 17β-HSD1 inhibitors, are being analysed as potential anticancer agents, especially in cases of steroid-dependent cancer (prostate cancer) [55]. Additionally, steroid conjugates can act by binding to receptors (e.g. antiestrogens or antiprogestogens), making them multi-targeted tools in anticancer therapy. Antiestrogens, such as tamoxifen, are widely used in the treatment of estrogen-dependent breast cancer [56]. Antiprogestins (such as mifepristone) have shown promising results in the context of hormone-dependent cancers, including endometrial and ovarian cancer [57]. Simultaneous blockade of steroid-metabolising enzymes and tumor-promoting receptors allows for multi-level effects on cancer cells. Steroid coupling is aimed at obtaining a less toxic structure and, at the same time, has high bioavailability. Therefore, the development of steroid conjugates is considered a promising therapeutic strategy in the treatment of hormone-dependent cancers.

2.1. Steroid conjugates with doxorubicin

Estrogens contribute to the development of breast cancer. The mammary gland produces more type β cells than type α. Whereas breast cancer cells do the complete opposite and overexpress abnormal α-type cells. This significant difference has provoked interest in estrogens as potential transport vehicles for cytotoxic agents. Initial attempts to bind estrogen to anthracyclines were unsuccessful. Only coupling the C-3 and C-17 positions of estradiol with doxorubicin *via* an amide bond brought better results. Conjugate (**12**) (Fig. 3) was effective against MCF-7 cells (IC_{50} = 0.7 μM, doxorubicin IC_{50} = 0.5 μM). In addition, the estradiol derivative showed 10-fold lower activity against ER-negative breast cancer cells and K562 leukaemia cells (IC_{50} = 10.5 μM) [58].

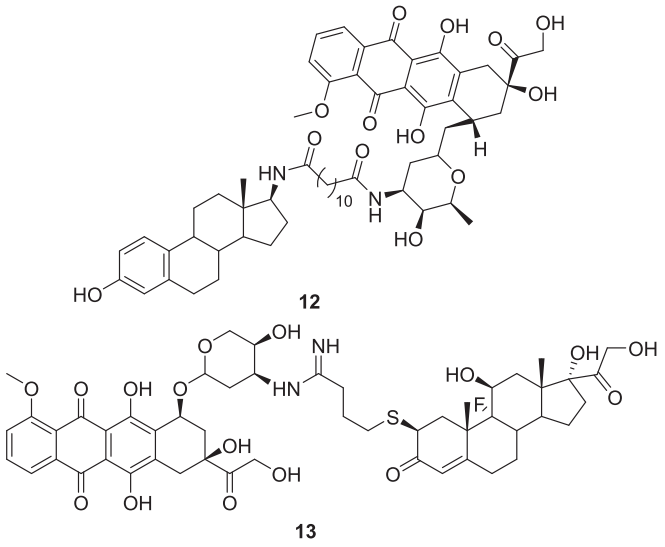

Fig. 3. A conjugate of doxorubicin with estradiol (**12**) and dexamethasone (**13**).

Chaikomon et al., on the other hand, synthesised a compound between dexamethasone and doxorubicin called DexDOX (**13**) (Fig. 3). The critical step in this reaction was the extremely simple conjugation of the 3′ amino group of doxorubicin with a dexamethasone molecule. DexDOX showed comparatively lower cytotoxicity than doxorubicin against MCF-7 cells (IC_{50} = 90.3 and 2.8 μg/ml, respectively). However, based on the results of flow cytometry analysis, a clear difference was found in the mechanism of cytotoxicity of these two compounds. Moreover, the lipophilicity of dexamethasone resulted in greater cellular penetration of the conjugate than doxorubicin alone. On the other hand, it suppressed the effects of P-gp overexpression, which is why it showed high potential for therapy for treating drug-resistant cancers [59].

2.2. Carbohydrate derivatives

Steroid glycosides comprise glycone (a sugar radical) and an aglycone (a steroid radical. They have been used in the treatment of congestive heart failure. Literature reports indicate their increasing cytotoxicity against many cancer cell lines [60]. Dioscine (**14**) (Fig. 4) inhibits the development of HL-60 leukemia cells. In addition, it has antiviral, antifungal, and anti-inflammatory properties [61]. Isolated from the roots *Polygonatum zanlanscianennse* saponins were characterised by an IC_{50} of 5.06 μg/ml against HeLa cells [62]. In contrast, other saponins derived from the plant *Myriopteron extensum K. Schum.* differ in the presence of an unsaturated lactone ring at C-17β. This feature of structure is crucial for anticancer properties. This is why extensumside A (**15**) (Fig. 4) showed IC_{50} in the range of 0.29 to 0.47 μg/ml against several cancer cell lines (including the highest efficacy against A549 cells). Extensumside B was inactive due to the lack of a lactone ring [63]. This highlights the importance of steroid saponins as natural hybrids for drug discovery.

Mimaki et al. successfully isolated and identified a cholestane glycoside (**16**) (Fig. 5) from onion *Ornithogalum saundersiae*. Studies have shown that OSW-1 has much higher activity against HL-60 cancer cells than etoposide or Adriamycin [64]. Many low-yield attempts have been made to synthesise this natural compound (using sugars such as D-xylose or L-arabinose) [65,66]. In addition, due to the cytotoxicity of cholestane glycoside, it was necessary to modify its structure. As a result, several transformations were made, such as replacing cholestane with estrane (conjugate with IC_{50} = 0.43–0.7 μM) or synthesising OSW-1 analogues of 22-deoxy-23-oxa [67,68]. Artificial steroid glycosides (**17–18**) (Fig. 5), in which the length of the side cholesteryl chain was increased to 8–11 carbon atoms, were characterised by low IC_{50} values (i.e. from 6.1 to 8 nM) for CEM and G361 cells.

Other compounds with antiproliferative activity were the dansyl derivatives of polyphyllin D and dioscin. Conjugate obtained (**19**) (Fig. 5) and its analogues showed activity against HeLa cells (IC_{50} = 15–18 μM), as well as formed self-assembled micelles [69].

It is worth noting that for the HeLa cell tumour line, cytotoxic was also created by the CuAAC method (*Copper(I)-Catalyzed Azide Alkyne Cycloaddition*) (**20**) (Fig. 6). The bioconjugate of secosterone monosaccharide -D- exhibited an IC_{50} of 20 μM, which is almost twice as low as standard cisplatin (IC_{50} = 42.6 μM). It has been proven that the presence of acetylated carbohydrates and oxime in part of the secosteroid affects anticancer activity [70].

2.3. Alkaloid and curcumin conjugates

Liu et al. designed the synthesis of taxols linked to hyaluronic acid, folic acid, monoclonal antibodies, and 3,17β-estradiol. They aimed to improve solubility and increase selectivity against ER-positive breast

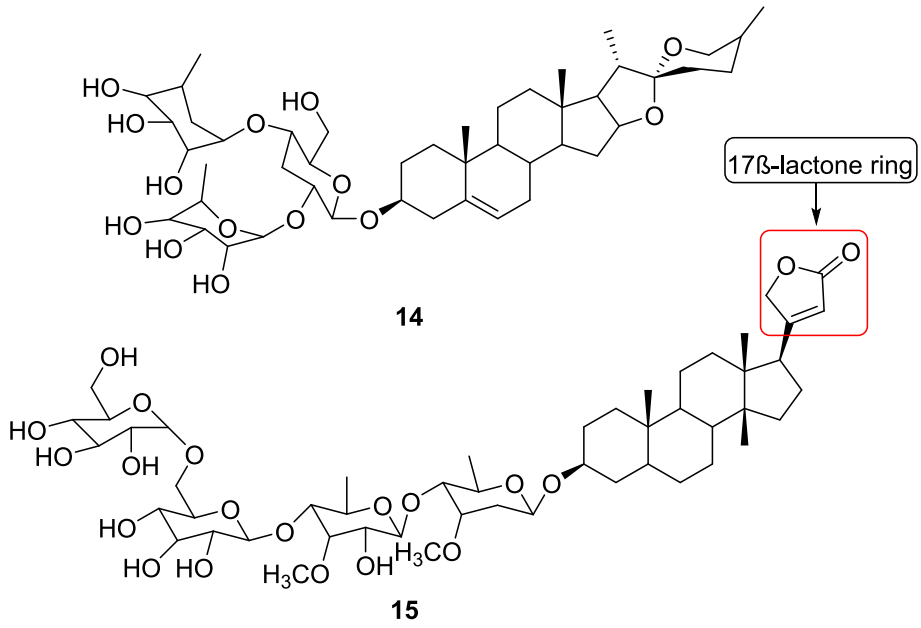

Fig. 4. Dioscine (**14**) and extensumside A (**15**) are cytotoxic to cancer cell lines.

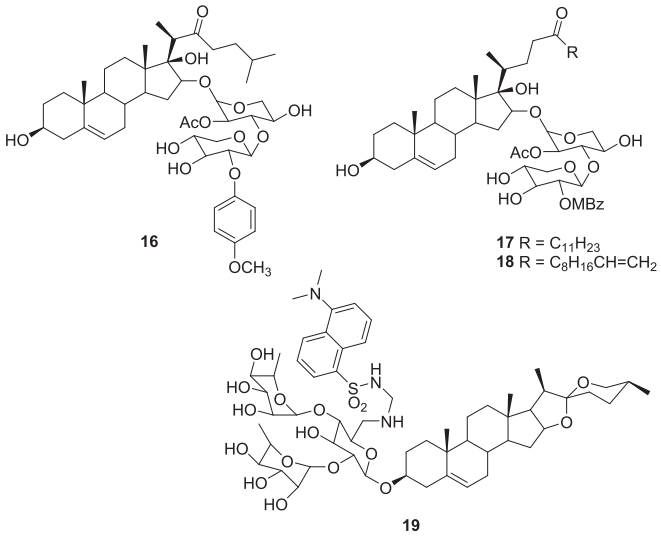

Fig. 5. Steroid glycosides (**16**–**19**) with biological activity.

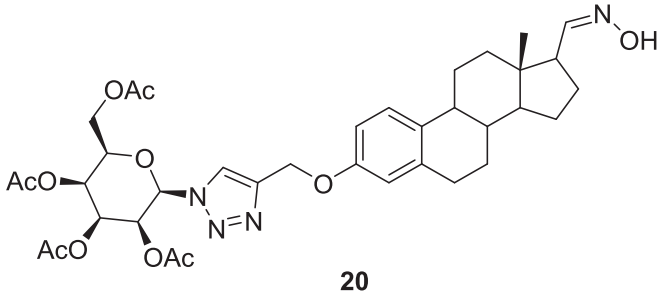

Fig. 6. The conjugate (**20**) was obtained by the CuAAC method.

cancer. Conjugation was used via bonds at C-2′, C-7 or C-10 in the taxol moiety with the C-11 or C-16 position in the steroid moiety. Bioconjugate (**21**) (Fig. 7) was distinguished by the highest effectiveness (IC_{50} = 40 nM against MCF-7), as was the estradiol analogue substituted in the C-11 position. On the other hand, taxol modified at the C-7 position showed good activity against the PC-3 cell line (IC_{50} = 1.7–4.2 μM). Studies have confirmed higher anticancer efficacy against ER-α positive cell lines but still lower than for the parent taxol (IC_{50} for taxol against MCF-7 and MDA-31 cells was 4.9 and 4.5 nM, respectively) [71].

Curcumin encapsulated in liposomes as a cationic lipid based on cholesterol and curcumin (**23**) (Fig. 7). Following synthesis, Apiratikul et al. performed antitumor activity tests for several cancer cell lines, such as HeLa, A549 (epithelial lung adenoma), HepG2 (liver cancer), K562 (erythromyeloblastoid leukaemia) and 1301 (*T*-cell lymphoblastic leukaemia), as well as for the human kidney (HEK293). Encapsulated curcumin was safe for regular human embryonic kidney cells. It has also been found to have up to 8 times higher cytotoxic activity than ordinary curcumin (**22**). Although the efficacy of encapsulated curcumin was not as high as expected, the results were in the IC_{50} range of 3.1–10 μM (see Table 1) [72].

2.4. Steroid-amino acid conjugates

Platinum complexes are of great importance as agents used in chemotherapy. Kvasnica et al. described the synthesis of platinum (II) conjugate with steroidal esters of L-methionine and L-histidine. The corresponding steroid esters were synthesised by esterification of Boc-protected amino acids with the hydroxyl group of various steroids (such as cholesterol, diosgenin, etc.). The Boc group was then removed using trifluoroacetic acid. Platinum(II) complexes were obtained by reacting the resulting steroid esters with potassium tetrachloroplatinate in aqueous dimethylformamide. Amphiphilicity cholesterol and estrone were used. The steroid part had the function of transporting the active substance to the breast cancer cells. Research *in vitro* showed that the platinum (II) complex of estrone with L-methionine (**24**) (Fig. 8) has a destructive effect on CEM cells (IC_{50} = 14 and 20 μmol/L). Among other compounds, pregnenolone esters (**25, 26**) (Fig. 8) with L-methionine and L-histidine. Their effectiveness against CEM cells oscillated around IC_{50} = 18–23 μmol/L. It is worth noting that all the obtained complexes were not toxic to normal human fibroblasts [73].

A synthesised cholesterol-phosphotyrosine conjugate (**27**) (Fig. 9) was evaluated to determine its properties against HeLa cancer cell lines and platinum-resistant AC780cis cells. Compound (**28**) had efficacy at IC_{50} = 16 and 13 μM against HeLa and AC780*cis*, respectively (where

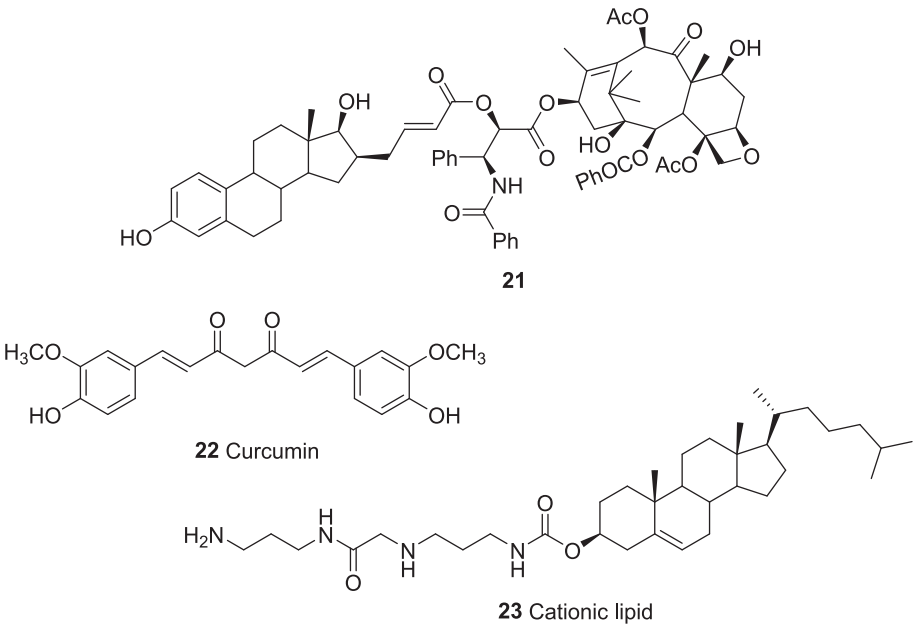

Fig. 7. Taxol derivative (**21**) and cholesterol-based curcumin and cationic lipid structure (**23**).

Table 1
Anticancer activity of curcumin and its encapsulated steroid derivative (**23**).

Compound	IC_{50} (μM)				
	HeLa	A549	HepG2	K562	1301
Curcumin	17	50	30	20	8
23	8	10	4	2,5	3,1
Empty liposomes	180	210	105	165	90

IC_{50} = 71 μM for cisplatin). In addition, studies suggest that enzyme dephosphorylation affects apoptosis. The dephosphorylated compound (**28**) (Fig. 9) showed lower activity against AC780*cis* (IC_{50} = 50 μM) [74].

Fusidic acid (**29**) (Fig. 10) is an antibiotic effective in treating bacterial infections, especially of the skin. It may have anticancer effects, especially when combined with amino acids. The synthesis focused mainly on the protection of the acid group of fusidic acid by esterification with benzyl bromide. The next step included coupling with Boc-protected amino acids (such as glycine, alanine, leucine, and lysine). The obtained conjugates were converted into hydrochloride salts using HCl in dioxane. Studies on fusidic acid derivatives have demonstrated their anticancer activity against various cancer cell lines, such as cervical cancer (HeLa), glioma (U87), multidrug-resistant epidermal oral carcinoma (KBV), and gastric cancer (MKN45). Compound (**33**) (Fig. 10) proved to be the most promising, showing excellent activity against all cancer cell lines tested (cell viability 8 %, 18 %, 9 %, and 8 %, respectively). Compounds (**30**) and (**32**) (Fig. 10) induced apoptosis of KBV and HeLa cells less than 30 %, while compound (**31**) was ineffective only against MKN54 (less than 33 % for other cell lines) [75].

Aromatic amide derivatives of bile acids and amino acids (**34**–**38**) (Fig. 11) were obtained (using HOBt and EDC-HCl) to test their antiproliferative properties against colon (HT29), breast (MDAMB231), and glioma (U87MG) cancers. They were also tested for cytotoxicity to the human normal kidney cell line (HEK293T). Better selectivity from cisplatin against breast cancer cell lines was shown by phenyl (**34**), benzothiazole (**35**), and 4-methylphenyl (**37**) derivatives (IC_{50} = 1.35, 1.41 and 4.52 μM, respectively). On the other hand, bile acid derivatives (**36–38**) distinguished activity against U87MG cells in the range of 1.62–2.49 μM (for doxorubicin IC_{50} = 2.60 μM, for cisplatin IC_{50} = 3.60 μM). Almost all the compounds were non-toxic to an average human HEK293T cell line (at a concentration of 25 μM). Moreover, bile acid conjugates containing an aryl group in the side chain were more active than heteroaryl derivatives [76].

Another critical group of steroids is the phytosterols, which are components of plant membranes (Fig. 12). These compounds, isolated mainly from vegetable oils, are involved in the proper growth of plants and lower blood cholesterol levels. Most importantly, phytosterols prevent the production of carcinogenic compounds, prevent the development of cancer cells, and cause their apoptosis [77]. Several conjugates of γ-oryzanol (**43**) (Fig. 12) were obtained by conjugation of the 4-hydroxyl ferulate ester γ-oryzanol with fatty acids, phenolic acids, amino acids, lipoic acid, retinoic acid, curcumin, and *trans*-resveratrol. A C-3 bond was also formed in the steroid backbone of selected phytosterols, such as cycloartenol (**39**), 24-methylene cycloartenol (**40**), campesterol (**41**), and β-sitosterol (**42**) (Fig. 12). All new structures were tested for anticancer activity, among other things. Studies have shown that phytosterol conjugated with cystine (**44**) has activity against HeLa and DAOY cells (where IC_{50} ranges from 1.4 to 8.3 μM; for γ-oryzanol IC_{50} > 10 μM) [78].

Chang et al. designed the efficient synthesis of lithocholic acid-amino acid conjugates acting as potential inhibitors of the enzyme sialyltransferase. Sialyltransferase is involved in hypersialylation. It is a crucial biological process during cancer cell metastasis, invasion, cell adhesion, or immune defence [79]. The tests performed showed that the conjugates (**45–47**) (Fig. 13) have enzyme inhibitory activity at IC_{50} of 6, 7, and 5 μM, respectively [80].

The CuAAC reaction was also used to synthesise triazolyl-13α-estrone conjugates with nucleosides. The multi-step synthesis included, among others, the reaction of the nucleoside protected with the 5-O-(4,4-dimethoxy trityl (DMTr)) group with acetic anhydride in pyridine, then deprotection with boron trifluoride in a solution of hexafluoroisopropanol and nitromethane, tosylation with tosyl chloride in pyridine at room temperature. Finally, after tosyl–azide substitution in DMF at 50 °C, the azide was formed, which was subjected to a click reaction with 3-O-propargyl-13α-estrone in the presence of DIPEA and a solvent. To obtain triazole conjugates of 13α-estrone with the nucleoside, the acyl derivative was deprotected in an ammonia solution in methanol at 50 °C. Interestingly, an adequately protected cytidine derivative (**48**) (Fig. 14) was more active than the unprotected thymidine derivative (**49**) (IC_{50} = 9.0–10.4 μM and 19 μM, respectively) versus

Table 2
Anticancer activity of steroid-based bioconjugates.

Type of steroid's conjugate	Bioactive compounds	Cell lines	Activity (IC_{50})	References
Hormone-doxorubicin	**12**	MCF-7 K562	0.7 μM 10.5 μM	[58]
DexDOX	**13**	MCF-7	90.3 μM	[59]
Dioscine	**14**	HeLa	5.06 μg/ml	[62]
Extensumside A	**15**	HL-60 HeLa A549	0.29–0.47 μg/ml	[63]
Steroid glycosides	**16**	HL-60	0.43–0.7 μg/ml	[64]
	17 **18**	CEM	6.1–8.0 nM	[67,68]
Dioscin's derivative	**19**	HeLa	15–18 μM	[69]
Carbohydrate-triazole-steroid	**20**	HeLa	20 μM	[70]
Taxol-steroid	**21**	MCF-7	40 nM	[71]
Curcumin-sterol	**23**	HeLa A549 HepG2 K562 1301	8 μM 10 μM 4 μM 2.5 μM 3.1 μM	[72]
Steroid-platinum (II)-amino acids	**24** **25** **26**	CEM	14–26 μM 18–23 μM	[73]
Sterol-amino acid	**27** **28**	HeLa AC780cis	16 μM 13 μM 50 μM	[74]
Fusidic acid-amino acid	**30**	HeLa KBV	< 30 %	[75]
	31	HeLa KBV U87	< 33 %	
	32	HeLa KBV	< 30 %	
	33	HeLa U87 KBV MKN45	8 % 18 % 9 % 8 %	
Bile acid-amino acid	**34** **35**	MDAMB231	1.35 μM 1.41 μM	[76]
	36	U87MG	1.62–2.49 μM	
	37	MDAMB231 U87MG	4.52 μM 1.62–2.49 μM	
	38	U87MG	1.62–2.49 μM	
Ester of γ-oryzanol	**44**	HeLa DAOY	1.4–8.3 μM	[78]
Lithocholic acid- amino acid	**45** **46** **47**	inhibitors of the sialyltransferase	6 μM 7 μM 5 μM	[80]
Triazole-steroid-nucleoside	**48** **49**	inhibitors of the 17β-HSD1	9.0–10.4 μM 19 μM	[81]
	50	K562	42.9 μM	[82]
	51	K562 HCT116	16.5 μM 22 μM	
	53	K562 Jurkat	8.51 ± 4.05 μM 10.47 ± 2.64 μM	[83,84]
Steroid-rhodamine B	**55** **56** **57**	MCF-7	59 nM 0.2 μM 0.1 μM	[88]

17β-HSD1. However, it is worth noting that 13α-estrone showed a higher inhibitory potential than all estrone-nucleoside conjugates [81].

Similar triazole bile acid-nucleoside bioconjugates were developed by Navacchia et al., and their antiproliferative activity against K562, HCT116 cancer cells, and normal human skin fibroblast cells were studied. The conjugate (**50**) (dU-*nor*-CDC) (Fig. 14) was effective against K562 cells (IC_{50} = 42.9 μM), whereas the compound (**51**) (dU-UDC) caused apoptosis of both cancer cell lines (IC_{50} = 16.5 and 22.0 μM) [82].

Perrone et al. developed and synthesised bile acid and deoxyadenosine conjugates linked by a triazole system (**52**–**54**) (Fig. 15). The three-step synthesis of 3α-azido bile acid derivatives began with the reaction of their methyl esters with iodine and triphenylphosphine in the presence of imidazole and 1,3-dioxolane. These compounds were then reacted with NaN_3 in DMF to form 3α-azido derivatives. Alkenyl deoxyadenosine derivatives were obtained from 8-bromodeoxyadenosine and hexynothiol in the presence of a palladium catalyst. Finally,

3α-azido bile acid derivatives were coupled with alkenyl deoxyadenosine derivatives using $CuSO_4$*$5H_2O$, sodium ascorbate, and THF: *t*-BuOH: H_2O (room temperature or microwave at 50 °C) to form the corresponding 1,2,3-triazole conjugates (**52**–**54**). The modification of the C-3 position of the steroid part was aimed at assessing the antitumour activity of the obtained structures. Compound (**53**) with the highest cytotoxicity against leukaemia cancer cells, K562 and Jurkat, had an IC_{50} of 8.51 ± 4.05 μM and 10.47 ± 2.64 μM, respectively [83,84]. Interestingly, other literature reports indicate that deoxyadenosine conjugated only with chenodeoxycholic acid has a better apoptotic effect on the K562 cell line (IC_{50} = 16.2 ± 2.2 μM) than its triazole derivative [82].

2.5. Steroid and rhodamine B conjugates

Chemotherapy-induced cell death can be induced in various ways. Studies show that mitochondria are vital in deciding whether a cell survives or dies [85]. There is growing interest in agents that directly target mitochondria and induce controlled cell death, called mitocans. Dysfunction of the mitochondria is associated with many diseases, including neurodegenerative, metabolic and cardiovascular diseases [86].

Rhodamine B, known mainly as a natural biosensor, is being studied for its potential anticancer properties. One of the mechanisms of its action is the induction of oxidative stress in cancer cells, leading to programmed cell death. This compound can be a scaffold for the formation of bioactive cationic molecules. The mitochondrial membranes of cancer cells have a higher membrane potential than non-cancer cells. Mitocans with a lipophilic cation, such as the rhodamine structure, show high selectivity for these cells [87].

Serbian et al. described the synthesis of steroid conjugates based on testosterone, prednisone, and abiraterone with rhodamine B (Fig. 16) [88]. In the coupling reaction, rhodamine B acyl chloride was coupled with steroids by adding triethylamine in dichloromethane (DCM). The conjugates (**55**–**57**) underwent cytotoxicity studies against several human cancer cell lines. They were shown to be active in the low μM to nM range. The testosterone conjugate (**55**) had an EC_{50} of 59 nM against MCF-7 cancer cells and acted mainly through necrosis. In contrast, the prednisone conjugate (**56**) was less cytotoxic (EC_{50} = 0.2 μM) but mostly worked through apoptosis. Interestingly, the compound showed higher selectivity for A2780 cancer cells than NIH 3 T3 fibroblasts. In contrast, the rhodamine B derivative and abiratone (**57**) showed average cytotoxicity and selectivity.

3. Steroid conjugates with antibacterial and antifungal activity

The increasing drug resistance of bacteria to antibiotics and constant mutations force scientists to look for analogues of active substances available on the market (Table 3). One of the first natural antibiotics was squalamine (**58**) (Fig. 17). This natural conjugate of sterol and spermidine was extracted from the stomach of spinfish *Squalus acanthias*. Squalamine has a biocidal effect on Gram-positive and Gram-negative bacteria, resulting in cell death [89]. Attempts have been made to synthesise its analogues, so squalamine is considered the beginning of

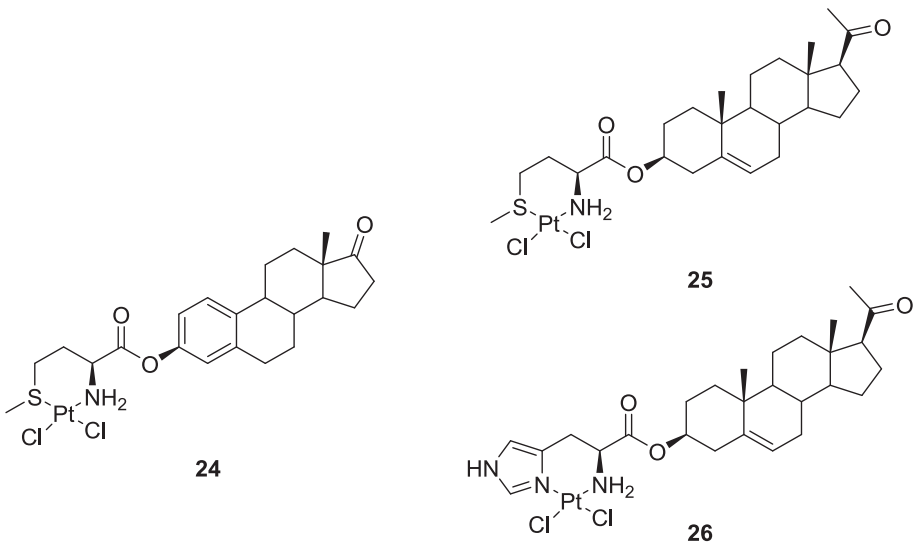

Fig. 8. Anticancer derivatives of estrone (**24**) and pregnenolone (**25**, **26**).

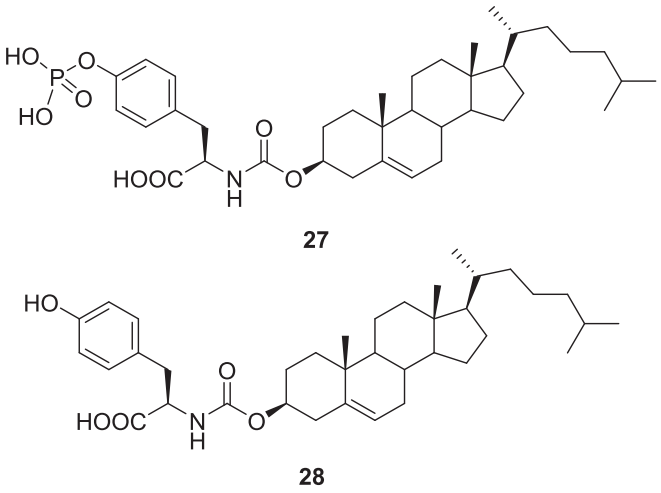

Fig. 9. Cholesterol conjugates with phosphotyrosine (**27**) and tyrosine (**28**).

steroid conjugate chemistry [90–92].

Novel chiral amides of amino alcohols, cholic acid, and deoxycholic acid were synthesised to test them for antimicrobial activity. Hazra et al. found that the bioconjugate of deoxycholic acid and (-R)-2-amino-cyclohexanol (**62**) (Fig. 18) is toxic to most Gram-positive bacteria (especially *E. coli* ATCC 25922 and *S. aureus* ATCC 25923, with MIC = 45 and 15 μg/ml, respectively) [93]. In contrast, another compound (1R, 2R)-1-phenyl-2-deoxycholicacetatamidopropane-1,3-diol) was active against the pathogenic fungus, where IC_{50} = 62.5 μg/ml.

Mishra et al. investigated the characterisation of eight new amide derivatives of chloramphenicol (**63**–**70**) (Fig. 19) [94]. This natural antibiotic has been extracted from actinomycete *Streptomyces venezuelae*. To synthesise steroid-amino alcohol conjugates, deoxycholic acids, cholic acid, (1R,2R)-1-phenyl-2-amino-1,3-propanediol, (1S,2S)-1-phenyl-2-amino-1, 3-propanediol, (1R,2R)-1-*para*-nitrophenyl-2-amino-1,3-propanediol, (1S,2S)-1-*para*-nitrophenyl-2-amino-1,3-propanediol, were used. Biocidal activity tests against Gram-positive and Gram-negative bacteria showed deoxycholic acid conjugates (**68**) and (**70**) (IC_{50} < 60 μg/ml), particularly for the *Cryptococcus neoformans*.

Vatmurge et al. developed a conjugation of bile acids with β-lactam

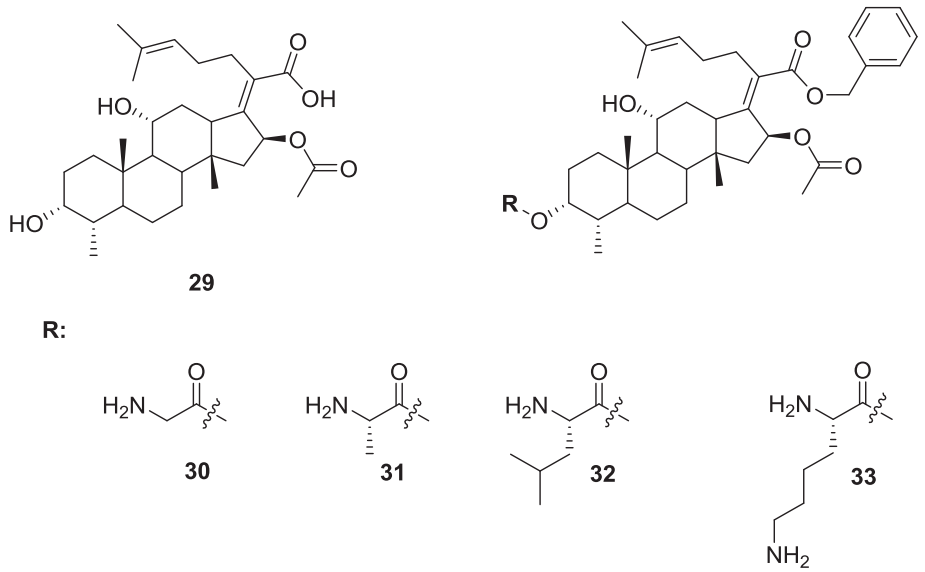

Fig. 10. Fusidic acid (**29**) and its benzyl derivatives with amino acids (**30**–**33**).

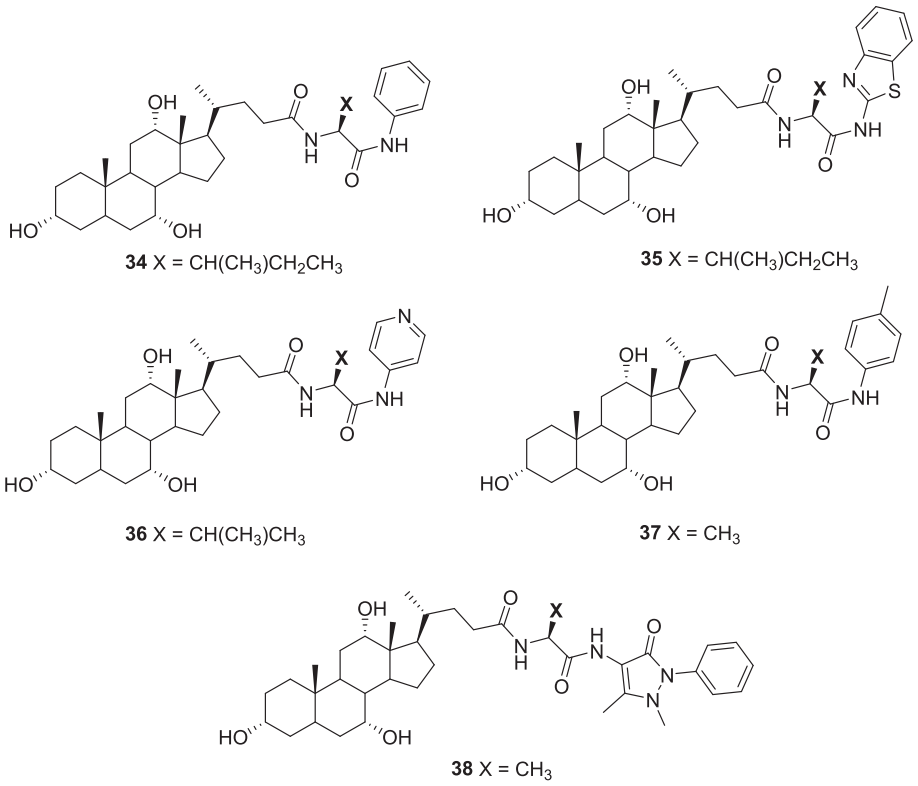

Fig. 11. Aromatic amide derivatives of cholic acid (**34**–**38**).

rings *via* ester or amide bonds. Antibiotics containing the azetidine-2-one unit are widely known. The conjugate created (**71**) (Fig. 20) was most active against yeasts *Yarrowia lipolytica* (8 μg/ml) as well as against fungal strains *Candida albicans* (128 μg/ml) and *Benjaminiella poitrasii* (32 μg/ml). The amide conjugate was characterised by efficacy at concentrations of 16, 8, and 32 μg/ml against *C. albicans*, *B. poitrasii,* and *Y. lipolytica* [95].

A series of aminocholestanes combined with an imidazole or pyridine ring was described by Kim et al. *vitro* demonstrated that the link (**72**) (Fig. 20) caused the death of several strains of bacteria *S. aureus* (MIC $<$ 4 μg/ml). In contrast, the 3,7-di(imidazole) steroid exhibited intense antibacterial activity against most bacterial cells at MIC ~ 4 μg/ml [96].

Cationic amphiphilic conjugates of cholic acid and lysine also exhibited antibacterial properties. The conjugate (**73**) (Fig. 20) was active against *S. aureus*, *E. coli,* and *C. albicans* with MIC $<$ 8 μg/ml. Researchers also observed that another cholic acid derivative exhibited antibacterial potential against resistant strains *S. aureus* 1704, *E. coli* 4052, and *Candida auris*. Most importantly, the compound (**73**) was safe for erythrocytes, causing changes only in the cell membranes of microbial strains [97].

Tetrapeptides glycine and β-alanine combined with cholic acid in position C-3β (**74**–**77**) (Fig. 21) with antibiotic properties comparable to fluconazole or erythromycin (FIC $<$ 0.5 against *E. coli* and *C. albicans*) [98]. On the other hand, the scientific report of Yadav et al. shows that the peptide derivative of cholic acid with valine and glycine (**78**) (Fig. 21) exhibit antimicrobial activity against bacterial strains *E. coli*, *Klebsiella pneumoniae,* and *Acinetobacter baumannii* (MIC_{99} = 4, 8 and 4 μM, respectively) [53,99].

Amphiphilicity plays a vital role in the destruction of biological membranes of microbes. Kong et al. extracted a steroid amino acid from an Irish sea sponge *Polymastia boletiformis*. After evaluation of antimicrobial activity (disc test, 1/4 in.), it was found that the conjugate (**79**) (Fig. 22) was toxic to strains *S. aureus*, *C. albicans,* and *Pythium ultimum* (MIC = 100, 75, and 25 μg/disc, respectively) [100]. Recent literature reports indicate that isolated analogs of steroid amino acids (**81**,**82**) (Fig. 22) were active against fungi of the genus *Cladosporium cucumerinum* (1D and 2D analysis of NMR, ZOI = 8.0 mm and 10.1 mm at 60 and 30 μg/disc, respectively). The conjugate activity (**82**) was the highest against *C. albicans*, with the ZOI being 9.8 mm (100 μg/disc) [101].

Tuberculosis (TB) is a deadly infectious disease that, despite being wholly cured with short-term therapy, is becoming increasingly resistant to available anti-tuberculosis drugs. Consequently, this leads to multidrug-resistant tuberculosis (MDR-TB). Using corticosteroids with a functional hydroxyl group at the C11 position is beneficial, especially in severe central nervous system or pericardial involvement cases. Steroid hormones with biological activity, such as fluticasone or dexamethasone, are an important therapeutic option [102]. Researchers seeking to develop effective inhibitors for *Mycobacterium tuberculosis* focused on bile acid derivatives with a substituted hydroxyl group at the C-11α position. It has been shown that compounds (**83**) and (**84**) (Fig. 23) show significant stunted growth in *M. tuberculosis* at a concentration of 30 μg/ml [103]. This is a decisive step in the fight against this dangerous disease.

4. Steroid conjugates with antiviral activity

HIV and AIDS continue to pose a considerable challenge to medicine. According to the World Health Organization (WHO), in 2022, about 39 million people were HIV positive, including 1.5 million children [96]. Although this virus no longer takes such a deadly toll, new therapeutic agents are still being sought [104].

Mayaux et al. developed the synthesis of betulinic acid (triterpenoid with a steroid-like skeleton) conjugates to assess their HIV-inhibiting activity. It was found that the selectivity and effectiveness of the obtained molecules depended to a large extent on their structural characteristics, especially on the length of the side chain. Therefore, the highest inhibitory activity of HIV replication was assessed for the compound (**85**) (gamma amino acid, a derivative of (3S,4S)-4-amino-3-hydroxy-6-methylheptanoic acid) (Fig. 24) at a concentration lower than

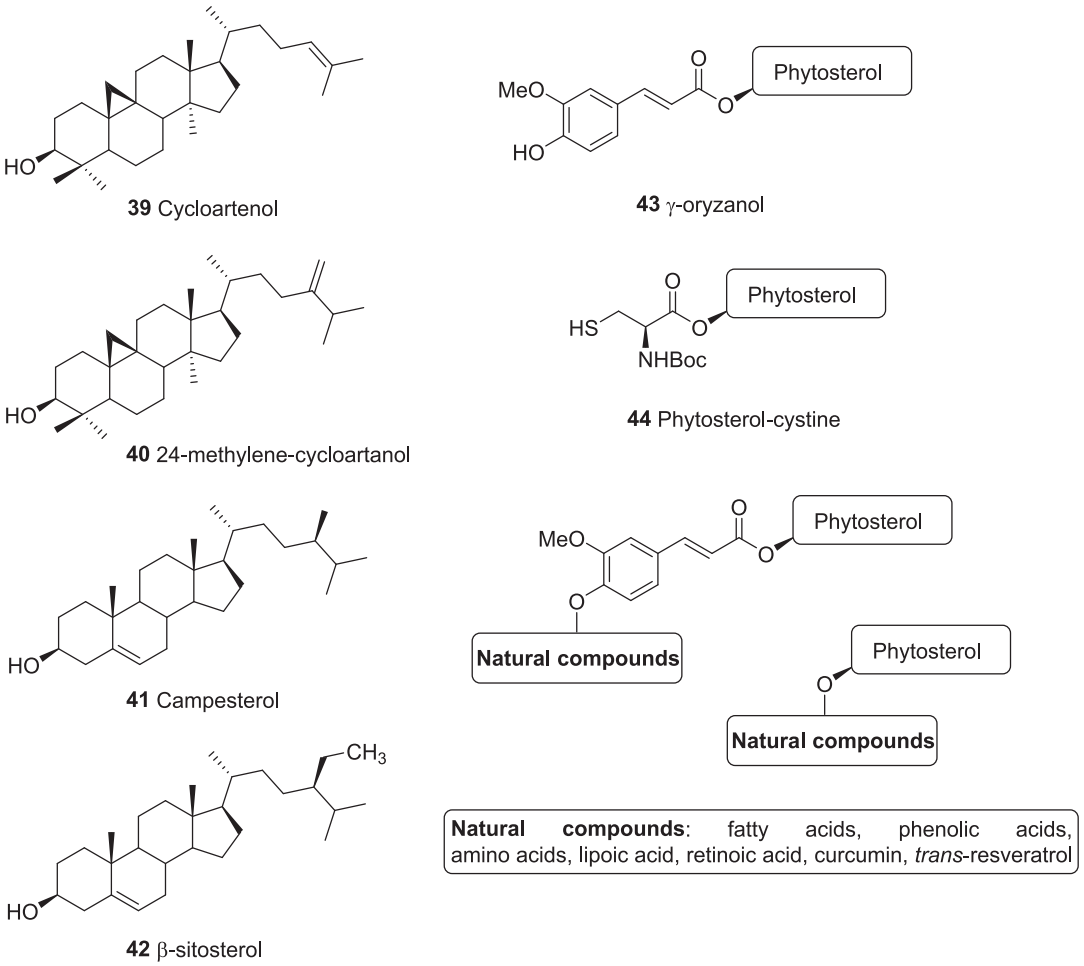

Fig. 12. Phytosterol analogues with antitumor activity (**39**–**44**).

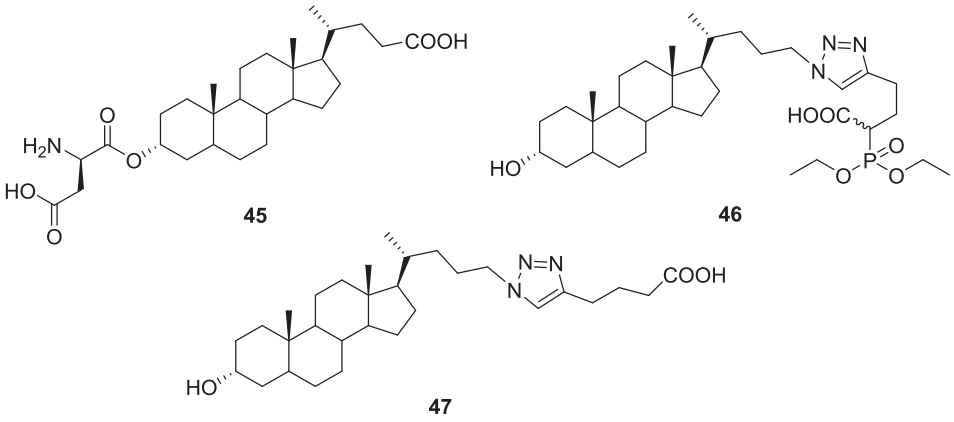

Fig. 13. Lithocholic acid conjugates (**45**–**47**) as sialyltransferase inhibitors.

0.02 μg/ml [105].

Bile acids' transport properties were used in synthesising cholic acid conjugates with small molecule peptides. Compounds (**86**–**88**) (Fig. 24) were investigated to determine their HIV-1 protease inhibitory capacity. The modification of the steroid backbone consisted of attaching the peptide part to the C-24 position. Tests showed that the compound β-benzyl-D-asp-cholic acid (**88**) had a moderate HIV-1 protease inhibitory potential (IC_{50} = 125 μM) [106].

Another type of deadly disease is the measles virus. Despite the availability of vaccines containing the measles antigen virus (MV), it is a common cause of death among children. MV's hemagglutinin glycoprotein (H) activates the cell membrane and facilitates viral penetration. Immunogenic H protein triggers an immune response. Scientific reports report that the hemagglutinin loop (HNE) epitope on the H protein (sequence H386-395 CKGKIQALCE) has an amphiphilic loop-like structure with an embedded disulfide bridge [107,108].

Vaccines containing peptides with the core sequence HNE, cystine, and a steroid nucleus were designed. The rigid steroid system provided the proper conformation for peptide coupling. As a result, the newly formed molecule resembled a loop with amphiphilic properties. An

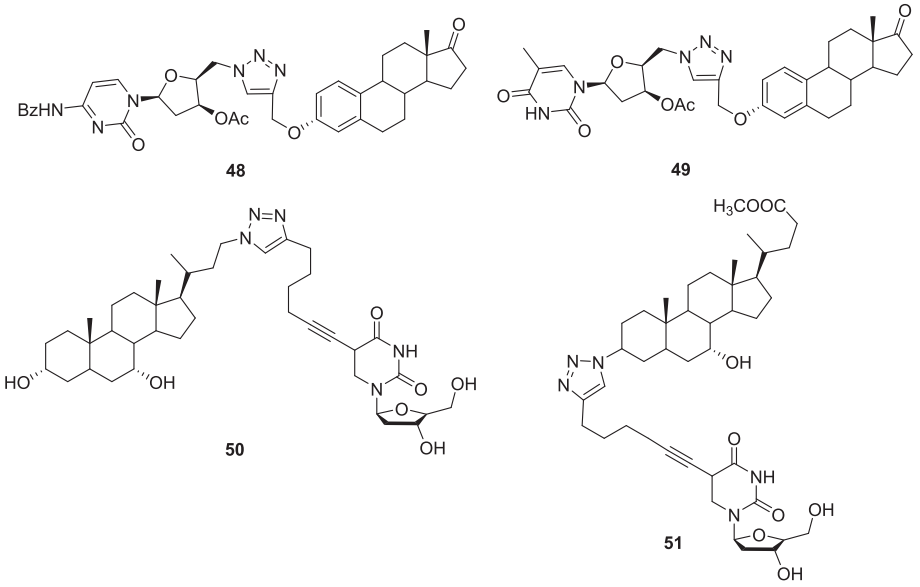

Fig. 14. Triazole steroid conjugates (**48**–**51**) as anticancer agents.

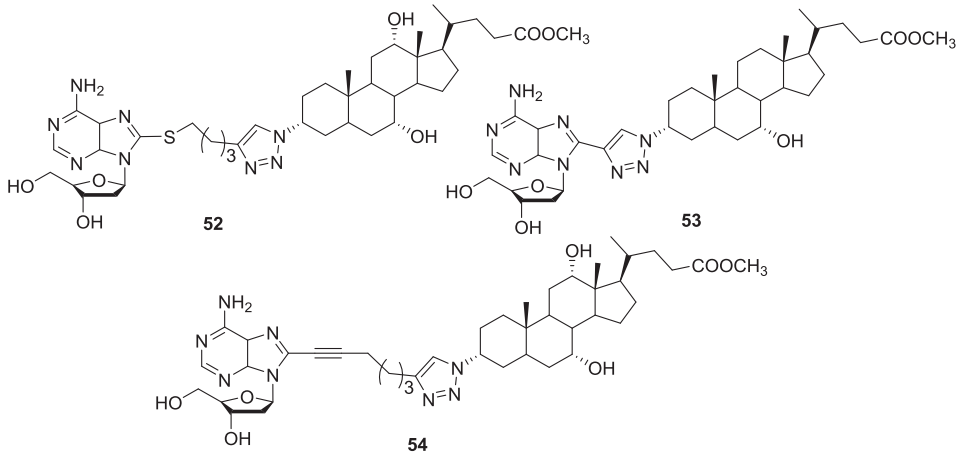

Fig. 15. Bile acid-deoxyadenosine conjugates linked by a triazole system (**52**–**54**).

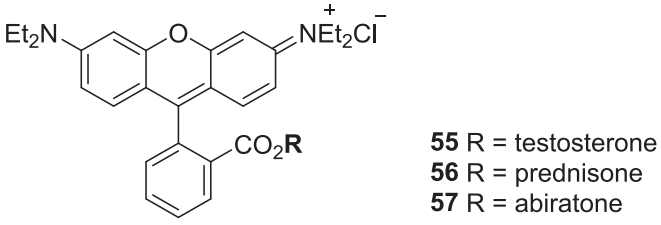

Fig. 16. Rhodamine B steroid esters (**55**–**57**).

appropriately protected bile acid derivative (**89**) was modified with a photolabile linker to obtain a compound (**90**) (Fig. 25). A series of successive selective transformations (such as group deprotection and finally coupling with a Gln-Ala-Cys-Lys tetrapeptide the same as the MV-HNE sequence) of the C-3 and C-12 positions of the steroid led to the production of a target macrocyclic peptidosteroid (**91**) (Fig. 25) [109]. This compound was supposed to be a precursor for new measles vaccines. Subsequently, Bode et al. synthesised a similar peptidosteroid (**89**) (Fig. 25) containing an additional disulfide bond (as in the HNE loop of the measles virus). The conjugate (**92**) had better bioavailability and stability than linear peptides. Subsequent studies have found that this macrocyclic compound also exhibits increased binding affinity for the monoclonal antibodies BH216 and BH21 compared to linear and non-steroidal peptides [110]. Therefore, the conjugate (**92**) can be considered a breakthrough in the design of vaccines to prevent the measles virus.

Yang et al. described and synthesised dehydroepiandrosterone (DHEA) conjugates with potential activity against H1N1 and H3N2 type A (IAV) influenza viruses. Bioconjugate containing 2-OH-Ph residue (**93**) (Fig. 26) inhibited viral RNA synthesis and protein expression. Based on the MTT test, it was concluded that the compound (**93**) was most effective at $CC_{50} = 111 \pm 7.1$ μg/ml [111].

Yang et al. report further effective thiazoline conjugates based on their promising activity against steroid-derived DNA and RNA viruses [39]. Assessment *in vitro* demonstrated that the link (**94**) (Fig. 26) was cytotoxic to enterovirus 71 (EV71) and Coxsackie B3 virus (CVB3). The results were compared with antiviral agents such as ribavirin and pyrodavir (IC_{50} = 1327 and 836; 431 and 397 μmol/l, respectively). Again, based on the MTT test, it was found that the DHEA derivative (**94**) exhibits activity against RD and Hep-2 cells at IC_{50} = 305.3 and 44.7 μmol/l, respectively. The legitimate antiviral properties of dehydroepiandrosterone bioconjugates place it at the forefront of potential antiviral drugs.

Table 3
Antibacterial and antiviral activity of steroid-based bioconjugates.

Type of steroid's conjugate	Bioactive compounds	Cell lines	Activity (IC_{50})	References
Bile acid-aminoalcohol	**62**	*E. coli* *S. aureus*	45 μg/ml 15 μg/ml	[93]
	68 **70**	*C. neoformans*	< 60 μg/ml	[94]
Bile acid-β-lactam	**71**	*Y. lipolytica* *C. albicans* *B. poitrassi*	8 μg/ml 128 μg/ml 32 μg/ml	[95]
Aminocholestanes	**72**	*S. aureus*	< 4 μg/ml	[96]
Bile acid-amino acid	**73**	*S. aureus* *E. coli* *C. albicans*	< 8 μg/ml	[97]
	74 **75** **76** **77**	*E. coli* *C. albicans*	< 0.5 μg/ml	[98]
	78	*E. coli* *K. pneumoniae* *A. baumanii*	4 μM 8 μM 4 μM	[99]
Steroid amino acid	**79**	*C. albicans* *S. aureus* *P. ultimum*	75 μg/disc 100 μg/disc 25 μg/disc	[100]
	81 **82**	*C. cucumerinum* *C. albicans*	60 μg/disc 30 μg/disc 100 μg/disc	[10171]
Bile acid-substitution of C-11α	**83** **84**	*M. tuberculosis*	30 μg/ml	[103]
Betulinic acid-amino acid	**85**	HIV replication inhibitor	< 0.02 μg/ml	[105]
Bile acid-peptide	**88**	anti-HIV1	125 μM	[106]
Macrocyclic peptidosteroid	**92**	binding of monoclonal antibodies BH216 and BH21	–	[109]
DHEA conjugate	**93**	H1N1 H3N2 type of A (IAV)	111 ± 7.1 μg/ml	[111]
Steroid-thiazoline	**94**	Enterovirus 71 (EV71) Coxsackie B3 (CVB3)	305.3 μmol/l 44.7 μmol/l	[39]
Bile acid-acyclovir	**96**	better bioavailability than acyclovir	–	[113–115]
	97	affinity for hASBT	K_i = 35 x M	[116]

Acyclovir (**95**) (Fig. 27) is a medicine used to inhibit the herpes virus [112]. Poor absorption in the intestine and low oral bioavailability (about 20 %) were the impetus for the design of its new derivative. Valacyclovir (**96**) (Fig. 27) is an ester derivative of L-valine with much better therapeutic potential [113]. Bile acid conjugation with valacyclovir resulted in a total of 4 novel prodrugs. Tests *in vitro* with esterase in HBSS showed that after two hours, acyclovir was again obtained from the prodrug [114,115].

In 2004, Tolle-Sander et al. developed similar analogues of acyclovir and valine-linked bile acids. Assessment *in vitro* and *in vivo* demonstrated that the prodrug acyclovir valylchenodeoxycholate (**97**) (Fig. 27) was characterised by an affinity for hASBT (i.e., a human sodium-dependent apical bile acid transporter) comparable to cholic acid (K_i = 35 x M and

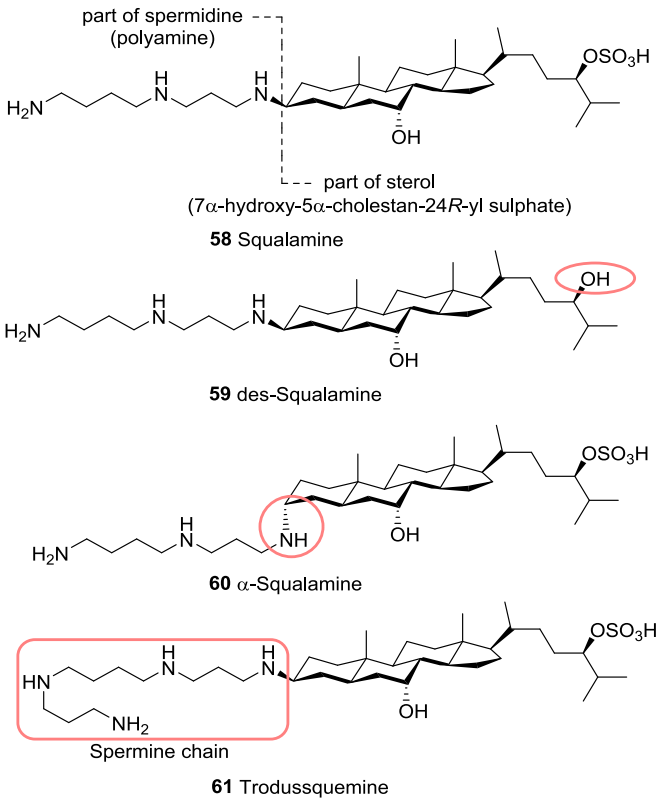

Fig. 17. Structures of squalamine (**58**) and its modified analogues (**59**–**61**).

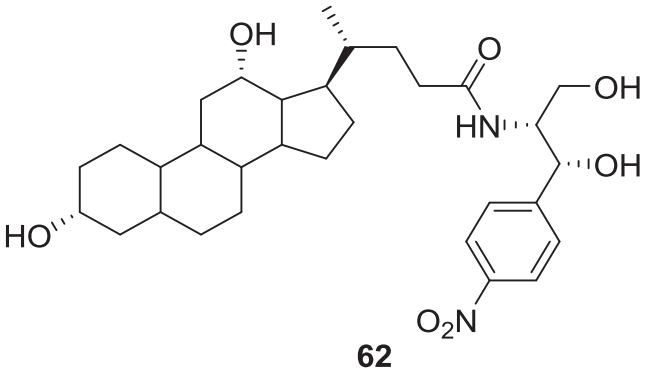

Fig. 18. Bioconjugate of deoxycholic acid and (-R)-2-aminocyclohexanol (**62**).

K_i = 25 x M, respectively). Most importantly, the steroidal acyclovir conjugate was about 16 times more selective for hASBT-COS cells than acyclovir alone. In addition, acyclovir valineoxycholate showed significantly stronger passive permeability. On the other hand, an assessment of oral bioavailability in rats showed that the compound (**97**) is twice the bioavailability of acyclovir [116].

5. Anti-inflammatory steroid conjugates

The pharmacological potential of glucocorticoids is used to treat many autoimmune diseases, asthma, intestinal disorders, and rheumatoid arthritis. The consequence of frequent use of steroids may be the occurrence of osteoporosis or a decrease in the immunity of the immune system [117,118].

Efforts to develop more safe and effective anti-inflammatory drugs have led to the development of so-called „anti-drugs". Loteprednol etabonate can be applied topically [119]. Once they enter the

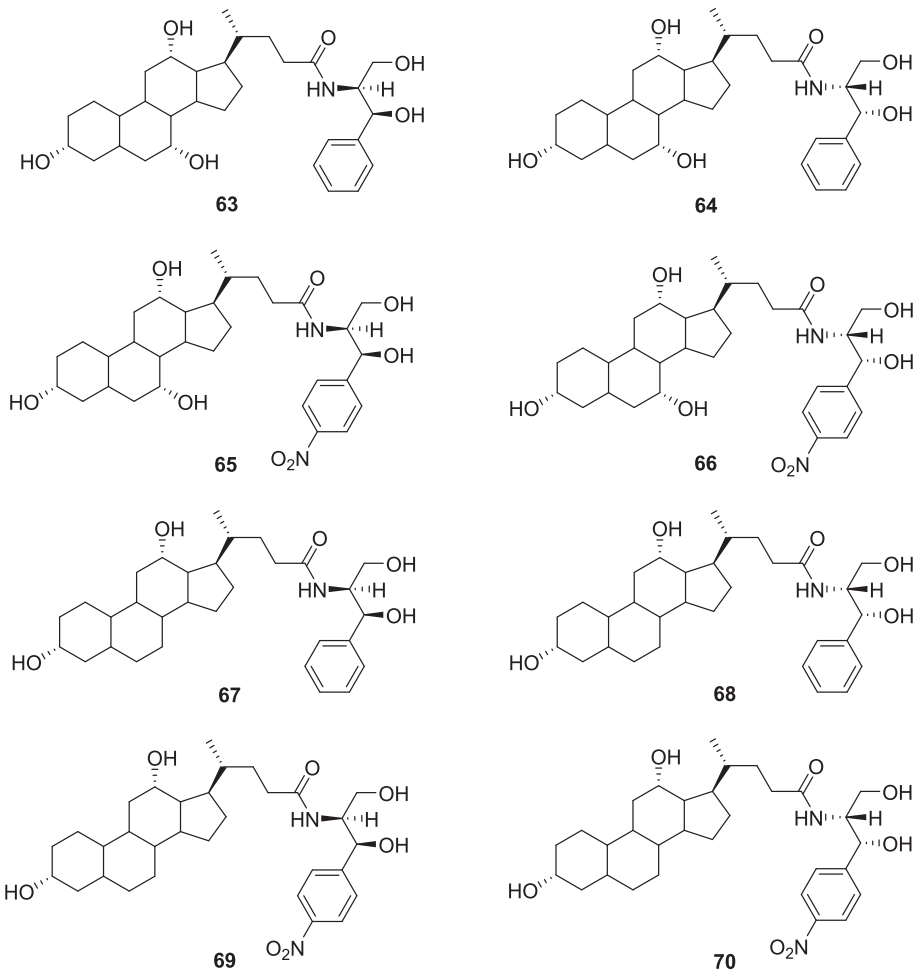

Fig. 19. Bile acid and chloramphenicol conjugates (**63**–**70**) with biocidal activity.

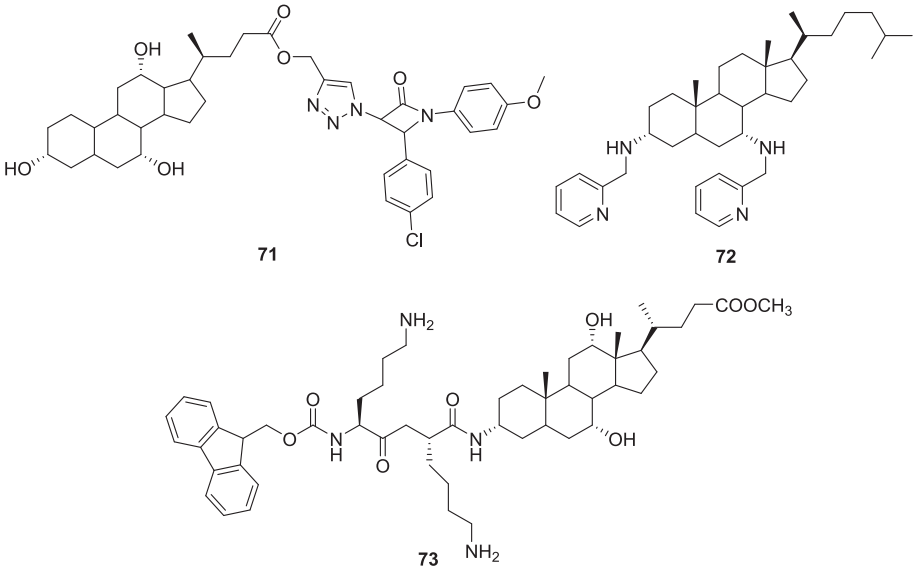

Fig. 20. Conjugates (**71**–**73**) with antibacterial and antifungal properties.

bloodstream, the „anti-drugs" are converted into inactive metabolites and are removed from the body [120]. The final molecule is formed by conjugating steroidal „anti-drugs" with non-steroidal anti-inflammatory drugs. Specific conjugates have been synthesised to prevent a potential increase in potency, such as the combination of prednisolone with non-steroidal anti-inflammatory medications such as indomethacin and ibuprofen [121]. Biological studies of ibuprofen-prednisolone conjugate (**98**) (Fig. 28) showed a slight increase in anti-inflammatory effects

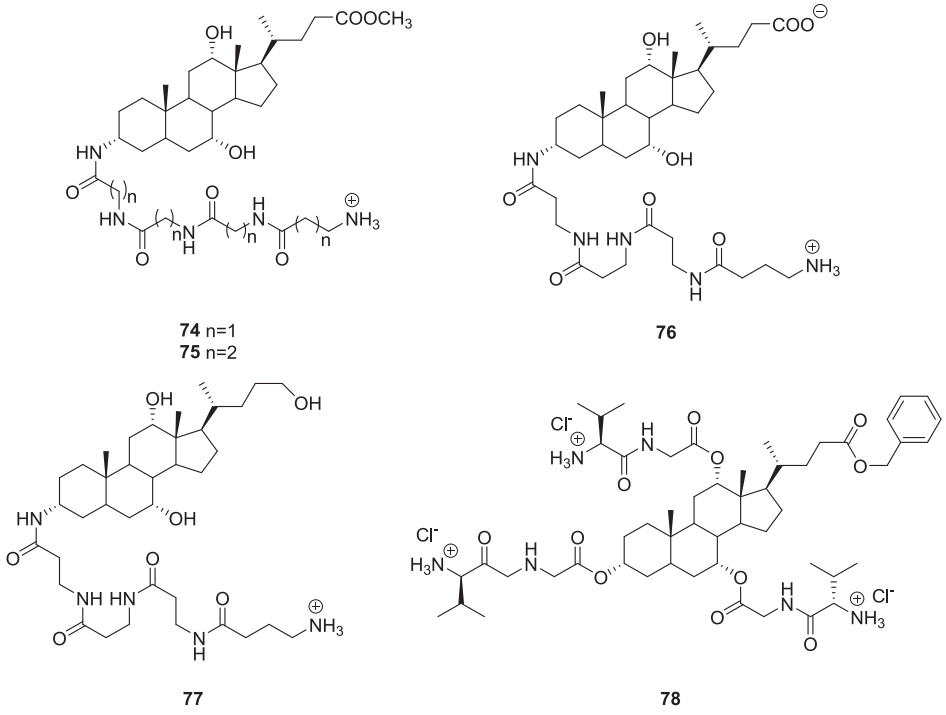

Fig. 21. Tetrapeptides and dipeptides of cholic acid and amino acids (**74**–**78**).

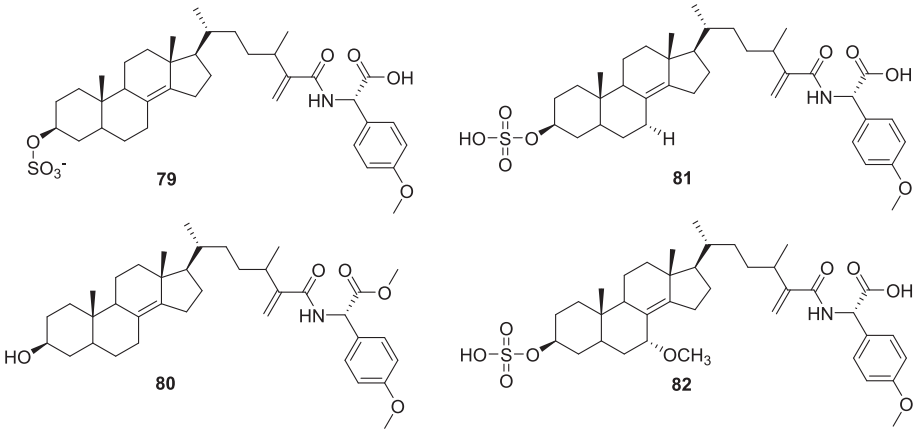

Fig. 22. Natural steroid amino acids (**79**–**82**) with antimicrobial activity.

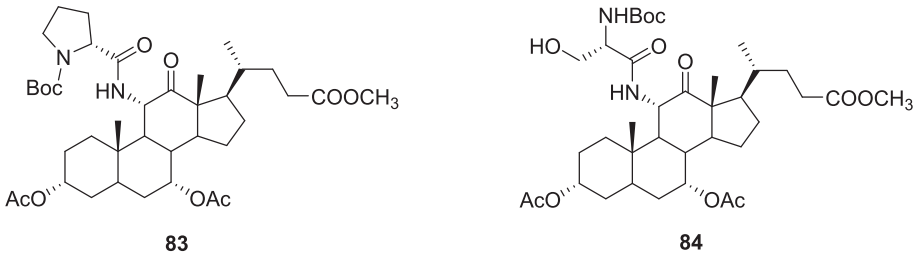

Fig. 23. Bile acid derivatives (**83**–**84**) as tuberculosis factor inhibitors.

(62.5 % inhibition) compared to prednisolone alone. In contrast, indomethacin and prednisolone bioconjugate did not show systemic anti-inflammatory activity.

Liu et al. designed steroid hybrids with C_{60} to determine their anti-inflammatory properties [122]. Tests *in vivo* in mice showed that a dexamethasone derivative (**99**) (Fig. 29) eliminated the swelling initiated by xylene administration in 47 % [123]. Hydrophobic steroid scaffolds have been used as carriers of selective oligonucleotides in gene therapy [124]. Thus, the second generation of micellar cholesterol polyamidoamine (**100**) (Fig. 29) conjugated to resveratrol and the heme oxygenase-1 (HO-1, pDNA) gene [125]. Its therapeutic potential for treating acute lung injury (ALI) was then evaluated. Studies in an animal

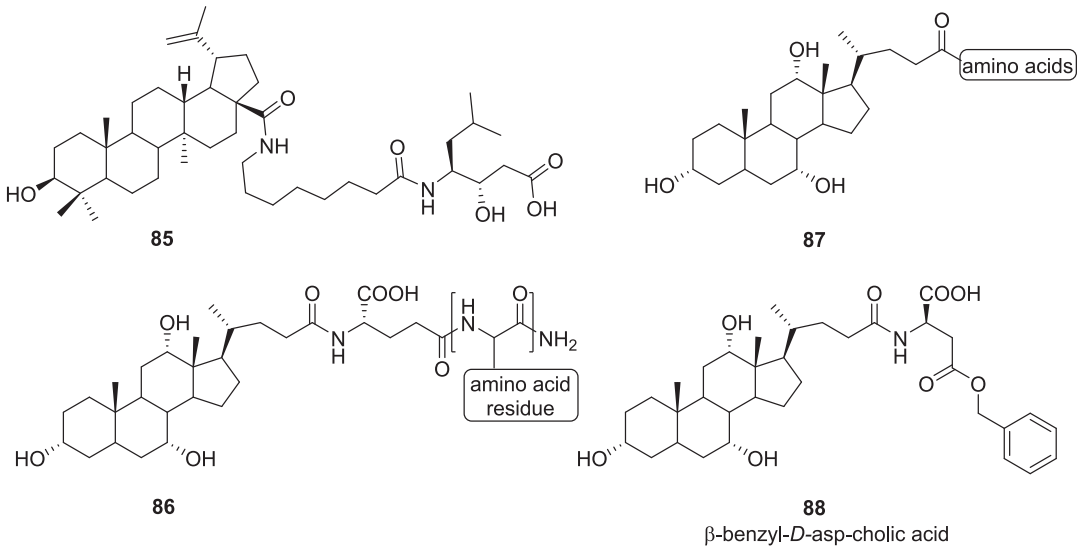

Fig. 24. Steroid conjugates (**85**–**88**) as inhibitors of HIV replication.

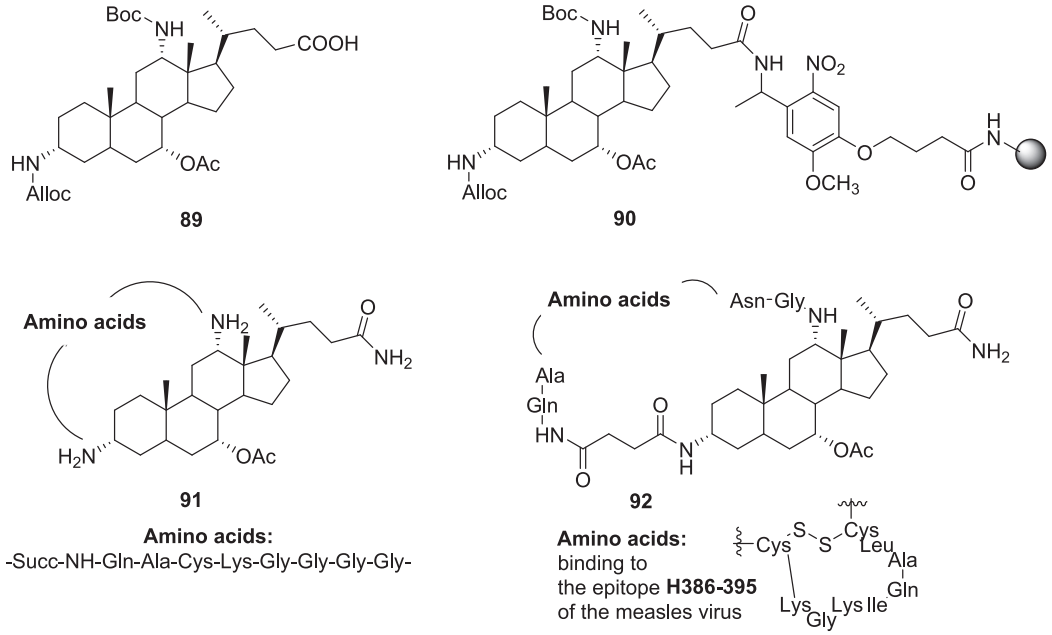

Fig. 25. Peptidosteroids (**89**–**92**) showing activity against measles virus.

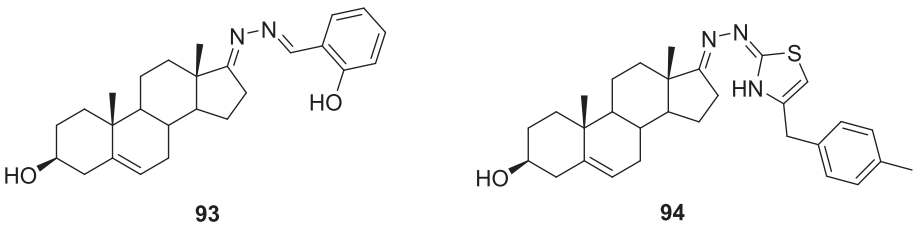

Fig. 26. DHEA conjugates (**93**–**94**) with antiviral activity.

liposaccharide (LPS)-induced ALI model showed that the conjugate (**100**) containing the drug and pDNA reduces the production of cytokines (critical micelle concentration of 0,22 mg/ml^{-1}). Subsequent reports have found that polyamidoamine and cholesterol micelles similar to curcumin and the HO-1 gene also reduce the levels of pro-inflammatory cytokines [126].

6. Steroid conjugates as antioxidant agents

Fullerenes (common C_{60} molecules or radical sponges) are effective at scavenging free radicals, which is why they are used as pharmacological antioxidants [127]. Due to their low solubility in polar and non-polar solvents, it is necessary to modify them. Multiple interfaces of

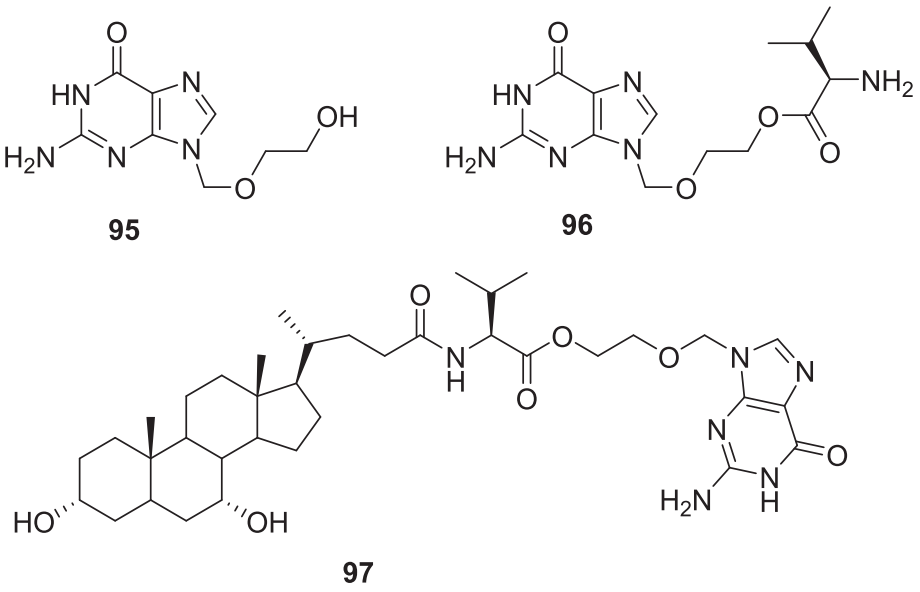

Fig. 27. Acyclovir (**95**) and its derivative (**96**–**97**) with chenodeoxycholic acid.

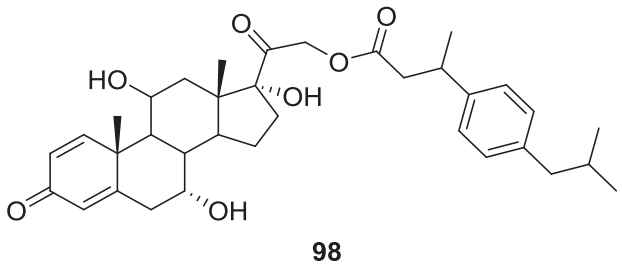

Fig. 28. A conjugate of prednisolone and ibuprofen (**98**) with anti-inflammatory activity.

fullerenes with steroids, amino acids, and peptides were performed to improve solubility and increase interaction with the membrane and interior of the target cell [128–130]. Bioconjugate (**101**) (Fig. 30) containing a linker of γ-aminobutyric acid (GABA) between estradiol and fullerenpyrrolidine showed 3 times higher antioxidant activity (ED_{50} = 20.2 μM) than fullerene alone (ED_{50} = 64.1 μM) [131]. The improved antioxidant properties of the carbon clusters resulted from a lipophilic steroid system, which was also confirmed by morphological, electrochemical, and theoretical analyses [132].

7. Steroid conjugates in anticoagulant therapy

Heparin is an effective anticoagulant drug composed of glycosaminoglycans weighing about 15 kDa. Unfractionated heparin (UFH) is

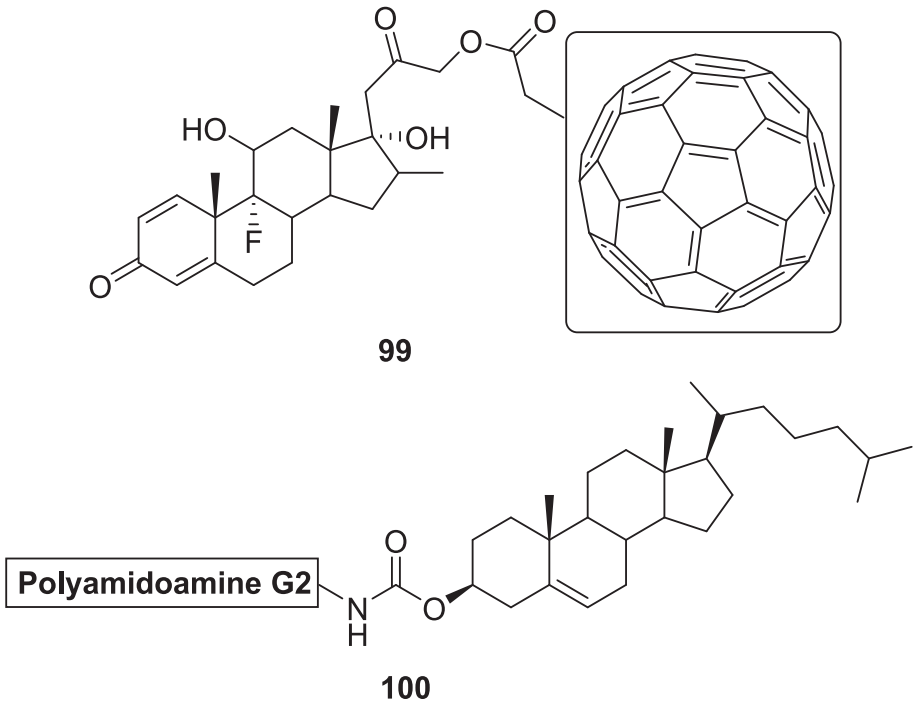

Fig. 29. A derivative of dexamethasone (**99**) and cholesterol (**100**) with potential use in anti-inflammatory drugs.

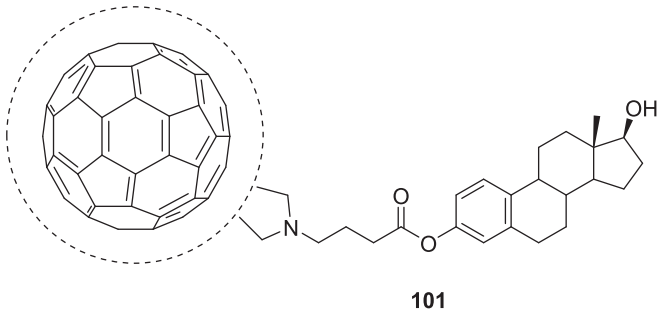

Fig. 30. A steroid conjugate of fullerene (**101**) with antioxidant properties.

administered intravenously and subcutaneously with low molecular weight heparin (LMWH). UFH works by binding to antithrombin III, strongly inhibiting the action of thrombin (unlike LMWH) and factor X_a [133]. Heparins are conjugated with lipids and other molecules to increase oral bioavailability by modifying free groups (such as sulfate, carboxylic, hydroxyl, or amine) [134]. Studies suggest that the DOCA-heparin conjugate (**102**) (Fig. 31) has a higher bioactivity than the cholesterol-heparin conjugate [135–137]. In addition, increased intestinal absorption was confirmed for the bis-DOCA-heparin conjugate (**103**) (Fig. 31) [138]. Preclinical studies *in vivo* showed that the conjugate (**102**) is safe and non-mutagenic [36]. The DOCA-heparin conjugate containing the ethylenediamine linker between the carboxyl groups positively affected wound recovery after surgery (anticoagulant activity = 86 IU/mg) [139]. Similar anticoagulant properties are possessed by the conjugate (**104**) (109.8 IU/mg) (Fig. 31). On the other hand, for the LMWH-tetraDOCA compound, an increase in oral bioavailability (19.9 %) and anticoagulant activity (33.5 %) was observed [140]. Literature data indicate that a dose of 5 mg/kg (for mice) inhibits thrombosis formation during cancer [141].

8. Steroid conjugates as glucocorticoid antagonists

11β-hydroxysteroid dehydrogenases (11βHSD, including 11βHSD1 and 11βHSD2) are responsible for the proper level of glucocorticoids in the body. Excessive production of these enzymes interferes with converting cortisone to cortisol (or *vice versa*), leading to metabolic syndrome or fatty liver without obesity [142]. Inhibition of 11βHSD2 leads to cortisol activating mineralocorticoid receptors, which retain sodium and water [143]. 11βHSD2 inhibitors are used in patients on hemodialysis to prevent potassium loss caused by cortisol activation of MR in the colon [144]. MR activation can adversely affect the heart and metabolism [145]. Inhibition of 11βHSD is a promising direction in the treatment of atherosclerosis, osteoporosis, hyperlipidemia, and type 2 diabetes. This is why MR antagonists and 11βHSD inhibitors are needed. Progesterone and its metabolites bind to MR and inhibit 11βHSD [146,147]. The conjugation of amino acids and 11α-hydroxyprogesterone by modification at the 11β position yielded compounds (**105–107**) (Fig. 32). The conjugates were found to be suitable inhibitors of 11βHSD2 (IC_{50} = 2.41; 2.69 and 6.76 μM), although they did not match the inhibitory activity of 11α-hydroxyprogesterone (IC_{50} = 0.40 μM) [148].

9. Insulin-stimulating steroid conjugates

Insulin is a hormone produced by the beta cells of the pancreas. Its primary function is to regulate blood glucose levels. Insulin allows the body's cells to absorb glucose from the blood and use it as energy. In addition, it supports the storage of glucose in the liver as glycogen and inhibits the breakdown of fats. Insulin deficiency, or the body's improper response to this hormone, leads to diabetes [149,150].

The deoxycholic acid-insulin derivative (**109**) (Fig. 32) was synthesised using the succinimide deoxycholate ester. In contrast, conjugation with the same amino group of the Lys residue^{B29} insulin through the succinimide bisdeoxycholyl-1-lysine ester (**108**) (Fig. 33) has given a link (**109**). Lee et al. found that the attachment of a large molecule of steroid acid did not affect insulin structure and the persistence of binding to insulin receptors on HepG2 cells. The results indicated that steroidal insulin conjugates are characterised by prolonged interaction with the body. Moreover, they were more active longer and did not break down faster than native insulin. The report shows that for the conjugate (**109**), the insulin receptor IC_{50} was 3.37 * 10^{-9} M, for conjugate (**110**) (Fig. 33) was 2.24 * 10^{-9} M, and for native insulin 1.28 * 10^{-9} M [151]. Bile acid derivatives may act as potential therapeutic agents during abnormal insulin secretion.

10. Sarsasapogenin conjugates in the treatment of neurodegenerative diseases

Alzheimer's disease is a chronic and progressive neurodegenerative disease. It manifests as a gradual loss of cognitive functions such as memory, thinking, orientation, and the ability to perform daily activities independently. It is the most common cause of dementia among the

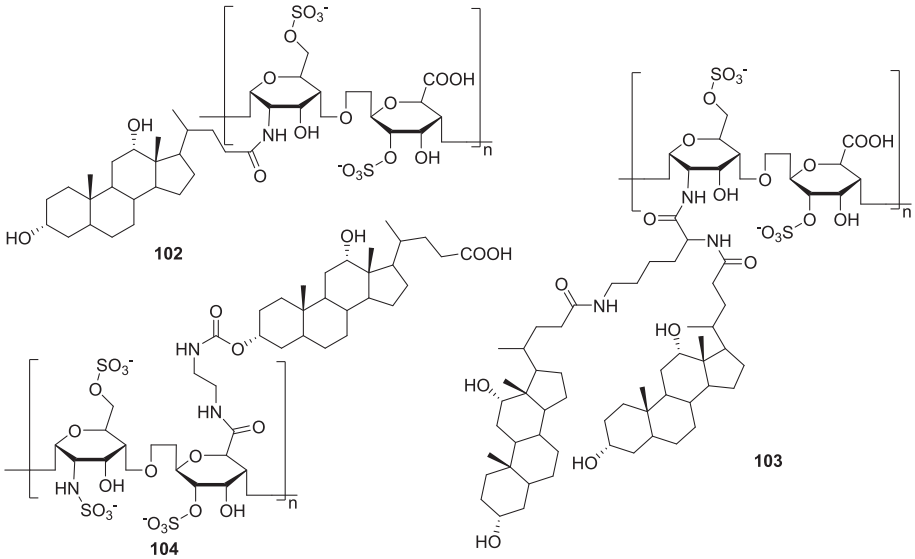

Fig. 31. Heparin steroid conjugates (**102–104**) as potential anticoagulants.

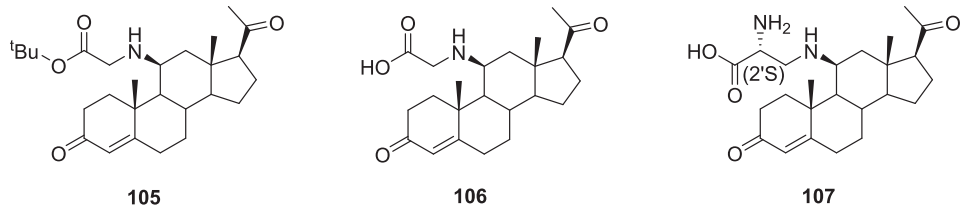

Fig. 32. 11α-progesterone derivatives (**105**–**107**) inhibiting 11βHSD2 dehydrogenase.

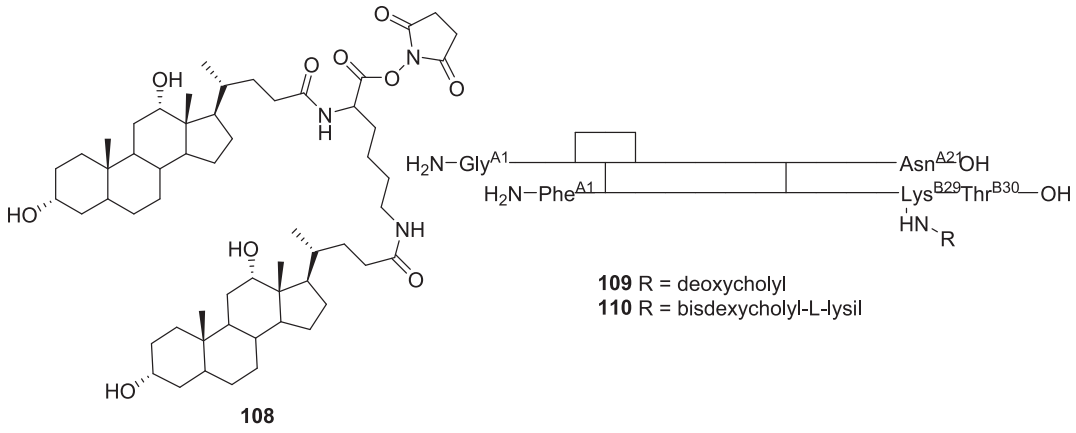

Fig. 33. Insulin steroid conjugates (**108**–**110**).

elderly. Characteristic symptoms are memory disorders, speech problems, confusion, and changes in personality and behaviour. In the brain of people with Alzheimer's, there is a build-up of amyloid plaques and neurofibrillary plexuses. As a result, nerve cells become damaged and die. The causes of the disease are not fully understood. Treatment focuses mainly on alleviating symptoms and slowing their progression [152]. Natural steroid conjugates have greatly improved the treatment of this disease (see Table 4) [153].

Table 4
Potential biological properties of steroid-based conjugates.

Type of steroid's conjugate	Number of bioactive compounds	Bioactivity	References
Steroid-ibuprofen	**98**	anti-inflammatory,	[121]
Dexamethasone derivative	**99**	inhibition of swelling	[123]
Liposaccharide-steroid	**100**	cute lung injury-ALI (reduced cytokine production, MIC = 0.22 mg/ml)	[125,126]
Steroid-fullerene	**101**	Antioxidative	[131]
DOCA-heparin	**102**	anticoagulant	[135–138]
	103	(86 j.m./mg)	
	104	anticoagulant (109.8 j.m./mg)	[140]
Progesterone derivatives		inhibitors of 11βHSD2	[148]
	105	2.41 μM	
	106	2.69 μM	
	107	6.76 μM	
Bile acid-insulin	**109**	insulin receptor ($3.37 * 10^{-9}$ M)	[151]
	110	insulin receptor ($2.24 * 10^{-9}$ M)	
Sarsasapogenin-amino acid	**111**	neuroprotective activity against the SH-SHY5Y (Alzheimer's disease)	[47]
	112		
	113		
	114		
	115		
Bile acid-amino acid	**116**	inhibitor NAFLD	[158]

Sarsasapogenin isolates neurons that are vulnerable to damage from hydrogen peroxide. Studies on an animal model have also shown that it can minimise memory loss [154]. In combination with 3-carbamate, it has a neuroprotective effect [155].

The conjugates of sarsasapogenin (**11**) (Fig. 2) with the C-26 amino acid methyl ester (**111–115**) (Fig. 34) were synthesised to determine their neuroprotective activity against the SH-SHY5Y cell line. Derivative (**115**) conjugated to phenylalanine at position C-26 had almost 4 times stronger neuroprotective properties than sarsasapogenin (102.2 % and 27.3 %, respectively). As a result of such significant neuroprotective activity of the conjugate (**115**) was found to minimise peroxide-induced neuronal apoptosis by inhibiting the activity of cleaved poly(ADP-ribose) polymerase (PARP for short) and cleaved caspase-3. In addition, such an effect also increases the expression of neurotrophic brain factor (BDNF), as well as its receptor tyrosine kinase B (TrkB). Compounds with the methoxyl group at the C-3 position showed the highest neuroprotective potential. Wang et al. suggest that the resulting sarsasapogenin conjugates may be of breakthrough importance for patients with Alzheimer's disease [47].

11. Steroid conjugates for the treatment of liver damage

Fatty liver, or non-alcoholic steatohepatitis (NASH), is an incurable type of non-alcoholic fatty liver disease (NAFLD). It is known that the main effects of NAFLD are hepatocellular carcinoma (HCC), cirrhosis of the liver, and end-stage liver disease [156]. Due to the coupling between

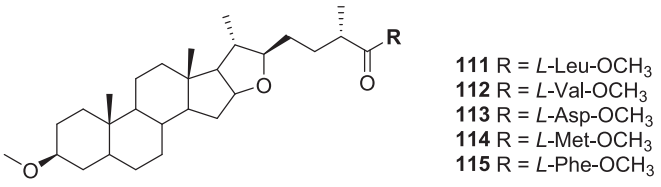

Fig. 34. Conjugates of sarsasapogenin and amino acids (**111**–**115**) with promising activity in treating Alzheimer's disease.

bile acid receptor G (TGR5) and farnesoid X receptor (FXR) ligands, bile acids have great potential in the treatment of NAFLD [157].

Chenodeoxycholic acid L-arginine ethyl ester bioconjugate (CDCArg) (**116**) (Fig. 35) was tested in a mouse model to determine its cytotoxicity as well as its effect on cholesterol accumulation in the liver [158]. Voloshin et al. suggest that adding the CDCArg compound to the diet of high-fat mice does not cause excess cholesterol in the liver and its destruction. It has also been observed that the conjugate (**116**) protects the liver and prevents weight gain. Steroidal amino acid conjugates can be precursors as therapeutic agents in inhibiting NAFLD.

12. Steroid conjugates as organic gels

Organogels are gels in which an organic solvent is used as a dispersing medium for the three-dimensional lattice formed by gelling molecules. These are soft materials that have both liquid and solid properties. Steroid amino acids can be crucial in the formation of organogels. Due to their unique structural and chemical properties, steroid amino acids can act as effective gelling molecules. They can stabilise the structure of organogels through intermolecular interactions such as hydrogen bonding, van der Waal's, or hydrophobic interactions. Biocompatible steroid amino acids have a vast potential due to the ability to customise the gel structure to meet specific needs.

Conjugates of bile acid methyl esters and L-methionine (**117–119**) (Fig. 36) were evaluated for gelling properties in several organic solvents. It was concluded that the compound (**117**) was highly susceptible to gelation. On the other hand, the association (**119**) formed strong and colourless gels. In addition, X-ray powder diffraction tests have shown that temperature reduction to –150 °C affects reversible conformational changes in the solid state of the conjugate (**117**) [159].

Svobodova et al. synthesised stigmasterol derivatives with amino acids (**120–122**) (Fig. 37) [160]. Amino acids (glycine, L-leucine, L-phenylalanine) were adequately secured at the *N*-terminus of Fmoc, which was then removed using piperidine. Then, after conjugation with stigmasterol, hydrochloride salts (**123–125**) were formed to investigate their gelling potential against derivatives of other amines compared to inert phytosterols. Tests showed that stigmasterol amino acid conjugates exhibited significant gelling properties. It was also observed that there were gel-forming salts only under polar alcoholic conditions (such as stigmasterol hydrochloride with glycine and 1-taurine) and those with the ability to form gels only under non-polar aromatic conditions (stigmasterol hydrochloride with 1-phenylalanine).

In the literature, bile and amino acids conjugates with gelling activity are also known [161]. Phenylalanine conformers conjugated urea compounds to bile acids. The most minor crystal structure was shown by

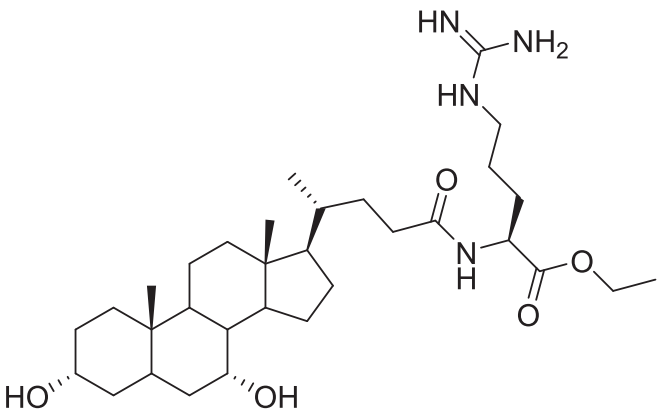

116

Fig. 35. CDCArg (**116**) as a potential drug to inhibit NAFLD.

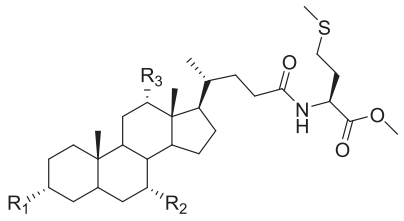

117 R_1 = OH, R_2 = R_3 = H
118 R_1 = R_3 = OH, R_2 = H
119 R_1 = R_2 = R_3 = OH

Fig. 36. Bile acid and L-methionine conjugates (**117–119**) with gelling properties.

the cholic acid conjugate (**128**) (Fig. 38). Based on the results of the analyses (DSC, powder XRD, or ^{13}C NMR from the solid phase), it was found that the polymorphism of cholic acid derivatives (**128**) and (**129**) (Fig. 38) affects their broad organogelling potential. In addition, all derivatives of lithocholic, deoxycholic, and cholic acids showed better-gelling properties in 1,2-disubstituted aromatic solvents (e.g., 1,2-dimethylbenzene) compared to solvents substituted in position 1,3 or 1,4.

Based on the good gelling properties of bile acid amino acids, Maitra et al. designed further derivatives of α-amino acids [162]. Conjugate hydrochlorides (**130–137**) (Fig. 39) were synthesised using ethyl chloroformate. It was determined that the obtained structures showed good hydrogelling properties at pH within the range of 7–8 as molecules with low mass and appropriate hydrophilic-hydrophobic balance. This rigid structure has been used to synthesise gold and ZnO nanoparticles.

Finally, the Maitra research group published a report on the behaviour of bile acid-based gelling agents with glycine and phenylalanine (**138–139**) (Fig. 40) depending on the pH [163,164]. Interestingly, deoxycholic and cholic acid derivatives did not form gels, probably due to the presence of additional hydroxyl groups. A hydrogel matrix of a derivative of lithocholic acid was used to synthesise silver and gold nanoparticles. A photoreduction analysis was performed to document the immobilisation of these nanoparticles on gels, compounds (**138**), and (**139**). A silver-doped conjugate (**138**) is resistant to colour change caused by exposure to solar radiation. On the other hand, after adding $NaBH_3CN$ and after one minute, the silver-doped compound (**139**) turned pink, and after 1 h, it turned dark pink and finally yellow.

13. Conclusions

Due to their structure and multidirectional biological profile, steroid compounds have long attracted interest in bioorganic chemistry. Conjugates of steroids with diverse groups, such as polyamines, amino acids, carbohydrates, bioactive heterocycles and bis-conjugates, show significant pharmacological potential. This review discusses numerous conjugates of these compounds with bioactive molecules and diverse biological activity. The derivatives are primarily focused on combating cancers, pathogens and microorganisms. There are also examples in the literature of bioconjugates acting on metabolic disorders and performing antioxidant or antithrombotic functions. These compounds are excellent materials for designing new molecules with improved bioavailability. They can act as drug carriers or be used as hydrogels. Future studies should focus on further exploration of new conjugation techniques. They will allow us to overcome the current limitations related to bioavailability and selectivity of action. Furthermore, additional research could focus on therapeutic applications in treating metabolic diseases. The development of multi-target conjugates is also crucial. This could significantly increase the effectiveness and safety of therapy for many serious diseases.

List of abbreviations

11βHSD	11β-Hydroxysteroid Dehydrogenases (including 11βHSD1 and 11βHSD2)
^{13}C NMR	Carbon-13 Nuclear Magnetic Resonance
17β-HSD1	17β-Hydroxysteroid dehydrogenase 1

(*continued on next page*)

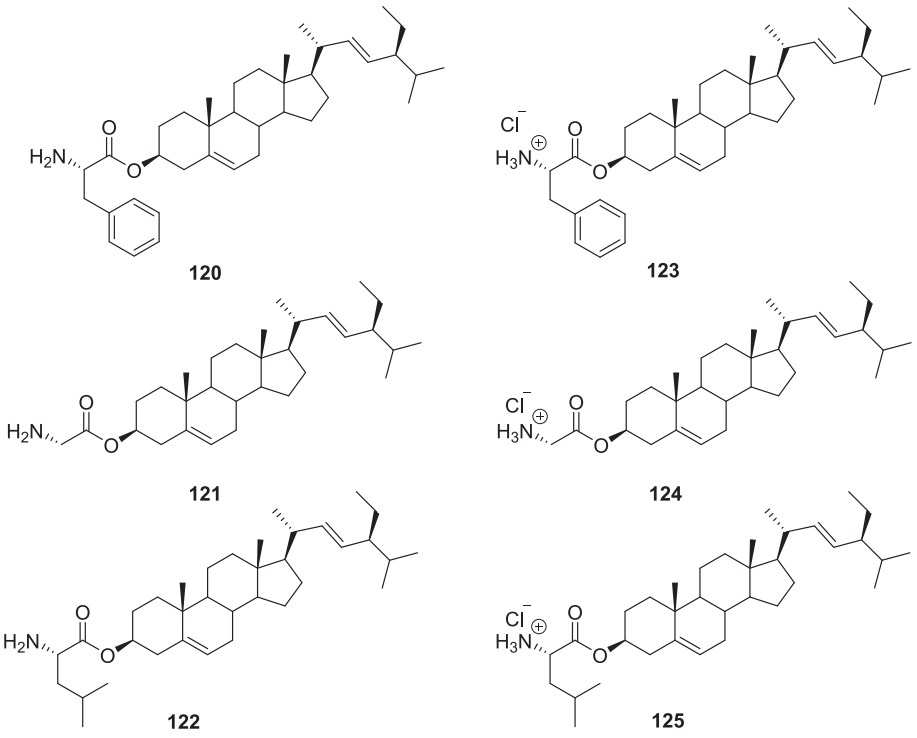

Fig. 37. Conjugates of stigmasterol with amino acids (**120–122**) and their salts (**123**–**125**) as potential gels.

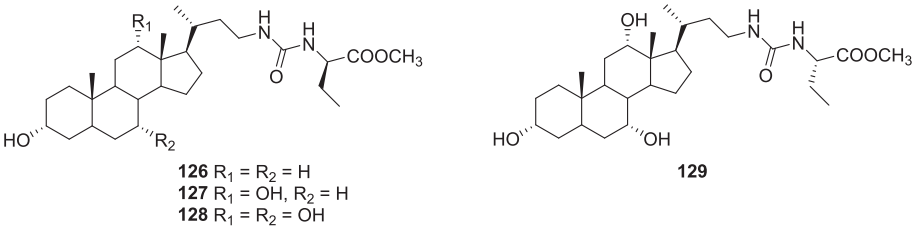

Fig. 38. Bile acids combined with amino acids (**126**–**129**) as organogelators.

(*continued*)

List of abbreviations	
1D NMR	One-Dimensional Nuclear Magnetic Resonance
2D NMR	Two-Dimensional Nuclear Magnetic Resonance
ADP	Adenosine Diphosphate
AIDS	Acquired Immunodeficiency Syndrome
Ala	Alanine
ALI	Acute Lung Injury
BDNF	Brain-Derived Neurotrophic Factor
CC_{50}	Concentration of Cytotoxicity 50 %
CDCArg	Chenodeoxycholic Acid L-arginine ethyl ester bioconjugate
COS	monkey kidney fibroblast cell line
CuAAC	Copper(I)-Catalyzed Azide Alkyne Cycloaddition
CVB3	Coxsackie B3 Virus
Cys	Cysteine
DCC	Dicyclohexyl Carbodiimide
DHEA	Dehydroepiandrosterone
DIPEA	*N, N*-Diisopropylethylamine
DNA	Deoxyribonucleic Acid
DOCA-heparin	Heparin-Deoxycholic Acid conjugate
DSC	Differential Scanning Calorimetry
ED_{50}	Effective Dose for 50 % of the population
EDC	1-Ethyl-3-(3-(Dimethylamino)propyl)Carbodiimide Hydrochloride
ER	Estrogen Receptor
EV71	Enterovirus 71
FDA	U.S. Food and Drug Administration
Fmoc	Fluorenylmethoxycarbonyl Chloride

(*continued on next column*)

(*continued*)

List of abbreviations	
FXR	Farnesoid X Receptor
GABA	γ-Aminobutyric Acid
Gln	Glycine
H	Hemagglutinin glycoprotein
hASBT	Human Sodium-dependent Apical Bile Acid Transporter
HCC	Hepatocellular Carcinoma
HeLa	Human Epithelial Adenocarcinoma cell line
HIV	Human Immunodeficiency Virus
HNE	Hemagglutinin Loop Epitope
HO-1	Heme Oxygenase-1
HOBt	Hydroxybenzotriazole
IAV	Influenza A Virus
IC_{50}	Half-maximal Inhibitory Concentration
Ile	Isoleucine
K_i	Inhibitory Constant
Leu	Leucine
LMWH	Low Molecular Weight Heparin
LPS	Liposaccharide
Lys	Lysine
MCF-7	Michigan Cancer Foundation-7
MDR-TB	Multidrug-Resistant Tuberculosis
MIC	Minimum Inhibitory Concentration
MR	Mineralocorticoid Receptor
MTT	3-(4,5-dimethylthiazol-2-yl)-2,5-diphenyl-2H-tetrazolium bromide
MV	Measles Virus
NAFLD	Non-Alcoholic Fatty Liver Disease

(*continued on next page*)

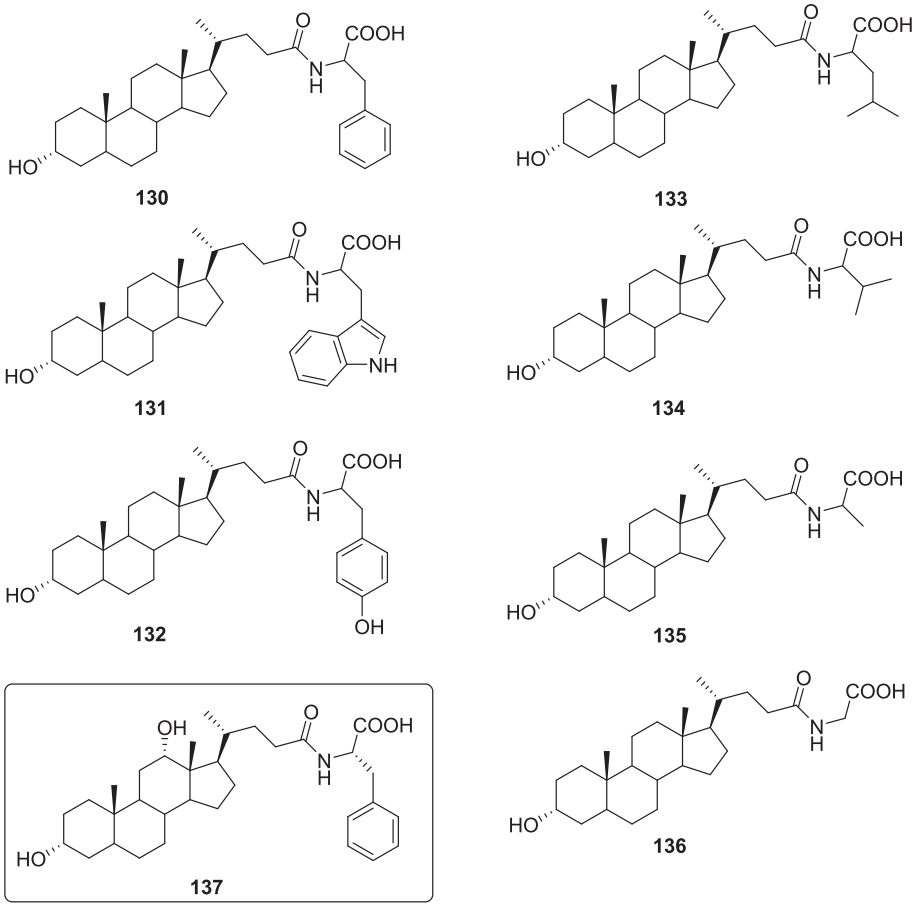

Fig. 39. Derivatives of α-amino acids with lithocholic acid (**130–136**) and deoxycholic acid (**137**).

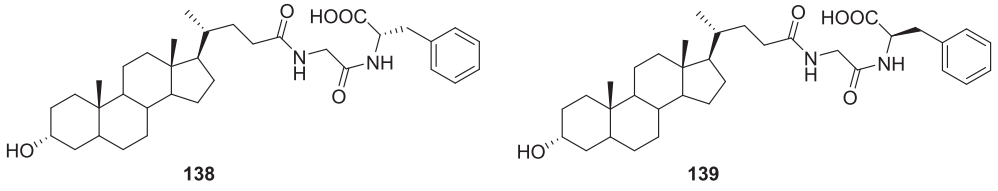

Fig. 40. Bile acid derivatives with phenylalanine and glycine (**135–136**) were used to synthesise gold and silver nanoparticles.

(*continued*)

List of abbreviations	
NASH	Non-Alcoholic Steatohepatitis
OSW-1	Orsaponin
PARP	Poly(ADP-Ribose) Polymerase
PC-3	Prostate Cancer cell line
pDNA	plasmid Deoxyribonucleic Acid
PEGylated	Polyethylene Glycol
P-gp	Permeability Glycoprotein
RD	Rhabdomyosarcoma line cells
RNA	Ribonucleic Acid
TB	Tuberculosis
TGR5	bile acid receptor G
TrKB	Tyrosine Kinase B
UFH	Unfractionated Heparin
WHO	World Health Organization
X-ray	X radiation
XRD	X-ray Diffraction
ZOI	Zone of Inhibition

CRediT authorship contribution statement

Anna Kawka: Writing – review & editing, Writing – original draft, Visualization, Validation, Resources, Project administration, Methodology, Investigation, Formal analysis, Data curation, Conceptualization. **Hanna Koenig:** Writing – review & editing, Validation, Supervision, Project administration, Formal analysis. **Tomasz Pospieszny:** Writing – review & editing, Visualization, Validation, Supervision, Project administration, Methodology, Formal analysis, Conceptualization.

Declaration of competing interest

The authors declare that they have no known competing financial interests or personal relationships that could have appeared to influence the work reported in this paper.

Data availability

No data was used for the research described in the article.

References

[1] H.G. Floss, Natural products derived from unusual variants of the shikimate pathway, Nat. Prod. Rep. 14 (1997) 433.
[2] S. Simić, E. Zukić, L. Schmermund, K. Faber, C.K. Winkler, W. Kroutil, Shortening synthetic routes to small molecule active pharmaceutical ingredients employing biocatalytic methods, Chem. Rev. 122 (2022) 1052–1126.
[3] Z.-R. Lu, J.-G. Shiah, S. Sakuma, P. Kopečková, J. Kopeček, Design of novel bioconjugates for targeted drug delivery, J. Control. Release 78 (2002) 165–173.
[4] T. Matsuda, Device-directed therapeutic drug delivery systems, J. Control. Release 78 (2002) 125–131.
[5] A. Vaidya, A. Agarwal, A. Jain, R.K. Agrawal, S.K. Jain, Bioconjugation of polymers: A novel platform for targeted drug delivery, Cur. Pharm. Des. 17 (2011) 1108–1125.
[6] A. Ulu, B. Ates, Immobilization of l -Asparaginase on carrier materials: a comprehensive review, Bioconjugate Chem. 28 (2017) 1598–1610.
[7] D.W. De Melo, R. Fernandez-Lafuente, R.C. Rodrigues, Enhancing biotechnological applications of l-asparaginase: Immobilization on amino-epoxy-agarose for improved catalytic efficiency and stability, Biocatal. Agric. Biotechnol. 52 (2023) 102821.
[8] F. Li, R.I. Mahato, Bioconjugate therapeutics: Current progress and future perspective, Mol. Pharmaceutics 14 (2017) 1321–1324.
[9] Y. Singh, N. Spinelli, E. Defrancq, P. Dumy, A novel heterobifunctional linker for facile access to bioconjugates, Org. Biomol. Chem. 4 (2006) 1413.
[10] G.T. Hermanson, Introduction to bioconjugation, in: Bioconjugate techniques, Elsevier, 2013: pp. 1–125.
[11] D.B. Salunke, B.G. Hazra, V.S. Pore, Steroidal conjugates and their pharmacological applications, Curr. Med. Chem. 13 (2006) 813–847.
[12] P. Singla, D.B. Salunke, Recent advances in steroid amino acid conjugates: Old scaffolds with new dimensions, Eur. J. Med. Chem. 187 (2020) 111909.
[13] Z. Du, G. Li, H. Ge, X. Zhou, J. Zhang, Design, synthesis and biological evaluation of steroidal glycoconjugates as potential antiproliferative agents, Chem. Med. Chem. 16 (2021) 1488–1498.
[14] A.R. Gomes, A.S. Pires, F.M.F. Roleira, E.J. Tavares-da-Silva, The structural diversity and biological activity of steroid oximes, Molecules 28 (2023) 1690.
[15] F.F. Davis, T.V. Es, N.C. Palczuk, Non-immunogenic polypeptides, US4179337A (1979).
[16] A.I. Graul, The year's new drugs, Drug News Perspect. 14 (2001) 12–31.
[17] L.D. Williams, M.S. Hershfield, S.J. Kelly, M.G.P. Saifer, M.R. Sherman, PEG-urate oxidase conjugates and use thereof, US7723089B2, 2010.
[18] K. Traynor, Recap of FDA product approvals – 2002, Am. J. Health Syst. Pharm. 60 (2003) 310.
[19] C.D. Godwin, R.P. Gale, R.B. Walter, Gemtuzumab ozogamicin in acute myeloid leukemia, Leukemia 31 (2017) 1855–1868.
[20] A. Younes, U. Yasothan, P. Kirkpatrick, Brentuximab vedotin, Nat. Rev. Drug Discov. 11 (2012) 19–20.
[21] Ado-Trastuzumab Emtansine (Kadcyla®) National Drug Monograph December 2014, (2014).
[22] M.M. Cruz Silva, J. António Ribeiro Salvador, Introductory Chapter: Chemistry and biological activity of steroids - scope and overview, in: J. António Ribeiro Salvador, M. Manuel Cruz Silva (Eds.), Chemistry and Biological Activity of Steroids, IntechOpen, 2020.
[23] M.C. di Gregorio, J. Cautela, L. Galantini, Physiology and physical chemistry of bile acids, Int. J. Mol. Sci. 22 (2021) 1780.
[24] C. Bai, A. Schmidt, L.P. Freedman, Steroid hormone receptors and drug discovery: Therapeutic opportunities and assay designs, ASSAY Drug Dev. Tech. 1 (2003) 843–852.
[25] S. Kandi, V. Godishala, P. Rao, K.V. Ramana, Biomedical significance of terpenes: an insight, Biomed, Biotechnol. 3 (2015) 8–10.
[26] T. Pospieszny, Chapter 6 - Steroidal Conjugates: Synthesis, Spectroscopic, and Biological Studies, in: Atta-ur-Rahman (Ed.), Studies in Nat. Prod. Chem. Elsevier, 2015: pp. 169–200.
[27] A. Bendi, C. Vashisth, S. Yadav, R. Pundeer, N. Raghav, Recent advances in the synthesis of cholesterol-based triazoles and their biological applications, Steroids 211 (2024) 109499.
[28] J.R. Hanson, Steroids: partial synthesis in medicinal chemistry, Nat. Prod. Rep. 27 (2010) 887–899.
[29] P. Borah, P. Chowdhury, Steroid hybrid systems: New molecular entities with potential therapeutical spectrum, CDTH 12 (2017) 3–22.
[30] L. Reguera, C.I. Attorresi, J.A. Ramírez, D.G. Rivera, Steroid diversification by multicomponent reactions, Beilstein J. Org. Chem. 15 (2019) 1236–1256.
[31] D. Bastien, R. Hanna, V. Leblanc, É. Asselin, G. Bérubé, Synthesis and preliminary *in vitro* biological evaluation of 7α-testosterone–chlorambucil hybrid designed for the treatment of prostate cancer, Eur. J. Med. Chem. 64 (2013) 442.
[32] S. Mistry, M. Thakkar, A.K. Singh, D. Patel, Synthesis, *in vitro* cytotoxic activity and molecular docking study of androstene and estrone derivatives, Steroids 197 (2023) 109259.
[33] A. Gupta, B. Sathish Kumar, A.S. Negi, Current status on development of steroids as anticancer agents, J. Steroid Biochem. Mol. Biol. 137 (2013) 242–270.
[34] M. Garrido, A. González-Arenas, I. Camacho-Arroyo, M. Cabeza, B. Alcaraz, E. Bratoeff, Effect of new hybrids based on 5,16-pregnadiene scaffold linked to an anti-inflammatory drug on the growth of a human astrocytoma cell line (U373), Eur. J. Med. Chem. 93 (2015) 135–141.
[35] C. Lin, Y. Wang, M. Le, K.-F. Chen, Y.-G. Jia, Recent progress in bile acid-based antimicrobials, Bioconjugate Chem. 32 (2021) 395–410.
[36] J. Kim, O.-C. Jeon, H.T. Moon, S.R. Hwang, Y. Byun, Preclinical safety evaluation of low molecular weight heparin-deoxycholate conjugates as an oral anticoagulant: Preclinical safety evaluation of oral heparin-deoxycholate conjugates, J. Appl. Toxicol. 36 (2016) 76–93.
[37] V. Dobričić, B. Marković, N. Milenković, V. Savić, V. Jaćević, N. Rančić, S. Vladimirov, O. Čudina, Design, Synthesis, and local anti-inflammatory activity of 17β-carboxamide derivatives of glucocorticoids, Archiv. Der, Pharmazie. 347 (2014) 786–797.
[38] M.L. Mascotti, M.A. Palazzolo, F.R. Bisogno, M. Kurina-Sanz, Biotransformation of dehydro-*epi*-androsterone by *Aspergillus parasiticus*: Metabolic evidences of BVMO activity, Steroids 109 (2016) 44–49.
[39] S. Ke, N. Li, T. Ke, L. Shi, Z. Zhang, W. Fang, Y.-N. Zhang, K. Wang, R. Zhou, Z. Wan, Z. Yang, G. Zhang, Y. Wei, Synthesis and evaluation of steroidal thiazoline conjugates as potential antiviral agents, Future, Med. Chem. 10 (2018) 2589–2605.
[40] Y. Sun, P. Gao, L. Zhu, Z. Li, R. Zhao, C. Li, L. Shan, Synthesis and biological evaluation of 17-cyanopyridine derivatives of pregnenolone as potential anti-prostate cancer agents, Steroids 171 (2021) 108841.
[41] O. Jurček, Z. Wimmer, H. Svobodová, B. Bennettová, E. Kolehmainen, P. Drašar, Preparation and preliminary biological screening of cholic acid–juvenoid conjugates, Steroids 74 (2009) 779–785.
[42] M.S. Bjelaković, T.J. Kop, M. Vlajić, J. Đorđević, D.R. Milić, Design, synthesis, and characterization of fullerene–peptide–steroid covalent hybrids, Tetrahedron 70 (2014) 8564–8570.
[43] A. Hryniewicka, M. Malinowska, T. Hauschild, K. Pieczul, J.W. Morzycki, Synthesis and antimicrobial properties of steroid-based imidazolium salts, J. Steroid Biochem. Mol. Biol. 189 (2019) 65–72.
[44] S. Mostarda, D. Passeri, A. Carotti, B. Cerra, C. Colliva, T. Benicchi, A. Macchiarulo, R. Pellicciari, A. Gioiello, Synthesis, physicochemical properties, and biological activity of bile acids 3-glucuronides: novel insights into bile acid signaling and detoxification, Eur. J. Med. Chem. 144 (2018) 349–358.
[45] D.B. Salunke, D.S. Ravi, V.S. Pore, D. Mitra, B.G. Hazra, Amino functionalized novel cholic acid derivatives induce HIV-1 replication and syncytia formation in T. cells, J. Med. Chem. 49 (2006) 2652–2655.
[46] S. Kumar, J. Thakur, K. Yadav, M. Mitra, S. Pal, A. Ray, S. Gupta, N. Medatwal, R. Gupta, D. Mishra, P. Rani, S. Padhi, P. Sharma, A. Kapil, A. Srivastava, U. D. Priyakumar, U. Dasgupta, L. Thukral, A. Bajaj, Cholic acid-derived amphiphile which combats Gram-positive bacteria-mediated infections *via* disintegration of lipid clusters, ACS Biomater. Sci. Eng. 5 (2019) 4764–4775.
[47] Z.-D. Wang, G.-D. Yao, W. Wang, W.-B. Wang, S.-J. Wang, S.-J. Song, Synthesis and evaluation of 26-amino acid methyl ester substituted sarsasapogenin derivatives as neuroprotective agents for Alzheimer's disease, Steroids 125 (2017) 93–106.
[48] R. Bansal, A. Suryan, A comprehensive review on steroidal bioconjugates as promising leads in drug discovery, ACS Bio. Med. Chem. Au. 2 (2022) 340–369.
[49] D.S. Agarwal, R. Sakhuja, R.M. Beteck, L.J. Legoabe, Steroid-triazole conjugates: A brief overview of synthesis and their application as anticancer agents, Steroids 197 (2023) 109258.
[50] S. Peter, S. Alven, R.B. Maseko, B.A. Aderibigbe, Doxorubicin-based hybrid compounds as potential anticancer agents: A review, Molecules 27 (2022) 4478.
[51] R. Zhang, L. Hao, P. Chen, G. Zhang, N. Liu, Multifunctional small-molecule theranostic agents for tumor-specific imaging and targeted chemotherapy, Bioorg. Chem. 137 (2023) 106576.
[52] A. Boes, J.M. Brunel, A. Derouaux, F. Kerff, A. Bouhss, T. Touze, E. Breukink, M. Terrak, Squalamine and aminosterol mimics inhibit the peptidoglycan glycosyltransferase activity of PBP1b, Antibiotics 9 (2020) 373.
[53] K. Yadav, S. Kumar, D. Mishra, M. Asad, M. Mitra, P.S. Yavvari, S. Gupta, M. Vedantham, P. Ranga, V. Komalla, S. Pal, P. Sharma, A. Kapil, A. Singh, N. Singh, A. Srivastava, L. Thukral, A. Bajaj, Deciphering the role of intramolecular networking in cholic acid–peptide conjugates on the lipopolysaccharide surface in combating Gram-negative bacterial infections, J. Med. Chem. 62 (2019) 1875–1886.
[54] C. Palmieri, A. Januszewski, S. Stanway, R.C. Coombes, Irosustat: a first-generation steroid sulfatase inhibitor in breast cancer, Expert Review of Anticancer Therapy 11 (2) (2011) 179–183.
[55] D. Poirier, Synthesis and biological testing of steroid derivatives as inhibitors, J. Steroid Biochem. Mol. Biol. 137 (2013) 174–175.
[56] A. Howell, S.J. Howell, Tamoxifen evolution, Br. J. Cancer 128 (2023) 421–425.
[57] C.R. Tieszen, A.A. Goyeneche, B.N. Brandhagen, C.T. Ortbahn, C.M. Telleria, Antiprogestin mifepristone inhibits the growth of cancer cells of reproductive and non-reproductive origin regardless of progesterone receptor expression, BMC Cancer 11 (2011) 207.
[58] H. Sadeghi-Aliabadi, J. Brown, Synthesis, Analysis and biological evaluation of novel steroidal estrogenic prodrugs for the treatment of breast cancer, Pharma. Biol 42 (2004) 367–373.
[59] K. Chaikomon, S. Chattong, T. Chaiya, D. Tiwawech, Y. Sritana-anant, A. Sereemaspun, K. Manotham, Doxorubicin-conjugated dexamethasone induced MCF-7 apoptosis without entering the nucleus and able to overcome MDR-1-induced resistance, Drug Des. Devel. Ther. 12 (2018) 2361–2369.
[60] V. Pongrakhananon, Anticancer properties of cardiac glycosides, in: Cancer treatment – Conventional and innovative approaches, IntechOpen, 2013.
[61] Z. Wang, J. Zhou, Y. Ju, H. Zhang, M. Liu, X. Li, Effects of two saponins extracted from the *Polygonatum Zanlanscianense* pamp on the human leukemia (HL-60) Cells, Biol. Pharm. Bull. 24 (2001) 159–162.
[62] J.-M. Jin, Y.-J. Zhang, H.-Z. Li, C.-R. Yang, Cytotoxic steroidal saponins from *Polygonatum zanlanscianense*, J. Nat. Prod. 67 (2004) 1992–1995.

[63] M.-F. Yang, Y.-Y. Li, X.-P. Gao, B.-G. Li, G.-L. Zhang, Steroidal saponins from *Myriopteron extensum* and their cytotoxic activity, Planta Med. 70 (2004) 556–560.

[64] Y. Mimaki, M. Kuroda, A. Kameyama, Y. Sashida, T. Hirano, K. Oka, R. Maekawa, T. Wada, K. Sugita, J.A. Beutler, Cholestane glycosides with potent cytostatic activities on various tumor cells from *Ornithogalum saundersiae* bulbs, Bioorg. Med. Chem. Lett. 7 (1997) 633–636.

[65] S. Deng, B. Yu, Y. Lou, Y. Hui, First total synthesis of an exceptionally potent antitumor saponin, OSW-1, J. Org. Chem. 64 (1999) 202–208.

[66] W. Yu, Z. Jin, Total synthesis of the anticancer natural product OSW-1, J. Am. Chem. Soc. 124 (2002) 6576–6583.

[67] Y. Matsuya, S. Masuda, N. Ohsawa, S. Adam, T. Tschamber, J. Eustache, K. Kamoshita, Y. Sukenaga, H. Nemoto, Synthesis and antitumor activity of the estrane analogue of OSW-1, Eur. J. Org. Chem. 2005 (2005) 803–808.

[68] J. Maj, J.W. Morzycki, L. Rárová, J. Oklešťková, M. Strnad, A. Wojtkielewicz, Synthesis and biological activity of 22-deoxo-23-oxa analogues of saponin OSW-1, J. Med. Chem. 54 (2011) 3298–3305.

[69] Z. Yang, E. Lai-Ming Wong, T. Yuen-Ting Shum, C.-M. Che, Y. Hui, Fluorophore-appended steroidal saponin (dioscin and polyphyllin D) derivatives, Org. Lett. 7 (2005) 669–672.

[70] B. Bodnár, E. Mernyák, J. Szabó, J. Wölfling, G. Schneider, I. Zupkó, Z. Kupihár, L. Kovács, Synthesis and *in vitro* investigation of potential antiproliferative monosaccharide–d-secoestrone bioconjugates, Bioorg. Med. Chem. Lett. 27 (2017) 1938–1942.

[71] C. Liu, J.S. Strobl, S. Bane, J.K. Schilling, M. McCracken, S.K. Chatterjee, R. Rahim-Bata, D.G.I. Kingston, Design, Synthesis, and bioactivities of steroid-linked taxol analogues as potential targeted drugs for prostate and breast cancer, J. Nat. Prod. 67 (2004) 152–159.

[72] N. Apiratikul, T. Penglong, K. Suksen, S. Svasti, A. Chairoungdua, B. Yingyongnarongkul, *In vitro* delivery of curcumin with cholesterol-based cationic liposomes, Bioorg. Chem. 39 (2013) 497–503.

[73] M. Kvasnica, M. Budesinsky, J. Swaczynova, V. Pouzar, L. Kohout, Platinum(II) complexes with steroidal esters of l-methionine and l-histidine: Synthesis, characterization and cytotoxic activity, Bioor, Med. Chem. 16 (2008) 3704–3713.

[74] H. Wang, Z. Feng, D. Wu, K.J. Fritzsching, M. Rigney, J. Zhou, Y. Jiang, K. Schmidt-Rohr, B. Xu, Enzyme-regulated supramolecular assemblies of cholesterol conjugates against drug-resistant ovarian cancer cells, J. Am. Chem. Soc. 138 (2016) 10758–10761.

[75] J. Ni, M. Guo, Y. Cao, L. Lei, K. Liu, B. Wang, F. Lu, R. Zhai, X. Gao, C. Yan, H. Wang, Y. Bi, Discovery, synthesis of novel fusidic acid derivatives possessed amino-terminal groups at the 3-hydroxyl position with anticancer activity, Eur. J. Med. Chem. 162 (2019) 122–131.

[76] D.S. Agarwal, H.S. Anantaraju, D. Sriram, P. Yogeeswari, S.H. Nanjegowda, P. Mallu, R. Sakhuja, Synthesis, characterization and biological evaluation of bile acid-aromatic/heteroaromatic amides linked via amino acids as anti-cancer agents, Steroids 107 (2016) 87–97.

[77] N. Shahzad, W. Khan, S. Md, A. Ali, S.S. Saluja, S. Sharma, F.A. Al-Allaf, Z. Abduljaleel, I.A.A. Ibrahim, A.F. Abdel-Wahab, M.A. Afify, S.S. Al-Ghamdi, Phytosterols as a natural anticancer agent: Current status and future perspective, Biomed. Pharm. 88 (2017) 786–794.

[78] G. Lesma, A. Luraghi, T. Bavaro, R. Bortolozzi, G. Rainoldi, G. Roda, G. Viola, D. Ubiali, A. Silvani, Phytosterol and γ-oryzanol conjugates: Synthesis and evaluation of their antioxidant, antiproliferative, and anticholesterol activities, J. Nat. Prod. 81 (2018) 2212–2221.

[79] L.K. Mahal, N.W. Charter, K. Angata, M. Fukuda, D.E. Koshland, C.R. Bertozzi, A small-molecule modulator of poly-α2,8-sialicacid expression on cultured neurons and tumor cells, Science 294 (2001) 380–381.

[80] K.-H. Chang, L. Lee, J. Chen, W.-S. Li, Lithocholic acid analogues, new and potent α-2,3-sialyltransferase inhibitors, Chem. Commun. 629 (2006).

[81] B. Bodnár, E. Mernyák, J. Wölfling, G. Schneider, B. Herman, M. Szécsi, I. Sinka, I. Zupkó, Z. Kupihár, L. Kovács, Synthesis and biological evaluation of triazolyl 13α-estrone–nucleoside bioconjugates, Molecules 21 (2016) 1212.

[82] M. Navacchia, E. Marchesi, L. Mari, N. Chinaglia, E. Gallerani, R. Gavioli, M. Capobianco, D. Perrone, Rational Design of nucleoside–bile acid conjugates incorporating a triazole moiety for anticancer evaluation and SAR exploration, Molecules 22 (2017) 1710.

[83] D. Perrone, O. Bortolini, M. Fogagnolo, E. Marchesi, L. Mari, C. Massarenti, M. L. Navacchia, F. Sforza, K. Varani, M.L. Capobianco, Synthesis and *in vitro* cytotoxicity of deoxyadenosine–bile acid conjugates linked with 1,2,3-triazole, New J. Chem. 37 (2013) 3559.

[84] S. Ikonen, H. Macíčková-Cahová, R. Pohl, M. Šanda, M. Hocek, Synthesis of nucleoside and nucleotide conjugates of bile acids, and polymerase construction of bile acid-functionalized DNA, Org. Biomol. Chem. 8 (2010) 1194.

[85] B. Yan, L. Dong, J. Neuzil, Mitochondria: An intriguing target for killing tumour-initiating cells, Mitochondrion 26 (2016) 86–93.

[86] J. Neuzil, L.F. Dong, J. Rohlena, J. Truksa, S.J. Ralph, Classification of mitocans, anti- cancer drugs acting on mitochondria, Mitochondrion 13 (3) (2013) 199–208.

[87] S. Hoenke, I. Serbian, H.P. Deigner, R. Csuk, Mitocanic di- and triterpenoid rhodamine B conjugates, Molecules 25 (22) (2020) 5443.

[88] I. Serbian, S. Hoenke, R. Csuk, Synthesis of some steroidal mitocans of nanomolar cytotoxicity acting by apoptosis, E. J. Med. Chem. 199 (2020) 112425.

[89] K.S. Moore, S. Wehrli, H. Roder, M. Rogers, J.N. Forrest, D. McCrimmon, M. Zasloff, Squalamine: an aminosterol antibiotic from the shark, Proc. Natl. Acad. Sci. u.s.a. 90 (1993) 1354–1358.

[90] J. Brunel, C. Salmi, C. Loncle, N. Vidal, Y. Letourneux, Squalamine: A polyvalent drug of the future? Curr. Cancer Drug Targets 5 (2005) 267–272.

[91] R. Limbocker, R. Staats, S. Chia, F.S. Ruggeri, et al., Squalamine and its derivatives modulate the aggregation of Amyloid-β and α-Synuclein and suppress the toxicity of their oligomers, Front. Neurosci. 15 (2021) 680026.

[92] B. Brycki, H. Koenig, T. Pospieszny, Quaternary alkylammonium conjugates of steroids: Synthesis, molecular structure, and biological studies, Molecules 20 (11) (2015) 20889–20900.

[93] B.G. Hazra, V.S. Pore, S. Dey, S. Datta, M.P. Darokar, D. Saikia, S.P.S. Khanuja, A. P. Thakur, Bile acid amides derived from chiral amino alcohols: novel antimicrobials and antifungals, Bioorg. Med. Chem. Lett. 14 (2004) 773–777.

[94] S. Mishra, S. Patel, Design, Synthesis, and anti-bacterial activity of novel deoxycholic acid- amino alcohol conjugates, Med. Chem. 16 (2020) 385–391.

[95] N.S. Vatmurge, B.G. Hazra, V.S. Pore, F. Shirazi, P.S. Chavan, M.V. Deshpande, synthesis and antimicrobial activity of β-lactam–bile acid conjugates linked via triazole, Bioorg. Med. Chem. Lett. 18 (2008) 2043–2047.

[96] H.-S. Kim, J.R. Jadhav, S.-J. Jung, J.-H. Kwak, Synthesis and antimicrobial activity of imidazole and pyridine appended cholestane-based conjugates, Bioorg. Med. Chem. Lett. 23 (2013) 4315–4318.

[97] P. Singla, M. Kaur, A. Kumari, L. Kumari, S.V. Pawar, R. Singh, D.B. Salunke, Facially amphiphilic cholic acid-lysine conjugates as promising antimicrobials, ACS Omega 5 (2020) 3952–3963.

[98] S.N. Bavikar, D.B. Salunke, B.G. Hazra, V.S. Pore, R.H. Dodd, J. Thierry, F. Shirazi, M.V. Deshpande, S. Kadreppa, S. Chattopadhyay, Synthesis of chimeric tetrapeptide-linked cholic acid derivatives: Impending synergistic agents, Bioorg. Med. Chem. Lett. 18 (2008) 5512–5517.

[99] S. Gupta, J. Thakur, S. Pal, R. Gupta, D. Mishra, S. Kumar, K. Yadav, A. Saini, P. S. Yavvari, M. Vedantham, A. Singh, A. Srivastava, R. Prasad, A. Bajaj, Cholic acid-peptide conjugates as potent antimicrobials against interkingdom polymicrobial biofilms, Antimicrob. Agents. Chemother. 63 (2019) e00520–e00619.

[100] F. Kong, R.J. Andersen, Polymastiamide A, a novel steroid/amino acid conjugate isolated from the Norwegian marine sponge Polymastia boletiformis (Lamarck, J. Org. Chem. 58 (1993) (1815) 6924–6927.

[101] V. Smyrniotopoulos, M. Rae, S. Soldatou, Y. Ding, C. Wolff, G. McCormack, C. Coleman, D. Ferreira, D. Tasdemir, Sulfated steroid–amino acid conjugates from the Irish marine Sponge Polymastia boletiformis, Marine Drugs 13 (2015) 1632–1646.

[102] M.S. Tendolkar, R. Tyagi, A. Handa, Review of advances in diagnosis and treatment of pulmonary tuberculosis, Indian J. Tuberc. 68 (2021) 510–515.

[103] V.S. Pore, J.M. Divse, C.R. Charolkar, L.U. Nawale, V.M. Khedkar, D. Sarkar, Design and synthesis of 11α-substituted bile acid derivatives as potential anti-tuberculosis agents, Bioorg. Med. Chem. Lett. 25 (2015) 4185–4190.

[104] HIV data and statistics, (n.d.). https://www.who.int/teams/global-hiv-hepatitis-and-stis-programmes/hiv/strategic-information/hiv-data-and-statistics (accessed May 13, 2024).

[105] R. Takeuchi, K. Ogihara, J. Fujimoto, K. Sato, N. Mase, K. Yoshimura, S. Harada, T. Narumi, Design, synthesis, and bio-evaluation of novel triterpenoid derivatives as anti-HIV-1 compounds, Bioorg. Med. Chem. Lett. 69 (2022) 128768.

[106] J.F. Mayaux, A. Bousseau, R. Pauwels, T. Huet, Y. Hénin, N. Dereu, M. Evers, F. Soler, C. Poujade, E. De Clercq, Triterpene derivatives that block entry of human immunodeficiency virus type 1 into cells, Proc. Natl. Acad. Sci. u.s.a. 91 (1994) 3564–3568.

[107] M. Kågedahl, P.W. Swaan, C.T. Redemann, M. Tang, C.S. Craik, F.C. Szoka, S. Øie, Use of the intestinal bile acid transporter for the uptake of cholic acid conjugates with HIV-1 protease inhibitory activity, Pharm. Res. 14 (1997) 176–180.

[108] Department of Pediatrics, The University of Calgary, Calgary, Alberta, Canada, A. K. Leung, K. Hon, K. Leong, C. Sergi, Measles: a disease often forgotten but not gone, Hong Kong Med. J. (2018).

[109] M.M. Coughlin, A.S. Beck, B. Bankamp, P.A. Rota, Perspective on global measles epidemiology and control and the role of novel vaccination strategies, Viruses 9 (2017) 11.

[110] C.A. Bodé, C.P. Muller, A. Madder, Validation of a solid-phase-bound steroid scaffold for the synthesis of novel cyclic peptidosteroids, J. Pept. Sci. 13 (2007) 702–708.

[111] C.A. Bodé, T. Bechet, E. Prodhomme, K. Gheysen, P. Gregoir, J.C. Martins, C. P. Muller, A. Madder, Towards the conformational mimicry of the measles virus HNE loop: design, synthesis and biological evaluation of a cyclic bile acid–peptide conjugate, Org. Biomol. Chem. 7 (2009) 3391–3399.

[112] Q. Yang, Q. Mao, M. Liu, K. Wang, Z. Wu, W. Fang, Z. Yang, P. Luo, S. Ke, L. Shi, The inhibitory effect of dehydroepiandrosterone and its derivatives against influenza A virus in vitro and in vivo, Arch. Virol. 161 (2016) 3061–3072.

[113] P. De Miranda, M.R. Blum, Pharmacokinetics of acyclovir after intravenous and oral administration, J. Antimicrob. Chemother. 12 (1983) 29–37.

[114] M.A. Jacobson, Valaciclovir (BW256U87): The L-valyl ester of acyclovir, J. Med. Virol. 41 (1993) 150–153.

[115] J. Soul-Lawton, E. Seaber, N. On, R. Wootton, P. Rolan, J. Posner, Absolute bioavailability and metabolic disposition of valaciclovir, the L-valyl ester of acyclovir, following oral administration to humans, Antimicrob. Agents Chemother. 39 (1995) 2759–2764.

[116] K.H. Fife, R.A. Barbarash, T. Rudolph, B. Degregorio, R. Roth, Valaciclovir versus acyclovir in the treatment of first-episode genital herpes infection: Results of an international, multicenter, double-blind, randomized clinical trial, Sex. Transm. Dis. 24 (1997) 481–486.

[117] S. Tolle-Sander, K.A. Lentz, D.Y. Maeda, A. Coop, J.E. Polli, Increased acyclovir oral bioavailability *via* a bile acid conjugate, Mol. Pharmaceutics 1 (2004) 40–48.

[118] S. Vandevyver, L. Dejager, J. Tuckermann, C. Libert, New insights into the anti-inflammatory mechanisms of glucocorticoids: An emerging role for glucocorticoid-receptor-mediated transactivation, Endocrinology 154 (2013) 993–1007.
[119] U. Baschant, N.E. Lane, J. Tuckermann, The multiple facets of glucocorticoid action in rheumatoid arthritis, Nat. Rev. Rheumatol. 8 (2012) 645–655.
[120] I. Szelenyi, G. Hochhaus, S. Heer, S. Kuesters, D. Marx, H. Poppe, J. Engel, Loteprednol etabonate: A soft steroid for the treatment of allergicdiseases of the airways, Drugs of Today 36 (2000) 313.
[121] M.O.F. Khan, H.J. Lee, Synthesis and pharmacology of anti-inflammatory steroidal antedrugs, Chem. Rev. 108 (2008) 5131–5145.
[122] H.M. McLean, H.J. Lee, Synthesis and pharmacological evaluation of conjugates of prednisolone and non-steroidal anti-inflammatory agents, Steroids 54 (1989) 421–439.
[123] R. Liu, J. Yin, W. Li, Synthesis of glucocorticoid-C60 hybrids, Carbon 44 (2006) 387–388.
[124] R. Liu, X. Cai, J. Wang, J. Li, Q. Huang, W. Li, Research on the bioactivities of C_{60}-dexamethasone, J. Nanosci. Nanotechnol. 9 (2009) 3171–3176.
[125] X.M. Anguela, K.A. High, Entering the modern era of gene therapy, Annu. Rev. Med. 70 (2019) 273–288.
[126] G. Kim, C. Piao, J. Oh, M. Lee, Self-assembled polymeric micelles for combined delivery of anti-inflammatory gene and drug to the lungs by inhalation, Nanoscale 10 (2018) 8503–8514.
[127] G. Kim, C. Piao, J. Oh, M. Lee, Combined delivery of curcumin and the heme oxygenase-1 gene using cholesterol-conjugated polyamidoamine for anti-inflammatory therapy in acute lung injury, Phytomedicine 56 (2019) 165–174.
[128] Q. Cui, X. Yang, A. Ebrahimi, J. Li, Fullerene-biomolecule conjugates and their biomedicinal applications, Int. J. Nanomedicine 77 (2013).
[129] J. Yang, L.B. Alemany, J. Driver, J.D. Hartgerink, A.R. Barron, Fullerene-derivatized amino acids: Synthesis, characterization, antioxidant properties, and solid-phase peptide synthesis, Chem. Eur. J. 13 (2007) 2530–2545.
[130] R. Bakry, R.M. Vallant, M. Najam-ul-Haq, M. Rainer, Z. Szabo, C.W. Huck, G. K. Bonn, Medicinal applications of fullerenes, Int. J. Nanomedicine 2 (2007) 639–649.
[131] L. Tanzi, M. Terreni, Y. Zhang, Synthesis and biological application of glyco- and peptide derivatives of fullerene C60, Eur. J. Med. Chem. 230 (2022) 114104.
[132] M.S. Bjelaković, D.M. Godjevac, D.R. Milić, Synthesis and antioxidant properties of fullero-steroidal covalent conjugates, Carbon 45 (2007) 2260–2265.
[133] M. Bjelaković, T. Kop, R. Baošić, M. Zlatović, A. Žekić, V. Maslak, D. Milić, Electrochemical, theoretical, and morphological studies of antioxidant fullerosteroids, Monatsh. Chem. 145 (2014) 1715–1725.
[134] E.A. Yates, T.R. Rudd, Recent innovations in the structural analysis of heparin, Int. J. Cardiol. 212 (2016) S5–S9.
[135] J. Harenberg, Past, present, and future perspectives of heparins in clinical settings and the role of impaired renal function, Int. J. Cardiol. 212 (2016) S10–S13.
[136] J.W. Park, O.C. Jeon, S.K. Kim, T.A. Al-Hilal, H.T. Moon, C.Y. Kim, Y. Byun, Anticoagulant efficacy of solid oral formulations containing a new heparin derivative, Mol. Pharmaceutics 7 (2010) 836–843.
[137] S.K. Kim, J. Huh, S.Y. Kim, Y. Byun, D.Y. Lee, H.T. Moon, Physicochemical conjugation with deoxycholic acid and dimethylsulfoxide for heparin oral delivery, Bioconjugate Chem. 22 (2011) 1451–1458.
[138] R. Paliwal, S.R. Paliwal, G.P. Agrawal, S.P. Vyas, Recent advances in search of oral heparin therapeutics, Med. Res. Rev. 32 (2012) 388–409.
[139] S.K. Kim, K. Kim, S. Lee, K. Park, J.H. Park, I.C. Kwon, K. Choi, C.-Y. Kim, Y. Byun, Evaluation of absorption of heparin-DOCA conjugates on the intestinal wall using a surface plasmon resonance, J. Pharm. Biomed. Anal. 39 (2005) 861–870.
[140] J.S. Eom, K.S. Koh, T.A. Al-Hilal, J.W. Park, O.C. Jeon, H.T. Moon, Y. Byun, Antithrombotic efficacy of an oral low molecular weight heparin conjugated with deoxycholic asset on microsurgical anastomosis in rats, Thrombosis Res. 126 (2010) 220–224.
[141] T.A. Al-Hilal, J. Park, F. Alam, S.W. Chung, J.W. Park, K. Kim, I.C. Kwon, I.-S. Kim, S.Y. Kim, Y. Byun, Oligomeric bile acid-mediated oral delivery of low molecular weight heparin, J. Control. Release 175 (2014) 17–24.
[142] T.A. Al-Hilal, F. Alam, J.W. Park, K. Kim, I.C. Kwon, G.H. Ryu, Y. Byun, Prevention effect of orally active heparin conjugate on cancer-associated thrombosis, J. Control. Release 195 (2014) 155–161.
[143] H. Masuzaki, J. Paterson, H. Shinyama, N.M. Morton, J.J. Mullins, J.R. Seckl, J. S. Flier, A Transgenic Model of Visceral Obesity and the Metabolic Syndrome, Science 294 (2001) 2166–2170.
[144] P.M. Stewart, R. Valentino, A.M. Wallace, D. Burt, C.H.L. Shackleton, C.R. W. Edwards, Mineralocorticoid activity of liquorice: 11-beta-hydroxysteroid dehydrogenase deficiency comes of age, The Lancet 330 (1987) 821–824.
[145] S. Farese, A. Kruse, A. Pasch, B. Dick, B.M. Frey, D.E. Uehlinger, F.J. Frey, Glycyrrhetinic acid food supplementation lowers serum potassium concentration in chronic hemodialysis patients, Kidney Int. 76 (2009) 877–884.
[146] A. Odermatt, D.V. Kratschmar, Tissue-specific modulation of mineralocorticoid receptor function by 11β-hydroxysteroid dehydrogenases: An overview, Mol. Cell. Endocrinol. 350 (2012) 168–186.
[147] G.W. Souness, S.A. Latif, J.L. Laurenzo, D.J. Morris, 11α- and 11ß-hydroxyprogesterone, potent inhibitors of 11ß-hydroxysteroid dehydrogenase (isoforms 1 and 2), confer marked mineralocorticoid activity on corticosterone in the ADX rat, Endocrinology 136 (1995) 1809–1812.
[148] D.J. Morris, S.A. Latif, M.P. Hardy, A.S. Brem, Endogenous inhibitors (GALFs) of 11β-hydroxysteroid dehydrogenase isoforms 1 and 2: Derivatives of adrenally produced corticosterone and cortisol, J. Steroid Biochem. Mol. Biol. 104 (2007) 161–168.
[149] K. Pandya, D. Dietrich, J. Seibert, J.C. Vederas, A. Odermatt, Synthesis of sterically encumbered 11β-aminoprogesterone derivatives and evaluation as 11β-hydroxysteroid dehydrogenase inhibitors and mineralocorticoid receptor antagonists, Bioorg. Med. Chem. 21 (2013) 6274–6281.
[150] J.M. Podskalny, S. Takeda, R.E. Silverman, D. Tran, J. Carpentier, L. Orci, P. Gorden, Insulin receptors and bioresponses in a human liver cell line (Hep G-2), Eur. J. Biochem. 150 (1985) 401–407.
[151] W.T. Cefalu, Concept, Strategies, and feasibility of noninvasive insulin delivery, Diabetes Care 27 (2004) 239–246.
[152] S. Lee, K. Kim, T.S. Kumar, J. Lee, S.K. Kim, D.Y. Lee, Y. Lee, Y. Byun, Synthesis and biological properties of insulin−deoxycholic acid chemical conjugates, Bioconjugate Chem. 16 (2005) 615–620.
[153] V.L. Villemagne, S. Burnham, P. Bourgeat, B. Brown, K.A. Ellis, O. Salvado, C. Szoeke, S.L. Macaulay, R. Martins, P. Maruff, D. Ames, C.C. Rowe, C.L. Masters, Amyloid β deposition, neurodegeneration, and cognitive decline in sporadic Alzheimer's disease: a prospective cohort study, Lancet Neurol. 12 (2013) 357–367.
[154] N.H. Mustafa, M. Sekar, S. Fuloria, M.Y. Begum, S.H. Gan, N.N.I.M. Rani, S. Ravi, K. Chidambaram, V. Subramaniyan, K.V. Sathasivam, S. Jeyabalan, S. Uthirapathy, S. Ponnusankar, P.T. Lum, V. Bhalla, N.K. Fuloria, Chemistry, biosynthesis and pharmacology of sarsasapogenin: A potential natural steroid molecule for new drug design, development and therapy, Molecules 27 (2022) 2032.
[155] Y. Hu, Z. Xia, Q. Sun, A. Orsi, D. Rees, A new approach to the pharmacological regulation of memory: Sarsasapogenin improves memory by elevating the low muscarinic acetylcholine receptor density in brains of memory-deficit rat models, Brain Res. 1060 (2005) 26–39.
[156] H. Pan, P. Van Khang, D. Dong, R. Wang, L. Ma, Synthesis and SAR study of novel sarsasapogenin derivatives as potent neuroprotective agents and NO production inhibitors, Bioorg. Med. Chem. Lett. 27 (2017) 662–665.
[157] M. Barigou, L. Favre, M. Fraga, F. Artru, New trends in non-alcoholic fatty liver diseases (NAFLD), Rev. Med. Suisse 16 (2020) 586–591.
[158] Q. Yu, Z. Jiang, L. Zhang, Bile acid regulation: A novel therapeutic strategy in non-alcoholic fatty liver disease, Pharm. Therap. 190 (2018) 81–90.
[159] I. Voloshin, M. Hahn-Obercyger, S. Anavi, O. Tirosh, L-arginine conjugates of bile acids-a possible treatment for non-alcoholic fatty liver disease, Lipids Health Dis. 13 (2014) 1–11.
[160] V. Noponen, M. Nonappa, A. Lahtinen, H. Valkonen, E. Salo, E. Kolehmainen, Sievänen, Bile acid–amino acid ester conjugates: gelation, structural properties, and thermoreversible solid to solid phase transition, Soft Matter 6 (2010) 3789–3796.
[161] H. Svobodová, Z. Nonappa, E. Wimmer, Kolehmainen, Design, synthesis and stimuli responsive gelation of novel stigmasterol–amino acid conjugates, J. Colloid Interface Sci. 361 (2011) 587–593.
[162] V. Sanjayan Sajisha, U. Maitra, Remarkable isomer-selective gelation of aromatic solvents by a polymorph of a urea-linked bile acid–amino acid conjugate, RSC Advances 4 (2014) 43167–43171.
[163] M. Maity, U. Maitra, Supramolecular gels from conjugates of bile acids and amino acids and their applications, Eur. J. Org. Chem. 2017 (2017) 1713–1720.
[164] M. Maity, V.S. Sajisha, U. Maitra, Hydrogelation of bile acid–peptide conjugates and in situ synthesis of silver and gold nanoparticles in the hydrogel matrix, RSC Advances 5 (2015) 90712–90719.

ACS OMEGA

Open Access

http://pubs.acs.org/journal/acsodf

Article

Exploring Triazole-Connected Steroid-Pyrimidine Hybrids: Synthesis, Spectroscopic Characterization, and Biological Assessment

Anna Kawka,* Damian Nowak, Hanna Koenig, and Tomasz Pospieszny

Cite This: *ACS Omega* 2024, 9, 37995−38014

Read Online

ACCESS | Metrics & More | Article Recommendations | Supporting Information

ABSTRACT: Molecules originating from natural sources are physicochemically and biologically diverse. The conjugation of two active biomolecules has become the foundation for medical and pharmaceutical sciences. An effective synthesis of 11 new steroid-pyrimidine conjugates containing 1,2,3-triazole rings was carried out. The group of 3α−OH bile acids (lithocholic, deoxycholic, cholic) and 3β−OH sterols (cholesterol, cholestanol) were respectively modified to azidoacetates. 2-thiouracil was converted into N(1)S and N(3)S dipropargyl derivatives. Azide−alkyne cycloaddition in the presence of copper(I) of the obtained compounds led to the preparation of 1,2,3-triazole derivatives. Based on a series of spectroscopic (^{1}H NMR, ^{13}C NMR, Fourier-transform infrared (FT-IR)), spectrometric analyses (Electrospray ionization-mass spectrometry (ESI-MS), electron impact-mass spectrometry (EI-MS)), and semiempirical calculations, the structures of all compounds were confirmed. *In silico* biological tests and molecular docking (for domain 1KZN, 2H94, 5V5Z, 1EZF, 2Q85) were performed for selected compounds. The tests performed indicate the theoretical antimicrobial potential of the obtained ligands.

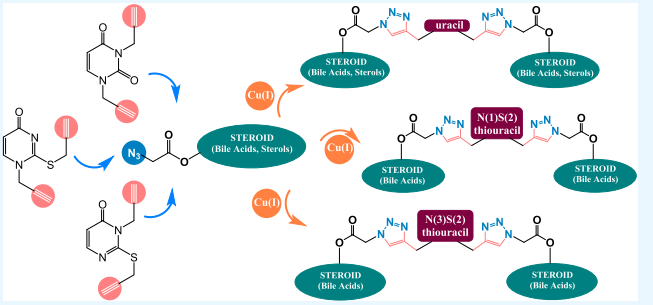

1. INTRODUCTION

Two highly significant classes of natural compounds, pyrimidine bases and steroids, are pivotal in numerous biological processes. Among these, thio derivatives of pyrimidine bases such as 2-thiouracil emerge as noteworthy constituents of t-RNA.[1,2] Beyond their role in biological systems, these compounds have made substantial contributions to the realms of pharmacology, medicine, and medicinal chemistry. Their *S*-, *N*-, or *S*, *N*-disubstituted analogues have displayed notable therapeutic potential, mainly exhibiting antiviral, antithyroid, and antitumor activities.[3−6] They have also been identified as valuable in biosensing applications and radioprotectors.[7,8] Nucleobases have been found to have broad applications as precursors capable of forming strong hydrogen bonds in the design of new biomaterials or complex nanostructures.[9,10]

The prototropic tautomerism exhibited by thio derivatives of pyrimidine bases has garnered significant interest (Scheme 1). The equilibrium between tautomeric forms, particularly in the case of 2-thiouracil, plays a pivotal role in dictating its chemoselectivity and regioselectivity. Moreover, this equilibrium is intricately influenced by factors such as temperature and the physical state of the compound, whether in solution or the solid phase.[11]

Steroids are essential for medicinal chemistry because they involve all metabolic pathways. The rigid skeleton of cyclopentaneperhydrophenanthrene provides steroid conjugates with the proper arrangement of other molecules and several physicochemical properties.[12] Bile acids act as an emulsifier, helping with the digestion and absorption of fats, while sterols such as cholesterol are essential for cell structure and the biosynthesis of steroid hormones.[13,14] Modifications of functional groups such as 3α−OH, 7α−OH, 12α−OH or 3β−OH and amphiphilic properties resulted in their wide use in bioorganic synthesis.[15] Their 1,2,3−triazole derivatives with anticancer properties are particularly important.[16,17] These compounds can inhibit the growth of cancer cells through various mechanisms, such as induction of apoptosis, blocking DNA synthesis, or inhibiting angiogenesis.[18−20] Some studies suggest that bile acid derivatives with 1,2,3-triazole systems may have antiviral activity. They may inhibit viral replication or penetration into host cells.[21,22] Moreover, they have been used as potential drugs in treating cholestasis and research tools for studying the mechanisms of drug action, especially in the context of interactions with cell receptors and signaling pathways.[23−25]

Received: May 21, 2024
Revised: August 16, 2024
Accepted: August 22, 2024
Published: August 29, 2024

Scheme 1. Selected Forms of 2-Thiouracil Tautomerization

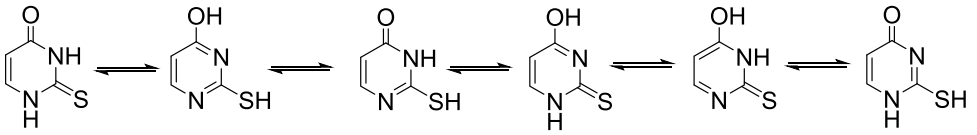

Scheme 2. Synthesis of Uracil (3) and 2-Thiouracil (4−5) Propargyl Derivatives

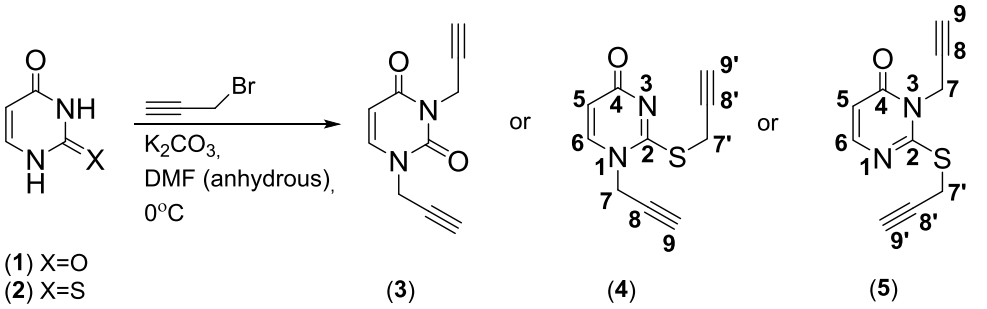

Scheme 3. Synthesis of Substituted Derivatives of Methyl Esters of Bile Acids (9−11) and Sterols (14−15)

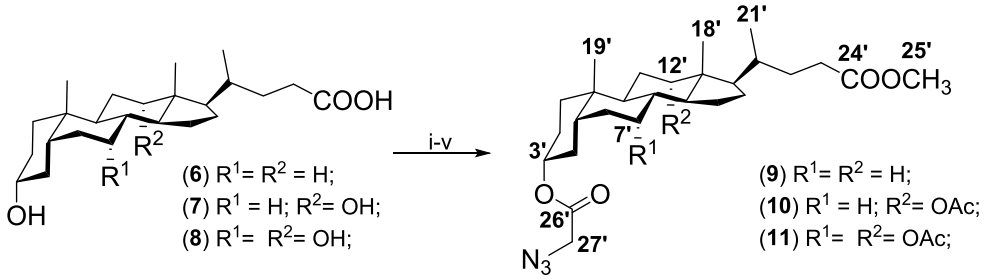

(i) MeOH, *p*-TsOH,(ii) Ac_2O, Py (**2**) & (**3**),(iii) K_2CO_3, MeOH (**2**) & (**3**),(iv) $BrCH_2COBr$, $CH_2Cl_{2(dry)}$,(v) NaN_3, THF, 50°C

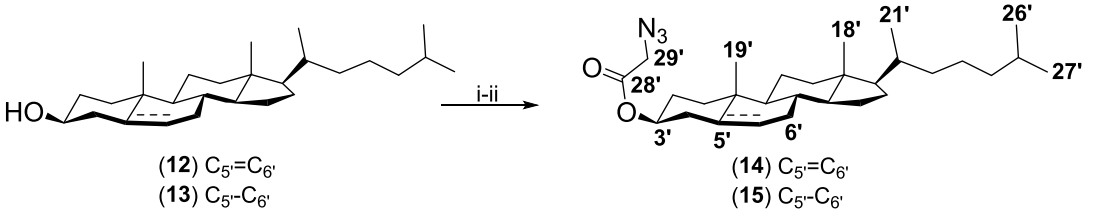

(i) $BrCH_2COBr$, $CH_2Cl_{2(dry)}$,(ii) NaN_3, THF, 50°C

The main route for the synthesis of 1,2,3−triazole derivatives is the "click" chemistry reaction. This technique involves the rapid, efficient, and specific formation of new chemical bonds between two reactants.[26] Typically, 1,3−dipolar reactions are used, such as the reactions of azides with alkynes in the presence of copper(I) ions, which lead to triazole linkers.[27] This method is beneficial in supramolecular chemistry, biochemistry, and nanotechnology, as well as in creating materials with advanced properties. Its advantages are ease and versatility, high reaction efficiency, and minor byproducts.[28,29]

The combination of steroids with pyrimidines can lead to the creation of compounds with unique biological activity.[30] Conjugation of a carrier molecule with a biologically active substance brings many benefits, such as nontoxicity, minimizing side effects, and overcoming drug resistance of the target cell.[31] These compounds may have therapeutic, anticancer, antiviral, anti-inflammatory, or neuroprotective effects.[32−35] Steroid-pyrimidine conjugates may be more stable compared to uncombined components. Bile acid and uracil conjugates are being investigated for their potential anticancer effects. Research suggests that these compounds may have antiproliferative and apoptotic activity against cancer cells, which opens the possibility of their use in anticancer therapy.[36−38] Bile acid and uracil conjugates can be carriers in gene therapy. Thanks to their ability to bind to deoxyribonucleic acid (DNA), they can deliver genetic material to target cells, which opens the possibility of using them to treat genetic and cancer diseases. These are promising compounds with potential therapeutic applications in oncology, hepatology, virology, and gene therapy.[39−42]

2. RESULTS AND DISCUSSION

2.1. Synthesis. The studies describe efficient syntheses of obtaining new steroid-pyridine bioconjugates linked by 1,2,3−triazole rings. Bile acids (lithocholic, deoxycholic, cholic), sterols (cholesterol, cholestanol) with appropriately modified 3α− or 3β−$OCOCH_2N_3$ groups, such as uracil and 2-thiouracil dipropargyl were used as a reactant. According to the literature,

https://doi.org/10.1021/acsomega.4c04800
ACS Omega 2024, 9, 37995−38014

Scheme 4. Synthesis of Steroids−pyrimidine Conjugates (16−26)

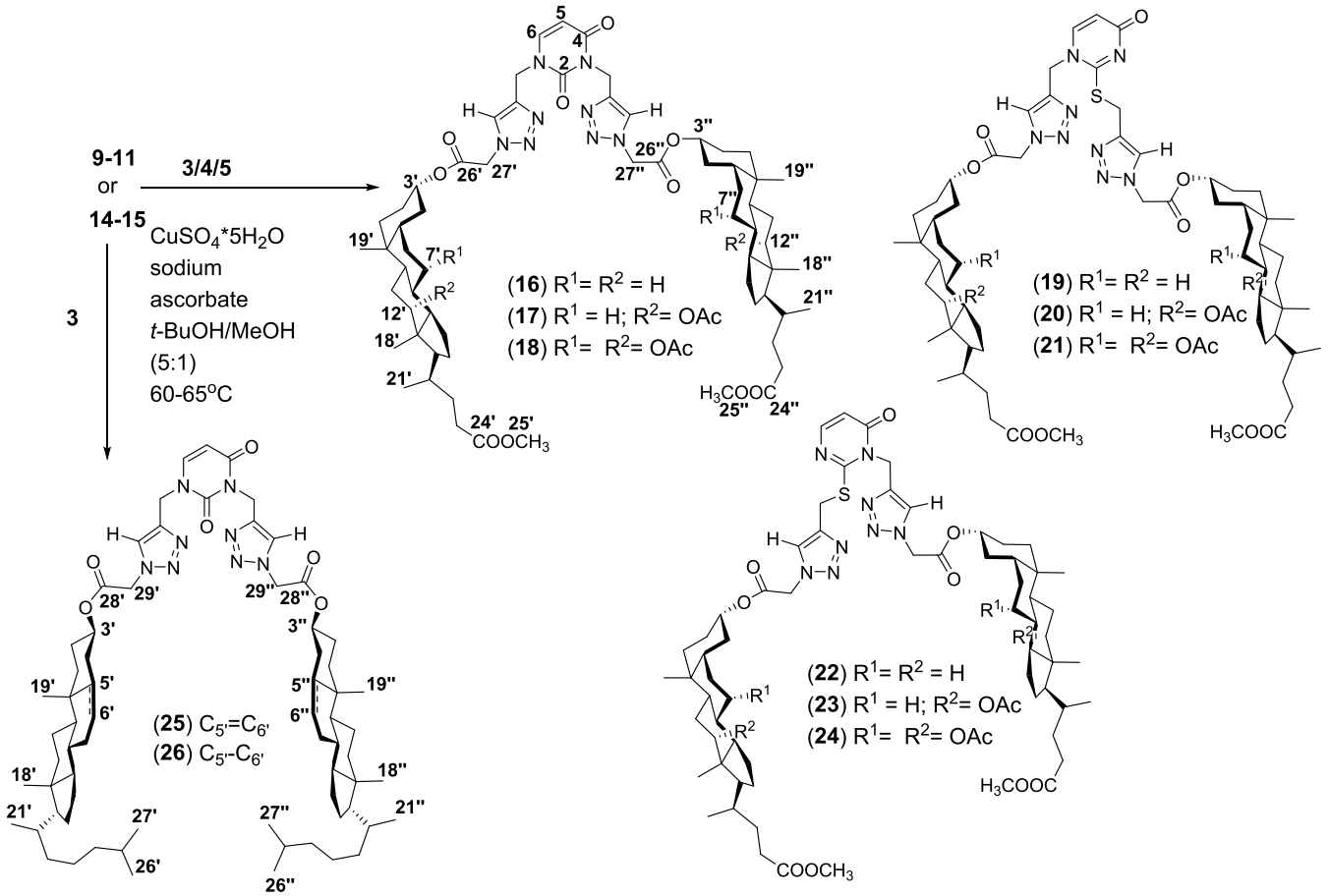

the synthesis of two propargyl derivatives of 2-thiouracil (*N*(1)*S* and *N*(3)*S*), as well as 11 new bile/sterol−pyrimidine conjugates containing 1,2,3-triazole systems, has not been described so far. The created compounds align with the modern trend of synthesis of macrocyclic systems, which are the foundation in the search for new structures with biological activity.

The structures of two propargyl disubstituted derivatives of 2-thiouracil (**4**) and (**5**), as well as all synthesized conjugates (**16**−**26**), were determined based on their ^{1}H and ^{13}C NMR, Fourier-transform infrared (FT-IR), electrospray ionization-mass spectrometry (ESI-MS), and electron impact-mass spectrometry (EI-MS) spectra. Moreover, the PM5 calculation method was performed for all compounds. The syntheses of substrates (**3**−**5**), (**9**−**11**), (**14**−**15**), and conjugates (**16**−**26**) are shown in Schemes 2, 3, and 4, respectively.

2.2. Spectroscopic Characteristics. The structural characterization of all synthesized compounds was accomplished by analyzing their ^{1}H and ^{13}C NMR, FT-IR, ESI-MS, and EI-MS spectra. In addition, PM5 calculations were conducted for each compound further to explore their properties and characteristics.[43−45]

The six substrates: methyl 3*α*-azidoacetoxy-5*β*-cholan-24-oate (**9**), methyl 3*α*-azidoacetoxy-12*α*-acetoxy-5*β*-cholan-24-oate (**10**), methyl 3*α*-azidoacetoxy-7*α*,12*α*-diacetoxy-5*β*-cholan-24-oate (**11**), cholester-3*β*-yl 2-azidoacetate (**14**), 5*α*-cholestan-3*α*-yl azidoethanoate (**15**) and *N*1, *N*3-bis(prop-2-yne-1-yl)uracil (**3**) have been described and characterized in the literature.[46−48]

In the ^{1}H NMR spectrum of dipropargyl derivatives of 2-thiouracil (**4**, **5**), characteristic doublets were observed at 8.30 and 7.77 ppm from CH-6 protons and at 6.50 and 6.26 from CH-5 (Figure 1). Signals from CH_2−N(1) protons appear as double singlets at 5.03 and 4.85 ppm, similar to CH_2−S protons at 4.02 and 3.91 ppm. In the 2.53−2.19 ppm range, characteristic triplets originating from C≡CH protons were observed.

Diagnostic signals from protons from 1,2,3-triazole rings were observed for all conjugates (**16**−**26**) as singlets in the 7.90−7.70 ppm range (Figure 2). Characteristic doublets from protons at CH-6 and CH-5 were observed at 8.26−8.25 and 6.45 ppm (for compounds **22**−**24**), 7.77−7.75 and 6.22−6.20 ppm (for compounds **19**−**21**), 7.46−7.45 and 5.75−5.74 ppm (for compounds **16**−**18**, **25**, **26**). Protons present in the methylene groups N−CH_2−triazole ring and S-CH_2−triazole ring give singlets with values of 5.54−5.52, respectively (N(3)), 5.34−5.33 (N(1)) and 4.56−4.50 ppm. Signals appeared in the ^{1}H NMR spectra of steroid−uracil conjugates (**16**−**18**, **25**−**26**) at 5.25−5.23 and 5.13−5.11 ppm from protons of the CH_2 methylene groups connecting the steroid skeleton with the triazole ring. For compounds (**19**−**24**), similar singlets were observed at 5.15−5.08 ppm. In the ^{1}H NMR spectra of all compounds (**16**−**26**), there are characteristic multiplets in the 4.86−4.61 ppm belonging to 3′*α*-H and 3′*β*-H. Additionally, in the case of conjugates (**17**−**18**), (**20**−**21**), (**23**−**24**), a singlet appears from the 12′*β*-H proton at 5.11−5.09, while for (**18**), (**21**), (**24**) multiplets originating with the 7′*β*-H proton at 4.93−4.91 ppm. A cholesterol derivative (**26**) diagnostic is a broad singlet for C6′-H at 5.38 ppm. The proton spectra of all bile

https://doi.org/10.1021/acsomega.4c04800
ACS Omega 2024, 9, 37995−38014

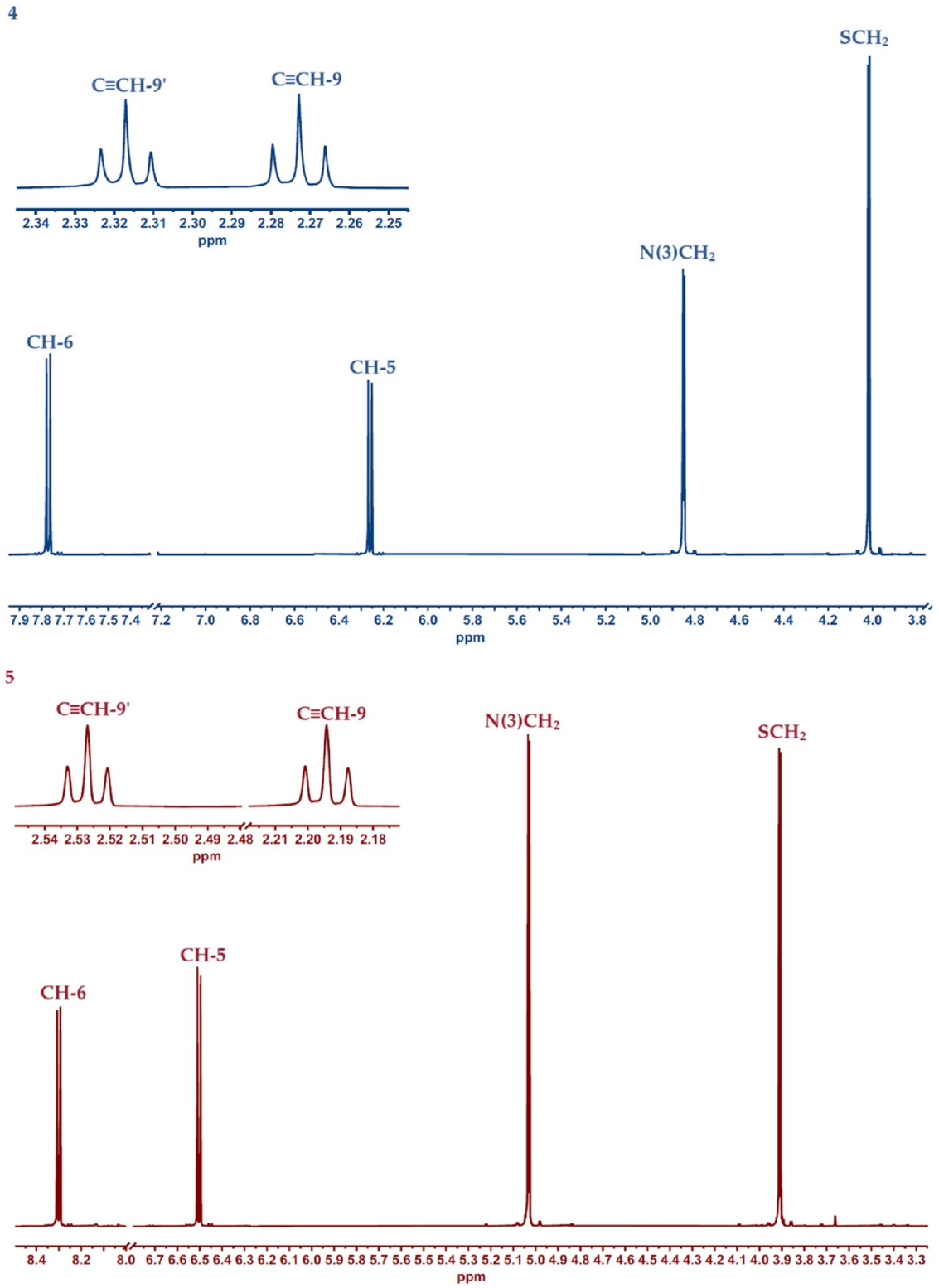

Figure 1. Spectra ^{1}H NMR of new compounds (**4**) and (**5**).

acid−pyrimidine compounds are characterized by a singlet at 3.67−3.65 ppm coming from protons from the ester group CH_3-25′. Moreover, for derivatives of deoxycholic and cholic acids, characteristic singlets from hydrogens present in the 7′α−$OCOCH_3$ and 12′α−$OCOCH_3$ groups can be observed at 2.15 and 2.11−2.09 ppm, respectively. In the ^{1}H NMR spectra of all compounds (**16**−**26**), signals coming at the hydrogens from the methyl groups CH_3-18′, CH_3-19′, and CH_3-21′ were observed at 0.73−0.65, 1.04−0.90, and 0.93−0.91 ppm, respectively. Moreover, for sterol derivatives (**25**−**26**), doublets appear in the range of 0.86−0.85 ppm, characteristic of the CH_3-26′ and CH_3-27′ groups.

The ^{13}C NMR spectra of compounds (**4**) and (**5**) show signals from carbons C(4)═O, C(2)-S, C(6)═(C5), at 169.8−

https://doi.org/10.1021/acsomega.4c04800
ACS Omega 2024, 9, 37995−38014

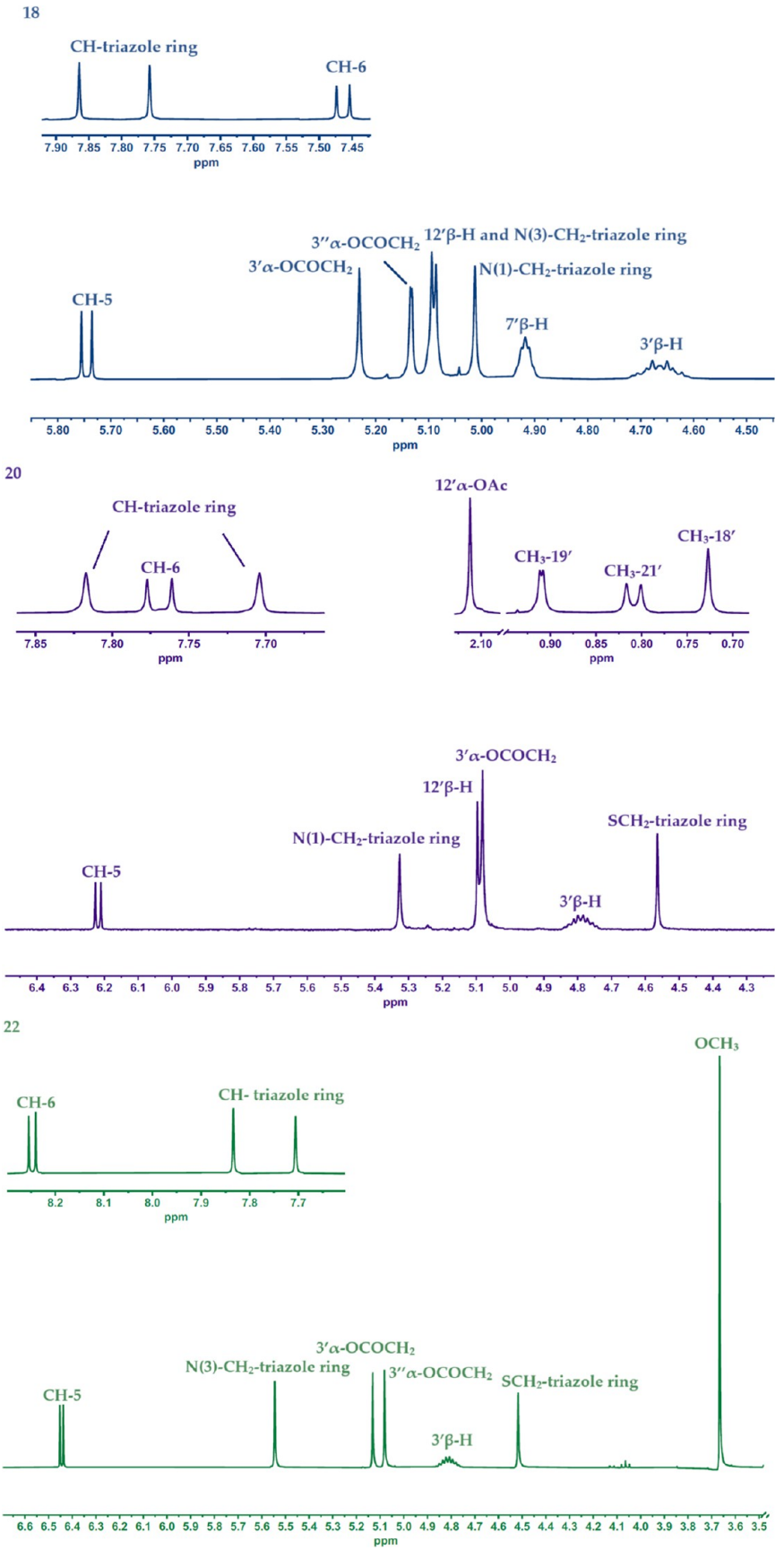

Figure 2. Diagnostic signals in spectra ^{1}H NMR conjugates (**18**, **20**, **22**).

https://doi.org/10.1021/acsomega.4c04800
ACS Omega 2024, 9, 37995−38014

Scheme 5. Fragmentation of Compounds (4) (a) and (5) (b) during EI-MS

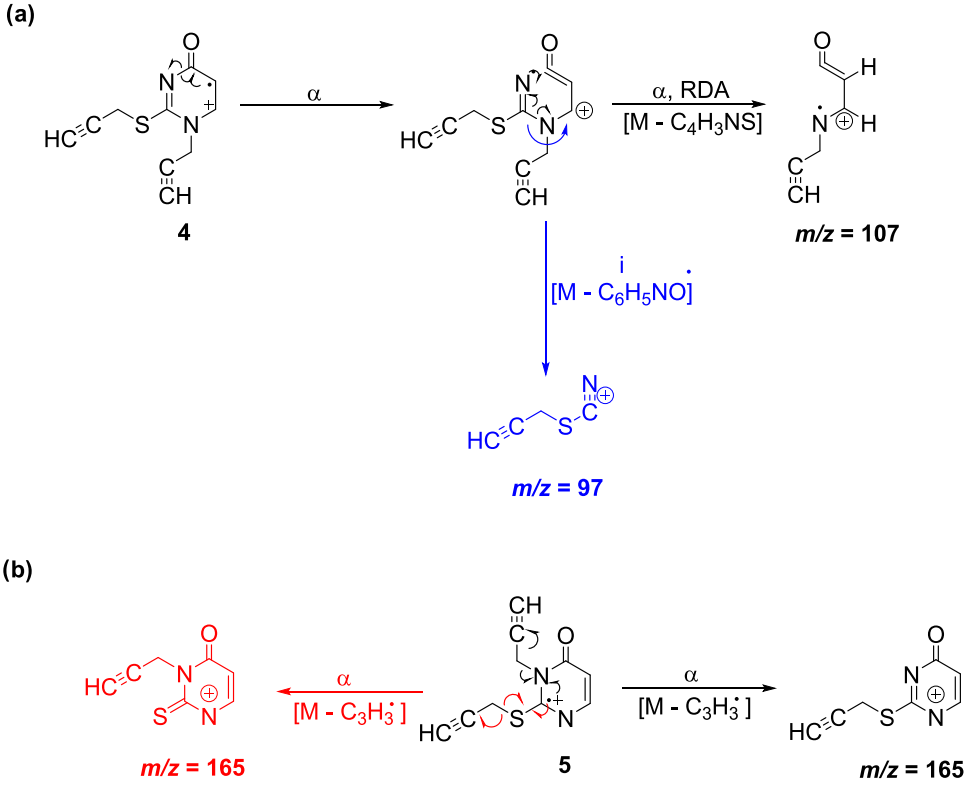

160.7, 167.5−160.7, 157.8−151.9 and 110.8−104.1 ppm, respectively. Signals from C≡C atoms were observed in the 79.7−70.5 ppm range, while signals from carbons from methylene groups CH_2 were observed in the 54.1−19.4 ppm range.

In the ^{13}C NMR spectra of all conjugates (**16**−**26**), signals from carbons from methyl groups C-18′, C-21′, and C-19′ were observed about 12.4−11.8, 18.7−17.5, 23.0−20.8 ppm, and additionally for compounds (**25**, **26**) at 21.2−19.2 ppm from atoms C-26′ and C-27′. However, carbon atoms in the carbonyl group in positions 3′α (or 3′β)-OC═O resonate in the 165.7−165.4 ppm range. The carbon atoms of the 12′α-OC═O steroid skeleton gave signals in the range of 170.5−170.4 ppm. However, the carbon of the 7′α-OC═O gave a signal at 170.5−170.2 ppm. The signals of C(24′)═O, C(4)═O, and C(2)-S appeared in the range of 174.7−174.5, 170.4−162.0, and 168.1−151.1 ppm, respectively. Moreover, unsaturated carbon atoms at the C(5)═C(6) bond can be seen at 111.0−102.0 and 157.6−142.4 ppm. However, the diagnostic carbon atoms from the triazole ring, such as C═CH, give signals at 145.7−138.8 and 125.4−123.3 ppm, respectively. On the other hand, the methylene carbon atom of the steroid skeleton-CH_2−triazole ring was observed at 51.2−51.0 ppm.

2.3. Infrared Spectroscopy. The most characteristic feature of the FT-IR spectra of compound (**4**, **5**) is the band at 3287−3228 cm^{-1} assigned to the ν(≡C−CH) group. The steroid skeleton is a saturated hydrocarbon, so it does not provide many useful IR features. Stretching solid vibrations of C−H bonds are identified at 2972 and 2927 cm^{-1}. Additionally, for synthesis, the new compounds of thiouracil are requisite and analytical bands at 2122 cm^{-1}, which are specific attributes of ν(C≡C) group. Moreover, for all products (**16**−**26**) are also observed two characteristic solid bands at 1748−1661 cm^{-1} and 1248−1211 cm^{-1} are assigned respectively to the symmetric group ν(C═O) and ν(C−O). In addition, characteristic stretching vibrations of C−H bonds are present in 2965−2852 cm^{-1}.

2.4. Electron Impact Mass Spectrometry. In the $N(1)$ S substitution, there are ions with molecular masses of 107 and 97, which are not present in the $N(3)S$ substitution spectrum. The presence of the m/z 165 ion in $N(3)S$ with an intensity of 100% indicates the possibility of its formation in two ways mass fragmentation (Scheme 5).

2.5. Electrospray Ionization. The ESI-MS spectra were acquired using methanol as the solvent. In all instances, the molecular ion $[M]^+$ is detected, indicating the presence of a positively charged ion with a proton, alkali metals, or halides in positive ion mode (ES^+) as well as negative ion mode (ES^-).

Figure 3 displays the ESI-MS spectra of conjugates (**16**), (**19**), and (**20**). In this spectrum, ion peaks are observed at m/z at 1174 (20%) $[C_{64}H_{94}N_8O_{10} + K]^+$ and 1158 (100%) $[C_{64}H_{94}N_8O_{10} + Na]^+$ (compound **16**), 1189 $[C_{64}H_{94}N_8O_9S + K]^+$ (10%) and 1174 (100%) $[C_{64}H_{94}N_8O_9S + Na]^+$ (compound **19**), 1306 $[C_{68}H_{98}N_8O_{13}S + K]^+$ and 1290 (100%) $[C_{68}H_{98}N_8O_{13}S + Na]^+$ (compound **20**).

2.6. PM5 Calculations. The PM5 semiempirical calculations were performed using the WinMopac 2003 program. The final heat of formation (HOF) of compounds (**3**, **4**, **5**) and conjugates (**16**−**26**) is presented in Table 1, and Figure 4 shows their molecular models. Theoretical values of calculations are very often used in comparing crystallographic structures or in determining molecular docking.

The obtained HOF values indicate that the most stable are triazole systems of cholic acid with uracil or thiouracil (**18**, **21**, **24**). This results from blocked hydroxyl groups in the steroid skeleton at the C-7′ and C-12′ atoms. Acetate groups (7′α-OAc and 12′α-OAc) predispose to the formation of intramolecular interactions, such as hydrogen bonds or electrostatic inter-

https://doi.org/10.1021/acsomega.4c04800
ACS Omega 2024, 9, 37995−38014

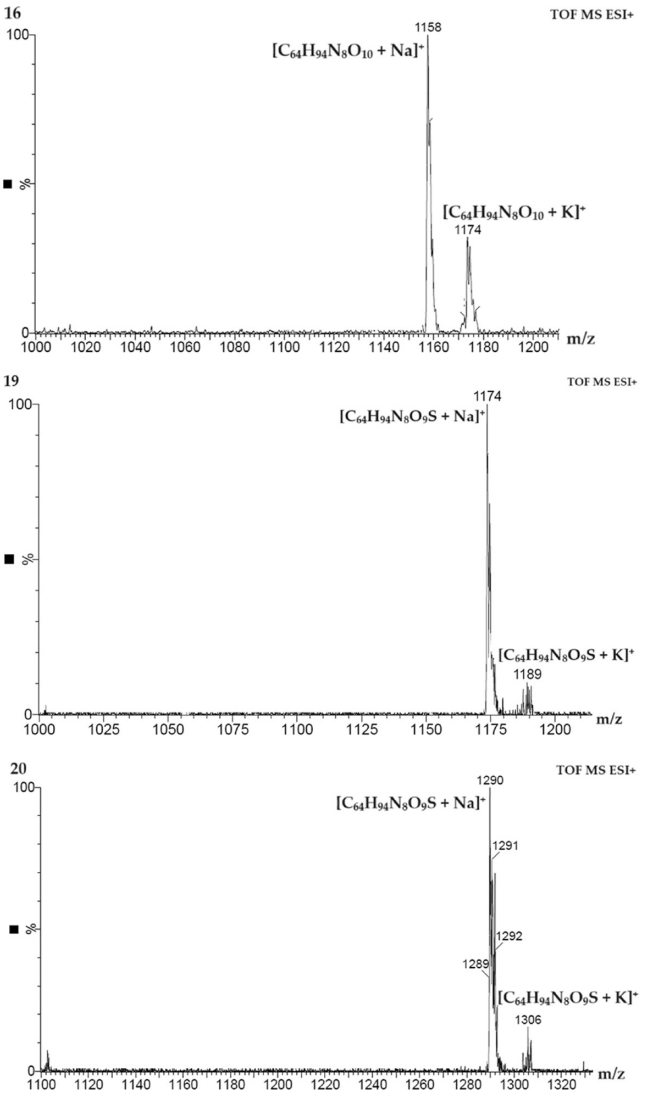

Figure 3. ESI-MS spectra of bioconjugates (**16**), (**19**), and (**20**).

Table 1. Heat of Formation [kcal/mol] of Compounds (3, 4, 5) and (16−26)

compound	heat of formation [kcal/mol]
3	28.9829
4	97.0622
5	90.6298
16	−439.5148
17	−606.8373
18	−784.1348
19	−370.6792
20	−546.0568
21	−712.6079
22	−379.0817
23	−548.2400
24	−712.2926
25	−272.6631
26	−321.9369

actions. Therefore, the obtained compounds can form stable host−guest complexes. The HOF values in each bile acid conjugate increase with decreasing OAc groups. The lowest HOF values are observed for 1,2,3-triazole derivatives of

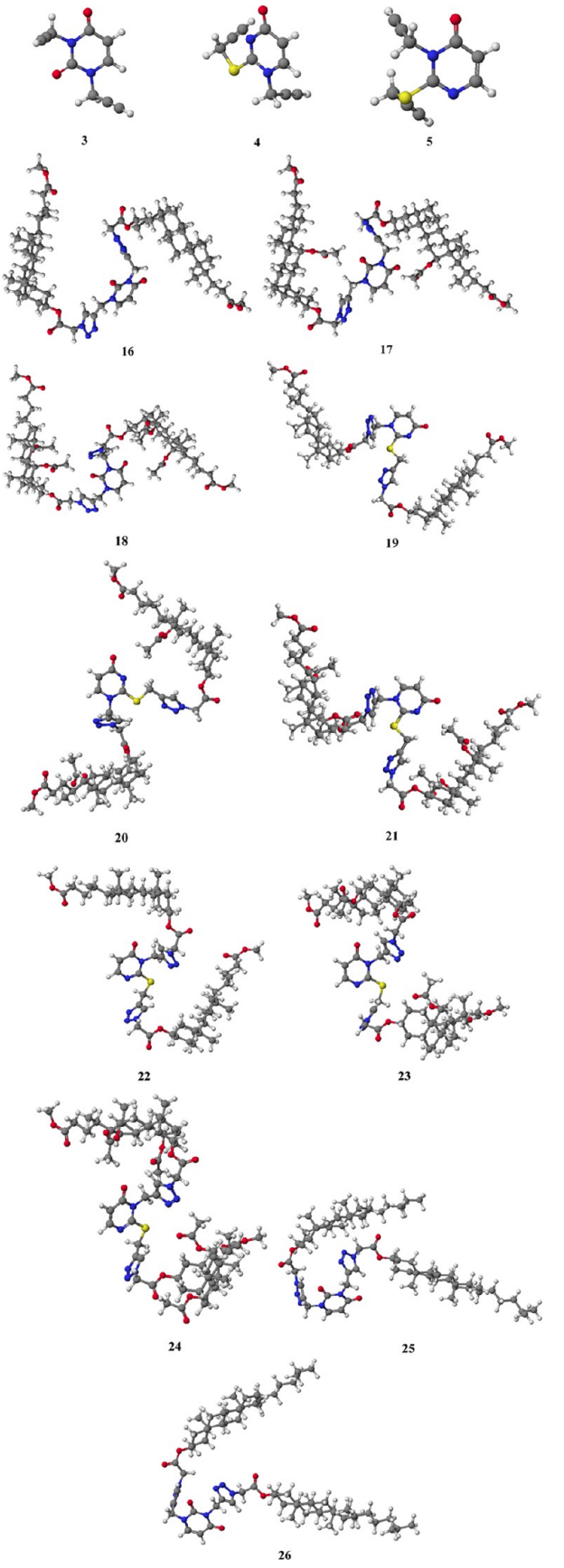

Figure 4. Molecular models of representative compounds (**4**) and (**5**), as well as (**16−26**), were calculated by the PM5 method.

https://doi.org/10.1021/acsomega.4c04800
ACS Omega 2024, 9, 37995−38014

Table 2. "Probability to be Active" (PA) Values for the Predicted biological Activity of (4−5), as well as (16, 19, 22, 25, 26)

	compound						
focal predicted activity (PA > 50%) (4, 5) − substrates; (16, 19, 22, 25, 26) − conjugates	4	5	16	19	22	25	26
electron-transferring-flavoprotein dehydrogenase inhibitor	64	74	−	−	−	−	−
mannotetraose 2-α-*N*-acetylglucosaminyl transferase inhibitor	59	59	−	−	−	−	−
chloride peroxidase inhibitor	56	56	−	−	−	−	−
proteasome ATPase inhibitor	51	79	−	−	−	−	54
muramoyltetrapeptide carboxypeptidase inhibitor	−	74	−	−	−	−	−
chenodeoxycholoyltaurine hydrolase inhibitor	−	62	−	−	−	−	−
formaldehyde transketolase inhibitor	−	58	−	−	−	−	−
ferredoxin-NAD + reductase inhibitor	−	57	−	−	−	−	−
naphthalene 1,2-dioxygenase inhibitor	−	57	−	−	−	−	−
glutathione thiol esterase inhibitor	−	58	−	−	−	−	−
glyceryl-ether monooxygenase inhibitor	−	52	71	69	69	61	73
alkylacetylglycerophosphatase inhibitor	−	−	68	−	52	−	71
antieczematic	−	−	69	59	−	64	67
cytoprotectant	−	−	61	57	60	−	−
biliary tract disorder treatment	−	−	56	−	−	−	61
dermatologic	−	−	57	52	54	59	57
anti-infertility, female	−	−	53	−	−	58	57
prostate disorders treatment	−	−	53	−	−	58	53
Myc inhibitor	−	−	52	50	50	58	54
antipruritic, allergic	−	−	52	−	−	54	54
CYP17 inhibitor	−	−	−	−	−	65	−
DELTA14-sterol reductase inhibitor	−	−	−	−	−	60	−

Table 3. Search Space of Each of the Protein Domains[a]

PDB ID/search parameter	1EZF	1KZN	2H94	2Q85	5V5Z
search size	66,60,64	62, 54, 60	62, 62, 56	60, 50, 50	72, 70, 50
search center	−12.596, 43.347, 32.218	18.320, 30.783, 36.761	25.643, 43.019, 89.938	13.168, 2.780, 2.799	−38.038, − 19.282, 24.569

[a]The values are given in *x*, *y*, and *z* coordinates and the Angstrom unit.

lithocholic acid (**16**, **19**, **22**) and sterols (**25**, **26**). This is due to the lack of additional groups to create stable interactions. Moreover, due to the C5′═C6′ double bond, the cholesterol conjugate (**25**) has a higher HOF value than the cholestanol conjugate (**26**). The positive HOF values for compounds (**3**, **4**, **5**) result from two propargyl groups in each molecule. Alkyne bonds make uracil/thiouracil derivatives the least stable and can be easily modified.

2.7. Prediction of Activity Spectra for Substances. The pharmacological activities of the synthesized compounds were determined using the in silico Prediction of Activity Spectra for Substances (PASS) program, which is based on computer analysis of structure−activity relationships. This program uses a heterogeneous training set containing approximately 250,000 biologically active compounds from various chemical series, covering approximately 4500 different types of biological activity. Because PASS only requires the structural formula of a chemical compound to predict, it can be used in the early stages of research. Many examples of successful applications of PASS have led to the development of new pharmacological agents.[49−52] This program is also helpful in studying the biological activity of secondary metabolites. The present study focused on the activities predicted with the highest probability for a potential compound (focal activities).

Biological activity prediction analysis could only be performed for compounds whose mass does not exceed 1200 g/mol. Therefore, the potential pharmacotherapeutic properties of two new propargyl thiouracil derivatives (**4** and **5**) and conjugates (**16**, **19**, **22**, **25**, **26**) have been described. Table 2 lists the target compounds against which the conjugates show the highest probability of biological activity. According to the research results, the most frequently predicted types of activity for compounds (**4**) and (**5**) are proteasome ATPase inhibitor, electron-transferring-flavoprotein dehydrogenase inhibitor, muramoyltetrapeptide carboxypeptidase inhibitor and chloride peroxidase inhibitor. However, *in silico* tests for the new steroid-pyrimidine conjugates (**16**, **19**, **22**, **25**, **26**) obtained show the highest activity against glyceryl-ether monooxygenase inhibitor, alkylacetylglycerophosphatase inhibitor, antieczematic, cytoprotectant and CYP17 inhibitor. The obtained triazole derivatives show different biological activity than thiouracil substrates. Their predicted effects can be used in the design of hypolipemic, antispot, cholesterol-lowering and even prostate cancer treatments.

2.8. Molecular Docking. The molecular docking process started by converting the SMILES[53] representation of conjugated chemical structures (new ligands) into three-dimensional (3D) structures, and the Gasteiger[54] charges were added to each new ligand. It was accomplished through the application of OpenBabel tool version 3.1.1.[55,56] Subsequently, the protein domains corresponding to the PDB[57] IDs 1EZF[58,59] 1KZN,[60,61] 2H94,[62,63] 2Q85[64,65] and 5V5Z[66,67] were prepared in accordance with the standard AutoDock tool 1.5.7 scheme.[68] Molecular dockings were then carried out using AutoDock Vina,[69] with the specific parameters outlined in Table 3 for each docking search.

The determination of molecular docking centers was based on the ligands in the raw PDB files.[70] UCSF Chimera software,

https://doi.org/10.1021/acsomega.4c04800
ACS Omega 2024, 9, 37995−38014

version 1.1670, was employed to visualize the three-dimensional aspects.

2.9. Selected Protein Domains. Their specific biological functions guided the selection of protein domains within the physiological system:

- antifungal activity (PDB IDs: 1EZF, 5V5Z)
- antibacterial activity (PDB IDs: 1KZN, 2Q85)
- Both antifungal and antibacterial activity (PDB ID: 2H94)

These proteins belong to different enzyme classes:[71]

- transferases (1EZF) - transfer specific functional groups from one molecule to another
- isomerases (1KZN) - facilitate intramolecular rearrangements within a single molecule
- oxidoreductases (2H94, 2Q85, and 5V5Z) - catalyze oxidation−reduction reactions by transferring electrons between molecules

The protein domain 1EZF[58] corresponds to squalene synthase, which catalyzes squalene production, a precursor to ergosterol, an essential component of fungal cell membranes. Inhibiting squalene synthase disrupts ergosterol biosynthesis, making it a classic target for antifungal drugs. Understanding the structure and function of squalene synthase aids in developing antifungal agents to combat fungal infections.[59,72]

The protein domain 1KZN,[60] known as gyrase, is crucial in bacterial DNA replication and transcription by catalyzing negative supercoiling of circular DNA. Targeting DNA gyrase with antibacterial agents can lead to bacterial death. Compounds like quinolones, coumarins, and cyclothialidines have been developed to inhibit gyrase, offering potential avenues for antibacterial drug discovery.[61,73]

The protein domain 2H94[62] shows the shape of a human enzyme called Lysine-Specific Demethylase-1 (LSD1). This enzyme helps control how genes are turned on or off by removing certain chemical marks from proteins called histones. These marks are like little tags on the histone tails. Interestingly, the products of this enzyme can also have antifungal properties. Some bacteria and fungi depend on specific chemical reactions for their survival. By interfering with these reactions, the LSD1 enzyme can slow down the growth of these microbes.[63,74]

The protein domain 2Q85[64] corresponds to *Escherichia coli* MurB, associated with antibacterial activity. MurB is an enzyme involved in the peptidoglycan biosynthesis pathway of bacteria, making it a potential target for antibacterial agents. Inhibiting MurB could disrupt bacterial cell wall formation, leading to bacterial death.[65,75,76]

The protein domain 5V5Z[66] represents the structure of CYP51 from the pathogen *Candida albicans*, known as lanosterol 14α-demethylase (LDM). LDM is the target of azole drugs used to treat fungal infections, but their efficacy is limited by drug resistance and suboptimal cure rates, especially in immunocompromised patients. Understanding the structure of CYP51 aids in developing new antifungal agents to combat drug-resistant fungal pathogens and improve treatment outcomes for fungal infections.[67,76,77]

2.10. Similarities and Differences between Novel and Endogenous Ligands. To visualize the differences between native ligand and new ligands, the molecular some of QED (Quantitative Estimate of Druglikeness)[78] descriptors were calculated with RDKit python library,[80] as shown in Table 4.

Both the native and new ligands exhibit a wide range of molecular weights. The new ligands have more molecular weight than the native ligands. The number of hydrogen bonds acceptors of new ligands is similar to the number of hydrogen bonds acceptors in native ligands. In the case of hydrogen bonds donors, the new ligands do not have any of them. The polar surface area is generally higher than in the case of new ligands. The lipophilicity is much different for the new ligands exposed to higher alogP values.[79] It indicates that new ligands are exhibiting much higher lipophilicity compared to native ligands, which may lead to low solubility and poor absorption.[80] There is also variability in the number of rotatable bonds, meaning that the flexibility of the ligands is different. To conclude, it can be said that the new ligands are not very similar to native ligands. Thus, they can be potent ligands that do good activity.

Table 4. Comparison of Native Ligands and New Ligand Molecular Descriptors

name	molecular weight [g/mol]	HB acceptors	HB donors	polar surface area Å^2	*a* log *P*	rotatable bonds
1EZF	539	7	3	133.24	1.09	9
1KZN	664	11	4	186.35	2.07	9
2H94	763	20	10	363.61	−0.98	13
2Q85	763	20	10	363.31	−0.98	13
5V5Z	667	9	0	104.70	1.73	11
4	204	3	0	34.89	0.60	3
5	204	3	0	34.89	0.60	3
16	1136	14	0	210.62	9.60	18
17	1252	18	0	263.22	8.69	20
18	1368	22	0	315.82	7.78	22
19	1152	15	0	201.51	11.09	19
20	1268	19	0	254.11	10.17	21
21	1384	23	0	306.71	9.25	23
22	1152	15	0	201.51	11.09	19
23	1268	19	0	254.11	10.17	21
24	1384	23	0	306.71	9.25	23
25	1128	10	0	158.02	13.20	20
26	1132	10	0	158.02	13.36	20

2.11. Molecular Docking. The RMSD (Root-Mean-Square Deviation) values of atomic positions are provided in Table 5.

Table 5. Quantitative Assessment of the Structural Differences between the Endogenous Ligands Raw Pose and the Endogenous Ligands Predicted Pose through Molecular Docking

PDB ID	1EZF	1KZN	2H94	2Q85	5V5Z
RMSD (Å)	1.30	0.50	0.54	1.54	1.65

RMSD measures the average distance between the atoms of two superimposed molecules. It is commonly used to quantify the structural similarity between two molecules in space. In the context of molecular docking, RMSD describes how far the predicted pose of a ligand differs from the native pose. Lower RMSD values indicate higher accuracy in pose prediction.

Table 6 presents the results of molecular docking studies conducted via AutoDock Vina software.[69] The five protein domains have been studied. Three of them are related to antibacterial activity (1KZN and 2Q85), one to anticancer (2H94), and the others (1EZF and 5V5Z) are related to antifungal activity.

2.12. 1EZF Protein Domain. Regarding antifungal activity, protein domain 1EZF reveals that the newly discovered ligands have affinities comparable to the native ligand's binding energy.

https://doi.org/10.1021/acsomega.4c04800
ACS Omega 2024, 9, 37995−38014

Table 6. Results− Binding Energies (Affinities) are Given in [kcal/mol] Unit

protein domain ID/ligand name	1EZF	1KZN	2H94	2Q85	5V5Z
native	−11.9	−9.1	−14.6	−10.9	−10.5
4	−5.7	−5.7	−6.2	−5.9	−5.9
5	−6.2	−5.2	−5.6	−5.7	−5.6
16	−11.4	−7.1	−9.5	−11.3	−11.3
17	−11.4	−8.3	−9.9	−12.7	−10.8
18	−11.1	−6.4	−9.6	−9.7	−10.6
19	−10.8	−8.0	−10.7	−11.3	−11.2
20	−10.9	−7.1	−9.9	−10.7	−10.6
21	−10.2	−8.0	−9.3	−11.6	−9.7
22	−11.3	−8.8	−10.2	−11.2	−11.9
23	−10.9	−7.6	−10.2	−9.5	−10.8
24	−10.4	−8.2	−9.3	−10.1	−10.1
25	−11.4	−8.7	−10.3	−11.6	−12.1
26	−11.6	−7.4	−10.0	−10.8	−11.3

Only in a few cases do the binding energies of new ligands deviate by more than 1 kcal/mol. Nevertheless, their affinities fall within the same range as the native ligand. The RMSD for the native ligand, in this case, is 1.30 Å (Table 5).[81] Figure 5 shows how a protein and a molecule called a **26** ligand might bond together. They could form up to 11 hydrogen bonds, like tiny bridges holding them together. However, some of these bonds compete with each other, meaning only about six can form at the same time.

The **26** ligand can form hydrogen bonds with several specific amino acids in the 1EZF protein domain. These hydrogen bonds help hold the ligand and protein together. The shorter the distance between the atoms involved in a hydrogen bond, the stronger the bond. These hydrogen bonds involve the following atoms and distances:

- Ligand's keto-ester oxygen atom (acceptor) to LYS 117 A amine (donor): 2.15 Å
- Ligand's keto-ester oxygen atom (acceptor) to ARG 52 A amine (donor): 2.91 Å
- Ligand's 1,2,3-triazole nitrogen (acceptor) to ARG 77 A amine (donor): 1.97 Å (more likely) or 2.95 Å
- Ligand's other ester oxygen atom (acceptor) to ASN 215 A amine (donor): 2.71 or 2.78 Å
- Ligand's keto-ester oxygen atom (acceptor) to THR 214 A amine (donor): 2.94 Å
- Ligand's other 1,2,3-triazole nitrogen (acceptor) to ARG 218 A amine (donor): 2.15 or 2.43 Å
- Ligand's other 1,2,3-triazole nitrogen (acceptor) to THR 299 A amine (donor): 2.50 or 2.84 Å

2.13. 1KZN Protein Domain. These ligands exhibit similar or lower binding energies than the native ligand for the 1KZN protein domain. Specifically, ligands such as **17**, **22**, **24**, and **25** demonstrate similar affinities (within ±1 kcal/mol) to the native ligand, while others (**4**, **5**, **16**, **18**, **19**, **20**, **21**, **23** and **26**) exhibit lower affinities. The reduced affinities of these ligands can be attributed to their larger sizes compared to the native ligand. Notably, the root-mean-square deviation (RMSD) between the initial pose of the native ligand and its reduced pose is 0.50 Å (Table 5), indicating an accurate recreation of the native ligand's binding configuration.[81] Figure 6 shows how a protein and a molecule called a **25** ligand might bond together. They could form up to six hydrogen bonds, like tiny bridges holding them together. However, some of these bonds compete with each other, meaning only about four can form at the same time.

The **25** ligand can form hydrogen bonds with specific amino acids in the 1KZN protein domain. These hydrogen bonds involve the following atoms and distances:

- Ligand's keto-ester oxygen atom (acceptor) to ASN 46 A amine (donor): 2.83 Å
- Ligand's 1,2,3-triazole nitrogen (acceptor) to ARG 76 A amine (donor): 2.43 and 2.61 Å
- Ligand's ester oxygen atom (acceptor) to ARG 76 A amine (donor): 2.25, 2.26, and 2.45 Å

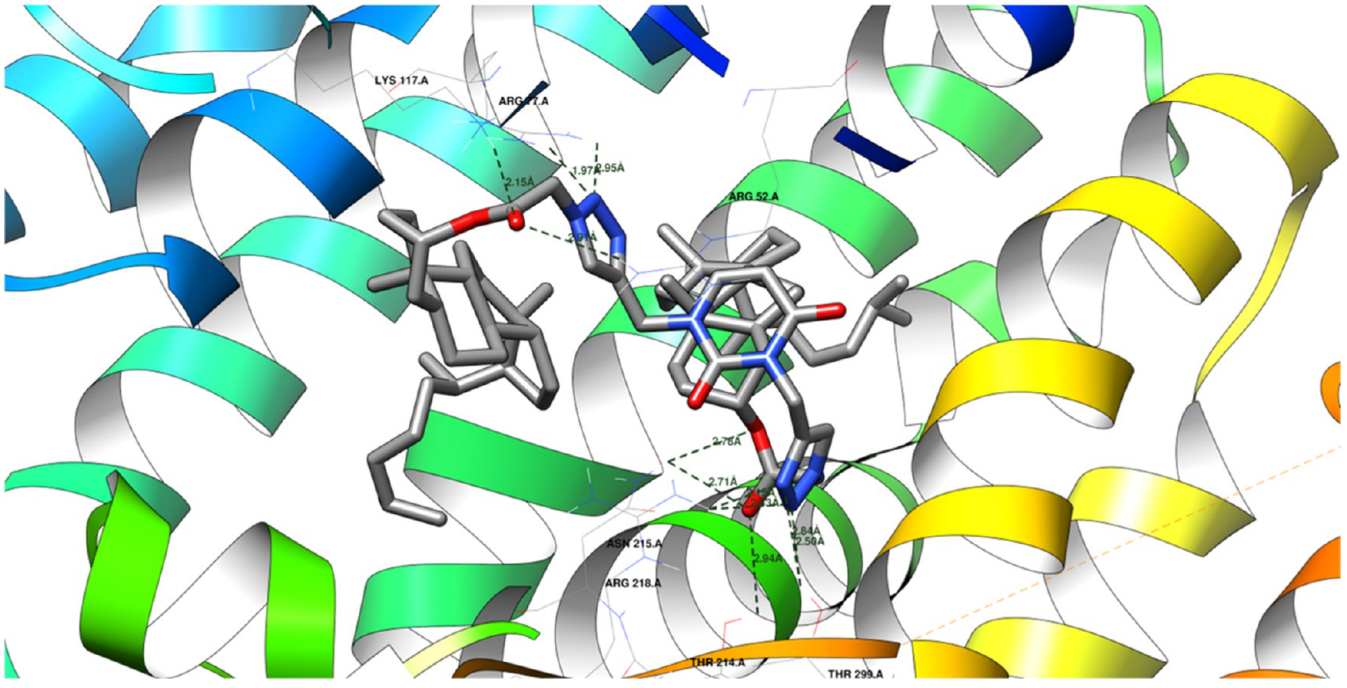

Figure 5. Potential hydrogen bonds between **26** ligand and the 1EZF protein domain.

https://doi.org/10.1021/acsomega.4c04800
ACS Omega 2024, 9, 37995−38014

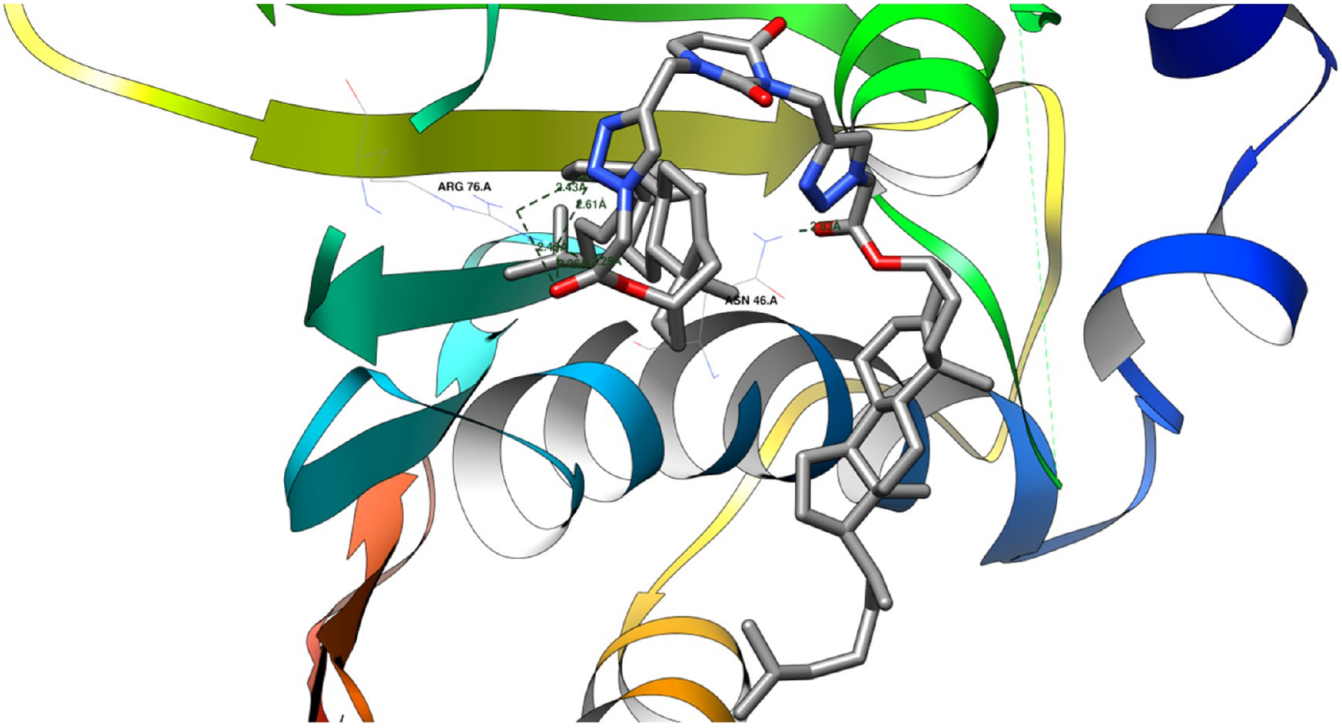

Figure 6. Potential hydrogen bonds between ligand **25** and the 1KZN protein domain.

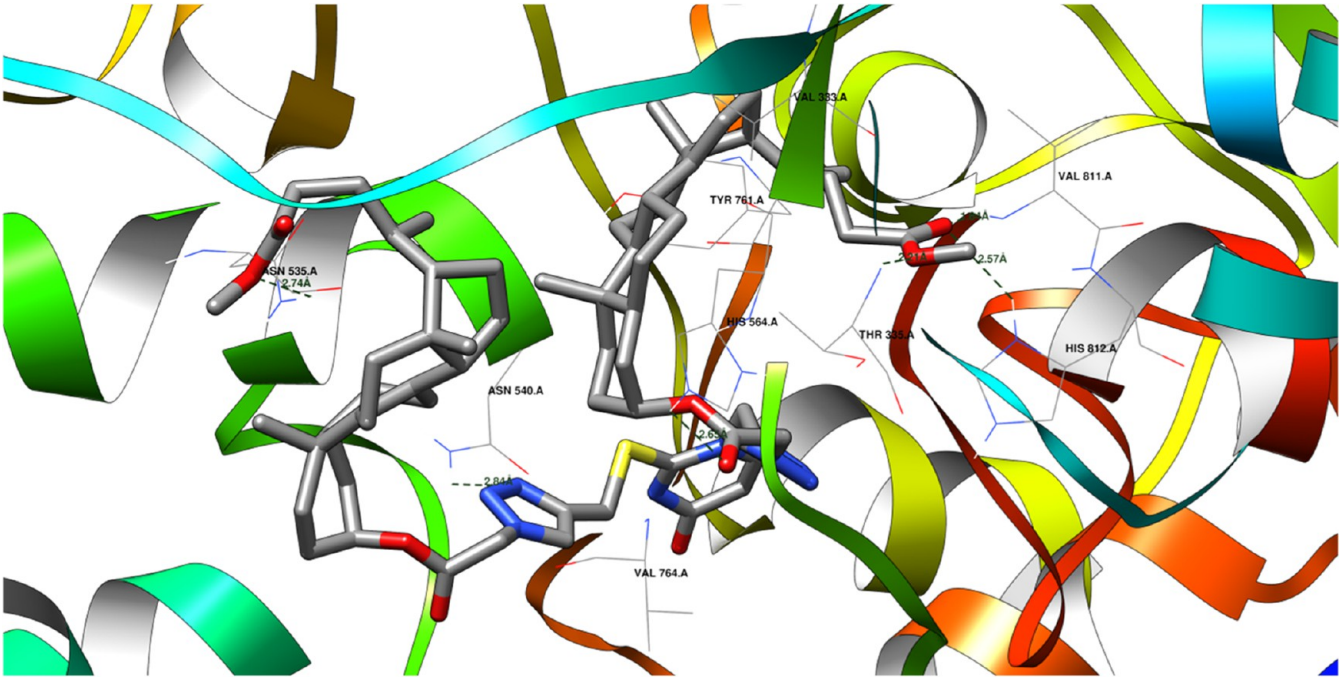

Figure 7. Potential hydrogen bonds between ligand **19** and the 2H94 protein domain.

2.14. 2H94 Protein Domain. For protein domain 2H94, the newly discovered ligands consistently exhibit significantly lower affinities than the native ligand. Despite this, their affinities are still noteworthy, suggesting potential anticancer activity. In this case, the RMSD for the initial pose recreation is 0.54 Å (Table 5), demonstrating faithful reproduction of the native ligand's pose.[81] Figure 7 shows how a protein and a molecule called a **19** ligand might bond together. They could form up to six hydrogen bonds, like tiny bridges holding them together. However, some of these bonds compete with each other, meaning only about five can form at the same time.

The **19** ligand can form hydrogen bonds with specific amino acids in the 2H94 protein domain. These hydrogen bonds involve the following atoms and distances:

- Ligand's keto-ester oxygen atom (acceptor) to ASN 535 A amine (donor): 2.74 Å
- Ligand's 1,2,3-triazole nitrogen (acceptor) to ASN 540 A amine (donor): 2.84 Å

https://doi.org/10.1021/acsomega.4c04800
ACS Omega 2024, 9, 37995−38014

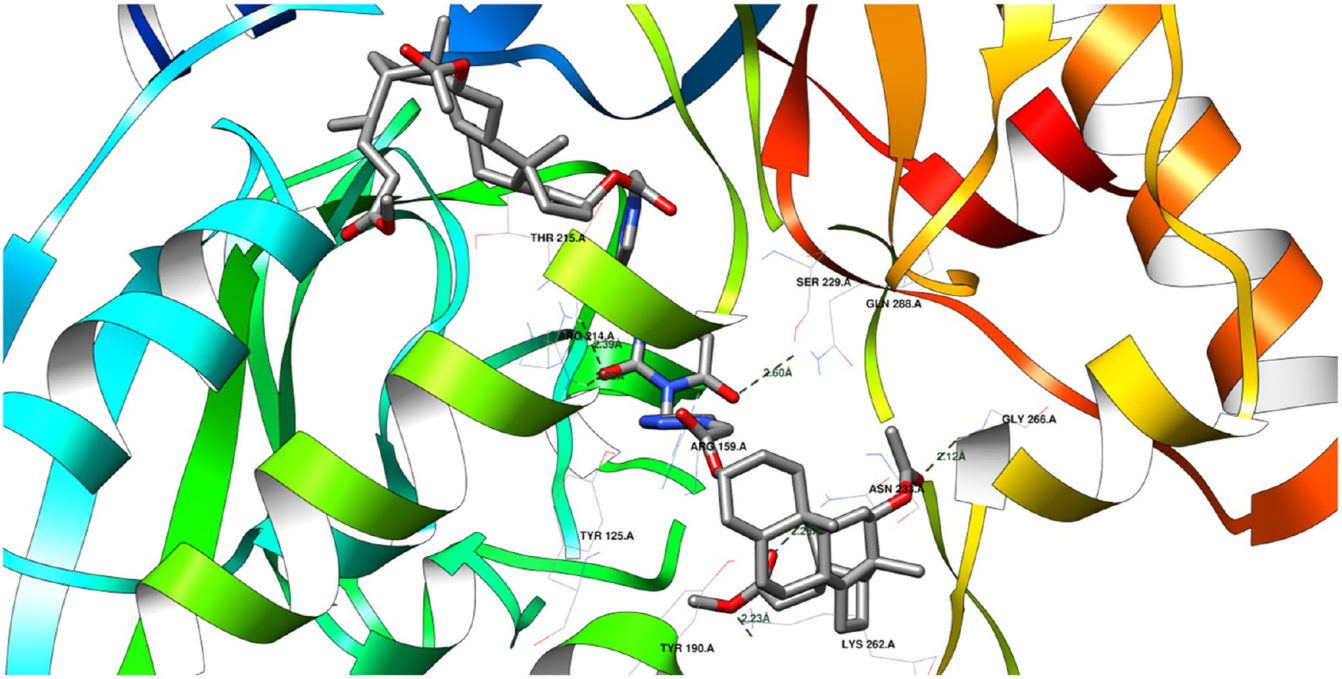

Figure 8. Potential hydrogen bonds between ligand **17** and the 2Q85 protein domain.

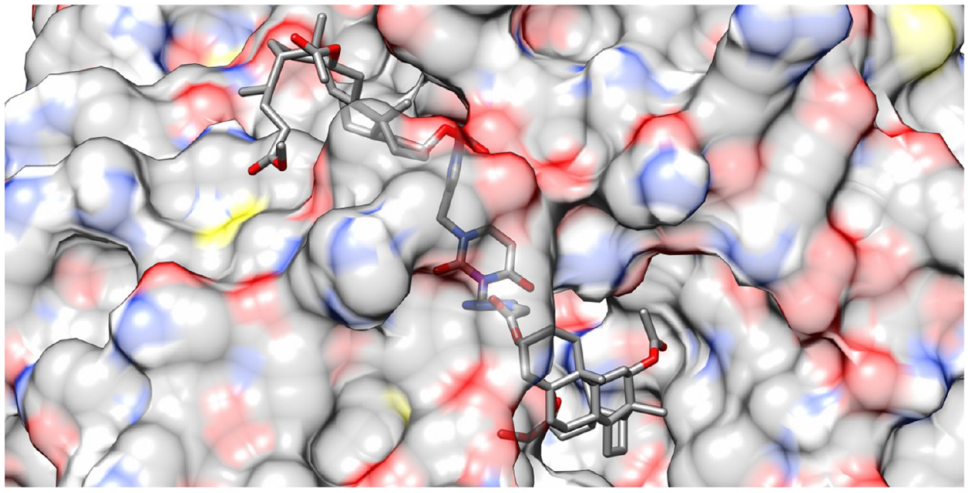

Figure 9. Illustration of the fitting of the **17** ligand into the binding site of the 2Q85 protein domain.

- Ligand's keto-ester oxygen atom (acceptor) to HIS 564 A amine (donor): 2.65 Å
- Ligand's keto-ester oxygen atom (acceptor) to VAL 811 A amine (donor): 1.84 Å
- Ligand's keto-ester oxygen atom (acceptor) to THR 335 A amine (donor): 2.21 Å
- Ligand's keto-ester oxygen atom (acceptor) to HIS 812 A amine (donor): 2.57 Å

2.15. 2Q85 Protein Domain. In the case of protein domain 2Q85, some new ligands exhibit affinities similar to or even better than the initial ligand. Notably, the **17** ligand shows significantly higher affinity. However, most other ligands have lower affinities than the native ligand, indicating antibacterial activity. The RMSD for this domain is 1.54 Å (Table 5), indicating reasonable pose reproduction.[81] Figure 8 shows how a protein and a molecule called a **17** ligand might bond together. They could form up to six hydrogen bonds, like tiny bridges holding them together. However, some of these bonds compete with each other, meaning only about five can form at the same time. Figure 9 shows the same ligand bound to the 2Q85 protein domain similarly. The protein is shown as a surface instead of a ribbon, but the interactions remain the same.

The **17** ligand can form hydrogen bonds with specific amino acids in the 2Q85 protein domain. These hydrogen bonds involve the following atoms and distances:

- Ligand's keto-ester oxygen atom (acceptor) to ASN 233 A amine (donor): 2.26 Å
- Ligand's ether oxygen atom (acceptor) to LYS 262 A amine (donor): 2.23 Å
- Ligand's keto-ester oxygen atom (acceptor) to GLY 266 A amine (donor): 2.12 Å
- Ligand's uracil oxygen atom (acceptor) to ARG 214 A amine (donor): 2.08 and 2.39 Å

https://doi.org/10.1021/acsomega.4c04800
ACS Omega 2024, 9, 37995−38014

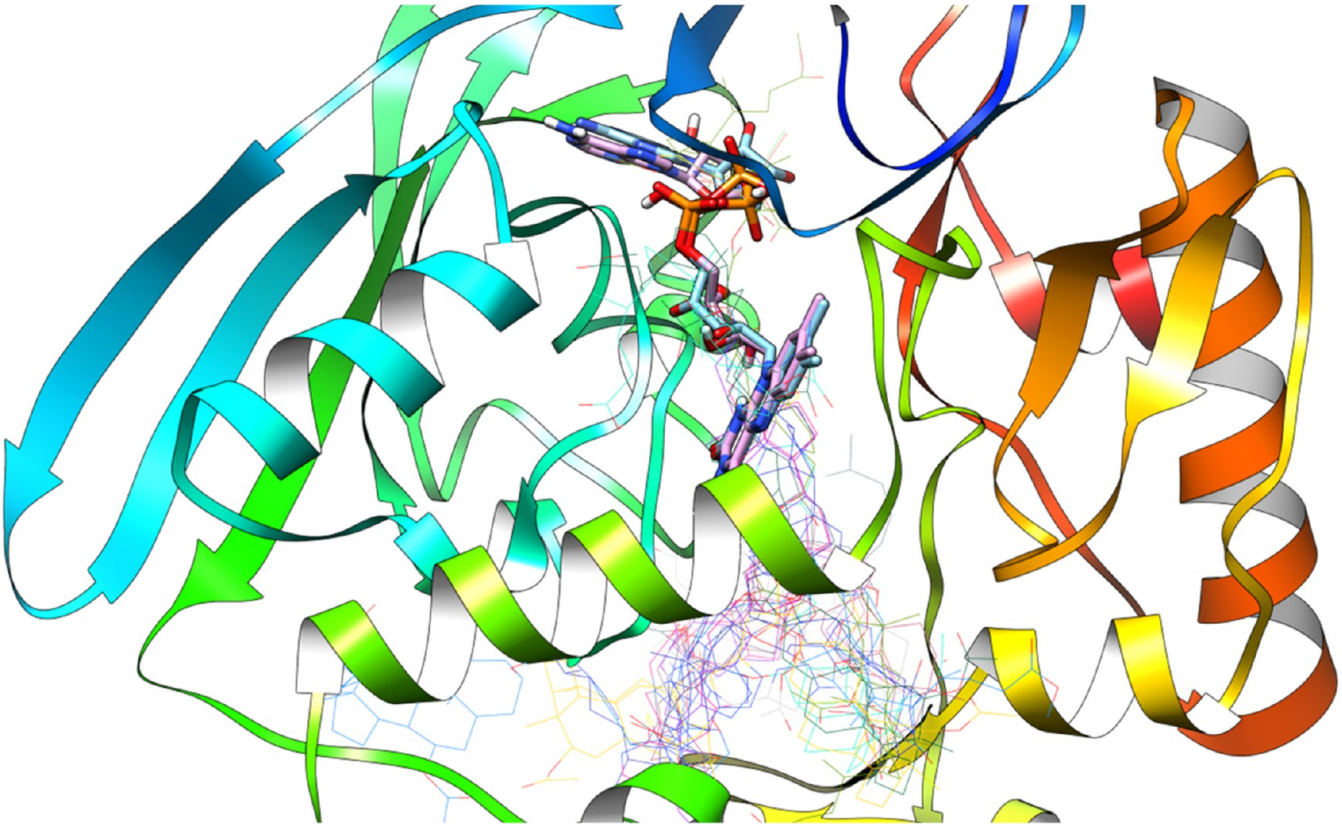

Figure 10. Native ligand, redocked ligand (sticks), and all new ligands at once are wired representations within the 2Q85 protein domain's active site.

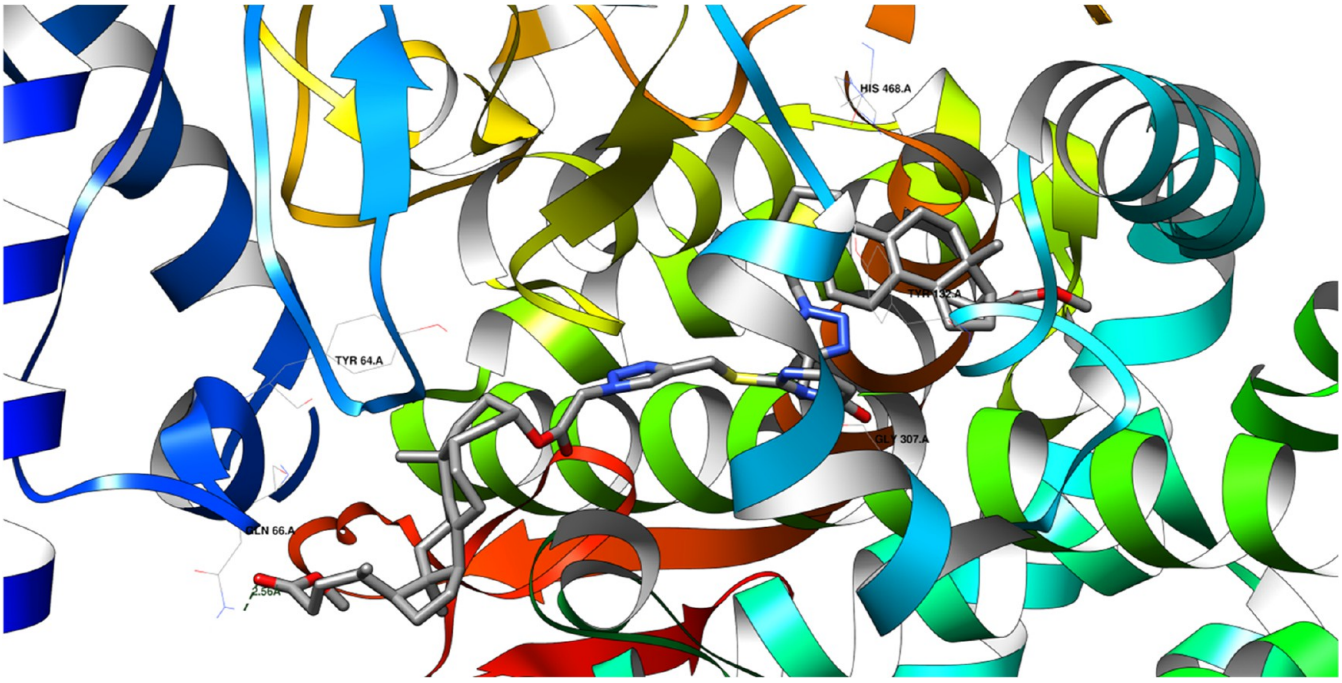

Figure 11. Potential hydrogen bonds between ligand **22** and the 5V5Z protein domain are shown in the figure. One hydrogen bond will likely be formed between the ligand's keto-ester oxygen atom (an acceptor) and the GLN 66 A residue of the domain. The length of this hydrogen bond is 2.56 Å.

- Ligand's uracil oxygen atom (acceptor) to SER 229 A hydroxyl group (donor): 2.60 Å

In this case, the hydrogen bonds between the ligand's keto-ester oxygen and ASN 233 A, ether oxygen and LYS 262 A, and keto-ester oxygen and GLY 266 A are likely the strongest because they have the shortest distances.

Figure 10 shows all the different ligands docked into the 2Q85 protein domain. The docked ligands are shown as wireframe

https://doi.org/10.1021/acsomega.4c04800
ACS Omega 2024, 9, 37995−38014

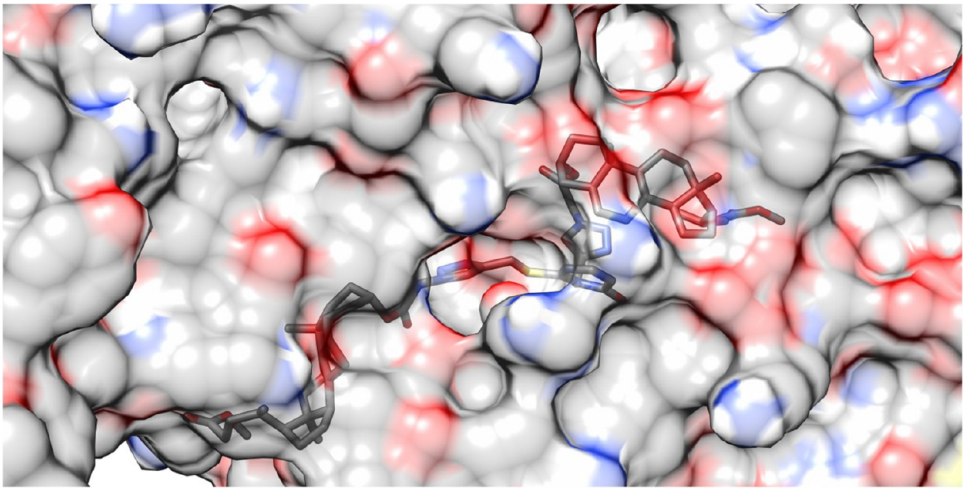

Figure 12. Illustration of the fitting of the **22** ligand into the binding site of the 5V5Z protein domain.

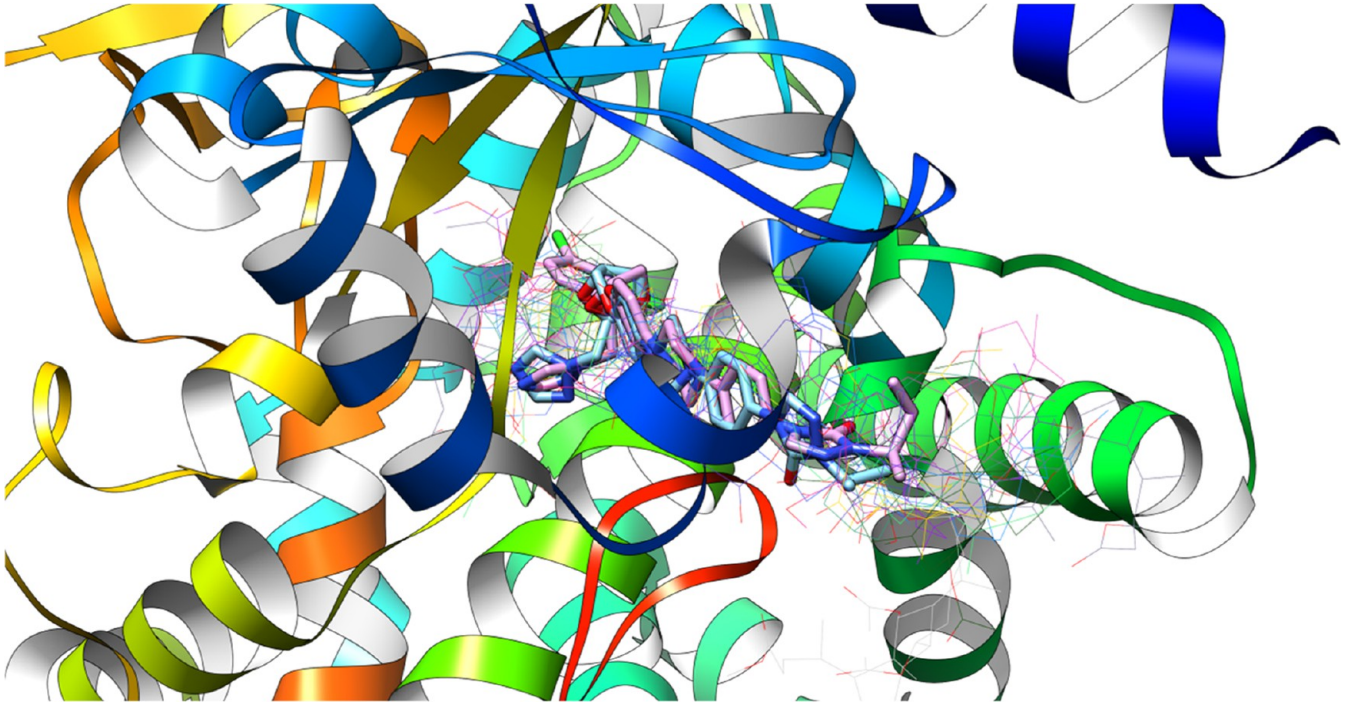

Figure 13. Native ligand, redocked ligand (sticks), and all new ligands at once are wired representations within the 5V5Z protein domain's active site.

models, while the native ligand (the ligand that the protein naturally binds to) and the redocked ligand (a ligand that was docked back into the binding site) are shown as solid models.

The low RMSD (Root Mean Square Deviation) value indicates that the docked ligands occupy the same binding site as the native ligand. RMSD is a measure of how closely two structures match up. A lower RMSD value means that the structures are more similar.

In this case, the low RMSD value means that the docked ligands bind to the protein, similarly to the native ligand. This suggests that the docking procedure found the ligands' correct binding site.

2.16. 5V5Z Protein Domain. Finally, for protein domain 5V5Z, the new ligands exhibit similar or higher affinities than the native ligand, suggesting genuine antifungal activity. Notably, the energy-favorable pose (out of the top 10 poses) has been chosen based on the lowest root-mean-square error (RMSE), which equals 1.65 Å (Table 5).[81]

Figure 11 shows the potential hydrogen bonds between the protein domain and the **22** ligand. There is the possibility of formation of at least one hydrogen bond. Figure 12 shows the same ligand in the binding site of the 5V5Z protein domain but with the protein surface instead of the ribbon.

Figure 13 shows all the docked ligands (represented as wireframes) and the native and redocked ligands. The low value of RMSD (root-mean-square deviation) can be explained by the fact that all the ligands occupy the same binding site of the 5V5Z protein domain.

All the ligands occupying the same binding site suggest competing for the same binding site. This could have implications for drug design, as it could be possible to design ligands that are more selective for the binding site and, therefore, have a higher affinity for the protein.

https://doi.org/10.1021/acsomega.4c04800
ACS Omega 2024, 9, 37995−38014

3. EXPERIMENTAL SECTION

3.1. Synthesis. *3.1.1. General Procedure for the Synthesis of Compounds (**3**–**5**).* Uracil (**1**) or 2-thiouracil (**2**) (11.9 mmol) was dissolved in 5 mL of anhydrous DMF, then K_2CO_3 was added and left for 30 min. The mixture was cooled to 0 °C, and propargyl bromide (26.2 mmol) was added. After 24 h of stirring, the reaction was stopped. DMF was evaporated, and the crude product obtained was dissolved in 10 mL of ethyl acetate. The organic layer was washed with brine (2 × 15 mL) and dried over anhydrous Na_2SO_4. As an eluent, the crude compound was purified by column chromatography on silica gel using ethyl acetate/hexane (1.5:1). Two new compounds were isolated: **4** (323 mg, 26%) and **5** (443 mg, 34%).

*3.1.2. General Procedure for the Synthesis of Compounds (**16**–**26**).* The synthesis of azidoacetyl-substituted bile acids (**9**–**11**) or sterols (**14**–**15**) derivatives has been described previously.[46]

An azidoacetate derivative of lithocholic acid (**9**) (201 mg, 0.426 mmol) or sterol (**14**) was dissolved in a *tert*-butanol/methanol mixture (5:1, 6 mL). A propargyl derivative of uracil (**3**) or 2-thiouracil (**4**/**5**) (40 mg, 0.213 mmol) was added at 65 °C (in a water bath). $CuSO_4{\cdot}5H_2O$ (3 mg, 3 mol %) and sodium ascorbate (9 mg, 20 mol %) in water (0.3 mL) were then added to the dissolved mixture. The mixture was heated to 60–65 °C in a water bath for 1 h. The resulting mixture was extracted with chloroform (10 mL), washed with brine (15 mL), and dried using anhydrous Na_2SO_4. After evaporating the solvent and purifying the residue over silica gel ($CHCl_3$/EtOAc, 20:1), a total of 162 mg (72%) of the product (**16**) and 155 mg (65%) of the product (**25**) were obtained.

*3.1.2.1. N(1),N(3)-Di(prop-2-yne-1-yl) Uracil (**3**).* White solid (1120 mg, 63%). ^{1}H NMR (400 MHz, $CDCl_3$): δ ppm 7.49 (d, J = 8.0 Hz, 1H, CH-5), 5.86 (d, J = 8.0 Hz, 1H, CH-6), 4.72 (ds, J = 2.5 Hz, 2H, N(3)CH_2−7′), 4.62 (ds, J = 2.6 Hz, 2H, N(1)CH_2−7), 2.52 (d, J = 2.6 Hz, 1H, CH-9), 2.19 (d, J = 2.5 Hz, 1H, CH-9′); ^{13}C {^{1}H} NMR (101 MHz, $CDCl_3$) δ 161.6 (C-4), 150.3 (C-2), 140.7 (C-6), 102.2 (C-5), 77.8 (C-8), 75.9 (C-8′), 75.8 (C-9), 70.4 (C-9′), 37.4 (C-7), 30.4 (C-7′); FT-IR (KBr, cm^{-1}) ν_{max}: 3303, 2306, 1717, 1676, 1275.

*3.1.2.2. N(1)-(Prop-2-yne-1-yl)-S(2)-(prop-2-yn-1-yl) Thiouracil (**4**).* White solid (323 mg, 26%). ^{1}H NMR (400 MHz, $CDCl_3$): δ ppm 7.77 (d, J = 6.5 Hz, 1H, CH-6), 6.26 (d, J = 6.5 Hz, 1H, CH-5), 4.85 (ds, J = 2.5 Hz, 2H, N(3)CH_2), 4.02 (ds, J = 2.7 Hz, 2H, SCH_2), 2.32 (t, J = 2.5 Hz, 1H, CH-9′), 2.27 (t, J = 2.7 Hz, 1H, CH-9); ^{13}C {^{1}H} NMR (101 MHz, $CDCl_3$) δ 160.8 (C-4), 160.7 (C-2), 152.0 (C-6), 110.8 (C-5), 77.7 (C-8′), 75.8 (C-8), 73.1 (C-9′), 72.0 (C-9), 33.1 (C-7), 21.1 (C-7′); FT-IR (KBr, cm^{-1}) ν_{max}: 3281, 3228, 3174, 2973, 2927, 2122, 1691, 1560, 1495; EI-MS (m/z, % int.): 203 (M^+, 100), 107 (10), 78 (25).

*3.1.2.3. N(3)-(Prop-2-yne-1-yl)-S(2)-(prop-2-yn-1-yl) Thiouracil (**5**).* White solid (443 mg, 34%). ^{1}H NMR (400 MHz, $CDCl_3$): δ ppm 8.30 (d, J = 5.7 Hz, 1H, CH-6), 6.50 (d, J = 5.7 Hz, 1H, CH-5), 5.03 (ds, J = 2.5 Hz, 2H, N(3)CH_2), 3.91 (ds, J = 2.6 Hz, 2H, SCH_2), 2.53 (t, J = 2.4 Hz, 1H, CH-9′), 2.19 (t, J = 2.6 Hz, 1H, CH-9); ^{13}C {^{1}H} NMR (101 MHz, $CDCl_3$) δ 169.8 (C-4), 167.5 (C-2), 157.8 (C-6), 104.1 (C-5), 79.7 (C-8′), 77.8 (C-8), 75.3 (C-9′), 70.5 (C-9), 54.1 (C-7), 19.4 (C-7′); FT-IR (KBr, cm^{-1}) ν_{max}: 3287, 3173, 2972, 2927, 2122, 1560, 1435, 1344, 1306, 1013; EI-MS (m/z, % int.): 204 (25), 164 (100), 69 (23).

*3.1.2.4. N(1),N(3)-Di[2-(methyl 5β- cholan-24-oate)-2-oxoethyl-1H-1,2,3-triazole-1-(3-carboxylate)] Uracil (**16**).* Oil (224 mg, 72%). ^{1}H NMR (400 MHz, $CDCl_3$): δ ppm 7.84 (s, 1H, CH-triazole ring), 7.74 (s, 1H, CH-triazole ring), 7.45 (d, J = 7.9 Hz, 1H, CH-6), 5.74 (d, J = 7.9 Hz, 1H, CH-5), 5.25 (s, 2H, CH_2−27′), 5.12 (s, 2H, CH_2−27″) 5.08 (s, 2H, N(3)−CH_2−triazole ring), 5.03 (s, 2H, N(1)−CH_2−triazole ring), 4.86–4.81 (m, 2H, 3′β-H and 3″β-H), 3.66 (s, 6H, OCH_3-25′ and OCH_3-25″), 0.93 (d, J = 6.4 Hz, 6H, CH_3-21′ and CH_3-21″), 0.92 (s, 6H, CH_3-19′ and CH_3-19″), 0.65 (s, 6H, CH_3-18′ and CH_3-18″); ^{13}C {^{1}H} NMR (101 MHz, $CDCl_3$) δ 174.7 (C-24′/24″), 165.7 (3′α−OCO), 165.6 (3″α−OCO), 162.4 (C-4), 151.1 (C-2), 143.3 (C-6), 142.4 (C-triazole ring), 142.2 (C-triazole ring), 125.3 (CH-triazole ring), 125.0 (CH-triazole ring), 102.0 (C-5), 76.7 (C-3′/C-3″), 56.4, 56.3, 56.0, 55.9, 51.5 (C-25′/25″), 51.0 (C-27′/27″), 50.9, 44.3, 42.7, 41.8, 40.4, 40.4, 40.0, 37.8, 36.0 (N(1)−CH_2), 35.7, 35.3, 34.8, 34.5, 32.0, 31.0, 30.9, 30.4 (N(3)−CH_2), 28.1, 26.9, 26.4, 26.2, 24.1, 23.2 (C-19′/19″), 20.8, 18.2 (C-21′/21″), 12.0 (C-18′/18″); FT-IR (KBr, cm^{-1}) ν_{max}: 2941, 2867, 1741, 1667, 1451, 1217; ESI-MS (m/z): 1174 $[C_{64}H_{94}N_8O_{10} + K]^+$, 1171 $[C_{64}H_{94}N_8O_{10} + Cl]^-$, 1158 $[C_{64}H_{94}N_8O_{10} + Na]^+$.

*3.1.2.5. N(1),N(3)-Di[2-(methyl 12α-acetoxy-5β-cholan-24-oate)-2-oxoethyl-1H-1,2,3-triazole-1-(3-carboxylate)] Uracil (**17**).* Oil (188 mg, 63%). ^{1}H NMR (400 MHz, $CDCl_3$): δ ppm 7.85 (s, 1H, CH-triazole ring), 7.75 (s, 1H, CH-triazole ring), 7.46 (d, J = 7.9 Hz, 1H, CH-6), 5.74 (d, J = 7.9 Hz, 1H, CH-5), 5.24 (s, 2H, CH_2−27′), 5.12 (s, 2H, CH_2−27″) 5.09 (d, 2H, 12′β-H and 12″β-H), 5.08 (s, 2H, N(3)−CH_2−triazole ring), 5.02 (s, 2H, N(1)−CH_2−triazole ring), 4.80–4.78 (m, 2H, 3′β-H and 3″β-H), 3.67 (s, 6H, OCH_3-25′ and OCH_3-25″), 2.11 (s, 6H, 12′α-OAc and 12″α-OAc), 0.91 (s, 6H, CH_3-19′ and CH_3-19″), 0.83 (d, J = 6.4 Hz, 6H, CH_3-21′ CH_3-21″), 0.73 (s, 6H, CH_3-18′ and CH_3-18″); ^{13}C {^{1}H} NMR (101 MHz, $CDCl_3$) δ 174.6 (C-24′/24″), 170.4 (12′/12″α−OCO), 165.7 (3′α−OCO),165.5 (3″α−OCO), 162.4 (C-4), 151.1 (C-2), 143.3 (C-6), 142.4 (C-triazole ring), 142.2 (C-triazole ring), 125.2 (CH-triazole ring), 125.0 (CH- triazole ring), 102.0 (C-5), 75.82 (C-12′/12″), 75.79 (C-3′/3″), 51.5 (C-25′/25″), 51.0 (C-27′/27″), 50.1, 49.4, 49.3, 47.5, 45.0, 44.2, 41.8, 36.0 (N(1)−CH_2), 35.6, 34.7, 34.5, 34.4, 34.0, 32.0, 31.0, 30.8 (N(3)−CH_2), 27.3, 25.8, 25.6, 23.4, 23.0 (C-19′/19″), 21.4 (C-29′/29″), 17.5 (C-21′/21″), 12.4 (C-18′/18″); FT-IR (KBr, cm^{-1}) ν_{max}: 2950, 2870, 1736, 1667, 1451, 1246, 1216; ESI-MS (m/z): 1289 $[C_{68}H_{98}N_8O_{14}+K]^+$, 1286 $[C_{68}H_{98}N_8O_{14} + Cl]^-$, 1274 $[C_{68}H_{98}N_8O_{14} + Na]^+$.

*3.1.2.6. N(1),N(3)-Di[2-(methyl 7α,12α-diacetoxy-5β- cholan-24-oate)-2-oxoethyl-1H-1,2,3-triazole-1-(3-carboxylate)] Uracil (**18**).* Oil (140 mg, 78%). ^{1}H NMR (400 MHz, $CDCl_3$): δ ppm 7.86 (s, 1H, CH-triazole ring), 7.76 (s, 1H, CH-triazole ring), 7.46 (d, J = 7.9 Hz, 1H, CH-6), 5.75 (d, J = 7.9 Hz, 1H, CH-5), 5.23 (s, 2H, CH_2−27′), 5.13 (ds, 2H, CH_2−27″) 5.09 (s, 4H, 12′β-H, 12″β-H and s, 2H, N(3)−CH_2−triazole ring), 5.01 (s, 2H, N(1)−CH_2−triazole ring), 4.93–4.91 (m, 2H, 7′β-H and 7″β-H), 4.72–4.61 (m, 2H, 3′β-H and 3″β-H), 3.66 (s, 6H, OCH_3-25′ and OCH_3-25″), 2.15 (s, 6H, 7′α-OAc and 7″α-OAc), 2.11 (s, 6H, 12′α-OAc and 12″α-OAc), 0.93 (s, 6H, CH_3-19′ and CH_3-19″), 0.82 (d, J = 6.3 Hz, 6H, CH_3-21′ and CH_3-21″), 0.73 (s, 6H, CH_3-18′ and CH_3-18″); ^{13}C {^{1}H} NMR (101 MHz, $CDCl_3$) δ 174.5 (C-24′/24″), 170.5 (12′α−OCO), 170.4 (12″α−OCO), 170.3 (7′α−OCO), 170.2 (7″α−OCO), 165.6 (3′α−OCO), 165.5 (3″α−OCO), 162.4 (C-4), 151.1 (C-2), 143.3 (C-6), 142.4 (C-triazole ring), 142.2 (C-triazole ring),

https://doi.org/10.1021/acsomega.4c04800
ACS Omega 2024, 9, 37995−38014

125.3 (CH-triazole ring), 125.1 (CH-triazole ring), 102.0 (C-5), 76.5 (C-12′/12″), 75.3 (C-3′/3″), 70.5 (C-7′/7″), 51.5 (C-25′/25″), 51.0 (C-27′/27″), 47.3, 45.0, 44.2, 43.3, 40.8, 37.7, 35.9 (N(1)−CH_2), 34.6, 34.4, 34.2, 31.2, 30.8, 30.7 (N(3)−CH_2), 28.8, 27.1, 26.7, 25.5, 22.8 (C-19′/19″), 22.4, 21.6 (C-29′/29″), 21.4 (C-31′/31″), 17.5 (C-21′/21″), 12.2 (C-18′/18″); FT- IR (KBr, cm^{-1}) ν_{max}: 2952, 2872, 1736, 1668, 1452, 1238; ESI-MS (m/z): 1406 $[C_{72}H_{102}N_8O_{18} + K]^+$, 1402 $[C_{72}H_{102}N_8O_{18} + Cl]^-$, 1390 $[C_{72}H_{102}N_8O_{18} + Na]^+$.

*3.1.2.7. N(1),S(2)-[2-(methyl 5β-cholan-24-oate)-2-oxoethyl-1H-1,2,3-triazole-1-(3-carboxylate)] Thiouracil (**19**).* Oil (76 mg, 34%). ^{1}H NMR (400 MHz, $CDCl_3$): δ ppm 7.81 (s, 1H, CH-triazole ring), 7.77 (d, J = 6.4 Hz, 1H, CH-6), 7.70 (s, 1H, CH-triazole ring), 6.21 (d, J = 6.5 Hz, 1H, CH-5), 5.34 (s, 2H, N(1)−CH_2−triazole ring), 5.09 (ds, J = 5.2 Hz, 4H, CH_2−27′ and CH_2−27″), 4.84−4.76 (m, 2H, 3′β-H and 3″β-H), 4.57 (s, 2H, SCH_2−triazole ring), 3.67 (s, 6H, OCH_3-25′ and CH_3-25″), 0.93 (d, J = 6.4 Hz, 6H, CH_3-21′ and CH_3-21″), 0.92 (s, 6H, CH_3-19′ and CH_3-19″), 0.65 (s, 6H, CH_3-18′ and CH_3-18″); ^{13}C {^{1}H} NMR (101 MHz, $CDCl_3$) δ 174.7 (C-24′/24″), 165.6 (3′α−OCO), 165.5 (3″α−OCO), 162.0 (C-4), 161.6 (C-2), 151.9 (C-6), 143.8 (C-triazole ring), 141.9 (C-triazole ring), 125.3 (CH-triazole ring), 124.2 (CH-triazole ring), 110.7 (C-5), 75.0 (C-3′/3″), 69.2, 56.4, 56.4, 56.0, 51.4 (C-25′/25″), 51.1 (C-26′/26″), 42.7, 41.9 (N(1)−CH_2), 40.5, 40.4, 40.1, 40.0, 35.8, 35.3, 34.9, 34.5, 32.1, 32.0, 31.1, 31.0, 28.1, 27.3, 26.9, 26.5, 26.6, 26.3, 24.2, 23.2 (SCH_2), 20.8 (C-19′/19″), 18.3 (C-21′/21″), 16.5, 12.0 (C-18′/18″); FT-IR (KBr, cm^{-1}) ν_{max}: 2940, 2866, 1740, 1684, 1489, 1216; ESI-MS (m/z): 1189 $[C_{64}H_{94}N_8O_9S + K]^+$, 1186 $[C_{64}H_{94}N_8O_9S + Cl]^-$, 1174 $[C_{64}H_{94}N_8O_9S + Na]^+$.

*3.1.2.8. N(1),S(2)-Di[2-(methyl 12α-acetoxy-5β-cholan-24-oate)-2-oxoethyl-1H-1,2,3-triazole-1-(3-carboxylate)] Thiouracil (**20**).* Oil (88 mg, 47%). ^{1}H NMR (400 MHz, $CDCl_3$): δ ppm 7.82 (s, 1H, CH-triazole ring), 7.77 (d, J = 6.4 Hz, 1H, CH-6), 7.70 (s, 1H, CH-triazole ring), 6.22 (d, J = 6.5 Hz, 1H, CH-5), 5.33 (s, 2H, N(1)−CH_2−triazole ring), 5.10 (d, 2H, 12′β-H and 12″β-H), 5.08 (s, 4H, CH_2−27′ and CH_2−27″), 4.83−4.77 (m, 2H, 3′β-H and 3″β-H), 4.56 (s, 2H, SCH_2−triazole ring), 3.67 (s, 6H, OCH_3-25′ and CH_3-25″), 2.11 (ds, J = 2.6 Hz, 6H, 12′α-OAc and 12″α-OAc) 0.91 (s, 6H, CH_3-19′ and CH_3-19″), 0.81 (d, J = 6.4 Hz, 6H, CH_3-21′ and CH_3-21″), 0.73 (s, 6H, CH_3-18′ and CH_3-18″); ^{13}C {^{1}H} NMR (101 MHz, $CDCl_3$) δ 174.5 (C-24′/24″), 170.4 (12′α−OCO and 12″α−OCO), 165.6 (3′α−OCO), 165.5 (3″α−OCO), 162.1 (C-4), 161.7 (C-2), 151.9 (C-6), 143.7 (C-triazole ring), 142.0 (C-triazole ring), 125.4 (CH-triazole ring), 124.2 (CH-triazole ring), 110.7 (C-5),, 75.9 (C-12′/12″), 75.3 (C-3′/3″), 51.5 (C-25′/25″), 51.1 (C-27′/27″), 49.4, 47.6, 45.0, 41.8 (N(1)−CH_2), 40.0, 35.7, 34.7, 34.6, 34.5, 34.4, 34.0, 32.1, 31.0, 30.8, 27.3, 26.8, 26.5, 25.8, 25.6, 23.4 (SCH_2), 23.0 (C-19′/19″), 21.4 (C-29′/29″), 17.5 (C-21′/21″), 12.4 (C-18′/18″); FT-IR (KBr, cm^{-1}) ν_{max}: 2950, 2869, 1737, 1683, 1490, 1246, 1241; ESI-MS (m/z): 1346 $[C_{68}H_{98}N_8O_{13}S + Br]^-$, 1306 $[C_{68}H_{98}N_8O_{13}S + K]^+$, 1303 $[C_{68}H_{98}N_8O_{13}S + Cl]^-$, 1290 $[C_{68}H_{98}N_8O_{13}S + Na]^+$.

*3.1.2.9. N(1),S(2)-Di[2-(methyl 7α,12α-diacetoxy-5β-cholan-24-oate)-2-oxoethyl-1H-1,2,3-triazole-1-(3-carboxylate)] Thiouracil (**21**).* Oil (42 mg, 43%). ^{1}H NMR (400 MHz, $CDCl_3$): δ ppm 7.90 (s, 1H, CH-triazole ring), 7.75 (d, J = 6.4 Hz, 1H, CH-6), 7.80 (s, 1H, CH-triazole ring), 6.20 (d, J = 6.3 Hz, 1H, CH-5), 5.34 (s, 2H, N(1)−CH_2−triazole ring), 5.11 (d, 2H, 12′β-H and 12″β-H), 5.09 (s, 4H, CH_2−27′ and CH_2−27″), 4.92 (s, 2H, 7′β-H and 7″β-H) 4.69−4.64 (m, 2H, 3′β-H and 3″β-H), 4.51 (s, 2H, SCH_2−triazol ring), 3.66 (s, 6H, OCH_3-25′ and CH_3-25″), 2.15 (s, 6H, 7′α-OAc and 7″α-OAc), 2.11 (s, 6H, 12′α-OAc and 12″α-OAc), 0.92 (s, 6H, CH_3-19′ and CH_3-19″), 0.82 (d, J = 6.3 Hz, 6H, CH_3-21′ and CH_3-21″), 0.73 (s, 6H, CH_3-18′ and CH_3-18″); ^{13}C {^{1}H} NMR (101 MHz, $CDCl_3$) δ 174.5 (C-24′/24″), 170.5 (12′α−OCO), 170.5 (12″α−OCO), 170.4 (7′α−OCO), 170.3 (7″α−OCO), 165.6 (3′α−OCO), 165.4 (3″α−OCO), 164.1 (C-4), 161.4 (C-2), 152.1 (C-6), 143.8 (C-triazole), 141.9 (C-triazole), 125.3 (CH-triazole), 124.2 (CH-triazole), 111.0 (C-4), 75.3 (C-12′/12″), 75.0 (C-3′/3″), 70.5 (C-7′/7″), 60.2, 59.1, 51.52 (C-25′/25″), 51.2 (C-27′/27″), 47.3, 45.0, 43.3, 40.8 (N(1)−CH_2), 37.7, 34.6, 34.4, 34.2, 31.2, 30.9, 30.7, 29.7, 28.8, 27.1, 26.7, 25.5, 22.8 (SCH_2), 22.5 (C-19′/19″), 21.7 (C-29′/29″), 21.4 (C-31′/31″), 17.5 (C-21′/21″), 12.2 (C-19′/19″); FT-IR (KBr, cm^{-1}) ν_{max}: 2965, 2875, 1741, 1675, 1485, 1241, 1232; ESI-MS (m/z): 1290 $[C_{68}H_{98}N_8O_{13}S + Na]^+$.

*3.1.2.10. N(3),S(2)-[2-(methyl 5β-cholan-24-oate)-2-oxoethyl-1H-1,2,3-triazole-1-(3-carboxylate)] Thiouracil (**22**).* Oil (135 mg, 60%). ^{1}H NMR (400 MHz, $CDCl_3$): δ ppm 8.25 (d, J = 5.7 Hz, 1H, CH-6), 7.83 (s, 1H, CH-triazole ring), 7.70 (s, 1H, CH-triazole ring), 6.45 (d, J = 5.7 Hz, 1H, CH-5), 5.54 (s, 2H, N(3)−CH_2−triazole ring), 5.13 (s, 2H, CH_2−27′), 5.08 (s, 2H, CH_2−27″), 4.85−4.78 (m, 2H, 3′β-H and 3″β-H), 4.52 (s, 2H, SCH_2−triazole ring), 3.67 (s, 6H, OCH_3-25′ and CH_3-25″), 0.93 (s, 6H, CH_3-19′ and CH_3-19″), 0.91 (d, J = 6.4 Hz, 6H, CH_3-21′ and CH_3-21″), 0.65 (s, 6H, CH_3-18′ and CH_3-18″); ^{13}C {^{1}H} NMR (101 MHz, $CDCl_3$) δ 174.7 (C-24′/24″), 170.4 (C-4), 168.1 (C-2), 165.7 (3′α−OCO), 165.6 (3″α−OCO), 157.6 (C-6), 145.7 (C-triazole ring), 143.1 (C-triazole ring), 125.2 (CH-triazole ring), 123.7 (CH-triazole ring), 104.5 (C-5), 76.7 (C-3′/3″), 59.4, 56.4, 56.0, 51.4 (C-25′/25″), 51.1 (C-27′/27″), 42.7, 41.9 (N(3)−CH_2), 40.5, 40.1, 35.8, 35.3, 34.9, 34.6, 32.1, 31.1, 31.0, 28.1, 27.0, 26.5, 26.3, 25.7, 24.2, 23.2 (SCH_2), 20.8 (C-19′/19″), 18.3 (C-21′/21″), 12.0 (C-18′/18″); FT-IR (KBr, cm^{-1}) ν_{max}: 2935, 2852, 1741, 1666, 1472, 1211; ESI-MS (m/z): 1188 $[C_{64}H_{94}N_8O_9S + K]^+$, 1186 $[C_{64}H_{94}N_8O_9S + Cl]^-$, 1174 $[C_{64}H_{94}N_8O_9S + Na]^+$.

*3.1.2.11. N(3),S(2)-Di[2-(methyl 12α-acetoxy-5β-cholan-24-oate)-2-oxoethyl-1H-1,2,3-triazole-1-(3-carboxylate)] Thiouracil (**23**).* Oil (169 mg, 78%). ^{1}H NMR (400 MHz, $CDCl_3$): δ ppm 8.25 (d, J = 5.7 Hz, 1H, CH-6), 7.83 (s, 1H, CH-triazole ring), 7.71 (s, 1H, CH-triazole ring), 6.45 (d, J = 5.7 Hz, 1H, CH-5), 5.53 (s, 2H, N(3)−CH_2−triazole ring), 5.14 (s, 2H, CH_2−27′), 5.09 (s, 4H, 12′β-H, 12″β-H and CH_2−27″), 4.83−4.76 (m, 2H, 3′β-H and 3″β-H), 4.51 (s, 2H, SCH_2−triazole ring), 3.67 (s, 6H, OCH_3-25′ and CH_3-25″), 2.11 (6H, 12′α-OAc and 12″α-OAc), 0.91 (s, 6H, CH_3-19′ and CH_3-19″), 0.81 (d, J = 6.2 Hz, 6H, CH_3-21′ and CH_3-21″), 0.72 (s, 6H, CH_3-18′ and CH_3-18″); ^{13}C {^{1}H} NMR (101 MHz, $CDCl_3$) δ 174.6 (C-24′/24″), 170.4 (12′α−OCO, 12″α−OCO and C-4), 168.1 (C-2), 165.7 (3′α−OCO), 165.6 (3″α−OCO), 157.6 (C-6), 145.7 (C-triazole ring), 143.2 (C-triazole ring), 125.2 (CH-triazole ring), 123.7 (CH-triazole ring), 104.5 (C-5), 75.9 (C-12′/12″), 75.8 (C-3′/3″), 59.4, 51.5 (C-25′/25″), 51.1 (C-27′/27″), 49.4, 47.6, 45.0, 41.8 (N(3)−CH_2), 35.6, 34.7, 34.6, 34.4, 34.0, 32.1, 31.0, 30.8, 27.3, 26.8, 26.5, 25.8, 25.7, 25.6, 23.5 (SCH_2), 23.0 (C-19′/19″), 21.4 (C-29′/29″), 17.5 (C-21′/21″), 12.4 (C-18′/18″); FT-IR (KBr, cm^{-1}) ν_{max}: 2951, 2872, 1735, 1563, 1377, 1248; ESI-MS (m/z): 1406 $[C_{72}H_{102}N_8O_{17}S + Na]^+$.

3.1.2.12. N(3),S(2)-Di[2-(methyl 7α,12α-diacetoxy-5β-cholan-24-oate)-2-oxoethyl-1H-1,2,3-triazole-1-(3-carboxylate)]

https://doi.org/10.1021/acsomega.4c04800
ACS Omega 2024, 9, 37995−38014

*Thiouracil (**24**).* Oil (124 mg, 67%). ^{1}H NMR (400 MHz, $CDCl_3$): δ ppm 8.26 (d, J = 5.8 Hz, 1H, CH-6), 7.83 (s, 1H, CH-triazole ring), 7.71 (s, 1H, CH-triazole ring), 6.45 (d, J = 5.7 Hz, 1H, CH-5), 5.52 (s, 2H, N(3)−CH_2−triazole ring), 5.15 (s, 2H, CH_2−27′), 5.10 (s, 2H, 12′β-H and 12″β-H), 5.08 (s, 2H, CH_2−27″), 4.91 (s, 2H, 7′β-H and 7″β-H), 4.72−4.62 (m, 2H, 3′β-H and 3″β-H), 4.50 (s, 2H, SCH_2−triazole ring), 3.66 (s, 6H, OCH_3-25′ and CH_3-25″), 2.15 (s, 6H, 7′α-OAc and 7″α-OAc), 2.09 (s, 6H, 12′α-OAc and 12″α-OAc), 0.92 (s, 6H, CH_3-19′ and CH_3-19″), 0.82 (d, J = 6.3 Hz, 6H, CH_3-21′ and CH_3-21″), 0.73 (s, 6H, CH_3-18′ and CH_3-18″); ^{13}C {^{1}H} NMR (101 MHz, $CDCl_3$) δ 174.5 (C-24′/24″), 170.5 (12′α−OCO and 12″α−OCO), 170.3 (7′α−OCO, 7″α−OCO and C-4), 168.1 (C-2), 165.7 (3′α−OCO), 165.6 (3″α−OCO), 157.6 (C-6), 145.6 (C-triazole ring), 143.2 (C-triazole ring), 125.2 (CH-triazole ring), 123.7 (CH-triazole ring), 104.5 (C-5), 75.3 (C-12′/12″), 75.0 (C-3′/3″), 70.5 (C-7′/7″), 60.4, 59.4, 51.5 (C-25′/25″), 51.1 (C-27′/27″), 47.3, 45., 43.3, 40.8 (N(3)−CH_2), 37.7, 34.6, 34.4, 34.2, 31.2, 30.9, 30.7, 28.8, 27.2, 26.7, 25.6, 25.5, 22.8 (SCH_2), 22.5 (C-19′/19″), 21.6 (C-31′/31″), 21.4 (C-29′/29″), 21.0, 19.1, 17.5 (C-21′/21″), 16.5, 14.2, 13.7, 12.2 (C-18′/18″); FT-IR (KBr, cm^{-1}) ν_{max}: 2949, 2869, 1736, 1563, 1439, 1246, 1214; ESI-MS (m/z): 1290 $[C_{68}H_{98}N_8O_{13}S + Na]^+$.

*3.1.2.13. N(1),N(3)-Di[2-(methyl cholest-5-ene)-2-oxoethyl-1H-1,2,3-triazole-1-(3-carboxylate)] Uracil (**25**).* Oil (115 mg, 65%). ^{1}H NMR (400 MHz, $CDCl_3$): δ ppm 7.84 (s, 1H, CH-triazole ring), 7.74 (s, 1H, CH-triazole ring), 7.45 (d, J = 7.9 Hz, 1H, CH-6), 5.75 (d, J = 7.8 Hz, 1H, CH-5), 5.38 (bs, 2H, CH-6′ and CH-6″), 5.25 (s, 2H, CH_2−29′), 5.12 (s, 2H, CH_2−29″), 5.08 (s, 2H, N(3)−CH_2−triazole ring), 5.02 (s, 2H, N(1)−CH_2−triazole ring), 4.69−4.64 (m, 2H, 3′α-H and 3″α-H), 1.04 (s, 6H, CH_3-19′ and CH_3-19″), 0.91 (d, J = 6.4 Hz, 6H, CH_3-21′ and CH_3-21″), 0.86 (dd, J_1 = 6.6 Hz, J_2 = 1.8 Hz, 12H, CH_3-26′/26″ and CH_3-27′/27″), 0.68 (s, 6H, CH_3-18′ and CH_3-18″); ^{13}C {^{1}H} NMR (101 MHz, $CDCl_3$) δ 165.6 (3′β−OCO), 165.5 (3″β−OCO), 162.4 (C-4), 151.1 (C-2), 142.4 (C-6 and C-5′/5″), 138.9 (C-triazole ring), 138.8 (C-triazole ring), 123.4 (CH-triazole ring), 123.3 (CH-triazole ring and C-6′/6″), 102.0 (C-5), 76.4 (C-3′/3″), 56.6, 56.1, 51.0 (C-29′/29″), 49.9, 44.3, 42.3, 39.7, 39.5, 37.8, 36.8, 36.5 (N(1)−CH_2), 36.1, 36.0, 35.8, 31.8, 31.8, 29.7, 28.2, 28.0 (N(3)−CH_2), 27.6, 24.2, 23.8, 22.8, 22.5 (C-19′/19″), 21.0 (C-26′/26″ and C-27′/27″), 19.2, 18.7 (C-21′/21″), 14.2, 11.8 (C-18′/18″); FT-IR (KBr, cm^{-1}) ν_{max}: 3447, 2947, 1748, 1706, 1661, 1222; ESI-MS (m/z): 1151 $[C_{68}H_{102}N_8O_6 + Na]^+$.

*3.1.2.14. N(1),N(3)-Di[2-(methyl 5β-cholestan)-2-oxoethyl-1H-1,2,3-triazole-1-(3-carboxylate)] Uracil (**26**).* Oil (75%). ^{1}H NMR (400 MHz, $CDCl_3$): δ ppm 7.84 (s, 1H, CH-triazole ring), 7.73 (s, 1H, CH-triazole ring), 7.45 (d, J = 7.9 Hz, 1H, CH-6), 5.74 (d, J = 7.9 Hz, 1H, CH-5), 5.25 (s, 2H, CH_2−29′), 5.11 (s, 2H, CH_2−29″) 5.07 (s, 2H, N(3)−CH_2−triazole ring), 5.02 (s, 2H, N(1)−CH_2−triazole ring), 4.83−4.72 (m, 2H, 3′α-H and 3″α-H), 0.90 (d, J = 6.4 Hz, 6H, CH_3-21′ and CH_3-21″), 0.86 (dd, J_1 = 6.4 Hz, J_2 = 2.4 Hz, 12H, CH_3-26′/26″ and CH_3-27′/27″), 0.82 (s, 6H, CH_3-19′ and CH_3-19″), 0.65 (s, 6H, CH_3-18′ and CH_3-18″); ^{13}C {^{1}H} NMR (101 MHz, $CDCl_3$) δ 165.7 (3′β−OCO), 165.6 (3″β−OCO), 162.4 (C-4), 151.1 (C-2), 143.3 (C-6), 142.4 (C-triazole ring), 142.2 (C-triazole ring), 125.3 (CH-triazole ring), 125.1 (CH-triazole ring), 102.0 (C-5), 76.5 (C-3″), 76.3 (C-3′), 56.3, 56.2, 56.2, 54.1, 51.1 (C-29′), 50.9, 44.6, 44.3, 42.5, 39.9, 39.5, 36.5 (N(1)−CH_2), 36.1, 35.9, 35.8, 35.4, 33.8, 31.9, 28.5, 28.20, 28.0 (N(3)−CH_2), 27.3, 24.1, 23.8, 22.8, 22.5 (C-19′/19″), 21.2 (C-26′/26″ and C-27′/27″), 18.6 (C-21′/21″), 12.2 (C-18″), 12.0 (C-18′); FT-IR (KBr, cm^{-1}) ν_{max}: 3440, 2935, 1740, 1620, 1215; ESI-MS (m/z): 1171 $[C_{68}H_{106}N_8O_6 + K]^+$.

4. CONCLUSIONS

An effective synthesis, comprehensive spectroscopic characterization, and theoretical studies of the biological properties of 11 new steroid-pyrimidine bioconjugates connected with 1,2,3-triazole rings were carried out. The synthesis involved the strategic incorporation of triazole rings that linked steroid and pyrimidine units, which could offer synergistic effects in biological activity. Detailed spectroscopic and spectrometric analyses provided detailed structural information, confirming the successful formation of the bioconjugates. Additionally, the potential biological activities of the synthesized compounds were investigated in theoretical studies, such as molecular docking simulations. Computational methods provided insight into the molecular interactions between bioconjugates and target biological receptors. The combined experimental and theoretical approach confirmed the structural integrity of the synthesized compounds. It also provided valuable information about their potential biological activities, opening a promising avenue for further pharmaceutical development. Molecular docking studies predicted that the new ligands may have potential antibacterial and antifungal activities. Affinity energy for selected ligands is lower than the affinity energy of the native ligand toward *E. coli* MurB and against *C. albicans* fungi. This is a promising path for the development of new drugs, especially in the fight against infections resistant to currently available therapies. However, further experimental studies are required to confirm these predicted activities. In particular, *in vitro* and *in vivo* studies can provide valuable information on their efficacy and safety profile, enabling more informed decisions regarding drug development.

■ ASSOCIATED CONTENT

Data Availability Statement

The study's data are available in the published article and its Supporting Information.

Supporting Information

The Supporting Information is available free of charge at https://pubs.acs.org/doi/10.1021/acsomega.4c04800.

General information and copies of ^{1}H and ^{13}C NMR, ESI-MS, EI-MS, and FT-IR spectra (PDF)

■ AUTHOR INFORMATION

Corresponding Author

Anna Kawka − *Department of Bioactive Products, Faculty of Chemistry, Adam Mickiewicz University, 61-614 Poznań, Poland;* orcid.org/0000-0001-9281-7103; Email: anna.kawka@amu.edu.pl

Authors

Damian Nowak − *Department of Quantum Chemistry, Faculty of Chemistry, Adam Mickiewicz University, 61-614 Poznań, Poland;* orcid.org/0000-0003-3739-3306

Hanna Koenig − *Department of Bioactive Products, Faculty of Chemistry, Adam Mickiewicz University, 61-614 Poznań, Poland*

Tomasz Pospieszny − *Department of Bioactive Products, Faculty of Chemistry, Adam Mickiewicz University, 61-614 Poznań, Poland;* orcid.org/0000-0001-5071-7016

https://doi.org/10.1021/acsomega.4c04800
ACS Omega 2024, 9, 37995−38014

Complete contact information is available at:
https://pubs.acs.org/10.1021/acsomega.4c04800

Author Contributions

Conceptualization, A.K. and T.P.; molecular docking, D.N.; methodology, A.K., H.K. and D.N.; formal analysis, A.K., H.K., D. N. and T.P.; investigation, T.P.; PASS and theoretical calculation (PM5), T.P.; resources, H.K. and T.P.; data curation, T.P.; writing−original draft preparation, A.K., H.K., D.N. and T.P.; writing−review and editing, T.P.; visualization, A.K., H.K. and T.P.; supervision, T.P.; project administration, T.P.; funding acquisition, T.P. All authors have read and agreed to the published version of the manuscript.

Notes

The authors declare no competing financial interest.
The obtained compounds were obtained under laboratory conditions. The compounds have not been subjected to cytotoxicity tests. Therefore, their effect on human or animal cells is not known.

■ ACKNOWLEDGMENTS

This work was financially supported by the Research Subsidy at the Faculty of Chemistry of the Adam Mickiewicz University in Poznan.

■ REFERENCES

(1) Seeman, N. C. At the Crossroads of Chemistry, Biology, and Materials: Structural DNA Nanotechnology. *Chem. Biol.* **2003**, *10* (12), 1151−1159.
(2) Sharma, A.; Vaghasiya, K.; Verma, R. K.; Yadav, A. B. DNA Nanostructures: Chemistry, Self-Assembly, and Applications. In *Emerging Applications of Nanoparticles and Architecture Nanostructures*; Barhoum, A.; Makhlouf, A. S. H., Eds.; Elsevier, 2018; Chapter 3, pp 71−94.
(3) Chimirri, A.; Monforte, P.; Rao, A.; Zappalà, M.; Monforte, A. M.; De Sarro, G.; Pannecouque, C.; Witvrouw, M.; Balzarini, J.; De Clercq, E. Synthesis, Biological Activity, Pharmacokinetic Properties and Molecular Modelling Studies of Novel 1H,3H-Oxazolo[3,4-a]-Benzimidazoles: Non-Nucleoside HIV-1 Reverse Transcriptase Inhibitors. *Antiviral Chem. Chemother.* **2001**, *12* (3), 169−174.
(4) Cortés-Percino, A.; Vega-Baez, J. L.; Romero-Lopez, A.; Puerta, A.; Merino-Montiel, P.; Meza-Reyes, S.; Padron, J. M.; Montiel-Smith, S. Synthesis and Evaluation of Pyrimidine Steroids as Antiproliferative Agents. *Molecules* **2019**, *24* (20), No. 3676.
(5) Kumar, K.; Liu, N.; Yang, D.; Na, D.; Thompson, J.; Wrischnik, L. A.; Land, K. M.; Kumar, V. Synthesis and Antiprotozoal Activity of Mono- and Bis-Uracil Isatin Conjugates against the Human Pathogen *Trichomonas Vaginalis*. *Bioorg. Med. Chem.* **2015**, *23* (16), 5190−5197.
(6) Andreeva, O. V.; Garifullin, B. F.; Zarubaev, V. V.; Slita, A. V.; Yesaulkova, I. L.; Volobueva, A. S.; Belenok, M. G.; Man'kova, M. A.; Saifina, L. F.; Shulaeva, M. M.; Voloshina, A. D.; Lyubina, A. P.; Semenov, V. E.; Kataev, V. E. Synthesis and Antiviral Evaluation of Nucleoside Analogues Bearing One Pyrimidine Moiety and Two D-Ribofuranosyl Residues. *Molecules* **2021**, *26* (12), No. 3678.
(7) Raj, C. R.; Behera, S. Mediatorless Voltammetric Oxidation of NADH and Sensing of Ethanol. *Biosens. Bioelectron.* **2005**, *21* (6), 949−956.
(8) Chu, X.; Duan, D.; Shen, G.; Yu, R. Amperometric Glucose Biosensor Based on Electrodeposition of Platinum Nanoparticles onto Covalently Immobilized Carbon Nanotube Electrode. *Talanta* **2007**, *71* (5), 2040−2047.
(9) Arenas-González, A.; Mendez-Delgado, L. A.; Merino-Montiel, P.; Padrón, J. M.; Montiel-Smith, S.; Vega-Báez, J. L.; Meza- Reyes, S. Synthesis of Monomeric and Dimeric Steroids Containing [1,2,4]-Triazolo[1,5-*a*]Pyrimidines. *Steroids* **2016**, *116*, 13−19.
(10) Yu, B.; Shi, X. J.; Zheng, Y. F.; Fang, Y.; Zhang, E.; Yu, D. Q.; Liu, H. M. A Novel [1,2,4] Triazolo [1,5-*a*] Pyrimidine-Based Phenyl-Linked Steroid Dimer: Synthesis and Its Cytotoxic Activity. *Eur. J. Med. Chem.* **2013**, *69*, 323−330.
(11) Civcir, P. Ü. A Theoretical Study of Tautomerism of Cytosine, Thymine, Uracil and their 1-Methyl Analogues in the Gas and Aqueous Phases Using AM1 and PM3. *J. Mol. Struct.* **2000**, *532* (1), 157−169.
(12) Dewick, P. M. *Medicinal Natural Products: A Biosynthetic Approach*, 3rd ed.; Wiley, A John Wiley and Sons, Ltd., 2009; pp 247−298.
(13) Horáčková, Š.; Plocková, M.; Demnerová, K. Importance of Microbial Defence Systems to Bile Salts and Mechanisms of Serum Cholesterol Reduction. *Biotechnol. Adv.* **2018**, *36* (3), 682−690.
(14) Fleisman, J. S.; Kumar, S. Bile acids metabolism and signaling in health and disease: molecular mechanisms and therapeutic targets. *Signal Transduction Targeted Ther.* **2024**, *9*, No. 97.
(15) Shansky, Y.; Bespyatykh, J. Bile Acids: Physiological Activity and Perspectives of Using in Clinical and Laboratory Diagnostics. *Molecules* **2022**, *27* (22), No. 7830.
(16) Patel, S.; Challagundla, N.; Rajput, R. A.; Mishra, S. Design, Synthesis, Characterization and Anti-cancer Activity Evaluation of Deoxycholic Acid-Chalcone Conjugates. *Bioorg. Chem.* **2022**, *127*, No. 106036.
(17) Stathopoulou, M. E. K.; Zoupanou, N.; Banti, C. N.; Douvalis, A. P.; Papachristodoulou, C.; Marousis, K. D.; Spyroulias, G. A.; Mavromoustakos, T.; Hadjikakou, S. K. Organotin Derivatives of Cholic Acid Induce Apoptosis into Breast Cancer Cells and Interfere with Mitochondrion; Synthesis, Characterization and Biological Evaluation. *Steroids* **2021**, *167*, No. 108798.
(18) Zhang, Y. L.; Li, Y. F.; Wang, J. W.; Yu, B.; Shi, Y. K.; Liu, H. M. Multicomponent Assembly of Novel Antiproliferative Steroidal Dihydropyridinyl Spirooxindoles. *Steroids* **2016**, *109*, 22−28.
(19) Yu, B.; Qi, P.-P.; Shi, X. J.; Huang, R.; Guo, H.; Zheng, Y. C.; Yu, D. Q.; Liu, H. M. Efficient Synthesis of New Antiproliferative Steroidal Hybrids Using the Molecular Hybridization Approach. *Eur. J. Med. Chem.* **2016**, *117*, 241−255.
(20) Navacchia, M. L.; Marchesi, E.; Perrone, D. Bile Acid Conjugates with Anti-cancer Activity: Most Recent Research. *Molecules* **2021**, *26* (1), No. 25.
(21) Kim, J.; Jeon, O. C.; Moon, H. T.; Hwang, S. R.; Byun, Y. Preclinical Safety Evaluation of Low Molecular Weight Heparin-Deoxycholate Conjugates as an Oral Anticoagulant: Preclinical Safety Evaluation of Oral Heparin-Deoxycholate Conjugates. *J. Appl. Toxicol.* **2016**, *36* (1), 76−93.
(22) Marchesi, E.; Gentili, V.; Bortolotti, D.; Preti, L.; Marchetti, P.; Cristofori, V.; Fantinati, A.; Rizzo, R.; Trapella, C.; Perrone, D.; Navacchia, M. L. Dihydroartemisinin-Ursodeoxycholic Bile Acid Hybrids in the Fight against SARS-CoV-2. *ACS Omega* **2023**, *8* (47), 45078−45087.
(23) Mehiri, M.; Jing, B.; Ringhoff, D.; Janout, V.; Cassimeris, L.; Regen, S. L. Cellular Entry and Nuclear Targeting By a Highly Anionic Molecular Umbrella. *Bioconjugate Chem.* **2008**, *19* (8), 1510−1513.
(24) Singla, P.; Kaur, M.; Kumari, A.; Kumari, L.; Pawar, S. V.; Singh, R.; Salunke, D. B. Facially Amphiphilic Cholic Acid-Lysine Conjugates as Promising Antimicrobials. *ACS Omega* **2020**, *5* (8), 3952−3963.
(25) Altinkok, C.; Acik, G.; Karabulut, H. R. F.; Ciftci, M.; Tasdelen, M. A.; Dag, A. Synthesis and Characterization of Bile Acid-Based Polymeric Micelle as a Drug Carrier for Doxorubicin. *Polym. Adv. Technol.* **2021**, *32* (12), 4860−4868.
(26) Hein, J. E.; Fokin, V. V. Copper−Catalyzed Azide−Alkyne Cycloaddition (CuAAC) and beyond: New Reactivity of Copper(I) Acetylides. *Chem. Soc. Rev.* **2010**, *39* (4), 1302−1315.
(27) González-Olvera, R.; Urquiza-Castro, C. I.; Negrón-Silva, G. E.; Ángeles-Beltrán, D.; Lomas-Romero, L.; Gutiérrez-Carrillo, A.; Lara, V. H.; Santillan, R.; Morales-Serna, J. A. Cu−Al Mixed Oxide Catalysts for Azide−Alkyne 1,3-Cycloaddition in Ethanol−Water. *RSC Adv.* **2016**, *6* (68), 63660−63666.
(28) Tron, G. C.; Pirali, T.; Billington, R. A.; Canonico, P. L.; Sorba, G.; Genazzani, A. A. Click Chemistry Reactions in Medicinal

Chemistry: Applications of the 1,3-Dipolar Cycloaddition between Azides and Alkynes. *Med. Res. Rev.* **2008**, *28* (2), 278−308, DOI: 10.1002/med.20107.
(29) Aflak, N.; El Ayouchia, H. B.; Bahsis, L.; El Mouchtari, E. M.; Julve, M.; Rafqah, S.; Anane, H.; Stiriba, S. E. Sustainable Construction of Heterocyclic 1,2,3-Triazoles by Strict Click [3 + 2] Cycloaddition Reactions Between Azides and Alkynes on Copper/Carbon in Water. *Front. Chem.* **2019**, *7*, No. 81.
(30) Hammouda, M. M.; Elattar, K. M.; Rashed, M. M.; Osman, A. M. A. Synthesis, biological activities, and future perspecitives of steroidal monocyclic pyridines. *RSC Med. Chem.* **2023**, *14* (10), 1934−1972.
(31) Simić, S.; Zukić, E.; Schmermund, L.; Faber, K.; Winkler, C. K.; Kroutil, L. Shortening synthetic routes to small molecule active pharmaceutical ingredients employing biocatalytic methods. *Chem. Rev.* **2022**, *122*, 1052−1126.
(32) Gregorić, T.; Sedić, M.; Grbčić, P.; Paravić, A. T.; Kraljević Pavelić, S.; Cetina, M.; Vianello, R.; Raić-Malić, S. Novel Pyrimidine-2,4-Dione−1,2,3-Triazole and Furo[2,3-*d*]Pyrimidine-2-One−1,2,3-Triazole Hybrids as Potential Anti-Cancer Agents: Synthesis, Computational and X-Ray Analysis and Biological Evaluation. *Eur. J. Med. Chem.* **2017**, *125*, 1247−1267.
(33) Kumar, K.; Sagar, S.; Esau, L.; Kaur, M.; Kumar, V. Synthesis of Novel 1*H*-1,2,3-Triazole Tethered C-5 Substituted Uracil−Isatin Conjugates and Their Cytotoxic Evaluation. *Eur. J. Med. Chem.* **2012**, *58*, 153−159.
(34) Miyakoshi, H.; Miyahara, S.; Yokogawa, T.; Endoh, K.; Muto, T.; Yano, W.; Wakasa, T.; Ueno, H.; Chong, K. T.; Taguchi, J.; Nomura, M.; Takao, Y.; Fujioka, A.; Hashimoto, A.; Itou, K.; Yamamura, K.; Shuto, S.; Nagasawa, H.; Fukuoka, M. 1,2,3-Triazole-Containing Uracil Derivatives with Excellent Pharmacokinetics as a Novel Class of Potent Human Deoxyuridine Triphosphatase Inhibitors. *J. Med. Chem.* **2012**, *55* (14), 6427−6437.
(35) Lahmidi, S.; Anouar, E. H.; El Hamdaoui, L.; Ouzidan, Y.; Kaur, M.; Jasinski, J. P.; Sebbar, N. K.; Essassi, E. M.; El Moussaouiti, M. Synthesis, Crystal Structure, Spectroscopic Characterization, Hirshfeld Surface Analysis, DFT Calculations and Antibacterial Activity of Ethyl 2-(4-Vinylbenzyl)-2-(5-Methyl-[1,2,4]Triazolo[1,5-a]Pyrimidin-7-Yl)-3-(4-Vinylphenyl)Propanoate. *J. Mol. Struct.* **2019**, *1191*, 66−75.
(36) Abdelkhalek, A. S.; Attia, M. S.; Kamal, M. A. Triazolopyrimidine Derivatives: An Updated Review on Recent Advances in Synthesis, Biological Activities and Drug Delivery Aspects. *Curr. Med. Chem.* **2024**, *31* (14), 1896−1919.
(37) Kaishap, P. P.; Baruah, S.; Shekarrao, K.; Gogoi, S.; Boruah, R. C. A Facile Method for the Synthesis of Steroidal and Nonsteroidal 5-Methyl Pyrazolo[1,5-*a*]Pyrimidines. *Tetrahedron Lett.* **2014**, *55* (19), 3117−3121.
(38) Romero-López, A.; Montiel-Smith, S.; Meza-Reyes, S.; Merino-Montiel, P.; Vega-Baez, J. L. Synthesis of Steroidal Derivatives Containing Substituted, Fused and Spiro Pyrazolines. *Steroids* **2014**, *87*, 86−92.
(39) Monier, M.; El-Mekabaty, A.; Abdel-Latif, D.; Mert, B. D.; Elattar, K. M. Heterocylic steroids: Efficient routes for annulation of pentacyclic steroidal pyrimidines. *Steroids* **2020**, *154*, No. 108548.
(40) Agarwal, D. S.; Krishna, V. S.; Sriram, D.; Yogeeswari, P.; Sakhuja, R. Clickable Conjugates of Bile Acids and Nucleosides: Synthesis, Characterization, in Vitro Anti-cancer and Antituberculosis Studies. *Steroids* **2018**, *139*, 35−44.
(41) Corrales, R. C. N. R.; de Souza, N. B.; Pinheiro, L. S.; Abramo, C.; Coimbra, E. S.; Da Silva, A. D. Thiopurine Derivatives Containing Triazole and Steroid: Synthesis, Antimalarial and Antileishmanial Activities. *Biomed. Pharmacother.* **2011**, *65* (3), 198−203.
(42) Negrón-Silva, G.; González-Olvera, R.; Angeles-Beltrán, D.; Maldonado-Carmona, N.; Espinoza-Vázquez, A.; Palomar-Pardavé, M. E.; Romero-Romo, M. A.; Santillan, R. Synthesis of New 1,2,3-Triazole Derivatives of Uracil and Thymine with Potential Inhibitory Activity against Acidic Corrosion of Steels. *Molecules* **2013**, *18* (4), 4613−4627.
(43) *CAChe 5.04 UserGuide*; Fujitsu: Chiba, Japan, 2003.
(44) Stewart, J. J. P. Optimization of parameters for semiempirical methods. III Extension of PM3 to Be, Mg, Zn, Ga, Ge, As, Se, Cd, In, Sn, Sb, Te, Hg, Tl, Pb, and Bi. *J. Comput. Chem.* **1991**, *12*, 320−341.
(45) Stewart, J. J. P. Optimization of parameters for semiempirical methods I. Method. *J. Comput. Chem.* **1989**, *10*, 209−220.
(46) Kawka, A.; Hajdaś, G.; Kułaga, D.; Koenig, H.; Kowalczyk, I.; Pospieszny, T. Molecular Structure, Spectral and Theoretical Study of New Type Bile Acid−Sterol Conjugates Linked via 1,2,3-Triazole Ring. *J. Mol. Struct.* **2023**, *1273*, No. 134313.
(47) Pospieszny, T. Design and Synthesis of New Bile Acid−Sterol Conjugates Linked *via* 1,2,3-Triazole Ring. *Helv. Chim. Acta* **2015**, *98* (10), 1337−1350.
(48) Hakimelahi, G. H.; Gassanov, G. S.; Hsu, M.-H.; Hwu, J. R.; Hakimelahi, S. A Novel Approach towards Studying Non-Genotoxic Enediynes as Potential Anti-cancer Therapeutics. *Bioorg. Med. Chem.* **2002**, *10*, 1321−1328.
(49) Pharma Expert Predictive Services ©20112013, Version 2.0. http://www.pharmaexpert.ru/PASSOnline/.
(50) Poroikov, V. V.; Filimonov, D. A.; Borodina, Y. V.; Lagunin, A. A.; Kos, A. Robustness of biological activity spectra predicting by computer program PASS for noncongeneric sets of chemical compounds. *J. Chem. Inf. Comput. Sci.* **2000**, *40*, 1349−1355.
(51) Poroikov, V. V.; Filimonov, D. A. How to acquire new biological activities in old compounds by computer prediction. *J. Comput.-Aided Mol. Des.* **2002**, *16*, 819−824.
(52) Poroikov, V. V.; Filimonov, D. A. *Predictive Toxicology*; Helma, C., Ed.; Taylor and Francis: Boca Raton, Florida, USA, 2005; pp 459−478.
(53) Weininger, D. SMILES, a Chemical Language and Information System. 1. Introduction to Methodology and Encoding Rules. *J. Chem. Inf. Comput. Sci.* **1988**, *28* (1), 31−36.
(54) Mortier, W. J.; Van Genechten, K.; Gasteiger, J. Electronegativity Equalization: Application and Parametrization. *J. Am. Chem. Soc.* **1985**, *107* (4), 829−835.
(55) O'Boyle, N. M.; Banck, M.; James, C. A.; et al. Open Babel: An open chemical toolbox. *J. Cheminf.* **2011**, *3*, No. 33.
(56) Open Babel Development Team. Open Babel, Version: 3.1.1. 2020 http://openbabel.org/wiki/Main_Page. (accessed on April 25, 2024).
(57) Berman, H. M. The Protein Data Bank. *Nucleic Acids Res.* **2000**, *28* (1), 235−242.
(58) Pandit, J.; Danley, D. E.; Schulte, G. K.; Mazzalupo, S. M.; Pauly, T. A.; Hayward, C. M.; Hamanaka, E. S.; Thompson, J. F.; Harwood, H. J. Crystal Structure of Human Squalene Synthase. *J. Biol. Chem.* **2000**, *275*, 30610−30617, DOI: 10.1074/jbc.m004132200.
(59) Pandit, J.; Danley, D. E.; Schulte, G. K.; Mazzalupo, S.; Pauly, T. A.; Hayward, C. M.; Hamanaka, E. S.; Thompson, J. F.; Harwood, H. J. Crystal Structure of Human Squalene Synthase. *J. Biol. Chem.* **2000**, *275* (39), 30610−30617.
(60) Lafitte, D.; Lamour, V.; Tsvetkov, P. O.; Makarov, A. A.; Klich, M.; Deprez, P.; Moras, D.; Briand, C.; Gilli, R. Crystal Structure of *E. coli* 24 kDa Domain in Complex with Clorobiocin. 2002.
(61) Lafitte, D.; Lamour, V.; Tsvetkov, P. O.; Makarov, A. A.; Klich, M.; Deprez, P.; Moras, D.; Briand, C.; Gilli, R. DNA Gyrase Interaction with Coumarin-Based Inhibitors: The Role of the Hydroxybenzoate Isopentenyl Moiety and the 5′-Methyl Group of the Noviose. *Biochemistry* **2002**, *41* (23), 7217−7223.
(62) Stavropoulos, P.; Blobel, G.; Hoelz, A. Crystal Structure of human Lysine-Specific Demethylase-1. *Nat. Struct. Mol. Biol.* **2006**, *13*, 626−632, DOI: 10.1038/nsmb1113.
(63) Stavropoulos, P.; Blobel, G.; Hoelz, A. Crystal Structure and Mechanism of Human Lysine-Specific Demethylase-1. *Nat. Struct. Mol. Biol.* **2006**, *13* (7), 626−632.
(64) Chopra, R.; Bard, J.; Svenson, K.; Mansour, T. Crystal Structure of *E. Coli* Mur B bound to a Naphthyl Tetronic Acid inihibitor. 2007.
(65) Mansour, T.; Caulfield, C. E.; Rasmussen, B.; Chopra, R.; Krishnamurthy, G.; Morris, K. M.; Svenson, K.; Bard, J.; Smeltzer, C.; Naughton, S.; Antane, S.; Yang, Y.; Severin, A.; Quagliato, D.; Petersen,

https://doi.org/10.1021/acsomega.4c04800
ACS Omega 2024, 9, 37995−38014

P. J.; Singh, G. Crystal Structure of *E. Coli* Mur B bound to a napthyl tetronic acid inhibitor. To be published.
(66) Keniya, M. V.; Sabherwal, M.; Wilson, R. K.; Sagatova, A. A.; Tyndall, J. D. A.; Monk, B. C. Structure of CYP51 from the pathogen *Candida albicans*. 2017.
(67) Keniya, M. V.; Sabherwal, M.; Wilson, R. K.; Woods, M. A.; Sagatova, A. A.; Tyndall, J. D. A.; Monk, B. C. Crystal Structures of Full-Length Lanosterol 14α-Demethylases of Prominent Fungal Pathogens *Candida albicans* and *Candida glabrata* Provide Tools for Antifungal Discovery. *Antimicrob. Agents Chemother.* **2018**, *62* (11), No. 10-1128.
(68) Morris, G. M.; Huey, R.; Lindstrom, W.; Sanner, M. F.; Belew, R. K.; Goodsell, D. S.; Olson, A. J. AutoDock4 and AutoDockTools4: Automated docking with selective receptor flexibility. *J. Comput. Chem.* **2009**, *30*, 2785−2791.
(69) Trott, O.; Olson, A. J. AutoDock Vina: Improving the speed and accuracy of docking with a new scoring function, efficient optimization, and multithreading. *J. Comput. Chem.* **2010**, *31*, 455−461.
(70) Pettersen, E. F.; Goddard, T. D.; Huang, C. C.; Couch, G. S.; Greenblatt, D. M.; Meng, E. C.; Ferrin, T. E. UCSF Chimera—A visualization system for exploratory research and analysis. *J. Comput. Chem.* **2004**, *25*, 1605−1612.
(71) Robinson, P. K. Enzymes: Principles and Biotechnological Applications. *Essays Biochem.* **2015**, *59*, 1−41.
(72) Song, J.; Shang, N.; Baig, N.; Yao, J.; Shin, C.; Kim, B. K.; Li, Q.; Malwal, S. R.; Oldfield, E.; Feng, X.; Guo, R.-T. Aspergillus Flavus Squalene Synthase as an Antifungal Target: Expression, Activity, and Inhibition. *Biochem. Biophys. Res. Commun.* **2019**, *512* (3), 517−523.
(73) Collin, F.; Karkare, S.; Maxwell, A. Exploiting Bacterial DNA Gyrase as a Drug Target: Current State and Perspectives. *Appl. Microbiol. Biotechnol.* **2011**, *92* (3), 479−497.
(74) Han, D.; Lu, J.; Fan, B.; Lu, W.; Xue, Y.; Wang, M.; Liu, T.; Cui, S.; Gao, Q.; Duan, Y.; Xu, Y. Lysine-Specific Demethylase 1 Inhibitors: A Comprehensive Review Utilizing Computer-Aided Drug Design Technologies. *Molecules* **2024**, *29*, No. 550.
(75) El Zoeiby, A.; Sanschagrin, F.; Levesque, R. C. Structure and Function of the Mur Enzymes: Development of Novel Inhibitors. *Mol. Microbiol.* **2003**, *47* (1), 1−12.
(76) Nadaraia, N. S.; Amiranashvili, L. S.; Merlani, M.; Kakhabrishvili, M. L.; Barbakadze, N. N.; Geronikaki, A.; Petrou, A.; Poroikov, V.; Ciric, A.; Glamoclija, J.; Sokovic, M. Novel Antimicrobial Agents' Discovery among the Steroid Derivatives. *Steroids* **2019**, *144*, 52−65.
(77) Hargrove, T. Y.; Friggeri, L.; Wawrzak, Z.; Qi, A.; Hoekstra, W. J.; Schotzinger, R. J.; York, J. D.; Guengerich, F. P.; Lepesheva, G. I. Structural Analyses of *Candida Albicans* Sterol 14α-Demethylase Complexed with Azole Drugs Address the Molecular Basis of Azole-Mediated Inhibition of Fungal Sterol Biosynthesis. *J. Biol. Chem.* **2017**, *292* (16), 6728−6743.
(78) Bickerton, G. R.; Paolini, G. V.; Besnard, J.; Muresan, S.; Hopkins, A. L. Quantifying the Chemical Beauty of Drugs. *Nat. Chem.* **2012**, *4* (2), 90−98.
(79) Landrum, G. RDKit: Open-Source Cheminformatics Software. 2022.
(80) Ghose, A. K.; Viswanadhan, V. N.; Wendoloski, J. J. Prediction of Hydrophobic (Lipophilic) Properties of Small Organic Molecules Using Fragmental Methods: An Analysis of ALOGP and CLOGP Methods. *J. Phys. Chem. A* **1998**, *102* (21), 3762−3772.
(81) Ramírez, D.; Caballero, J. Is It Reliable to Take the Molecular Docking Top Scoring Position as the Best Solution without Considering Available Structural Data? *Molecules* **2018**, *23*, No. 1038.

https://doi.org/10.1021/acsomega.4c04800
ACS Omega 2024, 9, 37995−38014

Chapter 8

From squalamine to triazole ring derivatives: Exploring the versatility of steroidal bioconjugates

Anna Kawka, Hanna Koenig and Tomasz Pospieszny*

Department of Bioactive Products, Faculty of Chemistry, Adam Mickiewicz University Poznań, Poland

**Corresponding author: E-mail: tposp@amu.edu.pl.*

Introduction

In recent years, there has been a significant increase in interest in technologies for isolating, synthesizing, and modifying steroid conjugates. Compounds of natural origin have a broad spectrum of physicochemical, biological, and pharmacotherapeutic properties. Progress in the design of steroid derivatives with polyamines, polyalcohols, alkaloids, or nucleobases opens the way to obtaining highly effective drugs, carriers of biomolecules, organogelators, or complex compounds. Steroid structures are becoming increasingly important in pharmacology, biomimetics, supramolecular chemistry, and medicine [1,2].

Among all natural products, steroids form a large group of compounds showing significant and diverse biological activity [3]. Sterols (e.g., cholesterol, ergosterol, and stigmasterol) are part of the cell membrane of prokaryotes and eukaryotes (Fig. 8.1) [4]. Bile acids (e.g., lithocholic, deoxycholic, and cholic) as surfactants reduce surface tension and emulsify fats. In addition, they significantly affect the solubility of cholesterol contained in bile (Fig. 8.1) [5]. Hormones (e.g., estrogens, androgens, and gestagens) are responsible for gene expression, normal protein synthesis, and the basic regulatory and modification activities of target tissues (Fig. 8.1). In contrast, brassinosteroids (brassinolide) and withanolides (e.g., vitaferin A) are hormones of plant origin (Fig. 8.1). Their primary tasks include the proper course

Studies in Natural Products Chemistry. https://doi.org/10.1016/B978-0-443-15756-1.00009-4

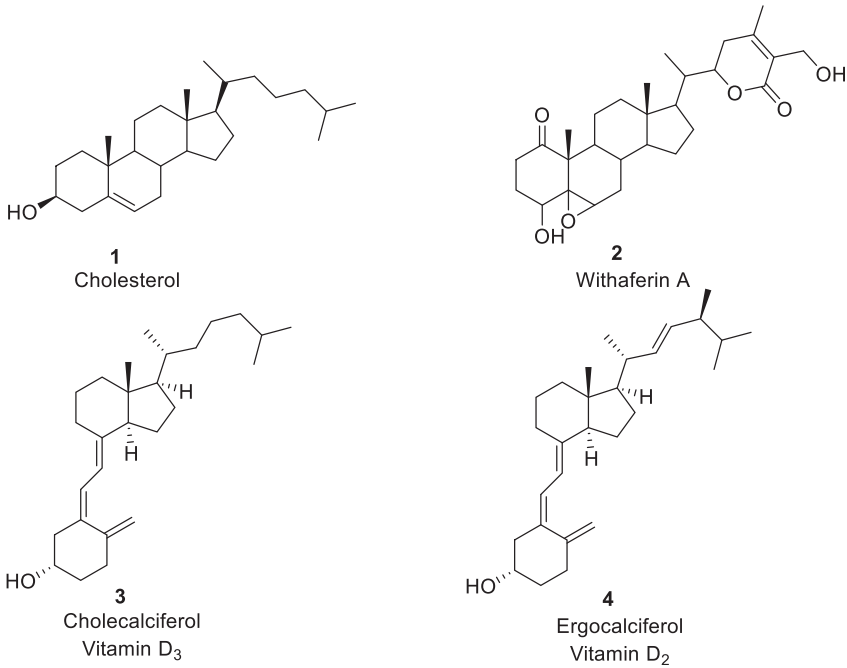

FIGURE 8.1 Structures of selected steroids [3].

of the photosynthesis process, good plant growth, or the action of other phytohormones [6,7]. Withanolides also have immunosuppressive, anticancer, antiviral, and antibacterial properties [8]. In turn, vitamin D (ergocalciferol and cholecalciferol) are responsible for the proper calcium-phosphate metabolism and maintaining the functioning and structures of the skeletal system (Fig. 8.1) [9,10].

The essential structural element of all steroids is the cyclopentano[α] perhydrophenanthrene skeleton, formed of four condensed rings A, B, C, and D. The spatial arrangement of the rings, the type of substituents, the side chains of different lengths, and the degree of unsaturation determine the diversity of steroids. The connection of the condensed A/B rings in the skeleton of 1,2-cyclopentanoperhydrophenanthrene picks the *allo* series (as in *trans*-decaline) or normal steroids (as in *cis*-decaline) (Fig. 8.2). All natural steroids usually have *trans* stereochemistry of the B/C and C/D rings [11,12].

A significant group of steroids are bile acids. Their natural biosynthesis occurs in the liver, forming products of cholesterol metabolism (among others, oxidation of cholesterol by cytochrome P450) (Scheme 8.1). Then steroid acids combine with amino acids (glycine and taurine) and are stored as salts in

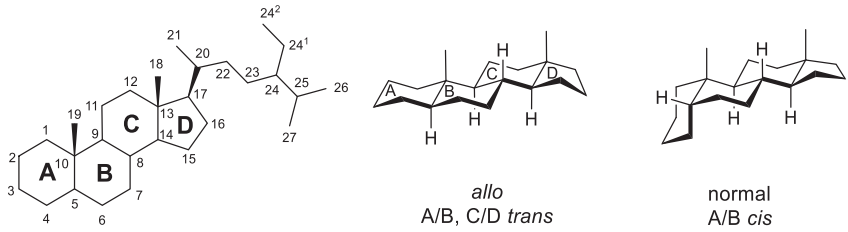

FIGURE 8.2 Atomic numbering and stereochemistry in steroid skeleton [11].

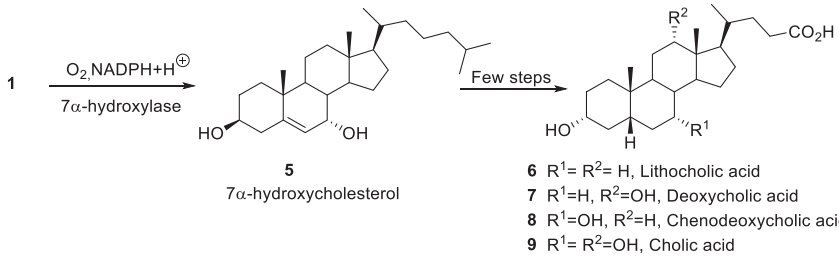

SCHEME 8.1 The part of multistep biosynthesis of bile acids [13].

the gallbladder. The resulting "primary bile acids" (glycocholic acid, taurocholic acid) undergo further modifications. Under intestinal bacteria's influence, the amino acid molecule and hydroxyl group are detached at the 7α carbon atom. This consequently leads to the preparation of deoxycholic and lithocholic acids [13,14].

All steroid acids are derived from 5β-cholan-24-oic acid [15]. Compounds of this type are characterized by the presence of hydroxyl groups (3α; 3α,7α; 3α,12α or 3α,7α,12α) and a side chain with a carboxyl group at the C-17 atom [15,16]. Due to the rigid arrangement of alicyclic rings, curved skeleton, different reactivity of hydroxyl groups, and amphipathic properties, bile acids (lithocholic, deoxycholic, and cholic) have been used in the design of new macrocyclic compounds [17–19]. The biological activity of bile acids is mainly related to their spatial structure. Therefore, they are a precursor to preparing new substances with pharmacotherapeutic properties, used as drugs in treating liver and gastrointestinal tract disease [20–25]. In addition, their derivatives are known as receptors that detect molecules in solutions (e.g., biomarkers detecting organic anions or polypeptides) and can form inclusion complexes [26,27]. Bile acids play a significant role in supramolecular chemistry. Their derivatives are the primary material for synthesizing artificial molecular receptors susceptible to detecting foreign molecules in host cells [28,29].

Squalamine as steroid-polyamine conjugate with diverse biological activities

Control and regulation of life processes in organisms are usually carried out with the help of biogenic amines. These compounds are the main products of the decarboxylation of neutral and basic amino acids essential in the biological system; biogenic amines are often found as conjugates of fundamental neurohormones.

Squalamine (**10**) is one of the most essential natural steroid-polyamine conjugates (Fig. 8.3). It was first isolated from the liver cells of spiny dogfish (*Squalus acanthias*) [31]. This aminosterol antibiotic is a bioconjugate of spermidine and 7α,24-ζ-dihydroxy-5α-cholestane 24-sulfate. It dissolves well in water thanks to a hydrophobic steroid skeleton, a polar hydroxyl group, and hydrophilic amino groups [31,32]. The specific stereochemistry and charge of squalamine allow it to penetrate the cell membrane. Thanks to this, it is possible to transport proteins associated with electrostatic interactions with the inner part of the cytoplasmic membrane. Squalamine prevents the development of Parkinson's disease by inhibiting the early aggregation of α-synuclein. It exhibits competitive effects against toxic proteins, separating α-synuclein from the membranes of synaptic vesicles responsible for the transport of neurotransmitters. Consequently, no harmful aggregates are formed, while previously formed sums become less toxic [33–36]. This compound has high biocidal activity against gram-positive, gram-negative, protozoa, fungi, and viruses (including HIV) [37–39]. In addition, squalamine slows the development of brain tumors by suppressing the growth of new blood vessels. Most

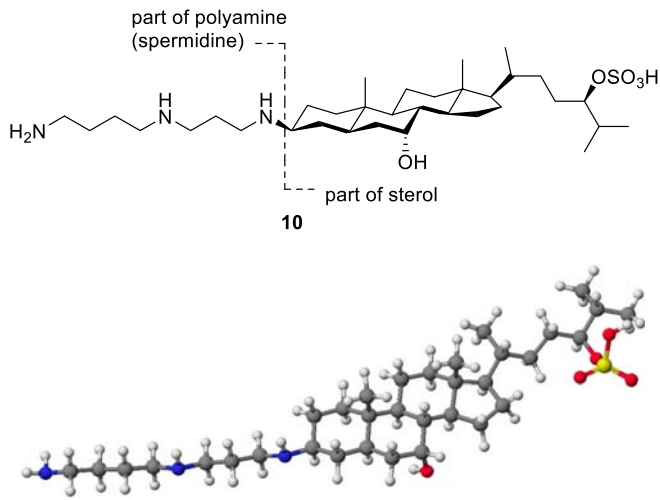

FIGURE 8.3 Squalamine and its molecular model [30].

importantly, squalamine intensifies the antitumor properties of cytotoxic agents against lung, breast, ovarian, and prostate cancers [40–46].

The antimicrobial activity of squalamine was compared with several natural peptide antibiotics, such as *Magainin-II*, CPF, and ampicillin. Table 8.1 presents the results of antimicrobial activity studies on squalamine conducted by Moore et al. [31] The activity of squalamine in inhibiting the development of candidiasis is two orders lower than for other compounds studied. The MIC value of this compound on *Candida albicans* (*C. albicans*) was 4–8 μg/mL. Most importantly, the antibiotic's action does not cause erythrocyte hemolysis [47].

Steroid-amino conjugates

Steroid-amino conjugates, often referred to as steroid-amino acid conjugates, are a class of molecules that combine a steroid skeleton with an amino acid moiety. These conjugates are a unique hybrid molecule that merges the biological activities of steroids and amino acids. The conjugation of steroids with amino acids can alter their properties, such as solubility and bioavailability, and may lead to distinct biological activities. Steroid-amino conjugates have been of interest in medicinal chemistry and drug development due to their potential to enhance the therapeutic effects or targeting of steroids while minimizing their side effects. These conjugates can also serve as valuable research tools to study the interactions between steroids and amino acids in biological systems.

Consequently, there are many reports in the chemical literature concerning the synthesis of squalamine and its derivatives [48–55]. The main criterion for the synthesis of biologically active steroid-polyamine conjugates is based on a rigid hydrophobic "tail" and an adjustable hydrophilic chain with a polar hydroxyl group constituting the "head" [56]. In turn, hydroxyl or carboxylate groups can easily remove or replace the current sulfate groups. However, only the steroid part is susceptible to modification [56].

Kim et al. synthesized an analog of squalamine from bisnoralcohol (**11**) (Scheme 8.2). The compound (**13**) showed significant activity against *M. luteus* 9341, *Staphylococcus aureus* (*S. aureus*) 6538P, *K. pneumoniae* 10031, *S. equi* 6580C, and *B. subtilis* 6633. However, it was inactive against *Escherichia coli* (*E. coli*) 25922, *P. aeruginosa* 27853, *P. mirabilis* 25933, *S. marcescens* 27117, and *S. typhimurium* 14028. It should be emphasized that the antibacterial activity of the compound (**13**) is lower than that of squalamine [57].

Shu et al. obtained squalamine derivatives with a side chain modified with an amino (**14**) or hydroxyl (**15**) group [58]. In contrast, stereoselective synthesis of new squalamine derivatives with transformations in the B ring led to compounds (**16**) and (**17**) [59]. It is worth noting that the above conjugates manifested similar biocidal properties to squalamine (Fig. 8.4).

TABLE 8.1 Antimicrobial activity of squalamine and other selected biologically active compounds [31].

Compound	Antimicrobial activity (MIC), μg/mL							
	(1)	*(2)*	*(3)*	*(4)*	*(5)*	*(6)*	*(7)*	*(8)*
Squalamine	1–2	4–8	1–2	1–2	4–8	>125	4–8	4–8
CHAPS (detergent)	>500	>500	>500	250–500	>500	>500	>500	>260
Taurolithocholic acid 3-sulfate	>500	>500	>500	>500	>500	>500	>500	>260
Spermidine	>500	>500	>500	250–500	>500	>500	>500	>260
Melittin (disambiguation)	8–16	16–31	8–16	4–16	16–31	>250	16–31	2–4
Magainin-II amide	31–62	31–62	>250	>250	125–250	>250	125–250	33–65
Amide-CPF	8–16	8–31	8–16	31–62	62–125	>125	62–125	4–8
Conessine	>500	>500	>500	>500	>500	>500	31–62	16–33
Holothurin	>500	>500	>500	>250	>500	>500	>500	130–260
Ampicillin	2–4	62–125	<1	<125	8–16	4–62	>125	>65

(1) *Escherichia coli*; (2) *Pseudomonas aeruginosa*; (3) *Staphylococcus aureus*; (4) *Streptococcus faecalis*; (5) *Proteus vulgaris*; (6) *Serratia marcescens*; (7) *Candida albicans*; (8) *Paramecium caudatum*.

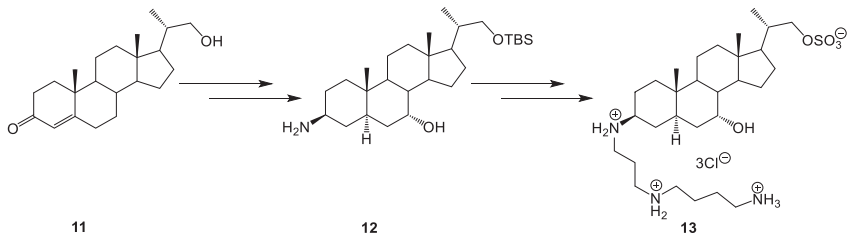

SCHEME 8.2 Synthesis of a squalamine analog (**13**) [57].

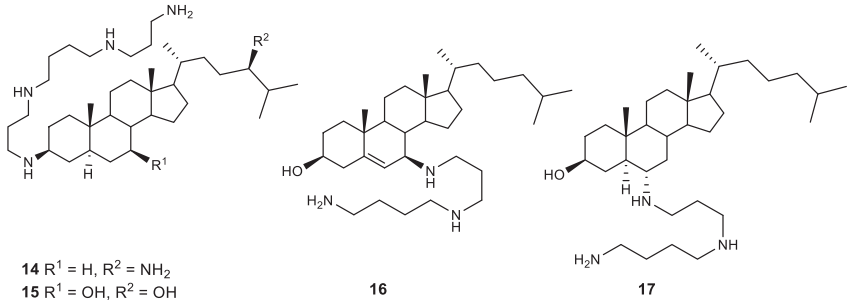

FIGURE 8.4 Synthetic derivatives of squalamine (**14**–**17**) [58,59].

The synthesis of many new squalamine derivatives distinguished by significant biological activity was developed by Kim et al. Their study included the effect of stereochemistry at the C(3)/C(5) position of the steroid ring on the lethality of pathogens. The type of polyamine attached to the steroid A ring's C(3) position was also important. The obtained conjugates showed antiseptic solid activity. All 3α (or β)-aminosteroids were characterized by considerable in vitro activity against gram-positive bacteria. Notably, compound (**25**) with a configuration of 3β, 5β and a polyamine chain containing four ammonium groups at the C(3) position of the steroid A ring showed the most muscular toxicity against *S. aureus* ATCC25923P, *M. luteus* ATCC9341, and *B. subtilis* ATCC6633. The highest biocidal activity against *S. aureus* ATCC25923P was demonstrated by the compound (**18**) among the 3α, 5α configurations. Conjugates (**20**, **24**) with a 3α, 5β configuration had less antibacterial activity (Fig. 8.5) [60].

Several new synthetic derivatives of squalamine were presented by Brunel and Letourneux [61,62]. Similarly, the biological activity of conjugates is determined by the stereochemistry of sterols and the chain length of the attached polyamine (spermine or spermidine) to the C(3) position of the steroid skeleton. A stereoisomer with a 3β configuration exhibits much better biocidal properties than a 3α compound (Fig. 8.6).

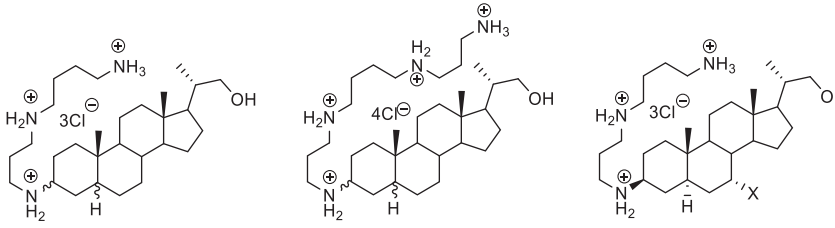

18 3α,5α; **19** 3β,5α
20 3α,5β; **21** 3β,5β

22 3α,5α; **23** 3β,5α
24 3α,5β; **25** 3β,5β

26 X = OH;
27 X = F
28 X = $NH_3^{\oplus}$

FIGURE 8.5 Synthetic steroid-polyamine conjugates (**18**–**28**) [60].

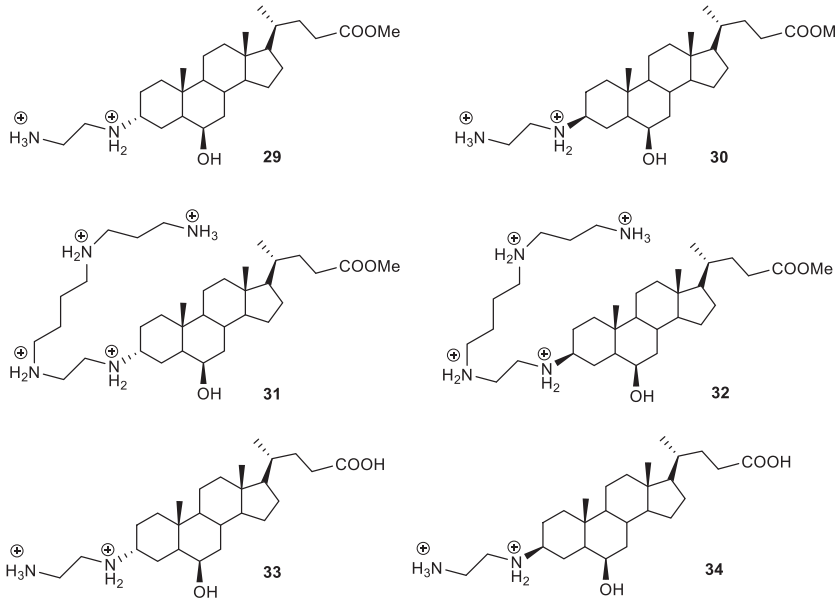

FIGURE 8.6 Analogs of squalamine (**29**–**34**) [61,62].

Rao et al. described novel squalamine derivatives isolated from dogfish liver cells (Fig. 8.7) [63]. Their content in liver cells was much lower (20–100 mg) than the concentration of squalamine (400–800 mg). Still, their antibacterial activity was equally interesting. The structure of all conjugates (**35**–**41**) was determined using spectral methods (2D NMR, HR FAB-MS).

Table 8.2 presents the activity of isolated aminosterols and squalamine against selected microbial species. The lowest aseptic activity was shown by

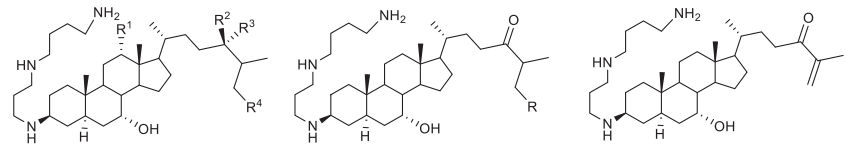

35 R^1 = H, R^2 = OH, R^3 = H, R^4 = OSO_3H
36 R^1 = OH, R^2 = OSO_3H, R^3 = H, R^4 = H
37 R^1 = H, R^2 = OSO_3H, R^3 = CH_2OH, R^4 = H
38 R^1 = H, R^2 = OSO_3H, R^3 = R^4 = H

39 R = $SCH_2CH(NH_2)CO_2H$
40 R = OSO_3H,

41

FIGURE 8.7 Natural analogs of squalamine (**35**–**41**) [63].

TABLE 8.2 MIC of squalamine and selected aminosterols [63].

	MIC μg/mL			
Compound	*S. aureus*	*E. coli*	*P. aeruginosa*	*C. albicans*
35	4–8	128	32	16
36	8–16	16	16	32
37	2	8	16	32
38	1	4	16	16
39	8–16	256	256	128
40	8	128	128	32
41	2	16	16	2
Squalamine	1	4	16	16

conjugate (**39**). The compounds (**35**, **40**) showed weak activity against *E. coli* and *P. aeruginosa*.

A series of analogs (**43**–**52**) of the MSI-1436 conjugate has been characterized by Shu et al. [58]. The multistep (9–13 steps) and compelling synthesis of compounds confirmed the critical influence of stereochemistry at the C(3) and C(7) positions on their biological activity. Notably, the change in stereochemistry at the carbon atom C(24) of the side chain had a negligible effect on bioactivity (Fig. 8.8).

Conjugates of steroid-polyamine with antimicrobial activities

Innovative methods enable the efficient synthesis of steroid conjugates with different pharmacological activities. The conjugation reaction of cholesteryl

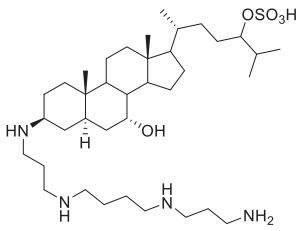

42

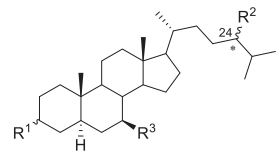

C(24) mixed isomers

43 R^1 = α–spermine, R^2= NH_2, R^3 = H
44 R^1 = β–spermine, R^2= NH_2, R^3 = H
45 R^1 = α–spermine, R^2= OH, R^3 = H
46 R^1 = β–spermine, R^2= OH, R^3 = H
47 R^1 = α–spermine, R^2= OH, R^3 = OH
48 R^1 = β–spermine, R^2= OH, R^3 = OH

C(24) stereoisomer

49 R^1 = α–spermine, R^2= (*R*)OH, R^3 = OH
50 R^1 = β–spermine, R^2= (*R*)OH, R^3 = OH
51 R^1 = α–spermine, R^2= (*R*)OSO_3H, R^3 = OH
52 R^1 = β–spermine, R^2= (*R*)OSO_3H, R^3 = OH

FIGURE 8.8 Structure of MSI-1436 (**42**) and its analogs (**43**–**52**) [58].

ester (**53**) and 5′-azido-5′-deoxythymidine (**54**) using "click" chemistry allows obtaining compounds that enhance the uptake of oligonucleotides by the cell (Scheme 8.3). In addition, as carriers, they transmit them inside the cell. Instead, conjugates (**55**, **56**) effectively inhibit hepatitis C [64,65].

It is worth noting that steroid-polyamine conjugates are also used in other fields of medicine than combating microorganisms. In vitro and in vivo studies have shown that Genzyme GL-67 (**57**) and bis(guanidine)tren-cholesterol (**58**) are highly effective in gene transfection (Fig. 8.9) [66,67].

Gołebiewski et al. described using cosalane (**59**) as a highly effective agent against HIV-1 and HIV-2 [68–70]. Cell membranes can be chemically altered to facilitate the uptake of macromolecules. Peterson's research group obtained a conjugate (**60**), allowing antibody uptake and forming protein complexes bound in mammalian cells [70]. They also effectively synthesized

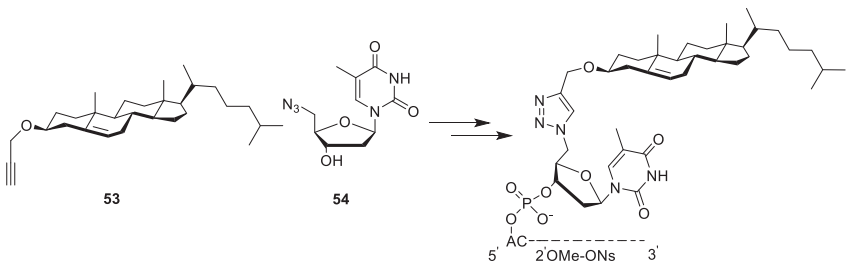

53 **54**

55 LON^{Chol}: 3'-CGGCUCAUCACAACCCAT^{Chol}-5'
56 LON^{Chol}: 3'F*-CGGCUCAUCACAACCCAT^{Chol}-5'
F*: fluorescent element

SCHEME 8.3 Synthesis of conjugates (**55**) and (**56**) inhibiting the development of HCV [64,65].

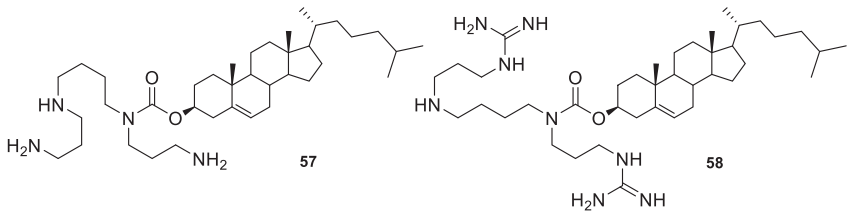

FIGURE 8.9 Spermidine and guanidine-cholesterol conjugates [66,67].

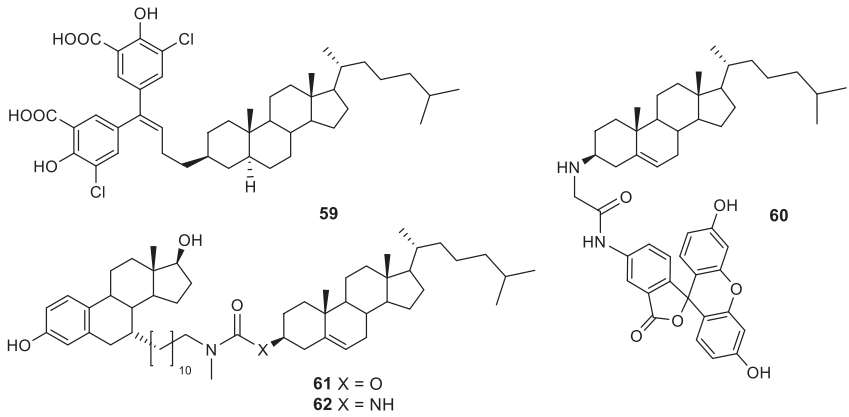

FIGURE 8.10 Steroid conjugates with different biological activity [68].

7α-substituted, cholesterol-modified derivatives of β-estradiol (**61**) and (**62**) (Fig. 8.10). These compounds showed a significant affinity for estrogen receptors [71,72].

Degteva et al. designed the synthesis of *p*-[*N*,*N*-bis-(2-chloroethyl)amino] phenylacetate 3β-hydroxy-5-cholestane (**63**), which was characterized by vigorous antitumor activity [73]. In turn, the compound (**64**) described by Ji et al. selectively delivers boron atoms to cancer cells [74]. Wall et al. synthesized a conjugate (**65**) that showed high activity against various tumors and leukemia (Fig. 8.11) [75].

Synthesis of steroid's organogels

Conjugate (**66**) was also effectively obtained, the structure of which is similar to cationic surfactants commonly used in the polycondensation reaction (Fig. 8.12). This compound exhibited significant gelling properties [76].

In turn, Ono, Jung, et al. designed the synthesis of a gelator (**67**) made of cholesterol structure and corona ether moiety [77–79]. This compound

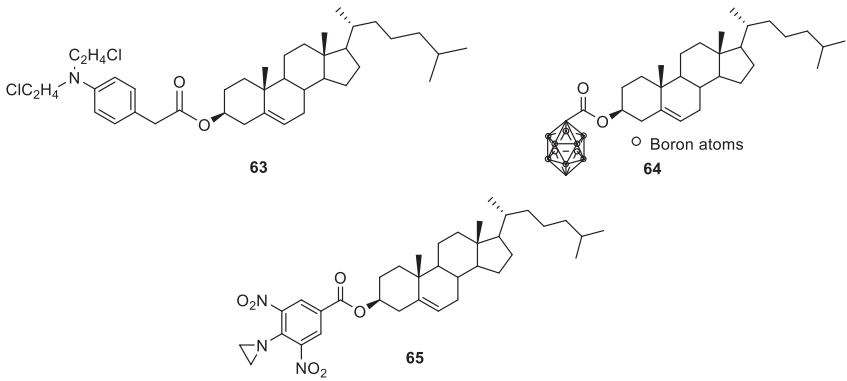

FIGURE 8.11 Biologically active steroid conjugates [73–75].

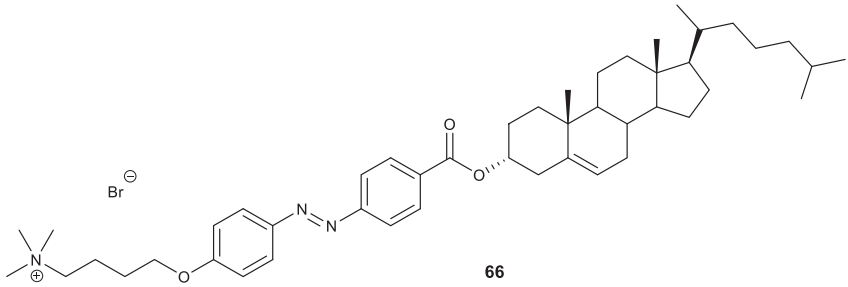

FIGURE 8.12 Steroid conjugate with gelling properties [76].

showed good selectivity toward the binding of potassium ions. It did not form complexes with lithium, sodium, rubidium, or cesium ions. Another conjugate (**68**) containing corona ether aza was used as a template for the polycondensation reaction sol-gel (Fig. 8.13). Importantly, it formed only in the presence of metals, and in their absence, it assumed a granular structure [80].

Studies on the structure and biological properties of squalamine and its analogs provided data on the formation of new compounds with pharmacological potential. Compounds of this type should be characterized by a giant, rigid hydrophobic skeleton that is easily modified and a polar hydrophilic chain. The structure of polyamine is not essential. In contrast, the sulfone group can be easily replaced by another group (carboxyl or hydroxyl) or removed. The stereochemistry of the polyamine chain at the C(3), C(5), and C(7) positions of the steroid has a crucial influence on biological activity (Fig. 8.14). Many literature papers have analyzed the strong biocidal properties of squalamine and its derivatives [56,81,82].

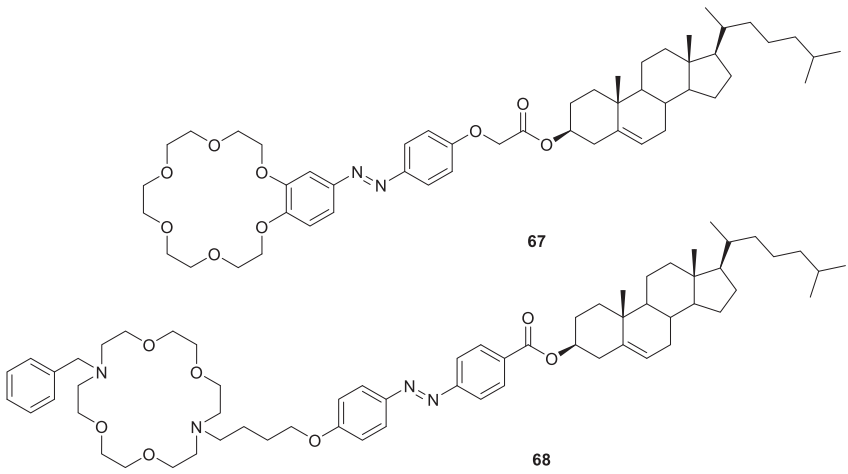

FIGURE 8.13 Steroid conjugates exhibit selective reactivity to cations [77–80].

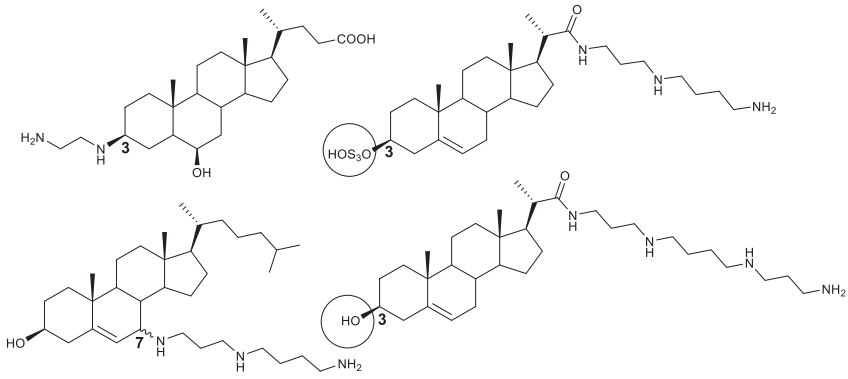

FIGURE 8.14 Selected structures with group modification.

Bile acid conjugates by the "click" chemistry method

The "click" chemistry is a relatively new and desirable method of modern organic synthesis. The products of this reaction are stable in solvents of different polarities (e.g., in water) and resistant to oxidation, reduction, or metabolic degradation. In addition, 1,2,3-triazole rings are very often involved in forming hydrogen bonds. As a consequence, the durability of the tested system increases. Crucial is the method using catalytic amounts of Cu(I) in 1,3-dipolar cycloaddition, also called the Huisgen reaction (Scheme 8.4). This straightforward way of synthesizing 1,2,3-triazole rings uses terminal alkynes

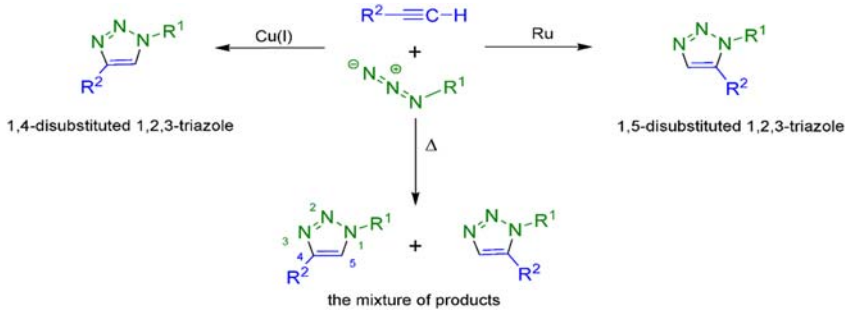

SCHEME 8.4 The reaction of formation of 1,4- and/or 1,5-disubstituted 1,2,3-triazole [87].

and azides as reactants [83,84]. The Huisgen reaction's use in forming macromolecular bile acid derivatives is exceptionally functional [85,86].

A rigid skeleton, high activity of polar hydroxyl and carboxyl groups, and amphipathic characteristics distinguish bile acids. Several valuable properties determine their massive impact on the pharmaceutical industry. Steroid acids are an excellent biological material used to synthesize macrocyclic compounds (e.g., molecular pincers), elements of the structure of organisms, or fluconazole derivatives [88–91].

Fluconazole (**69**) is a potent medicinal substance with antifungal and antimicrobial properties (Fig. 8.15). It consists of a triazole ring bound to fluoridated benzene and contains a hydroxide group. Due to the increasing drug resistance of bacteria and the decrease in its effectiveness, it was necessary to modify the structure of fluconazole. The synthesis of new fluconazole derivatives was performed using the amphiphilic properties of bile acids. A conjugate of deoxycholic acid (**71**,**73**) and cholic acid (**72**,**74**) was obtained, connected with a 1,2,3-triazole ring to a drug molecule (Fig. 8.16). According to the assumption, the bile acid unit acts as a carrier of the drug substance. At the same time, fluconazole is an inhibitor of the enzymes of the relevant bacterial strains. The new structure has gained many benefits from the possibility of hydrogen bond formation. However, from a biological perspective, exceptional resistance to metabolic degradation was an additional

FIGURE 8.15 Fluconazole (**69**) and its alkyne derivative (**70**) [88].

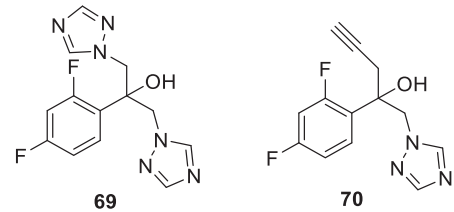

69 **70**

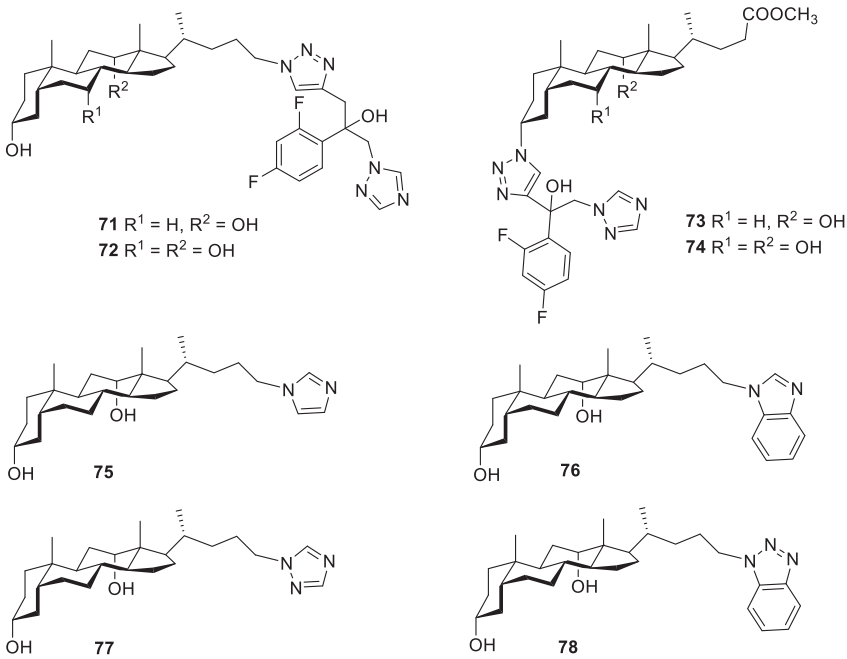

FIGURE 8.16 Bile acid and fluconazole conjugate with antifungal properties [90–92].

attribute. Most importantly, the biocidal compounds obtained showed almost 100% lethality against microorganisms belonging to *Candida* strains, such as *C. parapsilosis*, *C. albicans,* and *Sporothrix schenckii* [90–92]. The novel bioconjugates (**71–74**) exhibited antifungal activity in the MIC range of 3.12–6.25 mg/mL [90]. In contrast, a molecule of imidazole/benzimidazole (**75/76**) or triazole/benzotriazole (**77/78**) attached in the C-24 position of bile acid showed slight antifungal activity (Fig. 8.16).

Bile acids-purine with antiparasitic activity

Corrales et al. obtained new cholic acid and 6-thiopurine derivatives linked by a 1,2,3-triazole system [93]. Based on in vivo studies, compounds with higher antimalarial activity than chloroquine were evaluated (**79–82**). In vitro evaluation confirmed the excellent training of the compound (**83**) against Leishman's parasite (Fig. 8.17). Notably, the synthesized derivatives are nontoxic to the mammal's cells. The lack of cytotoxicity was most likely due to intracellular biochemical or metabolic differences in parasite-host cells [94]. From an anatomical perspective, mammalian cells are enriched with drug outflow pumps, thanks to which it is possible to transport lipophilic nucleoside analogs

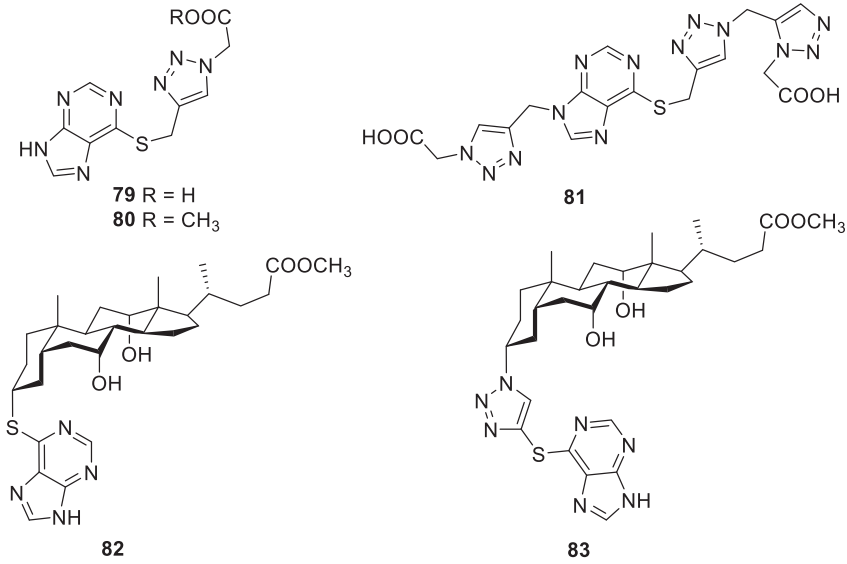

FIGURE 8.17 Steroid-thiopurine conjugates with antiparasitic activity [93–95].

outside the cell. That is why thiopurine-steroid conjugates are distinguished by considerable activity against malaria or antileishmanial. In turn, derivatives of 1,2,3-triazoles (**79**, **81**, **82**) were also obtained by 1,3-dipolar cycloaddition of final alkynes to the azide group in a molecule of acetic acid or cholic acid in the presence of Cu(I) and DMSO [95]. The condensation compound (**83**) showed antimalarial activity similar to chloroquine at the same dose on days 7 and 9. In contrast, after 12 days, all the new bioconjugates showed more excellent biocidal activity than chloroquine [96].

Antinarelli et al. obtained amino choline-steroid conjugates with considerable activity against the Leishman parasite and *Mycobacterium tuberculosis* (*M. tuberculosis*) than similar intermediate alkyne structures. An excellent percentage of inhibition against *M. tuberculosis* (MIC = 8.8 μM) was obtained for the compound (**84**), which can be compared with the activity of popular *antituberculosis* drugs. In addition, all new conjugates (**85–87**) exhibited potent toxicity to *promastigote* and *amastigota L. major*, leishmanicidal, and antituberculosis effects, indicating the great potential of steroids as drug carriers (Scheme 8.5) [97].

Synthesis of bile acids-nucleosides derivatives with 1,2,3-triazole rings

Efficient synthesis of new bile acid conjugates and nucleosides connected by a 1,2,3-triazole ring was also carried out (Scheme 8.6). Based on in vitro

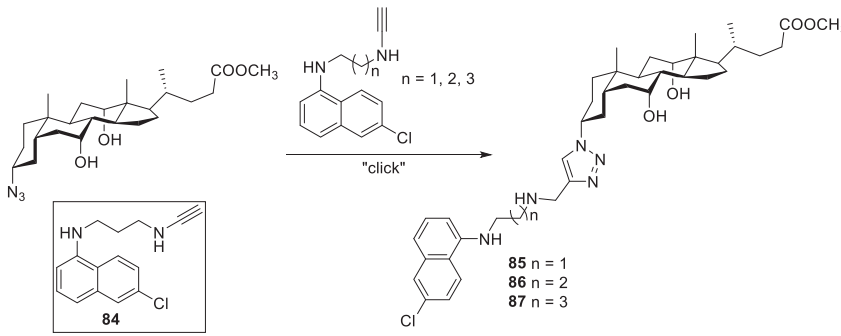

SCHEME 8.5 Synthesis of amino choline and cholic acid conjugates [97].

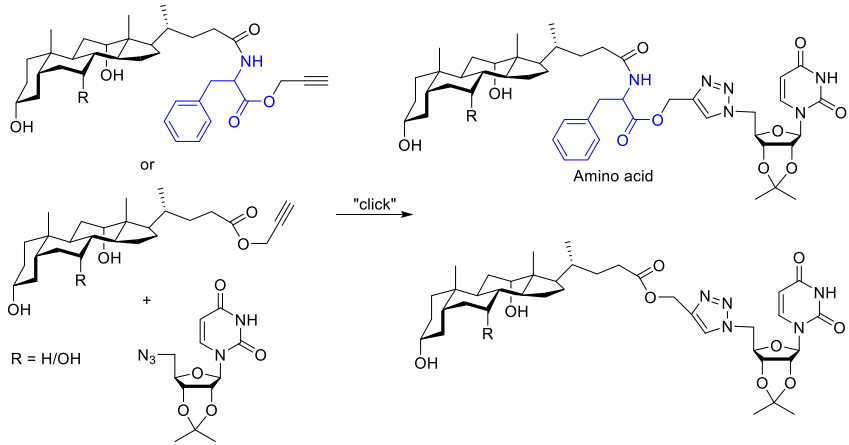

SCHEME 8.6 Synthesis of steroid-uridine triazole derivatives [98].

metabolism, their antitumor activity against three cancer cell lines, PC-3, MCF-7, and IMR-32, and antimycobacterial activity against *M. tuberculosis* H37Rv (ATCC strain 27294) were estimated.

The highest activity against MCF-7 and IMR-32 (ICP = 8.084 and 8.71 μM, respectively) was shown by the compounds cholic acid-uridine-triazole (**91**) and cholic acid-uridine-triazole linked by the phenylalanine moiety (**89**). In contrast, the conjugate deoxycholic acid-adenosine triazole (**92**) was distinguished by the best antituberculosis properties (MIC = 4.09 μM). The new products (**88**–**95**) showed no toxicity to the average human embryonic kidney cell line (HEK 293 T) (Fig. 8.18). In vitro evaluation confirmed their significant antitumor and antituberculous potential [98].

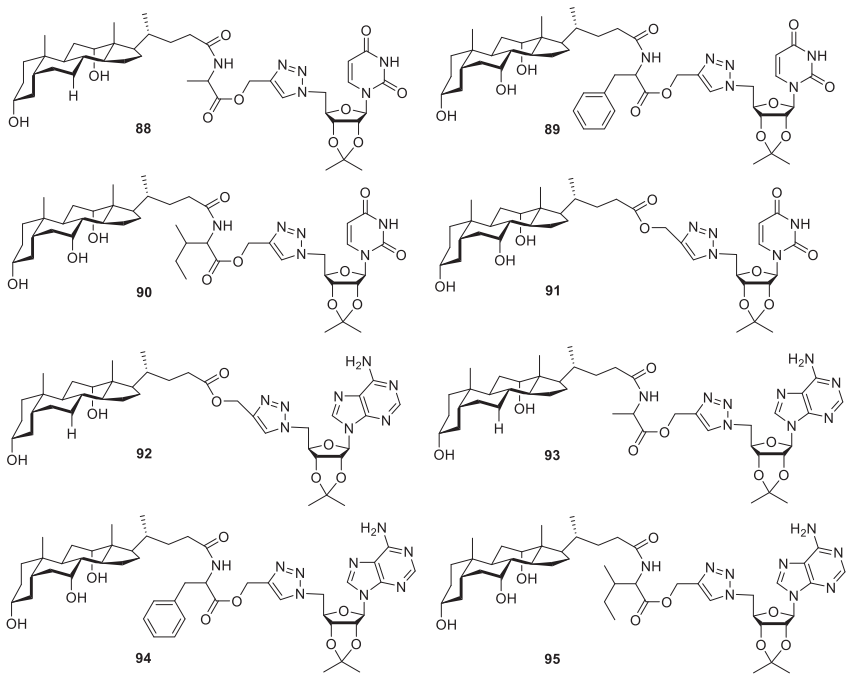

FIGURE 8.18 Conjugates bile acid-nucleoside containing 1,2,3-triazole rings [98].

Synthesis of macrocycles with 1,2,3-triazole rings

Steroids are made of rigid chiral tetras of the acyclic core. Due to curved structures, amphiphilicity, and unequal polarity, hydrophilic and hydrophobic ends can form self-assembling micelles (Fig. 8.19). Modifying hydroxyl or carboxyl groups through esterification, etherification, oxidation, or reduction strives to design new structures with a wide range of applications. Pharmacological conjugates, chemical sensors, biosensors, drug precursors, and molecular carriers are particularly important [99].

Chemoselective 1,3-dipolar azide-alkyne cycloaddition (CuAAC) is an attractive building block for joining to synthesize macrocyclic structures such as clusters, dendrimers, polymers, or polypeptides. In addition, the chemical inertness of the triazole ring significantly affects their physicochemical properties, such as blocking parts of the molecule, polarity, or susceptibility to interaction with the "guest."

Khaligh et al. synthesized menthol conjugation with bile acids using "click" chemistry. Methylated menthol was reacted with sodium azide in DMF, while efficient esterification of bile acid with propargyl bromide in the presence of potassium carbonate gave a second reactant to form 1,2,3-triazole.

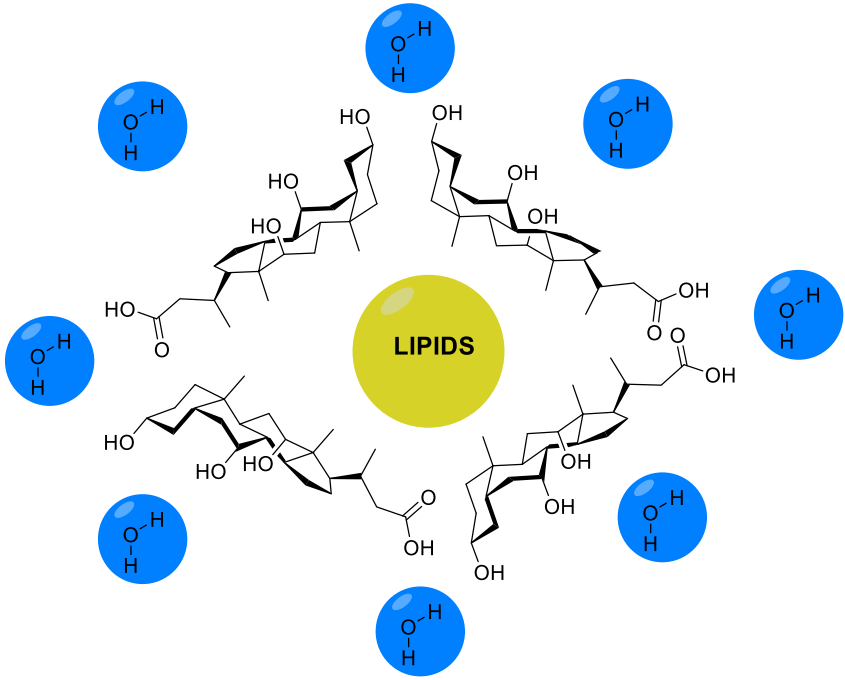

FIGURE 8.19 Bile acids form micelles.

The conjugates obtained by the "click" reaction (**96**–**98**) were evaluated for biological activity (Scheme 8.7). In vitro studies have shown that their antibacterial activity against *Enterococcus faecium* is higher (MIC < 10 μM) than for menthol (MIC = 410 μM), free bile acids (MIC = 10, 20, 157, 410 μM), and even the strong antibiotic cefixime (MIC = 35410 μm) [100].

The "click" chemistry method was also used to obtain dimers of deoxycholic acid derivatives (Scheme 8.8) [101]. The introduction of the azide group took place successively by securing hydroxyl groups (**99**), reducing the carboxyl group, and reacting nucleophilic S_N2 with sodium azide (**100**). In contrast, the propargyl ester (**101**) was formed under the Mitsunobu reaction conditions. The steroid dimer (**102**) was subjected to calculations (PM3, CaChe Fujitsu). It was found that the conformer in orientation was more energy stable than the *anti*conformer in direction.

Anandkumar et al. synthesized steroidal "molecular pocket" type dendrimers with excellent anticancer activity (Scheme 8.9) [102]. First-generation chlorodendrimers were formed by a "click" reaction from 1,3,5-tris(aminomethyl)arene and 3,1 equivalent to 1,3-bis(chloromethyl)-5-(propargyl oxy)-benzene. Subsequently, it was converted into suitable

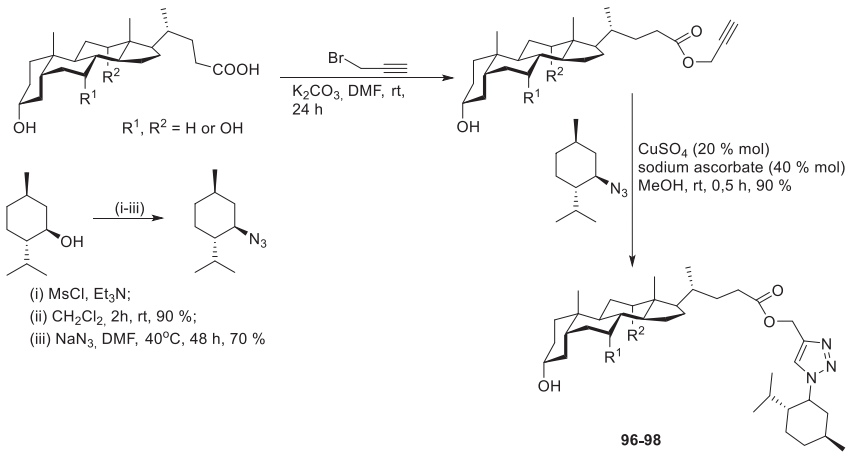

SCHEME 8.7 Bile acid and menthol bioconjugate preparation (**96**–**98**) [100].

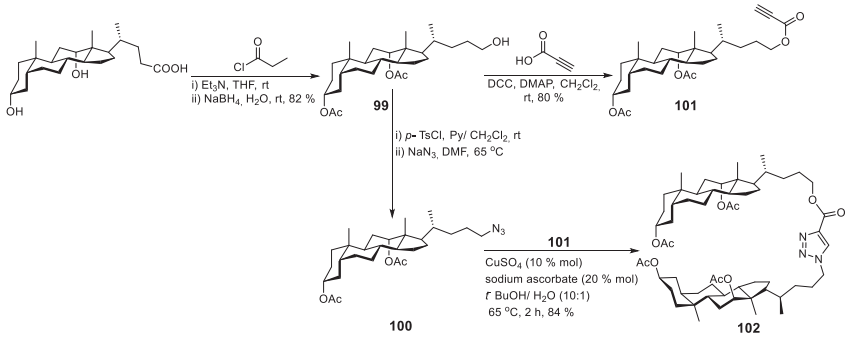

SCHEME 8.8 Synthesis of steroid dimer (**102**) [101].

azidodendrimers, and during the next "click" reaction, second-generation azidodendrimers were obtained. In contrast, the corresponding bile acids (cholic/deoxycholic) were modified by reaction with propargyl bromide and *p*-TsOH and acylated to safeguard the alkyne group. The design performance of the steroid platforms was best for zero-generation dendrimers and lowest for second-generation dendrimers. The MTT assessment of activity against C6 glioma cancer cells confirmed the highest efficacy for second-generation compounds (**107, 108**), with an IC50 value of 10.48 μM.

Conjugates bile acids-triazole as ligands

Another type of macrocyclic compound susceptible to anion binding is cholophanes (Scheme 8.10). The 3α-OH group of the deoxycholic acid derivative was

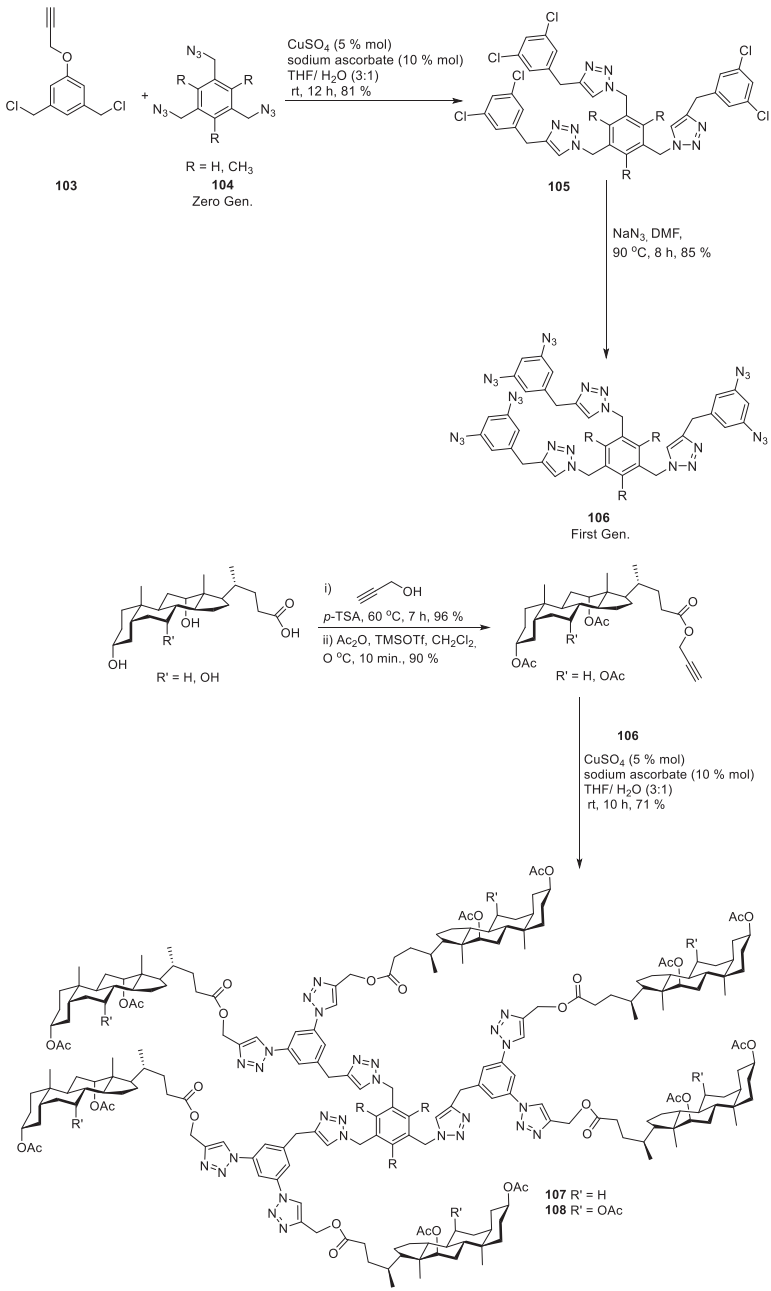

SCHEME 8.9 Synthesis of steroidal dendrimers [102].

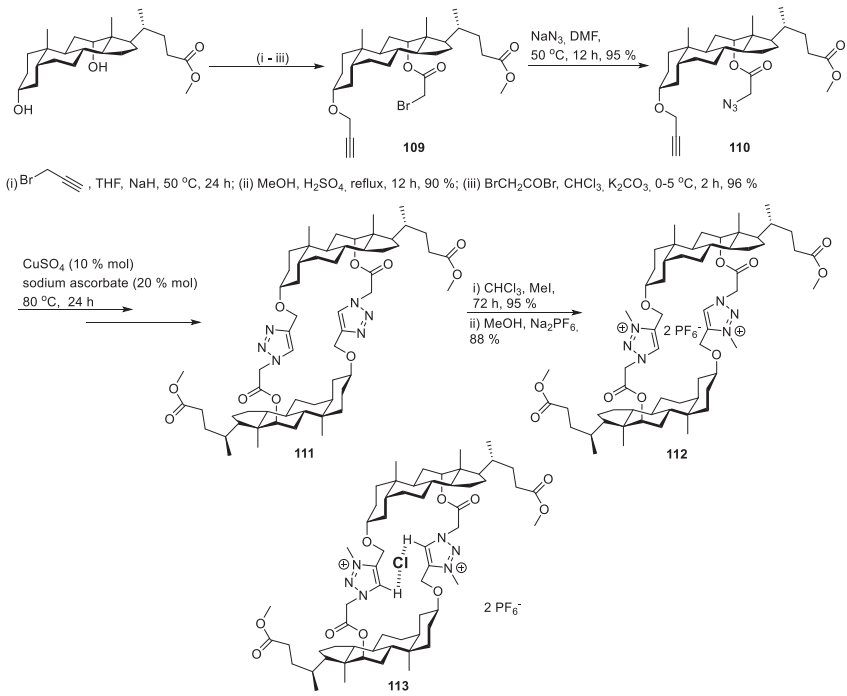

SCHEME 8.10 Synthesis of cholophane (**111**, **112**) and exemplary interaction with chloride anion (**113**) [103,104].

modified in the presence of propargyl bromide, NaH in THF, and then acylated with bromoacetyl bromide with the addition of potassium carbonate in chloroform. The resulting monoester (**109**) was then converted to an azide derivative (**110**), after which a cholophane (**111**) was formed in a "click" reaction with good efficiency. Due to the more efficient formation of hydrogen bonds by alkyl-1,2,3-triazole (**112**), methylation with methyl iodide and the exchange of anions were performed. To analyze the donor properties of cholophane, titration with $Bu_4N^+X^-$ salts in $CDCl_3$ was carried out and controlled by NMR. On the spectrum, a change in the shift of signals from protons in the triazole ring and acetylmethylene was observed, which resulted from interaction with the anion. In addition, association constants were estimated according to the order $Cl^- > H_2SO_4^- > F^- > Br^- > CH_3COO^- > H_2PO_4^{2-}$. A higher affinity for chloride ion binding ($K_a = 3700^{M-1}$) may result from the most stable binding to hydrogen [103,104].

Li et al. synthesized a steroid dimer with a similar structure [105,106]. The side chain of bile acid was coupled to the hydroxyl group at the C-3 α position (Scheme 8.11). The spectroscopic analysis of ^{1}H NMR excluded the participation of protons from hydroxyl groups in anion binding. In contrast, the new

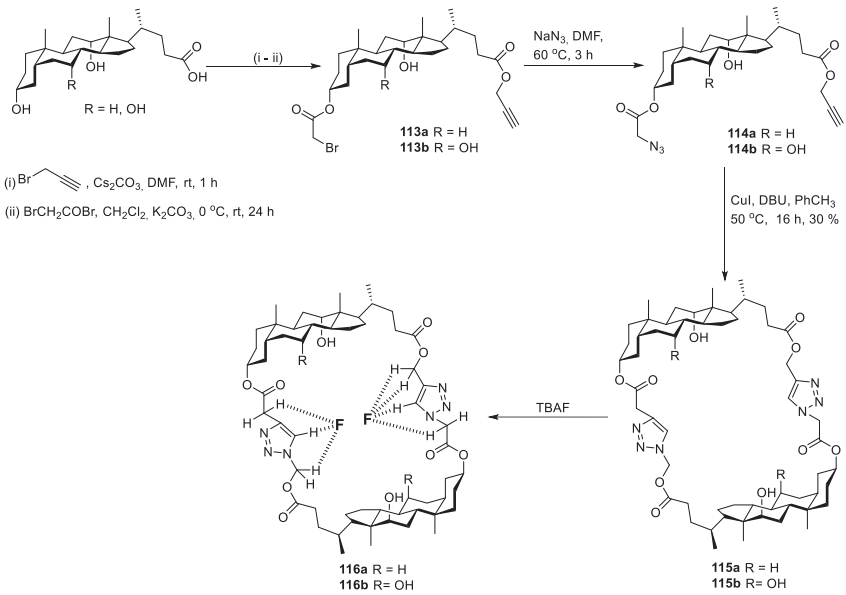

SCHEME 8.11 Synthesis of a head-to-tail steroid dimer [105,106].

conjugate steroid-triazole (**115a**, **115b**) was the most highly selective for fluoride ions. The calculated constants of K_1 and K_2 were 560 (±8) and 18 (±3) $^{M-1}$, respectively. TBAF appendix (2 eq.) caused the signal loss from the aliphatic proton while strengthening two hydrogen bonds in the dimer structure (**116a**, **116b**).

Nayal et al. have described cholapods containing units with colorimetric properties [107]. The highly efficient reaction under click chemistry (efficiency > 80%) allowed for the effective binding of selected anions (Scheme 8.12). For compound (**120a**), after adding $Bu_4N^+H_2PO_4^-$ (in $CHCl_3$), its color changed to yellow, while the UV absorption band at 360 nm was reduced and shifted to 400 nm. The second compound (**120b**) showed a similar decrease at 380 nm and an increase at 600 nm while turning blue in the presence of TBAF, $BuNCH_3CO_2$ (in $Bu_4N^+H_2PO_4^-$). Cholapods (**120a**, **120b**) were characterized by increased selectivity for $H_2PO_4^-$ ions (**121a**, **121b**) than for Cl^- ions. This is a significant difference compared to macrocyclic compounds.

The "click" chemistry allowed the design of new functionalized hybrids of bile acids and calixarene [108]. The synthesis of these triazole conjugates consisted again of the conjugation of a steroid triazide (**118**) and calixarene, previously enriched with a propargyl group (**123**) (Scheme 8.13). The resulting compound (**124**) showed two absorption peaks derived from the triazole and

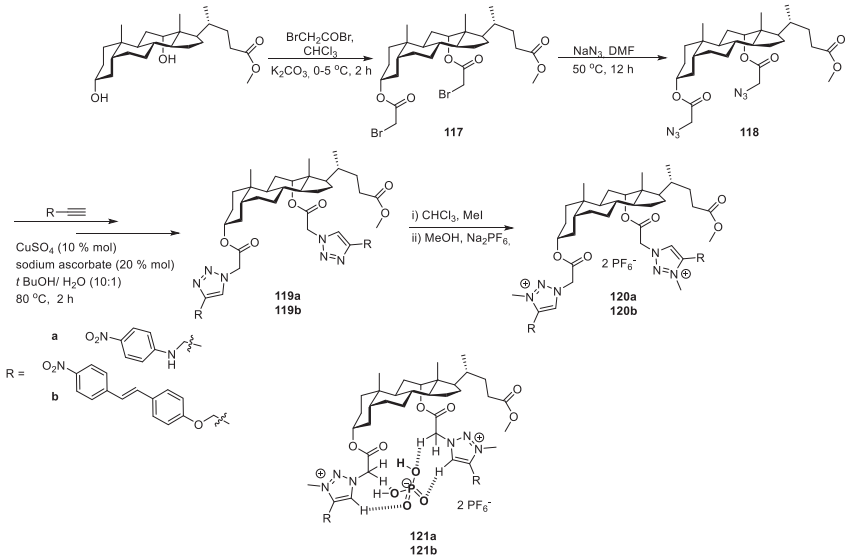

SCHEME 8.12 Synthesis of cholapods [107].

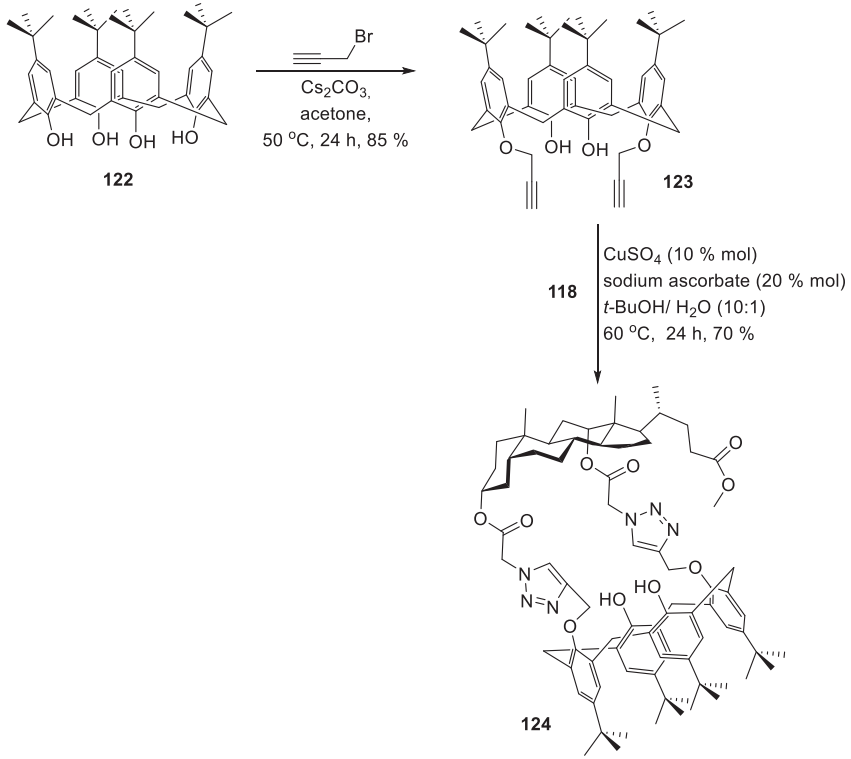

SCHEME 8.13 Synthesis of bile acid-calixarene hybrids (**124**) [108].

calixarene rings at 284 and 289 nm, respectively. The peaks were suppressed in the presence of selected metal perchlorates in CH_3CN. Two isometric points were observed at wavelengths of 276 and 302 nm. The hybrid receptor's binding analysis showed the highest mercury affinity ($K_a = 1.2 * 10^4\ M^{-1}$). The critical power of other metal ions was as follows: $Hg^{2+} > Cd^{2+} > Zn^{2+} > Pb^{2+} > Li^{+} > Mn^{2+} > Cu^{2+}$.

Synthesis of other derivatives of bile acids with 1,2,3-triazole rings

Another compound type is bile acid-sterol dimers (**135**−**140**) connected by a 1,2,3-triazole ring (Scheme 8.14). Corresponding azido acetoxy substituted bile acid derivatives and propionyl sterol derivatives were reacted by adding Cu(I) ions. The newly obtained products were confirmed by spectroscopic analysis and mass spectrometry. In silico studies conducted by the PASS method indicated their outstanding biological activity (Table 8.3) [109].

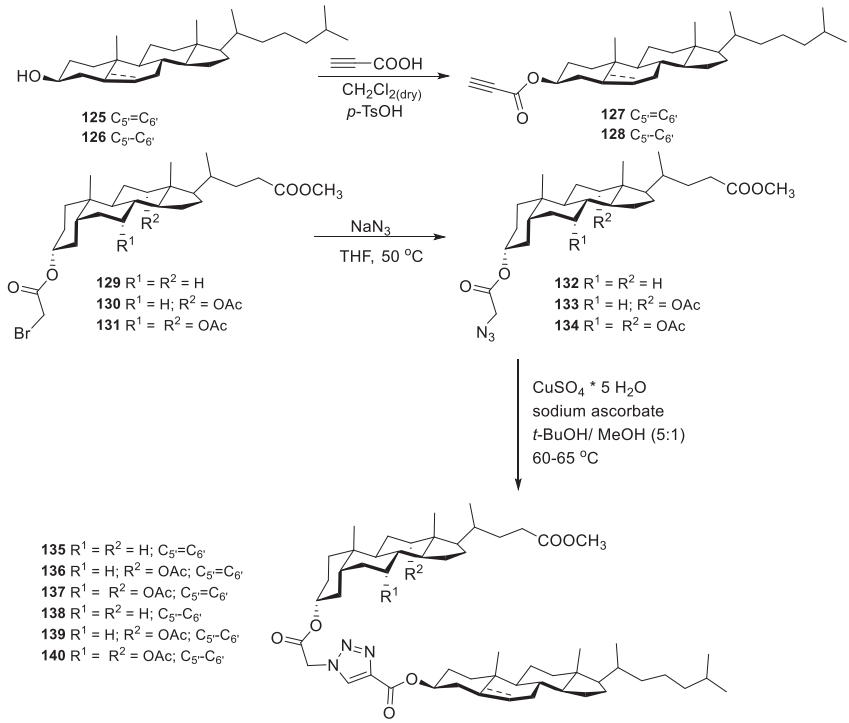

SCHEME 8.14 Synthesis of new steroid conjugates (**125**−**140**) [109].

TABLE 8.3 Values obtained during PASS analysis [109].

Focal predicted activity (PA > 0.70)	131	132	133	134	135	136	137	138	139	140
Acylcarnitine hydrolase inhibitor	0.96	0.96	0.95	0.95	–	–	–	–	–	–
Alkenyl glycerophosphocholine hydrolase inhibitor	0.93	0.90	0.89	0.83	–	–	–	–	–	–
Alkylacetylglycerophosphatase inhibitor	0.93	0.90	0.90	0.86	–	–	–	–	–	–
Dextranase inhibitor	0.89	0.83	0.85	0.75	–	–	–	–	–	–
Glyceryl-ether monooxygenase inhibitor	0.82	0.85	0.80	0.83	–	0.71	0.75	0.72	0.75	0.79
Peptidoglycan glycosyltransferase inhibitor	0.81	0.75	0.80	0.73	–	–	–	–	–	–
Cholesterol antagonist	0.79	0.76	–	–	0.84	0.76	0.76	0.71	–	–
Protein-disulfide reductase (glutathione) inhibitor	0.80	0.72	0.76	–	–	–	–	–	–	–
Adenomatous polyposis treatment	0.79	0.80	0.76	0.78	–	–	–	–	–	–
Cytoprotectant	0.74	0.76	0.73	0.75	–	–	–	–	–	–
Hypolipemic	–	0.71	–	0.74	0.76	0.78	0.85	–	–	0.78
Antihypercholesterolemic	–	–	0.73	0.79	0.73	–	0.75	–	–	–
Pancreatic disorders treatment	–	–	–	–	0.83	0.80	0.79	0.90	0.86	0.84

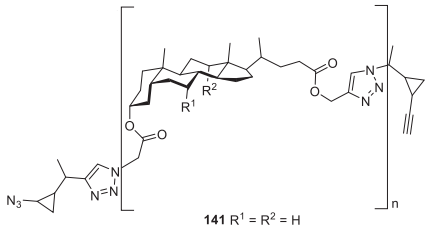

141 $R^1 = R^2 = H$
142 $R^1 = H$, $R^2 = OH$
143 $R^1 = R^2 = OH$

FIGURE 8.20 Polymers of bile acid-triazole rings [110].

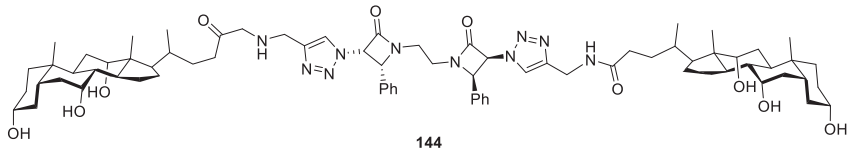

144

FIGURE 8.21 Conjugate cholic acid β-lactam [111].

Another example of using bile acid molecules in combination with a 1,2,3-triazole ring is a model leading to the formation of polymers (Fig. 8.20). These products make it possible to maintain the stabilization of silver nanoparticles, which have been used in a modern approach to the selective recognition of iodide anions by colorimetric methods [110].

S. Vatmurge et al. designed the synthesis of steroid conjugates with β-lactams linked to 1,2,3-triazole rings (Fig. 8.21) [111]. This was due to the newly emerging strains of pathogens showing high drug resistance to medicinal substances containing β-lactam groups. In the era of the development of pharmaceuticals and medicine and the appearance of yet-unidentified pathogenic microorganisms, there is a great need to synthesize effective compounds with antimicrobial properties. The conjugates obtained by Vatmurge were characterized by high pharmacotherapeutic potential against the following strains: *C. albicans*, *Cryptococcus neoformans*, *Yarrowia lipolytica*, *Fusarium oxysporum*, *Benjaminiellapoitrasii,* and bacteria of the following types: *E. coli* and *S. aureus*.

The new quasi-podands containing 1,2,3-triazole rings were synthesized by Pospieszny et al. (Scheme 8.15). A "click" reaction between the corresponding propargylic esters of bile derivatives (**145**−**147**) and 1,3,5-tris(azidomethyl) benzene resulted in conjugates (**148**−**150**) having a rigid benzyl platform with high efficiency (>85%) [87]. The structure with an aromatic ring promotes the formation of conformers that can interact with the surface of biopolymers as anchors.

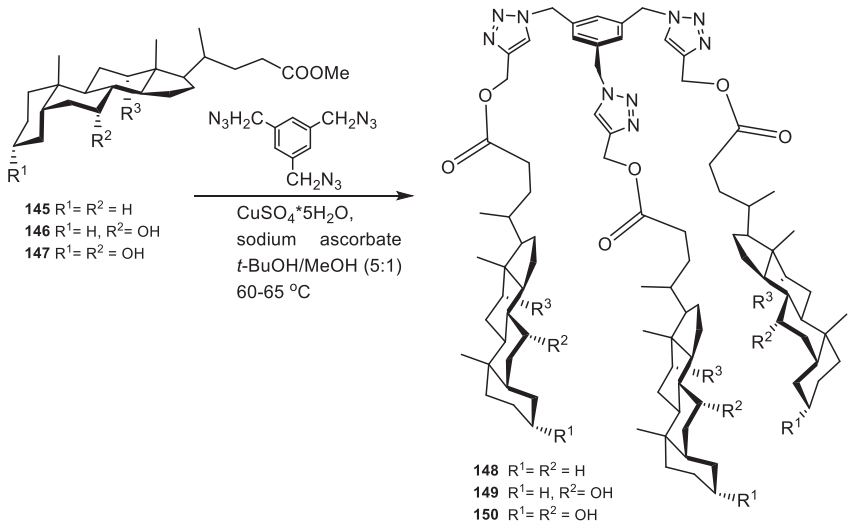

SCHEME 8.15 Synthesis of quasi-podands of method "click" chemistry [87].

Based on excellent physicochemical properties, the synthesis of three new bile acid dimers connected by 1,2,3-triazole rings (**151**−**153**) and two dimers substituted in the C-3 position with bromoacetoxy groups (**154**,**155**) was designed (Fig. 8.22) [112]. Complete spectroscopic analysis (^{1}H NMR,

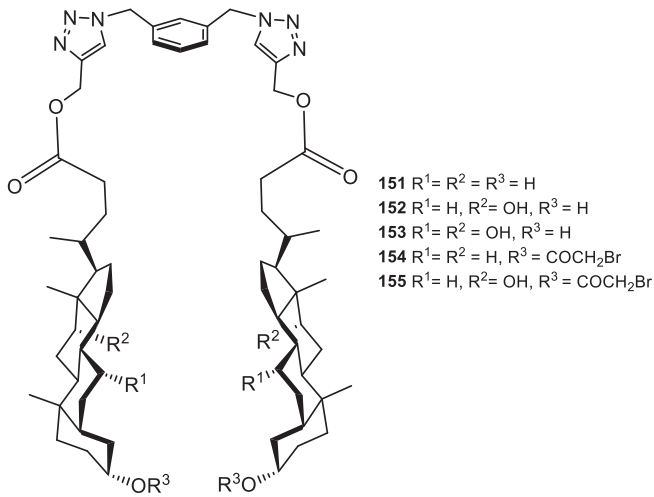

FIGURE 8.22 Synthesis of bile acid dimers containing 1,2,3-triazole systems [112].

^{13}C NMR) and mass spectrometry (ESI-MS, MALDI) confirmed their structure, and their molecular models were determined using the semiempirical PM5 method.

Subsequently, the obtained conjugates were used as ligands to synthesize adducts with phthalic, terephthalic, and 4-aminobenzoic acid (PABA, vitamin B_{10}). Studies have shown that adducts are formed due to the formation of hydrogen bonds between the hydroxyl groups of the steroid skeleton and the carboxyl groups of added aromatic acids. Fig. 8.23 shows the spectrum of ^{1}H NMR of the conjugate (**153**) and its adducts with phthalic, terephthalic, and 4-aminobenzoic acids. A characteristic feature

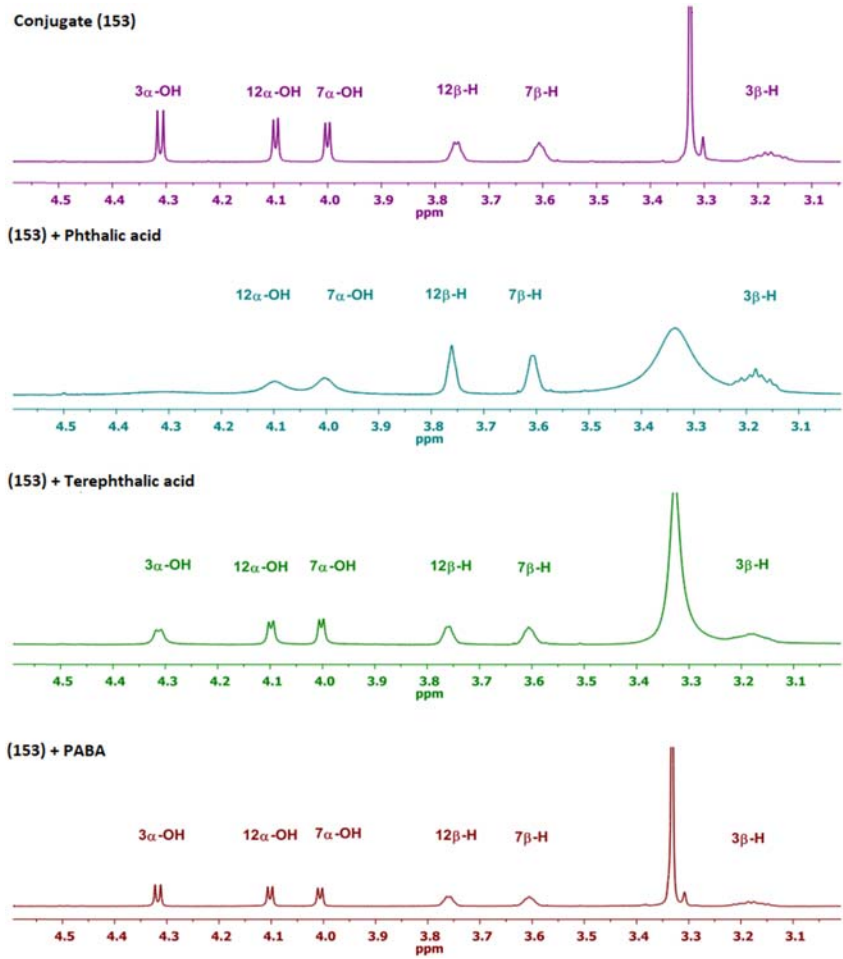

FIGURE 8.23 ^{1}H NMR in 4.5−3.0 ppm region of dimers (**153**) and its adducts with phthalic acid, terephthalic and PABA in DMSO-d_6 [112].

appearing in the ^{1}H NMR spectra of the corresponding adducts is the presence of extended 3β-H and 12β-H proton signals and expanded and flattened signals coming from protons of 3α-OH and 12α-OH groups. In the ^{1}H NMR spectrum of the dimer adduct (**153**) with phthalic acid, it can be seen that the signals coming from the protons of the 7α-OH and 12α-OH groups have been significantly flattened, and the signal coming from the proton of the 3α-OH group disappears. This is related to these groups' participation in forming intermolecular hydrogen bonds, which is also facilitated by the location of carboxyl groups in the phthalic acid molecule in the ortho position. The presence of blocking groups at the C(3) position of the steroid skeleton in conjugates (**154**) and (**155**) prevents the formation of hydrogen bonds between conjugates and aromatic acids and the construction of adducts. It follows that only hydroxyl groups participate in forming hydrogen bonds, while nitrogen atoms of the triazole ring do not.

Conclusions

The synthesis of new steroid conjugates and the application of click chemistry are essential for developing science for several vital reasons. Firstly, by creating novel steroid conjugates, scientists can fine-tune the properties of steroids, making them more effective for therapeutic purposes. This can lead to the development of new and improved drugs with enhanced efficacy and reduced side effects. Secondly, steroid conjugates can be used to investigate the complex interactions between steroids and other biomolecules in biological systems. This helps researchers gain a deeper understanding of physiological processes and disease pathways. Whereas "click" chemistry, a highly efficient and selective chemical reaction, facilitates the precise conjugation of molecules. Its use in steroid conjugate synthesis enables the creation of complex molecules with high precision, offering new possibilities for drug design and biomaterial development. Steroid conjugates can target specific tissues or cells, allowing for more targeted therapies. This can reduce off-target effects and improve treatments' overall safety and efficacy. The versatility of steroid conjugates and click chemistry extends beyond drug development to materials science, diagnostics, and biotechnology. This broadens the impact of these research areas across various scientific disciplines. The synthesis of new steroid conjugates and the application of click chemistry are pivotal in advancing scientific knowledge and innovation. They contribute to the development of better drugs, an improved understanding of biological processes, and the creation of innovative materials and technologies, ultimately benefiting both scientific research and society.

References

[1] J.L. Atwood, J.W. Steed, Supramolecular Chemistry, second ed., Wiley, Hoboken, New Jersey, 2013.

[2] K.C. Nicolaou, T. Montagnon, Molecules that Changed the World, John Wiley & Sons, Ltd., UK, 2008, pp. 79–90.

[3] S. Kandi, V. Godishala, P. Rao, K.V. Ramana, Biomedical significance of terpenes: an insight, Biomedicine 3 (2015) 8–10.

[4] K. Bloch, Sterol molecule: structure, biosynthesis, and function, Steroids 57 (1992) 378–383.

[5] Š. Horáčková, M. Plocková, K. Demnerová, Importance of microbial defence systems to bile salts and mechanisms of serum cholesterol reduction, Biotechnol. Adv. 36 (2018) 682–690.

[6] P.M. Dewick, Medicinal Natural Products: A Biosynthetic Approach, third ed., Wiley, A John Wiley and Sons, Ltd., Publication, Chichester, West Sussex, United Kingdom, 2009, pp. 275–277.

[7] J. Tang, Z. Han, J. Chai, Q&A: what are brassinosteroids and how do they act in plants? BMC Biol. 14 (2016) 113.

[8] V. Kumar, A. Dey, M.B. Hadimani, T. Marcovic, M. Emerald, Chemistry and pharmacology of withania somnifera: an update, Cell Med. 5 (2015), 1.1–1.13.

[9] M. Makishima, T.T. Lu, W. Xie, G.K. Whitfield, H. Domoto, R.M. Evans, M.R. Haussler, D.J. Mangelsdorf, Vitamin D receptor as an intestinal bile acid sensor, Science 296 (2002) 1313–1316.

[10] W.H. Okamura, M.M. Midland, M.W. Hammond, N.A. Rahman, M.C. Dormanen, I. Nemere, A.W. Norman, Chemistry and conformation of vitamin D molecules, J. Steroid Biochem. Mol. Biol. 53 (1995) 603–613.

[11] I. Kirson, E. Glotter, Recent developments in naturally occurring ergostane-type steroids. A review, J. Nat. Prod. 44 (1981) 633–647.

[12] R.E. Summons, A.S. Bradley, L.L. Jahnke, J.R. Waldbauer, Steroids, triterpenoids and molecular oxygen, Philos. Trans. R. Soc. Lond. B Biol. Sci. 361 (2006) 951–968.

[13] S. Mukhopadhyay, U. Maitra, Chemistry and biology of bile acids, Curr. Sci. 87 (2004) 18.

[14] Y. Shansky, J. Bespyatykh, Bile acids: physiological activity and perspectives of using in clinical and laboratory diagnostics, Molecules 27 (2022) 7830.

[15] H. Gao, J.R. Dias, Selective protection of the various hydroxy groups of cholic acid and derivatives. A review, Org. Prep. Proced. Int. 31 (1999) 145–166.

[16] J.Y.L. Chiang, Bile acids: regulation of synthesis: thematic review series: bile acids, J. Lipid Res. 50 (2009) 1955–1966.

[17] K.M. Bhattarai, A.P. Davis, J.J. Perry, C.J. Walter, S. Menzer, D.J. Williams, A new generation of "cholaphanes": steroid-derived macrocyclic hosts with enhanced solubility and controlled flexibility, J. Org. Chem. 62 (1997) 8463–8473.

[18] C. Altinkok, H.R.F. Karabulut, M.A. Tasdelen, G. Acik, Bile acid bearing poly(vinyl chloride) nanofibers by combination of CuAAC click chemistry and electrospinning process, Mater. Today Commun. 25 (2020) 101425.

[19] C. Altinkok, G. Acik, H.R.F. Karabulut, M. Ciftci, M.A. Tasdelen, A. Dag, Synthesis and characterization of bile acid-based polymeric micelle as a drug carrier for doxorubicin, Polym. Adv. Technol. 32 (2021) 4860–4868.

[20] L. Xiao, E. Yu, H. Yue, Q. Li, Enhanced liver targeting of camptothecin *via* conjugation with deoxycholic acid, Molecules 24 (2019) 1179–1185.

[21] K. Sue, M.M. Cadelis, T. Troia, F. Rouvier, M.L. Bourguet-Kondracki, J.M. Brunel, B.R. Copp, Investigation of α,ω-disubstituted polyamine-cholic acid conjugates identifies hyodeoxycholic and chenodeoxycholic scaffolds as non-toxic, potent antimicrobials, Antibiotics 12 (2023) 404.

[22] P. Singla, M. Kaur, A. Kumari, L. Kumari, S.V. Pawar, R. Singh, D.B. Salunke, Facially amphiphilic cholic acid-lysine conjugates as promising antimicrobials, ACS Omega 5 (2020) 3952−3963.

[23] J. Wu, T.T. Yu, R. Kuppusamy, M.M. Hassan, A. Alghalayini, C.G. Cranfield, M.D.P. Willcox, D.S. Black, N. Kumar, Cholic acid-based antimicrobial peptide mimics as antibacterial agents, Int. J. Mol. Sci. 23 (2022) 4623.

[24] J. Kim, O.C. Jeon, H.T. Moon, S.R. Hwang, Y. Byun, Preclinical safety evaluation of low molecular weight heparin-deoxycholate conjugates as an oral anticoagulant: preclinical safety evaluation of oral heparin-deoxycholate conjugates, J. Appl. Toxicol. 36 (2016) 76−93.

[25] M.E.K. Stathopoulou, N. Zoupanou, C.N. Banti, A.P. Douvalis, C. Papachristodoulou, K.D. Marousis, G.A. Spyroulias, T. Mavromoustakos, S.K. Hadjikakou, Organotin derivatives of cholic acid induce apoptosis into breast cancer cells and interfere with mitochondrion; Synthesis, characterization and biological evaluation, Steroids 167 (2021) 108798.

[26] D. Bariya, V. Anand, S. Mishra, Recent advances in the bile acid based conjugates/derivatives towards their gelation applications, Steroids 165 (2021) 108769.

[27] R. Thakare, H. Gao, R.E. Kosa, Y.A. Bi, M.V.S. Varma, M.A. Cerny, R. Sharma, M. Kuhn, B. Huang, Y. Liu, A. Yu, G.S. Walker, M. Niosi, L. Tremaine, Y. Alnouti, A.D. Rodrigues, Leveraging of rifampicin-dosed cynomolgus monkeys to identify bile acid 3-*O*-sulfate conjugates as potential novel biomarkers for organic anion-transporting polypeptides, Drug Metab. Dispos. 45 (2017) 721−733.

[28] E. Virtanen, E. Kolehmainen, Use of bile acids in pharmacological and supramolecular applications, Eur. J. Org. Chem. 2004 (2004) 3385−3399.

[29] H. Masuno, Y. Kazui, A. Tanatani, S. Fujii, E. Kawachi, T. Ikura, N. Ito, K. Yamamoto, H. Kagechika, Development of novel lithocholic acid derivatives as vitamin D receptor agonists, Bioorg. Med. Chem. 27 (2019) 3674−3681.

[30] B. Brycki, H. Koenig, T. Pospieszny, Quaternary alkylammonium conjugates of steroids: synthesis, molecular structure, and biological studies, Molecules 20 (2015) 20887−20900.

[31] K.S. Moore, S. Wehrli, H. Roder, M. Rogers, J.N. Forrest, D. McCrimmon, M. Zasloff, Squalamine: an aminosterol antibiotic from the shark, Proc. Natl. Acad. Sci. USA 90 (1993) 1354−1358.

[32] S.L. Wehrli, K.S. Moore, H. Roder, S. Durell, M. Zasloff, Structure of the novel steroidal antibiotic squalamine determined by two-dimensional NMR spectroscopy, Steroids 58 (1993) 370−378.

[33] R.A. Hauser, D. Sutherland, J.A. Madrid, M.A. Rol, S. Frucht, S. Isaacson, F. Pagan, B.N. Maddux, G. Li, W. Tse, B.L. Walter, R. Kumar, D. Kremens, M.F. Lew, A. Ellenbogen, O. Oguh, A. Vasquez, W. Kinney, M. Lowery, M. Resnick, N. Huff, J. Posner, K.V. Ballman, B.E. Harvey, M. Camilleri, M. Zasloff, D. Barbut, Targeting neurons in the gastrointestinal tract to treat Parkinson's disease, Clin. Park. Relat. Disord. 1 (2019) 2−7.

[34] C.L. West, Y.K. Mao, T. Delungahawatta, J.Y. Amin, S. Farhin, R.M. McQuade, S. Diwakarla, R. Pustovit, A.M. Stanisz, J. Bienenstock, D. Barbut, M. Zasloff,

J.B. Furness, W.A. Kunze, Squalamine restores the function of the enteric nervous system in mouse models of Parkinson's disease, J. Parkinsons Dis. 10 (2020) 1477–1491.

[35] J. Xu, L. Wang, X. Chen, W. Le, New Understanding on the pathophysiology and treatment of constipation in Parkinson's disease, Front. Aging Neurosci. 14 (2022) 917499.

[36] S.R.W. Stott, R.K. Wyse, P. Brundin, Novel approaches to counter protein aggregation pathology in Parkinson's disease, Prog. Brain Res. 252 (2020) 451–492.

[37] M. Zasloff, A.P. Adams, B. Beckerman, G.C.L. Wong, Squalamine as a broad-spectrum systemic antiviral agent with therapeutic potential, Proc. Natl. Acad. Sci. USA 108 (2011) 15978–15983.

[38] F. Vigant, N.C. Santos, B. Lee, Broad-spectrum antivirals against viral fusion, Nat. Rev. Microbiol. 13 (2015) 426–437.

[39] M. Nicol, M.A.B. Mlouka, T. Berthe, P. Di Martino, T. Jouenne, J.M. Brunel, E. Dé, Anti-persister activity of squalamine against *Acinetobacter baumannii*, Int. J. Antimicrob. Agents 53 (2019) 337–342.

[40] J.H. Schiller, G. Bittner, Potentiation of platinum antitumor effects in human lung tumor xenografts by the angiogenesis inhibitor squalamine: effects on tumor neovascularization, Clin. Cancer Res. 5 (1999) 4287–4294.

[41] J.I. Williams, S. Weitman, C.M. Gonznalez, C.H. Jundt, J. Marty, S.D. Stringer, K.J. Holroyd, M.P. Mclane, Q. Chen, M. Zasloff, D.D. Von Hoff, Squalamine treatment of human tumors in nu/nu mice enhances platinum-based chemotherapies, Clin. Cancer Res. 7 (2001) 724–733.

[42] C. Sterling, D. Márquez-Garbán, J.V. Vadgama, R.J. Pietras, Squalamines in blockade of tumor-associated angiogenesis and cancer progression, Cancers 14 (2022) 5154.

[43] A. Bosseboeuf, A. Baron, E. Duval, A. Gautier, P. Sourdaine, P. Auvray, A potential antineoplastic peptide of human prostate cancer cells derived from the lesser spotted dogfish (*Scyliorhinus canicula L.*), Mar. Drugs 17 (2019) 585.

[44] D. Li, J.I. Williams, R.J. Pietras, Squalamine and cisplatin block angiogenesis and growth of human ovarian cancer cells with or without HER-2 gene overexpression, Oncogene 21 (2002) 2805–2814.

[45] D.C. Márquez-Garbán, M. Gorrín-Rivas, H.W. Chen, C. Sterling, D. Elashoff, N. Hamilton, R.J. Pietras, Squalamine blocks tumor-associated angiogenesis and growth of human breast cancer cells with or without HER-2/neu overexpression, Cancer Lett. 449 (2019) 66–75.

[46] S. Carmona, J.M. Brunel, R. Bonier, V. Sbarra, S. Robert, P. Borentain, D. Lombardo, E. Mas, R. Gerolami, A squalamine derivative, NV669, as a novel PTP1B inhibitor: *in vitro* and *in vivo* effects on pancreatic and hepatic tumor growth, Oncotarget 10 (2019) 6651–6667.

[47] R. Stone, *Deĵà vu* guides the way to new antimicrobial steroid, Science 259 (1993) 1125.

[48] K. Alhanout, J.M. Brunel, D. Raoult, J.M. Rolain, *In vitro* antibacterial activity of aminosterols against multidrug-resistant bacteria from patients with cystic fibrosis, J. Antimicrob. Chemother. 64 (2009) 810–814.

[49] R.M. Moriarty, S.M. Tuladhar, L. Guo, S. Wehrli, Synthesis of squalamine. A steroidal antibiotic from the shark, Tetrahedron Lett. 35 (1994) 8103–8106.

[50] S.R. Jones, W.A. Kinney, X. Zhang, L.M. Jones, B.S. Selinsky, The synthesis and characterization of analogs of the antimicrobial compound squalamine: 6 beta-hydroxy-3-aminosterols synthesized from hyodeoxycholic acid, Steroids 61 (1996) 565–571.

[51] X.D. Zhou, F. Cai, W.S. Zhou, A stereoselective synthesis of squalamine, Tetrahedron 58 (2002) 10293–10299.

[52] K. Okumura, Y. Nakamura, S. Takeuchi, I. Kato, Y. Fujimoto, N. Ikekawa, Formal synthesis of squalamine from desmosterol, Chem. Pharm. Bull. 51 (2003) 1177−1182.

[53] B. Choucair, M. Dherbomez, C. Roussakis, L. El kihel, Synthesis of 7α- and 7β-spermidinylcholesterol, squalamine analogues, Bioorg. Med. Chem. Lett 14 (2004) 4213−4216.

[54] W.H. Chen, C. Wennersten, R.C. Moellering Jr., S.L. Regen, Towards squalamine mimics: synthesis and antibacterial activities of head-to-tail dimeric sterol-polyamine conjugates, Chem. Biodivers. 10 (2013) 385−393.

[55] J.R. Jadhav, H.S. Kim, J.H. Kwak, *N*-cholesteryl amino acid conjugates and their antimicrobial activities, Eur. J. Pharmaceut. Sci. 50 (2013) 208−214.

[56] D.B. Salunke, B.G. Hazra, V.S. Pore, Steroidal conjugates and their pharmacological applications, Curr. Med. Chem. 13 (2006) 813−847.

[57] H.S. Kim, B.S. Choi, K.C. Kwon, S.O. Lee, H.J. Kwak, C.H. Lee, Synthesis and antimicrobial activity of squalamine analogue, Bioorg. Med. Chem. 8 (2000) 2059−2065.

[58] Y. Shu, S.R. Jones, W.A. Kinney, B.S. Selinsky, The synthesis of spermine analogs of the shark aminosterol squalamine, Steroids 67 (2002) 291−304.

[59] B. Choucair, M. Dherbomez, C. Roussakis, L. El kihel, Synthesis of spermidinylcholestanol and spermidinylcholesterol, squalamine analogues, Tetrahedron 60 (2004) 11477−11486.

[60] H.S. Kim, S.N. Khan, J.R. Jadhav, J.W. Jeong, K. Jung, J.H. Kwak, A concise synthesis and antimicrobial activities of 3-polyamino-23,24-bisnorcholanes as steroid-polyamine conjugates, Bioorg. Med. Chem. Lett. 21 (2011) 3861−3865.

[61] J.M. Brunel, Y. Letourneux, Recent advances in the synthesis of spermine and spermidine analogs of the shark aminosterol squalamine, Eur. J. Org. Chem. 2003 (2003) 3897−3907.

[62] J. Brunel, C. Salmi, C. Loncle, N. Vidal, Y. Letourneux, Squalamine: a polyvalent drug of the future? Curr. Cancer Drug Targets 5 (2005) 267−272.

[63] M.N. Rao, A.E. Shinnar, L.A. Noecker, T.L. Chao, B. Feibush, B. Snyder, I. Sharkansky, A. Sarkahian, X. Zhang, S.R. Jones, W.A. Kinney, M. Zasloff, Aminosterols from the dogfish shark *Squalus acanthias*, J. Nat. Prod. 63 (5) (2000) 631−635.

[64] G. Godeau, C. Staedel, P. Barthélémy, Lipid-conjugated oligonucleotides *via* "click chemistry" efficiently inhibit *Hepatitis C Virus* translation, J. Med. Chem. 51 (2008) 4374−4376.

[65] X. Li, K. Feng, L. Li, L. Yang, X. Pan, H.S. Yazd, C. Cui, J. Li, L. Moroz, Y. Sun, B. Wang, X. Li, T. Huang, W. Tan, Lipid−oligonucleotide conjugates for bioapplications, Natl. Sci. Rev. 7 (2020) 1933−1953.

[66] E.R. Lee, J. Marshall, C.S. Siegel, C. Jiang, N.S. Yew, M.R. Nichols, J.B. Nietupski, R.J. Ziegler, M.B. Lane, K.X. Wang, N.C. Wan, R.K. Scheule, D.J. Harris, A.E. Smith, S.H. Cheng, Detailed analysis of structures and formulations of cationic lipids for efficient gene transfer to the lung, Hum. Gene Ther. 7 (1996) 1701−1717.

[67] C. Jiang, S.P. O'Connor, S.L. Fang, K.X. Wang, J. Marshall, J.L. Williams, B. Wilburn, Y. Echelard, S.H. Cheng, Efficiency of cationic lipid-mediated transfection of polarized and differentiated airway epithelial cells *in vitro* and *in vivo*, Hum. Gene Ther. 9 (1998) 1531−1542.

[68] W.M. Gołebiewski, J.P. Bader, M. Cushman, Design and synthesis of cosalane, a novel anti-HIV agent, Bioorg. Med. Chem. Lett 3 (1993) 1739−1742.

[69] M. Cushman, W.M. Gołebiewski, J.B. McMahon, R.W. Buckheit, D.J. Clanton, O. Weislow, R.D. Haugwitz, J.P. Bader, L. Graham, W.G. Rice, Design, synthesis, and biological evaluation of cosalane, a novel anti-HIV agent which inhibits multiple features of virus reproduction, J. Med. Chem. 37 (1994) 3040−3050.

[70] R.F. Keyes, W.M. Gołebiewski, M. Cushman, Correlation of anti-HIV potency with lipophilicity in a series of cosalane analogs having normal alkenyl and phosphodiester chains as cholestane replacements, J. Med. Chem. 39 (1996) 508−514.

[71] S.L. Hussey, E. He, B.R. Peterson, A synthetic membrane-anchored antigen efficiently promotes uptake of antifluorescein antibodies and associated protein a by mammalian cells, J. Am. Chem. Soc. 123 (2001) 12712−12713.

[72] S.L. Hussey, E. He, B.R. Peterson, Synthesis of chimeric 7α-substituted estradiol derivatives linked to cholesterol and cholesterylamine, Org. Lett. 4 (2002) 415−418.

[73] S.A. Degteva, L.F. Larionov, Toxicity and antitumor effect of β-sitosterol and cholesterol esters of *p*-bis(2-chloroethyl)-aminophenylacetic acid, Vopr. Onkl. 12 (1966) 51−53.

[74] B. Ji, G. Peacock, D.R. Lu, Synthesis of cholesterol-carborane conjugate for targeted drug delivery, Bioorg. Med. Chem. Lett 12 (2002) 2455−2458.

[75] M.E. Wall, G.S. Abernethy Jr., F.I. Carroll, D.J. Taylor, The effects of some steroidal alkylating agents on experimental animal mammary tumor and leukemia systems, J. Med. Chem. 12 (1969) 810−818.

[76] Y. Ono, K. Nakashima, M. Sano, Y. Kanekiyo, K. Inoue, S. Shinkai, M. Sano, J. Hojo, Organic gels are useful as a template for the preparation of hollow fiber silica, Chem. Commun. (1998) 1477−1478.

[77] Y. Ono, K. Nakashima, M. Sano, J. Hojo, S. Shinkai, Template effect of cholesterol-based organogels on sol-gel polymerization creates novel silica with a helical structure, Chem. Lett. 28 (1999) 1119−1120.

[78] J.H. Jung, Y. Ono, S. Shinkai, Novel silica structures which are prepared by transcription of various superstructures formed in organogels, Langmuir 16 (2000) 1643−1649.

[79] J.H. Jung, H. Kobayashi, M. Masuda, T. Shimizu, S. Shinkai, Helical ribbon aggregate composed of a crown-appended cholesterol derivative which acts as an amphiphilic gelator of organic solvents and as a template for chiral silica transcription, J. Am. Chem. Soc. 123 (2001) 8785−8789.

[80] J.H. Jung, Y. Ono, S. Shinkai, Sol-gel polycondensation of tetraethoxysilane in a cholesterol-based organogel system results in chiral spiral silica, Angew. Chem. Int. Ed. Engl. 39 (2000) 1862−1865.

[81] B.T. Walker, T.A. Houston, Squalamine and its derivatives as potential antitubercular compounds, Tuberculosis 93 (2013) 102−103.

[82] O. Kazakova, G. Giniyatullina, D. Babkov, Z. Wimmer, From marine metabolites to the drugs of the future: squalamine, trodusquemine, their steroid and triterpene analogues, Int. J. Mol. Sci. 23 (2022) 1075.

[83] H.C. Kolb, M.G. Finn, K.B. Sharpless, Click chemistry: diverse chemical function from a few good reactions, Angew. Chem. Int. Ed. Engl. 40 (2001) 2004−2021.

[84] N.K. Devaraj, M.G. Finn, Introduction: click chemistry, Chem. Rev. 121 (2021) 6697−6698.

[85] J. Luo, Y. Chen, X.X. Zhu, Invertible amphiphilic molecular pockets made of cholic acid, Langmuir 25 (2009) 10913−10917.

[86] J. Zhang, M.J.N. Junk, J. Luo, D. Hinderberger, X.X. Zhu, 1,2,3-triazole-containing molecular pockets derived from cholic acid: the influence of structure on host−guest coordination properties, Langmuir 26 (2010) 13415−13421.

[87] T. Pospieszny, H. Koenig, I. Kowalczyk, B. Brycki, Synthesis, spectroscopic and theoretical studies of new quasi-podands from bile acid derivatives linked by 1,2,3-triazole rings, Molecules 19 (2014) 2557−2570.

[88] S. Kohmoto, K. Sakayori, K. Kishikawa, M. Yamamoto, Molecular cleft possessing a cholic acid moiety as a podant and its conformation, J. Chem. Soc. Perkin Trans. 2 (1999) 833−836.

[89] J. Ropponen, J. Tamminen, E. Kolehmainen, K. Rissanen, Synthesis and characterization of novel steroidal dendrons, Synthesis (2003) 2226−2230.

[90] V.S. Pore, N.G. Aher, M. Kumar, P.K. Shukla, Design and synthesis of fluconazole/bile acid conjugate using click reaction, Tetrahedron 62 (2006) 11178−11186.

[91] V.S. Pore, M.A. Jagtap, S.G. Agalave, A.K. Pandey, M.I. Siddiqi, V. Kumar, P.K. Shukla, Synthesis and antifungal activity of 1,5-disubstituted-1,2,3-triazole containing fluconazole analogues, Med. Chem. Commun. 3 (2012) 484.

[92] N.G. Aher, V.S. Pore, N.N. Mishra, A. Kumar, P.K. Shukla, A. Sharma, M.K. Bhat, Synthesis and antifungal activity of 1,2,3-triazole containing fluconazole analogues, Bioorg. Med. Chem. Lett 19 (2009) 759−763.

[93] R.C.N.R. Corrales, N.B. de Souza, L.S. Pinheiro, C. Abramo, E.S. Coimbra, A.D. Da Silva, Thiopurine derivatives containing triazole and steroid: synthesis, antimalarial and antileishmanial activities, Biomed. Pharmacother. 65 (2011) 198−203.

[94] M. Shiradkar, G.V. Suresh Kumar, V. Dasari, S. Tatikonda, K.C. Akula, R. Shah, Clubbed triazoles: a novel approach to antitubercular drugs, Eur. J. Med. Chem. 42 (2007) 807−816.

[95] V.D. Bock, H. Hiemstra, J.H. van Maarseveen, CuI-catalyzed alkyne−azide "click" cycloadditions from a mechanistic and synthetic perspective, Eur. J. Org. Chem. 2006 (2006) 51−68.

[96] S.N. Bavikar, D.B. Salunke, B.G. Hazra, V.S. Pore, R.H. Dodd, J. Thierry, F. Shirazi, M.V. Deshpande, S. Kadreppa, S. Chattopadhyay, Synthesis of chimeric tetrapeptide-linked cholic acid derivatives: impending synergistic agents, Bioorg. Med. Chem. Lett 18 (2008) 5512−5517.

[97] L.M. Antinarelli, A.M. Carmo, F.R. Pavan, C.Q.F. Leite, A.D. Da Silva, E.S. Coimbra, D.B. Salunke, Increase of leishmanicidal and tubercular activities using steroids linked to aminoquinoline, Org. Med. Chem. Lett. 2 (2012) 16.

[98] D.S. Agarwal, V. Siva Krishna, D. Sriram, P. Yogeeswari, R. Sakhuja, Clickable conjugates of bile acids and nucleosides: synthesis, characterization, *in vitro* anticancer and antituberculosis studies, Steroids 139 (2018) 35−44.

[99] A. Davis, Bile acid scaffolds in supramolecular chemistry: the interplay of design and synthesis, Molecules 12 (2007) 2106−2122.

[100] P. Khaligh, P. Salehi, M. Bararjanian, A. Aliahmadi, H.R. Khavasi, S. Nejad-Ebrahimi, Synthesis and *in vitro* antibacterial evaluation of novel 4-substituted 1-menthyl-1,2,3-triazoles, Chem. Pharm. Bull. 64 (2016) 1589−1596.

[101] I. Mądrzak-Litwa, A. Wojciechowska, Z. Paryzek, Synthesis of isomeric dimers of deoxycholic acid derivatives linked by 1,2,3-triazole, Synth. Commun. 45 (2015) 1222−1230.

[102] D. Anandkumar, P. Rajakumar, Synthesis and anticancer activity of bile acid dendrimers with triazole as bridging unit through click chemistry, Steroids 125 (2017) 37−46.

[103] A. Kumar, P.S. Pandey, Anion recognition by 1,2,3-triazolium receptors: application of click chemistry in anion recognition, Org. Lett. 10 (2008) 165−168.

[104] R.K. Chhatra, A. Kumar, P.S. Pandey, Synthesis of a bile acid-based click-macrocycle and its application in selective recognition of chloride ion, J. Org. Chem. 76 (2011) 9086−9089.

[105] W. Li, X. Li, W. Zhu, C. Li, D. Xu, Y. Ju, G. Li, Topochemical approach to efficiently produce main-chain poly(bile acid)s with high molecular weights, Chem. Commun. 47 (2011) 7728.

[106] W. Li, Q. Xu, Y. Li, W. Zhu, J. Cui, Y. Ju, G. Li, Neutral bile acid cyclic dimers exhibit fluoride coordination by cooperative aliphatic and triazole CH segments, Tetrahedron Lett. 54 (2013) 3868−3871.

[107] A. Nayal, P.S. Pandey, Bile acid-based triazole and triazolium receptors for colorimetric sensing of anions, Tetrahedron 71 (2015) 6991−6996.

[108] M.K. Jaiswal, P.K. Muwal, S. Pandey, P.S. Pandey, A novel hybrid macrocyclic receptor based on bile acid and calix[4]arene frameworks for metal ion recognition, Tetrahedron Lett. 58 (2017) 2153−2156.

[109] A. Kawka, G. Hajdaś, D. Kułaga, H. Koenig, I. Kowalczyk, T. Pospieszny, Molecular structure, spectral and theoretical study of new type bile acid−sterol conjugates linked via 1,2,3-triazole ring, J. Mol. Struct. 1273 (2023) 134313.

[110] A. Kumar, R.K. Chhatra, P.S. Pandey, Synthesis of click bile acid polymers and their application in stabilization of silver nanoparticles showing iodide sensing property, Org. Lett. 12 (2010) 24−27.

[111] N.S. Vatmurge, B.G. Hazra, V.S. Pore, F. Shirazi, P.S. Chavan, M.V. Deshpande, Synthesis and antimicrobial activity of β-lactam−bile acid conjugates linked *via* triazole, Bioorg. Med. Chem. Lett 18 (2008) 2043−2047.

[112] T. Pospieszny, M. Pakiet, I. Kowalczyk, B. Brycki, Design, synthesis and application of new bile acid ligands with 1,2,3-triazole ring, Supramol. Chem. 29 (2017) 81−93.

JOC The Journal of Organic Chemistry

pubs.acs.org/joc

Article

Quasi-Podands with 1,2,3-Triazole Rings from Bile Acid Derivatives: Synthesis, and Spectroscopic and Theoretical Studies

Anna Kawka, Hanna Koenig, Damian Nowak, and Tomasz Pospieszny*

Cite This: J. Org. Chem. 2024, 89, 7561−7572

Read Online

ACCESS | Metrics & More | Article Recommendations | Supporting Information

ABSTRACT: An innovative approach to producing derivatives of bile acids has been devised, utilizing the principles of "click" chemistry. By employing intermolecular [3 + 2] cycloaddition between the newly developed acyl propiolic esters of bile acids and the azide groups of 1,3,5-tris(azidomethyl)benzene, a novel class of quasi-podands featuring 1,2,3-triazole rings has been synthesized. Identifying and characterizing these six compounds involved comprehensive analysis through spectral techniques (^{1}H NMR, ^{13}C NMR, and FT-IR), mass spectrometry, and the PM5 semiempirical method. The synthesized compounds' pharmacotherapeutic potential has been evaluated, employing the Prediction of Activity Spectra for Substances (PASS) methodology. Additionally, molecular docking was performed for all molecules.

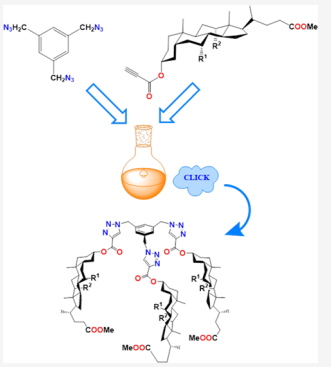

1. INTRODUCTION

"Click" chemistry is one of the most modern paths of design and synthesis of new compounds that can be used in medicine, pharmacology, biotechnology, or supramolecular chemistry. Sharpless optimized this innovative method's conditions for synthesizing new compounds used primarily as drugs.[1,2]

Obtaining new conjugates by "click" chemistry covers a broad spectrum of reactions leading to forming a carbon-heteroatom bond. Most importantly, it is characterized by extraordinary efficiency, selectivity, simple reaction conditions, and easy product isolation. Moreover, the product is stable in many solvents (e.g., in water).[3−5]

[3 + 2] Cycloaddition catalyzed by copper(I) is a representative example of a reaction based on "click" chemistry conditions (Scheme 1). The Huisgen reaction between azides and terminal alkynes is considered the primary method for synthesizing 1,2,3-triazoles, characterized by antimicrobial and antitumor properties. In biological systems, these compounds show high resistance to hydrolysis, oxidation, reduction, or metabolic degradation reactions. In addition, they can interact with biological molecules by forming hydrogen bonds or dipole−dipole interactions. Moreover, the bonds that are formed are resistant to cleavage even by proteases. The result may be triazole systems peptide bond analogues.[6,7] Literature data show that these are 1,2,3-triazole compounds characterized by unique pharmacotherapeutic effects, especially antihypertensive, antimalarial, antioxidant, antidepressant, antimicrobial, anti-inflammatory, and anticancer effects.[8−15] The "click" method was used to obtain new steroid conjugates containing 1,2,3-triazole rings.

Compounds of natural origin affect the proper functioning of all cells in living organisms. Bile acids as representatives of steroids are responsible for the digestion and absorption of lipids in the small intestine, the right amount of cholesterol, glucose metabolism, or the composition of the intestinal microbiota. Their biosynthesis begins in liver cells by the oxidation of cholesterol by cytochrome P450, and the final products are stored in the form of conjugated bile salts with the amino acids glycine and taurine. Bile acids (lithocholic acid, deoxycholic acid, and cholic acid) are distinguished by a large, curved steroid skeleton, A/B rings in *cis* geometry, enantiomeric purity, a long chain attached to the C(17) atom with a carboxyl group, amphipathic and polar hydroxyl groups with different chemical reactivity (3α−OH > 7α−OH > 12α−OH).[16−18] Their derivatives are valuable and essential for synthesizing macrocyclic compounds, steroid dimers, cholophanes, and drug-transporting molecules. Also, they can be used in designing molecular receptors capable of guest recognition in guest−host chemistry. Steroid conjugates have been used in medicine, pharmacology, supramolecular chemistry, biotechnology, and biomimetics.[19−22]

The growing interest in macromolecular derivatives of bile acids led to the development of the synthesis and use of molecular pockets[23−25] and umbrellas.[26−28] These compounds

Received: January 23, 2024
Revised: April 23, 2024
Accepted: May 7, 2024
Published: May 14, 2024

https://doi.org/10.1021/acs.joc.4c00195
J. Org. Chem. 2024, 89, 7561−7572

Scheme 1. Visual Representation Showing the Different Possible Reaction Routes During a "Click" Reaction

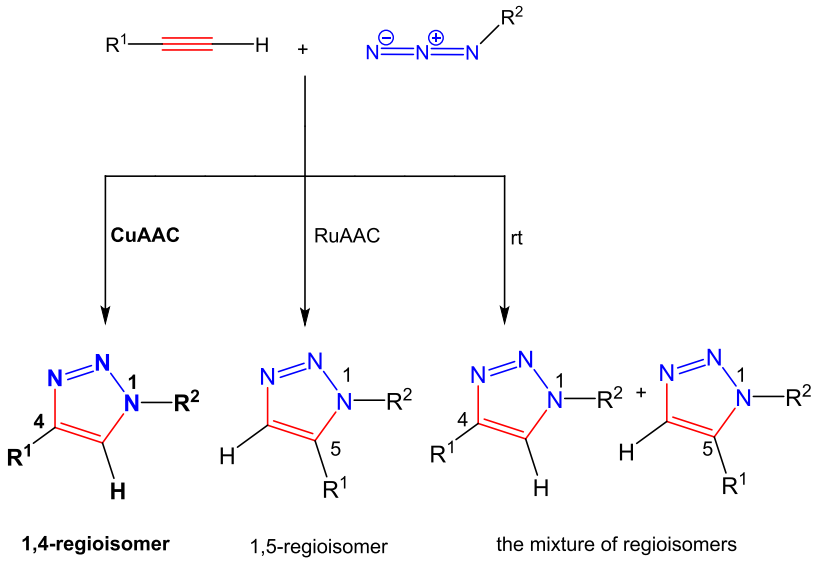

Scheme 2. Synthesis of Propionyl Esters of Bile Acids (4−6) and 1,3,5-Tris(azidomethyl)benzene (8)

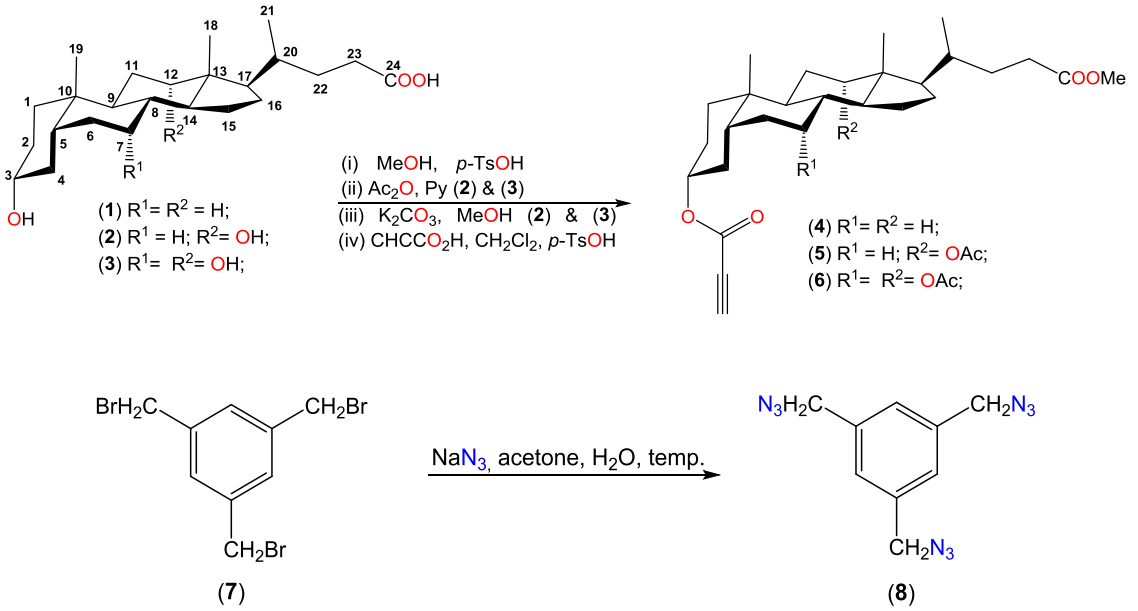

comprise at least two amphiphilic parts connected by a labile chain to the central atom. On the other hand, quasi-podands have a rigid benzene "platform" that allows them to obtain a conformer with appropriate geometry. Also, it can be crucial during interaction with the surface of biopolymers or acting as an "anchor" in biological systems.[29,30] Such systems have found application as carriers of biological molecules, hydrogelators, organogelators, or artificial receptors.[31−37]

The combination of beneficial physicochemical properties of bile acids, triazole systems, and the aromatic ring may lead to the preparation of new quasi-podands with great application potential. It is worth noting that podands are simple analogues of crown ethers and cryptands; thus, they can be valuable ligands in forming stable complexes with monovalent cations.[38,39] In addition, synthetic podands are easy to synthesize (as opposed to biological ones), and the spectrum of modification of their structures is endless.

2. RESULTS AND DISCUSSION

2.1. Synthesis. This study presents the synthesis and characterization of novel quasi-podands that are connected with a 1,2,3-triazole ring derived from propiolic esters of bile acids and 1,3,5-tris(azidomethyl)benzene. The propionyl esters of bile acids and 1,3,5-tris(azidomethyl)benzene were synthesized using previously established methods as described in Scheme 2.

The synthetic procedures for compounds **9**−**12** are presented in Scheme 3. Our experiments yielded trisubstituted products **10**−**12** as well as one disubstituted product **9**, which were isolated and characterized. Unlike molecular pocket or umbrella structures, these conjugates possess a rigid benzyl platform. This structural feature facilitates the formation of conformers with favorable geometries. The flat aromatic ring enables effective interactions with various surfaces, including biopolymers, making it function as a specific anchor. Previous research by Ghosh et al. has described similar connections achieved using cholesterol derivatives. Interestingly, these compounds exhibit

https://doi.org/10.1021/acs.joc.4c00195
J. Org. Chem. 2024, 89, 7561−7572

Scheme 3. "Click" Synthesis of Quasi-Podands of Bile Acids Derivatives Linked by 1,2,3-Triazole Ring (9−12)

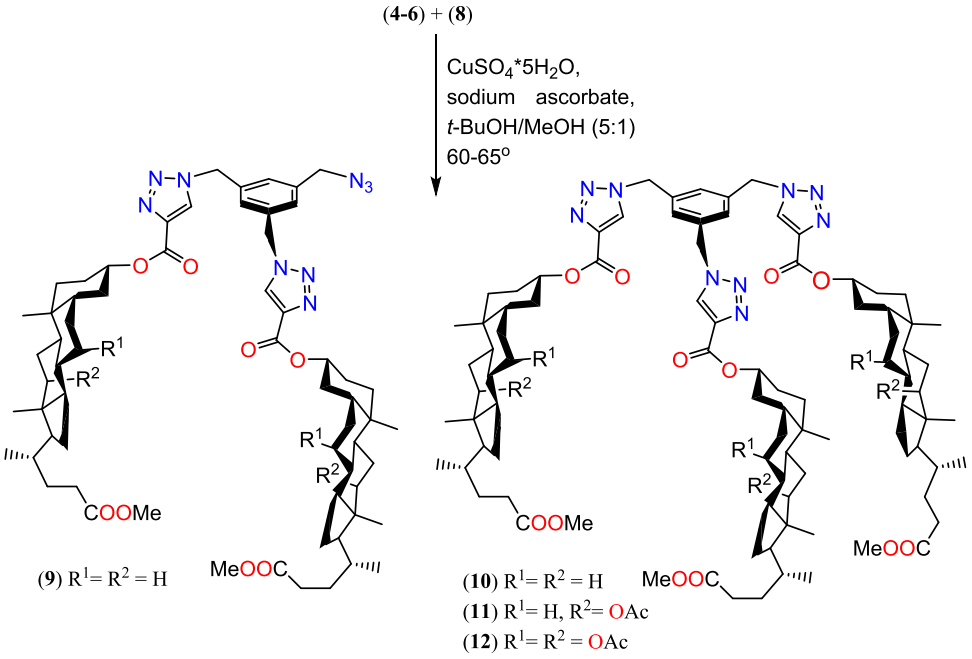

distinct gelling properties and detected ions Cu^{2+}, Ag^{+}, and Hg^{2+}.[40]

2.2. Spectroscopic Characteristic. The structural characterization of all synthesized compounds was accomplished through analysis of their ^{1}H and ^{13}C NMR, FT-IR, and ESI-MS spectra. In addition, PM5 calculations were conducted for each compound to further explore their properties and characteristics.[41−43]

The ^{1}H NMR spectra of compounds **9** and **10**−**12** exhibit distinctive patterns of signals. Notably, in the range of 5.07−4.81 ppm, characteristic multiplets are observed, which can be attributed to the C3β-H protons of the steroid skeleton. Additionally, two hydrogen singlets appear in the ranges of 0.73−0.64 and 0.95−0.94 ppm, accompanied by characteristic doublets at 0.92−0.81 ppm, assigned to CH_3-18, CH_3-19, and CH_3-21, respectively. In the spectra of compounds **11** and **12**, there are characteristic broad singlets observed in the range of 5.09−5.07 ppm, corresponding to the C12β-H protons. Furthermore, singlet in the range of 4.94−4.81 ppm is observed for the C7β-H protons in compound **12**. A distinctive signal at 4.37 ppm is observed in the ^{1}H NMR spectra of compound **9**, which can be attributed to the protons of the $-CH_2-N_3$ group. This signal serves as a diagnostic marker and is absent in the spectra of compounds **10**−**12**. The singlet at 5.55 ppm represents the signal for the two methylene protons of the Ph−CH_2−triazole ring group (refer to Figure 1).

Additionally, in the ^{1}H NMR spectrum of compound **9**, there is a distinctive and diagnostically significant singlet observed at 8.06 ppm, which can be attributed to the two protons of the triazole rings. Conversely, in the spectra of compounds **11**−**12**, three protons of the triazole rings are observed in the range of 8.10−8.06 ppm. Moreover, the ^{1}H NMR spectra of compounds **9**−**12** exhibit characteristic signals for the aromatic protons of the 1,3,5-trisubstituted benzene. These signals appear as singlets at 7.22−7.19 ppm for compound **9** and at 7.21−7.19 ppm for compounds **10**−**12**. These signals serve as prominent markers in the spectra of these compounds.

The ^{13}C NMR spectra of compounds **9**−**12** exhibit distinct peaks at the following chemical shifts: 12.4−12.0, 23.4−22.8, and 18.2−17.4 ppm, which correspond to CH_3-18, CH_3-19, and CH_3-21, respectively. However, the carbon atoms located in the 3α positions of the formyloxy groups exhibit resonance at 160.1−160.0 ppm. The carbon atoms within the C(12)=O steroid skeleton generate signals at 170.7 ppm, whereas the carbon atoms of C(7)=O are detected at 170.8 ppm. Alternatively, the carbon atoms of the C(24)=O group produce signals in the range of 174.8−174.5 ppm. The diagnostic signal for carbon atoms in the 1,2,3-triazole rings of compounds **9**−**12** is observed between 143.3−141.4 and 128.0−127.5 ppm, respectively. The carbon atoms within the CO_2-CH_2−triazole ring unit resonate within the range of 53.8−53.4 ppm (CH_2). In the ^{13}C NMR spectrum of compound **9**, the signal arising from the CH_2 group in the N_3-CH_2−Ph moiety is observed at 53.7 ppm. The spectra of compounds **10**−**12** display signals associated with the CH_2 atoms in the triazole ring-CH_2−Ph structure.

The FT-IR spectra of compounds **5** and **6** exhibit notable features. These include bands at 3251, 3292, and 3286 cm^{-1}, which are attributed to the stretching vibrations of the ν(≡C−H) group. The stretching vibrations of C−H bonds, forming a conjugate structure, merge into a broad band ranging from 2952 to 2869 cm^{-1}. Another significant observation is the presence of important analytical bands at 1737−1734 cm^{-1}, indicating the symmetric carbonyl group's ν(C=O) stretching vibration in the FT-IR spectrum. Additionally, strong characteristic bands in the region 1247−1246 cm^{-1} can be observed, which are assigned to the ν(C−O) vibration.

The FT-IR spectra of all synthesized compounds **9**−**12** exhibit a prominent feature characterized by bands at 2951−2866 cm^{-1}, which are assigned to the stretching vibrations of the ν(C−H) groups. Additionally, two strong characteristic bands appear in the regions of 1736−1733 and 1246−1228 cm^{-1}, which are attributed to the stretching vibrations of ν(C=O) and ν(C−O), respectively. Moreover, in the case of compound **9**

https://doi.org/10.1021/acs.joc.4c00195
J. Org. Chem. 2024, 89, 7561−7572

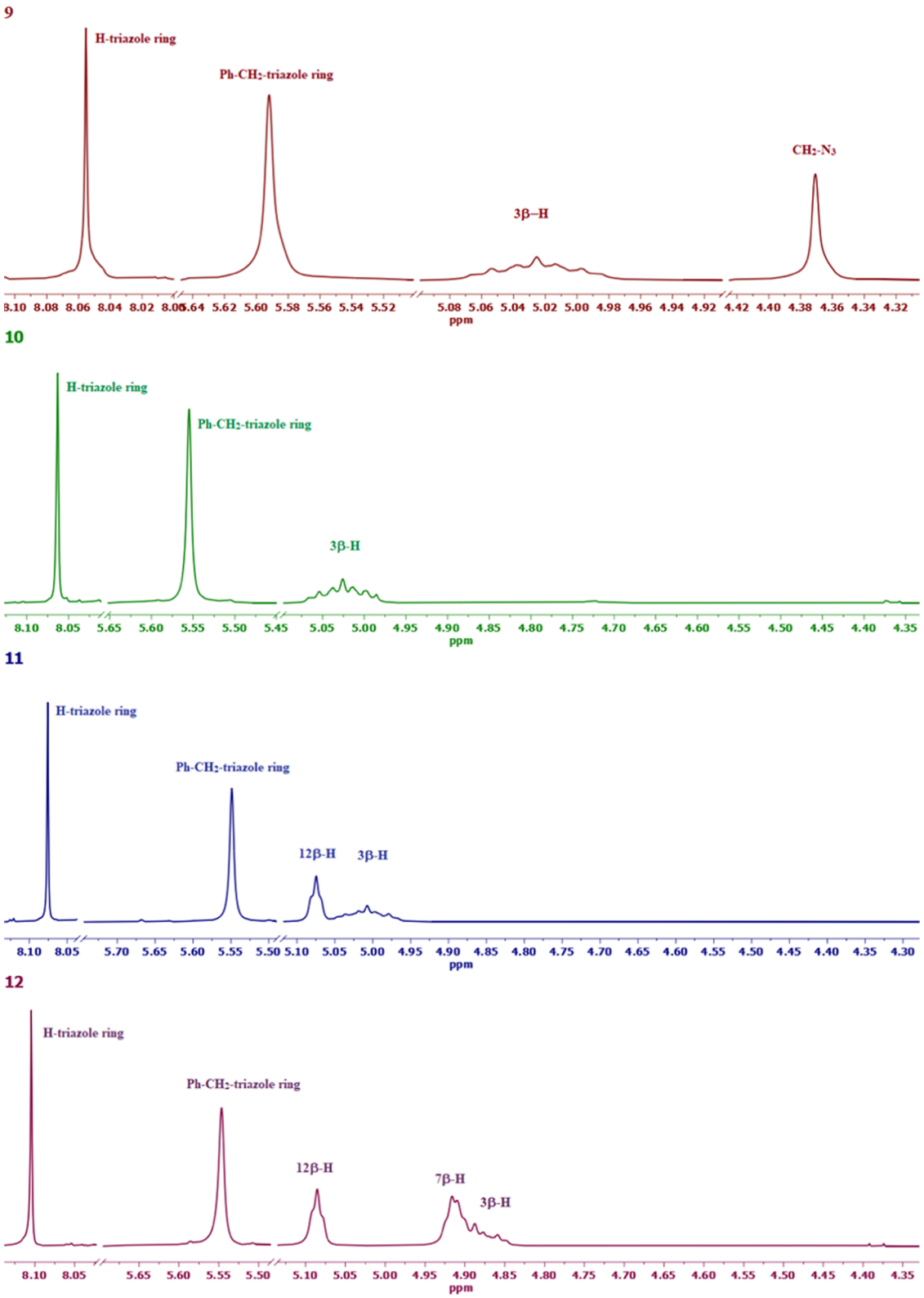

Figure 1. ^{1}H NMR spectra in the region (8.10−4.35 ppm) of the most characteristic signals of compounds (**9**−**12**).

a very strong band at 2099 cm^{-1} is observed, indicating the presence of $\nu(N = N^{+} = N^{-})$ groups (Figure 2).

The ESI-MS spectra were acquired using methanol as the solvent. In all instances, the molecular ion $[M]^{+}$ is detected, indicating the presence of a positively charged ion with a proton, alkali metals, or halides in positive-ion mode (ES^{+}) as well as negative-ion mode (ES^{-}). Figure 3 displays the ESI-MS spectrum of conjugates **11** and **12**. In this spectrum, ion peaks are observed at m/z 1820 (20%) $[C_{99}H_{141}N_9O_{18}+2K+H]^{+}$, m/z 1768 (95%) $[C_{99}H_{141}N_9O_{18}+Na]^{+}$ (for compound **11**), m/z 1942.2 (20%) $[C_{105}H_{147}N_9O_{24}+Na]^{+}$, and m/z 982.6 (100%) $[C_{105}H_{147}N_9O_{24}+2Na]^{2+}$ (for compound **12**). Furthermore, for

https://doi.org/10.1021/acs.joc.4c00195
J. Org. Chem. 2024, 89, 7561−7572

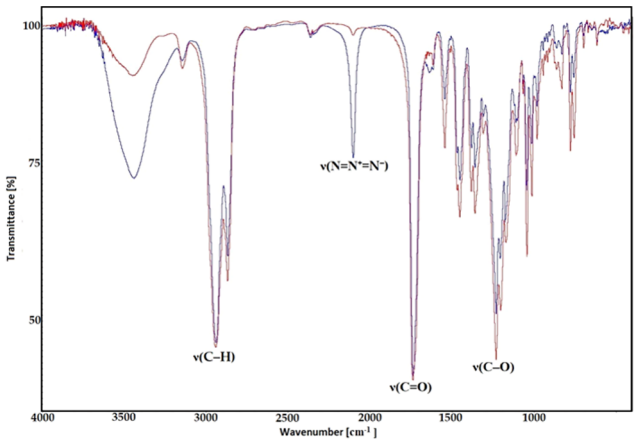

Figure 2. FT-IR spectra of **9** (blue) and **10** (red) in the region (3700–400 cm^{-1}).

these compounds, the ESI-MS spectrum in negative-ion mode exhibits the molecular ion at m/z 1801 (55%) $[C_{99}H_{141}N_9O_{18}+Hac-H]^-$ (for **11**), m/z 2016.2 (100%) $[C_{105}H_{147}N_9O_{24}+HSO_4]^-$, m/z 1954.2 (25%) $[C_{105}H_{147}N_9O_{24}+Cl]^-$, and m/z 2030.2 (55%) $[C_{105}H_{147}N_9O_{24}+TFA-H]^-$ (for **12**) (Figure 3).

2.3. PM5 Calculations. The PM5 semiempirical calculations were performed using the WinMopac 2003 program. The final heat of formation (HOF) of compounds **5** and **6** as well as quasi-podands **9**–**13** are presented in Table 1.

The molecular models of compounds **4**–**6** as well as **9**–**12** are shown in Figure 4. For the substrates **4**–**6**, the lowest values of HOF are observed for cholic acid derivatives **6**, where an increasing number of acetoxy groups facilitate the formation of intramolecular hydrogen bonds. It is noteworthy that mono-substituted derivatives of bile acids-linked 1,2,3-triazole ring (with two N_3 groups) are not formed because the heat of formation is very high. Also, disubstituted derivatives are occasionally observed. Only lithocholic acid derivatives could be obtained, and their stability was still low (higher HOF than substrate **5**).

In all quasi-podands, we observed $\pi-\pi$ stacking sandwich-type interactions between two triazole rings were observed. The calculated interplanar separation is about 5.8 Å. These distances are greater by about 1.7 Å in comparison to the classical $\pi-\pi$ stacking interactions because the triazole ring is attached to directly a rigid aromatic ring which imposes an increasing distance. Furthermore, this spatial arrangement of bile acids and 1,2,3-triazole rings can facilitate the formation of stable host–guest complexes.

2.4. *In Silico* Biological Activity Studies. The pharmacological activity of the synthesized compounds **5**, **6**, and **9**–**12** has been assessed using computer-aided drug discovery methods, specifically employing the Prediction of Activity Spectra for Substances (PASSs) program. This program utilizes a comprehensive analysis of structure–activity relationships within a diverse training set containing approximately 60,000 biologically active compounds from various chemical series, encompassing around 4500 types of biological activity. By simply providing the structural formula of a chemical compound, the PASS prediction can be obtained, making it a valuable tool for initial investigations. Numerous instances exist where the implementation of the PASS approach has resulted in the identification of novel pharmacological agents.[44−47]

Furthermore, the analysis of the biological activity spectra for the newly two synthesized esters presented in this study serves as a notable illustration of *in silico* investigations on chemical compounds. The PASS program was employed to predict the biological activity spectra for two substrates **5** and **6** and one specific compound, namely, compound **9**. Focusing on the potential compound with the highest probability (referred to as focal activities) (see Table 2), we identified several frequently predicted types of biological activity, including acylcarnitine hydrolase inhibitor, alkenylglycerophosphocholine hydrolase inhibitor, alkylacetylglycerophosphatase inhibitor, dextranase inhibitor, and CYP2C and CYP2B6 substrates for **5** and **6**. On the other hand, for the quasi-podands, an activity of more than 60% but less than 70% was observed. The following can be mentioned here: glyceryl-ether monooxygenase inhibitor, antifertility (female), antienzematic, cholesterol antagonist, as well as cytoprotectant. However, due to their molecular weight exceeding 1200 g/mol, the potential biological properties of compounds **10**–**12** could not be determined in this analysis.

2.5. Molecular Docking Studies. The macromolecular structure investigated in this study was identified by the PDB ID 1HW8. Below are the potential interactions observed between the analyzed structures and the protein domain. The graphical depictions illustrate the optimal ligand pose, determined by the binding site of the original ligands found within the raw PDB file 1HW8. These representations showcase the poses with the lowest binding energy observed inside the binding site. Figures 5–8 depict the interactions between the best poses of structures **9**, **10**, **11**, and **12**, respectively, and the protein domain of 1HW8.

For compound **9** (Figure 5), there exist three potential hydrogen bonds that could form between the ligand and the protein domain. The shortest among these potential interactions is identified between the ligand's keto ester oxygen and the hydrogen of residue SER 565 D, spanning a length of 2.07 Å. The second possible hydrogen bond measures 2.20 Å and involves the azide group's interaction with the hydrogen of residue ASP 690 C. The last interaction, furthest in distance, may occur between the ligand's nitrogen within the 1,2,3-triazole group and the SER 661 C residue of the protein.

For compound **10** (Figure 6), the potential number of hydrogen bonds is two. The shorter interaction, measuring 2.10 Å, occurs between the ligand's keto carboxyl oxygen and the hydrogen of residue ASN 810 D within the macromolecule.

According to the molecular docking studies, compound **11** (Figure 7) has the potential to form a total of four hydrogen bonds. These interactions are ranked in descending order of length:

- Another interaction involves the ligand's ester oxygen forming a bond (2.42 Å) with the hydrogen of ASN 755 C, which competes with the hydrogen bond formation between the same ligand's keto ester oxygen and the hydrogen of LYS 691 D residue (2.08 Å). The latter interaction is more favorable due to its shorter length.
- Additionally, another hydrogen bond is possible between another ligand's keto ester oxygen and the hydrogen of ARG 627 D, measuring 2.41 Å.
- The shortest hydrogen bond for compound **11** spans a length of 1.78 Å and can be established between yet another ligand's keto ester oxygen and the hydrogen of residue GLY 656 D.

The final compound investigated, ligand **12** (Figure 8), has the potential to form a total of five hydrogen bonds. However,

https://doi.org/10.1021/acs.joc.4c00195
J. Org. Chem. 2024, 89, 7561−7572

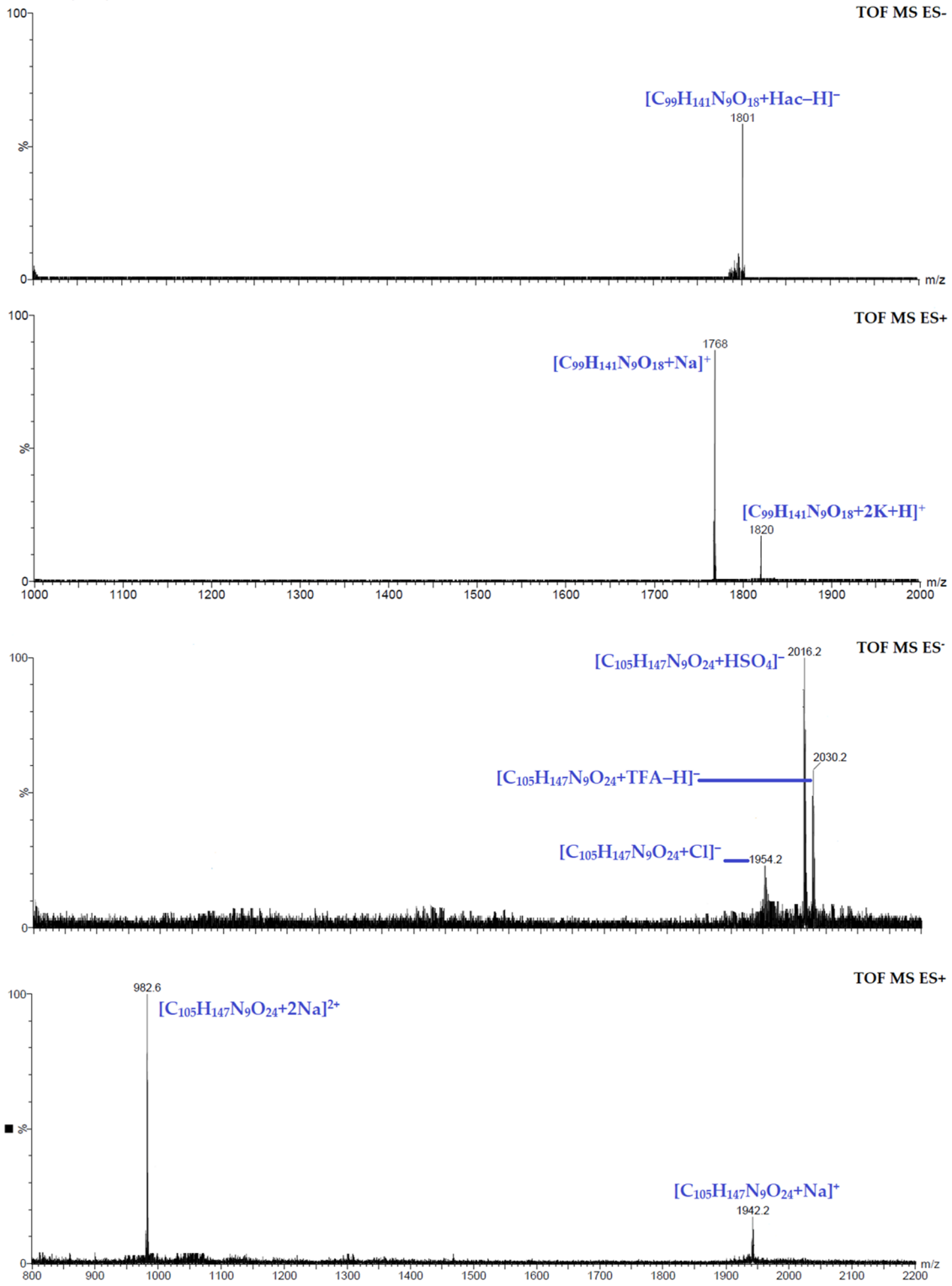

Figure 3. ESI-MS spectrum of conjugates **11** and **12**.

four of these interactions compete with each other, resulting in the effective formation of three hydrogen bonds. The longest possible hydrogen bond exists between the ligand's ester oxygen atom and the hydrogen of residue ASN 658 D.

Another competitive interaction involves the hydrogen of residue GLN 815 D forming a bond (2.40 Å) with the ketone oxygen of one of the ester groups. Additionally, an interaction occurs between the ether's oxygen within the ligand's ester group and the same hydrogen of the protein domain, measuring 2.25 Å. These interactions possess similar probabilities of formation due to their closely matching lengths.

The remaining two hydrogen bonds can be established between the ligand's ester keto oxygen and the hydrogen of residue ARG 590 D (2.20 Å in length), as well as between the same oxygen atom of the ligand and a different residue, namely,

https://doi.org/10.1021/acs.joc.4c00195
J. Org. Chem. 2024, 89, 7561−7572

Table 1. Heat of Formation (HOF) [kcal/mol] of Compounds5, 6, and 9−13

compound	heat of formation[kcal/mol]
4	−212.7209
5	−298.6465
6	−383.8356
9	−286.8410
10	−550.9153
11	−809.8199
12	−1063.6189

SER 661 D. These interactions similarly exhibit very close probabilities of formation.

The docked molecules exhibit a higher affinity toward the 1HW8 protein domain compared to the cocrystallized ligand, which demonstrated a binding energy of −7.5 kcal/mol, with an average binding energy of −6.2 kcal/mol. Similarly, they display a higher affinity compared to mevastatin, showing a binding energy of −6.9 kcal/mol, with an average binding energy of −6.8 kcal/mol. This suggests that these molecules have the potential to serve as effective inhibitors. However, it is essential to note that the sizes of ligands **9** through **12** are notably larger than those of the known activity inhibitors used for comparison, potentially influencing the sensitivity of this comparison. Figures 5−8 display binding energies, denoted in kcal/mol units (specified in the figures' descriptions).

3. CONCLUSIONS

In summary, an efficient synthesis of two new propiolic derivatives and four innovative bile acid bioconjugates with 1,2,3-triazole rings (compounds **9−12**) was designed using the "click" chemistry method. The reaction of propiolic or acyl propionic bile acid derivatives with 1,3,5-tris(azidomethyl)-benzene in a mixture of *tert*-butanol/methanol with the addition of sodium ascorbate and $CuSO_4$*5 H_2O at 60−65 °C yielded macrocyclic compounds containing rings 1,2,3-triazoles. The newly synthesized compounds were thoroughly characterized using spectroscopic techniques and molecular structure analysis. Additionally, the performed molecular docking indicates the potential inhibitory properties of the obtained structures. The Nobel Prize in Chemistry awarded for the study of "click" chemistry serves as conclusive evidence of the significance of this approach in organic synthesis. The growing interest in utilizing "click" chemistry for the synthesis of novel bioconjugates involving bile acids and sterols has a profound impact on the advancement of supramolecular chemistry, pharmacology, and

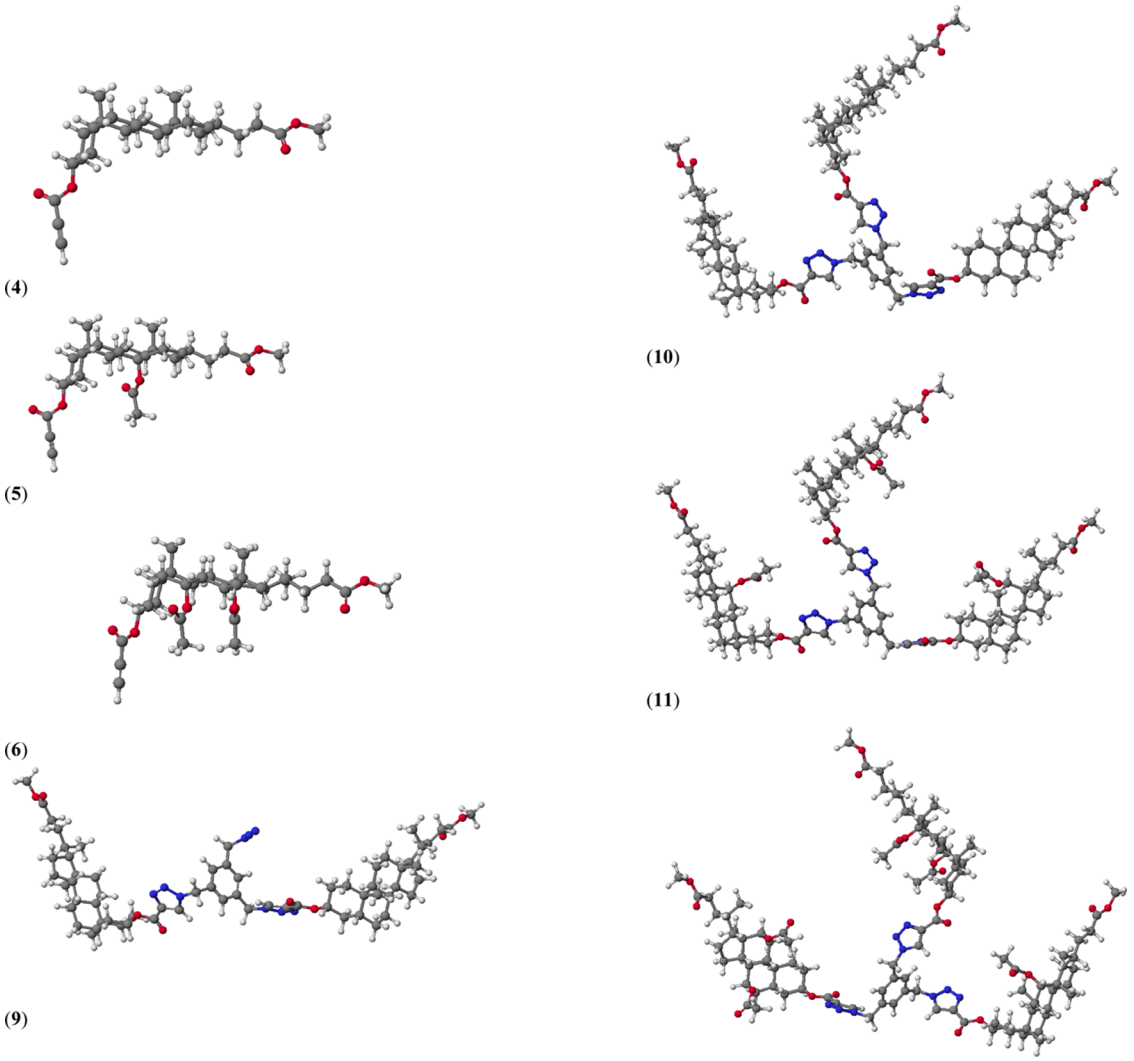

Figure 4. Molecular models of representative compounds **5** and **6** as well as **9−12** calculated by the PM5 method.

https://doi.org/10.1021/acs.joc.4c00195
J. Org. Chem. 2024, 89, 7561−7572

Table 2. PA (Probability "to be Active") Values for the Predicted Biological Activity of Substrates5 and 6 and Compounds9

focal predicted activity (PA > 80%) for **5** and **6**	compound		
focal predicted activity (PA > 60%) for **9**	**5**	**6**	**9**
glyceryl-ether monooxygenase inhibitor			66
antiinfertility (female)			62
antienzematic			67
cholesterol antagonist			60
cytoprotectant			60
acylcarnitine hydrolase inhibitor	96	96	
alkenylglycerophosphocholine hydrolase inhibitor	93	90	
alkylacetylglycerophosphatase inhibitor	93	90	
dextranase inhibitor	89	83	
CYP2C substrate	87	83	
CYP2B6 substrate	85	83	
respiratory analeptic	85		
analeptic	84		
protein-disulfide reductase (glutathione) inhibitor	84		
glyceryl-ether monooxygenase inhibitor	82	85	
peptidoglycan glycosyltransferase inhibitor	81		
CYP3A4 substrate	82	83	
CYP2C substrate		83	
flavin-containing monooxygenase inhibitor		82	
dextranase inhibitor		83	
hypolipemic		81	
adenomatous polyposis treatment		80	
CYP3A substrate		81	

medicine. The design and preparation of compounds incorporating the 1,2,3-triazole ring offer immense biological potential and a diverse range of physicochemical properties, enabling their application as artificial receptors, organogels, and novel complexing and drug delivery agents.

4. EXPERIMENTAL SECTION

4.1. Synthesis. *4.1.1. General Procedure for the Synthesis of Compounds **4**–**6**.* The methyl esters of bile acids were prepared according to a previously described procedure. In the case of compounds **4**, **5**, or **6**, the bile acids (1 equiv) were dissolved in 15 mL of dichloromethane. Subsequently, *p*-TsOH and propiolic acid (3 equiv) were added to the solution, and the reaction was allowed to proceed for 24 h at room temperature. After completion of the reaction, the mixture was subjected to a series of purification steps. It was first washed with cool water, followed by extraction with chloroform (20 mL). The chloroform layer was then washed with water and brine, and dried using Na_2SO_4. Finally, the solvent was removed under reduced pressure, yielding the following product yields: (45%) for **4**, (57%) for **5**, and (30%) for **6**.

*4.1.2. General Procedure for the Synthesis of Compounds **9**–**10**.* 1,3,5-Tris(azidomethyl)benzene (30 mg, 0.123 mmol) was dissolved in a mixture of *tert*-butanol and methanol (12 mL, 5:1). Propiolic lithocholic ester (163 mg, 0.369 mmol) was then added, and the resulting mixture was heated at 60−65 °C (in a water bath) for 30 min. Next, to the homogeneous solution, $CuSO_4$*$5H_2O$ (3 mg, 3 mol %) and sodium ascorbate (9 mg, 20 mol %) in water (0.3 mL) were added. The mixture was further heated to 60−65 °C (in a water bath) for 4 h. The resulting mixture was extracted with chloroform (10 mL), washed with brine (15 mL), and dried using anhydrous Na_2SO_4. After evaporating the solvent and purifying the residue over silica gel ($CHCl_3$/EtOAc, 25:1), 20.3 mg (11%) of product **9** and 169.7 mg (88%) of product **10** were obtained.

*Methyl 3α-Propynoyloxy-12α-acetoxy-5β-cholan-24-oate **(5)**.* Oil (130 mg, 57%). ^{1}H NMR (400 MHz, $CDCl_3$): δ ppm 5.08 (s, 1H, 12β-H), 4.88−4.80 (m, 1H, 3β-H), 3.66 (s, 3H, −OCH_3), 2.89 (s, 1H, −C≡CH), 2.11 (s, 3H, 12α-OAc), 0.91 (s, 3H, CH_3-19), 0.80 (d, *J* = 6.3 Hz, 3H, CH_3-21), 0.72 (s, 3H, CH_3-18). ^{13}C {^{1}H} NMR (101 MHz, $CDCl_3$) δ 174.6 (C-24), 170.5 (CO-12α), 152.1 (C-26), 75.8 (C-12), 75.8 (≡CH), 75.0 (C-3), 74.2 (−C≡), 51.5 (C-25), 49.3, 47.5, 45.0, 41.8, 35.6, 34.6, 34.6, 34.4, 34.0, 31.9, 30.9, 30.8, 27.2, 26.8, 26.3, 25.8, 25.6, 23.4, 23.0 (C-19), 21.4 (OAc-12α), 17.5 (C-21), 12.4 (C-18). FT-IR (KBr, cm^{-1}) ν_{max}: 3445, 3251, 2938, 2869, 2112, 1734, 1701, 1377, 1246, 1194. ESI-MS *m*/*z*: 523 $[M + Na]^+$, 539 $[M + K]^+$.

*Methyl 3α-Propynoyloxy-7α,12α-diacetoxy-5β-cholan-24-oate **(6)**.* Oil (153 mg, 30%), ^{1}H NMR (400 MHz, $CDCl_3$): δ ppm 5.09 (s, 1H, 12β-H), 4.92−4.91 (d, *J* = 3.1 Hz, 1H, 7β-H), 4.76−4.68 (m, 1H, 3β-H), 3.66 (s, 3H, −OCH_3), 2.91 (s, 1H, −C≡CH), 2.15 (s, 1H, 7α-OAc), 2.09 (s, 1H, 12α-OAc), 0.92 (s, 3H, CH_3-19), 0.81 (d, *J* = 6.4 Hz, 3H, CH_3-21), 0.73 (s, 3H, CH_3-18). ^{13}C {^{1}H} NMR (101 MHz, $CDCl_3$) δ 174.5 (C-24), 170.5 (CO-12α), 170.4 (CO-7α), 152.0 (C-26), 75.3 (C-12), 75.3 (≡CH), 75.0 (C-3), 74.4 (−C≡), 70.5 (C-7), 51.2 (C-25), 47.3, 45.0, 43.4, 40.9, 37.7, 34.6, 34.5, 34.3, 34.2, 31.2, 30.8, 30.7, 29.7, 28.9, 27.1, 26.5, 25.6, 22.8, 22.4 (C-19), 21.6 (OAc-7α), 21.5 (OAc-12α), 17.5 (C-21), 12.2 (C-18). FT-IR (KBr, cm^{-1}) ν_{max}: 3247, 2952, 2873, 2116, 1737, 1439, 1378, 1247. ESI-MS *m*/*z*: 581 $[M + Na]^+$, 597 $[M + K]^+$, 594 $[M + Cl]^-$.

*1-Azidomethylene-3,5-di[2-(methyl 5β-cholan-24-oate)-2-oxoethyl-1H-1,2,3-triazole- 4-(3-carboxylate)]benzene **(9)**.* Oil (34 mg, 11%). ^{1}H NMR (400 MHz, $CDCl_3$): δ ppm 8.06 (s, 2H, triazole ring), 7.22 and 7.19 (s, 3H, Ar−H), 5.59 (s, 4H, Ph−CH_2−triazole ring), 5.07−4.99 (m, 2H, 3β-H), 4.37 (s, 2H, CH_2−N_3), 3.67 (s, 6H, −OCH_3) 0.95 (s, 6H, CH_3-19), 0.92 (d, *J* = 6.5 Hz, 6H, CH_3-21), 0.64 (s, 6H, CH_3-18). ^{13}C {^{1}H} NMR (101 MHz, $CDCl_3$) δ 174.8 (C-24), 160.0 (C-26), 141.3 (C-27), 138.3 (Ar−CCH_2−triazole ring), 136.0 (Ar−CCH_2N_3), 127.9 (C-28), 127.5 (C−Ar), 127.2 (C−Ar), 75.7 (C-3), 56.4, 56.0, 53.8 (C-29), 53.7 (C-29'), 51.5 (C-25), 42.7, 41.9, 40.4, 40.1, 35.8, 35.3, 35.0, 34.6, 32.1, 31.0, 28.2, 27.0, 26.5, 26.4, 26.3, 24.2, 23.2 (C-19), 20.8, 18.2 (C-21), 12.0 (C-18). FT-IR (KBr, cm^{-1}) ν_{max}: 2933, 2866, 2099, 1733, 1228, 1203, 1043. ESI-MS (*m*/*z*): 1225 $[C_{65}H_{93}N_9O_8+HSO_4]^-$, 393 $[C_{65}H_{93}N_9O_8+H+2Na]^{3+}$, 413 $[C_{65}H_{93}N_9O_8+3K]^{3+}$, 565 $[C_{65}H_{93}N_9O_8+2H]^{2+}$.

*1,3,5-Tris[2-(methyl 5β-cholan-24-oate)-2-oxoethyl-1H-1,2,3-triazole-4-(3-carboxylate)] benzene **(10)**.* Crystal (170 mg, 88%), mp 130−133 °C. ^{1}H NMR (400 MHz, $CDCl_3$): δ ppm 8.06 (s, 3H, triazole ring), 7.20 (s, 3H, Ar−H), 5.55 (s, 6H, Ph−CH_2−triazole ring), 5.07−4.99 (m, 3H, 3β-H), 3.67 (s, 9H, OCH_3), 0.95 (s, 9H, CH_3-19), 0.92 (d, *J* = 6.5 Hz, 9H, CH_3-21), 0.65 (s, 9H, CH_3-18). ^{13}C {^{1}H} NMR (101 MHz, $CDCl_3$) δ 174.7 (C-24), 160.0 (C-26), 141.4 (C-27), 136.6 (Ar−C), 127.8 (CH-Ar), 127.5 (C-28), 75.8 (C-3), 56.4, 56.0, 53.4 (C-29), 51.5 (C-25), 42.7, 41.9, 40.3, 40.1, 35.8, 35.3, 35.0, 34.6, 32.1, 31.0, 31.0, 28.1, 27.0, 26.5, 26.3, 24.2, 23.2 (C-19), 21.0, 18.2 (C-21), 14.2, 12.0 (C-18). FT-IR (KBr, cm^{-1}) ν_{max}: 2939, 2866, 1736, 1228, 1040. ESI-MS (*m*/*z*): 533 $[C_{93}H_{135}N_9O_{12}+2H+Na]^{3+}$, 810 $[C_{93}H_{135}N_9O_{12}+2Na]^{2+}$.

*1,3,5-Tris[2-(methyl 12α-acetoxy-5β-cholan-24-oate)-2-oxoethyl]-1H-1,2,3-triazole-4-(3-carboxylate)benzene **(11)**.* Crystal (138 mg, 77%,), mp 136−139 °C. ^{1}H NMR (400 MHz, $CDCl_3$): δ ppm 8.08 (s, 3H, triazole ring), 7.19 (s, 3H, Ar−H), 5.55 (s, 6H, Ph−CH_2−triazole ring), 5.07 (d, 3H, 12β-H), 5.05−4.96 (m, 3H, 3β-H), 3.67 (s, 9H, OCH_3), 2.12 (s, 9H, 12α-OAc), 0.94 (s, 9H, CH_3-19), 0.80 (d, *J* = 6.3 Hz, 9H, CH_3-21), 0.73 (s, 9H, CH_3-18). ^{13}C {^{1}H} NMR (101 MHz, $CDCl_3$) δ 174.6 (C-24), 170.7 (C-31), 160.0 (C-26), 141.4 (C-27), 136.5 (Ar−C), 127.8 (Ar−CH), 127.7 (C-28), 75.8 (C-3 and C-12), 53.4 (C-29), 51.5 (C-25), 49.3, 47.5, 45.0, 42.0, 36.5, 34.2, 32.2, 30.9, 30.8, 27.3, 27.0, 26.6, 25.7, 23.4 (C-19), 23.1, 21.5 (OAc-12α), 17.5 (C-21), 12.4 (C-18). FT-IR (KBr, cm^{-1}) ν_{max}: 2950, 2869, 1736, 1672, 1245, 1195, 1041, 1020. ESI-MS (*m*/*z*): 1801 $[C_{99}H_{141}N_9O_{18}+Hac-H]^-$, 1768 $[C_{99}H_{141}N_9O_{18}+Na]^+$. 1820 $[C_{99}H_{141}N_9O_{18}+2K+H]^+$.

*1,3,5-Tris[2-(methyl 7α,12α-diacetoxy-5β-cholan-24-oate)-2-oxoethyl]-1H-1,2,3-triazole-4-(3-carboxylate)benzene **(12)**.* Crystal (176 mg, 57% yield), mp 136−139 °C. ^{1}H NMR (400 MHz, $CDCl_3$): δ ppm 8.10 (s, 3H, triazole ring), 7.21 (s, 3H, Ar−H), 5.55 (s, 6H, Ph−CH_2−triazole ring), 5.09 (d, 3H, 12β-H), 4.94−4.81 (m, 6H, 3β-H i 7β-H), 3.67 (s, 9H, OCH_3), 2.20 (s, 9H, 7α-OAc) 2.08 (s, 9H, 12α-OAc), 0.95 (s, 9H, CH_3-19), 0.81 (d, *J* = 6.2 Hz, 9H, CH_3-21),

https://doi.org/10.1021/acs.joc.4c00195
J. Org. Chem. 2024, 89, 7561−7572

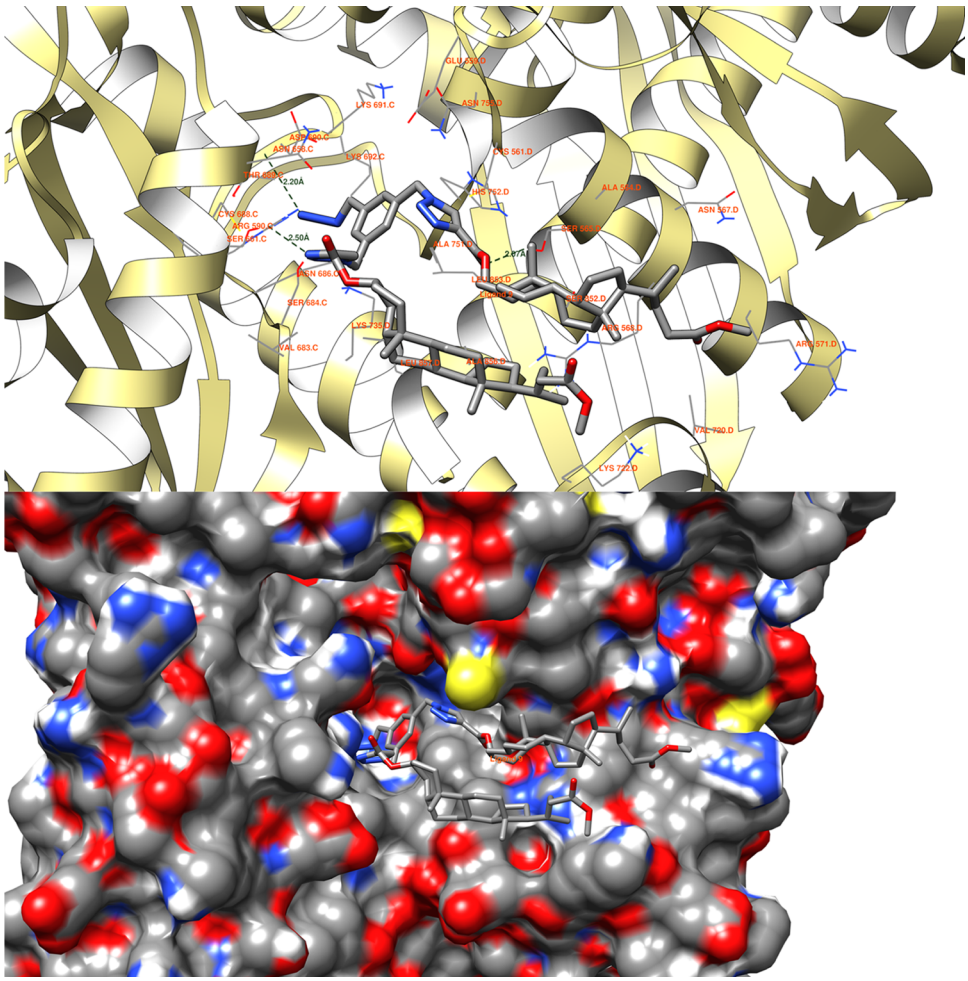

Figure 5. Ligand **9** possible hydrogen bonds between 1HW8 protein domain binding site. The binding energy equals −8.7 kcal/mol, with the average binding energy of −8.4 kcal/mol.

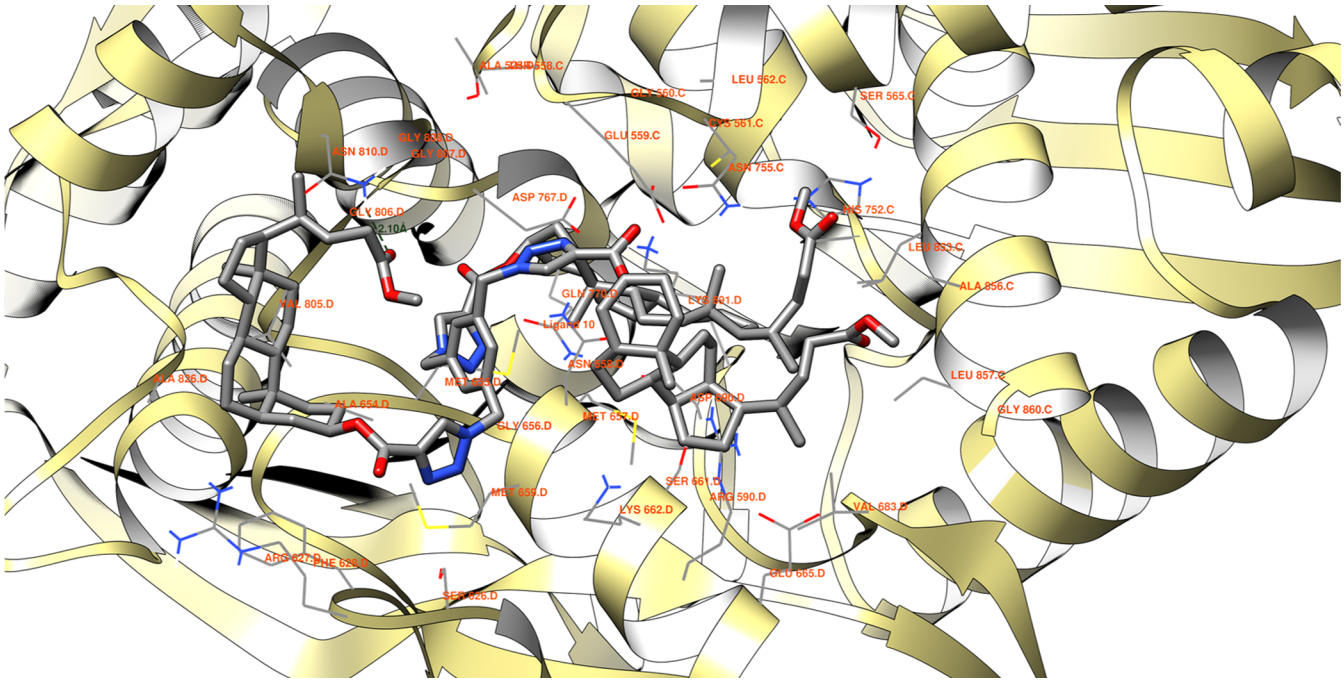

Figure 6. Ligand **10** possible hydrogen bonds between 1HW8 protein domain binding site. The binding energy equals −9.8 kcal/mol, with the average binding energy of −9.8 kcal/mol.

https://doi.org/10.1021/acs.joc.4c00195
J. Org. Chem. 2024, 89, 7561−7572

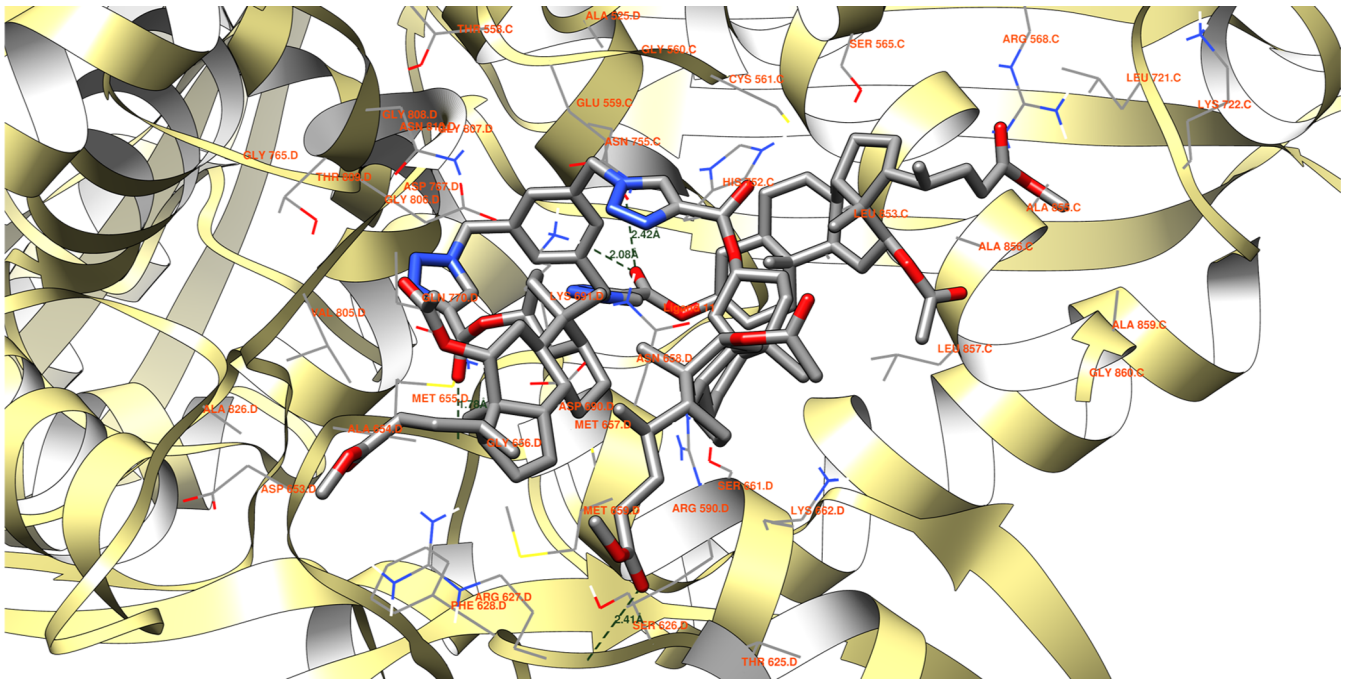

Figure 7. Ligand **11** possible hydrogen bonds between 1HW8 protein domain binding site. The binding energy equals −8.9 kcal/mol, with the average binding energy of −9.0 kcal/mol.

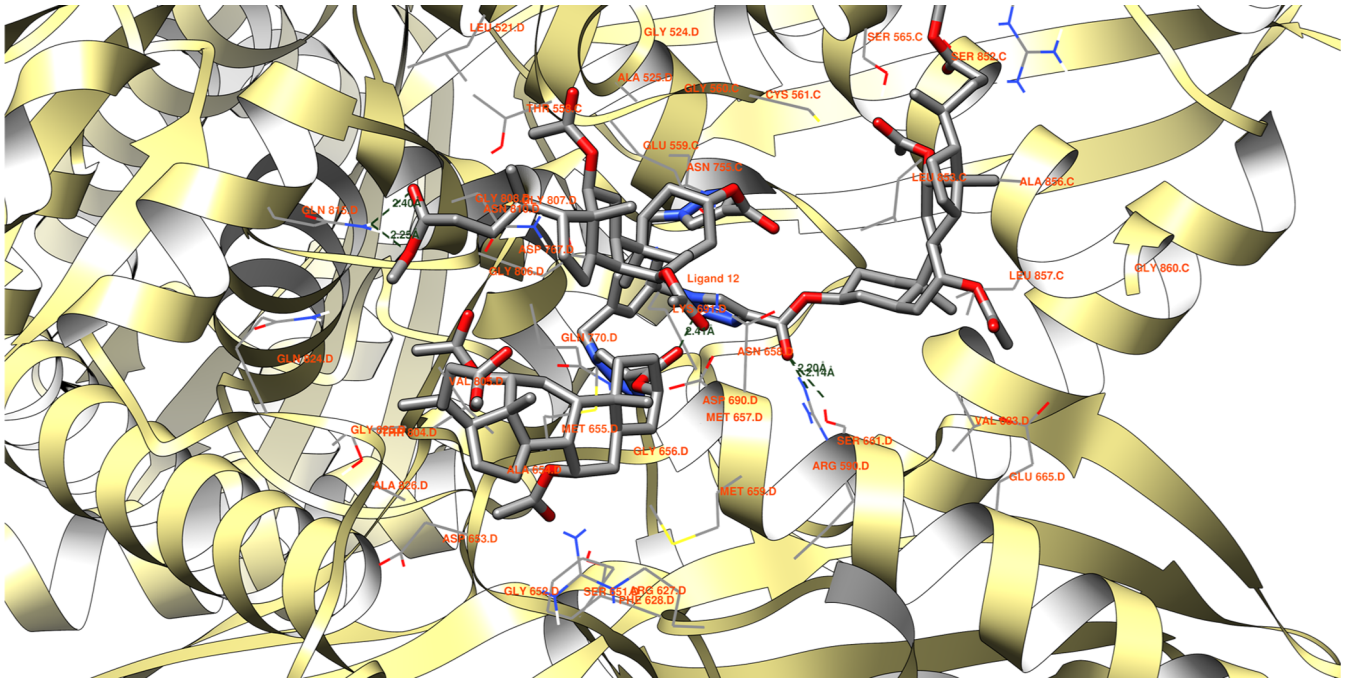

Figure 8. Ligand **12** possible hydrogen bonds between 1HW8 protein domain binding site. The binding energy equals −9.2 kcal/mol, with the average binding energy of −9.1 kcal/mol.

0.73 (s, 9H, CH_3-18). ^{13}C {^1H} NMR (101 MHz, $CDCl_3$) δ 174.5 (C-24), 170.8 (C-33), 170.6 (C-31), 160.1 (C-26), 141.4 (C-27), 136.5 (C−Ar), 128.0 (C-28 i CH-Ar), 75.7 (C-12), 75.3 (C-3), 70.5 (C-7), 53.4 (C-29), 51.5 (C-25), 47.3, 45.1, 43.4, 41.0, 37.7, 34.6, 31.3, 31.8, 30.7, 29.0, 27.1, 26.7, 25.7, 22.8 (C-19), 22.5 (OAc-7α), 21.7 (OAc-12α), 17.4 (C-21), 12.2 (C-18). FT-IR (KBr, cm^{-1}) ν_{max}: 2951, 2872, 1735, 1378, 1246, 1022. ESI-MS (m/z): 2016.2 $[C_{105}H_{147}N_9O_{24}+HSO_4]^-$, 1954.2 $[C_{105}H_{147}N_9O_{24}+Cl]^-$, 1942.2 $[C_{105}H_{147}N_9O_{24}+Na]^+$, 982.6 $[M+2Na]^{2+}$, 2030.2 $[C_{105}H_{147}N_9O_{24}+TFA-H]^-$.

4.2. Molecular Docking Studies. The molecular docking process utilized the OpenBabel software[48,49] to generate three-dimensional (3D) structures from SMILES representations of compounds. These structures were initially saved in *.pdb format and subsequently converted to the required *.pdbqt format for compatibility with the AutoDock Vina algorithm.[50] The receptor, represented by 1HW8 (PDB ID, HMG-CoA reductase), was prepared using AutoDock Tools 1.5.7.[51,52] The molecular docking methodology employed the AutoDock Vina algorithm utilizing the multiple CPU technique.[49] Visualizations of the best poses of the docked ligands and potential

https://doi.org/10.1021/acs.joc.4c00195
J. Org. Chem. 2024, 89, 7561−7572

hydrogen bond formations were performed using the Chimera tool (version 1.16).[53]

In this study, the receptor 1HW8 (PDB ID, HMG-CoA reductase) was selected for docking structures **9**, **10**, **11**, and **12** (refer to Figure 8), acquired from the Protein Data Bank (PDB).[54−56] This enzyme is pivotal in cholesterol production within the liver. Inhibiting the HMG-CoA reductase activity can potentially reduce cholesterol production, subsequently lowering its concentration in the bloodstream.[56]

The docked structures were targeted to the active site of the protein domain, analogous to the cocrystallized ligands. The search parameters utilized for 1HW8 were set as follows: center (*x*, *y*, *z*): 22.145, 21.402, 29.764, and size (*x*, *y*, *z*) (80 × 80 × 80) Å^3.

■ ASSOCIATED CONTENT

Data Availability Statement

The data underlying this study are available in the published article and its Supporting Information.

Supporting Information

The Supporting Information is available free of charge at https://pubs.acs.org/doi/10.1021/acs.joc.4c00195.

General information and copies of ESI-MS, ^{1}H and ^{13}C NMR, and FT-IR spectra (PDF)

■ AUTHOR INFORMATION

Corresponding Author

Tomasz Pospieszny − *Department of Bioactive Products, Faculty of Chemistry, Adam Mickiewicz University, 61-614 Poznań, Poland;* orcid.org/0000-0001-5071-7016; Email: tposp@amu.edu.pl

Authors

Anna Kawka − *Department of Bioactive Products, Faculty of Chemistry, Adam Mickiewicz University, 61-614 Poznań, Poland;* orcid.org/0000-0001-9281-7103

Hanna Koenig − *Department of Bioactive Products, Faculty of Chemistry, Adam Mickiewicz University, 61-614 Poznań, Poland*

Damian Nowak − *Department of Quantum Chemistry, Faculty of Chemistry, Adam Mickiewicz University, 61-614 Poznań, Poland;* orcid.org/0000-0003-3739-3306

Complete contact information is available at: https://pubs.acs.org/10.1021/acs.joc.4c00195

Author Contributions

Conceptualization: A.K. and T.P.; molecular docking: D.N.; methodology: A.K., H.K., and D.N.; formal analysis: A.K., H.K., D.N., and T.P.; investigation: H.K. and T.P.; resources: H.K. and T.P.; data curation: H.K. and T.P.; writing—original draft preparation: A.K., H.K., D.N., and T.P.; writing—review and editing: H.K. and T.P.; visualization: A.K., H.K., and T.P.; supervision: T.P.; project administration: T.P.; funding acquisition: T.P. All authors have read and agreed to the published version of the manuscript.

Notes

The authors declare no competing financial interest.

Safety Statement: The obtained compounds were obtained under laboratory conditions. The compounds have not been subjected to cytotoxicity tests; therefore, their effect on human or animal cells is not known.

■ ACKNOWLEDGMENTS

This work was financially supported by the Research Subsidy at the Faculty of Chemistry of the Adam Mickiewicz University in Poznan.

■ REFERENCES

(1) Kumar, V.; Lal, K.; Naveen; Tittal, R. K. The fate of heterogeneous catalysis & click chemistry for 1,2,3-triazoles: Nobel prize in chemistry 2022. *Catal. Commun.* **2023**, *176*, No. 106629.

(2) Narayan, S.; Muldoon, J.; Finn, M. G.; Fokin, V. V.; Kolb, H. C.; Sharpless, K. B. On Water": Unique Reactivity of Organic Compounds in Aqueous Suspension. *Angew. Chem., Int. Ed.* **2005**, *44*, 3275−3279.

(3) Woo, H.; Kang, H.; Kim, A.; Jang, S.; Park, J. C.; Park, S.; Kim, B. S.; Song, H.; Park, K. H. Azide-Alkyne Huisgen [3 + 2] Cycloaddition Using CuO Nanoparticles. *Molecules* **2012**, *17*, 13235−13252.

(4) Kumar, A.; Kumar, V.; Singh, P.; Tittal, K. R.; Lal, K. Ionic liquids for the green synthesis of 1,2,3-triazoles: a systematic review. *Green Chem.* **2024**, *26*, 3565−3594.

(5) da SM Forezi, L.; Cardoso, M. F. C.; Gonzaga, D. T. G.; da Silva, F. C.; Ferreira, V. F. Alternative Routes to the Click Method for the Synthesis of 1,2,3-Triazoles, an Important Heterocycle in Medicinal Chemistry. *Curr. Top. Med. Chem.* **2018**, *18* (17), 1428−1453.

(6) Bonandi, E.; Christodoulou, M. S.; Fumagalli, G.; Perdicchia, D.; Rastelli, G.; Passarella, D. The 1,2,3-Triazole Ring as a Bioisostere in Medicinal Chemistry. *Drug Discovery Today* **2017**, *22*, 1572−1581.

(7) Baraniak, D.; Boryski, J. Triazole-Modified Nucleic Acids for the Application in Bioorganic and Medicinal Chemistry. *Biomedicines* **2021**, *9* (6), 628.

(8) Rammohan, A.; Venkatesh, B. C.; Basha, N. M.; Zyryanov, G. V.; Nageswararao, M. Comprehensive review on natural pharmacophore tethered 1,2,3-triazoles as active pharmaceuticals. *Chem. Biol. Drug. Des.* **2023**, *101* (5), 1181−1203.

(9) Gonnet, L.; Baron, M.; Baltas, M. Synthesis of Biologically Relevant 1,2,3- and 1,3,4-Triazoles: From Classical Pathway to Green Chemistry. *Molecules* **2021**, *26* (18), 5667.

(10) Agarwal, D. S.; Krishna, V. S.; Sriram, D.; Yogeeswari, P.; Sakhuja, R. Clickable Conjugates of Bile Acids and Nucleosides: Synthesis, Characterization, in Vitro Anticancer and Antituberculosis Studies. *Steroids* **2018**, *139*, 35−44.

(11) Cui, X.; Zhang, X.; Wang, W.; Zhong, X.; Tan, Y.; Wang, Y.; Zhang, J.; Li, Y.; Wang, X. Regitz Diazo Transfer Reaction for the Synthesis of 1,4,5-Trisubstituted 1,2,3-Triazoles and Subsequent Regiospecific Construction of 1,4-Disubstituted 1,2,3-Triazoles via C−C Bond Cleavage. *J. Org. Chem.* **2021**, *86*, 4071−4080.

(12) Fang, Y.; Bao, K.; Zhang, P.; Sheng, H.; Yun, Y.; Hu, S.-X.; Astruc, D.; Zhu, M. Insight into the Mechanism of the CuAAC Reaction by Capturing the Crucial Au_4Cu_4 − π-Alkyne Intermediate. *J. Am. Chem. Soc.* **2021**, *143*, 1768−1772.

(13) Todorov, L.; Kostova, I. 1,2,3-Triazoles and their metal chelates with antimicrobial activity. *Front. Chem.* **2023**, *11*, 2023.

(14) Poonia, N.; Kumar, A.; Kumar, V.; Yadav, M.; Lal, K. Recent Progress in 1H-1,2,3-triazoles as Potential Antifungal Agents. *Curr. Top. Med. Chem.* **2021**, *21* (23), 2109−2133.

(15) Canseco-González, D.; Rodríguez-Victoria, I.; Apan-Ramírez, T.; Viviano-Posadas, A. O.; Serrano-García, J. S.; Arenaza-Corona, A.; Orjuela, A. L.; Alí-Torres, J.; Dorazco-González, A.; Morales-Morales, D. Facile, Single-Step Synthesis of a Series of D-Ring Ethisterones Substituted with 1,4−1,2,3-Triazoles: Preliminary Evaluation of Cytotoxic Activities. *ChemMedChem* **2023**, *18* (8), No. e202200659.

(16) Lednicer, D. *Steroid Chemistry at a Glance: Lednicer/Steroid Chemistry at a Glance*; John Wiley & Sons, Ltd: Chichester, UK, 2010.

(17) Silva, M. M. C.; Salvador, J. A. R. Introductory Chapter: Chemistry and Biological Activity of Steroids - Scope and Overview. In *Chemistry and Biological Activity of Steroids*; Salvador, J. A. R.; Silva, M. M. C., Eds.; IntechOpen, 2020.

(18) Monte, M. J.; Marin, J. J.; Antelo, A.; Vazquez-Tato, J. Bile Acids: Chemistry, Physiology, and Pathophysiology. *World J. Gastroenterol.* **2009**, *15*, 804.

(19) Li, X.; Zhao, T.; Cheng, D.; Chu, C.; Tong, S.; Yan, J.; Li, Q.-Y. Synthesis and Biological Activity of Some Bile Acid-Based Camptothecin Analogues. *Molecules* **2014**, *19*, 3761−3776.
(20) Xiao, L.; Yu, E.; Yue, H.; Li, Q. Enhanced Liver Targeting of Camptothecin via Conjugation with Deoxycholic Acid. *Molecules* **2019**, *24*, 1179−1185.
(21) Ermolenko, E. V.; Imbs, A. B.; Gloriozova, T. A.; Poroikov, V. V.; Sikorskaya, T. V.; Dembitsky, V. M. Chemical Diversity of Soft Coral Steroids and Their Pharmacological Activities. *Mar. Drugs* **2020**, *18*, 613.
(22) Kawka, A.; Hajdaś, G.; Kułaga, D.; Koenig, H.; Kowalczyk, I.; Pospieszny, T. Molecular Structure, Spectral and Theoretical Study of New Type Bile Acid−Sterol Conjugates Linked via 1,2,3-Triazole Ring. *J. Mol. Struct.* **2023**, *1273*, No. 134313.
(23) Zhang, J.; Junk, M. J. N.; Luo, J.; Hinderberger, D.; Zhu, X. X. 1,2,3-Triazole-Containing Molecular Pockets Derived from Cholic Acid: The Influence of Structure on Host−Guest Coordination Properties. *Langmuir* **2010**, *26*, 13415−13421.
(24) Zhang, J.; Luo, J.; Zhu, X. X.; Junk, M. J. N.; Hinderberger, D. Molecular Pockets Derived from Cholic Acid as Chemosensors for Metal Ions. *Langmuir* **2010**, *26*, 2958−2962.
(25) Peng, L.; Mo, F.; Zhang, Q. Cholate-Based Synthesis of Size-Tunable Cage Compounds. *J. Org. Chem.* **2015**, *80*, 1221−1228.
(26) Luo, J.; Chen, Y.; Zhu, X. X. Invertible Amphiphilic Molecular Pockets Made of Cholic Acid. *Langmuir* **2009**, *25*, 10913−10917.
(27) Janout, V.; Jing, B.; Regen, S. L. Molecular Umbrella-Assisted Transport of an Oligonucleotide across Cholesterol-Rich Phospholipid Bilayers. *J. Am. Chem. Soc.* **2005**, *127*, 15862−15870.
(28) Janout, V.; Regen, S. L. Bioconjugate-Based Molecular Umbrellas. *Bioconjugate Chem.* **2009**, *20*, 183−192.
(29) Janout, V.; Bienvenu, C.; Schell, W.; Perfect, J. R.; Regen, S. L. Molecular Umbrella−Amphotericin B Conjugates. *Bioconjugate Chem.* **2014**, *25*, 1408−1411.
(30) Pospieszny, T.; Koenig, H.; Kowalczyk, I.; Brycki, B. Synthesis, Spectroscopic and Theoretical Studies of New Quasi-Podands from Bile Acid Derivatives Linked by 1,2,3-Triazole Rings. *Molecules* **2014**, *19*, 2557−2570.
(31) Mishra, R.; Mishra, S. Updates in Bile Acid-Bioactive Molecule Conjugates and Their Applications. *Steroids* **2020**, *159*, No. 108639.
(32) Vatmurge, N. S.; Hazra, B. G.; Pore, V. S.; Shirazi, F.; Chavan, P. S.; Deshpande, M. V. Synthesis and Antimicrobial Activity of β-Lactam−Bile Acid Conjugates Linked via Triazole. *Bioorg. Med. Chem. Lett.* **2008**, *18*, 2043−2047.
(33) Karabulut, H. R. F.; Karatavuk, A. O.; Ozyildirim, H.; Doğanlar, O.; Doğanlar, Z. B. Synthesis of Novel Dimeric Compounds Containing Triazole Using Click Method and Their Selective Antiproliferative and Proapoptotic Potential via Mitochondrial Apoptosis Signaling. *Med. Chem. Res.* **2020**, *29*, 643−655.
(34) Bariya, D.; Anand, V.; Mishra, S. Recent Advances in the Bile Acid Based Conjugates/Derivatives towards Their Gelation Applications. *Steroids* **2021**, *165*, No. 108769.
(35) Nayal, A.; Muwal, P. K.; Pandey, P. S. Bile Acid Based Receptors for Multiple Metal Ion Recognition. *Tetrahedron* **2019**, *75*, 1968−1974.
(36) Kim, J.; Jeon, O.-C.; Moon, H. T.; Hwang, S. R.; Byun, Y. Preclinical Safety Evaluation of Low Molecular Weight Heparin-Deoxycholate Conjugates as an Oral Anticoagulant: Preclinical Safety Evaluation of Oral Heparin-Deoxycholate Conjugates. *J. Appl. Toxicol.* **2016**, *36*, 76−93.
(37) Kovacevic, B.; Jones, M.; Ionescu, C.; Walker, D.; Wagle, S.; Chester, J.; Foster, T.; Brown, D.; Mikov, M.; Mooranian, A.; Al-Salami, H. The Emerging Role of Bile Acids as Critical Components in Nanotechnology and Bioengineering: Pharmacology, Formulation Optimizers and Hydrogel-Biomaterial Applications. *Biomaterials* **2022**, *283*, No. 121459.
(38) Pospieszny, T. Molecular Pockets, Umbrellas and Quasi Podands from Steroids: Synthesis, Structure and Applications. *Mini-Rev. Org. Chem.* **2015**, *12*, 258−270.
(39) Bansal, R.; Suryan, A. A Comprehensive Review on Steroidal Bioconjugates as Promising Leads in Drug Discovery. *ACS Bio. Med. Chem. Au* **2022**, *2*, 340−369.
(40) Ghosh, K.; Panja, A.; Panja, S. Cholesterol appended bis-1,2,3-triazoles as simple supramolecular gelators for naked eye detection of Ag^{+}, Cu^{2+} and Hg^{2+} ions. *New J. Chem.* **2016**, *40* (4), 3476−3483.
(41) *CAChe 5.04 UserGuide*; Fujitsu: Chiba, Japan, 2003.
(42) Stewart, J. J. P. Optimization of parameters for semiempirical methods. III Extension of PM3 to Be, Mg, Zn, Ga, Ge, As, Se, Cd, In, Sn, Sb, Te, Hg, Tl, Pb, and Bi. *J. Comput. Chem.* **1991**, *12*, 320−341.
(43) Stewart, J. J. P. Optimization of parameters for semiempirical methods I. Method. *J. Comput. Chem.* **1989**, *10*, 209−220.
(44) Pharma Expert Predictive Services © 2011-2013, Version 2.0. http://www.pharmaexpert.ru/PASSOnline/.
(45) Poroikov, V. V.; Filimonov, D. A.; Borodina, Y. V.; Lagunin, A. A.; Kos, A. Robustness of biological activity spectra predicting by computer program PASS for noncongeneric sets of chemical compounds. *J. Chem. Inf. Comput. Sci.* **2000**, *40*, 1349−1355.
(46) Poroikov, V. V.; Filimonov, D. A. How to acquire new biological activities in old compounds by computer prediction. *J. Comput. Aided Mol. Des.* **2002**, *16*, 819−824.
(47) Poroikov, V. V.; Filimonov, D. A. *Predictive Toxicology*; Helma, C., Ed.; Taylor and Francis: Boca Raton, Florida, USA, 2005; pp 459−478.
(48) O'Boyle, N. M.; Banck, M.; James, C. A.; Morley, C.; Vandermeersch, T.; Hutchison, C. R. Open Babel: An Open Chemical Toolbox. *J. Cheminf.* **2011**, *3* (1), 33.
(49) The Open Babel Package, Version 3.1.1. http://openbabel.org (accessed Nov 2, 2023).
(50) Trott, O.; Olson, A. J. AutoDock Vina: Improving the Speed and Accuracy of Docking with a New Scoring Function, Efficient Optimization, and Multithreading. *J. Comput. Chem.* **2010**, *31* (2), 455−461.
(51) Sanner, M. F. Python: A Programming Language for Software Integration and Development. *J. Mol. Graphics Modell.* **1999**, *17*, 57−61.
(52) Morris, G. M.; Huey, R.; Lindstrom, W.; Sanner, M. F.; Belew, R. K.; Goodsell, D. S.; Olson, A. J. Autodock4 and AutoDockTools4: automated docking with selective receptor flexiblity. *J. Comput. Chem.* **2009**, *16*, 2785−2791.
(53) Pettersen, E. F.; Goddard, T. D.; Huang, C. C.; Couch, G. S.; Greenblatt, D. M.; Meng, E. C.; Ferrin, T. E. UCSF Chimera–a visualization system for exploratory research and analysis. *J. Comput. Chem.* **2004**, *25* (13), 1605−1612.
(54) Istvan, E. S.; Deisenhofer, J. Structural Mechanism for Statin Inhibition of HMG-CoA Reductase. *Science* **2001**, *292* (5519), 1160−1164.
(55) RCBS Protein DATA BANK. https://www.rcsb.org (accessed Oct 28, 2023).
(56) Berman, H. M. The Protein Data Bank. *Nucleic Acids Res.* **2000**, *28* (1), 235−242.

https://doi.org/10.1021/acs.joc.4c00195
J. Org. Chem. 2024, 89, 7561−7572

Journal of Molecular Structure 1273 (2023) 134313

Contents lists available at ScienceDirect

Journal of Molecular Structure

journal homepage: www.elsevier.com/locate/molstr

Molecular structure, spectral and theoretical study of new type bile acid–sterol conjugates linked via 1,2,3-triazole ring

Anna Kawka[a], Grzegorz Hajdaś[a], Damian Kułaga[b], Hanna Koenig[a], Iwona Kowalczyk[a], Tomasz Pospieszny[a,*]

[a] Department of Bioactive Products, Faculty of Chemistry, Adam Mickiewicz University, Uniwersytetu Poznańskiego 8 Street, 61–614 Poznań, Poland
[b] Department of Organic Chemistry and Technology, Faculty of Chemical Engineering and Technology, Cracow University of Technology, Warszawska 24 Street, 31-155 Kraków, Poland

ARTICLE INFO

Article history:
Received 27 June 2022
Revised 5 October 2022
Accepted 10 October 2022
Available online 11 October 2022

Keywords:
Bile acids
Sterols
Click chemistry
1,2,3-triazole ring
Semiempirical calculations
PASS
Molecular docking

ABSTRACT

New six steroid conjugates have been prepared from bile acids (tail part)and sterol (head part) derivatives using click chemistry method. The azide-alkyne Huisgen cycloaddition (intermolecular 1,3-dipolar cycloaddition) of the azide derivatives of lithocholic, deoxycholic, cholic acid and propiolate ester of cholesterol and cholestanol gave a new bile acid–sterol conjugates linked with a 1,2,3-triazole ring. Previously, bile acids were converted into bromoacetyl substituted derivatives by the reaction of propargyl esters of lithocholic, deoxycholic, cholic with bromoacetic acid bromide in toluene with TEBA and sodium hydride. Additionally, five of the reagents: bromoacetyl and azidoacetyl substituted derivatives of propargyl esters of deoxycholic and cholic acids as well as 5α-cholestan-3-yl-propynoatewere also obtained and characterized for the first time. All conjugates were obtained in good yields using an efficient synthesis method. The structures of all conjugates as well as four substrates were confirmed by spectral (^{1}H- and ^{13}C NMR, and FT-IR) analysis, mass spectrometry (ESI-MS), as well as PM5 semiempirical methods. Also B3LYP calculations have been carried out. The screening constants for ^{13}C and ^{1}H atoms have been calculated by the GIAO/B3LYP/6–311G(d,p) approach and analyzed. Theoretical vibrational parameters are compared with obtained experimental parameters. Estimation of the pharmacotherapeutic potential has been accomplished for the synthesized compounds on the basis of Prediction of Activity Spectra for Substances (PASS). Additionally molecular docking was performed for the selected conjugate.

1. Introduction

The properties of compounds of natural origin represent important benefits for organic chemistry. Steroids deserve special mention. They are chemical compounds that perform several functions ensuring the proper functioning of living organisms, such as participation in metabolic changes, components of plant and animal cell membranes, and a precursor to the production of many vitamins [1–7]. Transformation of the cholesterol structure under the influence of UV radiation leads to obtaining 1α,25-dihydroxycalciferol (vitamin D3) [8–10]. In addition, special attention is drawn to bile acids, plant sterols (ergosterol), sex hormones (estrogens, testosterone, progesterone), plant hormones (brassinosteroids) [11–13]. Organic syntheses, in which different functional groups attached to the core of all steroid compounds of the cyclopentanoperhydrophenanthrene skeleton are modified, lead to the production of derivatives with significantly higher biological activity [14–20].

Bile acids were isolated in 1828 by L. Gmelin from whale bile. The starting compound for their receipt in the liver is cholesterol. After biosynthesis, they form derivatives with the amino acids taurine and glycine and are stored in the form of salts in the gallbladder [21–24]. Bile acids are distinguished by a large curved skeleton, A/B rings adopting *cis* geometry, enantiomeric purity, chirality, and the presence of hydroxyl groups in a different position at carbon atoms (3α; 3α, 7α; 3α,7α,12α) [25–27]. Polarity, amphiphilic properties and high reactivity of hydroxide groups, varying respectively in the order of 3α>7α>12α, make these compounds have enormous potential as a precursor to the synthesis of organic macrocyclic steroid conjugates with high pharmacotherapeutic activity [28–34].

The possibility of modifying the 3α–OH group contributed to the increase in interest in bile acid and sterol derivatives, especially in the synthesis of dimers, molecular pliers, artificial receptors, cholophans or quasi-podands [35–42].

* Corresponding author.
E-mail address: tposp@amu.edu.pl (T. Pospieszny).

https://doi.org/10.1016/j.molstruc.2022.134313

"Click chemistry" is an innovative and modern method of synthesizing new steroid conjugates gaining importance in the pharmaceutical industry and medicine. The copper-alkyne azido-alkyne addition (CuAAC) described by K.B. Sharpless involves the formation of a new carbon-heteroatom bond in the ring [43–47]. Obtaining new conjugates by the "click" method is primarily a highly efficient, selective and effective synthesis. In addition, the resulting products are easy to isolate, stable in many solvents, including water, and resistant to metabolic degradation [44,48]. The 1.3-dipolar cycloaddition is crucial. The Huisgen reaction occurs in the presence of Cu(I) between terminal alkyne and azide. It is an extremely valuable method of synthesis of compounds containing 1,2,3-triazole rings [48–52]. The use of an appropriate catalyst and increased temperature determine the regioselectivity of the reaction, leading to the formation of 1,4- or 1,5-disubstituted 1,2,3-triazoles [53–57]. Conjugates containing 1,2,3-triazole rings in the structure have several important properties, especially they are distinguished by high resistance to oxidation reactions, reduction and hydrolysis of biological systems, invulnerability to metabolic degradation, anti-cancer activity and the possibility of forming hydrogen bonds [31,34,43,58-60].

2. Experimental

2.1. Instrumentation and chemicals

All of the synthesis reagents lithocholic, deoxycholic and cholic acids, cholesterol, cholestanol, acetic anhydride, pyridine, propiolic acid, sodium azide, sodium ascorbate were purchased from Sigma-Aldrich Corporation. Solvents chloroform, dichloromethane, toluene, hexane, *t*-butanol, methanol were obtained from common commercial sources (Merck, Fisher) and used with-out purification. General. IR Spectra: FT/IR-4600 type A in solid state or oil; ν in cm^{-1}. ^1H and ^{13}C NMR spectra: Varian Mercury 300 MHz spectrometer (Oxford, UK), operating at 300.07 and 75.4614 for ^1H and ^{13}C, resp.; δ in ppm rel. to Me_4Si as internal standard, J in Hz. Typical conditions for the H-atom spectra: pulse width 32°, acquisition time 5 s, FT size 32 K and digital resolution 0.3 Hz per point; and for the C-atom spectra: pulse width 60°, FT size 60 K and digital resolution 0.6 Hz per point, the number of scans varied from 1200 to 10.000 per spectrum. ESI-MS: Waters/Micromass (Manchester, UK) ZQ mass spectrometer equipped with a Harvard Apparatus (Saint Laurent, Canada), syringe pump; in *m/z*. The sample solns. were prepared in MeOH at the concentration of ca. 10^{-5} M. The standard ESI-MS mass spectra were recorded at the cone voltage 90 V.

2.2. Synthesis

Procedure for methyl esters of bile acids as well as their acetoxy derivatives (**4**–**6**) was described earlier. Procedure for 3-bromoacetoxy derivatives of bile acids (**7**–**9**): methyl 5β-cholan-24-oate (**4**), metyl 12α-acetoxy-5β-cholan-24-oate (**5**) or metyl 7α,12α-diacetoxy-5β-cholan-24-oate (**6**) was dissolved in 5 mL of anhydrous dichloromethane, and then subsequently, bromoacetic acid bromide was added drop wise and the reaction mixture was kept at room temperature for 24 h. Then the mixture was washed with $NaHCO_3$ (5%, 20 mL), brine (200 mL) and finally dried over Na_2CO_3. The solvent was evaporated under reduced pressure to give the crude product. Products were purified by chromatography on silica gel (Merck, type 60, 70–230 mesh) with chloroform/hexane as eluent and to give the products 50% of (**7**), 92% (**8**) and 70% of (**9**). Procedure for 3-azidoacetoxy derivatives of bile acids (**10**–**12**): 3-bromoacetoxy derivatives of bile acids (**7**–**9**) were dissolved in 15 mL of THF. Then, NaN_3 was added, the mixture was heated at 50 °C for 4 h. DMF was evaporated, extracted with toluene, washed with brine, and dried (Na_2SO_4) and to give the products 95% of (**10**), 88.6% (**11**) and 78% of (**12**). The sterols (cholesterol **13** or cholestanol **14**) was dissolved in 15 mL of dichloromethane, then *p*-TsOH and propiolic acid was added and the reaction was carried out for 24 h at room temperature. Next the mixture washed with cool water, extracted ethyl acetate and washed with water, brine, and dried (Na_2SO_4). The solvent was evaporated under reduced pressure to give the products: (53%) of (**15**) and (72%) of (**16**). Procedure for dimmers of bile acids and sterols derivatives (**17**–**22**): compounds (**10**–**12**) was dissolved in a mixture of *t*-BuOH/ MeOH (6 mL, 5:1). Then, 5-cholesten-3β-ol 3-propiolate (**15**) or 5-cholestan-3β-ol 3-propiolate (**16**) was added. Next, to the homogenous mixture were added $CuSO_4 \cdot 5H_2O$ (3 mg, 3 mol%) and sodium ascorbate (9 mg, 20 mol%) in water (0.3 mL). The reaction mixture was heated at 60 °C for 8 h and then extracted with chloroform, washed with brine and dried over anhydrous Na_2SO_4. The crude compound was purified by column chromatography on silica gel using chloroform/ethyl acetate (5:1) as an eluent.

2.3. Chemical characterization

2.3.1. Methyl 3α-bromoacetoxy-12α-acetoxy-5β-cholan-24-oate (8)

White solid (92.7%), melting point: 119–120 °C. ^1H NMR (400 MHz, $CDCl_3$) δ: 5.09 (d, J = 3.0 Hz, 1H, 12β–H), 4.81–4.72 (m, 1H, 3β–H), 3.81 (s, 2H, CH_2–27), 3.66 (s, 3H, CH_3–25), 2.10 (s, 3H, 12–OAc), 0.91 (s, 3H, CH_3–19), 0.81 (d, J = 6.3 Hz, 3H, CH_3–21), 0.73 (s, 3H, CH_3–18). ^{13}C NMR (101 MHz, $CDCl_3$) δ: 174.57 (C–24), 170.45 (12α–CO), 166.71 (C–26), 76.32 (C–12), 75.84 (C–3), 51.49 (C–25), 49.39, 47.54, 44.97, 41.75, 35.60, 34.67, 34.55, 34.35, 33.97, 31.84, 30.94, 30.90, 30.79, 27.30 (C–27), 26.78, 26.34, 26.32, 26.29, 25.79, 25.58, 23.38, 22.97 (C–19), 21.34 (12α–CO$\underline{C}H_3$), 17.47 (C–21), 12.37 (C–18). FT-IR (KBr) ν_{max}, cm^{-1}: 2936, 2865, 1733, 1281, 1250. ESI-MS (MeOH) *m/z* (%): 591 (100) $[M+Na]^+$, 607 (15) $[M + K]^+$.

2.3.2. Methyl 3α-bromoacetoxy-7α,12α-diacetoxy-5β-cholan-24-oate (9)

Oil (70%). ^1H NMR (400 MHz, $CDCl_3$) δ: 5.09 (t, J = 2.8 Hz, 1H, 12β–H), 4.91 (d, J = 3.1 Hz, 1H, 7β–H), 4.69–4.61 (m, 1H. 3β–H), 3.81 (d, J = 0.6 Hz, 2H, CH_2–27), 3.66 (s, 3H, CH_3–25), 2.15 (s, 3H, 7–OAc), 2.09 (s, 3H, 12–OAc), 0.92 (s, 3H, CH_3–19), 0.81 (d, J = 6.4 Hz, 3H, CH_3–21), 0.73 (s, 3H, CH_3–18). ^{13}C NMR (101 MHz, $CDCl_3$) δ: 174.50 (C–24), 170.50 (12α–CO), 170.31 (7α–CO), 166.74 (C–26), 76.06 (C–12), 75.32 (C–3), 70.61 (C–7), 51.51 (C–25), 47.33, 45.02, 43.35, 40.80, 37.69, 34.57, 34.43, 34.27, 34.22, 31.13, 30.85, 30.73, 28.86 (C–27), 27.15, 26.51, 26.28, 25.52, 22.76, 22.48 (C–19), 21.58 (12α–CO$\underline{C}H_3$), 21.40 (7α–CO$\underline{C}H_3$), 17.46 (C–21), 12.19 (C–18). FT-IR (KBr) ν_{max}, cm^{-1}: 1734, 1283, 1248. ESI-MS (MeOH) *m/z* (%): 651 (100) $[M+Na]^+$.

2.3.3. Methyl 3α-azidoacetoxy-12α-acetoxy-5β-cholan-24-oate (11)

White solid (88.6%), melting point: 129–131 °C. ^1H NMR (400 MHz, $CDCl_3$) δ: 5.09 (d, J = 3 Hz, 1H, 12β–H), 4.88–4.78 (m, 1H, 3β–H), 3.84 (s, 2H, CH_2–27), 3.66 (s, 3H, CH_3–25), 2.09 (s, 3H, 12–OAc), 0.92 (s, 3H, CH_3–19), 0.81 (d,J = 6.3 Hz, 3H, CH_3–21), 0.73 (s, 3H, CH_3–18). ^{13}C NMR (101 MHz,$CDCl_3$) δ: 174.57 (C–24), 170.43 (12α–CO), 167.70 (C–26), 76.13 (C–12), 75.83 (C–3), 51.47 (C–25), 50.54 (C–27), 49.40, 47.55, 44.98, 41.76, 35.60, 34.67, 34.58, 34.35, 33.96, 32.08, 30.95, 30.80, 27.30, 26.77, 26.51, 25.81, 25.57, 23.38, 22.95 (C–19), 21.28 (12α–CO$\underline{C}H_3$), 17.47 (C–21), 12.37 (C–18). FT-IR (KBr) ν_{max}, cm^{-1}: 2106, 1733, 1281, 1256, 1235, 1198. ESI-MS (MeOH) *m/z* (%): 554 (100) $[M+Na]^+$, 570 (10) $[M + K]^+$.

2.3.4. Methyl 3α-azidoacetoxy-7α,12α-diacetoxy-5β-cholan-24-oate (12)

Oil (78%). ^{1}H NMR (400 MHz, $CDCl_3$) δ: 5.09 (t, J = 2.8 Hz, 1H, 12β–H), 4.92 (d, J = 3.0 Hz, 1H, 7β–H), 4.74–4.66 (m, 1H. 3β–H), 3.85 (d, J = 1.8 Hz, 2H, CH_2–27), 3.66 (s, 3H, CH_3–25), 2.13 (s, 3H, 12–OAc), 2.08 (s, s, 3H, 7–OAc), 0.93 (s, 3H, CH_3–19), 0.82 (d, J = 6.4 Hz, 3H, CH_3–21), 0.73 (s, 3H, CH_3–18).^{13}C NMR (101 MHz, $CDCl_3$) δ: 174.48 (C–24), 170.44 (12α–CO), 170.28 (7α–CO), 167.63 (C–26), 75.90 (C–12), 75.30 (C–3), 70.60 (C–7), 51.48 (C–25), 50.56 (C–27), 47.34, 45.02, 43.32, 40.85, 37.72, 34.58, 34.51, 34.45, 34.25, 31.17, 30.86, 30.74, 28.81, 27.14, 26.75, 25.48, 22.78, 22.44 (C–19), 21.50 (12α–CO$\underline{C}$H$_3$), 21.30 (7α–CO$\underline{C}$H$_3$), 17.47 (C–21), 12.18 (C–18). FT-IR (KBr) ν_{max}, cm^{-1}: 2111, 1732, 1243, 1202. ESI-MS (MeOH) *m/z* (%): 612 (100) [M+Na]$^+$.

2.3.5. 5-cholestan-3β-ol 3-propiolate (16)

Oil (72%). ^{1}H NMR (300 MHz, $CDCl_3$) δ: 4.81–4.73 (m, 1H, 3′–H), 2.85 (s, 1H, CH–30), 0.90 (d, J = 6.5 Hz, 3H, CH_3–21′), 0.86 (dd, J_1 = 6.6, J_2 =1.4 Hz, 6H, CH_3–26′ and CH_3–27′), 0.82 (s, 3H, CH_3–19′), 0.64 (s, 3H, CH_3–18′).^{13}C NMR ($CDCl_3$) δ: 152.29 (C–28), 77.20, 76.37 (C–30), 75.12 (C–29), 74.03 (C–3′), 56.35, 56.21, 54.11, 44.61, 42.55, 39.91, 39.48, 36.63, 36.13, 35.78, 35.40, 33.94, 33.63, 31.92, 28.52, 28.22, 28.00, 27.17, 24.17, 23.81, 22.82 (C–19′), 22.55 (C–27′), 21.17 (C–26′), 18.64 (C–21′), 12.17, 12.05 (C–18′). FT-IR (KBr) ν_{max}, cm^{-1}: 3284, 2117, 1707, 1236. ESI-MS (MeOH) *m/z* (%): 463 (100) [M+Na]$^+$, 479 (40) [M + K]$^+$, 904 (55) [2M+Na]$^+$.

*2.3.6. 3β–hydroxy-5-cholestene 1-[2-(*methyl *5β*-cholan-*24*-oate*)–2*-oxoethyl*]–1H-1,2,3-triazole-4-(3-carboxylate) (17)*

Oil (79.7%). ^{1}H NMR (300 MHz, $CDCl_3$): δ 8.23 (s, 1H, CH–28), 5.42 (d, J = 5.0 Hz, 1H, 6′–H), 5.18 (s, 2H,CH_2–27), 4.98–4.89 (m, 1H, 3′α–H), 4.88–4.79 (m, 1H, 3β–H), 3.67 (s, 3H,CH_3–25), 1.05 (s, 3H, CH_3–19′), 0.93 (s, 3H, CH_3–19), 0.92 (d, J = 6.6 Hz, 3H, CH_3–21′*), 0.90 (d, J = 1.8 Hz, 3H, CH_3–21*), 0.87 (dd, J_1 = 6.6, J_2 = 1.8 Hz, 6H, CH_3–26′ and CH_3–27′), 0.69 (s, 3H, CH_3–18), 0.65 (s, 3H, CH_3–18′).^{13}C NMR (76 MHz, $CDCl_3$) δ: 174.73 (C–24), 165.12 (C–26), 160.03 (C–30), 141.02 (C–29), 139.48 (C–5′), 128.83 (C–28), 122.96 (C–6′), 77.48 (C–3), 77.20, 75.18 (C–3′), 51.47 (C–25), 51.21 (C–27), 50.05, 40.44, 40.05, 39.74,39.52, 32.04, 31.93, 31.87, 31.06, 31.01, 24.29, 24.16, 23.82, 23.23, 22.80 (C–19), 22.55 (C–19′), 21.05 (C–27′), 20.84 (C–26′), 19.23, 18.71 (C–21′), 18.28 (C–21), 12.03 (C–18), 11.85 (C–18′). FT-IR (KBr) ν_{max}, cm^{-1}: 2946, 2867, 1743, 1467, 1364, 1211. ESI-MS (MeOH) *m/z* (%): 935 (100) [M+Na]$^+$, 951 (10) [M + K]$^+$.

*2.3.7. 3β–hydroxy-5-cholestene 1-[2-(*methyl*12*-acetoxy-*5β*-cholan-*24*-oate*)–2*-oxoethyl*]–1H-1,2,3-triazole-4-(3-carboxylate) (18)*

Oil (55.7%). ^{1}H NMR (401 MHz, $CDCl_3$) δ: 8.24 (s, 1H, CH–28), 5.42 (d, 1H, 6′–H), 5.19 (s, 2H, CH_2–27), 5.08 (d, 1H, 12β–H), 4.98–4.87 (m, 1H, 3′α–H), 4.86–4.77 (m, 1H, 3β–H), 3.67 (s, 3H, CH_3–25), 2.10 (s, 3H, 12–OAc), 1.05 (s, 3H, CH_3–19′), 0.92 (s, 3H, CH_3–19), 0.92 (d, J = 6.8 Hz, 3H, CH_3–21′*), 0.87 (dd, J_1 = 6.6, J_2 = 1.8 Hz, 6H, CH_3–26′and CH_3–27′), 0.81 (d, J = 6.3 Hz, 3H, CH_3–21*), 0.73 (s, 3H, CH_3–18), 0.69 (s, 3H, CH_3–18′). ^{13}C NMR (101 MHz, $CDCl_3$) δ: 174.55 (C–24), 170.40 (12α–CO), 165.11 (C-26), 159.95 (C–30), 140.98 (C–29), 139.43 (C–5′), 128.74 (C–28), 122.95 (C–6′), 77.19 (C–12), 75.81 (C–3′),75.15 (C–3), 56.67, 56.12, 51.48 (C–25), 51.16 (C–27), 50.02, 49.37, 47.56, 44.99, 42.30, 41.76, 39.71, 39.49, 38.05, 36.98, 36.60, 36.16, 35.76, 35.60, 34.68, 34.50, 34.39, 33.94, 32.00, 31.90, 31.84, 30.97, 30.81, 28.20, 27.98, 27.73, 27.30, 26.75, 26.43, 25.77, 25.60, 24.26, 23.80, 23.38, 22.94 (C–19), 22.79, 22.53 (C–19′), 21.53 (12α–CO$\underline{C}$H$_3$), 21.33 (C–26′), 21.02 (C–27′), 19.29, 18.69 (C–21′), 17.48 (C–21), 12.38 (C–18), 11.83 (C–18′). FT-IR (KBr) ν_{max}, cm^{-1}: 2950, 2868, 1739, 1244, 1212. ESI-MS (MeOH) *m/z* (%): 993 [M+Na]$^+$.

*2.3.8. 3β–hydroxy-5-cholestene 1-[2-(*methyl *7α,12α*-diacetoxy-*5β*-cholan-*24*-oate*)–2*-oxoethyl*]–1H-1,2,3-triazole-4-(3-carboxylate) (19)*

Oil (60%). ^{1}H NMR (401 MHz, $CDCl_3$) δ: 8.24 (s, 1H, CH–28), 5.42 (d, J = 4.9 Hz, 1H, 6′–H), 5.22 (s, 2H, CH_2–27), 5.09 (d, 1H, 12β–H), 4.98–4.86 (m, 2H, 7β–H and 3′α–H), 4.74–4.64 (m, 1H, 3β–H), 3.66 (s, 3H, CH_3–25), 2.14 (s, 3H, 7–OAc), 2.09 (s, 3H, 12–OAc), 1.05 (s, 3H, CH_3–19′), 0.92 (s, 3H, CH_3–19), 0.92 (d, J = 3.2 Hz, 3H, CH_3–21′*), 0.87 (dd, J_1= 6.6, J_2 = 1.8 Hz, 6H, CH_3–26′ and CH_3–27′), 0.82 (d, J = 6.3 Hz, 3H, CH_3–21′), 0.73 (s, 3H, CH_3–18), 0.69 (s, 3H, CH_3–18′). ^{13}C NMR (101 MHz, $CDCl_3$) δ: 174.47 (C–24), 170.43 (12α–CO), 170.22 (7α–CO), 165.08 (C–26), 159.88 (C–30), 140.97 (C–29), 139.39 (C–5′), 128.77 (C–28), 122.97 (C–6′), 76.87 (C–12), 75.26 (C–3′), 75.16 (C–3), 70.52 (C–7), 56.66, 56.10, 51.49 (C–25), 51.18 (C–27), 50.00, 47.34, 45.02, 43.32, 42.28, 40.83, 39.70, 39.48, 38.04, 37.70, 36.96, 36.59, 36.15, 35.75, 34.58, 34.38, 34.22, 31.89, 31.83, 31.14, 30.87, 30.73, 28.82, 28.19, 27.97, 27.72, 27.14, 26.68, 25.50, 24.25, 23.79, 22.78 (C–19), 22.53 (C–19′), 22.43 (7α–CO$\underline{C}$H$_3$), 21.57 (12α–CO$\underline{C}$H$_3$), 21.36 (C–26′), 21.01 (C–27′), 19.28, 18.68 (C–21′), 17.47 (C–21), 12.19 (C–18), 11.82 (C–18′). FT-IR (KBr) ν_{max}, cm^{-1}: 2950, 2869, 1739, 1237. ESI-MS (MeOH) *m/z* (%): 1051 (100) [M+Na]$^+$, 1067 (20) [M + K]$^+$.

*2.3.9. 3β–hydroxy-5-cholestane 1-[2-(*methyl *5β*-cholan-*24*-oate*)–2*-oxoethyl*]–1H-1,2,3-triazole-4-(3-carboxylate) (20)*

Oil (51%). ^{1}H NMR (401 MHz, $CDCl_3$) δ: 8.22 (s, 1H, CH–28), 5.18 (s, 2H, CH_2–27), 5.04–4.98 (m, 1H, 3′α–H), 4.89–4.79 (m, 1H, 3β–H), 3.67 (s, 3H, CH_3–25), 0.93 (s, 3H, CH_3–19), 0.91 (d, J = 8.8 Hz, 3H, CH_3–21*), 0.90 (d, J = 6.8 Hz, 3H, CH_3–21′*), 0.86 (dd, J_1 = 6.4, J_2 = 2.4 Hz, 6H, CH_3–26′ and CH_3–27′), 0.85 (s, 3H, CH_3–19′), 0.66 (s, 3H, CH_3–18), 0.65 (s, 3H, CH_3–18′). ^{13}C NMR (101 MHz, $CDCl_3$) δ: 174.73 (C–24), 165.14 (C–26), 160.16 (C–30), 141.09 (C–29), 128.76 (C–28), 77.46 (C–3), 77.20, 75.03 (C–3′), 56.43, 56.39, 56.28, 55.97, 54.24, 51.45 (C–25), 51.19 (C–27), 44.74, 42.73, 42.60, 41.89, 40.44, 40.05, 39.99, 39.51, 36.79, 36.17, 35.79, 35.77, 35.49, 35.35, 34.85, 34.54, 33.99, 32.04, 31.99, 31.06, 31.01, 28.61, 28.23, 28.16, 28.00, 27.46, 26.93, 26.47, 26.25, 24.20, 24.15, 23.83, 23.23, 22.80 (C–19), 22.55 (C–19′), 21.22 (C–27′), 20.84 (C–26′), 18.66 (C–21′), 18.27 (C–21), 12.25 (C–18), 12.06, 12.03 (C–18′). FT-IR (KBr) ν_{max}, cm^{-1}: 2945, 2867, 1742, 1380, 1214. ESI-MS (MeOH) *m/z* (%): 937 (100) [M+Na]$^+$, 953 (5) [M + K]$^+$.

*2.3.10. 3β–hydroxy-5-cholestane 1-[2-(*methyl *12α*-acetoxy-*5β*-cholan-*24*-oate*)–2*-oxoethyl*]–1H-1,2,3-triazole-4-(3-carboxylate) (21)*

Oil (53%). ^{1}H NMR (401 MHz, $CDCl_3$) δ: 8.22 (s, 1H, CH–28), 5.18 (s, 2H, CH_2–27), 5.08 (d, 1H, 12β–H), 5.04–4.96 (m, 1H, 3′α–H), 4.86–4.77 (m, 1H, 3β–H), 3.66 (s, 3H, CH_3–25), 2.10 (s, 3H, 7–OAc), 0.91 (s, 3H, CH_3–19), 0.90 (d, J = 5.6 Hz, 3H, CH_3–21), 0.86 (dd, J_1 = 6.4, J_2 = 1.6 Hz, 6H, CH_3–26′ and CH_3–27′), 0.85 (s, 3H, CH_3–19′), 0.81 (d, J = 6.3 Hz,3H, CH_3–21′), 0.73 (s, 3H, CH_3–18), 0.65 (s, 3H, CH_3–18′). ^{13}C NMR (101 MHz,$CDCl_3$) δ: 174.56 (C–24), 170.42 (12α–CO), 165.12 (C–26), 160.06(C–30), 141.04 (C–29), 128.74 (C–28), 77.16 (C–12), 75.80 (C–3), 74.99 (C–3′), 51.49 (C–25),51.13 (C–27), 47.54, 27.30, 22.93 (C–19), 22.53 (C–19′),21.53 (12α–CO$\underline{C}$H$_3$), 21.34 (C–26′), 21.18 (C–27′), 18.63 (C–21′), 17.47 (C–21), 12.37 (C–18), 12.03 (C–18′). FT-IR (KBr) ν_{max}, cm^{-1}: 2948, 2867, 1738, 1244, 1212. ESI-MS (MeOH) *m/z* (%): 994 (100) [M+Na]$^+$, 1011 (30) [M + K]$^+$.

*2.3.11. 3β–hydroxy-5-cholestane 1-[2-(*methyl *7α,12α*-diacetoxy-*5β*-cholan-*24*-oate*)–2*-oxoethyl*]–1H-1,2,3-triazole-4-(3-carboxylate) (22)*

Oil (52%). ^{1}H NMR (401 MHz, $CDCl_3$) δ: 8.22 (s, 1H, CH–28), 5.17 (s, 2H, CH_2–27), 5.09 (d, 1H, 12β–H), 5.05–4.95 (m, 1H, 3′α–H), 4.92 (s, 1H, 7β–H), 4.75–4.64 (m, 1H, 3β–H), 3.67 (s, 3H, CH_3–25), 2.14 (s, 3H, 7–OAc), 2.09 (s, 3H, 12–OAc), 0.92 (s, 3H, CH_3–19), 0.90 (d, J = 6.5 Hz, 3H, CH_3–21), 0.86 (dd, J_1 = 6.8, J_2 = 2 Hz, 6H, CH_3–26′and CH_3–27′), 0.85 (s, 3H, CH_3–19′), 0.82 (d, J = 6.4 Hz, 3H, CH_3–21′), 0.73 (s, 3H, CH_3–18), 0.65 (s, 3H, CH_3–18′).^{13}C NMR (101 MHz, $CDCl_3$) δ: 174.50 (C–24), 170.45 (12α–CO), 170.25 (7α–CO), 165.10 (C–26), 160.04 (C–30), 141.13 (C–29), 128.69 (C–28), 76.92 (C–12), 75.30 (C–3), 75.06 (C–3′), 70.55 (C–7), 51.52 (C–25), 51.20 (C–27), 47.39, 45.06, 44.73, 43.35, 42.60, 40.86, 39.98, 39.51, 37.73, 36.78, 36.17, 35.79, 35.49, 34.62, 34.41, 34.25, 33.99, 31.98, 31.18, 30.91, 30.77, 28.85, 28.61, 28.24, 28.01, 27.47, 27.17, 26.71, 25.53, 24.20, 23.83, 22.80 (C–19), 22.55 (C–19′), 22.46 (7α–CO$\underline{C}H_3$), 21.60 (12α–CO$\underline{C}H_3$), 21.39 (C–26′), 21.22 (C–27′), 18.66 (C–21′), 17.51 (C–21), 12.26 (C–18), 12.22, 12.07 (C–18′). FT-IR (KBr) ν_{max}, cm^{-1}: 2948, 2868, 1739, 1237.ESI-MS (MeOH) *m/z* (%): 1053 (100) [M+Na]$^+$, 1069 (10) [M + K]$^+$.

2.4. Theoretical calculations

The PM5 semiempirical calculations were performed using the WinMopac 2003 program. The final heat of formation (HOF) for dimers of bile acids and sterols derivatives (**17**–**22**) linked 1,2,3-triazole ring is presented in Table 5. The molecular models of compounds all compounds are shown in Figs. 3 and 4.The calculations were performed using the Gaussian 09 program package [61] and B3LYP [62,63] method in conjunction with 6–311G(d,p) [64] basis set. The magnetic isotropic shielding tensors were calculated using the standard GIAO/B3LYP/6–311G(d,p) (Gauge-Independent Atomic Orbital) approach [65,66].

2.5. Docking experiments

Docking experiments were performed using Flare application available in Cresset Software [67]. Downloaded target pdb's from PDB protein data bank [68] were prepared in protein preparation module using normal calculating mode. Active site size was set at 6 Å. Ligands were prepared according to automatic settings. Docking calculations were performed according to very accurate but slow method. Grid box was centered on co-crystallized ligand. Number of runs was set at 8 and max poses at 10.

3. Results and discussion

In our previous work we described the synthesis method and characterization bile acid–sterol conjugates linked with a 1,2,3-triazole ring of propargyl esters of lithocholic, deoxycholic as well as cholic acids and ergo ster-3β-yl 2-azidoacetate and cholester-3β-yl 2-azidoacetate [69]. To the best of our knowledge, no work has been published on the synthesis or the physicochemical properties of 3-bromoacetoxy (**8,9**) and 3-azidoacetoxy derivatives of metyl 12α-acetoxy-5β-cholan-24-oate (**11**) and metyl 7α,12α-diacetoxy-5β-cholan-24-oate (**12**), 5-cholestan-3β-ol 3-propiolate (**16**) as well as new six conjugates of connected in a head-to-tail fashion of 3-azidoacetoxy derivatives of bile acids (tail) and propiolate esters of sterols (head) linked by a 1,2,3-triazole ring (**17**–**22**). This type of combination is a completely innovative approach to the preparation and research of a new type of steroid conjugates.

The structures of two bromoacetyl substituted derivatives of bile acids (**8**) and (**9**), azidoacetyl substituted derivatives of bile acids (**11**) and (**12**), 5-cholestan-3β-ol 3-propiolate (**16**) as well as all synthesized conjugates (**17**–**22**) were determined on the basis of their ^{1}H and ^{13}C NMR, FT-IR, and ESI-MS spectra. Moreover, PM5 and B3LYP calculation methods were performed for all compounds. The syntheses of substrates (**8,9**), (**11,12**) and (**16**), as well as conjugates (**17**–**22**), are shown in the Schemes 1 and 2, respectively.

3.1. Synthesis

The bile acid methyl esters, steroids bromoacetates and azidoacetates derivatives as well as propiolate esters of sterols were obtained with satisfactory yields. The methyl 3α-bromoacetoxy-5β-cholan-24-oate (**7**), methyl 3α-bromoacetoxy-12α-acetoxy-5β-cholan-24-oate (**8**), methyl 3α-bromoacetoxy-7α,12α-diacetoxy-5β-cholan-24-oate (**9**) was synthesized in the reaction of methyl esters of bile acids (**4**–**6**) with bromoacetic acid bromide in anhydrous dichloromethane. On the other hand methyl 3α-azidoacetoxy-5β-cholan-24-oate (**10**), methyl 3α-azidoacetoxy-12α-acetoxy-5β-cholan-24-oate (**11**), methyl 3α-azidoacetoxy-7α,12α-diacetoxy-5β-cholan-24-oate (**12**) was synthesized in the reaction of bromoacetate derivatives of bile acids *via* a substitution reaction with NaN_3 in DMF at 50°. This one-pot reaction leads to azide derivatives in very good yield. The estrification of cholesterol (**13**) or cholestanol (**14**) with propiolic acid in dichloromethane with *p*-TsOH presence gave 5-cholesten-3β-ol 3-propiolate (**15**) and 5-cholestan-3β-ol 3-propiolate (**16**).The azides of derivatives bile acids (**10**–**12**) and propargyl esters of sterols (**15**–**16**) were used as a substrates in the „click" chemistry reaction in the presence of $CuSO_4{\cdot}5H_2O$ and sodium ascorbate in *t*-BuOH/MeOH (5:1). A mixture of crude products (**17**–**22**) were obtained and separated by column chromatography. This reaction leads to dimers in saris factory yields.

3.2. Spectroscopic study

3.2.1. Nuclear magnetic resonance spectroscopy

The three substrates methyl 3α-bromoacetoxy-5β-cholan-24-oate (**7**), methyl 3α-azidoacetoxy-5β-cholan-24-oate (**10**) and 5-cholesten-3β-ol 3-propiolate (**15**) have been described and characterized in the literature [37,69]. The^{1}H and ^{13}C NMR data of compounds (**8**), (**9**), (**11**), (**12**) and (**17**–**22**) are shown in Tables 1–3 respectively. The ^{1}H NMR spectra in the region of 5.45–4.60 ppm for the most characteristic signals of compounds (**17**–**22**) are shown in Fig. 1.

In the ^{1}H NMR spectrum of methyl 3α-bromoacetoxy-12α-acetoxy-5β-cholan-24-oate (**8**), methyl 3α-bromoacetoxy-7α,12α-diacetoxy-5β-cholan-24-oate (**9**), methyl 3α-azidoacetoxy-12α-acetoxy-5β-cholan-24-oate (**11**) and methyl 3α-azidoacetoxy-7α,12α-diacetoxy-5β-cholan-24-oate (**12**) showed characteristic two hydrogen singlets in the range 0.73 and 0.93–0.91 ppm and doublet at 0.82–0.81 ppm assigned to CH_3–18, CH_3–19, and CH_3–21, respectively. The protons of CH_3–25 gave characteristic signal at 3.66 ppm. The protons of the 7α–CO_2CH_3 group gave signals in the range 2.15–2.13 ppm for compounds (**9**) and (**12**), and additionally 12α–CO_2CH_3 group gave signals in the range 2.08–2.10 ppm for compounds (**8**), (**9**) and (**11**) and (**12**).For all compounds show characteristic multiplets in the range 4.88–4.61 ppm assigned to axial positions of the C3β–H protons in steroid skeleton. In the spectrum of compounds (**9**) and (**12**) additionally is present positions of the C7β–H proton in the range 4.92–4.91 ppm. However, in the case of these acetoxy derivatives protons of C12β–H appear at 5.09 ppm. The ^{1}H NMR spectra of these compounds show characteristic singlets at 3.81 ppm for the protons of the 3α–CO_2CH_2Br group, whereas for compound (**8**)and (**9**). In turn for compounds (**11**) and (**12**) the protons of the 3α–$CO_2CH_2N_3$ group in the range 3.85–3.84 ppm. The proton of C≡CH group in compound (**16**) gave signal at 2.85 ppm. Two hydrogen singlets at 0.64, 0.82 as well as

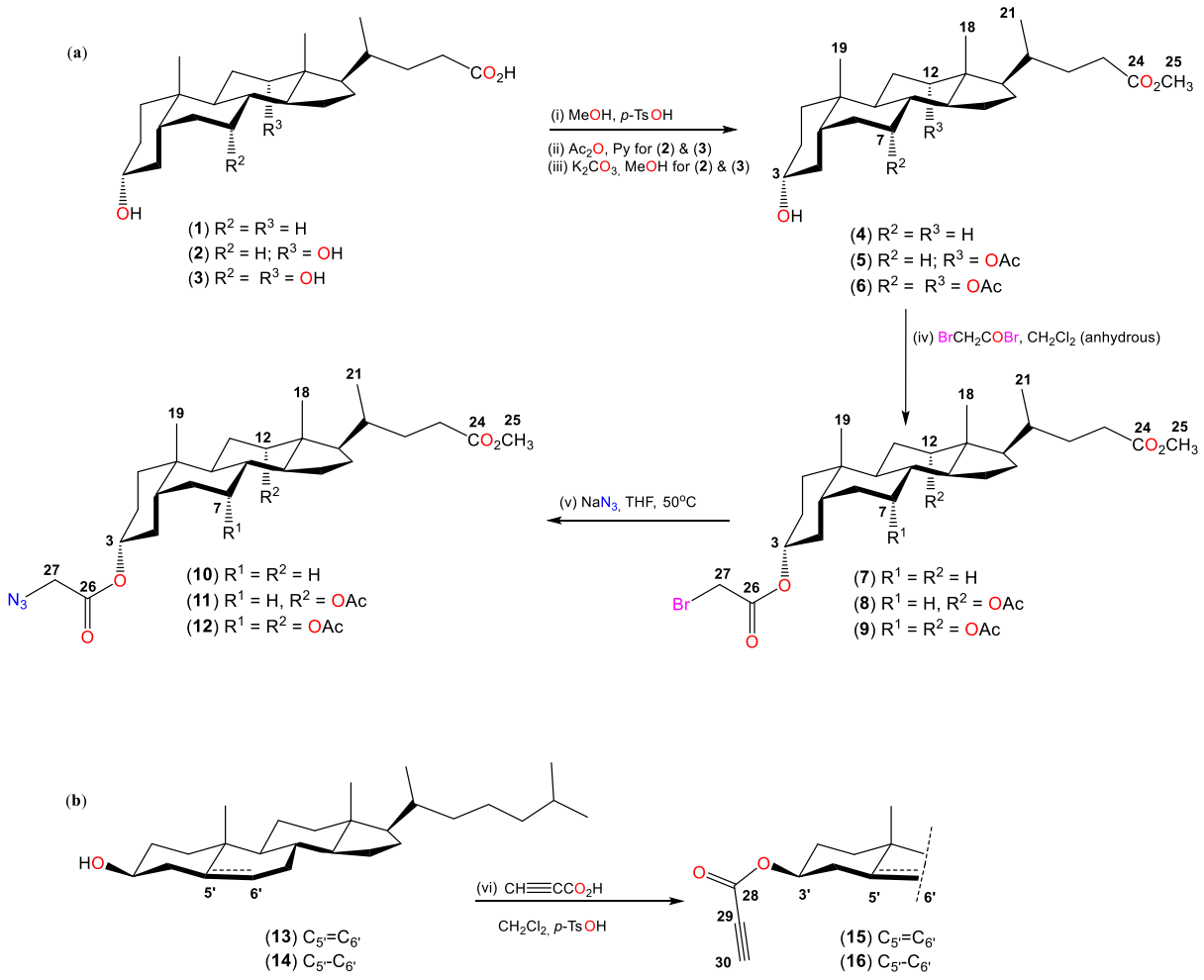

Scheme 1. Synthesis of bromoacetyl substituted derivatives of methyl esters of bile acids (**7**–**9**) and its azidoacetyl substituted derivatives (**10**–**12**) (**a**) as well as propargyl esters of cholesterol (**15**) and cholestanol (**16**) (**b**).

Table 1
^{1}H i^{13}C NMR chemical shift (ppm) of compounds (**8**–**9**) and (**11**–**12**) in $CDCl_3$.

No. of atoms	**8**		**9**		**11**		**12**	
	^{1}H	^{13}C	^{1}H	^{13}C	^{1}H	^{13}C	^{1}H	^{13}C
3	4.81–4.72	75.84	4.69–4.61	75.32	4.88–4.78	75.83	4.74–4.66	75.30
7	–	–	4.91	70.61	–	–	4.92	70.60
12	5.09	76.32	5.09	76.06	5.09	76.13	5.09	75.90
18	0.73	12.37	0.73	12.19	0.73	12.37	0.73	12.18
19	0.91	22.97	0.92	22.48	0.92	22.95	0.93	22.44
21	0.81	17.47	0.81	17.46	0.81	17.47	0.82	17.47
24	–	174.57	–	174.50	–	174.57	–	174.48
25	3.66	51.49	3.66	51.51	3.66	51.47	3.66	51.48
26	–	166.71	–	166.74	–	167.70	–	167.63
27	3.81	27.30	3.81	28.86	3.84	50.54	3.85	50.56
7α–CO	–	–	–	170.31	–	–	–	170.28
12α–CO	–	170.45	–	170.50	–	170.43	–	170.44
7α–CO$\underline{C}$H$_3$	–	–	2.15	21.40	–	–	2.13	21.30
12α–CO$\underline{C}$H$_3$	2.10	21.34	2.09	21.58	2.09	21.28	2.08	21.50

characteristic doublets at 0.90 ppm are assigned to CH_3–18′, CH_3–19′, and CH_3–21′, respectively. The doublets of doublets of protons of CH_3–26′ and CH_3–27′ gave signal at 0.86 ppm. The equatorial proton in positions of the C3α–H proton in cholestanol skeleton gave signal in the range 4.81–4.75 ppm.

The diagnostics proton signals of the triazole ring C28–H of all conjugates with 1,2,3-triazole ring (**17**–**22**) in $CDCl_3$ arise as a singlet at about 8.24–8.22 ppm. In turns, the protons of the methylene groups C27–H linked directly to the triazole ring give signals at about 5.22–5.17 ppm. The ^{1}H NMR spectra of (**17**–**22**) showed characteristic multiplets of protons of C3′α–H of sterol skeleton in the range of 5.04–4.86 ppm. In the same range there are also multiplets from the protons of C3β–H group of bile acid skeleton. In the spectra of compounds (**18**), (**19**)and (**21**)and (**22**) characteristic broad singlets in the range 5.09 ppm are observed which are due to the C12β–H protons. ^{1}H NMR spectra of conjugate (**19**)

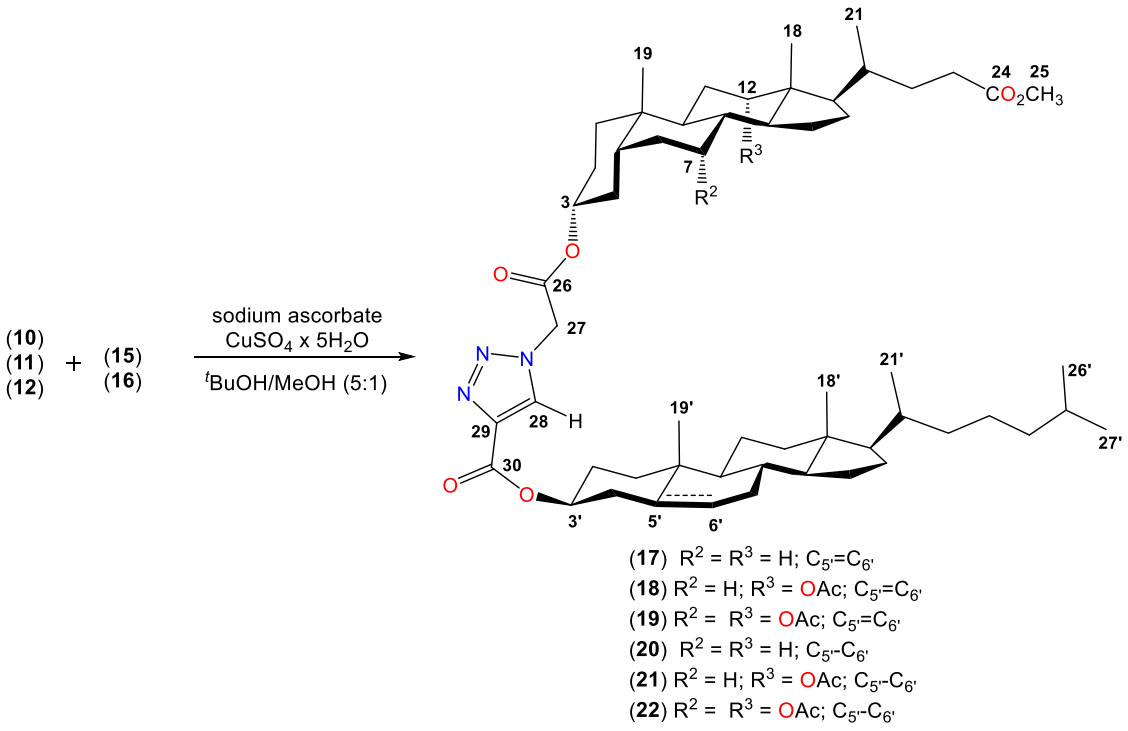

Scheme 2. Synthesis of dimers of bile acids and sterols derivatives (**17**–**22**) linked by 1,2,3-triazole ring.

Table 2
^{1}H NMR chemical shift (ppm) of compounds (**17**–**22**) in $CDCl_3$.

No. of atoms	Compounds					
	17	**18**	**19**	**20**	**21**	**22**
3β–H	4.88–4.79	4.86–4.77	4.74–4.64	4.89–4.79	4.86–4.77	4.75–4.64
7β–H	–	–	4.98–4.86	–	–	4.92
12β–H	–	5.08	5.09	–	5.08	5.09
18	0,69	0.73	0.73	0.66	0.73	0.73
19	0.93	0.92	0.92	0.93	0.91	0.92
21	0.90	0.81	0.82	0.91	0.90	0.90
25	3.67	3.67	3.66	3.67	3.66	3.67
27	5.18	5.19	5.22	5.18	5.18	5.17
28	8.23	8.24	8.24	8.22	8.22	8.22
7α–OAc	–	–	2.14	–	–	2.14
12α–OAc	–	2.10	2.09	–	2.10	2.09
3′α–H	4.98–4.89	4.98–4.87	4.98–4.86	5.04–4.98	5.04–4.96	5.05–4.95
6′–H	5.42	5.42	5.42	–	–	–
18′	0.65	0.69	0.69	0.65	0.65	0.65
19′	1.05	1.05	1.05	0.85	0.85	0.85
21′	0.92	0.92	0.92	0.90	0.81	0.82
26′	0.87	0.87	0.87	0.86	0.86	0.86
27′	0.87	0.87	0.87	0.86	0.86	0.86

show multiplets in the range of at 4.98–4.86 ppm but conjugate (**22**) gave singlet at 4.92 ppm assigned to the C7β–H protons of the bile acid skeleton. In the bile acids skeleton was observed two hydrogen singlets ranking from 0.73 to 0.66 and 0.93–0.91 ppm and characteristic doublet at 0.91–0.81 ppm assigned to CH_3–18, CH_3–19 and CH_3–21, respectively. On the other hand in the cholesterol part the characteristic hydrogen singlets in the range 0.69–0.65 and 1.05–0.85 ppm and doublet at 0.92–0.82 ppm assigned to CH_3–18′, CH_3–19′, and CH_3–21′, respectively. The ^{1}H–NMR spectra of (**17**–**22**) showed a doublet at 0.87 or 0.86 ppm for the protons of the CH_3–26′ and CH_3–27′ methyl groups. For cholesterol derivatives (**17**–**19**) diagnostics is doublet for C6'–H at 5.42 ppm. Additionally in the ^{1}H NMR spectra of all conjugates show characteristic singlets in the range 2.14 ppm and 2.10–2.09 ppm for the protons of the 7α–CO_2CH_3 and 12α–CO_2CH_3 group, respectively. The characteristic protons shifts for compounds (**15**–**18**) are collected in Table 3.

The ^{13}C NMR spectra of compounds (**8**–**9**) and (**11**–**12**) show characteristic signals at 12.37–12.18, 22.97–22.44 and 17.47–17.46 ppm which are assigned to CH_3–18, CH_3–19 and CH_3–21, respectively. On the other hand, carbon atoms in carbonyl group of bromoacetoxy groups in positions 3α resonate in the range of 167.70–166.71 ppm. The carbon atoms of the C(12)=O steroid skeleton gave signals in the range of 170.50–170.43 ppm. However, carbon of the C(7)=O gave signal at 170.31–170.28 ppm. The diagnostics signal for CH_2Br groups in compounds (**8**–**9**) is observed at 28.86–27.30 ppm. Whereas the characteristic signal for CH_2N_3 groups in compounds (**11**–**12**) is observed at 50.56–50.54 ppm. Additionally for compound (**16**) were observed five signals from methyl groups CH_3–18′, CH_3–19′ and CH_3–21′ as well as CH_3–26′

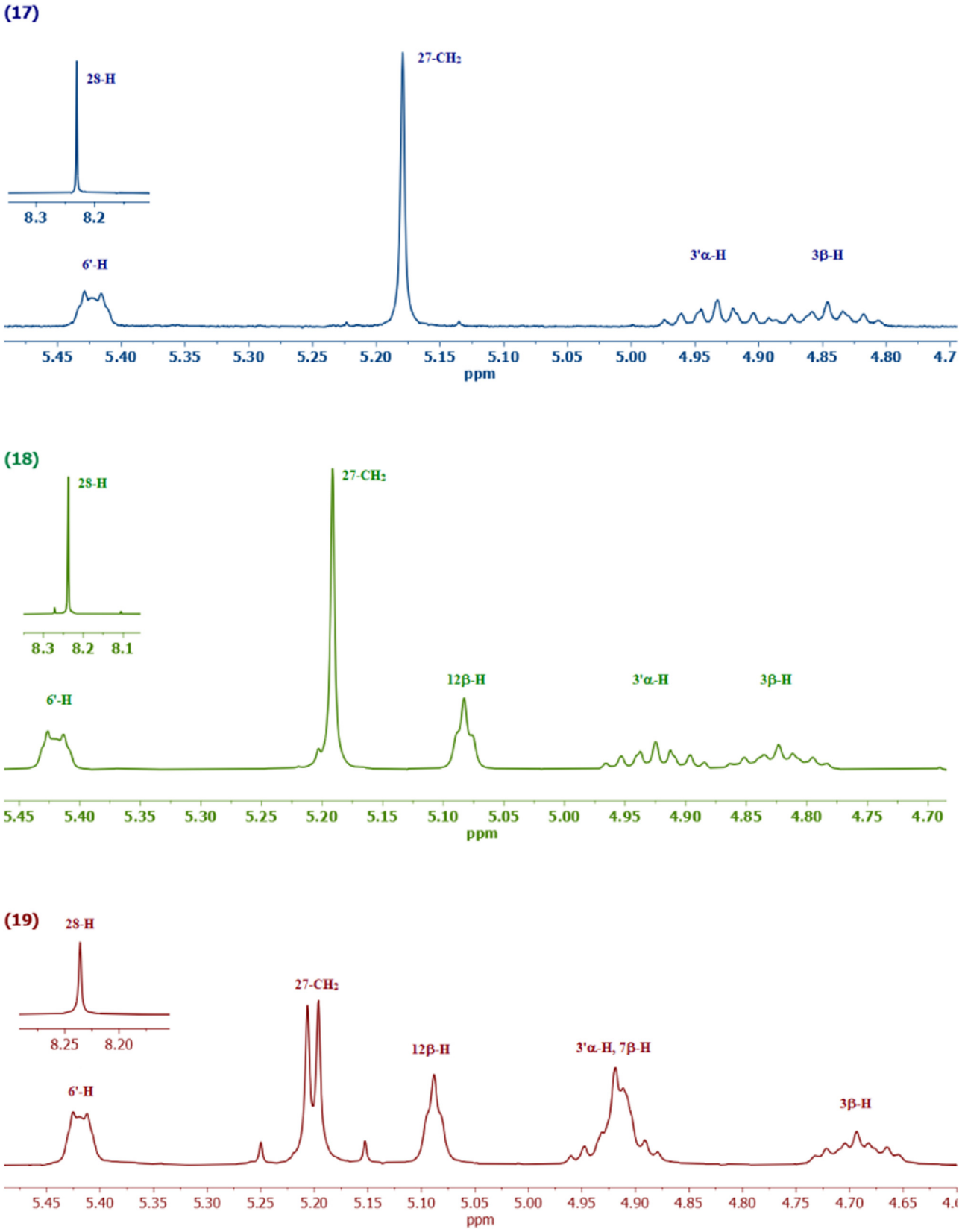

Fig. 1. ^{1}H NMR Spectra in the region of 5.45–4.65 ppm for the most characteristic signals of compounds (**17**–**19**).

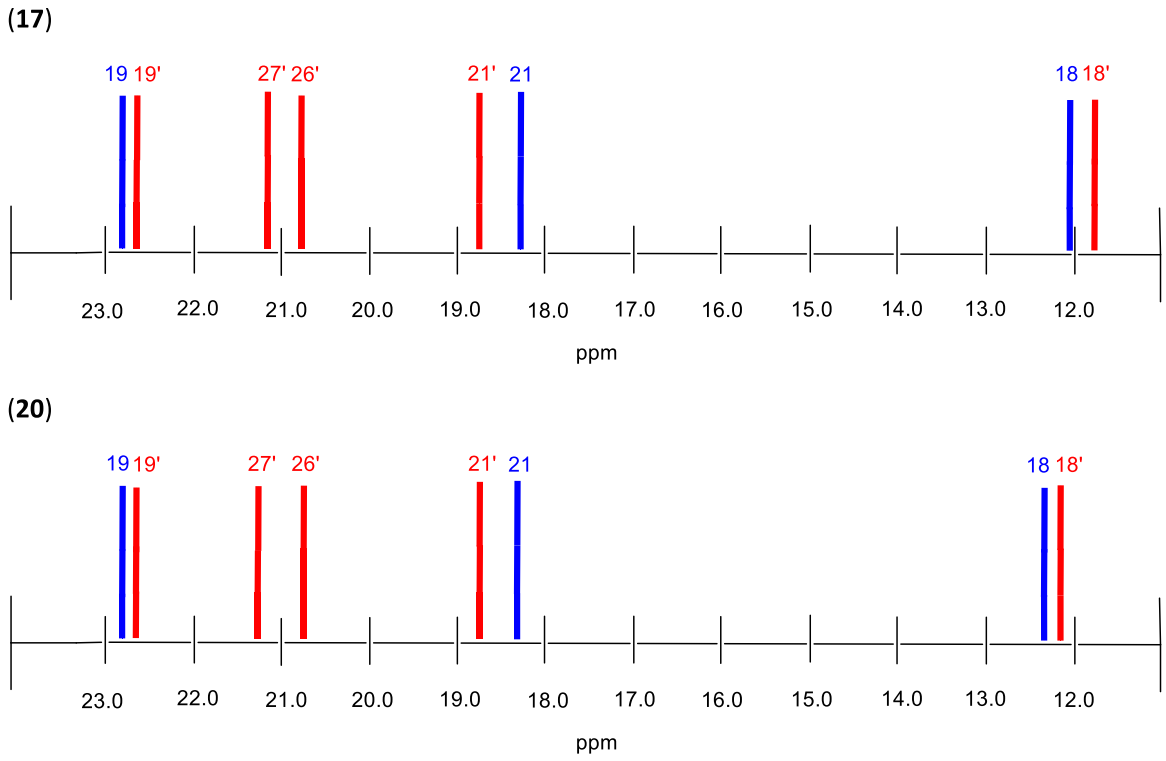

Fig. 2. Analytical differences of CH_3 groups of dimmers of lithocholic acid and cholesterol (**17**) and lithocholic acid and cholestanol (**20**) linked by 1,2,3-triazole ring in the corresponding ^{13}C NMR spectrum.

Table 3
^{13}C NMR chemical shift (ppm) of compounds (**17**–**22**) in $CDCl_3$.

No. of atoms	Compounds					
	17	**18**	**19**	**20**	**21**	**22**
3	77.48	75.15	75.16	77.46	75.80	75.30
7	–	–	70.52	–	–	70.55
12	–	77.19	76.87	–	77.16	76.92
7α–CO	–	–	170.22	–	–	170.25
12α–CO	–	170.40	170.43	–	170.42	170.45
7α–CO$\underline{C}H_3$	–	–	22.43	–	–	22.46
12α–CO$\underline{C}H_3$	–	21.53	21.57	–	21.53	21.60
18	12.03	12.38	12.19	12.25	12.37	12.26
19	22.80	22.94	22.78	22.80	22.93	22.80
21	18.28	17.48	17.47	18.27	17.47	17.51
24	174.73	174.55	174.47	174.73	174.56	174.50
25	51.47	51.48	51.49	51.45	51.49	51.52
26	165.12	165.11	165.08	165.14	165.12	165.10
27	51.21	51.16	51.18	51.19	51.13	51.20
28	128.83	128.74	128.77	128.76	128.74	128.69
29	141.02	140.98	140.97	141.09	141.04	141.13
30	160.03	159.95	159.88	160.16	160.06	160.04
3′	75.18	75.81	75.26	75.03	74.99	75.06
5′	139.48	139.43	139.39	–	–	–
6′	122.96	122.95	122.97	–	–	–
18′	11.85	11.83	11.82	12.03	12.03	12.07
19′	22.55	22.53	22.53	22.55	22.53	22.55
21′	18.71	18.69	18.68	18.66	18.63	18.66
26′	20.84	21.33	21.36	20.84	21.34	21.39
27′	21.05	21.02	21.01	21.22	21.18	21.22

and CH_3–27′ at 12.05 ppm, 22.85 ppm, 18.64 ppm and 27.17 and 22.55, respectively. The carbon atoms of the HC≡C–CO_2 group are observed in the range 152.29 ppm, and 75.12 ppm as well as at 76.37 ppm are assigned to CO_2,C≡C–H respectively.

The ^{13}CNMR spectra of dimers linked by 1,2,3-triazole ring in $CDCl_3$, showed signals at 12.38–12.03 ppm, 22.93–22.78 ppm, 18.28–17.47 ppm, which were assigned to CH_3–18, CH_3–19 and CH_3–21 of bile acids parts, respectively. In the case of cholesterol parts, the signals of C–atoms of CH_3–18′, CH_3–19′ and CH_3–21′ groups were situated in the ranges of 12.07–11.82, 22.55–22.53, and 18.71–18.63 ppm, respectively. The following characteristic shifts of methyl groups were present in the sterol side chain: CH_3–26′ and CH_3–27′are positioned in the range of 21.39–20.84 ppm and 21.22–21.01 ppm.

Analytical differences in the ^{13}C NMR spectra of the methyl groups of compound (**17**) and (**20**) are shown in Fig. 2. On the other hand, in the ^{13}C NMR spectra of compounds (**17**–**22**), the signals of the C(27)H_2 groups appeared in the range of 51.21–51.13 ppm. The carbon atoms from triazole ring: C(28) as well as C(29) groups resonated at 128.83–128.69 ppm and 141.13–140.97 ppm, respectively.

The signals of C(24)=O, C(26)=O and C(30)=O, appeared in the range of 174.73–174.47 ppm, 165.14–165.08 ppm and 160.16–159.95 ppm, respectively. However, carbon atoms in C = O of acetoxy groups in positions 7α and 12α resonate in the range of 170.45–170.22 ppm.

3.2.2. Infrared spectroscopy

The most characteristic feature of the FT-IR spectra of compound (**16**) is band at 3284 cm^{-1} assigned to the ν(≡C–CH) group. Regarding that the steroid skeleton is a saturated hydrocarbon, it doesn't provide many useful IR features. Strong stretching vibrations of C–H bonds are identified at 2933 cm^{-1} and 2865 cm^{-1}. For synthesized compounds (**10**), (**11**) and (**12**) are requisite and analytical bands at 2111–2106 cm^{-1}, which are specific attribute of ν(N = N^+=N^-) group. Moreover, for all substrates (**7**–**9**), (**10**–**12**) and (**15**–**16**) are also observed two strong characteristic bands at 1756–1707 cm^{-1} and 1283–1198 cm^{-1}, which are assigned respectively to the symmetric group ν(C = O) and ν(C–O). It worth mentioning that the most distinctive in the FT-IR spectra of conjugates steroids (**15**–**20**) are represented by ν(C = O) and ν(C–O) groups, two powerful bands in the 1743–1732 cm^{-1} and 1244–1211

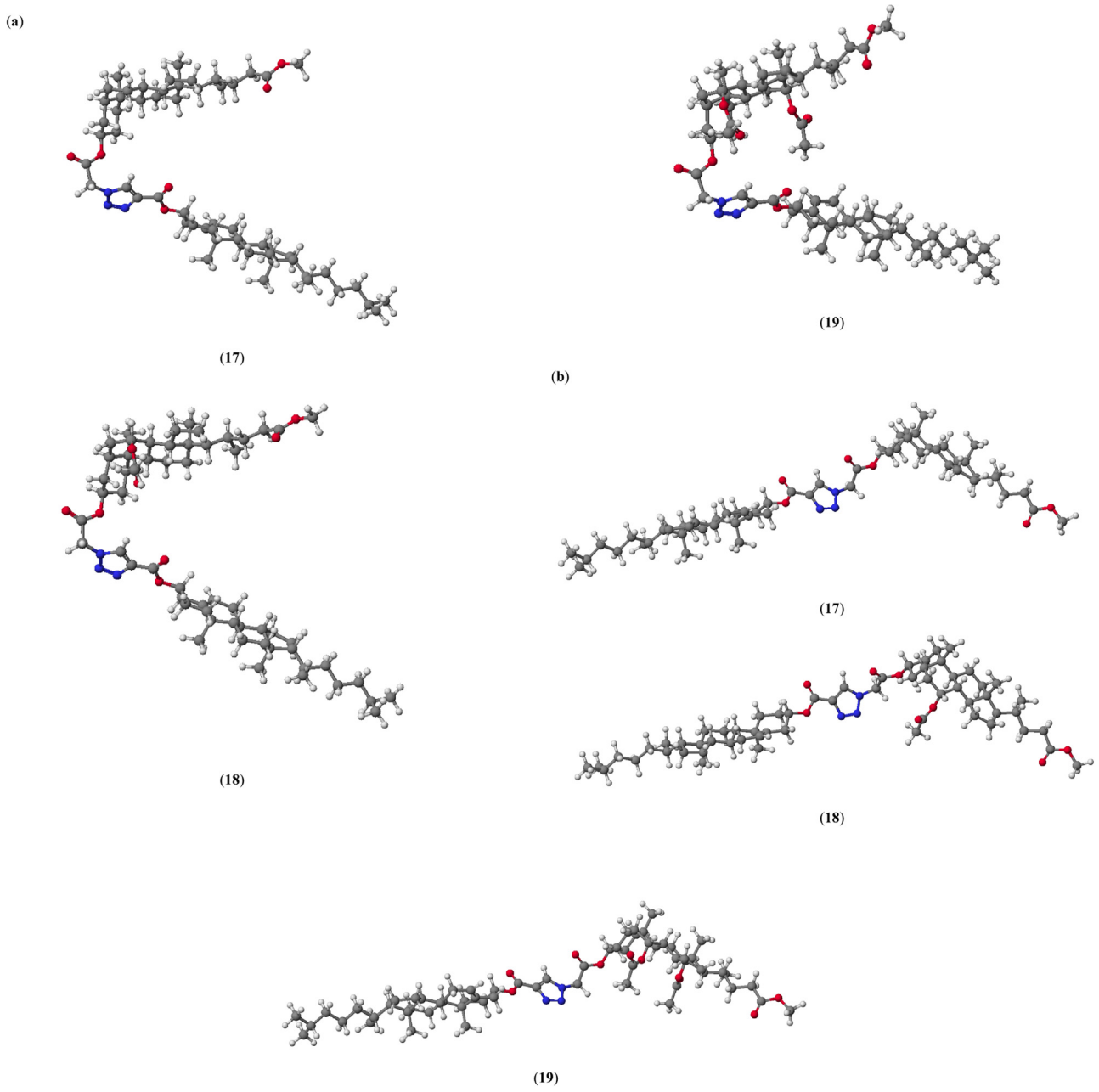

Fig. 3. Molecular models of conformers *syn* (**a**) and *anti* (**b**) for conjugates (**17**–**19**) calculated by PM5 method.

cm^{-1} region, appropriately. In addition, characteristic stretching vibrations of C–H bonds are present in the 2946–2867 cm^{-1}.

3.3. PM5 and B3LYP calculations

PM5 semiempirical calculations were performed using the WinMopac 2003 program. The molecular models of all conjugates are shown in Fig. 3. Representative conjugates (**19**) of bile acids in conformers *syn* and *anti* are shown in Fig. 4. The final heats of formation (HOF) for the bile acids (**1**–**3**), cholesterol (**13**) and cholestanol (**14**) as well as their conjugates (**17**–**22**) are presented in Table 4. It is worth mentioning that, in many works that describe the application of computational methods, one can find information on the comparison of theoretical results with crystallographic structures. Not without significance is the use of computational methods in determining the properties of the docking [70–72]. We were able to obtain a very good picture of molecular modeling using semiempirical calculations [73]. The lowest values of HOF for conjugates of bile acids and sterols (**17**–**22**) are observed for cholic acids and its conjugates (**19**) and (**22**). The number of hydroxyl groups in the steroid skeleton lowers the value of the determinant of HOF. We observe exactly the same relationship for blocked hydroxyl groups by bolting them with acetate groups. The OAc groups facilitate the formation of intramolecular H–bonds and stable host–guest complexes. These complexes may be stabilized by H–bonding or electrostatic interactions that arise from the OAc groups in the bile acid molecule. The HOF value decreases with the increasing number of OAc groups in the steroid skeleton. Furthermore, for *anti* conformers of deoxycholic and cholic acid derivatives, HOF is lower than for *syn* conformers. On the other hand, the *syn* conformer of the lithocholic acid derivatives (**17**) and (**20**) has a higher HOF value than the *anti* conformer and is therefore more durable as no

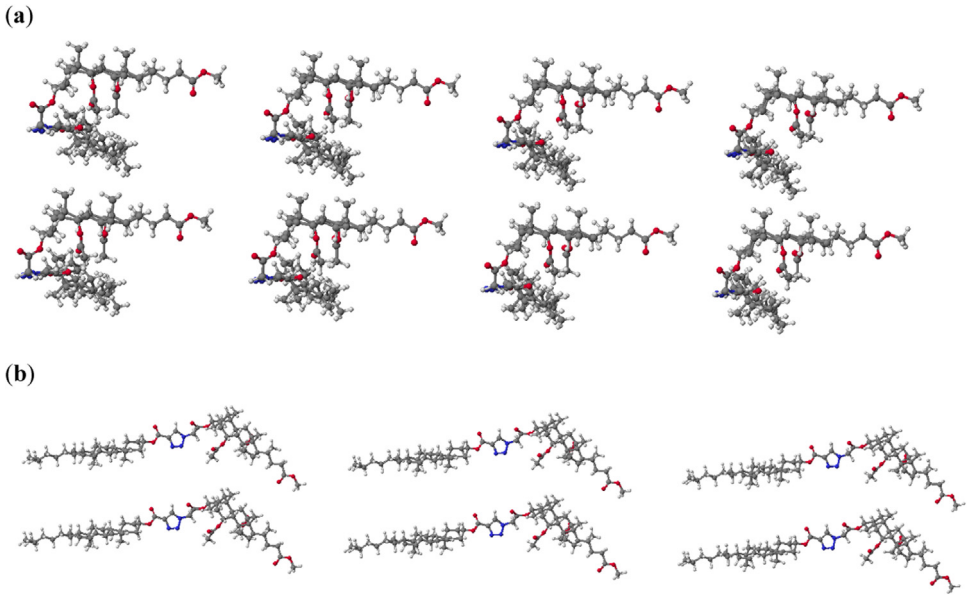

Fig. 4. Molecular models of conformers *syn* (**a**) and *anti* (**b**) of conjugate (**19**) calculated by PM5 method.

Table 4
Heat of formation (HOF) [kcal/mol] of bile acids (**1**–**3**), sterols (**13,14**) and conjugates (**17**–**22**).

Compound	HOF	HOF_{syn}	HOF_{anti}	ΔHOF_1	ΔHOF_2	ΔHOF_3	ΔHOF_4
1	−229.2756	–	–	–	–	–	–
2	−266.8560	–	–	–	–	–	–
3	−309.8662	–	–	–	–	–	–
13	−145.2016	–	–	–	–	–	–
14	−167.9130	–	–	–	–	–	–
17	–	−370.9984	−370.8825	−141.7228	−141.6069	−225.7968	−225.6809
18	–	−448.9483	−456.2749	−182.0923	−189.4189	−303.7467	−311.0733
19	–	−533.3628	−542.0610	−223.4966	−232.1948	−388.1612	−396.8450
20	–	−394.2004	−393.6084	−164.9248	−164.3328	−226.2874	−225.6954
21	–	−471.8692	−479.4003	−205.0132	−212.5443	−3,039,562	−311.4873
22	–	−557.2032	−557.2743	−247.3370	−247.4081	−389.2902	−389.3613

$\Delta HOF_1 = HOF_{conjugates\,syn(\mathbf{17}-\mathbf{22})} - HOF_{bile\ acids\ (\mathbf{1}-\mathbf{3})}$.
$\Delta HOF_2 = HOF_{conjugates\,anti\ (\mathbf{17}-\mathbf{22})} - HOF_{bile\ acids\ (\mathbf{1}-\mathbf{3})}$.
$\Delta HOF_3 = HOF_{conjugates\,syn(\mathbf{17}-\mathbf{22})} - HOF_{sterols(\mathbf{13}-\mathbf{14})}$.
$\Delta HOF_4 = HOF_{conjugates\,anti(\mathbf{17}-\mathbf{22})} - HOF_{sterols(\mathbf{13}-\mathbf{14})}$.

intramolecular interactions are formed. This is due to the absence of electron donating or acceptor groups in its molecule (without OAc groups). The preferential formation of *syn* conformers for conjugates (**17**) and (**20**) can therefore be explained by the formation of a molecule that is smaller in volume. However, for the remaining conjugates, deoxycholic and cholic acid derivatives (**18**–**19**) and (**21**–**22**), *anti* conformers with a lower HOF value are arranged in layers (Fig.3).

The relations between the experimental ^{13}C and ^{1}H chemical shifts (δ_{exp}) and the GIAO (Gauge-Independent Atomic Orbitals) magnetic isotopic shielding constants (σ_{calc}), which are widely used in an efficient implementation [65,66], are usually linear and described by the following equation: $\delta_{exp}=a + b\cdot\sigma_{calc}$. The slope and intercept of the least-squares correlation line is used to scale the GIAO magnetic isotopic shielding constants, σ_{calc}, and to predict the chemical shifts, $\delta_{pred}=a + b\cdot\sigma_{calc}$ (Fig. 5). The parameters a and b are given in Table 5. Usually, the correlations between the experimental chemical shifts and calculated magnetic isotopic shielding constants are better for carbon-13 atoms than for protons. The differences between the calculated and experimental shifts for protons are probably due to the fact that the shifts are calculated for single molecules in gas phase. As can be seen from Fig. 5 the correlationis good for both carbon atoms and for the protons.

3.4. Prediction of activity spectra for substances

Potential pharmacological activities of the synthesized compounds have been determined on the basis of computer-aided drug discovery approach with *in silico* Prediction of Activity Spectra for Substances (PASSs) program. It is based on a robust analysis of the structure-activity relationship in a heterogeneous training set currently including about 250.000 biologically active compounds from different chemical series with about 4.500 types of biological activities. Since only the structural formula of the chemical compound is necessary to obtain a PASS prediction, this approach can be used at the earliest stages of investigation. There are many examples of the successful use of the PASS approach leading to new pharmacological agents [74–78]. The PASS software is useful for the study of biological activity of secondary metabolites. We have selected the types of activities that were predicted for a potential compound with the highest probability (focal activities). If predicted activity is higher than 0.7 (PA > 0.7), the substance is very likely to exhibit the activity in experiment and the chance of the substance being the analogue of a known pharmaceutical agent is also high. If predicted activity is between 0.5 and 0.7 (0.5 < PA < 0.7), the substance is unlikely to exhibit the activity. In experiment and the similarity to known pharmaceutical substance is very limited. Additionally, analyses of the biolog-

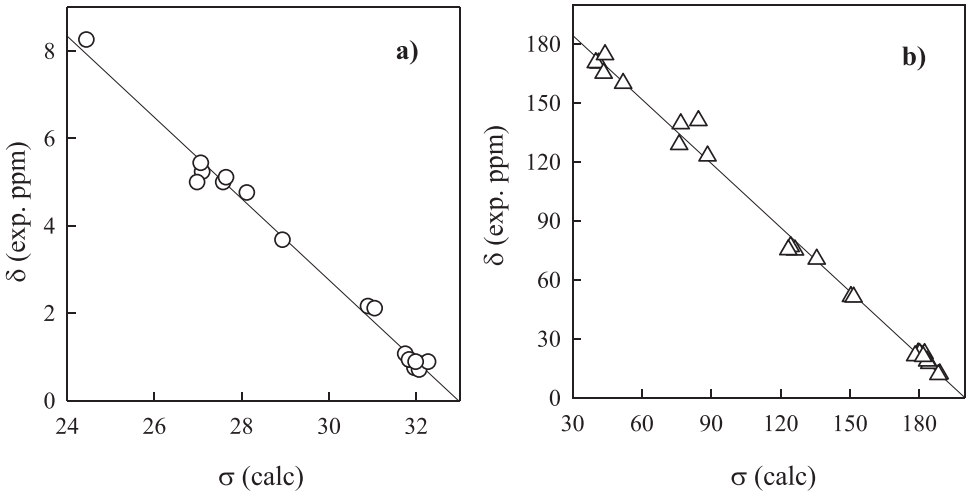

Fig. 5. Experimental chemical shifts (δ_{exp}, $CDCl_3$) in (**19**) vs isotropic magnetic shielding constants (σ_{calc}) from the GIAO/B3LYP/6–311G(d,p) calculations; (**a**) protons and (**b**) carbons-13.

Table 5
Chemical shifts (δ. ppm) in $CDCl_3$ and calculating GIAO nuclear magnetic shielding tensors (σ_{cal}) for (**19**). The predicted GIAO chemical shifts were computed from the linear equation $\delta_{exp.} = a + b{\cdot}\sigma_{calc}$ with a and b determined from the fit of the experimental data (r^2 is the correlation coefficient). .

	$\delta_{exp.}$	δ_{calc}	σ_{calc}		$\delta_{exp.}$	δ_{calc}	σ_{calc}
C(3)	75.16	80.50	126.30	H(3β))	4.74	4.49	28.14
C(7)	70.52	70.38	135.67	H(7β)	4.98	4.99	27.66
C(12)	76.87	82.54	124.41	H(12β)	5.09	4.93	27.58
C(7-CO)	170.22	172.33	41.27	H(18)	0.73	0.92	31.98
C(12-CO)	170.43	173.66	40.09	H(19)	0.92	1.02	31.86
C(7-$COCH_3$)	22.43	19.94	182.38	H(21)	0.82	0.77	32.14
C(12-$COCH_3$)	21.57	21.28	181.14	H(25)	3.66	3.73	28.95
C(18)	12.19	12.87	188.93	H(27)	5.22	5.45	27.11
C(19)	22.78	22.95	179.59	H(28)	8.24	7.91	24.46
C(21)	17.47	17.70	184.45	H(7α-OAc)	2.14	1.91	30.91
C(24)	174.47	169.26	44.12	H(12α-OAc)	2.09	1.77	31.06
C(25)	51.49	54.34	150.53	H(3′α)	4.98	5.55	26.78
C(26)	165.08	169.26	43.50	H(6′)	5.42	5.48	27.08
C(27)	51.18	53.11	151.66	H(18′)	0.69	0.82	32.08
C(28)	128.77	134.65	76.17	H(19′)	1.05	1.12	31.76
C(29)	140.97	125.66	84.47	H(21′)	0.92	1.03	31.85
C(30)	159.88	160.82	51.93	H(26′)	0.87	0.63	32.29
C(3′)	75.26	83.61	123.43	H(27′)	0.87	0.89	32.00
C(5′)	139.39	133.93	76.83	*a*			30.6665
C(6′)	122.97	121.41	88.42	*b*			−0.9303
C(18′)	11.82	13.45	188.39	r^2			0.9905
C(19′)	22.53	22.23	180.26				
C(21′)	18.68	18.72	183.51				
C(26′)	21.36	24.33	178.32				
C(27′)	21.01	20.59	181.78				
a			216.9071				
b			−1.848				
r^2			0.9942				

ical prediction activity spectra for the new bromoacetoxy derivatives of deoxy and cholic acids (**8**–**9**), azidoacetoxy derivatives of deoxy and cholic acids (**11**–**12**), and 5α-cholestan-3-yl-propynoate (**16**) as well as all conjugates (**17**–**22**) prepared herein are good examples of *in silico* studies of chemical compounds. We also selected the types of activity that were predicted for a potential compound with the highest probability (focal activities) (Table 6). According to these data the most frequently predicted types of biological activity for (**8**–**9**) and (**11**–**12**) are: acylcarnitine hydrolase inhibitor,alkenylglycerophosphocholine hydrolase inhibitor, alkylacetylglycerophosphatase inhibitor,dextranase inhibitor, glyceryl-ether monooxygenase inhibitor, peptidoglycan glycosyltransferase inhibitor. Additonaly5α-cholestan-3-yl-propynoate greater than 0.80 are: anesthetic general, respiratory analeptic, protein–disulfide reductase (glutathione) inhibitor, cholestanetriol 26-monooxygenase inhibitor, prostaglandyn-E2 9-reductase inhibitor, CYP2C, CYP3A, CYP2B6 and CYP3A4 substrates, flavin-containing monooxygenase inhibitor, alkenylglycerophosphoethanolamine hydrolase inhibitor, linoleate diol synthase inhibitorglucan Endo-1,3-beta-D-glucosidase inhibitor, antieczematic, analeptic. Conjugates have significantly lower predicted biological activity than the substrates discussed above.The most important include: pancreatic disorders treatment, glyceryl-ether monooxygenase inhibitor, cholesterol antagonist, antihypercholesterolemic, aypolipemic.

Table 6
"Probability to be Active" (PA) values for the predicted biological activity of (**8–9**)and (**11–12**), (**16**) as well as (**15–20**).

FocalPredicted Activity (PA>0.70)	Compounds										
	8	**9**	**11**	**12**	**16***	**17**	**18**	**19**	**20**	**21**	**22**
Acylcarnitinehydrolase inhibitor	0.96	0.96	0.95	0.95	0.96	–	–	–	–	–	–
Alkenylglycerophosphocholinehydrolase inhibitor	0.93	0.90	0.89	0.83	0.95	–	–	–	–	–	–
Alkylacetylglycerophosphatase inhibitor	0.93	0.90	0.90	0.86	0.95	–	–	–	–	–	–
Dextranase inhibitor	0.89	0.83	0.85	0.75	0.89	–	–	–	–	–	–
Glyceryl-ethermonooxygenase inhibitor	0.82	0.85	0.80	0.83	0.81	–	0.71	0.75	0.72	0.75	0.79
Peptidoglycanglycosyltransferase inhibitor	0.81	0.75	0.80	0.73	0.82	–	–	–	–	–	–
Cholesterol antagonist	0.79	0.76	–	–	0.89	0.84	0.76	0.76	0.71	–	–
Protein-disulfide reductase (glutathione) inhibitor	0.80	0.72	0.76	–	–	–	–	–	–	–	–
Adenomatouspolyposistreatment	0.79	0.80	0.76	0.78	0.83	–	–	–	–	–	–
Cytoprotectant	0.74	0.76	0.73	0.75	–	–	–	–	–	–	–
Hypolipemic	–	0.71	–	0.74	0,73	0.76	0.78	0.85	–	–	0.78
Antihypercholesterolemic	–	–	0.73	0.79	0,80	0.73	–	0.75	–	–	–
Pancreaticdisorderstreatment	–	–	–	–	–	0.83	0.80	0.79	0.90	0.86	0.84

* more examples in the text.

Table 7
Calculated docking scores for compounds (**19**) and (**22**).

	ΔG docking score [kcal/mol]			
Compound	2Q85	1KZN	5V5Z	1EZF
19	−6.877	−9.946	−15.856	−13.361
22	−0.238	−10.34	−15.388	−15.119

3.5. Molecular docking studies

Potential antibacterial and antifungal activity of two representative compounds was determined in docking study. In this case two of the most common molecular targets which are responsible for antibacterial activity were chosen: *E. coli* MurB (PDB ID: 2Q85) [79] and Gyrase (PDB ID: 1KZN) [80]. In terms of antifungal activity two of the most significant molecular targets are: $CYP51_{Ca}$ (PDB ID: 5V5Z) [81] and Squalene synthase (PDB ID: 1EZF) [82] and that targets were chosen for docking study. Based on calculated docking score (Table 7), most of considered compounds may exhibit potential antibacterial and antifungal activity, however antifungal activity seems to be stronger. All docked compounds occupy the same binding pocket as the parent co-crystallized ligands.

3.5.1. Docking to antibacterial drug targets

During dockinig to *E. coli* MurB protein (Fig. 6), forming of strong hydrogen bond with Arg327 was observed for both compounds. Ligands adopt bent conformation in the binding site. Ligand **19** exhibited forming of additional strong hydrogen bonds (bond length $\leq$ 2.1 Å) with Gln120 and Arg159. For the same ligand, we identified stabilizing hydrophobic contact (with Ile110, Leu290, Val291 and Pro111) as well. The binding mode for compound **19** is similar to those reported by A. Geronikaki [83]. Ligand **22** (Fig. 7) with the highest docking score (ΔG = −0.238 kcal/mol) exhibited many steric clashes which may suggest it does not fit to the binding pocket which may implies low activity. In terms of binding to gyrase (Table 7, 1KZN) both compounds exhibit low docking score and forming hydrogen bonds with Arg136 and Arg76 (bond length $\leq$ 2.2 Å) and cation-pi interaction between 1,2,3-triazole ring and Arg76. Some stabilizing hydrophobic interactions were identified as well as less number of steric clashes than for 2Q85.

3.5.2. Docking to antifungal drug targets

For both targets, docking study revealed the lowest docking scores and bent conformations for considered compounds. Ligand **19** (Fig. 8) forms strong hydrogen bond (bond length = 2.6 Å) between His377 and lanosterol 14 alpha-demethylase of C. albicans (Table 7, $CYP51_{Ca}$) whereas compound **22** (Fig. 8) forms hydrogen interaction with Met508 (bond length = 2.3 Å). In terms of stabilizing hydrophobic interactions (eg. Phe233 or Ile231) one of the most crucial is interaction between compound **19** and Hem601. This interaction was not observed for ligand **22**. For both ligands just a few steric clashes were identified which shows that ligands fit into binding pocket well. Docked ligand **19** to Squalene synthase (Fig. 9, Table 7) revealed forming of two strong hydrogen bonds with Arg218 and Arg52 (bond length $\leq$ 2.1 Å) while ligand **22** showed only one hydrogen bond with Gln212 (bond length $\leq$ 2.1 Å). Some weak stabilizing hydrophobic interactions were identified as well as a few steric clashes. Both compounds adopt bent conformation.

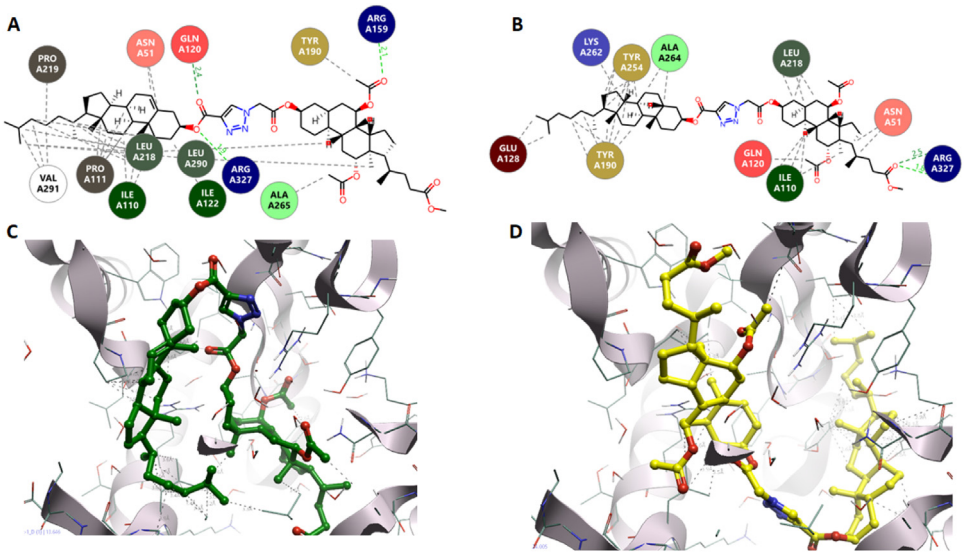

Fig. 6. Ligand interactions and binding mode for compound **19** and **22** in 2Q85. A, C – represents ligand **19** (green); B, D – represents ligand **22** (yellow).

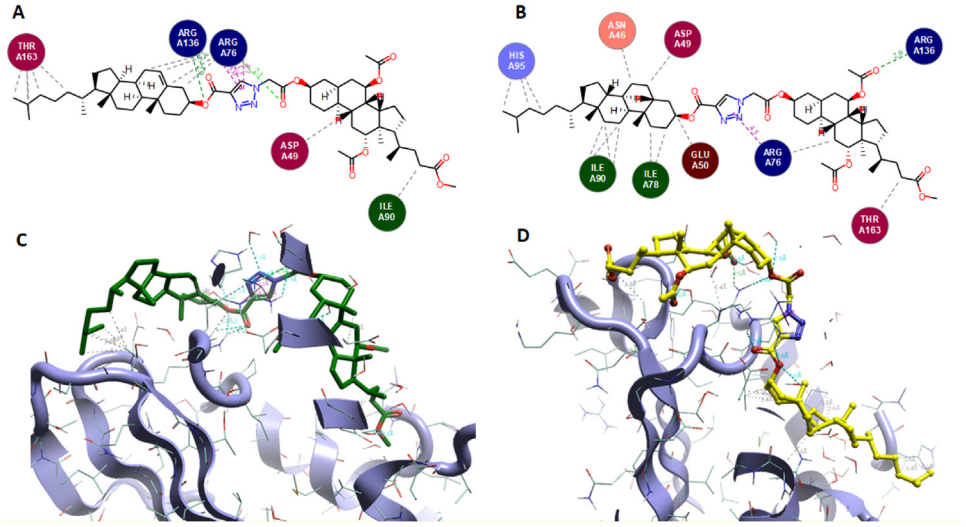

Fig. 7. Ligand interactions and binding mode for compound **19** and **22** in 1KZN. A, C – represents ligand **19** (green); B, D – represents ligand **22** (yellow).

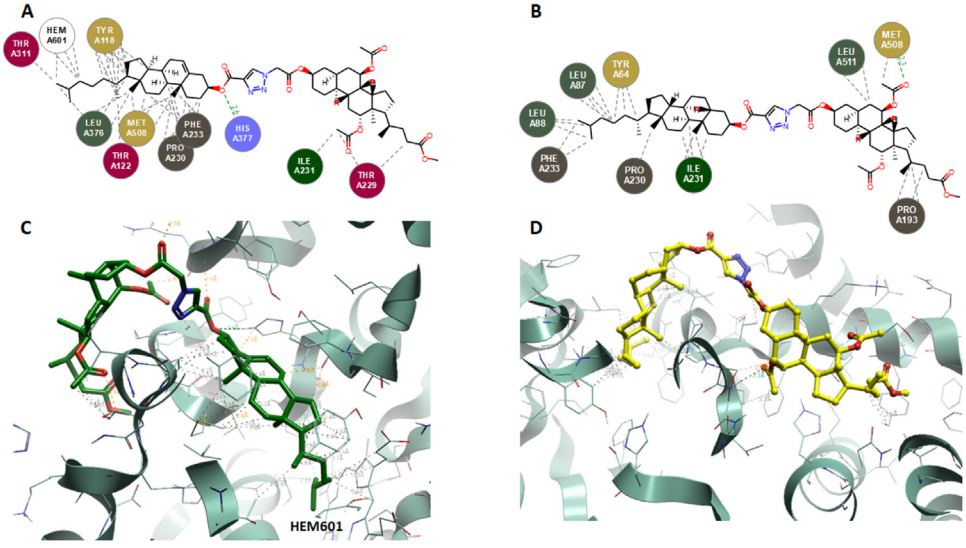

Fig. 8. Ligand interactions and binding mode for compound **19** and **22** in 5V5Z. A, C – represents ligand **19** (green); B, D – represents ligand **22** (yellow).

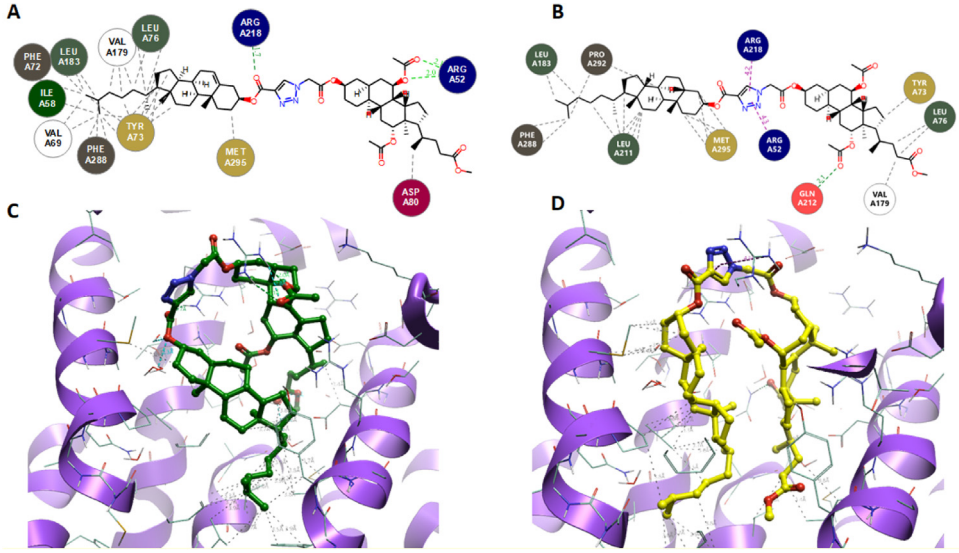

Fig. 9. Ligand interactions and binding mode for compound **19** and **22** in 1EZF. A, C – represents ligand **19** (green); B, D – represents ligand **22** (yellow).

4. Conlusions

The increasing interest in the synthesis of new bile acid conjugates using the click chemistry method significantly influences on the development of supramolecular chemistry, pharmacology and medicine. Design, preparation, enormous biological potential and a wide range of physicochemical properties of compounds containing the 1,2,3-triazole ring allow them to be used as artificial receptors, organogels or new complexing and transporting drugs. In conclusion, six new conjugates of bile acids and sterols linked with 1,2,3-triazole ring (**17**–**22**) in a way: head (sterol)–tail (bile acid) were prepared from cholesterol/cholestanol esters of propiolic acid and azidoacetyl substituted derivatives of bile acids in *t*-BuOH/MeOH mixture in the presence of $CuSO_4{\cdot}5H_2O$ and sodium ascorbate at 60 °C. Moreover, two bromoacetyl (**8**) and (**9**) as well as two azidoacetyl (**11**) and (**12**) substituted derivatives of bile acids were prepared from dehydrocholic or cholic acid in dry dichloromethane with bromoacetic acid bromide and in THF with sodium azide at 50 °C, appropriately. Additionally cholestanyl ester of propiolic acid (**16**) were prepared from cholestanol in dichloromethane. These new compounds linked with 1,2,3-triazole ring were characterized by analytical methods such as spectroscopic (NMR, FT-IR), spectrometry (ESI-MS), semiempirical calculation (PM5) and PASS. The effects of inter and intramolecular interactions and conformation of molecules have been precisely explained by comparison of experimental data taken in the condensed phase and calculation data (gas phase).The magnetic isotopic shielding constants, σ_{calc}, were calculated by the GIAO/B3LYP/6–311G(dp) level of theory. Linear correlations between the experimental ^{1}H and ^{13}C chemical shifts and the computed screening constants confirm the optimized geometry. The potential antibacterial and antifungal activity of two representative compounds were determined in the docking study. Based on the calculated docking score most of the considered compounds may exhibit potential antibacterial and antifungal activity, however, antifungal activity seems to be stronger.

5. Author contributions

The listed authors contributed to this work as described in the following. Anna Kawka performed the synthesis of cholesterol and bile acid derivatives. Grzegorz Hajdaś performed the synthesis of cholestanol and bile acid derivatives. Hanna Koenig was purifying compounds and interpreted the results. Iwona Kowalczyk performed quantum chemical calculations. Tomasz Pospieszny carried out of the synthetic work, interpretation of results, performed semiempirical calculations (PM5) and Prediction of Activity Spectra for Substances (PASS). Damian Kułaga performed and described molecular docking studies. All authors con tributed with valuable discussions and scientific in put and approved the final version.

Declaration of Competing Interest

The authors declare that they have no known competing financial interests or personal relationships that could have appeared to influence the work reported in this paper.

References

[1] T. Pospieszny, I. Małecka, Z. Paryzek, Synthesis and spectroscopic studies of new bile acid derivatives linked by a 1,2,3–triazole ring, Tetrahedron Lett. 53 (2012) 301–305, doi:10.1016/j.tetlet.2011.11.027.
[2] I. Kirson, E. Glotter, Recent developments in naturally occurring ergostane–type steroids. A review, J. Nat. Prod. 44 (1981) 633–647, doi:10.1021/np50018a001.
[3] T. Pospieszny, H. Koenig, I. Kowalczyk, B. Brycki, Spectroscopic methods and theoretical studies of bromoacetic substituted derivatives of bile acids, Acta Chim. Slov. 62 (2015) 15–27, doi:10.17344/acsi.2014.608.
[4] P.M. Dewick, Bile Acids, in: Medicinal Natural Products A Biosynthetic Approach, 3rd Ed, John Wiley and Sons, Ltd., Chichester, West Sussex, United Kingdom, 2009, pp. 275–277.
[5] H. Gao, J.R. Dias, Selective protection of the various hydroxy groups of cholic acid and derivatives. a review, Org. Prep. Proced. Int. 31 (1999) 145–166, doi:10.1080/00304949909355705.
[6] T. Pospieszny, H. Koenig, I. Kowalczyk, B. Brycki, Molecular structure, spectral and thermal properties and in silico biological activity of new bis–phthalimidopropylalkylammonium conjugates of bile acids, J. Mol. Struct. 1243 (2021) 130814, doi:10.1016/j.molstruc.2021.130814.
[7] J.Y.L. Chiang, Bile acids: regulation of synthesis: thematic review series: bile acids, J. Lipid Res. 50 (2009) 1955–1966, doi:10.1194/jlr.R900010-JLR200.
[8] K. Rajakumar, S.L. Greenspan, S.B. Thomas, M.F. Holick, Solar ultraviolet radiation and vitamin D, Am. J. Public Health. 97 (2007) 1746–1754, doi:10.2105/AJPH.2006.091736.
[9] P.L. Suarez, Z. Gándara, G. Gómez, Y. Fall, Vitamin D and click chemistry. Part 1: a stereoselective route to vitamin D analogues with triazole rings in their side chains, Tetrahedron Lett. 45 (2004) 4619–4621, doi:10.1016/j.tetlet.2004.04.117.
[10] M. Makishima, T.T. Lu, W. Xie, G.K. Whitfield, H. Domoto, R.M. Evans, M.R. Haussler, D.J. Mangelsdorf, Vitamin D receptor as an intestinal bile acid sensor, Science 296 (2002) 1313–1316, doi:10.1126/science.1070477.
[11] B. Brycki, H. Koenig, I. Kowalczyk, T. Pospieszny, Synthesis, spectroscopic and theoretical studies of new dimeric quaternary alkylammonium conjugates of sterols, Molecules 19 (2014) 9419–9434, doi:10.3390/molecules19079419.
[12] W.H. Okamura, M.M. Midland, M.W. Hammond, N.Abd. Rahman, M.C. Dormanen, I. Nemere, A.W. Norman, Chemistry and conformation of vitamin D molecules, J. Steroid Biochem. Mol. Biol. 53 (1995) 603–613, doi:10.1016/0960-0760(95)00107-B.

[13] D.S. Agarwal, H.S. Anantaraju, D. Sriram, P. Yogeeswari, S.H. Nanjegowda, P. Mallu, R. Sakhuja, Synthesis, characterization and biological evaluation of bile acid–aromatic/heteroaromatic amides linked via amino acids as anti–cancer agents, Steroids 107 (2016) 87–97, doi:10.1016/j.steroids.2015.12.022.

[14] Y. Li, J.R. Dias, Dimeric and Oligomeric Steroids, Chem. Rev. 97 (1997) 283–304, doi:10.1021/cr9600565.

[15] B. Brycki, H. Koenig, T. Pospieszny, Quaternary alkylammonium conjugates of steroids: synthesis, molecular structure, and biological studies, Molecules 20 (2015) 20887–20900, doi:10.3390/molecules201119735.

[16] M. Malkoch, R.J. Thibault, E. Drockenmuller, M. Messerschmidt, B. Voit, T.P. Russell, C.J. Hawker, Orthogonal approaches to the simultaneous and cascade functionalization of macromolecules using click chemistry, J. Am. Chem. Soc. 127 (2005) 14942–14949, doi:10.1021/ja0549751.

[17] I.A. Pikuleva, Cytochrome P450s and cholesterol homeostasis, Pharmacol. Ther. 112 (2006) 761–773, doi:10.1016/j.pharmthera.2006.05.014.

[18] L. Xiao, E. Yu, H. Yue, Q. Li, Enhanced liver targeting of camptothecin via conjugation with deoxycholic acid, Molecules 1179 (24) (2019) 1179–1185, doi:10.3390/molecules24061179.

[19] R. Mishra, S. Mishra, Updates in bile acid–bioactive molecule conjugates and their applications, Steroids 159 (2020) 108639, doi:10.1016/j.steroids.2020.108639.

[20] H. Woo, H. Kang, A. Kim, S. Jang, J.C. Park, S. Park, B.–S. Kim, H. Song, K.H. Park, Azide–alkyne Huisgen [3+2] cycloaddition using CuO nanoparticles, Molecules 17 (2012) 13235–13252, doi:10.3390/molecules171113235.

[21] K.Y. Tserng, D.L. Hachey, P.D. Klein, An improved procedure for the synthesis of glycine and taurine conjugates of bile acids, J. Lipid Res. 18 (1977) 404–407, doi:10.1016/S0022-2275(20)41691-8.

[22] S.M. Huijghebaert, A.F. Hofmann, Influence of the amino acid moiety on deconjugation of bile acid amidates by cholylglycine hydrolase or human fecal cultures, J. Lipid Res. 27 (1988) 742–752, doi:10.1016/S0022-2275(20)38791-5.

[23] A.F. Hofmann, L.R. Hagey, M.D. Krasowski, Bile salts of vertebrates: structural variation and possible evolutionary significance, J. Lipid Res. 51 (2010) 226–246, doi:10.1194/jlr.R000042.

[24] J.Y.L. Chiang, Bile acids: regulation of synthesis, J. Lipid Res. 50 (2009) 1955–1966, doi:10.1194/jlr.R900010-JLR200.

[25] S. Mukhopadhyay, U. Maitra, Chemistry and biology of bile acids, Curr. Sci 87 (2004) 1666–1683.

[26] B. Brycki, H. Koenig, I. Kowalczyk, T. Pospieszny, Synthesis, spectroscopic and theoretical studies of new quaternary N,N–dimethyl–3–phthalimidopropylammonium conjugates of sterols and bile acids, Molecules 19 (2014) 4212–4233, doi:10.3390/molecules19044212.

[27] J. Tamminen, E. Kolehmainen, Bile acids as building blocks of supramolecular hosts, Molecules 6 (2001) 21–46, doi:10.3390/60100021.

[28] D. Opsenica, G. Pocsfalvi, Z. Juranic, B. Tinant, J.P. Declercq, D.E. Kyle, W.K. Milhous, B.A. Solaja, Cholic acid derivatives as 1,2,4,5–tetraoxane carriers: structure and antimalarial and antiproliferative activity, J. Med. Chem. 43 (2000) 3274–3282, doi:10.1021/jm000952f.

[29] E. Virtanen, E. Kolehmainen, Use of bile acids in pharmacological and supramolecular applications, Eur. J. Org. Chem. 2004 (2004) 3385–3399, doi:10.1002/ejoc.200300699.

[30] D. Albert, M. Feigel, β–Loop, γ–loop, and helical peptide conformations in cyclopeptides containing a steroidal pseudo–amino acid, Helv. Chim. Acta. 80 (1997) 2168–2181, doi:10.1002/hlca.19970800716.

[31] T. Pospieszny, H. Koenig, Design, synthesis, spectral and theoretical study of new bile acid–sterol conjugates linked via 1,2,3–triazole ring, Steroids 176 (2021) 108934, doi:10.1016/j.steroids.2021.108934.

[32] D.S. Agarwal, V. Siva Krishna, D. Sriram, P. Yogeeswari, R. Sakhuja, Clickable conjugates of bile acids and nucleosides: synthesis, characterization, in vitro anticancer and antituberculosis studies, Steroids 139 (2018) 35–44, doi:10.1016/j.steroids.2018.09.006.

[33] H. Wang, W.–H. Chan, A cholic acid–based fluorescent chemosenor for the detection of ATP, Org. Biomol. Chem. 6 (2008) 162–168, doi:10.1039/B715086E.

[34] A. Kumar, R.K. Chhatra, P.S. Pandey, Synthesis of click bile acid polymers and their application in stabilization of silver nanoparticles showing iodide sensing property, Org. Lett. 12 (2010) 24–27, doi:10.1021/ol902351g.

[35] T. Pospieszny, Molecular pockets, umbrellas and quasi podands from steroids: synthesis, structure and applications, Mini–Rev. Org. Chem 12 (2015) 258–270, doi:10.2174/1570193x1203150429105154.

[36] P.S. Pandey, R. Rai, R.B. Singh, Synthesis of cholic acid–based molecular receptors: head–to–head cholaphanes, J. Chem. Soc. Perkin 1 (1) (2002) 918–923, doi:10.1039/B200320C.

[37] J. Ropponen, J. Tamminen, E. Kolehmainen, K. Rissanen, Synthesis and characterization of novel steroidal dendrons, Synthesis (Mass) (2003) 2226–2230, doi:10.1055/s-2003-41041.

[38] T. Pospieszny, H. Koenig, I. Kowalczyk, B. Brycki, Synthesis, spectroscopic and theoretical studies of new Quasi–Podands from bile acid derivatives linked by 1,2,3–triazole rings, Molecules 19 (2014) 2557–2570, doi:10.3390/molecules19022557.

[39] D. Verzele, S. Figaroli, A. Madder, Shortcut access to peptidosteroid conjugates: building blocks for solid–phase bile acid scaffold decoration by convergent ligation, Molecules 16 (2011) 10168–10186, doi:10.3390/molecules161210168.

[40] H. Wang, W.–H. Chan, Cholic acid–based fluorescent sensor for mercuric and methyl mercuric ion in aqueous solutions, Tetrahedron 36 (2007) 8825–8830, doi:10.1016/j.tet.2007.06.026.

[41] V. Noponen, H. Belt, M. Lahtinen, A. Valkonen, H. Salo, J. Ulrichová, A. Galandáková, E. Sievänen, Bile acid–cysteamine conjugates: structural properties, gelation, and toxicity evaluation, Steroids 77 (2012) 193–203, doi:10.1016/j.steroids.2011.11.006.

[42] D. Pasini, The click reaction as an efficient tool for the construction of macrocyclic structures, Molecules 18 (2013) 9512–9530, doi:10.3390/molecules18089512.

[43] T. Pospieszny, M. Pakiet, I. Kowalczyk, B. Brycki, Design, synthesis and application of new bile acid ligands with 1,2,3–triazole ring, Supramol. Chem. 29 (2017) 81–93, doi:10.1080/10610278.2016.1175568.

[44] H.C. Kolb, M.G. Finn, K.B. Sharpless, Click Chemistry: diverse Chemical Function from a Few Good Reactions, Angew. Chem. Int. Ed Engl. 40 (2001) 2004–2021, doi:10.1002/1521-3773(20010601)40:11⟨2004::AID-ANIE2004⟩3.0.CO;2-5.

[45] F. Himo, T. Lovell, R. Hilgraf, V.V. Rostovtsev, L. Noodleman, K.B. Sharpless, V.V. Fokin, Copper(I)–catalyzed synthesis of azoles. DFT study predicts unprecedented reactivity and intermediates, J. Am. Chem. Soc. 127 (2005) 210–216, doi:10.1021/ja0471525.

[46] J. Morales–Sanfrutos, M. Ortega–Muñoz, J. Lopez–Jaramillo, F. Hernandez–Mateo, F. Santoyo–Gonzalez, Synthesis of calixarene–based cavitands and nanotubes by click chemistry, J. Org. Chem. 73 (2008) 7768–7771, doi:10.1021/jo801325c.

[47] C.D. Hein, X.–M. Liu, D. Wang, Click chemistry, A powerful tool for pharmaceutical sciences, Pharm. Res. 25 (2008) 2216–2230, doi:10.1007/s11095-008-9616-1.

[48] J.E. Hein, V.V. Fokin, Copper–catalyzedazide–alkyne cycloaddition (CuAAC) and beyond: new reactivity of copper(I) acetylides, Chem. Soc. Rev. 39 (2010) 1302–1315, doi:10.1039/B904091A.

[49] R. Huisgen, Kinetics and mechanism of 1,3–dipolar cycloadditions, Angew. Chem. Int. Ed. Engl. 2 (1963) 633–645, doi:10.1002/anie.196306331.

[50] F. Amblard, J.H. Cho, R.F. Schinazi, Cu(I)–CatalyzedHuisgenAzide−alkyne 1,3–dipolar cycloaddition reaction in nucleoside, nucleotide, and oligonucleotide chemistry, Chem. Rev. 109 (2009) 4207–4220, doi:10.1021/cr9001462.

[51] G.C. Tron, T. Pirali, R.A. Billington, P.L. Canonico, G. Sorba, A.A. Genazzani, Click chemistry reactions in medicinal chemistry: applications of the 1,3–dipolar cycloaddition between azides and alkynes, Med. Res. Rev. 28 (2008) 278–308, doi:10.1002/med.20107.

[52] A. Kumar, P.S. Pandey, Steroidal 1,2,3–triazole–based sensors for Hg2+ ion and their logic gate behaviour, Tetrahedron Lett 50 (2009) 5842–5845, doi:10.1016/j.tetlet.2009.08.007.

[53] L. Liu, K. Sun, L. Su, J. Dong, L. Cheng, X. Zhu, C.–T. Au, Y. Zhou, S.–F. Yin, Palladium–catalyzed regio– and stereoselective coupling–addition of propiolates with arylsulfonyl hydrazides: a pattern for difunctionalization of alkynes, Org. Lett. 20 (2018) 4023–4027, doi:10.1021/acs.orglett.8b01585.

[54] J. Johansson, T. Beke–Somfai, A. Said Stålsmeden, N. Kann, Ruthenium–catalyzed azide alkyne cycloaddition reaction: scope, mechanism, and applications, Chem. Rev. 116 (2016) 14726–14768, doi:10.1021/acs.chemrev.6b00466.

[55] J. Palaniraja, S. Roopan, Ruthenium mediated cycloaddition reaction in organic synthesis – review, Chem. Sci. Rev. Lett. 3 (2014) 93–100 ISSN 2278-6783.

[56] B.C. Boren, S. Narayan, L.K. Rasmussen, L. Zhang, H. Zhao, Z. Lin, G. Jia, V.V. Fokin, Ruthenium–CatalyzedAzide−alkyne cycloaddition: scope and mechanism, J. Am. Chem. Soc. 130 (2008) 8923–8930, doi:10.1021/ja0749993.

[57] A. Kumar, P.S. Pandey, Anion recognition by 1,2,3–triazolium receptors: application of click chemistry in anion recognition, Org. Lett. 10 (2008) 165–168, doi:10.1021/ol702457w.

[58] X. Cui, X. Zhang, W. Wang, X. Zhong, Y. Tan, Y. Wang, J. Zhang, Y. Li, X. Wang, Regitz Diazo transfer reaction for the synthesis of 1,4,5–trisubstituted 1,2,3–triazoles and subsequent regiospecific construction of 1,4–disubstituted 1,2,3–triazoles via C–C bond cleavage, J. Org. Chem. 86 (2021) 4071–4080, doi:10.1021/acs.joc.0c02912.

[59] Y. Fang, K. Bao, P. Zhang, H. Sheng, Y. Yun, S.–X. Hu, D. Astruc, M. Zhu, Insight into the mechanism of the CuAAC reaction by capturing the crucial Au $_4$ Cu $_4$ $-\pi$–alkyne intermediate, J. Am. Chem. Soc. 143 (2021) 1768–1772, doi:10.1021/jacs.0c12498.

[60] R. Ramapanicker, P. ChauhanS. Chandrasekaran (Ed.), Click chemistry: mechanistic and synthetic perspectives, Click React. Org. Synth (2016) 1–24, doi:10.1002/9783527694174.ch1.

[61] R. Dennington II, T. Keith, T.J. Millam, Gauss View, Version 4.1.2, Semichem. Inc., Shawnee Mission, KS, 2007.

[62] M. Frisch, G.W. Trucks, H.B. Schlegel, G.E. Scuseria, M.A. Robb, J.R. Cheeseman, G. Scalmani, V. Barone, B. Mennucci, G.A. Petersson, H. Nakatsuji, M. Caricato, X. Li, H.P. Hratchian, A.F. Izmaylov, J. Bloino, G. Zheng, J.L. Sonnenberg, M. Hada, M. Ehara, K. Toyota, R. Fukuda, J. Hasegawa, M. Ishida, T. Nakajima, Y. Honda, O. Kitao, H. Nakai, T. Vreven, J.A. MontgomeryJr, J.E. Peralta, F. Ogliaro, M. Bearpark, J.J. Heyd, E. Brothers, K.N. Kudin, V.N. Staroverov, R. Kobayashi, J. Normand, K. Raghavachari, A. Rendell, J.C. Burant, S.S. Iyengar, J. Tomasi, M. Cossi, N. Rega, J.M. Millam, M. Klene, J.E. Knox, J.B. Cross, V. Bakken, C. Adamo, J. Jaramillo, R. Gomperts, R.E. Stratmann, O. Yazyev, A.J. Austin, R. Cammi, C. Pomelli, J.W. Ochterski, R.L. Martin, K. Morokuma, V.G. Zakrzewski, G.A. Voth, P. Salvador, J.J. Dannenberg, S. Dapprich, A.D. Daniels, O. Farkas, J.B. Foresman, J.V. Ortiz, J. Cioslowski, D.J. Fox, Gaussian 09, Revision D.01, Gaussian, Inc., Wallingford CT, 2009.

[63] A.D. Becke, Density-functional thermochemistry. V. Systematic optimization of exchange-correlation functionals, J. Chem. Phys. 107 (1997) 8554–8560, doi:10.1063/1.475007.

[64] P.J. Stephens, F.J. Devlin, C.F. Chabalowski, M.J. Frisch, Ab initio calculation of vibrational absorption and circular Dichroism spectra using density functional force fields density functional force fields, J. Phys. Chem. 98 (1994) 11623–11627, doi:10.1021/j100096a001.

[65] W.J. Hehre, L. Random, P.V.R. Schleyer, J.A. Pople, Ab Initio Molecular Orbital Theory, Wiley, New York, 1989.
[66] K. Wolinski, J.F. Hilton, P.J. Pulay, Efficient implementation of the gauge-independent atomic orbital method for NMR chemical shift calculations, J. Am. Chem. Soc. 112 (1990) 8251–8260, doi:10.1021/ja00179a005.
[67] Flare, version, Cresset®, Litlington, Cambridgeshire, UK; http://www.cresset-group.com/flare/; Copyright©, 2022 Cresset. All rights reserved.
[68] RCBS Protein DATA BANK; https://www.rcsb.org access: 27.09.2022.
[69] T. Pospieszny, Design and synthesis of new bile acid-sterol conjugates linked *via* 1,2,3-triazole ring, Helv. Chim. Acta 98 (2015) 1337–1350, doi:10.1002/hlca.201500118.
[70] Ž.B. Milanović, D.S. Dimić, E.H. Avdović, D.A. Milenković, J. Dimitrić-Marković, O.R. Klisurić, S.R. Trifunović, Z.S. Marković, Synthesis and comprehensive spectroscopic (X–ray, NMR, FTIR, UV–Vis), quantum chemical and molecular docking investigation of 3–acetyl–4–hydroxy–2–oxo–2H–chromen–7–yl acetate, J. Mol. Struc. 1225 (2021) 129256, doi:10.1016/j.molstruc.2020.129256.
[71] D. Milenković, E. Avdović, D. Dimić, S. Sudha, D. Ramarajan, Ž. Milanović, S. Trifunović, Z. Marković, Vibrational and Hirshfeld surface analyses, quantum chemical calculations, and molecular docking studies of coumarin derivative 3–(1–m–toluidinoethylidene)–chromane–2,4–dione and its corresponding palladium(II) complex, J. Mol. Struc. 1209 (2020) 127935 10.1016/j.molstruc.2020.127935.
[72] D. Dimić, Z. Marković, L. Saso, E. Avdović, J. Đorović, I. Petrović, D. Stanisavljević, M. Stevanović, I. Potočňák, Erika Samoľová, S. Trifunović, J. Dimitrić–Marković, Synthesis and characterization of 3–(1–((3,4–dihydroxyphenethyl)amino)ethylidene)–chroman–2,4–dione as a potential antitumor agent, Oxid. Med. Cell Longev (2019) 2069250–12, doi:10.1155/2019/2069250.
[73] T. Pospieszny, M. Pakiet, I. Kowalczyk, B. Brycki, Design, synthesis and applicationof new bile acid ligands with 1,2,3–triazole ring, Supramol. Chem. 29 (2) (2016) 81–93, doi:10.1080/10610278.2016.1175568.
[74] Way2Drug.com © 2011 - 2022 Version 2.0 Privacy Policy, http://www.pharmaexpert.ru/PASSOnline/.
[75] V.V. Poroikov, D.A. Filimonov, Y.V. Borodina, A.A. Lagunin, A. Kos, Robustness of biological activity spectra predicting by computer program PASS for noncongeneric sets of chemical compounds, J. Chem. Inf. Comput. Sci. 40 (2000) 1349–1355, doi:10.1021/ci000383k.
[76] V.V. Poroikov, D.A. Filimonov, How to acquire new biological activities in old compounds by computer prediction, J. Comput. Aided Mol. Des. 16 (2002) 819–824, doi:10.1023/A:1023836829456.
[77] V.V. Poroikov, D.A. Filimonov, in: Predictive Toxicology, Taylor and Francis, Boca Raton, FL, USA, 2005, pp. 459–478. Helma, C., Ed..
[78] A.V. Stepanchikova, A.A. Lagunin, D.A. Filimonov, V.V. Poroikov, Prediction of biological activity spectra for substances: evaluation on the diverse sets of drug–like structures, Curr. Med. Chem. 10 (2003) 225–233, doi:10.2174/0929867033368510.
[79] A.E. Zoeiby, F. Sanschagrin, R.C. Leves, Structure and function of the Mur enzymes: development of novel inhibitors, Mol. Microbiol. 47 (1) (2003) 1–12, doi:10.1046/j.1365-2958.2003.03289.x.
[80] F. Collin, S. Karkare, A. Maxwell, Exploiting bacterial DNA gyrase as a drug target: current state and perspectives, Appl. Microbiol. Biotechnol. 92 (2011) 479–497, doi:10.1007/s00253-011-3557-z.
[81] T.Y. Hargrove, L. Friggeri, Z. Wawrzak, A. Qi, W.J. Hoekstra, R.J. Schotzinger, J.D. York, F.P. Guengerich, G.I. Lepesheva, Structural analyses of *Candida albicans* sterol 14-demethylase complexed with azole drugs address the molecular basis of azole-mediated inhibition of fungal sterol biosynthesis, J. Biol. Chem. 292 (16) (2017) 6728–6743, doi:10.1074/jbc.M117.778308.
[82] J. Song, N. Shang, N. Baig, J. Yao, Ch. Shin, B.K. Kim, Q. Li, S.R. Malwal, E. Oldfield, X. Feng, R.-.T. Guo, *Aspergillus flavus* squalene synthase as an antifungal target: expression, activity, and inhibition, Biochem. Biophys. Res. Commun. 512 (2019) 517–523, doi:10.1016/j.bbrc.2019.03.070.
[83] N.Sh. Nadaraia, L.Sh. Amiranashvili, M. Merlani, M.L. Kakhabrishvili, N.N. Barbakadze, A. Geronikaki, A. Petrou, V. Poroikov, A. Ciric, J. Glamoclija, M. Sokovic, Novel antimicrobial agents' discovery among the steroid derivatives, Steroids 144 (2019) 52–65, doi:10.1016/j.steroids.2019.02.012.

Poznań, 5 maja 2025 r.

OŚWIADCZENIE

Oświadczamy, że w monografii „Triazole-Based Modification of Bile Acids: Promising Strategies for Combating Infections and Cancer – A Review" opublikowanej w książce *Na pograniczu chemii, biologii i fizyki – rozwój nauk. Tom 6* wkład wymienionych Autorów w przygotowanie publikacji jest następujący:

LP	Imię i nazwisko Autora	Wkład merytoryczny Autora	Podpis Autora
1	Dr inż. Hanna Koenig	Dyskusja wyników, współudział w opracowaniu oryginalnego manuskryptu	
2	Prof. UAM dr hab. Tomasz Pospieszny	Dyskusja wyników, współudział w opracowaniu oryginalnego manuskryptu	

Poznań, 5 maja 2025 r.

OŚWIADCZENIE

Oświadczamy, że w artykule „Steroid and Bioactive Molecule Conjugates: Improving Therapeutic Approaches in Disease Management" opublikowanym w czasopiśmie *Bioorganic Chemistry,* **2024**, *153,* 107933 wkład wymienionych Autorów w przygotowanie publikacji jest następujący:

LP	Imię i nazwisko Autora	Wkład merytoryczny Autora	Podpis Autora
1	Dr inż. Hanna Koenig	Dyskusja wyników, współudział w opracowaniu oryginalnego manuskryptu	
2	Prof. UAM dr hab. Tomasz Pospieszny	Dyskusja wyników, współudział w opracowaniu oryginalnego manuskryptu	

Poznań, 5 maja 2025 r.

OŚWIADCZENIE

Oświadczamy, że w artykule „Exploring Triazole-Connected Steroid-Pyrimidine Hybrids: Synthesis, Spectroscopic Characterization, and Biological Assessment" opublikowanym w czasopiśmie *ACS Omega*, **2024**, *9*, 37995–38014 wkład wymienionych Autorów w przygotowanie publikacji jest następujący:

LP	Imię i nazwisko Autora	Wkład merytoryczny Autora	Podpis Autora
1	Mgr Damian Nowak	Wykonanie oraz interpretacja wyników dokowania molekularnego, współudział w opracowaniu oryginalnego manuskryptu	PODPIS ZAUFANY DAMIAN NOWAK 13.05.2025 11:25:11 [GMT+2] Dokument podpisany elektronicznie podpisem zaufanym
2	Dr inż. Hanna Koenig	Dyskusja wyników, współudział w opracowaniu oryginalnego manuskryptu	
3	Prof. UAM dr hab. Tomasz Pospieszny	Dyskusja wyników, współudział w opracowaniu oryginalnego manuskryptu	

Poznań, 5 maja 2025 r.

OŚWIADCZENIE

Oświadczamy, że w rozdziale „From Squalamine to Triazole Ring Derivatives Exploring the Versatility of Steroidal Bioconjugates" opublikowanym w książce *Studies in Natural Products Chemistry* Edited by Atta-ur Rahman, Elsevier, Amsterdam, Netherlands **2024**, *82*, 247–283 wkład wymienionych Autorów w przygotowanie publikacji jest następujący:

LP	Imię i nazwisko Autora	Wkład merytoryczny Autora	Podpis Autora
1	Dr inż. Hanna Koenig	Dyskusja wyników, współudział w opracowaniu oryginalnego manuskryptu	
2	Prof. UAM dr hab. Tomasz Pospieszny	Dyskusja wyników, współudział w opracowaniu oryginalnego manuskryptu, autor korespondencyjny	

Poznań, 5 maja 2025 r.

OŚWIADCZENIE

Oświadczamy, że w artykule „Quasi-Podands with 1,2,3-Triazole Rings from Bile Acid Derivatives: Synthesis, and Spectroscopic and Theoretical Studies" opublikowanym w czasopiśmie *Journal of Organic Chemistry,* **2024**, *89* (11), 7561–7572 wkład wymienionych Autorów w przygotowanie publikacji jest następujący:

LP	Imię i nazwisko Autora	Wkład merytoryczny Autora	Podpis Autora
1	Dr inż. Hanna Koenig	Dyskusja wyników, współudział w opracowaniu oryginalnego manuskryptu	
2	Mgr Damian Nowak	Wykonanie i opisanie wyników dokowania molekularnego, współudział w opracowaniu oryginalnego manuskryptu	PODPIS ZAUFANY DAMIAN NOWAK 13.05.2025 11:25:23 [GMT+2] Dokument podpisany elektronicznie podpisem zaufanym
3	Prof. UAM dr hab. Tomasz Pospieszny	Dyskusja wyników, współudział w opracowaniu oryginalnego manuskryptu, autor korespondencyjny	

Poznań, 5 maja 2025 r.

OŚWIADCZENIE

Oświadczamy, że w artykule „Molecular Structure, Spectral and Theoretical Study of New Type Bile Acid–Sterol Conjugates Linked *via* 1,2,3-Triazole Ring" opublikowanym w czasopiśmie *Journal of Molecular Structure*, **2023**, *273*, 134313 wkład wymienionych Autorów w przygotowanie publikacji jest następujący:

LP	Imię i nazwisko Autora	Wkład merytoryczny Autora	Podpis Autora
1	Mgr inż. Grzegorz Hajdaś	Współudział w syntezie związków, dyskusja wyników	
2	Dr inż. Damian Kułaga	Wykonanie i opisanie wyników dokowania molekularnego	Podpisano przez/ Signed by: DAMIAN KUŁAGA Data/ Date: 12.05.2025 19:06 mSzafir
3	Dr inż. Hanna Koenig	Dyskusja wyników, współudział w interpretacji wyników i w opracowaniu oryginalnego manuskryptu	
4	Prof. UAM dr hab. Iwona Kowalczyk	Wykonanie i opisanie wyników obliczeń teoretycznych	
5	Prof. UAM dr hab. Tomasz Pospieszny	Dyskusja wyników, wykonanie obliczeń semiempirycznych i określenie potencjału biologicznego (PM5, PASS), współudział w opracowaniu oryginalnego manuskryptu, autor korespondencyjny	